F. L. MCMILLAN

ANL/RAS 73-21
(Revision 3)

Transmitted to AEC
by CKL-261-74
5/31/74

SAFETY ASSESSMENT REPORT FOR THE FUEL ELEMENT FAILURE PROPAGATION LOOP IN THE ENGINEERING TEST REACTOR

May 31, 1974

NOTE: This is a limited distribution report for the use of the recipients. It is not intended for and has not been reviewed for publication, and should not be given broader distribution without permission of the authors, or be referenced in publications.

REACTOR ANALYSIS AND SAFETY DIVISION
ARGONNE NATIONAL LABORATORY
9700 South Cass Avenue
Argonne, Illinois 60439

FEFPL PROJECT OFFICE
AEROJET NUCLEAR COMPANY
550 2nd Street
Idaho Falls, Idaho 83401

ANL/RAS 73-21
(Revision 3)

SAFETY ASSESSMENT REPORT FOR THE FUEL ELEMENT FAILURE PROPAGATION LOOP IN THE ENGINEERING TEST REACTOR

A report prepared jointly by the Argonne National Laboratory and the Aerojet Nuclear Company

May 31, 1974

NOTE: This is a limited distribution report for the use of the recipients. It is not intended for and has not been reviewed for publication, and should not be given broader distribution without permission of the authors, or be referenced in publications.

REACTOR ANALYSIS AND SAFETY DIVISION
ARGONNE NATIONAL LABORATORY
9700 South Cass Avenue
Argonne, Illinois 60439

FEFPL PROJECT OFFICE
Aerojet Nuclear Company
550 Second Street
Idaho Falls, Idaho 83401

ACKNOWLEDGEMENTS

The principal contributors to this report are:

W. A. Bezella, ANL
C. C. Bolta, ANL
E. S. Brown, ANC
J. J. English, ANL
H. K. Fauske, ANL
T. J. Hill, ANC
R. T. Johnson, ANC
W. B. Klingler, ANC
D. H. Lennox, ANL
R. D. Pierce, ANL
R. L. Rider, ANC
J. H. Tessier, ANL
R. W. Thomas, ANC

In addition, valuable assistance was given by E. Barts, J. Barghusen, C. Blomquist, W. Chen, D. Cho, R. Curtis, K. S. Dawson, W. Kaspic, B. D. LaMar, A. Oare, A. Padilla, D. Rose, L. Siefken, C. R. Snyder, D. H. Thompson, and N. C. Kaufman, P. Wang.

CONTENTS

CHAPTER 1.0

TABLE OF CONTENTS

LIST OF TABLES

LIST OF FIGURES

1.0 Introduction

The Fuel Element Failure Propagation Loop (FEFPL) is a doubly contained sodium loop designed for installation in the 175 MW Engineering Test Reactor (ETR). This loop will simulate a fast reactor environment and be used to investigate the potential consequences of certain postulated Liquid Metal Fast Breeder Reactor (LMFBR) malfunctions that may fail fuel. It is the purpose of this Safety Assurance Report (SAR) to show that such planned experiments can be conducted safely.

Analyses are presented that define the results of: a) experiments planned to produce gross fuel failure in the test section; b) malfunctions within the loop system; c) external disturbances that may challenge the loop integrity, such as ETR accidents or seismic events; and d) handling or industrial-type accidents. Of this wide range of potential accidents that were examined, even the most severe were found to pose no undue risk to the ETR facility, personnel, or the public.

In scope, this SAR covers all FEFPL-related activities within the Test Reactor Area (TRA) from the initial charging of the loop with sodium on through its operation in the reactor, removal and loading on the transporter for transfer to the Hot Fuel Examination Facility (HFEF). Safety issues that may arise during transportation to and subsequent examination of the loop at the HFEF will be discussed in separate reports.

The SAR is intended to provide a safety envelope for all experiments containing up to 37 full-length Fast Test Reactor (FTR)[1] fuel pins. These experiments can range in severity from those that may fail only a few fuel pins, to ones where flow to the test section is allowed to coast down or is completely blocked while the test section is operating at 15% over peak FTR linear power. Tests with more than 37 fuel pins are not precluded, provided it can be shown that their consequences fall within the loop safety envelope. For each experiment, a Test Plan that contains safety analysis will be submitted to the ETR operator (ANC) for review and approval to demonstrate that the specific experiment does indeed fall within the limits established by this SAR.

Although this report emphasizes the safety of the FEFPL-ETR system, certain additional precautions will be taken to protect the experiment itself from malfunctions and possible damage that would present a hazard to the reactor or public. Such experiment protection, however, does serve as an additional line of defense, even though it is not needed to ensure the safety of the system.

The SAR includes a brief review of key features of the FEFP loop system; a more complete description will be found in the System Design Description (SDD).[2] The safety philosophy, discussed in Chapter 3, that has evolved during the life of the project forms a basis for the design criteria in the SDD.

1.1 Safety Assessment

The potential hazards associated with the FEFPL operation all stem from one or more of four postulated events: a) sodium fires within the ETR building; b) handling errors involving the loop and/or loop handling machine (LHM); c) loss of loop containment integrity; and d) excessive reactivity feedback from loop to reactor. To guard against an accident in any of these categories, multiple lines of defense are provided, starting with intrinsic design features, supplemented by protection systems and, for backup, additional safety margin to counteract unlikely or unforeseen incidents. The effectiveness of these steps in limiting the risk to the ETR or personnel is demonstrated by the analyses described in Chapters 11, 12, and 13 of this report.

1.2 Design Approach

The FEFPL design, construction, and operational concept is patterned after the philosophy of three levels of safety. As part of the <u>first level</u>, the loop is designed both to satisfy the ETR Technical Specifications[3] and to maintain FEFPL/ETR integrity under the most severe experimental conditions. In addition, the design has a maximum tolerance for errors, off-normal operation and component malfunction. With respect to the containment of the maximum pressure pulse that may result from a fuel-coolant thermal reaction, FEFPL is designed - using appropriate standards such as ASME Section III, Code Case 1331- 7 to withstand pressures many times greater than expected from planned experiments or postulated accidents without permanent deformation of the primary vessel. Major loop components, including the heat exchanger and pump, are designed for continued operation during and after such events. Because the investigation of the propagative potential of possible fuel-coolant interactions is one experimental objective of the FEFP program, continued operation of the ETR is expected during test transients in order to simulate a local malfunction in a large fast reactor. Thus, the loop is designed to safely contain severe planned experiments without the necessity for an ETR scram.

Conservative calculational techniques are used to establish the structural capability of the loop. The pulse shape expected from a bounding molten fuel-coolant interaction (the "design envelope" MFCI) is converted to an equivalent static load to establish loop pressure containment requirements. In comparison with dynamic analyses, the use of this method <u>over estimates</u> the load the structure must be designed to withstand.

To contain molten fuel, and molten steel, that may come from cladding or test section components, a tungsten meltdown cup - backed up with Inconel - is provided. Its capacity is sufficient to hold 50% of the total fuel, plus associated clad and miscellaneous structural material in a test section of 37 full-length FTR pins, although much less is expected (this also amounts to 100% of the fuel that will be physically available during the first four FEFP experiments now planned; See Chapter 10). Cooling of this cup is effected by both forced and natural circulation of sodium within the loop; however, the latter alone is sufficient. The meltdown cup is designed to withstand the maximum pressures that may arise from a design envelope MFCI in the test section. In addition, the assumption is made that molten fuel may react with sodium in the cup itself; consequently, it is designed to withstand, without attenuation, these local events as well.

As additional criteria used to establish the <u>first level</u> of safety, the loop is designed to:

- accommodate all independent, single malfunctions without damage to ETR
- tolerate all ETR credible accidents without failure of loop containment

The <u>second level</u> of safety provides protection against incidents which might occur in spite of the care taken in design, construction, and operation. This additional level of protection is effected by reliable protection devices, redundancy in design, adequate safety margins, and extensive inspection, monitoring and testing to assure that these features are maintained.

For containment of the pressure pulse from a fuel-coolant interaction, two barriers, or vessels, are provided, each of which is independently able to contain the design envelope MFCI without permanent deformation. In the unlikely event that one vessel should fail, the other vessel is designed to contain the consequences with ample margin to ensure the safety of the ETR. Also, each vessel is designed to withstand alone, without buckling, the external loads that may arise from the ETR design basis accident - a double-ended pipe rupture.

Continuous monitoring of the loop containment margin is a function of the FEFPL Plant Protection System (PPS), as described in Chapter 7 of this report, and any significant reduction of this margin calls for an automatic ETR scram. Wall temperatures, pressures, and leak tightness are measured.

Although the loop pump and heat exchanger are built to function normally after an MFCI, the containment system still will prevent loss of sodium to the ETR should one or both fail.

Meltdown cup cooling is effected by circulation of sodium by forced convection if the loop pump is operating, or by natural convection if it is not. Backup heat removal capacity is provided by an annulus gas system that will automatically cool the primary vessel when a preselected temperature is reached. The vessel temperature is monitored continuously by the FEFPL PPS.

The FEFPL third level of safety is achieved through design features and system capability that safeguard the ETR and operating personnel, even if extremely unlikely and unforeseen events occur. To evaluate this extra safety margin, it is necessary to invent circumstances that have a severity level arbitrarily higher than would be associated with all reasonably postulated accidents. For example, the loop is designed to contain, with the primary vessel alone, pressures nearly five times greater than expected from a fuel-coolant interaction that may result from a planned experiment or a loop malfunction. To test the ultimate containment capability of both barriers, it was necessary to conceive - without a known logical precursor -

events that yield much higher pressures. A similar approach is used to establish the safety margin associated with the containment of molten fuel. If the assumption is made that somehow the multiple cooling systems that safeguard the primary vessel all fail, then it is shown that the loop secondary vessel can safely contain molten fuel, should the primary be breached.

These foregoing examples of the FEFPL design approach illustrate the application of three levels of safety. This philosophy of in-depth lines of defense applies to all potential accidents, such as handling errors, fires, and reactivity feedback from loop to reactor. They are discussed in detail in Chapters 11, 12, and 13.

An important component of, and check on, the multiple safety level approach is the additional precautions taken to ensure their effectiveness. These include a rigorous quality assurance program, extensive design review, meticulous inspection of key components, proof testing, and operational verification.

1.3 Experimental Program

The FEFP loop is a major LMFBR safety test vehicle with the capability to perform a wide range of experiments to support FFTF, demonstration and commercial reactor safety. A comprehensive examination of in-pile experiments which are likely to be required in the LMFBR Safety Program, as well as a system of priorities and an ideal schedule for these tests, is contained in ANL/RAS 70-06.[4] A very brief summary of this FEFP in-pile experimental program is provided here to orient the reader.

1.3.1 Experimental Objectives

The principal objectives of the FEFP Program are to:

- investigate the consequences of local malfunction within an LMFBR core
- establish the circumstances under which such malfunctions could cause failure propagation and thus involve a larger segment of the core
- investigate methods both for the detection of malfunctions and protection against their subsequent propagation
- study selected phenomena associated with whole core accidents

In furtherance of these overall program objectives, a comprehensive in-pile testing program has been developed to obtain specific data required in the accident evaluations of the FFTF reactor. A series of ten tests has been scheduled to study basic accident initiating malfunctions and their consequences. They include: end-of-life clad failure, loading error, and power-flow mismatch experiments.

1.3.2 Description of Planned Tests

The first series of FEFPL experiments, listed in Table 1.1, provides safety-related information for the FTR as well as for the reactor Closed Loop System (CLS). The test environment is based upon considerations directly related to FTR, including core geometry, nominal operating conditions, postulated accidents, and specific steps in the accident sequences for that reactor; consequently, the experiments are designed to be prototypical of conditions expected in FTR. These tests are planned on the basis of commitments made among HEDL, WARD, RRD, and they reflect current FTR priorities, but are subject to modification as information needs change. Test parameters, the design of test assemblies, and instrumentation will be selected to provide data needed to define limits for reactor events, to support analytical models of postulated accidents, and to study associated phenomenological events. ETR will be operated for the principal, if not the exclusive, use of the FEFP in-pile loop and will be maintained in a standby condition between experiments. Detailed descriptions of the first two experiments are contained in the "Test Requirements" documents, Refs. 5 and 6. The design of each experiment builds upon the knowledge gained from the totality of preceding tests. Results of experiments in other facilities, such as the TREAT tests with the Mark-II loops and static autoclaves, GETR capsule and Loopsule tests, and other tests now being planned, will provide the experience necessary to optimize later FEFPL experiments. In addition, the FEFPL test sequence progresses from mild to more severe experiments to confirm the safety of the system.

1.3.3 Fuel Element Description

Fuel elements for experiments P1 through P6 will be full-length, and built to FFTF Standards (RDT Standards E-13-1T to E-13-13T) insofar as

TABLE 1.1

REFERENCE FEFP IN-REACTOR EXPERIMENTAL PROGRAM

EXPERIMENT	DESCRIPTION	TEST CONDITIONS Fuel	No. Pins	Duct
P-1	Loop and System Checkout Fuel Pin Loading Error Release of Small Amount of Molten Fuel	S-BOL	19	
P-2	Flow Coastdown	BOL	19	BOL
P-3	Duct Integrity (inlet blockage)	BOL	19	BOL
P-4	Pipe Rupture	S-BOL	19	S-BOL
P-5	Flow Coastdown	S-BOL	37	S-BOL
P-6	Inlet Blockage - CLIRA	S-BOL	37	S-EOL
P-7	CLS Pump Loss (with scram)	EOL	37^{I}	
P-8	Internal Blockage	EOL	$19^{I}/37$	BOL
P-9	SA-to-SA Propagation (inlet blockage)	EOL	$19^{I}/37$	EOL
P-10	Gas Release Fuel Pin Loading Error	EOL	$\frac{24^{I}}{37}$	

Definition of Abbreviations

BOL - beginning of life
S - simulated
S-EOL - simulated end-of-life properties
EOL - end-of-life, these tests contain short (13.5 in) pins only
I - short pin, preirradiated in EBR-II
SA - subassembly

19/37 - 37 total elements, central 19 surrounded by duct
$\frac{24^{I}}{37}$ - fraction of preirradiated pins in single subassembly

feasible except for the enrichment of the uranium fraction, the processing to simulate end-of-life conditions in the fuel, and the instrumentation of the element. Those elements for experiments P7 through P10 will be shorter in both total length and in the fuel zone (60-7/8 and 13-1/2 in., respectively) because they will be preirradiated in EBR-II.

1.3.4 Simulation of FFTF Conditions

The test assemblies for each experiment are designed to provide the best practicable simulation of desired conditions in FTR, consistent with constraints imposed by loop design and flux source. They particularly are influenced by the anticipated relative sensitivity of the experiments to the following factors: temperatures, coolant hydrodynamics, and fuel-element properties. To provide a valid simulation of the thermal environment of a fast reactor under both steady-state and transient conditions, the FEFPL incorporates the following features:

1. A cadmium neutron filter is used to reduce the thermal-neutron component of the neutron spectrum and thus allow a temperature profile within a fuel element close to that found in a fast reactor.

2. A reasonably uniform radial distribution of coolant temperature in the test bundle is attained by reducing the peripheral flow area with smaller spacer wires between the outside elements and the hexagonal shroud.

3. Heat loss to FEFPL bypass flow is minimized with a double-wall hex shroud to simulate, with small fuel bundles, the thermal boundary conditions characteristic of a reactor-size subassembly.

In addition, the concentric FEFP loop design (shown in Fig. 1.1) closely simulates sodium-expulsion characteristics for gas-release and sodium-boiling (Ref. 7). Realistic coolant simulation behavior is attributed both to the relatively friction-free flow channel through the heat exchanger and pumps, and the low internal emf resistance of the pump. The calculated expulsion characteristics of the concentric loop with a 37-element test subassembly are in good agreement with those calculated for a FFTF subassembly. Smaller FEFP test subassemblies show a faster response than the 37-element bundle because they contain less sodium (i.e., have smaller flow area and require less change in coolant flow to produce the same displacement as in a large subassembly).

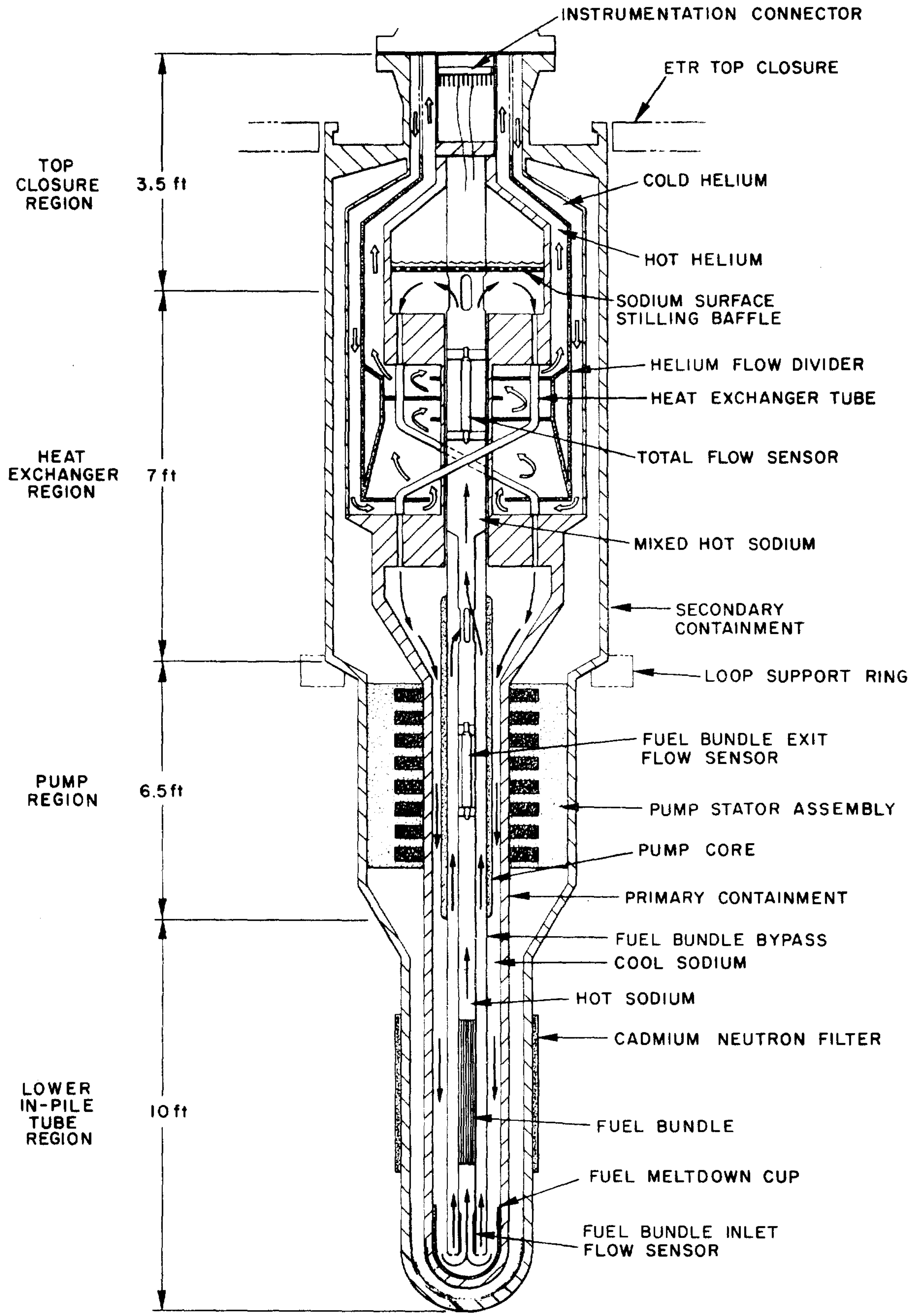

FIG. 1.1 - Schematic of the FEFP In-reactor Loop

1.3.5 ETR Operational Requirements

The FEFPL experimental program is based on the steady-state operation of the ETR with the exception of planned startup and shutdown to simulate the thermal cycling that fuel in an LMFBR may undergo. To achieve the peak linear power of an FTR start-of-life core (14.08 kW/ft) in the test fuel will require an ETR power, depending upon the specific test, around 140 MW - well within the 175 MW operating limit. Test Plan requirements for each experiment will dictate reactor operating power and will be approved as part of the core safety assurance submittal for each test.

1.4 General Loop Capabilities

The FEFP Loop System must be able to accommodate possible malfunctions as well as the following planned types of tests:

1. Gas release experiments, designed primarily to determine the possibility and mode of fuel-element failure and failure propagation caused by the release of fission gas into an FTR-type geometry.

2. Experiments that involve the release of small amounts of molten fuel, designed to determine whether or not propagation of the initial fuel-element failure occurs.

3. Experiments that involve the potential for release of large amounts of molten fuel, such as in a loss-of-flow accident, designed to determine the effects of fuel movement, coolant expulsion and reentry, and the energy release accompanying the molten fuel-coolant interaction.

To accomplish this program, specific experimental functions of the FEFP Loop System include:

- simulation of the FTR environment
- initiation of fuel failure or specific prototypical malfunctions
- containment of coolant and radioactive products under normal and abnormal conditions
- control of coolant temperature and flow conditions
- extraction of heat from the in-pile tests and transport to a heat dump
- retrieval of selected experimental data
- post-test examination of the experiment assembly

1.4.1 Summary Description of System

This brief description provides an introduction to the more extensive treatment contained in Chapter 5 and the System Design Description.

The FEFP Loop System includes the following subsystems:

- in-pile package loop
- test train
- data-acquisition system
- loop control system
- plant protection system
- loop secondary coolant (helium) system
- loop handling machine (LHM)
- loop handling machine transporter
- post-test examination system
- loop filling, storage and remelt (FS&R) system

The loop is 27 ft long, varies in diameter from 5-1/4 to 19 in., and with the test train inserted weighs 7000 lbs. Figure 1.2 shows the loop in place within the ETR.

The test train is considered to be a separate subsystem which fits inside the loop. It is 26 ft long and includes the flow divider, the fuel subassembly to be tested, and the associated test instrumentation. There are provisions for a total of 110 instrumentation leads from the test train. In addition, there are 82 instrumentation leads from the loop which are used to monitor loop operation and for the plant protection system. The loop is sized to accommodate physically a subassembly of up to 61 fuel elements to provide stretch capability for larger tests, should they be needed in the future. This SAR, however, is intended to provide an envelope for the more immediate tests containing up to 37 full-length pins.

As shown in Fig. 1.1, starting from the upper plenum, sodium flows down through the heat exchanger, the pump, the outside of the flow divider (where it removes the gamma heat generated in the primary containment), to the bottom of the loop, where it reverses direction and flows up through the fuel bundle and the bypass, through the inner hole in the pump core and the center tube of the heat exchanger, returning to the upper plenum region. The bypass flow stream mixes with the test-sample flow stream above the test sample, depending on experimental requirements. Mixed-mean sodium temperatures are specified to be a maximum of 1100°F, but sodium exiting the test unit can be higher, particularly during experimental transients. The loop contains about 30 gal of sodium which circulates at a rate up to 150 gpm.

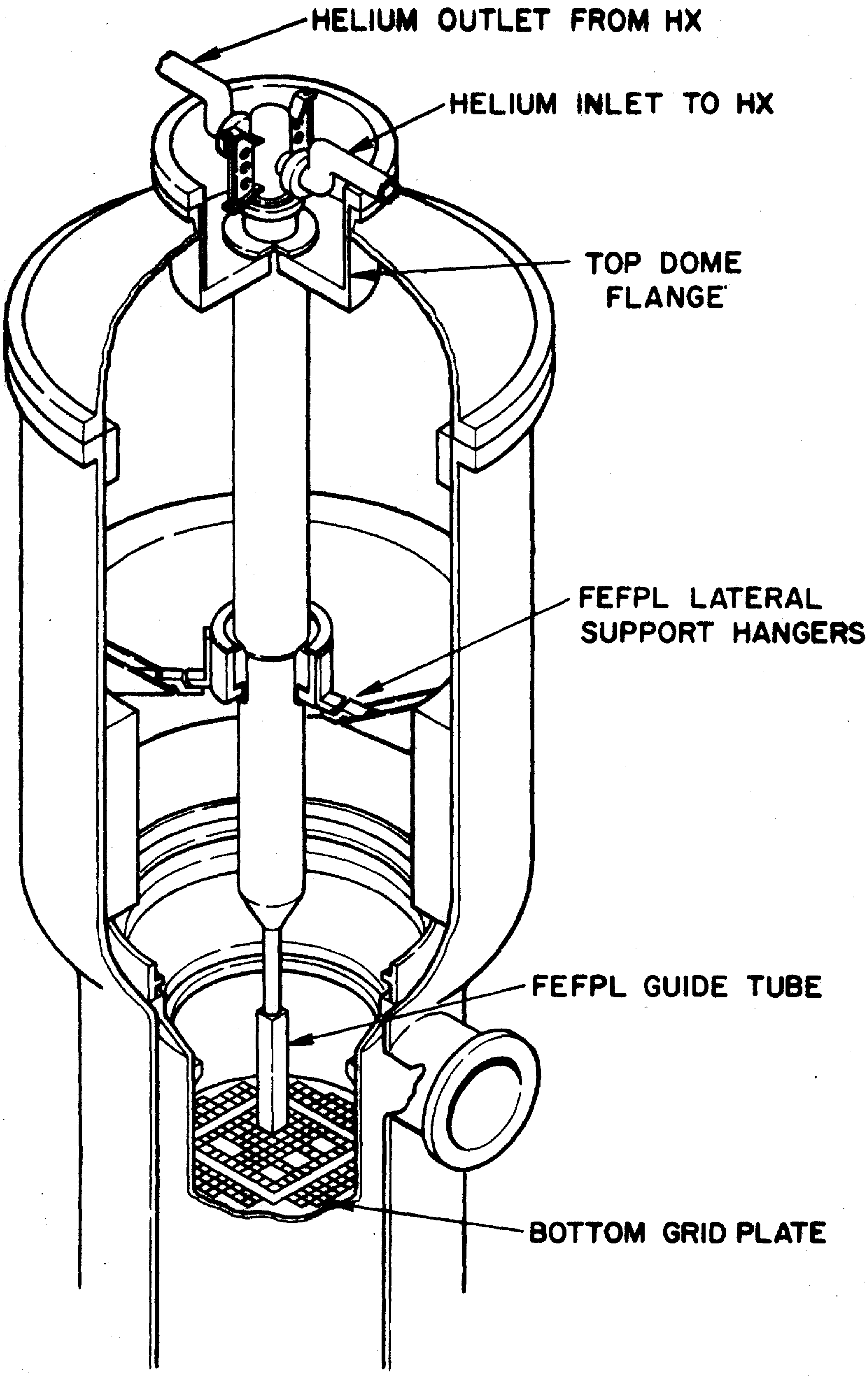

FIG. 1.2 - Loop in ETR

The annular linear induction pump (ALIP) is a counterflow design that can deliver up to 150 psi pressure at the design flowrate of 150 gpm. Heating necessary to compensate for heat losses during isothermal operations will be provided by the pump.

A helium-cooled heat exchanger (HX) is used: it has a heat removal capacity of 1500 kW with a sodium inlet temperature of 1050°F. The maximum helium pressure is 260 psia; HX helium is separated from the reactor water by two barriers - a shroud, plus the secondary vessel. A separate helium system is used for leak detection and backup cooling in the annulus between the primary and secondary vessels.

Table 1.2 lists the characteristics of the loop, and Fig. 1.3 gives a cross-section view.

Figure 1.4, a diagram of the FEFP in-pile system, shows all of the subsystems and assigned design and fabrication responsibilities. The Aerojet Nuclear Co., operator of the ETR, is responsible to the FEFP Project for the detailed design and fabrication of the loop facility; Argonne-West, operator of the Hot Fuel Examination Facility, is responsible to the FEFP Project for the design and fabrication of the post-test examination facility.

The loop facility includes, in addition to the loop, all the subsystems located at the ETR. The loop-control and data acquisition systems include a PDP-15 central computer, a control console, and various input/output and recording devices. There are provisions for both manual and automatic loop control and on-line monitoring of 133 data channels. The loop protection system interfaces with the ETR PPS and acts to terminate or prevent ETR operation unless loop double containment is maintained and thus guarantees a minimum condition for loop operation and not protection for the reactor. It is electrically isolated from the control and data-acquisition systems, and provides reactor shutdown signals. The loop-filling, storage, and remelt system consists of an oven for heating the loop, and a facility for both charging the loop with sodium and circulating loop sodium through an external cold trap to allow removal of impurities during cleanup and outgassing the loop.

A loop handling machine (LHM) will be used to remove the radioactive loop from the ETR and insert the loop into the Hot Fuel Examination Facility (HFEF). It will weigh 40 tons, of which approximately 23 tons will be depleted-uranium shielding. When the LHM is carrying the loop, the total load will be ~45 tons; it is necessary to increase the ETR crane capacity

TABLE 1.2

Characteristics of the FEFP In-reactor Loop

Loop	
Length	27 ft
Weight	up to 10^4 lb (including test train)
Diameter	19 in. above-core equipment region 5.25 in. in-reactor tube
Sodium content	∿210 lb
Cover gas volume	1.06 ft^3 (30 liters)
Heat Exchanger (sodium to helium)	
Type	tube and shell counterflow
Total length	∿81 in.
Capacity	950 kW @ 750°F sodium inlet temperature 1500 kW @ 1050°F sodium inlet temperature
Tubes (number and dimensions)	108, 0.75 in. OD, 0.049 in. wall
Pump	
Type	annular, linear induction
Length	∿65 in.
Design operating conditions	150 gpm @ 150 psi net pressure rise; 148 kW power input
Test Train (flow divider and internals)	
Length	26 ft
Weight	∿400 lb
Flow divider diameter	3.375 in. OD
Neutron Filter	
Thickness	0.040 in. Cd
Location	external to secondary vessel

FIG. 1.3 - Cross-section of Full-size FEFP Loop Test Section with 37-pin Bundle

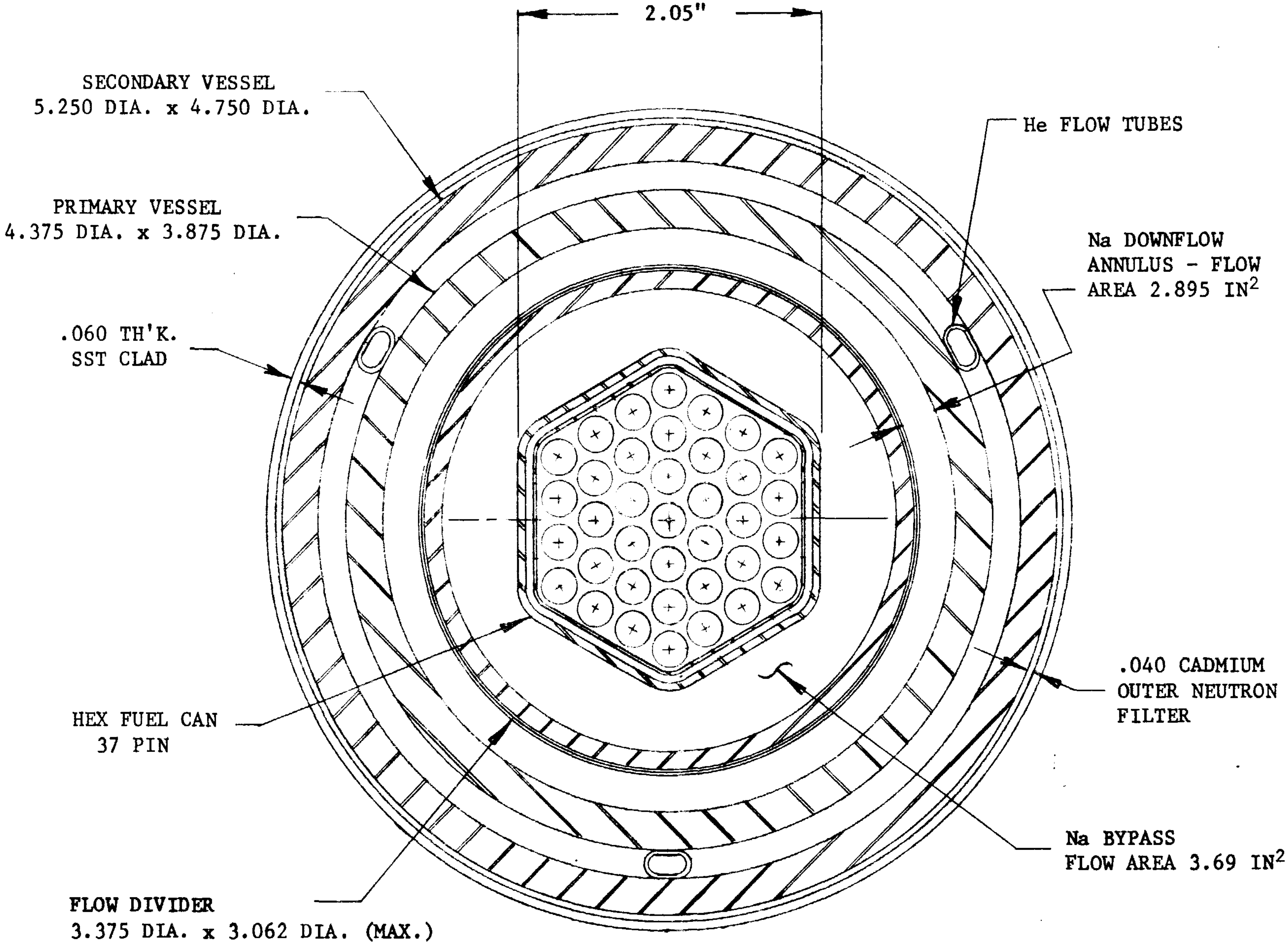

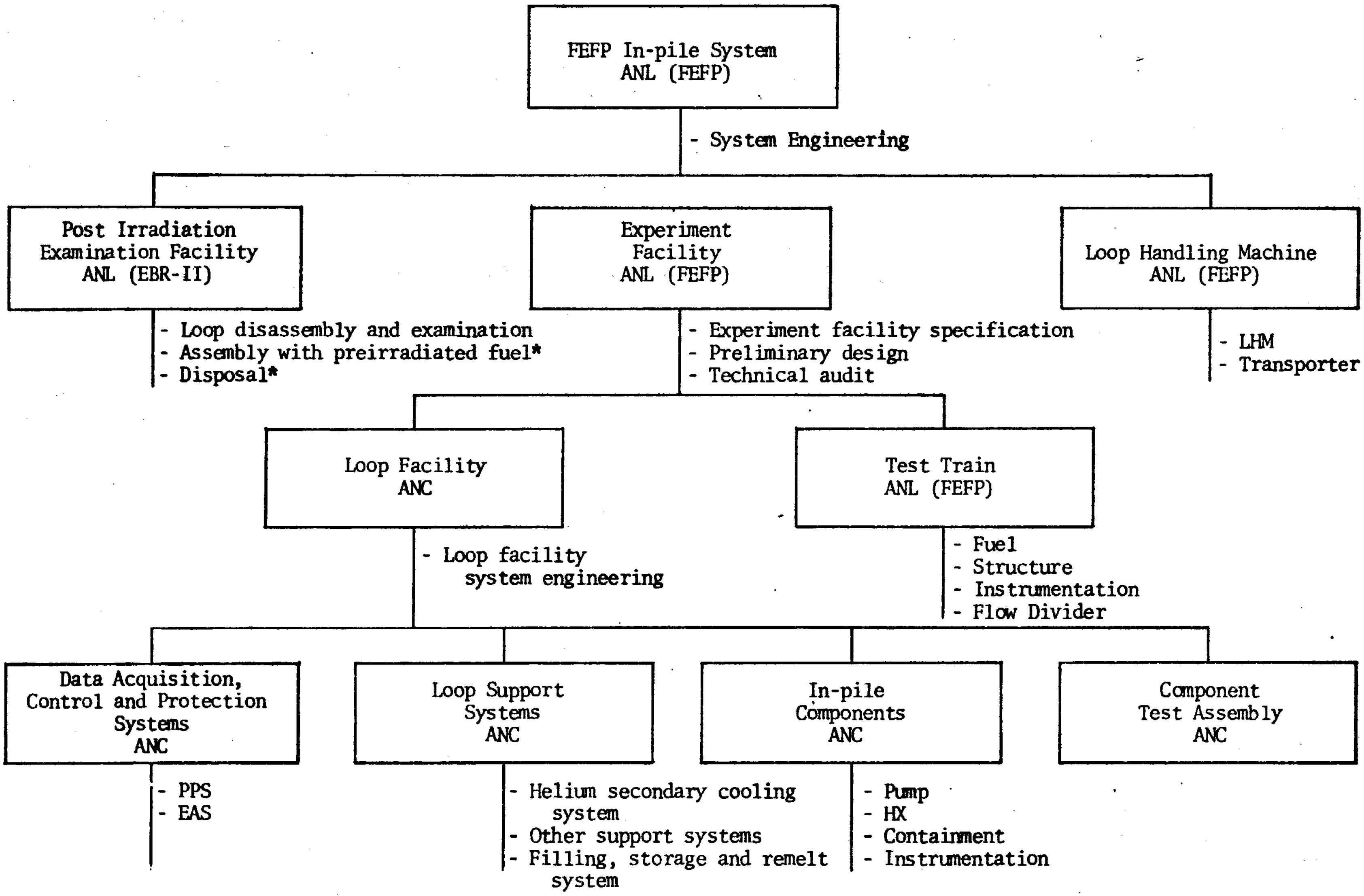

FIG. 1.4 - Diagram of FEFP In-pile Subsystems

*Tentative

from its present 30 tons to 50 tons to accommodate this requirement. The LHM will also be used to transport unirradiated loops containing pre-irradiated fuel elements. The LHM has provisions for keeping the sodium molten during transport and storage.

The HFEF also is located at NRTS, some 30 miles from the ETR. A transporter (see Fig. 1.5) will be used to transport the LHM between the ETR and HFEF.

The post-test examination system is composed of the equipment required to disassemble the loop and diagnostically examine the experiment and loop components. The equipment will be installed in the HFEF hot cells (see Fig. 1.6). Assembly of test trains and loops containing pre-irradiated fuel elements will also be done at HFEF.

1.4.2 Loop Operating Envelope

A design operating envelope for loop operation of 37-pin tests limited to 7.2 kg of $PU\text{-}0_2$ is identified in Chapter 6 in terms of the following:

a) Loop heat exchanger outlet sodium temperature - 450°F to 850°F
b) Loop heat exchanger inlet sodium temperature - less than 1100°F
c) sodium temperature differential across HX - less than 500°F
d) maximum loop heat rejection capability - 1.65 MW

Conservatively, the upper limit point of this design envelope (point C of Table 11.2) was assumed as the steady-state operating condition for the analysis of all upper limit operational accidents in Chapter 11. This upper limit results in the highest loop containment vessel temperature and therefore, conservatively represents the minimum allowable operating margin for the analysis of operational accidents. Normal steady-state operation of the loop will be conducted within the design envelope.

Specific loop and reactor operating setpoints will be identified in the experiment plan and core safety assurance package as the basis for approvals prerequisite to operation of each experiment.

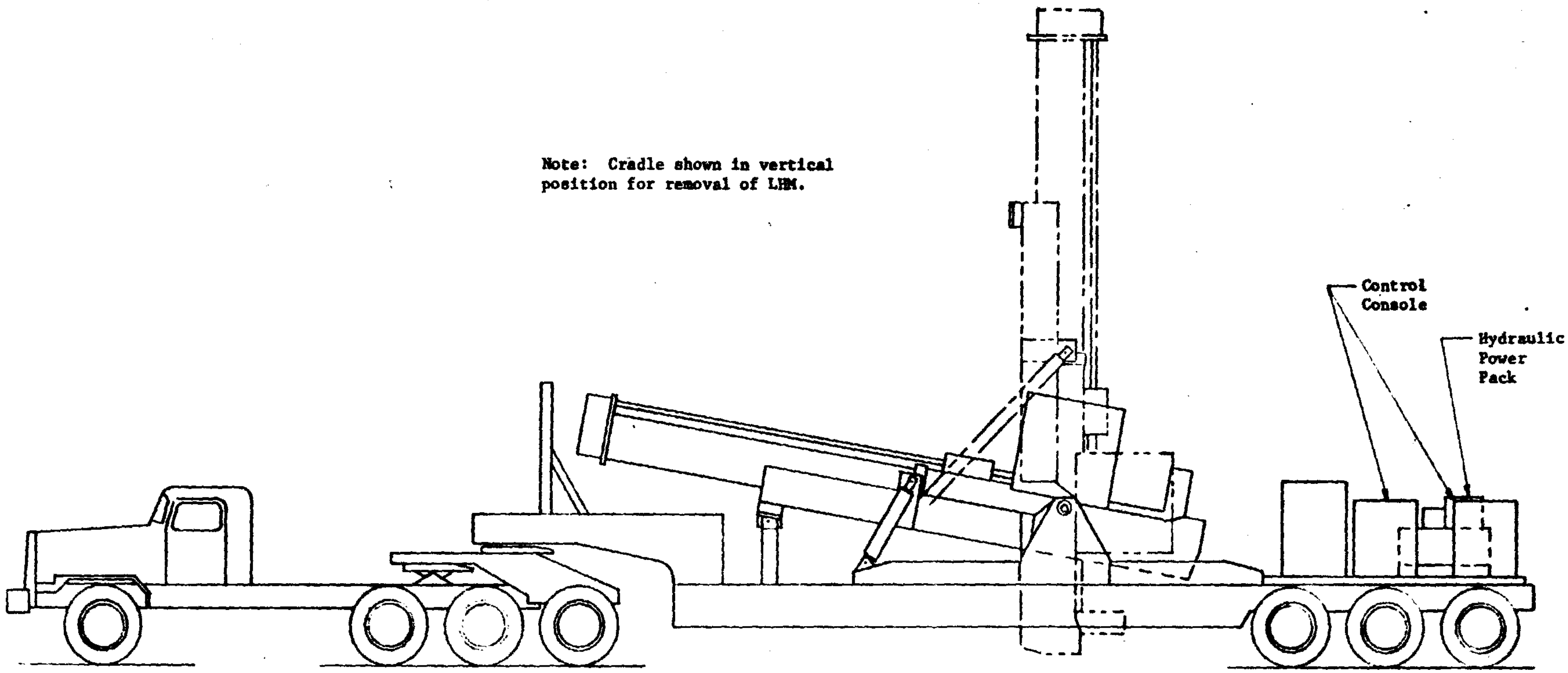

Gross Load - 168,439#

FIG. 1.5 - FEFPL Handling Machine Transporter

FIG. 1.6 - HFEF Hot Cell

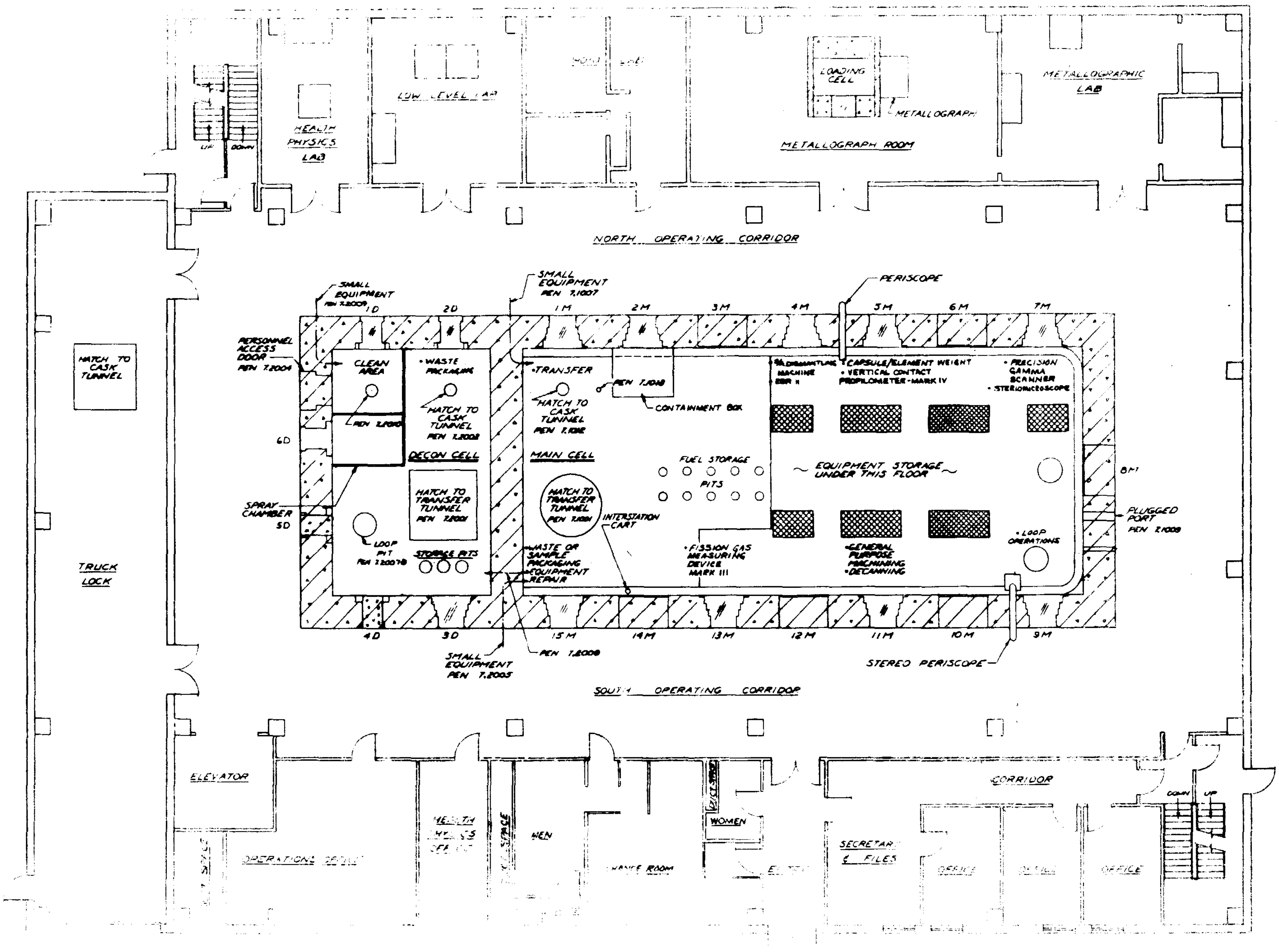

References

1. Fast Flux Test Facility design Safety Assessment, HEDL-TME-72-92, July, 1972.

2. "Fuel Element Failure Propagation Loop System Design Description," Vol. I, ANL Report R-1000-1001-SA, (May,1972).

*3. ETR Technical Specifications, CI-1233, February, 1972.

4. "Studies of LMFBR Safety Test Facilities," Vols. II and III, ANL/RAS 70-06.

5. "Test Requirements for Fuel Element Failure Propagation In-reactor Experiment P-1," ANL/RAS 72-9 (Rev. 1),(November, 1972).

6. "Test Requirements for Fuel Element Failure Propagation In-reactor Experiment P-2," ANL/RAS 72-22 (Rev. 1), (June, 1973)

7. "Thermal-hydraulic Simulation in the FEFP," ANL/RAS 71-17, (April, 1971).

---

*Under revision.

CHAPTER 2.0

TABLE OF CONTENTS

2.0 Summary

The safety of FEFPL-related operations conducted within the confines of the ETR building are evaluated and documented in this Safety Assessment Report. Fault tree analyses are used as an aid to a systematic search for possible accidents. The potential consequences of planned experiments, loop malfunctions, and handling accidents are examined. Postulated events that are independent of FEFPL activities, such as the ETR Design Basis Accidents (DBAs), also are evaluated to determine whether the presence of the loop may significantly compound the risk associated with them. Potential problems introduced by operations that involve liquid sodium are analyzed - a facility for charging FEFP loops with sodium is a new addition to the ETR complex; however, a previous ETR experimental loop did contain NaK. It is concluded, based upon studies of accidents ranging from the more probable to those considered to be hypothetical, that a) the FEFPL program can be conducted safely and without damage to the ETR or injury to personnel or the public, and b) the FEFPL will not affect the frequency of possible ETR malfunctions or escalate them into accidents more severe than previously analyzed.

Each of the pressure vessels in the loop double containment system is designed, with a margin of safety, to accommodate independently all experimental transients. The FEFPL-PPS continuously monitors loop containment to ensure that the safety margin designed into the system is preserved during operation. The adequacy of this safety margin is determined analytically by showing that the loop can tolerate overly severe, hypothetical events. Experimental confirmation will be obtained during an orderly FEFP test program that progresses from mild to the more energetic experiments and starts with a test (P1) whose principal objective is a thorough checkout of the loop system.

2.1 Safety Philosophy

The fundamental approach taken by the FEFP Project was to identify, assess, and resolve all foreseeable safety concerns. Starting early in the conceptual design of the in-reactor loop systems, repeated reviews were made to uncover possible problems that may have safety implications. They were then analyzed to assess what corrective feedback for design guidance may be required. Such action resulted in several comprehensive safety studies prior to this SAR[1,2,3] (the first, by the Aerojet Nuclear Company, was published in July 1969).

Final resolution of the issues thus identified, as well as the establishment of a tolerance by the loop system for unexpected problems, is achieved through an approach that utilizes three levels of safety as follows:

1) The FEFPL system, as designed and as it will be constructed, tested, operated, and maintained, provides a highly assured capability for reliable and predictable operation and an inherent capacity to prevent the occurrence of accidents. It is designed to meet the standards that have been prescribed for experiments in the ETR.[4]

2) The system is designed so that in the event of errors, malfunctions or off-normal conditions, protective systems and other features will arrest the event or limit its consequences to defined and acceptable levels.

3) The system design provides considerable additional margin for containment of extremely low probability or arbitrarily postulated hypothetical events without exceeding accepted guideline values for the protection of public health and safety.

Detailed information that relates to the identification, assessment, and resolution of specific safety concerns is contained within the sections of this report as listed below:

A. Identification

- Fault tree analyses of loop operation and handling accidents (Appendix A)
- Definition of the potential consequence of planned experiments or loop malfunctions (Chapter 10)

B. Assessment

- Evaluation of the effect of experimental transients on the loop integrity and reactivity coupling with ETR (Chapter 10)
- Analyses of the reaction of the FEFPL-ETR system to postulated operational accidents or seismic events (Chapter 11)
- Evaluation of potential handling accidents and sodium fires (Chapter 12)

C. Resolution

- Safety Philosophy (Chapter 3)
- Loop design features, standards, and test procedures (Chapter 5)
- Plant Protection System (Chapter 7)
- Administrative and Procedural Safeguards (Chapter 8)
- Loop safety margin for hypothetical events (Chapter 13)

2.2 Loop Operational Envelope

The FEFP loop is designed to: a) meet specific experimental performance requirements, b) safely contain the consequences of both planned experiments and possible malfunctions, c) satisfy the ETR standards[4] for in-reactor experiments, and d) tolerate all credible ETR accidents without loss of loop containment. Operational limits, with allowance made for adequate safety margin plus control and measurement uncertainties, are established consistent with these design characteristics. Such limits then define a normal operating envelope for all experiments which is independent of the design of a given test section. Steady-state limits for pressure and temperature are two principal loop parameters fixed by the operational envelope; operation within these limits is effected by the Control or Experiment Assurance System (CEAS). In addition, the PPS monitors parameters, such as vessel temperature, that affect the loop containment margin - if preset limits are exceeded, an ETR scram is initiated automatically.

Pressure Limits

Steady-state design pressure limits are established to ensure that the loop double containment system will protect the ETR from either planned experiments or possible loop malfunctions. Thus, a satisfactory design criterion would be that the containment system shall prevent damage to the ETR; however, a more conservative position is adopted. Namely, the primary vessel shall not be permitted to yield beyond the boundary established by the secondary even under internal pressure loads postulated for hypothetical events. Consequently, no deformation of the secondary vessel can occur or physical contact made with the core filler piece that surrounds the loop and provides an intermediate barrier between it and ETR fuel subassemblies. To meet the specified containment criterion satisfactorily, the loop may respond to an internal pressure load in one of the following three ways:

A. The primary containment vessel is entirely in the elastic region - no load is transmitted to the secondary vessel;

B. The primary containment vessel is fully plastic, but no credit is taken for strain hardening - no load is transmitted to the secondary vessel;

C. The primary containment vessel deforms plastically and contacts, but does not load the secondary vessel.

The static pressures (in psi) that the primary vessel may contain corresponding to the foregoing cases, as a function of temperature, are:

	800°F	1100°F	1300°F
Case A	1920	1799	1670
Case B	2960	2830	2590
Case C	3890	3640	3550

Although the primary vessel is capable of safely containing the higher pressures shown for Case C, the lower values given for Case B are used to establish conservative pressure limits for the loop.

The loop normal steady-state operating pressure from the pump (ALIP), sodium column, and gas plenum will be less than 300 psi. During an experiment deliberately planned to melt a significant fraction of the fuel in the test section, the most probable sustained pressure pulse that may arise from a molten fuel interaction with sodium is less than 150 psi. The same phenomena would prevail should a loop malfunction occur that also causes fuel to melt and possibly interact with sodium; therefore, the possible pressure pulse would be similar. This value is based upon analyses and interpretation of laboratory and in-reactor experiments. Using very conservative assumptions the maximum peak pressure that would be expected from a fuel coolant interaction is 69 atm. To establish the loop design, however, a peak pressure of 195 atm is postulated (Design Envelope MFCI) to provide additional safety margin (the third level of safety).

A comparison of the steady-state pressure containment capability of the primary vessel with the equivalent static load associated with a possible molten fuel-coolant interaction is given below:

	Load Applied To Primary	Pressure Capability / Applied Load
Most Probable MFCI	150 psi	18.8
Upper Limit MFCI	910 psi	3.1
Design Envelope MFCI	1516 psi	1.9

This indicates the magnitude of the safety margin for the primary vessel at its normal operating temperature (< 1100°F) and in the region that surrounds the test section. Elsewhere, the margins are greater due either to attenuation of the pressure pulse or structural characteristics of the loop.

Although the foregoing discussion is centered on limits for the primary vessel because it alone is affected by internally generated pressures, it should be noted that the secondary vessel also is designed with the capability to independently contain the same pressure source that may orginate within the test section.

Temperature Limits

Steady-state design temperature limits are established to preserve the containment margin and satisfy experimental needs. At a given ETR power level and corresponding gamma heating rate, the temperature of the loop structure and sodium is a function of the thermal balance at the loop heat exchanger. Hence, temperature limits are imposed on the heat exchanger which, in turn, are reflected throughout the loop.

The maximum sodium outlet temperature from the heat exchanger is limited to 850°F by control action to ensure that the highest temperature of the primary vessel does not exceed 1050°F. This provides a 250°F margin below the 1300°F design temperature limit. In the remote event that the loop control system (with operator backup available) does not hold the stipulated temperature limit, the FEFPL-PPS will automatically call for an ETR scram from high primary vessel temperature which then will cause a temperature drop.

Also, a minimum sodium outlet from the heat exchanger is established at 450°F which is well above the expected sodium plugging temperature (~ 260°F) or the 208°F freezing temperature.

Temperature limits are fixed for the loop secondary vessel as well as the primary in order to: a) ensure that the cadmium neutron filter does not approach the melting point, and b) maintain the margin of safety for pressure containment. In this case, however, the temperature is a function of the heat removal rate by the ETR cooling water, as well as direct gamma heating in the wall and some minor heat loss from the primary. The normal steady-state operating temperature of the cadmium filter is less than 500°F, taking into account possible uncertainties in the absolute gamma heating rate as well as variations that may be caused by ETR flux skew. Loss of cooling due to flow blockage of the ETR primary water surrounding the secondary vessel is precluded by the design of the core filler piece. Nevertheless, the FEFPL plant protection system is designed to effect an ETR scram well before the cadmium temperature reaches its melting point (609°F) due to overheating caused by unforeseeable circumstances.

ETR Technical Specifications

The ETR Technical Specifications[4] provide standards that all in-reactor experiments must meet. These specifically cover reactivity feedback to the ETR, heat transfer and gas leakage to the ETR coolant, and loop containment requirements.

Reactivity Limits

With respect to reactivity limits, an envelope has been established for an initiating accident of a +.75% ΔK/K step insertion and a secondary feedback reactivity insertion of +.15% ΔK/K applied as a step. The maximum possible total reactivity changes associated with fuel and sodium movement within the loop fall well within these limits; the specific values are:

- Total Sodium Voiding - + 0.015% ΔK/K
- Radial Redistribution and Compaction of all the Fuel - + 0.019% ΔK/K

. Fuel Meltdown and Axial Compaction + 0.12% ΔK/K

During experiments that are designed to investigate phenomena associated with fuel meltdown, only a fraction of the values listed above would be expected. In order to obtain larger reactivity additions, it is necessary to postulate gross movement of the loop, or cadmium filter, within the ETR core. Such movement is prevented mechanically by the loop structural support system. Loss of the cadmium filter is not considered credible because it is sealed within the secondary vessel and held at a temperature well below its melting point (temperature is monitored continuously by the FEFPL-PPS). In the improbable event that water should leak into the annulus between the secondary and primary vessels - this would require both overcoming the higher helium pressure head, plus an unexplained failure of the secondary vessel - the net reactivity change would be negative.

Heat Transfer Limits

Components that transfer heat to the ETR primary coolant, such as the FEFPL secondary vessel, must not present a high enough thermal load to approach within three standard deviations of either DNB or flow instability under conditions whereby the ETR coolant flow or power level may become abnormal. As shown below, these requirements are met with a margin of safety:

ETR Conditions	FEFPL Standard Deviations to Critical Heat Flux	FEFPL Standard Deviations to Flow Instability
Normal Power, Flow and Pressure	3.9	15.0
48% of Flow, Normal Power and Pressure	3.6	7.3
125% of Full Power, Normal Flow and Pressure	3.7	12.0
140 psig Inlet Pressure, Normal Power and Flow	3.7	13.1

Gas Leakage Limits

An experimental loop with a gas-filled annulus, such as the FEFPL, must provide leak monitoring so that the ETR can be shutdown to avoid potential heat transfer problems if a leak occurs that exceeds 2.2 standard cubic feet per minute. The FEFPL design meets these requirements. The integrity of the loop containment system is continuously monitored by the FEFPL-PPS, which is designed to the requirements of RDT Standard C16-1T. In the very low probability event of gas leakage through the secondary vessel, a scram signal would be initiated at a worst case trip point of 1.1 SCFM.

Containment Requirements

The remaining ETR experiment technical specification requires double containment for certain experiments. This is met by the FEFPL which is designed with a large containment safety margin. Continuous monitoring for leaks, overtemperature or overpressure is provided by the loop plant protection system to ensure the existence of this margin.

2.5 Experimental Transients

The first ten experiments planned will simulate specific LMFBR malfunctions that may lead to the failure of a large fraction of the fuel within a subassembly. It is the purpose of these experiments to determine the potential for propagation of such failures. Consequently, these experiments deliberately invoke conditions, such as loss of flow, that lead to fuel melting within the test section while the ETR remains at its specified power level. The loop is designed, with a large margin of safety, to contain the consequences of a postulated reference experiment which provides a more severe test of the containment system than planned experiments (or possible loop malfunctions that may lead to fuel meltdown in the test section). Hence, this reference experiment provides a safety envelope for all planned experiments. To define this reference experiment, it is postulated that a complete flow blockage occurs instantaneously in a 37-pin, full-length test fuel bundle that is operating at 15% overpower. It is further stipulated that this event is not arrested by an ETR scram. The loop is designed to contain the thermal and mechanical loads associated with this event without compromising the integrity of the primary containment or adversely affecting the operability of the loop pump or heat sink.

The first four experiments planned, however, will contain only half as much fuel as the postulated reference event; it is anticipated that they will verify the conservatism associated with this approach.

In addition to the more severe experiments that involve a planned flow decay followed by gross melting, other tests will investigate the potential effects of the local failure of one or a few pins only. These are not expected to challenge the loop containment system.

2.4 Protection Systems

The loop design incoporates multiple lines of defense against potential accidents which include: a) the Loop Control System, b) the Experiment Assurance System (EAS), c) the FEFPL Plant Protection System (PPS), and d) Double Containment.

It is the function of the control system to hold certain parameters within prescribed operational limits that are well within the loop safety envelope. The EAS is designed to prevent accidental damage to the experiment that may result from events leading to a power-flow mismatch in the test section, including loss of pump power, low sodium flow, high test section outlet temperature, and loss of heat sink. The action effected by the EAS, upon detection of these abnormalities, is to signal for an immediate ETR scram. The EAS is designed to conform, to the extent practical, to RDT Standard C16-1T.

An additional line of defense for the protection of the public and the plant is the FEFP loop double containment system. It is a passive protection system which provides an additional margin of safety over and above the other lines of defense.

The function of the FEFP Loop Plant Protection System is to ensure the continued existence of the containment safety margin provided by the containment system by continuously monitoring the integrity of the primary and the secondary containment vessels, and automatically terminating operation if the containment safety margin is reduced. The system is designed to detect leaks in either vessel or excessive vessel temperatures or pressures.

Detection of loss of integrity of either primary or secondary loop containment or a reduction in the containment safety margin will initiate an ETR scram.

The possible consequences of all experiments and postulated accidents, identified with the assistance of fault tree analyses, that may challenge the loop containment system are identified and assessed to establish PPS requirements. It is concluded that the containment system integrity can be verified and maintained by protective action that is a function of seven principal parameters:

A. Primary containment temperature in fuel zone,

B. Primary containment temperature in meltdown cup region,

C. Secondary containment temperature in fuel zone,

D. Sodium pressure pulse,

E. Primary containment integrity,

F. Secondary containment integrity,

G. Annulus gas system pressure.

Many of the accidents that have been analyzed for the purpose of determining PPS protective-function requirements would cause the EAS to take protective action before the PPS would be challenged. Thus, the EAS acts in a positive way to prevent or limit the severity of many postulated accidents. Although the EAS is not required to ensure containment safety margin (this is a PPS function) it does, however, form an additional line of defense.

2.5 Accident Analyses

During operation within the ETR, the FEFPL containment system may be subjected to internally produced, thermal-mechanical loads that arise from either planned experiments or possible malfunctions. The more severe loads stem from those events that lead to fuel meltdown; however, as a research tool, the FEFPL is designed to safely contain experiments that deliberately cause gross failure of fuel within the test section. A "worst case," or reference experiment, is used to establish a design envelope that will encompass all such planned tests as well as all possible accidents that also may lead to fuel meltdown.

The loop is designed to accommodate this reference experiment (which is defined as a sudden, complete flow blockage to the test section without intervention by either the EAS or PPS systems) without loss of containment integrity. That is, no permanent deformation of the loop primary vessel occurs; hence, no mechanical loads are transmitted to the secondary vessel or ETR core region. Also, no overheating of the loop primary or secondary vessels results. Major loop components, such as the pump and heat exchanger, remain operable.

Potential accidents that can lead to fuel melting in the test section (power-flow mismatch or loss of heat sink) are normally precluded by EAS action in order to protect the experiment against inadvertent damage. Nevertheless, these accidents are analyzed for the case whereby failure of the EAS is postulated and it is shown (Chapter 11) that the consequences are bounded by the envelope established by the reference experiment. Examples of the types of malfunctions considered include: a) loss of commercial power, b) loss of all electrical power, c) failure of the sodium pump (ALIP), d) sodium flow blockages, e) loss of loop heat sink, and f) failure of the FEFPL control system.

Also, the consequences of hypothetical events, such as accidental fuel meltdown, coupled with multiple, coincidental malfunctions, are examined to show that the loop has extra safety margin to tolerate such events (Chapter 13).

The three principal thermal sources that have the potential to overheat the primary vessel to approach the melting point are 1) direct contact with molten fuel, 2) an electrical short in the ALIP, or 3) continued operation of the ALIP with a complete loop flow blockage. All are precluded by design, with protection system backup. In the radial direction, molten fuel is separated from the primary vessel by two sodium-cooled barriers, in the axial direction a sodium-cooled refractory metal, meltdown cup provides protection. In addition, should the primary vessel approach 1300°F, the FEFPL-PPS signals for an ETR scram which will freeze molten fuel in the test section. Simultaneously, the annulus gas cooling system is actuated.

Although the ALIP is designed to preclude shorts that may directly affect the primary vessel, a backup alarm system is provided to detect faults before they can become a complete electrical short circuit. Should such a short occur, however, current limiting fuses will limit the current to a value insufficient to seriously heat the primary vessel.

An EAS function is provided to transfer the ALIP to reduced voltage emergency power and initiate a scram upon detection of a total flow blockage to decrease the loop thermal load.

Pressure loads on the primary vessel may stem from, internally, a MFCI or externally, the annulus gas system. It was shown previously that the maximum potential pressure expected from a MFCI is much less than the containment capability of the primary. The nominal pressure of the annulus gas system also is well below the buckling pressure for the primary. Redundant pressure relief systems provide protection against overpressure. In addition, the total head available from the helium system (∿480 psi) is less than the allowable design pressure for external loads on the primary vessel.

External sources of potential loads also are evaluated to ensure that the containment is adequate. These include seismic events and the ETR loss-of-flow, design basis accident, which leads to a 70 psi pressure pulse. The faulted buckling pressure of the secondary vessel at its weakest point, however, is 718 psi; consequently, this event does not pose a serious threat to the containment system. Likewise, seismic analyses indicate that the loop containment would not be damaged in the event an earthquake (similar to El Centro) were to occur near the ETR.

Handling Accidents

Safety of FEFPL handling operations also is assured through application of a defense indepth philosophy, expressed in terms of the three levels of safety discussed earlier. Thus, even though accident likelihood is remote, to the degree of being considered hypothetical, FEFPL handling operations within the ETR building were analyzed to identify potential accidents and evaluate their consequences. Particular attention was given to accidents that could be caused by failure of single components as identified by a fault tree analysis. These include failures of the overhead crane, the reactor building floor, the LHM and operator errors.

The postulated accidents were examined first in terms of the first two levels of safety, which demonstrated that the design methods, safety devices and strict adherence to detailed operating procedures provides safety during normal operation and maximum tolerance for assumed malfunctions or operator errors.

This was followed by examining the failures in terms of the third level of safety, which demonstrated that for extremely unlikely and hypothetical failures the design margin provides assured protection of the general public.

2.6 Hypothetical Events

A hypothetical event is a condition for which no real sequence of causitive events can be identified, but which is nevertheless considered in order to assess margins relative to protection of the public. Such events have been reduced to this category by design, redundant features, large safety factors, and comprehensive protection systems. Although the FEFPL-ETR system is not specifically designed to tolerate hypothetical events, nevertheless, certain of these are arbitrarily imposed on the loop as a test of its capability to function safely into a range well beyond that normally required. Three principal events that fall into this category are: a) containment system failures, b) reactivity additions, and c) large sodium fires.

Loss of Sodium Containment

The FEFPL containment system evolves from a "defense in depth" design philosophy which embodies the following multiple levels of safety.

First, the loop has two barriers between sodium and water everywhere except in the region of the heat exchanger, where there are three. Acting together, both vessels are designed to contain, without deformation, internal pressures at least a factor of four higher than postulated for a molten fuel-coolant interaction much more severe than expected. The FEFPL secondary vessel will not buckle if exposed to the external pressure loads that may result from the ETR loss-of-cooling DBA.

Second, during in-pile operation, the FEFPL Plant Protection System will continuously monitor the containment system to ensure that the safety margin is maintained. If a leak, overtemperature or overpressure occurs in either vessel, the ETR will be shutdown automatically.

Third, should it be postulated that one vessel fails for a reason not explained, and without detection by the FEFPL-PPS, an effective barrier still will separate the loop sodium from the ETR water. Each of the two containment vessels, primary and secondary, is designed to safely withstand alone the design envelope pressure pulse or the thermal effects of molten fuel. Additionally, analyses in Chapter 13 demonstrate that failure of one vessel will not propagate to the other.

Finally, it is shown that the loop containment system can withstand the consequences of arbitrarily postulated hypothetical events. When parametrically tested against hypothetical events that have even higher pressures than the accidents mentioned previously, the loop containment system maintains its integrity. Should, again for an unexplained reason, failures develop in both vessels that are not detectable, the potential sodium leak would not be great enough to endanger the ETR or personnel as discussed in Chapter 13.

Loss of Cadmium Neutron Filter

Because a reactivity insertion might result from the loss of the cadmium filter, which is used to attenuate the ETR thermal neutron flux to the experiment, a filter design has been developed which assures that it cannot move from its as-fabricated position. The filter geometry is such that, even should the outer steel jacket vanish, the circumferences of the cadmium and mating secondary containment vessel provide enough interference to prevent vertical displacement of the cadmium. The outer stainless steel sleeve is, however, welded in place to seal the cadmium (these welds are located outside the ETR core region). Containment is thus assured even if the cadmium were to melt due to excessive gamma heating or loss of ETR water cooling.

The FEFPL-PPS guards against cadmium melting by monitoring temperature on the secondary vessel ID near the core midplane. The ETR scram setpoint selected to prevent cadmium melting is based on the postulated transient that would occur if it were possible to block all ETR water flow between loop and core filler piece. (This accident actually is precluded by a filler piece design that provides for bypass flow around an inlet blockage.)

The following hypothetical sequence of coupled low-probability events must be postulated in order to provide a path for loss of cadmium:

a) complete blockage of cooling water around FEFPL secondary vessel coupled with blockage of at least three of the four auxiliary cooling holes in the core filler piece

or

ETR loss of flow or power excursion without scram,

b) failure of FEFPL-PPS to sense overheating of the secondary vessel or failure of ETR-PPS to respond to scram signal,

c) whole or partial melting of cadmium,

d) failure of stainless steel jacket at a site that permits significant loss of molten cadmium.

Four low-probability failures must occur in a mutually compatible fashion in order to lose cadmium; thus, it is considered to be hypothetical. Nevertheless, even if this should happen, it can be shown that tolerable reactivity additions result for physically realistic rates of cadmium motion. For holes in the stainless steel jacket that are postulated to be large, the melting rate can be controlling; whereas, for smaller ones, the exit and falling times will dominate.

In the hypothetical event that the cadmium could become molten by the combined loss of local ETR coolant flow and the secondary containment temperature detection system (PPS), in a stagnant coolant condition it would take in excess of one second due to gravity alone for the cadmium to leave the core region assuming it is lumped at the core midplane. Further time would be required for the molten cadmium to move within the 0.040 in. thick containment to the possible fault. Compared to the allowances made for ramp insertions in the Technical Specifications, which deal in msec, any postulated hypothetical FEFPL ramp would be considered slow (~1 sec), and hence, is not presently restricted by specific requirements.

An analysis using the ANC PARET computer code has been performed to determine the effect of cadmium loss for various insertion rates. Due to the difficulty of postulating a feasible mechanism for losing the filter, it was assumed that the loss would be radially linear with time. Only the scram rod insertion was considered for negative reactivity insertion (i.e., the negative temperature coefficient was neglected, which is conservative). The energy generated for the time period that the reactor was above 150% of 175 MW (262.5 MW) was shown to be less than 11 MW sec for ramp times of 2 sec or more. Duration above this power level trip point was 0.165 sec for the 2 sec ramp and .040 sec for ramps of 3 sec or longer. Peak power levels were less than 266 MW or only 2% above the trip level. These results indicate that the reactor control system greatly attenuates the effect of ramp cadmium loss. Thus, no damage to the ETR core or FEFPL fuel would result.

FS&R Fire under Hypothetical Conditions

Although there is no foreseeable way for the entire sodium inventory in the Charging Facility or Test Cell to spill over the maximum area required to optimize combustion, this postulated event is analyzed to determine whether the ETR or personnel would be adversely affected. It is shown (Chapter 13) that such hypothetical fires remain within their respective enclosures and do not propagate to the rest of the ETR facility. Normally, the Test Cell hatchway is closed, in the improbable event that it is damaged or open, smoke may enter the ETR facility. If radioactive contamination should be present, radiation monitoring will provide an automatic warning to personnel so evacuation measures can be effected if desirable. The maximum quantity of activity that could be present, however, would be well below permissible biological limits.

References:

1. D. R. de Boisblanc, et al., "Safety Study for the Fuel Element Failure Propagation Loop in the ETR," IN-1291, July 1969.
2. "Safety Study for the Fuel Element Failure Propagation Loop in the ETR," ANL/RAS-04, October 30, 1970 (prepared by Argonne National Laboratory and Aerojet Nuclear Company).
3. D. H. Lennox, et al., "Containment Study for the FEFP In-pile Loop," ANL/RAS 71-36, November 1971.

*4. S. A. Atkinson, et al., "ETR Technical Specifications," CI-1233, February 1972 (under AEC review).

---

*Under Revision

CHAPTER 3.0

TABLE OF CONTENTS

LIST OF TABLES

3.0 Safety Philosophy

3.1 General

The purpose of this SAR is to demonstrate that operation of FEFPL in ETR can be accomplished in a safe manner to meet the desired test objectives. To this end, safety concerns are identified, assessed, and fully resolved by systems design, the plant protective system, and other controls.

In a manner similar to that applied to the Fast Flux Test Facility Design Safety Assessment,[1] the approach to achieving safety is expressed in terms of three levels of safety, which can be summarized as follows:

1) The FEFPL system, as designed and as it will be constructed, tested, operated, and maintained, provides a highly assured capability for reliable and predictable operation and an inherent capacity to prevent the occurrence of accidents.

2) The system is designed so that in the event of errors, malfunctions or off-normal conditions, protective systems and other features will arrest the event or limit its consequences to defined and acceptable levels.

3) The system design provides considerable additional margin for containment of extremely low probability or arbitrarily postulated hypothetical events without exceeding accepted guideline values for the protection of public health and safety. (These three levels of safety are discussed further in Section 3.3).

The studies carried out verify that the FEFPL operation is within the parameters of the original ETR Engineering Design and Safeguards Report[2] and the updated ETR Technical Specification.[3]

3.2 Requirements

The primary safety requirement addressed in this SAR is that operation of the FEFPL system in the ETR shall not endanger the reactor, reactor operating personnel, or the general public. Specifically, it shall not be the cause of any significant damage to the core or core containment, and it shall not directly result in injury or overexposure to site personnel or the general public.

Malfunctions that only affect the acquisition and preservation of test data, but not the integrity of the FEFPL/ETR system, are not defined as safety problems, and consequently are not discussed here.

3.3 Approach to Assuring FEFPL Safety

3.3.1 First Level

Basic safety of the FEFPL operation in ETR is provided through intrinsic features of the design and the quality, redundancy, testability, and failsafe features of the components of the loop system. The design is such that the FEFPL in ETR will be unquestionably safe in all phases of operation* and has a maximum tolerance for errors, off-normal operation and component malfunction. Analyses are made and component tests conducted to find those types of malfunctions or faults that could affect reliability of operation, so that they can be guarded against by design, quality assurance, or failsafe features as appropriate. Key system parameters will be monitored to assure the continued integrity and capability of the loop system. Design, fabrication, and construction of the FEFPL are being performed under rigorous quality assurance procedures, and appropriate codes and standards are being applied.

The primary containment of the test train provides a high degree of assurance against the release of any of the primary coolant (sodium) from the loop into the ETR coolant. In addition, the secondary containment and the Plant Protection System (PPS) provide a second level of defense. The double containment precludes any sodium release into the ETR coolant. Both pressure boundaries will be constructed (materials, design, fabrication, examination and testing) in accordance with the requirements of the July, 1971, ASME Boiler and Pressure Vessel Code for Nuclear Vessels, Section III, Class I and supplemented by RDT Standard E15-2T and Code Case 1331-7.

FEFP loop was designed to thoroughly defined system and component function and performance requirements (as detailed in the SDD[4]) incorporating

---

*Includes both the normal operating procedure that precedes and follows the performance of an experiment and the performance of the preplanned experiment itself.

and emphasizing reliability and safety. These requirements have been made integral to the process of design and also of design verification, fabrication, construction, testing and operation. As part of this process of assuring a safe and reliable design, periodic independent and formal reviews are held for each subsystem and major component.

An extensive testing program will provide further substantiation of the system's capability to meet the program objectives and operate safely. Wherever feasible, major components and systems (pump, loop handling machine, data acquisition system, loop control system, loop secondary coolant (helium) system, etc.) will undergo a thorough test and/or checkout initially. Then, the complete loop system (using a dummy test train) will undergo a system test in the Filling, Storage and Remelt Facility, utilizing that facility's oven as a source of heat. Next, the loop system with the first experiment's test train inserted will undergo a complete preoperational checkout in the ETR before startup. The approach to full operating power itself will be carried out gradually, with periodic checkout of loop operation along the way, as a further test of satisfactory performance. Finally, the sequencing of the initial series of experiments to be carried out in the FEFP Program, all of which are well within the envelope of safe operation, is arranged to provide tests of increasing severity. The results of each test will therefore provide a high level of confidence for proceeding on to the next test. Detailed operating manuals and procedures for operation of the system, rigorously followed, provide a final measure of assurance that safe operation of the loop in the ETR will be accomplished.

The first level of safety is also served by many of the provisions made for optimizing the results of the FEFP experimental program. The Experiment Assurance System (EAS), which is part of the Loop Control System, primarily serves the economic and programmatic interests of the program by monitoring and controlling loop parameters to maximize experiment performance. While it does not, therefore, function directly as a safety system, it does often reinforce the first level of safety through the mitigation of an undesirable condition long before it approaches safety limits, thus avoiding the necessity for action by the plant protection system. Further, the EAS is designed generally in accord with the requirements of RDT Standard C16-1T,[5] where applicable and practical, and includes the capability of scramming the ETR.

3.3.2 Second Level

While the first-level factors given above assure safe operation of the loop in ETR, unexpected events during operation may alter loop conditions. Thus, in spite of the care taken in design, construction, and operation, it is assumed that such incidents may occur, and the second level provides fault detection equipment and design features which enable such occurrences to be prevented, arrested, or accommodated safely. The FEFPL Plant Protection System (PPS) is designed to sense and act on any parameter variations which may lead to a possible reduction of the original loop safety margin. The PPS will not only guard against violation of the requirements of the ETR technical specifications, but will also initiate corrective action if loop component conditions exceed setpoints which are well below the safety limits. In this way, the PPS provides continued assurance that the initial safe condition of the loop is not compromised. In recognition of the importance of this additional level of protection, the PPS will meet the requirements of RDT Standard C16-1T[5] for reactor plant safety systems. Conservative design practices, adequate safety margins, and parallel, independent, redundant detecting and actuating equipment (so that if one fails, others will be available to provide protective action) are used in the design and operation of this reactor protection system. In addition, this system is designed to be readily inspected and tested so that there is a high degree of assurance that it will operate reliably in the event it is required.

The double containment is a second level design feature which virtually precludes the release of primary coolant (sodium) from the loop into the ETR coolant. The design is such that either the primary or secondary vessel alone is capable of containing pressures in excess of any expected molten fuel-coolant interaction. This fact, plus the assurance that the PPS provides protection against any possible reduction of the original loop integrity, provides the redundancy characteristics of a second level of safety.

Another important second level design feature is the inclusion of a meltdown cup at the bottom of the test train, to contain the molten fuel debris that might result from an accident. Actually, the meltdown cup is also related to the first level of safety (since it will contain the small amounts, if any, of molten fuel anticipated with the planned experiments) and to the third level of safety (since it would also contain the molten debris even from hypothetical events). Further, the meltdown cup is designed to withstand the pressure resulting from a localized MFCI in the unlikely event one were to occur within the cup.

3.3.3 Third Level

The third level of safety assurance is provided through the study of extremely low-probability events and hypothetical events. Such studies are conducted to establish upper design bounds of low-probability accidents. Moreover, hypothetical events have been arbitrarily postulated to analyze and demonstrate safety margins inherent in those design bounds. Since no reasonable cause can be postulated for the hypothetical events, the fact that they are studied does not in any way mean they represent a design basis for the system or that their occurrence is acceptable. (Nevertheless, where design changes that would increase the margin of safety were identified and found practical, they have been incorporated.)

The studies reported in Chapter 13 show that the ETR-FEFPL systems have a large tolerance for the eventual consequences of these hypothetical occurrences.

3.4 Loop Safety Study Objectives

The experiment safety envelope is provided in the ETR Technical Specifications.[3] The limits stated in Section 2.2 of that document cover: (1) reactivity feedback from the experiment: (2) heat transfer and gas leakage to the ETR primary coolant; and (3) experiment containment. This SAR shows conformance of the FEFPL operation in ETR with all of these requirements.

It is a further objective of the studies reported in the SAR to show that the presence of the FEFPL does not produce a synergetic effect that would increase the severity of a mild ETR accident. In addition, it is shown that the presence of the FEFPL in ETR, during either of the two design basis accidents postulated for the reactor, will not significantly add to the consequences of such an event.

In addition to the safe operation of the loop in ETR, the SAR is also concerned with all other aspects of safety related to the loop when it is inside the ETR building, although not within the reactor proper. This includes movement of the loop handling machine within the ETR building (with or without the loop), insertion or removal of the loop from ETR, and insertion of the test train and filling of the loop with sodium. The safety studies reported herein demonstrate that adequate precautions are taken to minimize the likelihood of incidents or their consequences arising from these operations. These include the prevention of sodium fires and of radioactivity releases.

A summary of the safety concerns, their resolution, and the locations of the analyses and discussion of these various safety requirements and objectives, as well as of design documentation, are given in Table 3.1.

TABLE 3.1

Resolution of Key Safety Issues

ETR Technical Specification or Safety Objective	Resolution	Locations: SAR Accident Analyses	Locations: Design Documentation
Experiment Reactivity Insertion to ETR (Specifications 1 & 5)**	Analysis shows all reactivity changes but Cd filter-loss to be small. Loss of Cd filter is prevented by proper design	Chap. 10* Chap. 13	Chap. 5 SDD
Experiment Heat Transfer (Specification 2)	Analysis shows hot-spot heat flux and cooling water temperature rise within requirements of ETR Tech. Specs.	Chap. 6	FDR-05
Experiment Containment Requirements (Specification3)	Na is doubly contained. Maintenance of the safety margin is assured by the PPS (leak detection, pressure).		Chap. 5 Chap. 7 SDD FDR-09
Experiment Gas Leakage (Specification 4)	Secondary containment is continuously monitored for leaks. Gas makeup to annulus is physically restricted to values well below ETR Tech. Specs. limits.		Chap. 5 Chap. 7 SDD FDR-09
ETR DBA - Loss of Coolant Accident	Analysis shows that the FEFPL and supports will withstand resulting dynamic loads	Chap. 11 Chap. 13	Chap. 5 SDD CI-1231 FDR-05
ETR DBA - Reactivity Excursion	Analysis shows that neither the sample fuel or the Cd filter will experience melting due to the added heat generation or the effect of pressure loads on the loop.	Chap. 11	Chap. 5 CI-1231 SDD

* Chapter designations refer to this SAR.
** Pertains to five experiment standards given in Ref. 3, Section 2.2.

TABLE 3.1 (con't)

ETR Technical Specification or Safety Objective	Resolution	Locations: SAR Accident Analyses	Locations: Design Documentation
Handling Safety Assurance During Planned Movement of the FEFPL Within ETR Building	Adequate design of the handling equipment and stringent procedural controls are applied	Chap. 12	FDR-05
Assurance of Acceptable Sodium Fire Consequences	Limited sodium inventories in transfer lines, adequate tank design, enclosure control and accepted sodium fire-fighting techniques confines and controls the consequences of any possible fire	Chap. 12	SDD
Radioactive Material Control	Multiple containment and low inventories of active materials results in potential off-site doses far below guidelines.	Chap. 13	
Assurance of Acceptable Seismic Loading Consequences	Analysis shows that the loop will maintain containment integrity	Chap. 11	Chap. 5 SDD

3.5 Safety Assurance

Studies discussed in Chapters 5 through 13 show that the FEFPL is safe for operation in ETR. A disciplined approach, to assure that all significant safety questions have been treated, was made through the use of safety fault trees, and an accident summary table which are presented in Appendix A. For the operational accidents, a tabular listing of initiating events, their postulated results, and the provisions made to prevent or control them, is given in Chapter 11. It is noted that many events are extremely unlikely, or hypothetical, but are considered for completeness and to show that they cannot propagate to any serious consequences. Handling accidents are treated in Chapter 12.

3.6 Previous Experience with Na-Cooled Loops in Water Reactors

Precedent exists for the use of liquid metal loops and capsules in water reactors. Among these is the EURATOM program in the Belgian BR-2 reactor, which includes a liquid metal filled "FAFNIR" rig, a 0.5 MW in-pile sodium-cooled test loop,[6] and a NaK-filled "FASOLD" capsule.[7]

The Pratt and Whitney Loop (PW-19) irradiation program, using a packaged liquid metal loop design, was successfully accomplished in the ETR. The PW-19 Hazards Survey[8] was approved by the AEC Division of Reactor Development and Technology. Selected parameters for the PW-19 loop and the Fuel Element Failure Propagation Loop described in this study are shown in Table 3.3. Based on similarities between the PW-19 and FEFPL, such as operation with high temperature liquid metal, the use of 316 stainless steel welded construction, the irradiation environment, and incorporation of an experiment PPS, and taking account of the differences in design of the two loops, the PW-19 clearly provides a precedent for the safe insertion, operation, and removal of a doubly-contained liquid metal loop in ETR.

TABLE 3.2

Comparison of PW-19 and FEFPL

Design Condition	PW-19	FEFPL
Test Specimen Power, kW	100	1200
Primary Coolant	NaK	Na
Primary Coolant Inventory, lb	6.2	200
Primary Coolant Temperature (max), °F	1600	1300
Primary Coolant ΔT Through Heat Exchanger (max), °F	185	500
Primary Coolant Flow Rate (max), gpm	36	150
Primary Coolant Pump Type	Centrifugal Pump, Mechanical	Annular Linear Induction Pump, EM
Primary Coolant Pump ΔP, psi	63	150
Secondary Coolant	Air* (once through)	Helium (recirculating)
Secondary Coolant Flow Rate (max), lb/sec	0.7	1.59
Secondary Coolant ΔT (max), °F	---	950
Tertiary Coolant	Primary ETR cooling water	Secondary ETR cooling water
Material of Construction	Type 316 Stainless Steel	Type 316 Stainless Steel
Design Life, hr (max. irradiation time)	1000	1680
ETR Core Position	J-13 (6 × 6)	L-8 (6 × 6)

*Air and liquid metal separated by a stagnant inert-gas barrier.

Note: FEFPL conditions given are for steady state operation.

References:

1. "Fast Flux Test Facility Design Safety Assessment," HEDL-TME-72-92 (July 1972).

2. "ETR Engineering Design and Safeguards Report," IDO-24020 (July 1956).

*3. "ETR Technical Specifications," CI-1233 (February 1972).

4. "Fuel Element Failure Propagation Loop System Design Description," Vol. I, ANL Report R-1000-1001-SA-00 (May 1972).

5. "Supplementary Criteria and Requirements for RDT Reactor Plant Protection System," RDT-C16-1T, (December 1969).

6. "Development of Fast Reactors," NP-18809, pp. 1.1-33.

7. "Some BR2 Irradiation Devices for Fast Reactor Fuel and Fuel Elements," EUR-3632 (March 1971).

8. "PW-19 Hazards Survey," IDO-16545 (August 1959).

---

*Under Revision

CHAPTER 4.0

TABLE OF CONTENTS

TABLE OF CONTENTS (Contd.)

LIST OF TABLES

LIST OF FIGURES

LIST OF FIGURES (Contd.)

4.0 ETR Description

4.1 Summary Description

The ETR is a thermal heterogeneous light-water moderated and cooled high-flux test reactor located in the test reactor area (TRA) at the National Reactor Testing Station (NRTS) in southeastern Idaho. Conceptual design was performed by Phillips Petroleum Company, Atomic Energy Division. Design and construction was by the Atomic Power Equipment Department, General Electric Company, and the Nuclear Engineering Division of Kaiser Engineers. Much of the material in this chapter provides a description of the reactor as it was operated for previous experiments. Some changes to the ETR core, rod program and primary coolant system operating parameters will be made to specifically accommodate the FEFPL program. These modifications are not such that the conclusions of this report would be altered. Figures 4.1 through 4.17 present salient reactor and FEFPL experiment features.

The ETR was designed to perform engineering tests on fuel elements and components of nuclear plants. In order that these tests be made under conditions simulating the actual proposed application, certain requirements had to be met: (1) very high thermal and fast flux in the core holes; (2) test facilities (core holes) ranging in size from 3 x 3 x 36 in. to 9 x 9 x 36 in.; (3) a reasonably uniform flux from top to bottom of the core; and (4) closed loop-type facilities for circulating any coolant fluid.

All experiment facilities inside the reactor vessel are vertical, and experiments are supported from above the core by means that are integral with the vessel. The reactor control-rod drives are mounted below the reactor bottom head where they are least affected by the experiments. The vessel top head is near the first floor level because of the large clear height needed to remove experiments.

4.2 General

The ETR facility is a complete nuclear engineering test facility. It includes its own heat exchanger or process water building, electrical building, and office building. These are independently functioning buildings built with common dividing walls.

The reactor is housed in a building 112 by 136 ft, extending 58 ft above and 38 ft below grade. The reactor and building elevations are given in Table 4.2. The reactor vessel consists of the multidiameter vessel proper, removable ellipsoidal dome with flat top flange, flat bottom head, a discharge chute, inlet-water flow distributor, experiment hanger supports, experiment access nozzles, and the process-water inlet and outlet-line connections. The

Table 4.1

ETR Data Summary

Total Fuel Loading	- Approximately 22 to 27 kg ^{235}U
Fuel Matrix	- ^{235}U alloyed in Al. Fuel contains natural boron as burnable poison
Enrichment	- 93.4%
Fuel-plate Cladding	- 1100 Al
Burnable Poison	- Approximately 20 to 30 g ^{10}B
Active Core Size	- 76.2 x 76.2 x 91.4 cm high (includes irradiation positions)
Active Core Volume	- 530 liters
Coolant Inlet Pressure	- 200 psig
Core ΔP	- 43 psi
Total Coolant Flow	- 50,000 gpm
Active Core Flow	- 30,000 gpm
Coolant Velocity in Fuel	- 32 ft/sec
Inlet Temperature	- 110-120°F
Outlet Temperature	- 130-140°F
Fuel-plate Surface Temp (max)	- 330°F
Heat-transfer Area	- 1400 ft^2
Radial Peak/Avg Power	- 1.54
Axial Peak/Avg Power	- 1.33
Core Peak/Avg Power	- 1.60
Total Maximum Thermal Power	- 175 MW
Avg Power Density	- 6.5 kW/g
Maximum Power Density	- 21 kW/g
Avg Core Heat Flux	- 4.5×10^5 Btu/hr-ft^2
Avg Thermal Flux in Core	- 2×10^{14} n/cm^2-sec
Max Thermal Flux in Core	- 5×10^{14} n/cm^2-sec
Avg Integrated Flux in Core >1 MeV	- 3×10^{14} n/cm^2-sec
Max Integrated Flux in Core >1 MeV	- 1×10^{15} n/cm^2-sec
Temp Coef in Core	- -5×10^{-5}/°F
Nominal Excess Reactivity	
Shims	- 6% (11 to 12% Total Worth)
Burnable Poison	- 10.0%
Charge Life	- 34 days for 6000-MWd Cycle
Avg Gamma Flux	- 12 W/g of Al
Max Gamma Flux	- 25 W/g of Al
Number of Control Rods	- 16
Number of Safety Rods	- 4 to 8
Number of Shim Rods	- 8 to 12

NOTE: The preceding table is a summary of general information of typical ETR Core & Primary Coolant System parameters. Analysis presented in this document typically use bounding or accident ETR conditions and can be found in the appropriate reference material.

Table 4.2

Reactor and Building Elevations

1.	First floor	96 ft 6 in.
2.	Console floor	74 ft 0 in.
3.	Basement floor	58 ft 3 in.
4.	Canal parapet	99 ft 10-1/2 in.
5.	Canal water level (average)	98 ft 10-1/2 in.
6.	Canal floor	78 ft 10-11/16 in.
7.	Reactor-vessel top flange	99 ft 11-3/8 in.
8.	Top of discharge chute	87 ft 11-7/16 in.
9.	Top of inner tank	87 ft 3-1/4 in.
10.	Top of control-rod guide tube	84 ft 8-13/16 in.
11.	Top of core-filler piece and corner-filler piece	81 ft 8-3/4 in.
12.	Top of beryllium reflector	81 ft 7-7/8 in.
13.	Top of aluminum reflector	81 ft 7-3/4 in.
14.	Top of fuel-element fuel plates	81 ft 7-1/2 in.
15.	Centerline of active lattice	80 ft 1 in.
16.	Top of grid plate	78 ft 3-15/16 in.
17.	Top of support plate	73 ft 4-15/16 in.
18.	Bottom of reactor-vessel bottom head	68 ft 10-3/8 in.

NOTE: All the above elevations are relative to sea level datum of 4828.26 ft.

vessel contains the reactor core and provides space for nuclear radiation of the FEFPL experiment. Facilities also are provided for control rods, instrumentation, shielding of the vessel walls, directing coolant flow through the core, and support of all internal structures. Design pressures and temperature for the stainless steel-clad carbon steel and stainless steel reactor vessel are 250 psig and 200°F.

The reactor core is a square configuration of approximately 51 fuel elements, 12 shim control rods, 4 safety control rods, and 9 experimental facilities, and is approximately 30.4 in. square (see Fig. 4.2).

Material handling facilities include a new 50/5-ton bridge crane (replacing the present 30/5-ton), a 2-ton bridge crane, a 1-1/2-ton bridge crane, a freight elevator, a passenger elevator, and two hatch ways. The southeast hatchway near the stairs, consisting of an 11-ft x 11-ft opening in the main floor and a 10-ft x 10-ft opening immediately below in the console floor, is occupied by the Filling, Storage and Remelt Facility (FS&R) Test Cell (see Figure 4.7, First Floor Layout of Reactor Building).

The FEFP Loop Handling Machine (LHM) will not pass over the canal while suspended from the crane. Crane movement of the LHM will be restricted by limit switches and procedural controls to the reactor top and the east end of the reactor main floor. Usual operations will be transporter loading/unloading and experiment handling at the reactor and the Filling, Storage and Remelt Facility (FS&R) (see Figure 4.7, First Floor Layout of Reactor Building).

4.3 Reactor Building

The reactor building is designated MTR-642. The building is required to be closed to limit possible leakage during operation.

4.3.1 Building Description

The reactor building is a steel superstructure covered with insulated metal-sandwich panel siding. The interior surface of the siding is sealed and taped. The reactor-building integrity is assured by a manually operated sealed truck door, by self-closing and sealing access doors, and by remote manually controlled felt-lined dampers in the main supply and exhaust heating and ventilating systems. A complete description is contained in ETR Operating Manual, Volume VI, Heating, Ventilating and Air Conditioning Systems.

4.4 Reactor Pressure Vessel

A detailed description of the reactor pressure vessel is contained in IDO 24020, Engineering Test Reactor Engineering Design and Safeguards Report, July 1956. Figure 4.8 shows basic features, and reactor vessel dimensions are given in Table. 4.3.

4.4.1 Reactor Vessel Top Closure

The FEFPL experiment top flange closure (see Figure 4.9) is a vertical cylindrical element with the 5-1/4 in. thick x 4 ft 6-3/8 in. diameter head recessed into the 4 ft 6-7/8 in. ID reactor-vessel opening. The overall depth of the cylindrical element is approximately 3 ft 1-3/8 in. The cylindrical portion has an outer diameter of 4 ft 6-3/8 in. and is 1 in. thick. A 20 in. diameter hole in the recessed head mates with the FEFPL experiment inside the reactor vessel. The 20 in. hole is centered over the 6 × 6 core positions K-7, K-8, L-7, and L-8. Recessing of the head is a design requirement primarily dictated by the length of the FEFPL Loop Handling Machine, the maximum height of the crane hook and the inside dimensions of the biological shielding.

As a pressure retaining component in contact with reactor coolant, the top flange closure design, construction and installation satisfy the requirements of the applicable standards including ASME Section III, Class I and RDT E15-2T. An additional 28 RDT standards covering such items as forgings, fittings, pipe and the gland seal ring are used. These are listed in Appendix B of the SDD under Chart 14 covering the FEFP Loop Specification and Standards Tree No. R-1001-1000-SA-02.

4.5 Reactor Core and Reflector (see Figure 4.2)

4.5.1 FEFPL Experiment Position

The FEFPL experiment will occupy the southwest 6 x 6 portion of the 9 x 9 (M-7) experiment position and will be called the ANL L-8 facility.

4.5.2 Fuel Elements

The fuel elements are flat-plate, aluminum-boron-uranium assemblies containing nineteen 0.050-in.-thick, 37-in.-long fuel plates which are positioned and held by two aluminum side plates. The assembly is 54-1/16 in. long, and consists of an adapter or lower end box, fuel section, and a handle.

Table 4.3

Reactor Vessel Dimensions

Total height of vessel	35 ft 8 in.
Inside diameter of upper cylinder wall	11 ft 5 in.
Inside diameter of lower cylinder wall	7 ft 7 in.
Material	Stainless steel clad carbon steel and stainless steel
Thickness of upper cylinder wall	2-1/4 in.
Thickness of lower cylinder wall	1 in.
Opening in ellipsoidal top head	4 ft 6-7/8 in.
Diameter of opening in bottom head	5 ft 5 in.
Thickness of bottom head	8-1/2 in.
Thickness of FEFPL top flange	5-1/4 in.
Size of water-inlet pipe	36 in.
Elevation of water-inlet pipe	90 ft 9 in.
Size of water-outlet pipe	36 in.
Elevation of water-outlet pipe	83 ft 4 in.
Diameter of discharge chute	15 in.
Nozzles	
12 in. angular	4
12 in. horizontal	9
Nozzles	
8 in. angular	7
8 in. horizontal	3

Boron is used in these assemblies as a burnable poison. This is added to the aluminum-uranium alloy core to reduce the amount of reactivity that must be controlled over the reactor operating cycle, thereby allowing more fuel to be loaded into the reactor, and also to provide a more uniform flux distribution in the core over a given cycle.

4.5.3 Beryllium Reflector (see Figure 4.2)

The beryllium reflector consists of four rectangular slab assemblies arranged in a square array around the reactor core. The reflector is 4.5-in. thick, 37.5-in. high, and 30.4-in. square to the locating pads on the inner surface of the reflector. Each side is built up from ten beryllium pieces, the ten pieces being doweled together. The four sides are firmly held together at the ends by a full-length tie bar at each corner.

4.5.4 Aluminum Reflector (see Figure 4.2)

The aluminum reflector pieces surround the beryllium reflector and extend from the reflector to the inner tank wall.

4.6 Reactor Control

The ETR reactor safety control and regulating functions are accomplished by the use of sixteen control rods, two of which are used as regulating rods. The control rods are distributed within the core (see Figure 4.2).

Although the current work to update and revise the ETR Technical Specifications may identify changes to the control rod distribution (for example, seven of the control rods may be designated as safety rods instead of the present four). This is not expected to affect the safety assessment for FEFPL however. The description presented below describes the control system as it pertained to former ETR operation and generally applicable to FEFPL.

Four of the control rods (safety rods) are known as black position rods and are used for startup and shutdown only. In their lowest position, these four rods (safety rods) have a total worth of 7%. The other twelve control rods are known as grey poison rods and are used, not only for startup and shutdown, but also as power-level "coarse" controls during reactor operation. The nickel material of the grey rods was chosen so that its microscopic absorption cross section is approximately the same as that of the fuel elements. In this way, a minimum distortion of the thermal flux distribution in the core is obtained. In their lowest position, the twelve grey rods (shim rods) have a total worth of 11 to 12%.

Either the No. 10 or No. 13 grey control rod can be selected for use as a regulating rod. Only one regulating rod is used during operation of the reactor. The selected regulation rod is operated between 30 and 34 in. withdrawn and over this range has a worth of 0.3% $\Delta k/k$.

4.6.1 Control-rod Assemblies

The control-rod assembly (from top to bottom) consists of individual poison, fuel, and shock sections attached end-to-end and inserted in guide tubes which extend from the reactor bottom head up through the support plate and grid plate to a point approximately 3 ft above the top of the core. The lower end of the shock tube mates with the control-rod drive. Poison- and fuel-section cooling is accomplished by passage of primary coolant through the opening at the top of the rod, thence downward past the poison and fuel-plate sections, and finally out of the tube through slots placed in the shock section at a point approximately 3 ft below the grid plate.

4.7 ETR Plant Protection System

The ETR Plant Protection System (PPS) upgrade project is designed to eliminate existing areas of single failure vulnerability as identified in the ETR Single Failure Analysis CI-1225 and to upgrade other portions of the existing ETR PPS as required.

The modified and upgraded ETR PPS will provide two-channel redundancy and one-out-of-two coincident logic on all subsystems. The detailed upgrade work to be accomplished varies from subsystem to subsystem, but generally falls into three categories:

A. Replacement or addition of a complete new subsystem.
B. Addition of a second new channel to existing subsystems.
C. Modifications to existing subsystems to eliminate single failure vulnerability or to meet technical specification requirements.

Examples within these three categories are:

Category A:

1. Scram Logic Subsystem
2. Reactor ΔP Subsystem

Category B:

1. Inlet/Outlet Pressure Subsystem
2. Outlet Temperature
3. Emergency Flow Subsystem
4. Reactor ΔT Subsystem
5. Surge Tank Level Subsystem

Category C:

1. Neutron Level Subsystem
2. Pressurizer Flow Cutoff Subsystem
3. Control Rod Drive Interlocks Subsystem

The ETR PPS upgrade work is being accomplished in accordance with all applicable RDT Codes and Standards and, in particular, RDT C16-1T.

4.8 Overhead Cranes

Three independent crane facilities are provided in the ETR Reactor Building: (a) a 50/5-ton crane (presently being designed), (b) a 2-ton crane, and (c) a 1-1/2-ton crane. The 2-ton crane was modified after the original installation to give better control and safety. The 50/5-ton crane will replace the original 30/5-ton crane in order to provide the capacity to lift the maximum combined weight (50 tons) of the Loop Handling Machine (LHM) and FEFP Loop.

Design features of the new 50/5-ton crane are as follows:

Building runways will be strengthened as necessary.
New rails will be provided on the runways.
New bridge, trolley, and controls.
Hook height above main floor - 33 ft.
Total lift is 70 ft through the No. 2 hatchway.

All motors (hoist, bridge, and trolley) will be AC powered.
a 4 ft x 3 ft-4 in. opening in the trolley will accommodate the upper end of the LHM.
50 and 5-ton hoist speed - 2 to 14 ft/min. (Under full load)
Trolley - 5 to 55 ft/min.
Bridge - 5 to 100 ft/min.
Hoist Brakes - 1 holding brake for each hoist with capacity of 100% motor torque.
- 1 control brake for each hoist to limit hoist speed.
Bridge Brake - capacity 100% of motor torque.
Trolley Brake - 50% of motor torque

Two 25 ton load blocks are separately rigged to the 50 ton hoist drum. The load blocks will be equipped with 25-ton hooks for lifting the LHM or a 50-ton load beam with centrally mounted 50-ton hook. (See Section 12.2.3.1 for crane standards and specifications.)

Electrical interlocks prevent simultaneous operation of the 50/5-ton crane and the 2-ton crane. The 25 ton load blocks are maintained in a uniform horizontal plane within 1/4" under all load conditions.

The 2-ton crane operates over the central area of the reactor building with a coverage of 17 ft 7-1/2 in. north, 9 ft 3-1/4 in. south, 50 ft east, and 68 ft west of the reactor centerlines. It is mounted above the existing 30-ton crane with a clearance of approximately 4 in. when the 2-ton hook is in its highest position. The bridge speed is 110 ft/min and the trolley speed is 75 ft/min. The 2-ton hoist has three speed positions: low speed - 4 to 6 ft/min; medium speed - 14 ft/min; and high speed - 34 ft/min.

The 2-ton hoist has a two-speed motor with a magnetic clutch and a gear reducer assembly to obtain a third speed. This arrangement provides constant (reduced) speed independent of load.

The 1-1/2-ton crane is a top-riding bridge crane mounted above the 2-ton crane which serves a limited area over the reactor extending 3 ft north and south, 13 ft east, and 4-1/2 ft west of the reactor centerlines. Bridge speed is 8.4 ft/min, trolley speed is 9.8 ft/min, and hoist spees are 15 to 30 ft/min. The maximum hook height above the first floor is 50 ft 6 in.

4.9 FEFPL and FS&R Power and Utility Requirements

Ample capacity is available from the ETR system to meet the FEFPL and FS&R electrical power and utility requirements described below. (Refer to Figure 4.10, FEFPL/ETR Power Distribution System.)

FEFPL Electrical Power Requirements

Commercial Power Loads

LHM Power to ALIP		25 KVA
Primary Helium Circulators - 2		<360 KVA
Motor Control Center MCC E-107		<80 KVA
Helium Vacuum Pump M-32B	5 HP	
Bypass Valve GB-GG-114	1/5 HP	
Makeup Tank Compressor M-31B	15 HP	
Vacuum Booster Pump M-32A	7-1/2 HP	
Cubicle Air Handling Unit HVH-3	<2 HP	

MCC-113 (15 KVA transformer)		Note in use
ALIP Power MG Set		<350 KVA
Commercial-Diesel Transfer Switch		<40 KVA
30 KVA MG-5 Set		
Total Commercial Power Loads		<855 KVA
Diesel Power Loads		
Primary Helium Circulators - 2		<360 KVA
Motor Control Center MCC-E-106		<25 KVA
Makeup Tank Compressor M-31A	15 HP	
Circulator Valves GB-II-1,2,3,4		
Commercial-Diesel Transfer Switch		<40 KVA
30 KVA MG-5 Set (normally on commercial power)		
Total Diesel Power Loads		<425 KVA
Battery Backed ("H" Bus) Loads		
Instrument Power Distribution Panel MIP-108		<30 KVA
ALIP Emergency Power		60 KVA
Total Battery Backed ("H" Bus) Loads		<90 KVA
Battery Backed Instrument and Control Loads		
FEFPL Plant Protection System		<5 KVA
FS&R Facility Power Requirements		
Commercial Power Loads		
Distribution Panel No. 1		
Ventilation Blower	25 HP	40 KVA
ALIP Controller	36 kW	<45 KVA
Vacuum Pump Motor	1 HP	<2 KVA
37.5 KVA Transformer	Not in use	
Charging Facility Oper. Power		
30 KVA Transformer (Oper. & OCI Power)		<30 KVA
Drain Tank Heaters	3 kW	<5 KVA
Cleanup Tank Heaters	5 kW	<8 KVA
25 KVA Transformer (EM Pump & OCI Power)		<25 KVA
Total Commercial Power Load		<155 KVA
Diesel Power Loads		
Distribution Panel No. 2		<120 KVA
ALIP Controller	2 kW	
100 KVA Transformer		
Sodium Heaters	50 kW	
Oven	30 kW	
Lighting	3 kW	
Total Diesel Power Load		<120 KVA

Battery Backed ("H" Bus) Loads

Remelt Oven Blower	3 KVA
Distribution Panel No. 7	<5 KVA
Total Battery Backed Load	<8 KVA

FEFPL Utilities Requirements

Pneumatic Instrumentation 10 cfm Instrument Air

Approximately 20 transmitters and receivers

Cubicle Exhaust -- presently installed in Cubicle E-14

Helium (Charging and Makeup) - 12 bottles, 220 SCF each

Helium Compressors, Heat Exchangers and Mechanical Equipment

Cooling - 200 gpm high pressure demineralized water

60 gpm utility cooling water

FS&R Utilities Requirements

Pneumatic Instrumentation 7 cfm

Approximately 14 transmitters and receivers

4.10 Filling, Storage and Remelt (FS&R) Facility Description

The FS&R Facility will provide facilities for loop component assembly, loop sodium charging operations, and the preinsertion operational checkout of both irradiated and nonirradiated loops. The facility will also provide the capability to store loops that have been in the ETR. The facility will be constructed inside the existing ETR building so that maximum use can be made of existing equipment, facilities, and utilities.

System Design Requirements for the FS&R are given in FDR-03, Reference 1. The FS&R Facility design and construction is in accord with the FEFPL Specifications and Standards Tree Nos. 17 through 29 covering ventilation, fire detection, mechanical structure, electrical wiring and equipment, storage and remelt oven, and the test train cleaning facility. These are found in Appendix B to the SDD, Reference 2. ASME Section III, Class II, Code Case 1481 and RDT M 3-3T, RDT E 4-13T, RDT E 4-14T, RDT M 2-5T, and RDT E 15-2T are the principal standards applied to the sodium system. The standards and design requirements for the sodium and Pressure, Vent, and Vacuum Systems are specified in two design specifications, ANC-70014 and ANC-70015, References 3 and 4. These documents define the operating conditions and design parameters for the two systems.

The FS&R Facility will consist of the following subsystems:

Charging Facility

Charging Facility Instrumentation

Charging Facility Enclosure
Test Cell
Test Cell Instrumentation
Ventilation System
Erection Tower
Pump Assembly Station
Storage Oven
Test Train Sodium Cleaning System

Each of the preceding subsystems are described individually.

4.10.1 Charging Facility

The Charging Facility is a piping system designed to charge a FEFPL with liquid sodium, circulate the charge of sodium through the FEFPL to clean up the system, remove the sodium oxides entrapped in the sodium to a predetermined level, measure the amount of oxides with an on-line device, and collect a sample of sodium for chemical analysis at another facility.

Figure 4.11 is a flow sheet showing the direction of sodium flow through the Charging Facility. The Oxide Control and Plugging Indicating System (OCI) was purchased as a complete unit from MSA (Mine Safety Appliance Company) and the remainder of the system designed around it. Figure 4.12 is a flow sheet showing the direction of sodium flow through the Oxide Control and Plugging Indication System (OCI).

The Charging Facility piping system is constructed of 1-in. Schedule 40, ASTM A312, Type 304 Stainless Steel pipe. The system is of all-welded construction. Each pressure-containing weld will be radiographed to ASME Section III criteria. The Drain Tank, Cleanup Tank, Expansion Reservoir, and Filter are also of all-welded construction. Original charging facility equipment was designed to ASME Section VIII criteria. All new equipment and piping was designed to ASME Section III, Class II requirements. Design specification ANC-70014 delineate between new and old equipment and specify the design, quality assurance, acceptance testing and construction control requirements. A summary of system design conditions is as follows:

Pressure:	Design	1×10^{-4} torr to 50 psig	
	Operating	1×10^{-4} torr to 40 psig	
Temperature:	Design	Sodium vessels	1050°F
		Valves, Piping, and freeze vents	1000°F
		Vapor traps	330°F

Surrounding the pipe are wrap-on heaters capable of supplying sufficient energy to achieve and maintain the desired liquid-metal temperature. Additional contact heaters are located on the outside surface of the vessels, flowmeter, filter, and valves. The heaters are controlled in banks giving maximum versatility to control heatup, cooldown, and hot spots. All hot surfaces are insulated.

The electromagnetic pump is a commercial item supplied by Mine Safety Appliance Company. It is a Style III type pump with the following specifications:

Maximum Temperature	1000°F
Tube Size	1/2-in. OD, 0.049 in. wall
Tube Material	Type 304 Stainless Steel
Voltage	240
Capacity	3 gpm at 42 psid
Shutoff Head	48 psid

The pump has rectangular cross-section flow passage with magnetic and electric coils contacting the two opposite faces. The current intersecting the magnetic field at right angles causes a force to be exerted on the liquid metal in the tube.

The magnetic flowmeter is a commercial item supplied by Mine Safety Appliance Company. It is a FM-4 type flowmeter with the following specifications:

Flow Range	0-5 gpm
Maximum Temperature	1600°F
Pipe Size	1-in. Schedule 40
Pipe Material	Type 304 Stainless Steel

The flowmeter consists of a 1-in. Schedule 40 run of pipe which has a magnetic field passed through it. The field is obtained by placing the poles of a permanent magnet on both sides of the pipe. The liquid metal flowing through the magnetic field sets up a voltage that is proportional to the amount of flow. This voltage is measured and correlated to the flow.

The Mine Safety Appliance (MSA) Oxide Control and Plugging Indicating System (OCI) which was also purchased commercially, is designed to maintain and measure purity in liquid-metal systems. It operates on the principle that the solubility of oxide in liquid metals is temperature dependent, and when the temperature of the liquid metal is lowered slightly below the oxide saturation temperature, the oxide will precipitate from solution. This principle is used as the basis of operation of both the oxide control and oxide indicating sections of the system. For oxide control, a portion of the liquid-metal stream is withdrawn through an economizer into a cold trap where oxides are deposited. The effluent from the cold trap which is essentially oxide-free is reheated in the economizer and returned to the stream within 100°F of the stream temperature. An oxide indicating test is made by isolating the cold trap and passing a portion of the main stream through the oxide indicator when reducing the temperature of the liquid-metal stream at a constant rate. When the oxide saturation temperature is reached, solid oxide will precipitate and restrict the flow passages in the oxide indicator. Since constant pressure drop is maintained across the system, restriction of the flow passages will cause a decrease in flow. The liquid-metal temperature at this point is the saturation temperature.

The design conditions for the Oxide Control and Indicating System (OCI) are listed below:

Design Temperature	1050°F
Design Pressure	100 psig
Fluid	Sodium
Sodium Containment Material	304 H stainless steel

The inlet and outlet connections to the OCI system are 1/2-in. Schedule 40 seamless pipe and the interconnecting piping between components is 1/2-in. Schedule 40 seamless pipe.

The flowmeter used in the OCI system is a standard MSA unit, type FM-1. It has the following specifications:

Flow Rate	0-1 gpm
Maximum Temperature	1050°F
Pipe Size	1/2-in. Schedule 40

This flowmeter works on the same principle as the magnetic flowmeter that is in the Charging Facility piping.

The purpose of the economizer is to reduce the heat load on the cold trap and plugging indicator cooler and to reheat the returning liquid metal to reduce the heat loss to the main system. The economizer is a shell and tube type designed with a 1/2-in. tubing inside a 3/4-in. pipe.

The Plugging Indicator Cooler consists of a finned U-tube and a shell for directing air across the fins. Liquid metal from the economizer enters the cooler; a centrifugal blower with outlet damper and connecting ducting provides the necessary air for cooling.

The plugging indicator is a manual, remote-controlled electric-operated 1/2-in. bellows-sealed valve with a serrated seat. With the valve closed, sodium will pass through the serrated seat until the oxygen saturation temperature is reached, at which time oxide will precepitate out in the serrations and restrict the sodium flow, as indicated on the flowmeter. Following a plugging indicator run, the valve is opened and hot sodium flowing through the valve will redissolve the oxide deposit.

The cold trap is a 31-1/4-in. section of 10-in. pipe enclosing a 8-5/8-in. OD tube packed with stainless steel wire mesh. This trap has sufficient volume so the holdup time is at least five minutes and the oxide capacity is 29 pounds. Sodium capacity of the cold trap is 11 gallons. The sodium entering the cold trap flows down the outside of the 8-5/8-in. OD tube and is cooled below its oxide saturation temperature. The sodium then flows up through the packed tube and deposits the sodium oxide on the available surface. The sodium leaving the cold trap is free of sodium-oxide particles and is above the saturation temperature due to the economizer action of the cold trap. By circulation through the cold trap, the oxide saturation temperature of the system will be reduced to the temperature at which the cold trap is operating.

A blower is provided to supply the cooling air to the cold trap. A damper, with an electric damper operator, is mounted on the blower outlet to regulate the air supply. The external surface of the cold trap is covered with longitudinal fins. This surface, along with air blower, duct, and damper, is used to control the cold trap temperature. The cold trap will not drain back into the main system. This will prevent the material deposited in the cold trap from being flushed back through the system.

Two 1/2 in. bellows-sealed valves are used to regulate the plugging-indicator flow and cold trap flow. Each is furnished complete with an electric operator.

All sodium vessels are designed to ASME Section III, Class II. Design specification ANC-70013, Reference 5, gives the design requirements and ordering data for the vessels.

The Charging Facility Drain Tank and Cleanup Tank are located at the low point of the system. The Drain Tank acts as a reservoir in which the liquid metal in the system can be stored. The Drain Tank is normally at a low level and shut off from the system during circulation. The Cleanup Tank is in the loop and operates liquid-full during circulation for oxide removal before filling of the FEFP Loop. It is the source of sodium for filling a FEFPL in the Test Cell as well as the receiving vessel for sodium charging from a sodium shipping container. Both vessels are installed so as to allow movement due to thermal expansion of the piping.

Dump and Drain Tank specifications are: (Identical Vessels)

Design Temperature	1050°F
Design Pressure	50 psig
Vessel Capacity	21 gallons
Material	Type 304 Stainless Steel

Cleanup Tank specifications are:

Design Temperature	1050°F
Design Pressure	50 psig
Vessel Capacity	21 gallons
Material	Type 304 Stainless Steel

The Charging Facility filter is used to remove insoluble particles of 20 micron size and greater from the flowing sodium. The filter element is made of sintered stainless steel.

Filter specifications are:

Design Temperature	1000°F
Design Pressure	50 psig (rated pressure of 225 psig)
Material (pressure boundary)	Type 316 Stainless Steel

The Charging Facility Expansion Reservoir is located at the high point of the system. It contains the only free sodium surface while the system is in the circulation mode of operation. The vessel is installed so as to allow movement due to thermal expansion of the piping.

Expansion Reservoir specifications are:

Design Temperature	1050°F
Design Pressure	50 psig
Vessel Capacity	9 gallons
Material	Type 304 Stainless Steel

Mounted in series on all vessels are freeze vents and sodium vapor traps. The freeze vents are designed to RDT E 4-13T, Freeze Vent for Sodium Service and the vapor traps are designed to RDT E 4-14T, Vapor Trap Assemblies for Sodium Service. They are designed to prevent liquid sodium and sodium vapor, respectively, from entering into the pressure, vent, and vacuum system. Ordering data for the freeze vents and vapor traps are given in specification ANC-70016 and specification ANC-70017, respectively, References 6 and 7.

Design specifications are:

	Freeze Vents	Vapor Traps
Design Temperature	1000°F	330°F
Design Pressure	50 psig	50 psig
Material	304 SST	304 SST

All the piping and vessels (except vapor traps) are insulated to keep heat losses to a minimum and to keep surface temperatures below 140°F for personnel safety.

The Pressure, Vent, and Vacuum System interfaces with the sodium system at the four sodium vessels through the vapor traps and freeze vents. Design specification ANC 70015, Reference 4, give the design requirements. The major components in the system are a high pressure argon gas supply, pressure regulating and overpressure protection devices, low and high vacuum systems and associated pipe and valving.

4.10.2 Charging Facility Instrumentation

The Charging Facility instrumentation panels are located on the ETR main reactor floor adjacent to the charging facility enclosure. The panel arrangement is shown in Figure 4.14. These panels make pertinent system parameters necessary for safe operation available to the operator. Control of the system is maintained from these panels. An alarm system continually senses critical system parameters.

To assist the operator in safely operating the system, temperature, pressure, flow and level measurements are made. The system design is shown in Reference 8. The critical functions are listed in Table

Table 4.4 Charging Facility Instrumentation Functions

Measurement	Location	Action		
		Indication	Alarm	Shutdown
Temperature	Sodium Piping	X	X	Heaters
	Freeze Traps	X	X	
	Tank Surface Metal	X	X	Heaters
	Sodium in Tanks	X	X	Heaters
Flow	Sodium Piping	X	X	Pump
	Oxide Control Unit	X		
Pressure	EM Pump Outlet	X	X	Pump and Heaters
	Cleanup Tank Outlet	X	X	Pump and Heaters
Level	Cleanup Tank	X	X	
	Drain Tank	X	X	
	Dump Tank	X	X	
	Expansion Reservoir	X	X	Pump

The pressure, vent, and vacuum system that is used to transfer sodium in the charging facility is monitored for low and high pressure conditions. Alarm functions are provided, and protection from over-pressurization and under-pressurization is provided.

A FEFPL Fire Detection System is shown in Reference 8 and consists of the following subsystems:

a. Sodium leak detectors on the bellows-type sodium valves and the secondary enclosure surrounding the sodium transfer piping.
b. Photoelectric and ionization smoke detectors in the charging facility enclosure and the test cell enclosure.
c. Ionization detectors in the charging facility ventilation duct and the test cell ventilation duct.
d. Closed circuit television systems in the charging facility enclosure and the test cell enclosure.
e. Ambient temperature measurements in the charging facility enclosure and the test cell enclosure.

To avoid spuriously signaling the fire department that a sodium fire exists, two-of-the-three types of fire detection systems described above (Items a, b, and c) must be actuated. Two-out-of-three (2/3) logic is used to connect the FEFPL fire detection subsystems to the Central Facilities Fire Department.

Radiation monitoring, consisting of remote area monitors and constant air monitors, is provided for both the charging facility enclosure and the test cell enclosure. The locations of the radiation monitors are shown in Reference 8.

Detailed descriptions of the instrumentation channels are contained in Reference 12.

The electrical power distribution system for the charging facility is shown on drawing 404944 (Reference 11). Commercial power, failure-free power, and diesel-generated power are used to power the charging facility electrical components.

A failure mode analysis was conducted to determine in what ways the charging facility system components could fail and the consequences of the failures. No credible single event has been identified that can cause both a piping system failure and failure of critical operational instrumentation channels. Further details of the analysis may be found in References 9 and 10.

4.10.3 Charging Facility Enclosure

The Charging Facility Enclosure is constructed of concrete block with approximate outside dimensions of 11 ft wide by 28 ft long by 14 ft high. It houses the Charging Facility that is 8 ft wide by 16 ft long by 9-1/2 ft high. The Charging Facility Enclosure walls and floor are lined with carbon-steel sheet. Two 3 ft wide by 7 ft high metal doors are provided for personnel access to the front and rear of the Charging Facility for sodium sampling and maintenance purposes. A 10 ft x 10 ft metal door is provided for equipment insertion and removal. Concrete curbs or thresholds are provided at all floor level openings to prevent standing water from entering the enclosure. The floor of the Charging Facility is egg-crated to minimize the surface area of any potential sodium spill. Any four adjacent sections have a surface area of less than ten square feet and have a volumetric capacity to contain the maximum credible spill in the Charging Facility. The Charging Facility Enclosure is located on the ETR main reactor floor (see Fig. 4.7).

4.10.4 Test Cell

The Test Cell is a steel-lined concrete enclosure 13 ft by 13 ft by 38 ft high, built around existing hatchway openings in the ETR building main and console floors. The clear opening at the main floor is 11 ft square and the clear opening at the console floor is 10 ft square. Working and support platforms are installed at locations in the test cell which allow working near the top of the FEFPL during assembly and checkout, and support platforms are provided which support the FEFPL and associated equipment in the test cell. The ETR basement floor is excavated to bedrock beneath each of the four support columns and concrete pilings poured beneath them to allow for transfer of all loads imparted to the test cell to the lava bedrock. A 1/4-in.-thick carbon-steel plate is welded to the outside of the four support columns to line the test cell and provide a barrier between the test cell and shielding concrete. The floor of the test cell is lined with a 1/4-in. carbon-steel plate which slopes to a removable sodium spill container which incorporates a self-extinguishing design. Piping in the test cell will be double contained up to the in-pile tube isolation valves. A catch pan is provided for the remaining short length of piping into the glove box. A reinforced concrete hatch with a metal leveling plate including a removable plug is placed over the test cell at the ETR main floor level to support the LHM during insertion of the FEFPL for transfer to the ETR. Two doubly contained, insulated, and electrically trace-heated pipe lines bring and return sodium from the charging facility located in the Charging Facility Enclosure to the test cell. A dump tank in the test cell will catch the sodium when it is drained from the lines. Piping and dump tank design is as specified in 4.10.1. It will also receive the excess sodium from a FEFPL when the sodium level is lowered to the operating point. Sodium leak detectors are placed on the sodium supply lines and return lines. Inert gas lines for purging the FEFPL primary to secondary annulus and for leak checking during assembly are terminated inside the test cell. Vacuum lines to be used during leak checks and bake-out periods also terminate inside the test cell.

4.10.5 Test Cell Instrumentation

The Filling, Storage, and Remelt (FS&R) oven control panel is located at the west end of the helium control console on the ETR north console floor. This panel is used to control and regulate electrical power to the furnace heating elements. Zone heating of the FEFPL in-pile loop assembly may be required while the loop is in the oven. The oven control instrumentation has been designed to accomplish this zone heating.

Pertinent operating parameters of the in-pile loop assembly, while it is in the FS&R facility and in the ETR reactor, will be monitored by the FEFPL Data Acquisition System which is located on the north side of the ETR north console floor.

A fire detection system is provided for the test cell enclosure. This system is described in Section 4.10.2.

4.10.6 Ventilation System

The FS&R facility ventilation system is described in Section 4.11.6.

4.10.7 Erection Tower

The erection tower is a structural-steel framework 9 ft by 8-1/2 ft by 26 ft high with three working platforms. The tower will be used to remove FEFPL components from their shipping containers while in a vertical attitude and to attach instrument leads to the FEFPL primary vessel. Removable grating on each of the working platforms allows bringing the shipping containers into the center in order to remove the FEFPL components. The shipping containers are removed, the grating replaced, and then partial assembly can proceed. Final assembly of the secondary tube, primary tube, and test train will be accomplished in the test cell. The erection tower is located on the ETR main floor adjacent to an existing stairway and passenger elevator. The upper and lower platforms are located at the top of the stairway and elevator roofs to allow extended working areas on these platforms if needed for access or equipment storage. Handling associated with the work around the erection tower and test cell will be accomplished with the use of the 50/5-ton overhead traveling crane in the ETR building. Figure 4.13 shows plan and elevation views of the Erection Tower.

4.10.8 Pump Assembly Station

The pump assembly station located in the former north circular stair well will contain a fixture for assembling an annular linear induction pump to a primary FEFPL vessel.

4.10.9 Storage Oven

The storage oven, Figure 4.15, is located next to the Test Cell and extends down through the ETR building main and console floors. The storage oven will be a shielded storage area where FEFP Loops that have been irradiated in the ETR can be stored while keeping the sodium in a molten condition. The storage oven will also be used for charging a loop with sodium and conducting checkout tests prior to insertion in ETR.

4.10.10 Test Train Sodium Cleaning

The requirement for a test train sodium cleaning system has been eliminated. Figure 4.15 shows the proposed location of a conceptual design of the cleaning facility in the test cell.

4.11 Reactor Building, FEFPL Cubicle and FS&R Facility Ventilation

The reactor building, Building 642, is the only building in the ETR complex that interfaces directly with the FEFPL experiment and the FS&R facility. There are six other buildings in the complex that are adjacent to Building 642. These buildings have separate ventilation systems either completely independent of Building 642 or they exhaust to ducts going to the waste gas stack which also serves as the exhaust for Building 642.

The FEFPL cubicle (E-14) will be ventilated by air from the reactor building basement which will then enter the cubicle exhaust system and then go to the waste gas stack.

The FS&R Charging Facility and Test Cell will be cooled and ventilated by air drawn from the reactor main floor. After flowing through the Charging Facility and Test Cell the air will pass through a blower located on the low by roof (south side) of Building 642, and discharge to the atmosphere.

The following descriptions apply to the ETR building, Building 642. The FS&R facility ventilation system is an addition to the existing systems serving Building 642. The ventilation for the FEFPL cubicle, Cubicle E-14, is supplied by the existing ETR Cubicle Exhaust System. Figure 4.17 is a flow diagram of the Building 642 and FS&R facility ventilation systems (also see Figure 4.16).

4.11.1 Building 642 Ventilation System

Air flow in Building 642 is designed to flow from potentially low contamination areas to potentially high contamination areas, thence to the 250 ft high, reinforced-concrete waste gas stack, and finally to the atmosphere. In the event it is required to seal the building or purge it of contaminated air, two "Building Seal Push Buttons", No. 1 and No. 2, located on the reactor console in the reactor control room, can be activated. The "Building Seal Push Buttons" close dampers and shut down fans as follows:

Push Button No. 1

1. Console Supply Fan
2. First Floor Exhaust Fan and Building Seal Damper
3. First Floor Return Air Damper
4. Console Floor Return Air Damper
5. Console Floor Supply Air Damper
6. Console Floor Outside Air Damper
7. FS&R Facility Supply and Exhaust Motor Driven Dampers and Exhaust Blower. (D3, D4, D5, and D6 in Figure 4.16.)

Push Button No. 2

1. First Floor Supply Fan
2. Cubicle Exhaust Fans and Building Seal Damper
3. First Floor Supply Damper
4. First Floor Outside Air Damper
5. Cubicle Exhaust Dampers

On loss of power to the FS&R damper system, the FS&R facility is automatically sealed by dampers, D1 and D2, which are spring loaded shut.

4.11.2 Reactor Building First Floor

This system is designed to circulate first floor air four times per hour and maintain an area winter temperature of 65°F. Two of these hourly air changes shall be from fresh outside air and two by recirculation. This circulation is effected by means of one supply-air fan with a capacity of 48,000 cfm and one exhaust fan with a capacity of 24,000 cfm.

Maintenance of the desired atmospheric pressure in the first floor area is dependent upon balance between supply and exhaust air volumes.

4.11.3 Reactor Building Console Floor and Basement Area

This system is designed to heat and ventilate the console floor and basement areas of Building 642. The system maintains an air change rate equal to six times the total cubicle area per hour. To maintain this rate the two 7600 cfm cubicle exhaust fans will exahust a total of 15,200 cfm to the waste gas stack. The console floor supply fan provides 34,200 cfm to the area. This volume normally consists of 19,100 cfm of recirculated air and 15,100 cfm of fresh air from the outside.

The total exhaust through the cubicles exceeds the fresh supply by 100 cfm and maintains a slightly negative pressure in the basement and cubicle areas.

The exhaust air flow route is from the console floor through rectangular openings along the perimeter of the basement ceiling, to the cubicles, and then into the cubicle exhaust duct through the two cubicle exhaust fans. This exhaust air is expelled to the waste gas stack via a continuation duct.

Maintenance of the desired atmospheric pressure in the console floor and basement area is dependent upon balance between supply and exhaust air volumes.

4.11.4 Cubicle Exhaust System

The cubicle exhaust system is a continuation of the basement heating and ventilating system. The air flow is routed through rectangular openings along the perimeter of the basement ceiling to the experimental cubicles and then into the cubicle exhaust duct. Two 20-hp cubicle exhaust fans rated at 7,600 cfm discharge to the suction side of a booster fan. In the reactor building there are three exhaust ducts located at the working canal, storage canal and reactor top. These ducts penetrate the reactor main floor from beneath. Located in this duct on the console floor is an Axivane fan rated at 3,900 cfm and driven by a 2-hp motor which discharges into the suction side of the cubicle exhaust fans. This fan is two speed and the fan speed can be selected by the start-stop buttons located on the south side of the working canal parapet.

The booster fan, rated at 25,000 cfm, driven by a 75-hp motor is located in a room on top of the heat exchanger building and discharges to the waste gas stack via a continuation duct. Located in the same room as the booster fan is an exhaust fan rated at 5,000 cfm and driven by a 15-hp motor. This fan draws air from the heat exchanger building, Building 644, and discharges it to the suction side of the 75-hp booster fan.

4.11.5 Control Rod Drive Repair Room, Rod Access Room and Subpile Room

These three rooms located in the basement receive air from the basement area and are tied to the cubicle exhaust header. Air flow into the Rod Access Room and Subpile Room is by leakage only and they are at a slightly negative pressure with respect to the basement. The Control Rod Drive Repair Room is designed to have an air flow from the basement area to the cubicle exhaust header in order to prevent spread of contamination which might be released during disassembly, inspection, and repair of control rod drives. This room will be dismantled to accommodate construction of the FS&R Test Cell. Tentative plans are to relocate the Control Rod Drive Repair Room to the secondary experiment cubicle J-10, which will provide equivalent ventilation.

4.11.6 FS&R Charging Facility and Test Cell

The ventilation system consists of a two-speed blower, ductwork, dampers, and controls which provide ventilation to the test cell and charging facility enclosure. The system is designed to remove the estimated 32 kW of heat released to the atmosphere of the test cell and charging facility enclosure from components within these areas. It is also designed as part of the fire protection system; the ventilation system will operate at and maintain the system below 400°F (except at the immediate area of the fire) for three hours without damage to facilities during a maximum credible sodium spill. The system can replace the air in the test cell or the charging facility two and a half times a minute, thus removing the smoke and allowing access to the fire. The unaffected area (either test cell or charging facility) can be isolated to increase the ventilation flow rates through the affected area and the blower speed can also be increased. The system is tied into the building seal system to assure that the ETR main building can be properly sealed. The system is shown schematically in Figure 4.16.

4.12 Fire Protection Systems

As stated previously, the reactor building, Building 642, is the only building in the ETR complex that interfaces directly with the FEFPL experiment and the FS&R Facility. The fire protection systems for the six other buildings in the complex that are adjacent to Building 642 will not be described.

Except for the FS&R Test Cell and Charging Facility, FEFPL equipment will be protected by the present ETR Building 642 sprinkler systems.

Building 642 sprinkler systems on the three levels are:

Highbay and lowbay on main floor - wet pipe sprinkler system

Console Floor - preaction dry pipe sprinkler system

Basement - wet pipe sprinkler system (includes all cubicles)

Fire fighting capability on the spot consists of trained Fire Brigades composed of reactor operating personnel. The AEC Fire Department is summoned from Central Facilities Area by telephone or automatically by means of the ADT (American District Telegraph) System.

Fire protection provisions for the following FEFPL systems and equipment items will be described.

Helium System

- Cubicle E-14 in ETR Basement (Figure 4.6)
- Transmitter Panel adjacent to Cubicle E-14
- Transformers and Switchgear in ETR Basement
- Control Panel on Console Floor (same enclosure as FEFPL Instrumentation and Plant Protection System)
- Helium Circulator MG Sets on Main Floor

Annulus Gas System

- Cubicle TBD in ETR Basement
- Control Panel on Console Floor

Loop Handling Machine and Transporter

FEFP Loop

- Annular Linear Induction Pump (ALIP) MG Set on Main Floor
- Instrumentation and Plant Protection System (PPS) Panel Enclosure on Console Floor

Filling, Storage, and Remelt Facility

- Instrument Panels, Switchgear, and Transformers - Main Floor
- Erection Tower - Main Floor
- ALIP Assembly Fixture - North Circular Stairwell
- Charging Facility
- Test Cell

4.12.1 Helium System

Cubicle - Cubicle E-14 in the ETR Basement contains the following major items of mechanical equipment: helium circulators, shielded filter, helium coolers, makeup compressors, vacuum pump, helium makeup tank, and helium exhaust tank. Sprinkler fire protection for Cubicle E-14 is part of the ETR Basement wet-pipe sprinkler system.

Transmitter Panel - Adjacent to Cubicle E-14 - The wet-pipe sprinkler system in ETR Basement will not require modification to protect the transmitter panel.

Transformers and Switchgear in ETR Basement - The wet-pipe sprinkler system in the ETR Basement will not require modification to protect this equipment.

Control Panel on Console Floor - The Helium System control panel will be in the same air-conditioned enclosure as the FEFPL Data Acquisition and Plant Protection Systems. Location is the northeast corner of the console floor. The existing pre-action dry pipe sprinkler system for the console floor will be extended to provide four sprinkler heads and two detectors for complete coverage of the enclosure. Detectors operate on the rate of temperature rise principle backed up by a fusible link should the rate of rise be too low to activate entry of water into the system (also see 4.12.4).

Helium Circulators MG Sets - Two MG sets and associated switchgear for driving the four helium circulators are located on the main floor in the low bay area. The switchgear will be protected by the presently installed wet-pipe sprinkler system for this area.

4.12.2 Annulus Gas System

The building sprinkler systems provide fire protection for this area.

4.12.3 Loop Handling Machine (LHM) and Transporter

This equipment will be protected by the reactor main floor wet-pipe sprinkler system while inside the building. No modification to the system is required. It should be noted that the tractor portion of the transporter will be moved outside the building prior to lifting the LHM with the building crane.

4.12.4 Instrumentation and PPS Panel Enclosure

This approximately 16 ft x 24 ft enclosure located in the northeast corner of the console floor houses the Data Acquisition System, Plant Protection System (PPS) and the control instrumentation for the Helium System. Air temperature control for the enclosure and instrumentation will be provided by a 7-1/2-ton packaged air-conditioning unit. Since the interior will be totally isolated, the console floor dry pipe sprinkler system will be extended inside the enclosure. Four sprinkler heads and two heat activation devices (sensors) will be provided. A detector for combustion products will also be installed in the enclosure and will actuate an externally located alarm.

4.12.5 Annular Linear Induction Pump (ALIP) MG Set Enclosure

The enclosure for the ALIP MG set is to be located immediately east of the enclosure for the Helium Circulator MG sets on the reactor main floor. The low bay wet-pipe sprinkler system will be modified to cover the interior of the enclosure.

4.12.6 Filling, Storage, and Remelt System

Instrument Panels, Switchgear, and Transformers - This equipment located on the reactor main floor adjacent to the Test Cell and Charging Facility will be protected by the present main floor wet-pipe sprinkler system. Modification to the system is not required.

Erection Tower - Fire protection will be provided by the reactor main floor wet-pipe sprinkler system. Modification to the system is not required.

ALIP Assembly Fixture - Fire protection will be provided by the reactor main floor wet-pipe sprinkler system. Modification to the system is not required.

Test Cell and Charging Facility Enclosure - Fire protection for these areas is provided by fire detection systems as described in Section 4.10.2 and by stringent design requirements to prevent sodium spills. Sufficient fire-fighting materials are provided at each entrance to the area to extinguish the maximum credible fire. Reference 13 provides the details of the type and location of fire-fighting equipment. The ventilation system is described in Section 4.11.6.

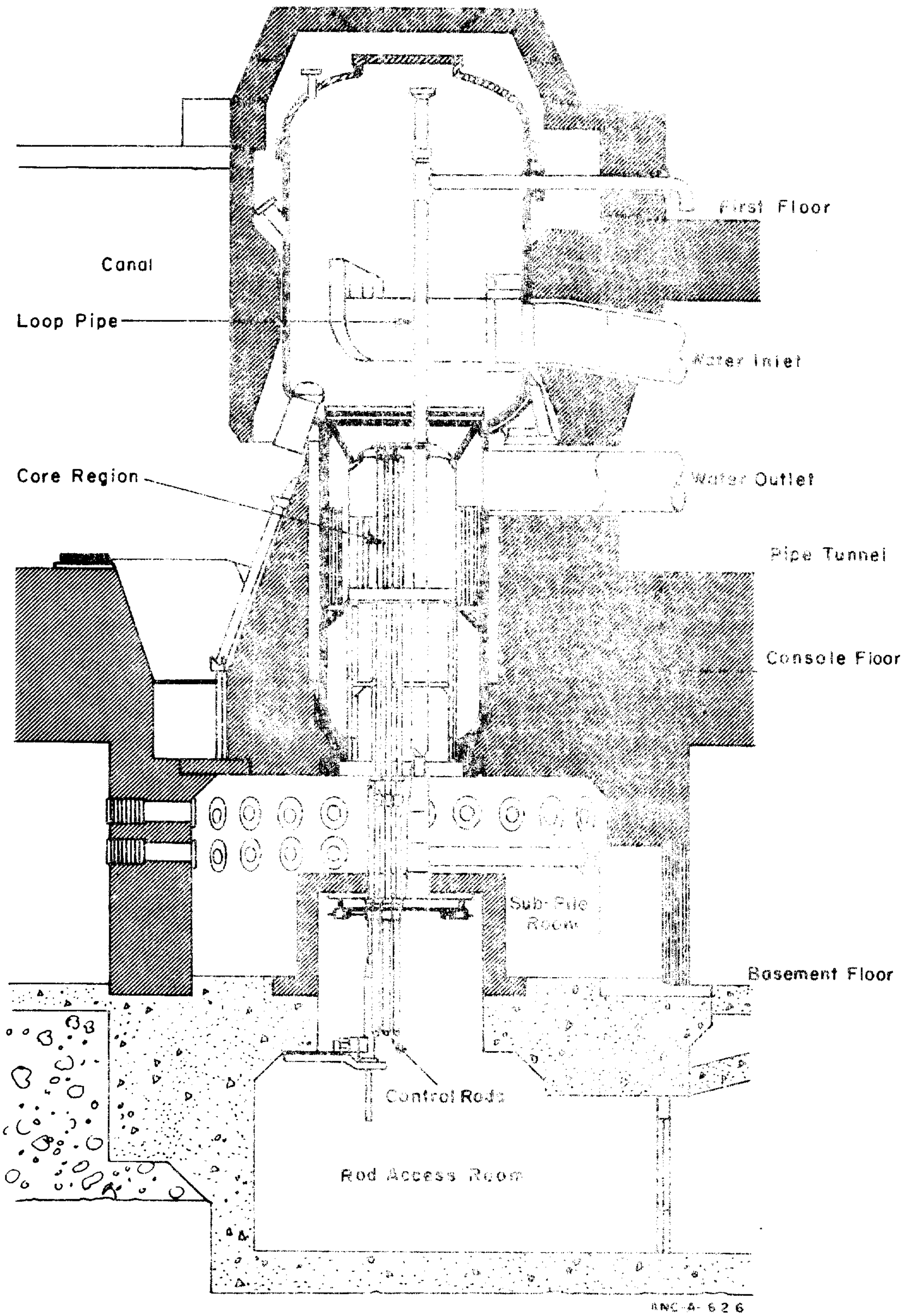

FIGURE 4.1 SIMPLIFIED DIAGRAM OF ETR

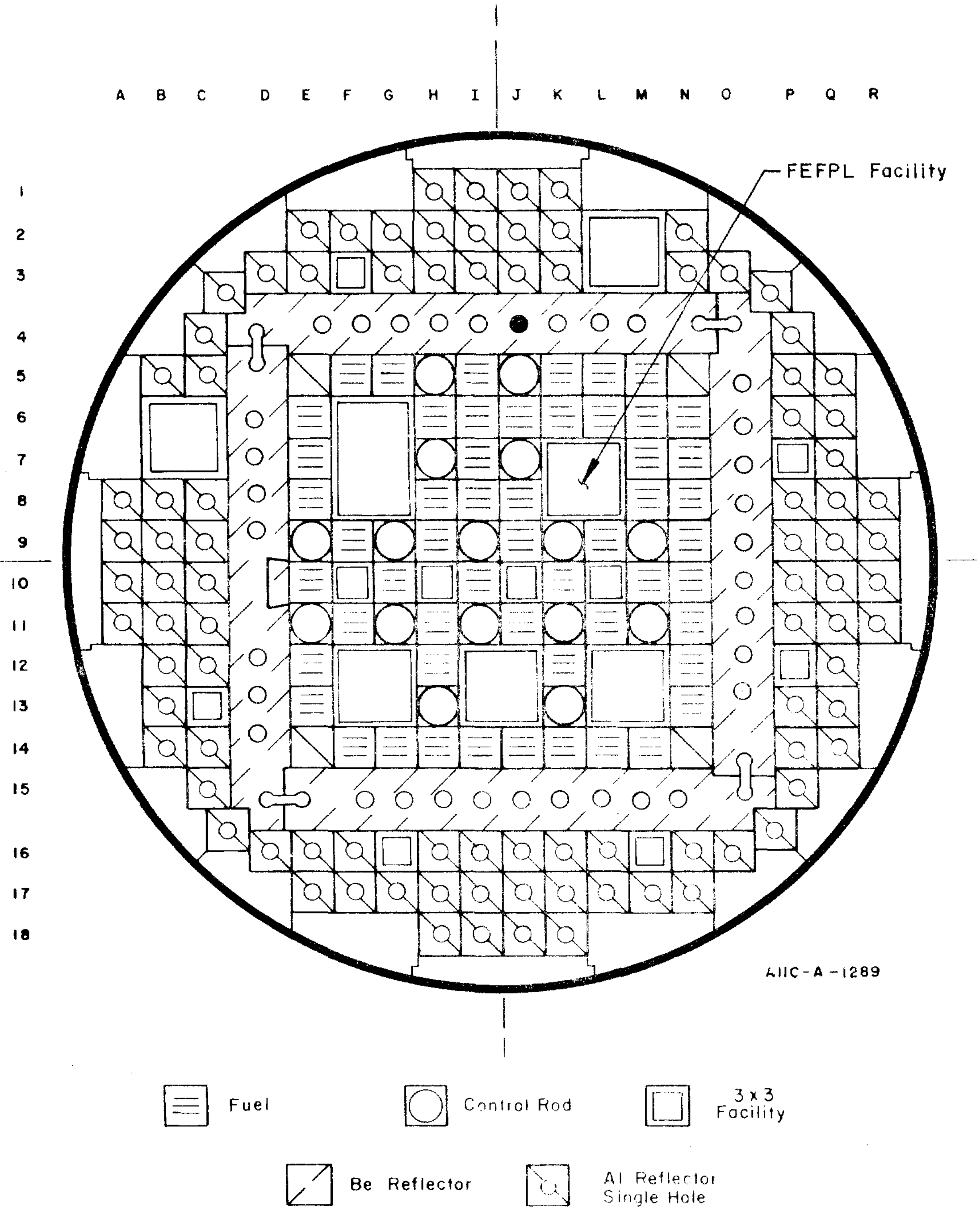

FIGURE 4.2 ETR LATTICE AND REFLECTOR HORIZONTAL CROSS SECTION ABOVE CORE

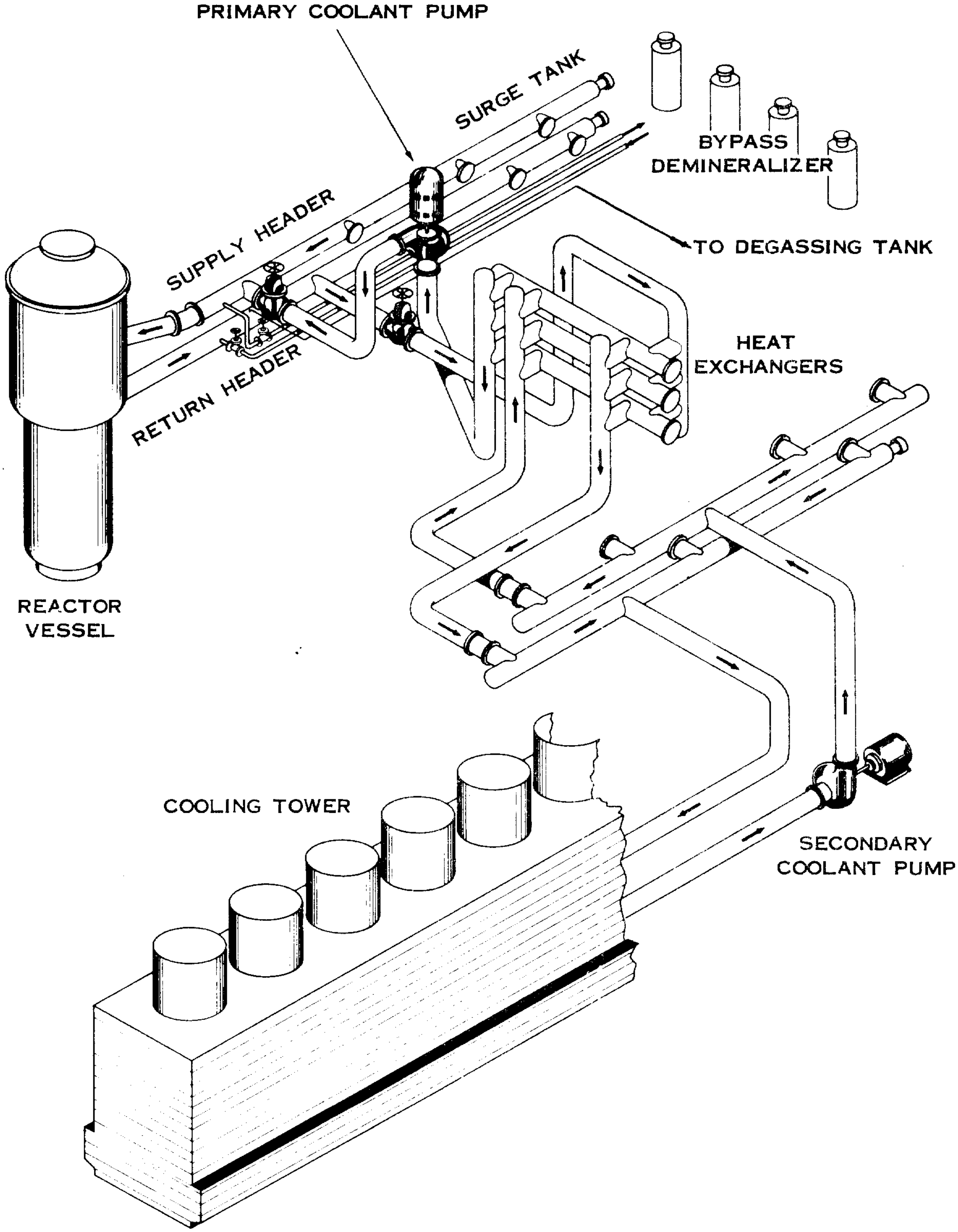

FIGURE 4.3 THE ETR COOLING SYSTEM

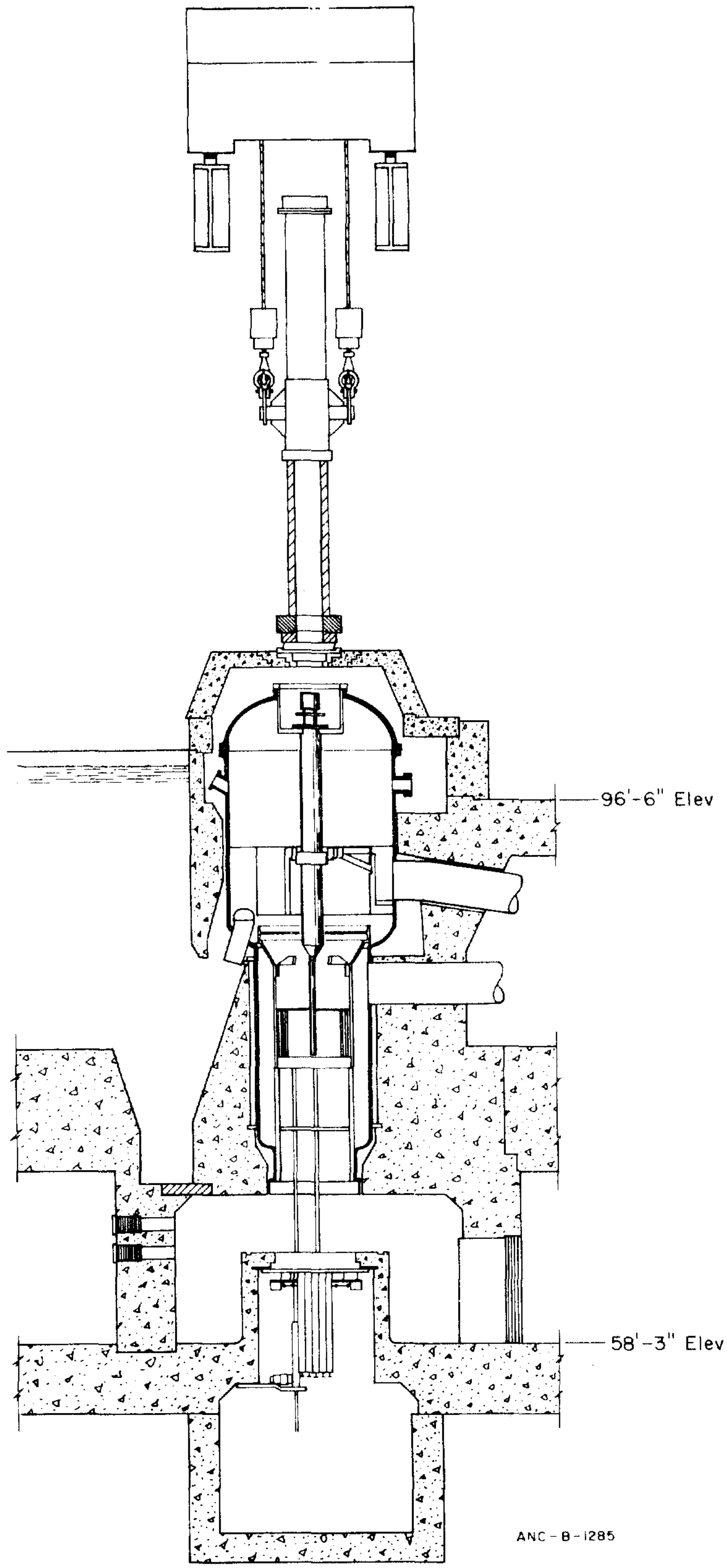

FIGURE 4.4 LOOP HANDLING MACHINE (LHM) SUSPENDED BY THE 50/5 TON CRANE OVER THE REACTOR

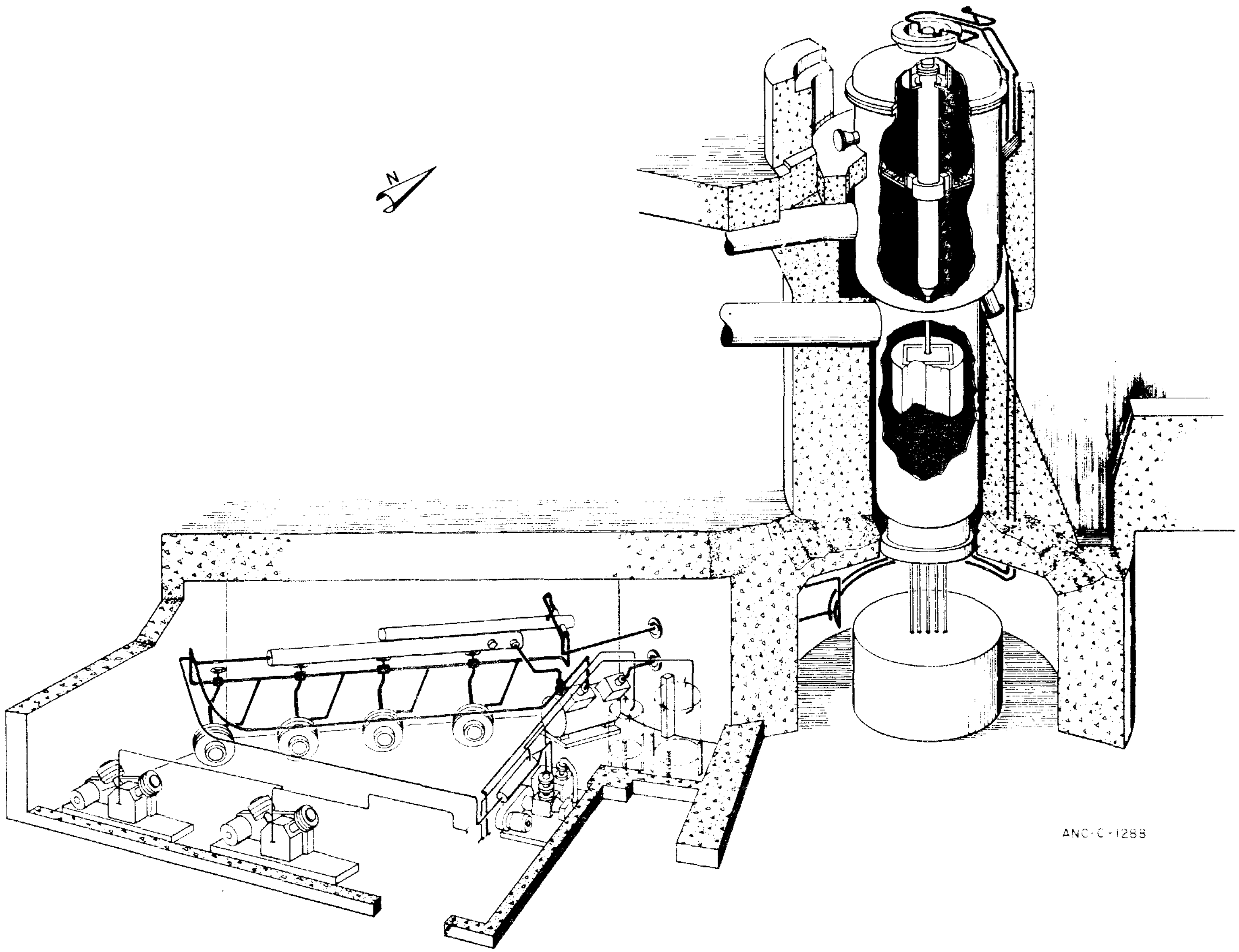

FIGURE 4.5 SIMPLIFIED DIAGRAM OF FEFP LOOP IN THE ETR AND THE HELIUM HEAT REMOVAL SYSTEM

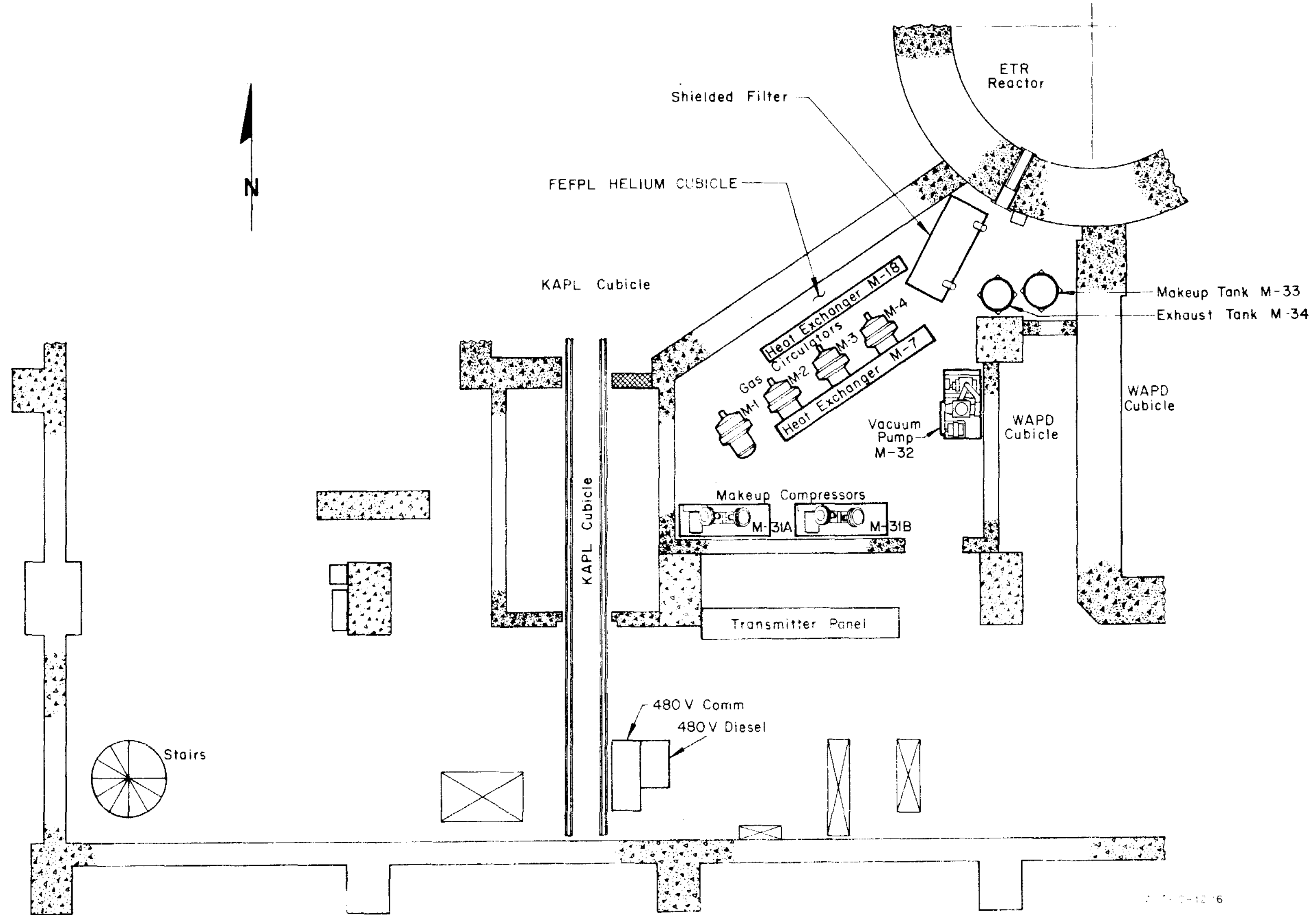

FIGURE 4.6 PLAN OF HELIUM CUBICLE MECHANICAL EQUIPMENT LAYOUT

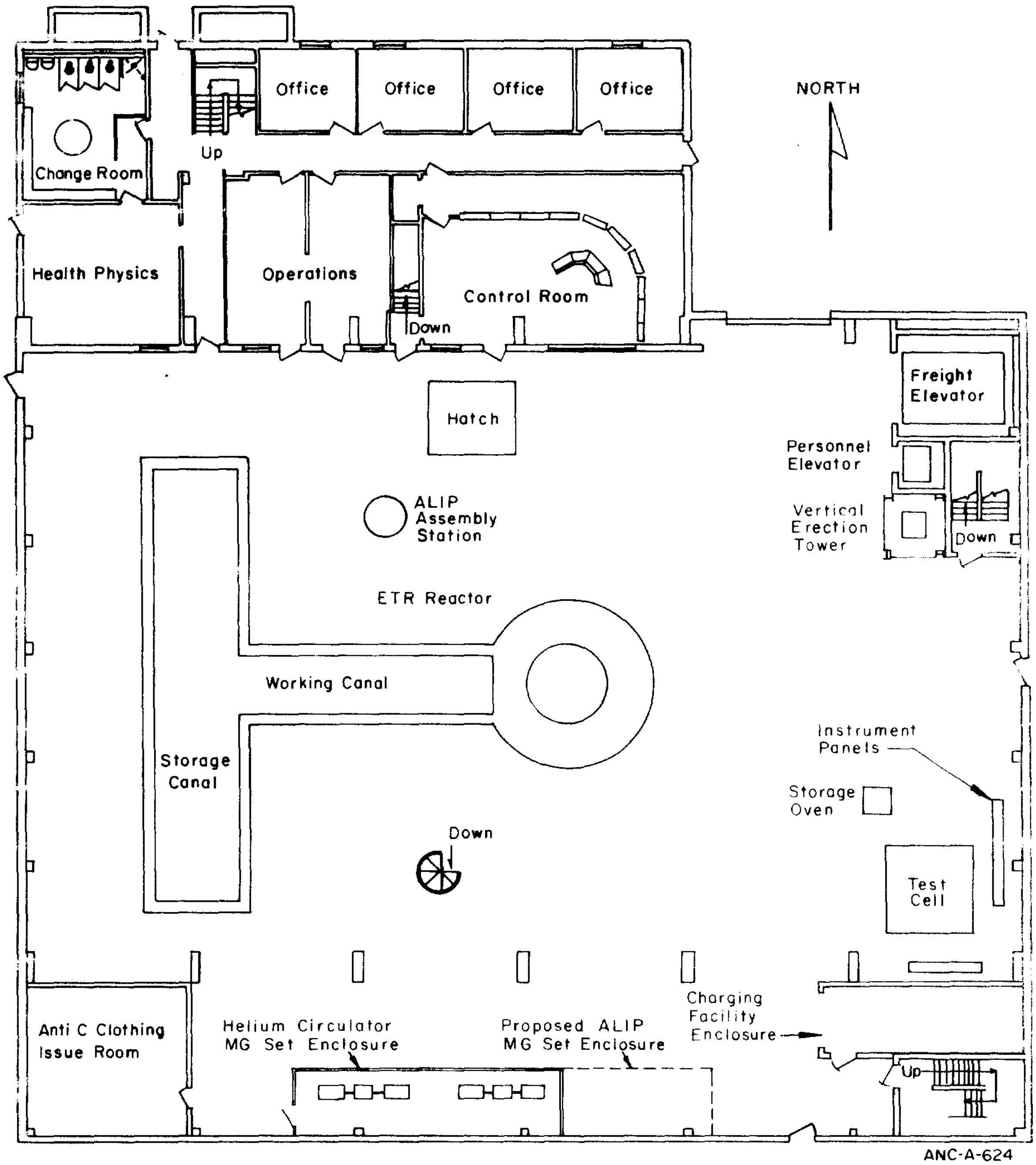

FIGURE 4.7 REACTOR BUILDING FIRST FLOOR LAYOUT

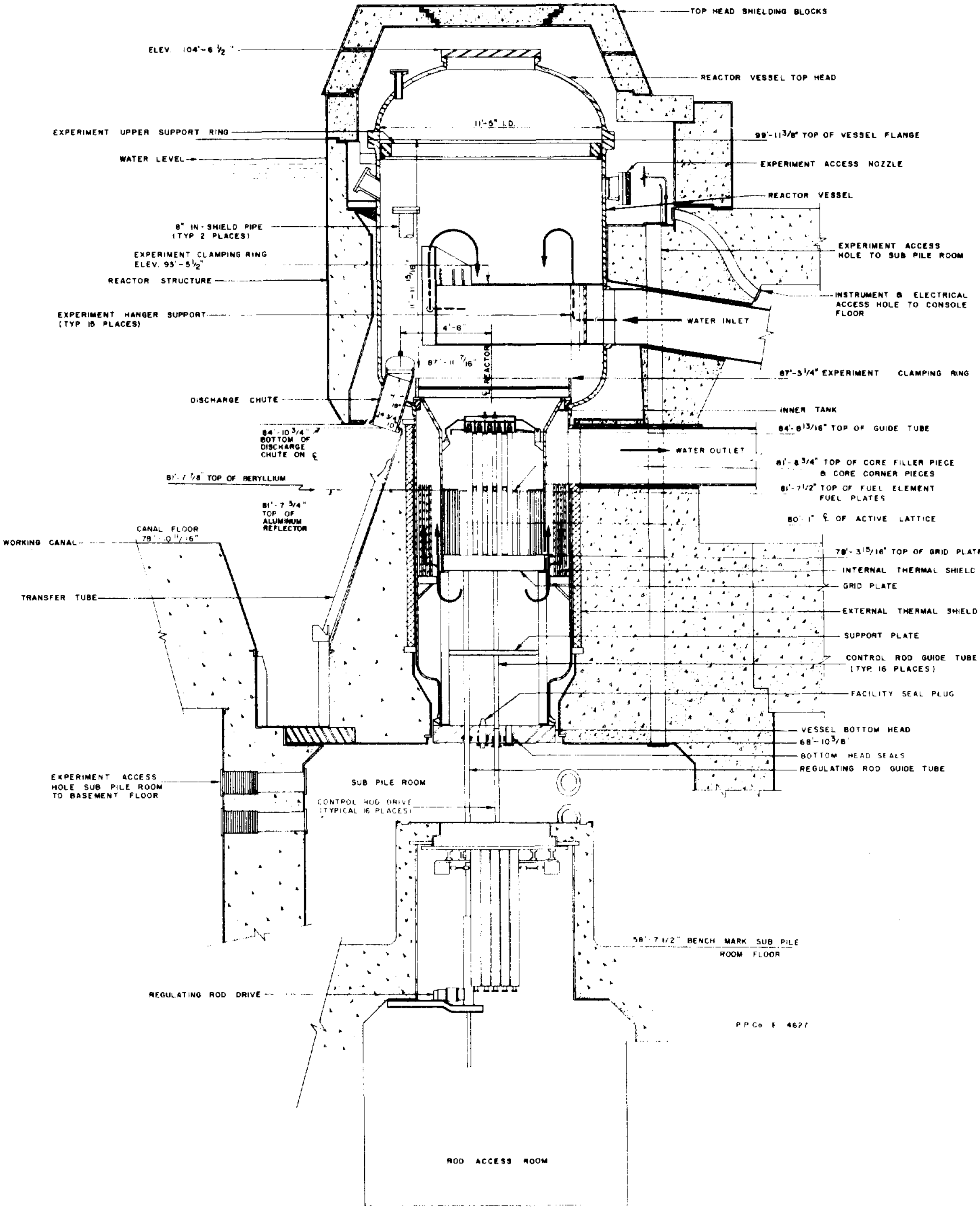

FIGURE 4.8 VERTICAL CROSS SECTION OF ETR STRUCTURE

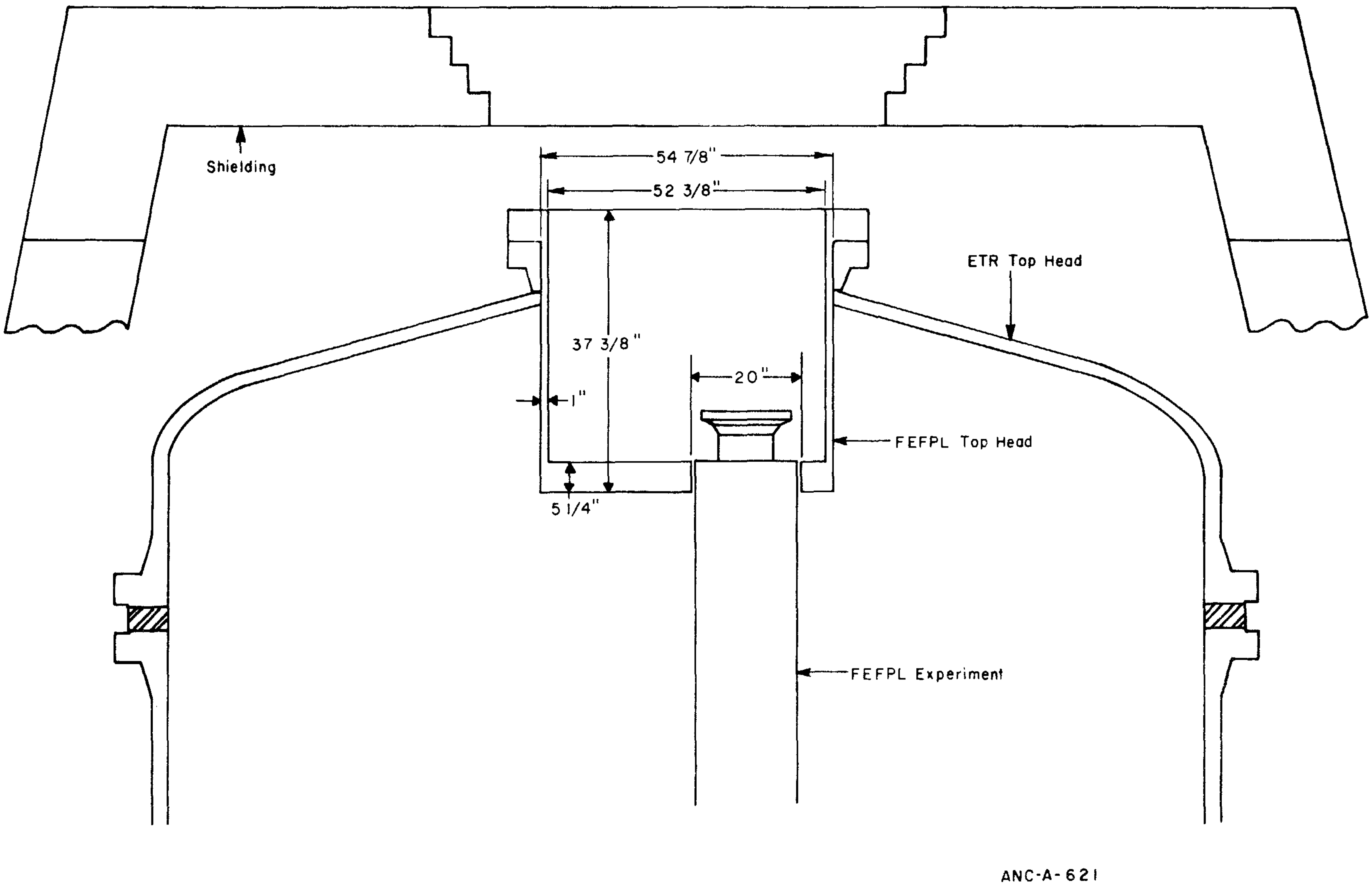

FIGURE 4.9 FEFPL TOP FLANGE CLOSURE

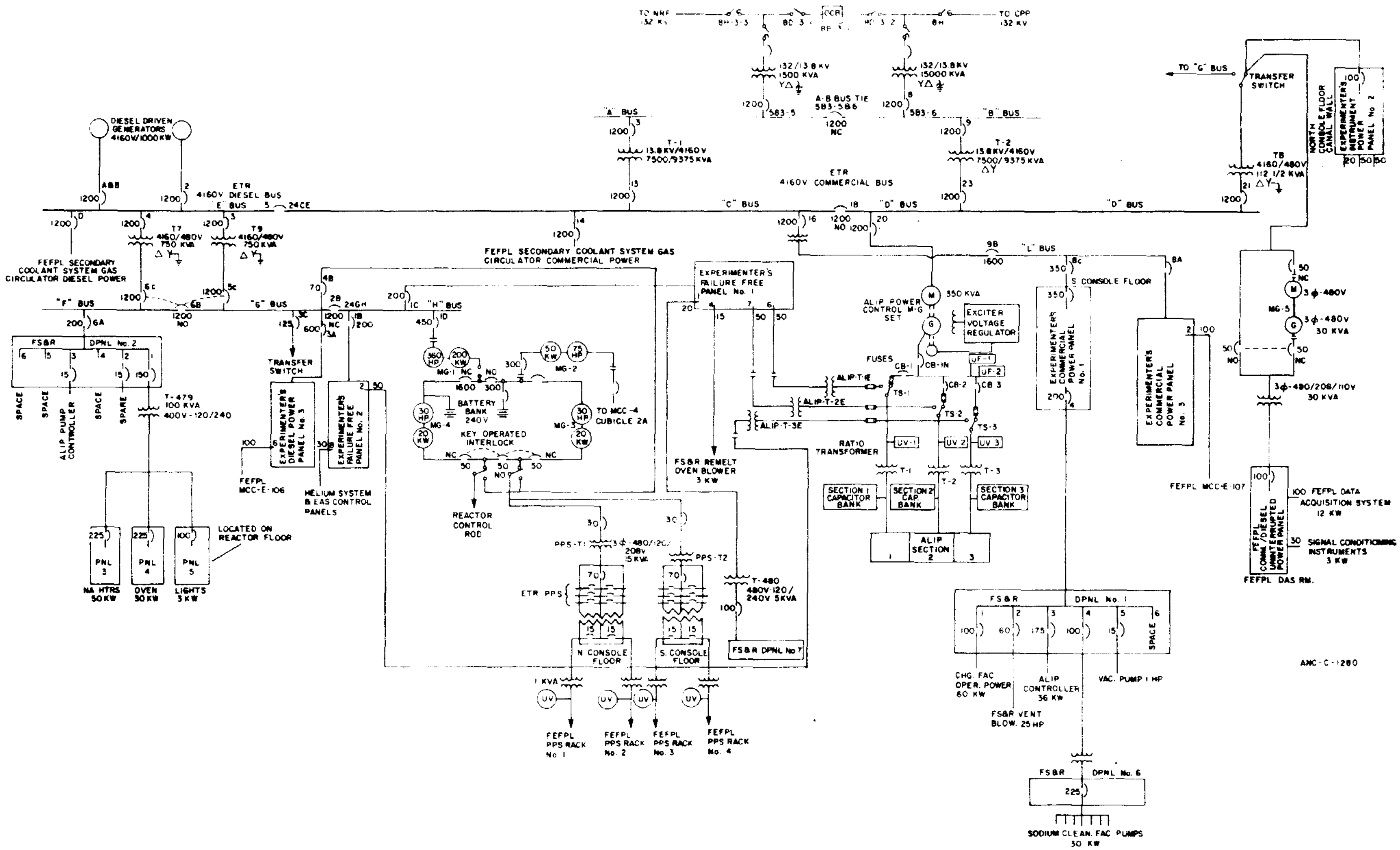

FIG. 4.10 - FEFPL/ETR Power Distribution System

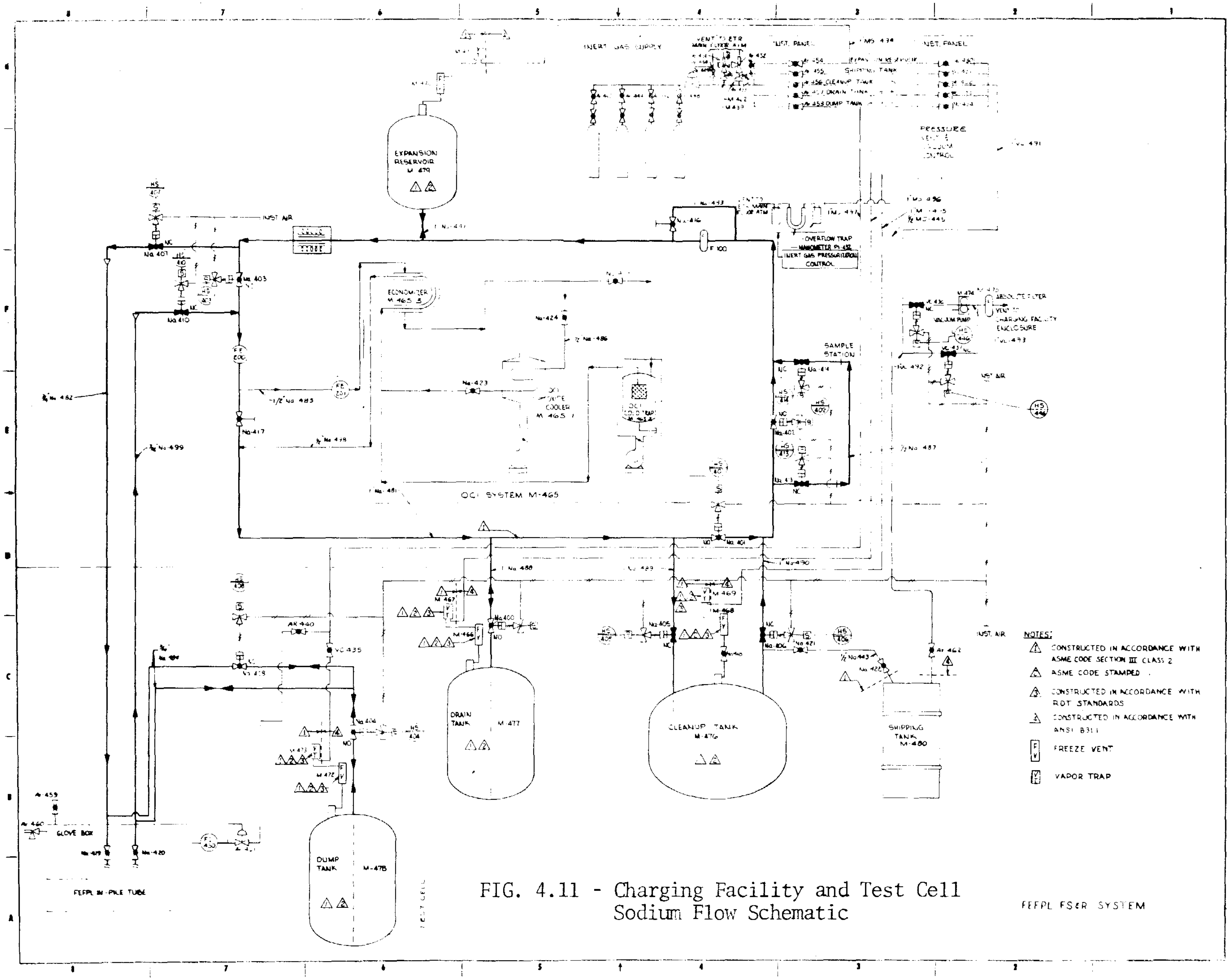

FIG. 4.11 - Charging Facility and Test Cell Sodium Flow Schematic

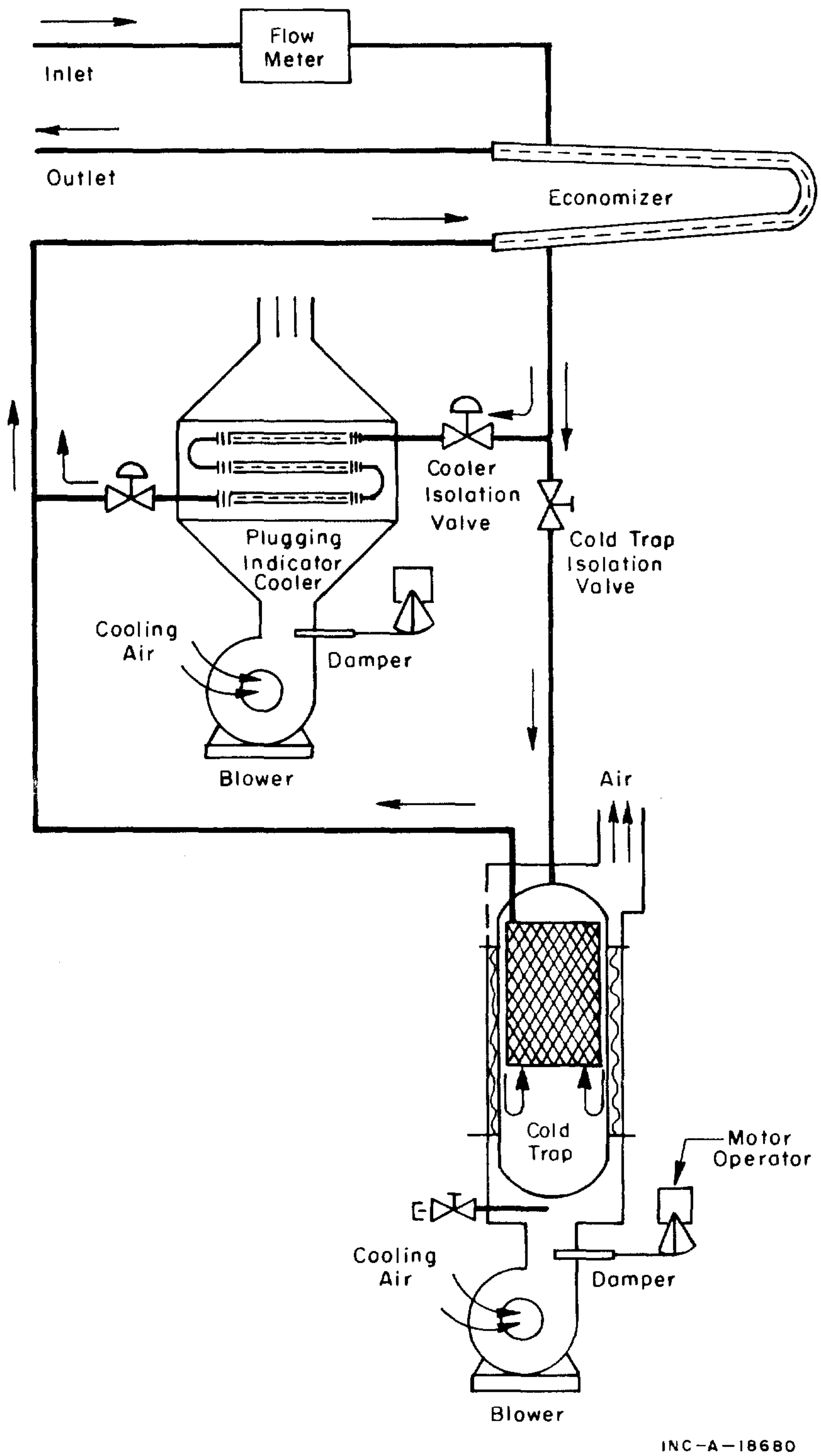

FIGURE 4.12 OXIDE CONTROL AND PLUGGING INDICATOR SYSTEM FLOW DIAGRAM

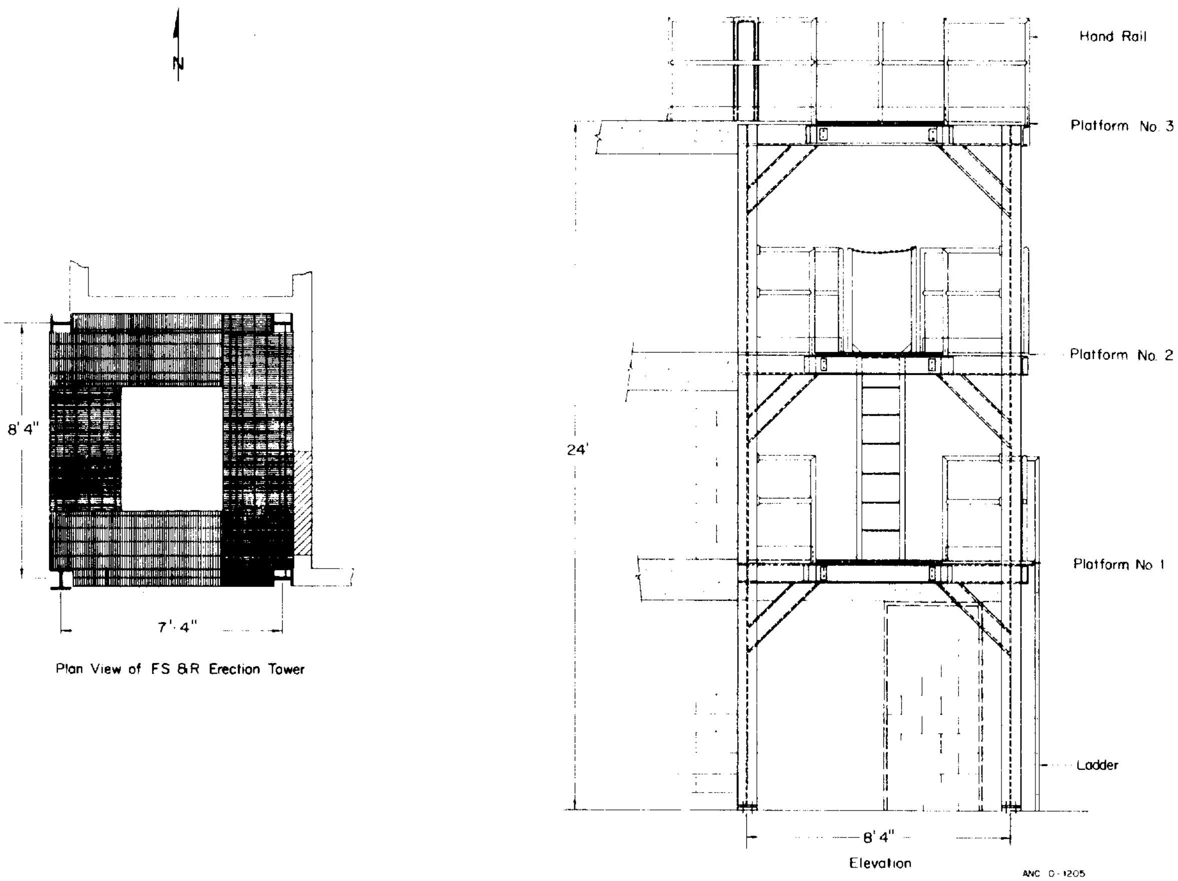

FIGURE 4.13 ERECTION TOWER

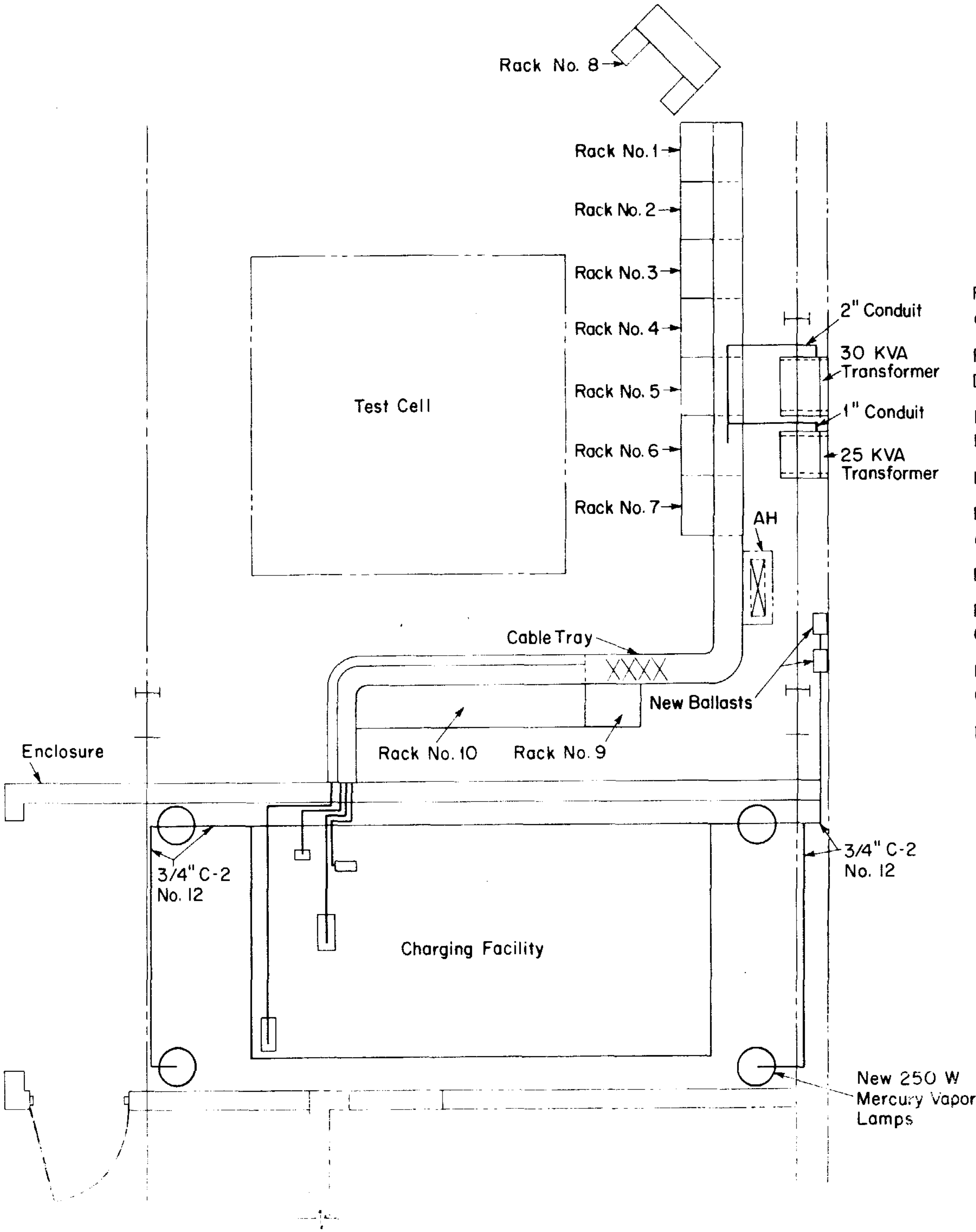

Racks 1 and 2 - Closed Circuit Television System (CCTV), and Fire Detection System

Rack 3 - Heater Control System for Transfer Lines and Dump Tank

Rack 4 - Dump Tank and Transfer Line Temperature Recorder and Dump Tank Level Channel

Rack 5 - Spare

Rack 6 - Annunciator System, Temperature Recorders, and Pressure Recorders

Rack 7 - Electrical Power Panel

Rack 8 - Charging Facility Piping and Tank Heater Control System

Rack 9 - Pressure, Vent and Vacuum (PVandV) Control Panel

Rack 10 - Charging Facility Control Panel

ANC-C-2069

FIG. 4.14 - Instrumentation Racks - Plan and Elevation

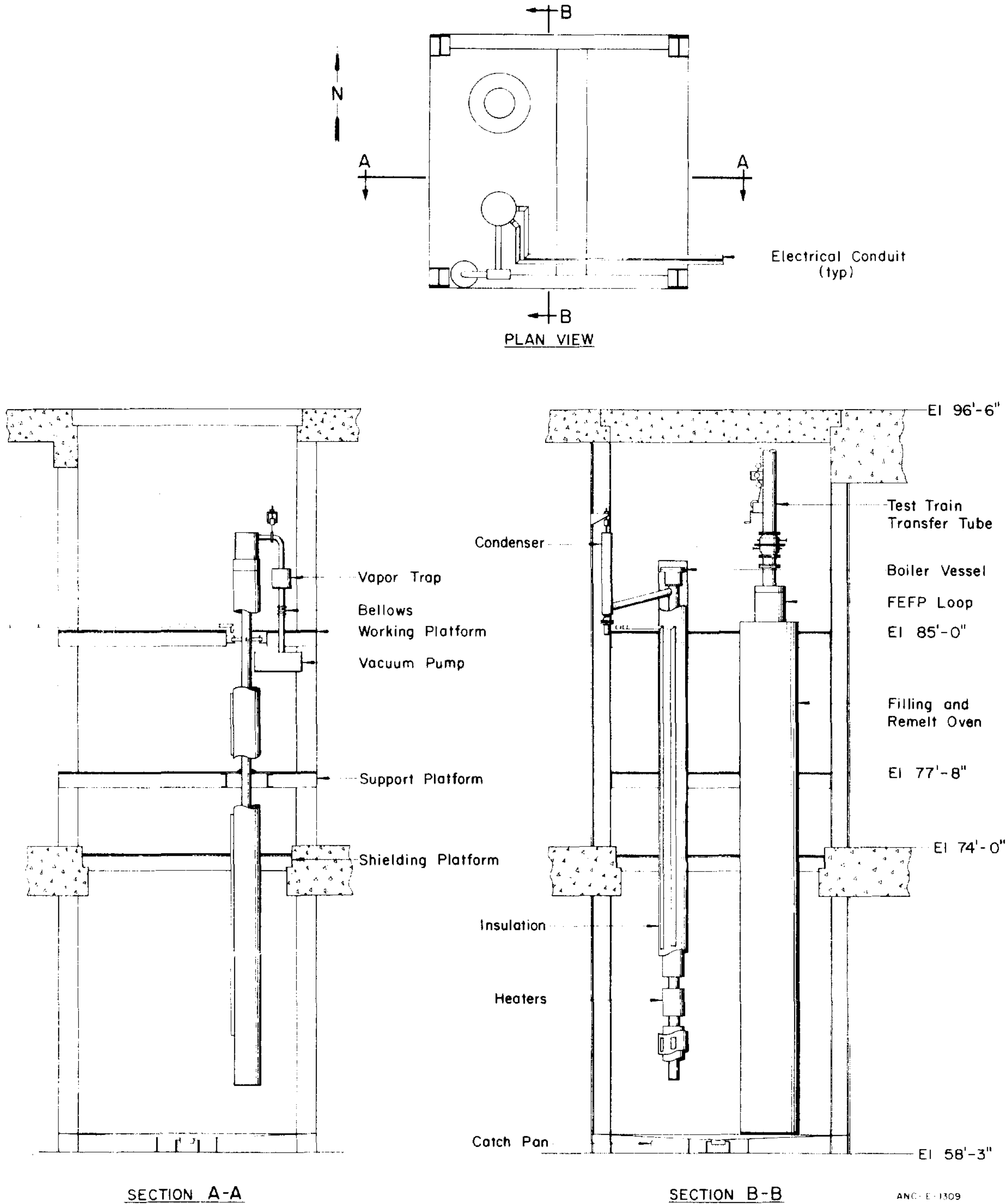

FIGURE 4.15 TEST CELL, STORAGE OVEN AND TEST TRAIN CLEANING SYSTEM

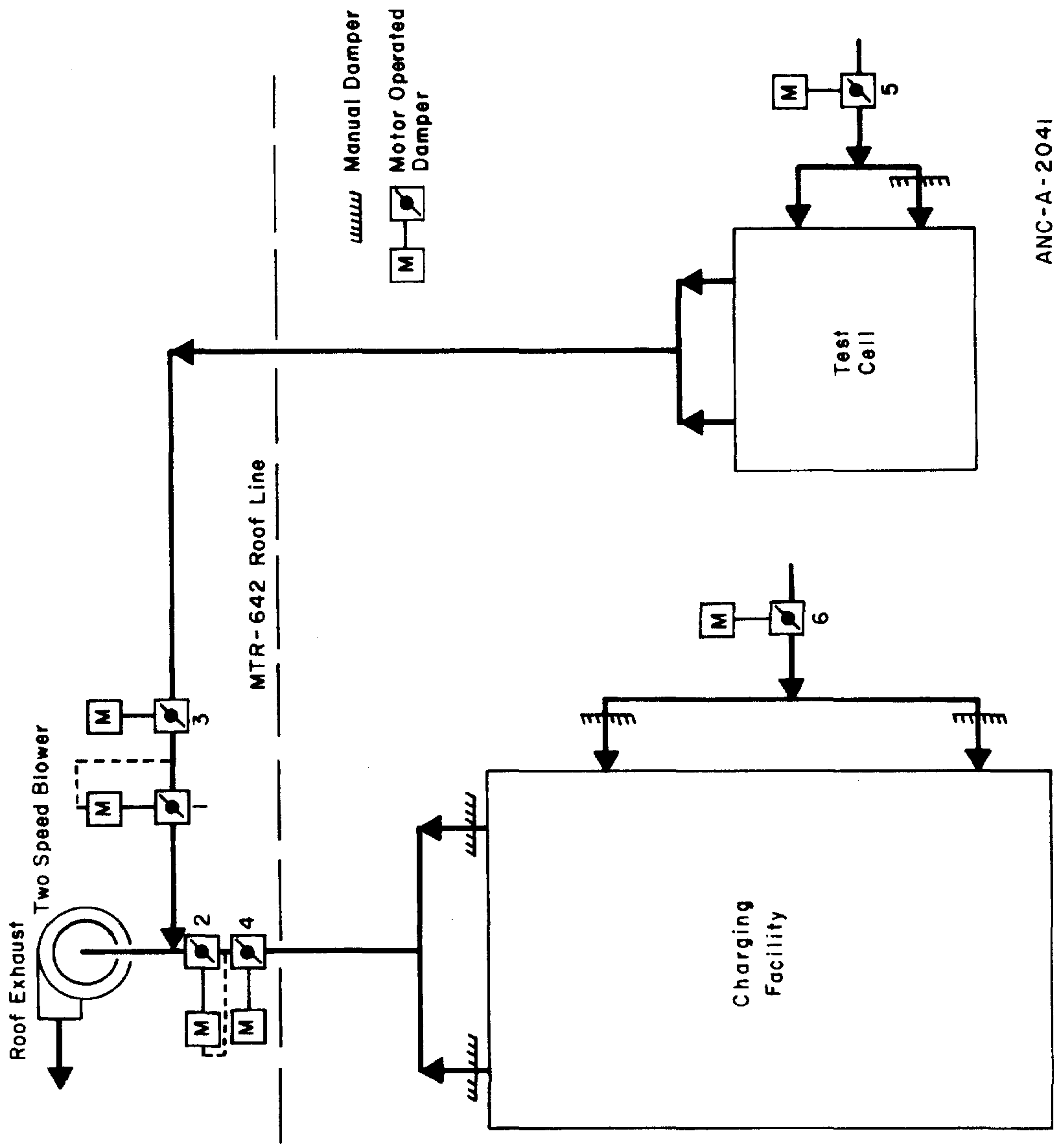

FIG. 4.16 - Charging Facility and Test Cell
Ventilation System Flow Diagram

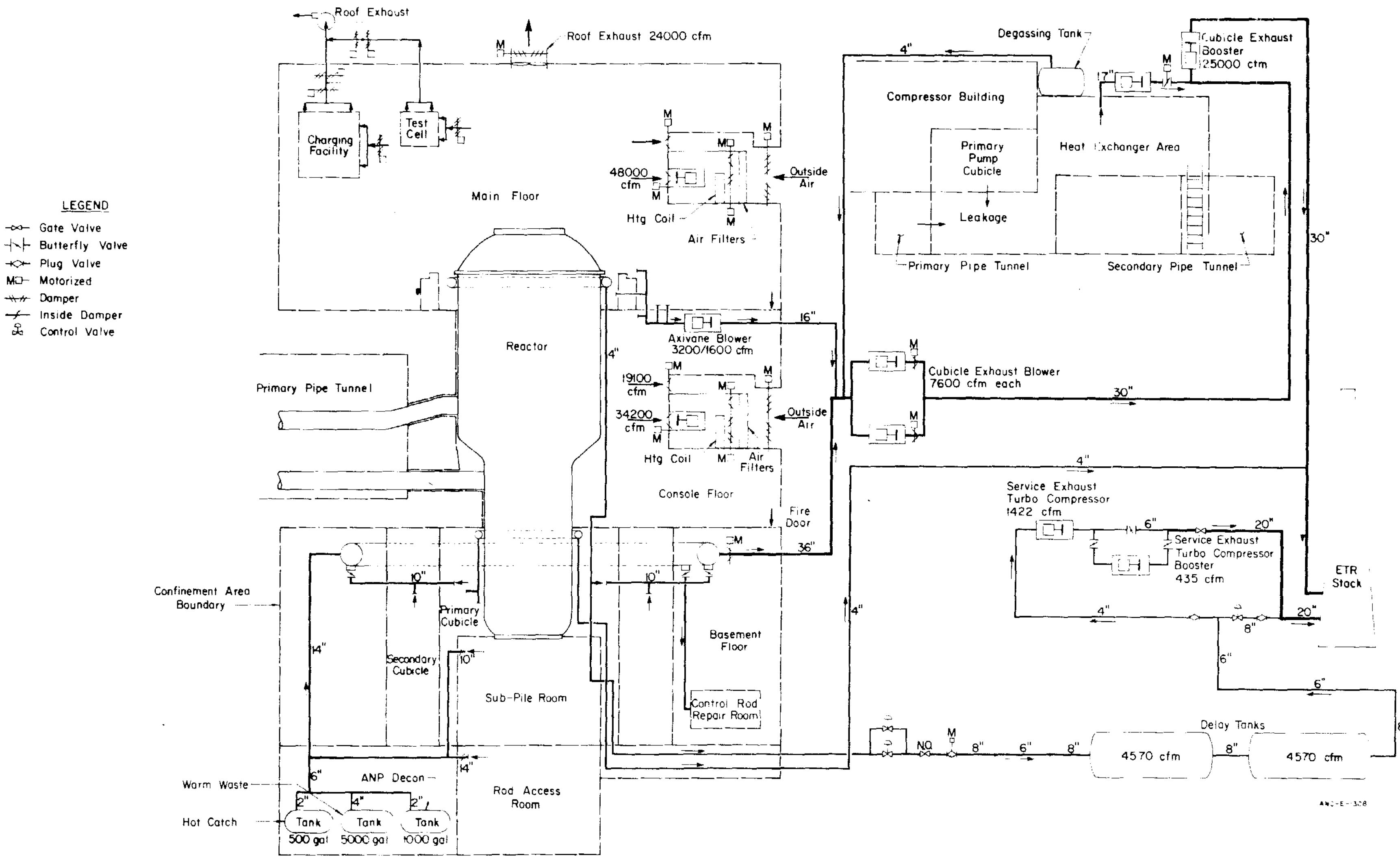

FIGURE 4.17 ETR BUILDING-642 VENTILATION SCHEMATIC

References

1. FDR-03, FEFPL Filling, Storage and Remelt System Design Requirements, Rev. No. 02, June 19, 1973.

2. R-1000-1001-SA, System Design Description of the Fuel Element Failure Propagation In-pile Loop System, Revision 2, October 1973.

3. Specification ANC-70014, Design Specification for the FEFPL Filling, Storage, and Remelt Sodium System, May 31, 1973.

4. Specification ANC-70015, Design Specification for the Filling, Storage, and Remelt System, Pressure, Vent, and Vacuum System, May 31, 1973.

5. Specification, ANC-70013, Design Specification and Ordering Data for the FEFPL Filling, Storage, and Remelt System Tanks, December 12, 1972.

6. Specification ANC-70016, Ordering Data for FS&R System Freeze Vent, May 14, 1973.

7. Specification ANC-70017, Ordering Data for FS&R System Vapor Trap, May 14, 1973.

8. ANC Drawing 403721, "ETR FEFPL FS&R Charging Facility Piping and Instrumentation Diagram.

9. EDF-895, "Charging Facility -- System Protective Parameter Review".

10. EDF-1113, "Design Basis and Failure Mode Analysis".

11. ANC Drawing 404944, "FS&R Electrical Distribution Power Diagram".

12. FEFPL Filling, Storage, and Remelt Facility Operating and Maintenance Manual, Section 3.15.

13. EDF-1043, Placement, Quantity, and Identification of FS&R Fire-Fighting Equipment.

CHAPTER 5.0

TABLE OF CONTENTS

LIST OF TABLES

LIST OF FIGURES

5.0 Loop System Description

(See SDD, R1000-1001-SA for system and component functions, design requirements and additional description.)[1] In Chapter 3.0, Safety Philosophy, it is pointed out that the FEFP Loop is designed to thoroughly defined system and component functions and performance requirements, as detailed in the SDD, incorporating and emphasizing reliability and safety. The disciplined approach to design of the system is itself a fundamental part of the approach to assuring FEFPL safety, particularly to the first level of safety as discussed in Section 3.3.1. In the detailed description that follows, selected design details are related to the three levels of safety discussed in Chapter 3.0, by way of examples.

5.1 FEFP Loop System

The FEFP Loop System consists of three major facilities or subsystems:

Experiment Facility - the in-pile loop, test train, and support systems located at the ETR, required to perform the safety tests specified in ANL/RAS 71-33.[2]

Loop Handling Machine and Transporter - the system required to insert the in-pile loop into the ETR, remove the loop, transport the loop to the Hot Fuel Examination Facility (HFEF), and insert it into the hot cell.

Postirradiation Examination Facility - the remotely operated system required to disassemble the in-pile loop; examine loop components, test train, and fuel elements; and assemble test trains containing pre-irradiated fuel elements.

5.2 Experiment Facility

The Experiment Facility includes the in-pile loop containing the instrumented test train, the data-acquisition system, the control system, the FEFP plant protection system, the closed-loop secondary-coolant (helium) system, the structural components for mechanical support, and the loop filling, storage, and remelt (FS&R) system. With these integrated systems, the Experiment Facility will be capable of performing all the safety tests specified in the Experiment Plan and of meeting the stated principle objectives.

5.2.1 Test Train

The functions of the test train and its design requirements are specified in the SDD[1] Section 2.2.1.

Test train instrument requirements are shown, for example, for experiment P1 in Table 5.1. A test requirements document will be issued for each experiment to provide similar details.

The test train consists of a fuel-element bundle, instrument sensors, failure-mechanism device,* e.g., planar blockage plate, gas release mechanism, etc., (as required), cable seal plug, and structural members which support the fuel bundle, sensors and special devices. Instrument sensors are provided to measure sodium flow, pressure and temperature. The test train is inserted in the FEFP Loop in the FS&R facility. A preirradiated test train can be removed from the loop, prior to a test in ETR, at the FS&R facility or the HFEF/N; whereas an irradiated loop can be handled only at FHEF/N.

The test train is 26 ft long and is surrounded by a 3-1/16-in.-ID flow divider. The first test train, shown in Fig. 5.1, contains 19 FTR fuel elements[3] and weighs approximately 400 lbs. The elements are spaced with 0.056-in.-dia, spiral-wrapped thermocouple cable. Sixteen of the 19 elements contain eddy-current-type pressure transducers to measure pressure in the fission-gas plenum. The fuel bundle is enclosed in an insulated hex can. Sodium flowing at the rate of 4.8 lb/sec enters the fuel bundle through a permanent-magnet-type flow-through flow sensor, is heated from 792 to 1215°F as it passes through the active section of the fuel bundle, and exits through an eddy-current probe type flow sensor. The remainder of the flow (bypass) mixes with the test section flow and then passes around two eddy-current flow sensors mounted in the upper tube. Forty-four thermocouples and 31 pressure sensors are located throughout the test train. The number of specific instruments may be varied, but the total number of instrument cables is usually 81 with 235 instrument leads.

The meltdown cup, shown in Fig. 5.2, is located at the bottom of the test train. It consists of a central 1-1/2 in. dia tungsten post inside a cylindrical tungsten cup - 2-7/8 in. ID, 9 in. long, with a 1/16-in. wall thickness. The tungsten cup is supported by an Inconel cup, which has a 5/32-in. wall thickness. The meltdown cup is sized to contain 3.5 kg of molten fuel (all the fuel in 19 elements, each 36 in. long) plus 3 kg of molten steel. If the fuel and steel collect in the cup as small solid pieces,

---

*The failure mechanism device provides the experimenter with a means of initiating, controlling, or terminating a particular malfunction, or of establishing circumstances leading to such a malfunction.

TABLE 5.1

P-1 Test Train Instrumentation

Type and Designation Number	Quantity	Description and Location	Wires	Cables	Cable Diameter
Flowsensors					
FE-1-1	1	Permanent Magnet Flowthrough at Fuel Bundle Inlet	2	1	0.125
FE-2-1	1	Eddy Current Probe Type at Fuel Bundle Outlet	4	2	0.125
FE-3-1,-2	2	Eddy Current Probe Type Above Sodium Mixing Level	8	4	0.125
Thermocouples					
TE-1-1,2,3,4	4	Sodium Temperature at Fuel Bundle Inlet	8	4	0.062
TE-2-1,2,3	3	Sodium Temperature at Fuel Bundle Outlet	6	3	0.062
TE-3-1,2,3,4	4	Spacer Wire Thermocouples in Fuel Bundle (Single Junction)	8	4	0.056
TE-4-1,2...9	9	Spacer Wire Thermocouples in Fuel Bundle (half size)	18	9	0.028
TE-5-1,2...6	6	Spacer Wire Thermocouples in Fuel Bundle (twin junction)	12	3	0.056
TE-6-1,2...12	12	Inner hex wall	24	4	0.062/0.160*
TE-7-1,2	2	Bypass Flow Temperature	4	2	0.062
TE-8-1,2,3	3	Mixed Mean Sodium Temperature	6	3	0.062
TE-9-1	1	Test Train Heater Temperature	2	1	0.062
Pressure Sensors					
PE-1-1,2	2	Type II - Fast Response at Fuel Bundle Inlet (Range 0-2000 psi)	8	4	0.062
PE-2-1,2	2	Type I - Slow Response at Fuel Bundle Inlet (Range 0-200 psia)	6	2	0.062
PE-3-1,2	2	Type II - Fast Response at Fuel Bundle Outlet (Ranges 0-2000, 0-10,000 psi)	8	4	0.062
PE-4-1,2	2	Type I - Slow Response at Fuel Bundle Outlet (Range 0-200 psia)	6	2	0.062
PE-5-1,2...16	16	Type III - Fuel Pin Plenum (Range 0-1000 psi)	48	16	0.062
PE-6-1,2	2	Type II - Fast Response Mixed Flow (Ranges 0-2000, 0-10,000 psi)	8	4	0.062
PE-7-1,2,3,4	4	Type I - Loop Plenum Gas Pressure (Range 0-200 psia)	12	4	0.062
Level Sensors					
LE-1-1	1	Relative Sodium Level in Loop Plenum	4	2	0.125
Acoustic Detectors					
PE-9-1,2	2	Acoustic Detector in Loop Sodium Plenum	2	2	0.125
Heater					
HE-1-1	1	Test Train Heater for Postirradiation Meltout (1500 w, approximately 15 ft)	2	1	0.125
		Total:	206	81	

*Assembly with three 0.062 TCs inside 0.160 sheath.

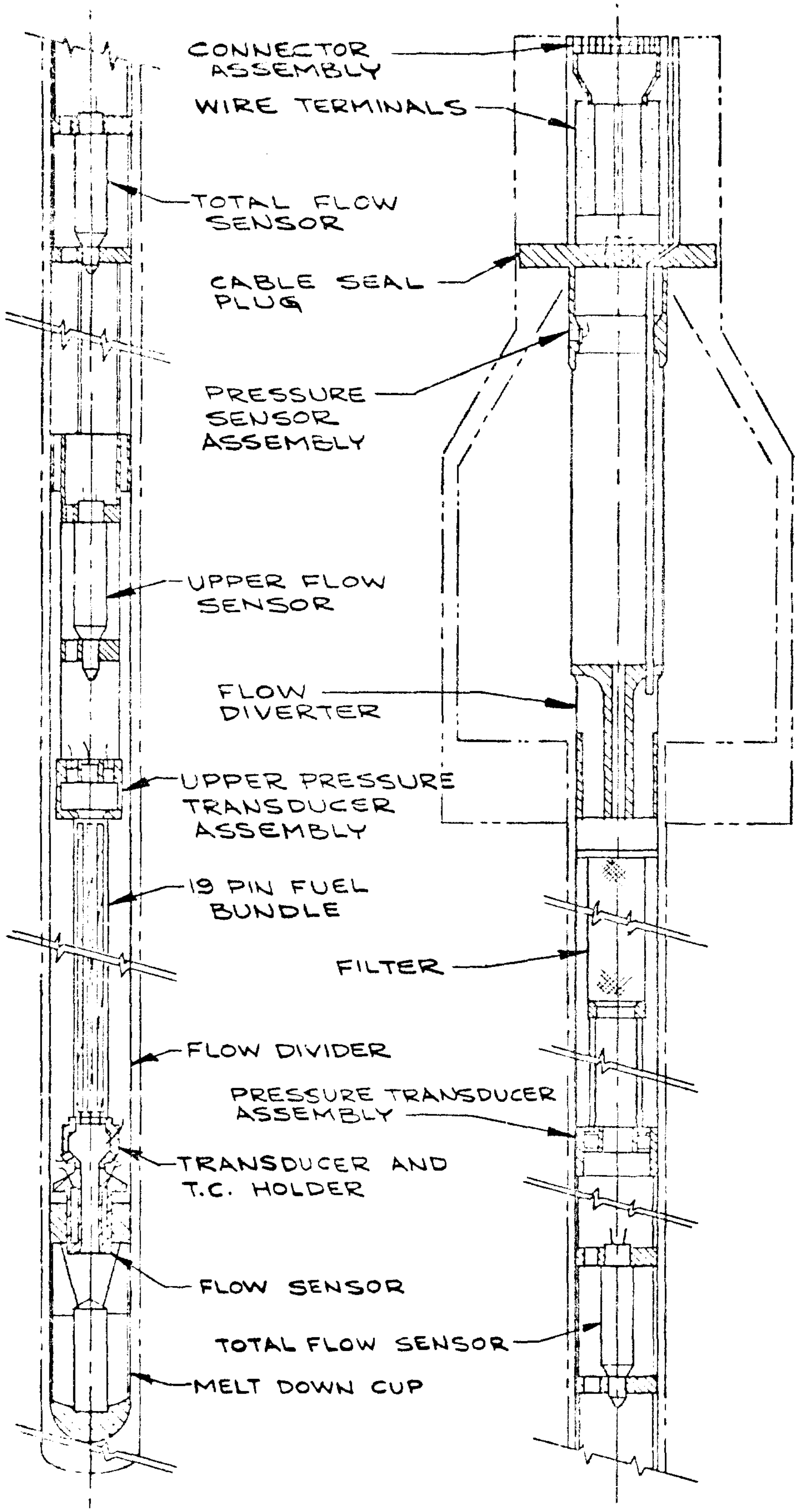

FIG. 5.1 - FEFPL Test Train, Experiment P-1

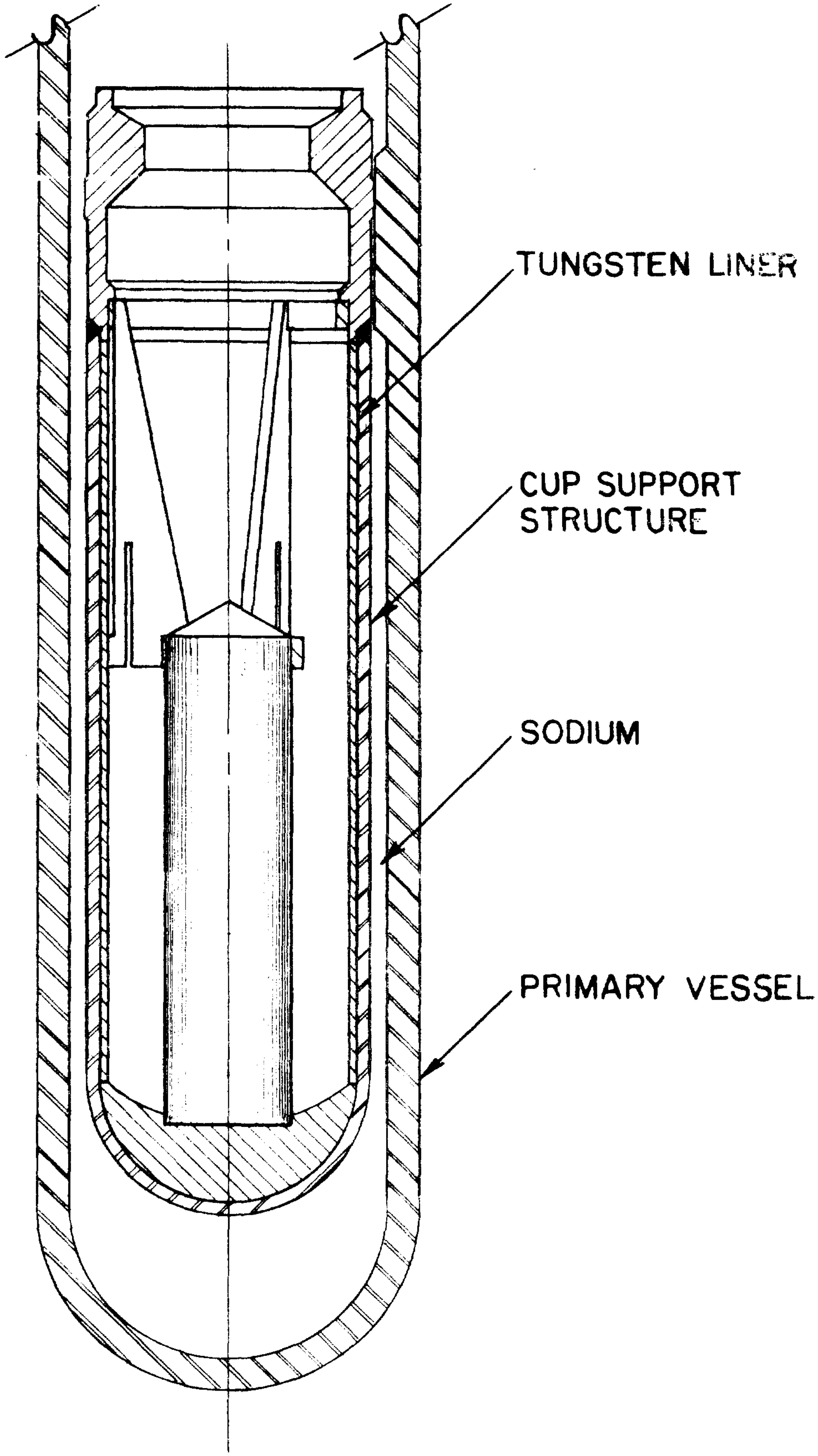

FIG. 5.2 - Meltdown Cup

the capacity is about 2 kg of such solid debris. The meltdown cup is related to all three levels of safety. To the first level, in terms of containing the small amounts, if any, of molten fuel anticipated with the planned experiments; to the second level, in terms of containing the consequences of postulated accidents; and to the third level, in terms of containing molten debris from hypothetical events.

5.2.2 In-pile Loop

The functions of the in-pile loop and its design requirements are specified in SDD,[1] Section 2.2.2.1.

The in-pile loop is a packaged assembly which will receive a test train, be filled with sodium, sealed, and inserted in the L-8 opening in the ETR core to perform a specified experiment. The loop is of a reentrant design and has two concentric vessels for isolation of the sodium primary loop coolant from water reactor primary coolant (second level of safety).

The primary vessel, shown in Fig. 1.1, fabricated of Type 316 stainless steel, contains a tube-and-shell sodium-to-helium heat exchanger (sodium on the tube side), an Annular Linear Induction Electro-magnetic Pump (ALIP), a sealed top closure with instrument-lead penetrations, and a cylindrical vessel cavity to accept a test train and flow divider. The primary vessel is essentially a closed sodium-circulation loop.

The secondary vessel, fabricated of Type 316 stainless steel, is flanged at the top to mate with the ETR top closure and completely surrounds the primary vessel. The minimum gap between the vessels is 3/16-in. and is filled with helium gas.

The portion of the secondary vessel which is within the ETR core has a cadmium filter surrounding its external surface to harden the neutron spectrum for the planned experiments. Lateral and vibration support of the primary vessel is provided by the secondary vessel.

The in-pile loop, less test train, weighs approximately 6600 lb and has an overall length of 27 ft. Dimensions of various sections of the loop are shown on the dimensional control drawing, Fig. 5.3.

5.2.2.1 Component Description

The thickness of the vessels has been selected to approach maximum strength at operating conditions, that is to say, vessels with thinner walls

FIG. 5.3 - FEFP Loop Dimensional Control Drawing

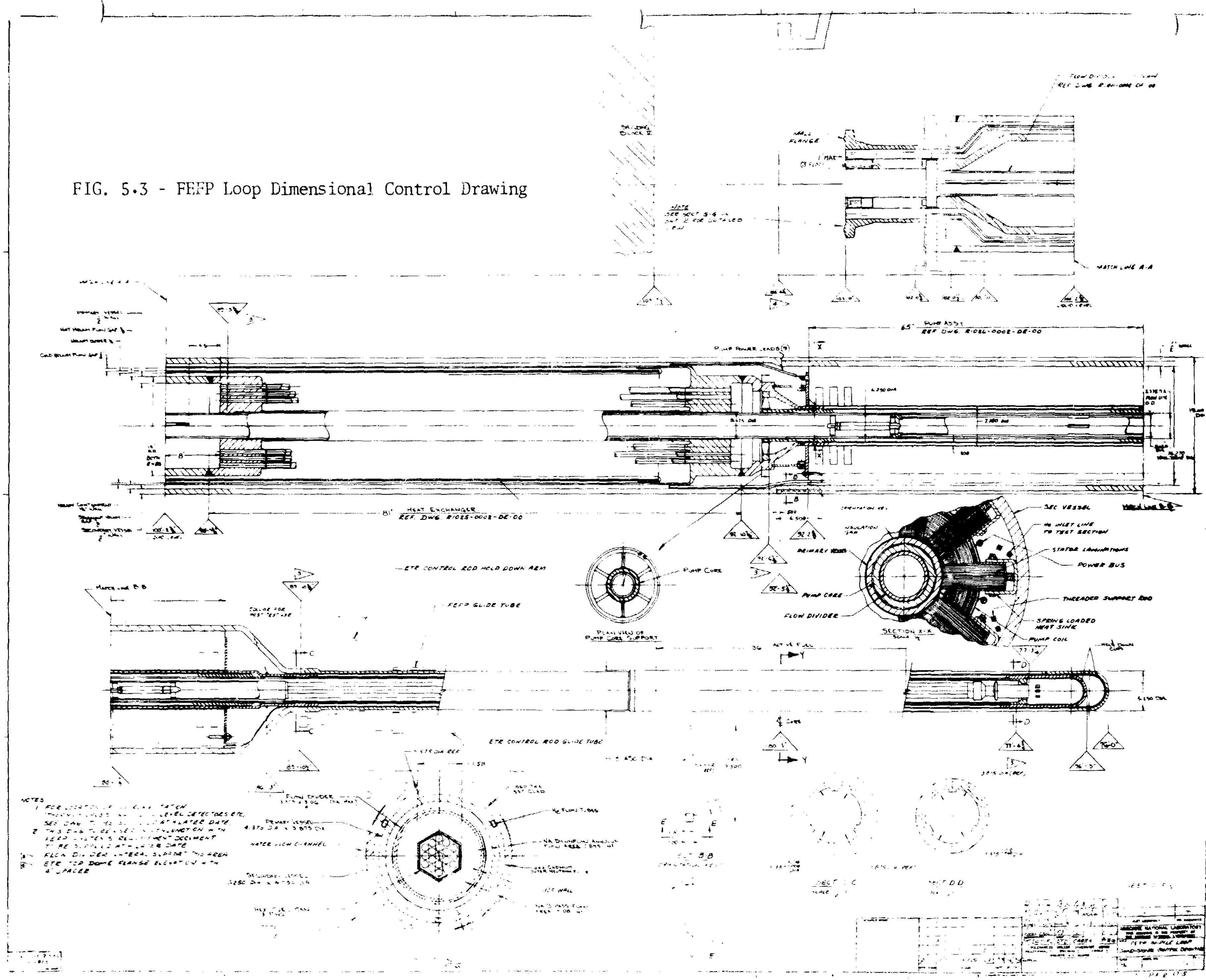

are weaker because of less structural cross-sectional area resisting load and thicker walls are weaker because of increased gamma heating and longer conduction heat paths resulting in high temperatures. The gamma field in the ETR (<15 W/g) causes the primary wall temperatures to exceed the sodium temperatures due to the gamma heat input and the low heat loss from the primary to the secondary vessel. If the vessels were thicker, the wall temperatures would be higher and material strength lower. An approach to optimization has been made.

The heat exchanger is shown in Fig. 5.4. It is located between the pump and top closure, and is a tube-and-shell design.

Sodium at temperatures up to 1050°F flows upward through the 3.06-in.-inner-diameter central tube to the loop top plenum. There the sodium flow direction is reversed and the hot sodium enters the heat-exchanger upper plenum. The flow is distributed at the upper tube sheet to a parallel array of 108 tubes. The tubes are of 0.75-in. inner-diameter with an 0.049-in. wall. The tubes in the lower 18 in. of the tube bundle are spiralled to provide for differential expansion between the heavy center tube and the smaller heat-transfer tubes. The center tube is insulated from the hot sodium flow to reduce the differential expansion. The sodium leaves the tubes and enters the heat-exchanger lower plenum before passing downward to the pump.

Secondary helium coolant at 150°F, flowing at rates up to 5750 lb/hr and pressures up to 260 psia, enters the annular space between the helium flow divider and the helium-containment jacket near the top of the loop. The jacket is sized to contain the high-pressure helium and provide double containment for the gas. The cold helium passes inside the jacket and down the heat exchanger to the region of the lower plenum where it reverses direction and flows upward on the shell side of the heat exchanger, countercurrent to the sodium flow direction. The helium is heated to temperatures up to 1050°F as it passes through the heat exchanger. There are eight baffle zones to direct the helium flow across the tubes. The helium leaves the heat exchanger through the annulus between the upper sodium plenum and the helium flow divider. A double-walled helium-flow separator is required to minimize regenerative heating of the inlet helium by the hot effluent helium.

The concentric, counterflow loop requires the sodium pump to be of the Annular Linear Induction (ALIP) type, using a counterflow geometry.

The flow rates required by the initial experiments in the loop set the design capacity of the sodium pump at an output of 150 gpm of 800°F sodium at a pressure of 150 psi.

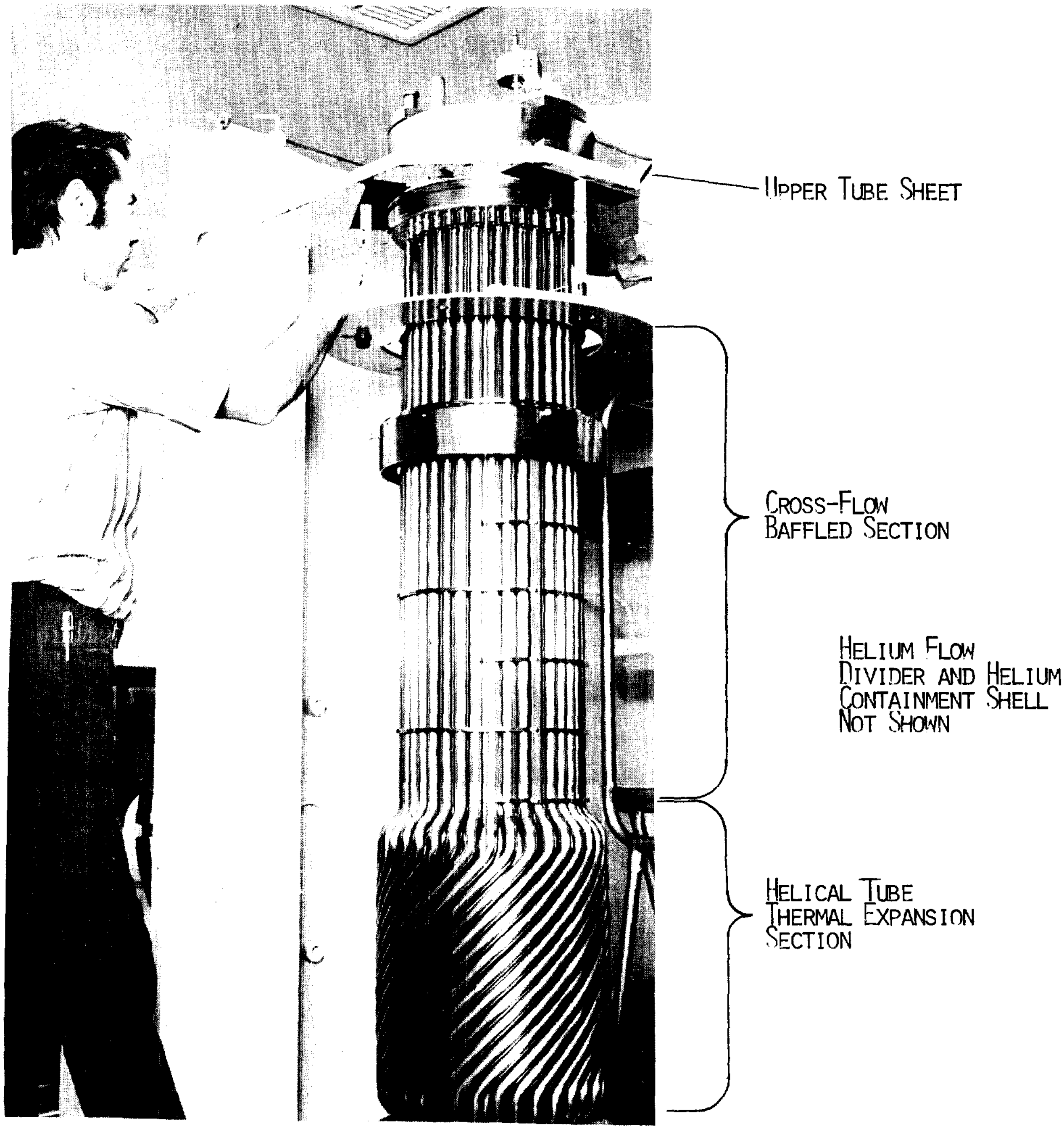

FIG. 5.4
HEAT FXCHANGER
DURING ASSEMBLY

The sodium-pump stator is located in the annulus between the primary and secondary vessels, in close thermal contact with the inner wall of the secondary vessel, and thermally insulated from the outer wall of the primary vessel. The ALIP is shown in the layout drawing of Fig. 5.5. The pump core is outside the flow divider and, with the inner wall of the primary vessel, defines the annulus of the induction pump.

The pumped flow of sodium is in the downward direction in the core/primary pump annulus, with the return flow of sodium upward from the test fuel section through the hollow pump core within the flow divider to the loop plenum. The sodium passes downward through the heat exchanger and is cooled before entering the pump annulus.

The thermal rating of the stator and the materials required for its construction are predetermined by the service life requirement (Item 12 in Table 5.2) of "720 hr at 900°F isothermal" loop temperature. For service at this temperature, the pump stator is constructed to a full Class C rating, which requires the use throughout of inorganic or ceramic electrical insulation, and limits the stator to temperatures dependent upon the properties of the electrical conductors and magnetic materials, rather than upon the insulation.

The pump core is fabricated from a solid, heavy-wall tube of mild steel (AISI C1026). The annular core is fitted at the upper end with a radially-spoked support ring, from which it is suspended by a recess machined in an interior shoulder provided inside the heat exchanger - power transition section. The pump core must be inserted into the primary vessel prior to welding the transition section to the heat exchanger, and can be removed only by cutting through the primary vessel at that point.

The ALIP for the FEFP Loop is a 9-pole pump, electrically divided into three parallel sections, with the poles series-connected within each section. Sectionalizing the stator is necessary to limit the current in the external supply leads to a value which can be carried by the size of cables that will fit in the restricted space between the heat exchanger and the secondary vessel, above the sodium pump. The three equivalent sections also provide fail-safe redundancy, in the event of failure of a portion of the pump stator (a second level of safety).

When installed in the ETR, the top end of the FEFP Loop (see Fig. 5.6) will extend above the ETR top dome so that none of the loop access penetrations need pass through reactor water, but rather are directly accessible. The loop's maximum diameter of 19 in. extends from the top end of the secondary down to a point below the heat exchanger. There is a sealing surface at

FIG. 5.5 - MSAR Layout for ALIP

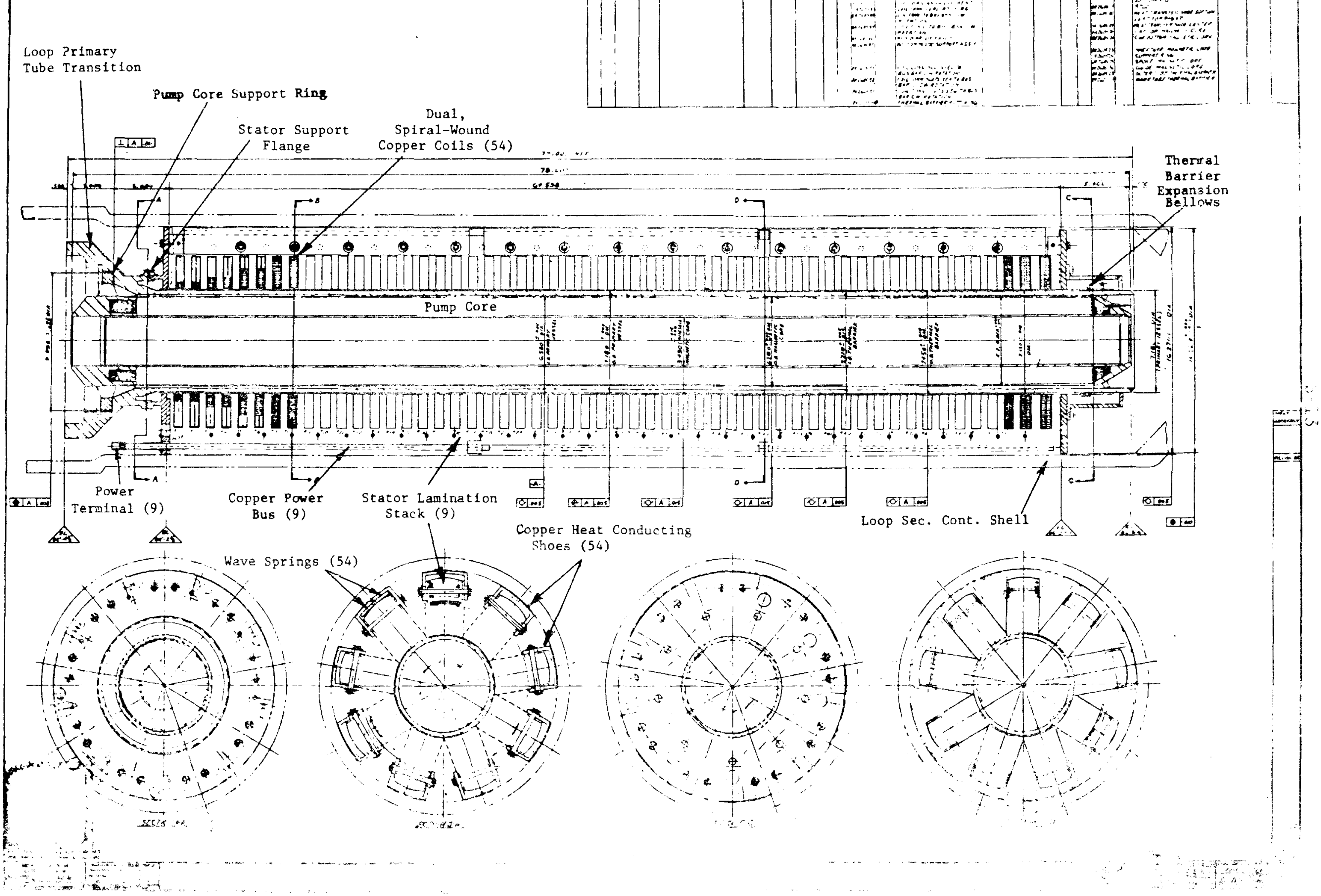

TABLE 5.2

Requirements for High-temperature, Electromagnetic, Counterflow Annular Linear Induction Pump Geometry and Performance

Item No.	Parameter	Data
1	Physical shape	Cylindrical
2	Stator length, maximum (in.)	65
3	Outer diameter, secondary vessel (in.)	18
4	Wall thickness, secondary vessel (in.)	0.500
5	Inner diameter of core (in.)	3.500
6	Design flowrate (gpm)	150
7	Pressure delivered at design flowrate (psid)	150
8	Temperature of sodium at pump inlet (°F)	800
9	Duct design pressure (primary vessel) (psig)	2000
10	Duct design temperature (primary vessel) (°F)	900
11	Pump stator cooling	Radial conduction and convection
12	Service life	720 hr at 900°F isothermal and 10% full design flow; 4500 hr at 450°F isothermal and 10% full design flow; 1700 hr at full design power and 800°F Na inlet
13	Type of service	Continuous
14	Minimum acceptable efficiency, at design flow and pressure (%)	10

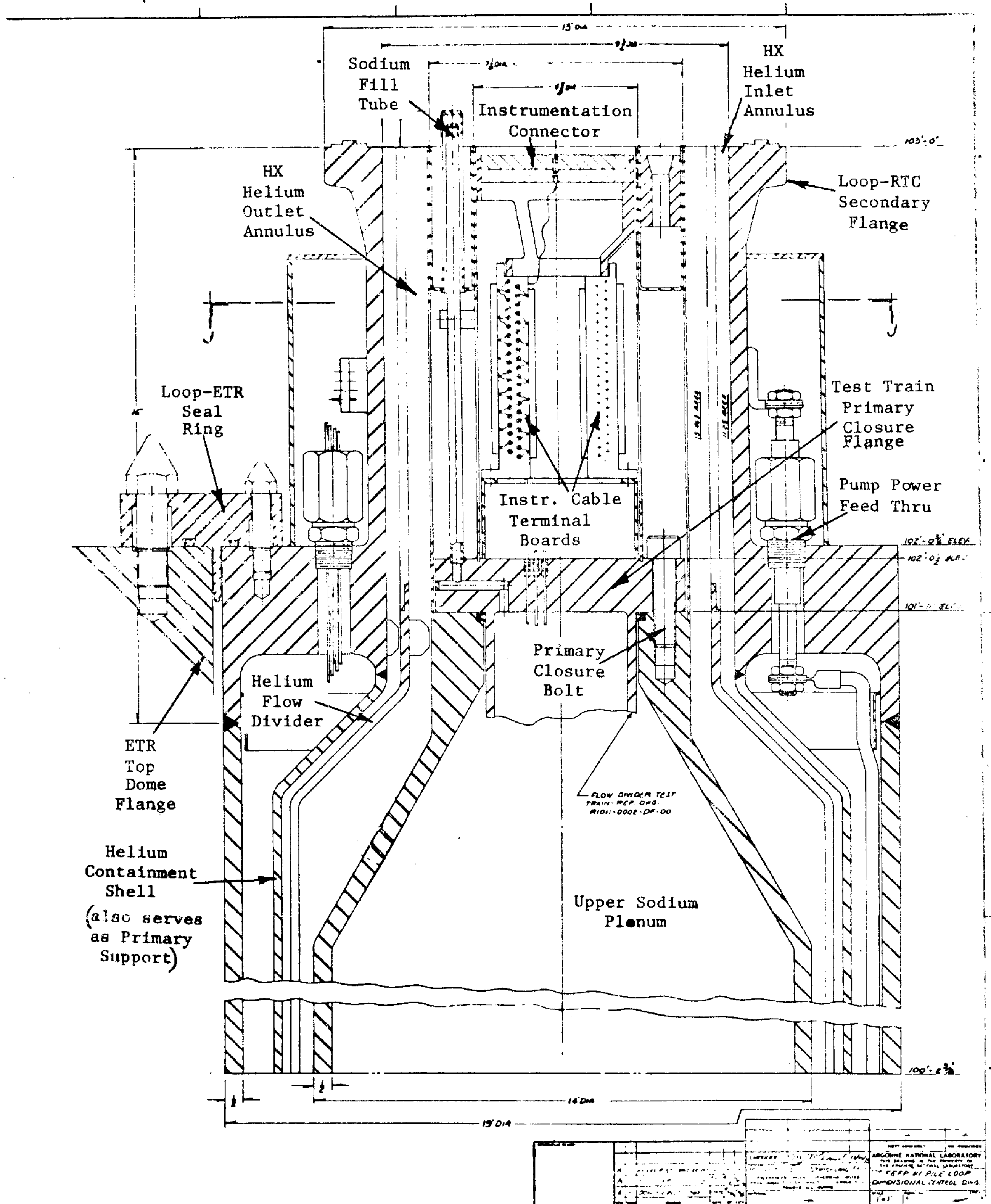

FIG. 5.6 - Dimensional Control Drawing for Top Closure

the top of this cylinder on which a double-flanged seal ring is attached, providing a means for sealing the gap between the ETR top and the loop. A 10-in., Schedule 80 pipe nozzle penetrates the center region of the top of the secondary vessel. Helium is supplied to the heat exchanger and is removed via two concentric flow annuli inside this nozzle. The primary-vessel closure consists of a 7-in.-outer diameter, bolted-flange cap through which the test-train instrument cables pass. Above this flange, a light-gauge metal sleeve encloses a space where the instrument cables are terminated, and heavier, flexible wires are connected to a multipin connector at the top of the sleeve. The connector face is flush with the nozzle flange. Two 3/8-in.-outer diameter tubes also penetrate the bolted flange as well as a smaller pressurizing tube of 3/16-in.-outer diameter and 1/16-in.-inner diameter. The larger tubes provide access to the primary vessel for sodium filling and circulating operations prior to a test. All three tubes are welded closed at a point slightly above the helium-pipe nozzle flange outside the connector diameter. A flow divider for the helium terminates at a mating surface in the helium annulus below the bolted joint face. The removable helium manifold assembly has a helium-flow-divider sleeve which mates with the loop flow divider.

The bolted primary flange cap is sealed to the top of the primary vessel by means of a metal "K" seal gasket ring. There are eight 5/8-in. high-strength alloy bolts designed for 1100°K service holding the closure cap in place. Two holes in the cap have internal threads so that lifting studs can be installed for handling the test train before and during installation. A ring is welded into place over the bolts as the final seal weld. This ring serves to back up the "K" seal and the tubing closure welds.

The nozzle flange is sealed by means of a double conical metallic seal with a cavity to monitor for leaks.

Quick-disconnect electrical connectors are arranged around the 10-in. pipe nozzle penetrating the top of the secondary vessel, and provides all loop instrumentation and pump power connections. Three tubing quick-disconnects provide means for utilizing an annulus purge gas to monitor the space between the primary and secondary vessels (a first level of safety).

The thermal neutron filter is an integral part of the secondary pressure vessel. It is 48-in. long and extends 6-in. above and below the ETR core. The filter contains a nominal 0.040 in. thickness of cadmium which is sandwiched between the secondary vessel outer wall and a nominal 0.060-in. thick stainless steel protective sheath.

The filter is fabricated by placing a flash coat of nickel (less than 0.0005 in.) on the inside surface of the sheath. The steel sheath is then electro-plated with a nominal 0.040-in. thick cadmium layer. The sheath is then assembled to the secondary vessel with an interference fit and both ends seal welded to the secondary vessel.

The design of the filter is such that the lower end of the sheath is flush with the surface of the secondary vessel, thus precluding any interference during insertion into the ETR core and subsequent filter damage.

5.2.2.2 Nondestructive Examination and Testing

To provide assurance that the FEFP Loop has been designed in accordance with Paragraphs 1.3.2 and 2.2.2.1 of the SDD[1] (which impose the design requirements of Section III of the ASME Boiler and Pressure Vessel Code, as supplemented by RDT Standard E 15-2T and ANC Design Specifications 70008 and 70009), and that the design has not been compromised during fabrication and assembly, the following nondestructive, proof and leak tests will be performed as indicated below. These tests are an important element of the first level of safety.

A. Nondestructive Examinations

1. Liquid Penetrant Examination

The liquid penetrant (LP) examination method is used for detecting the presence of surface discontinuities. This examination will be performed on the root pass and the completed weld after removal of the weld crown on all butt welds of the primary and secondary vessels, including the final closure weld that joins the primary and secondary vessels. The tube-to-tube sheet and the tube-to-tube welds on the heat exchanger are welds in the primary vessel and LP examination will be performed after each one of these welds has been completed.

Liquid penetrant examination will be performed on all accessible welds after proof test has been completed on the primary vessel, secondary vessel, and the heat exchanger.

2. Radiographic Examination

Radiographic examination by use of x-rays or gamma rays is used to detect discontinuities in material. Radiographic examination will be performed, after removal of the weld crown on the completed weld, on all the welds in the primary and secondary vessels including the tube-to-tube sheet and the tube-to-tube welds in the heat exchanger except as stated in Paragraph 3, "Ultrasonic Examination".

3. Ultrasonic Examination

Ultrasonic examination is another method of detecting discontinuities in material and will be used only when the configuration of the loop prevents the radiographs from being reviewed and interpreted to meet the design requirements, such as the interference of the heat exchanger tubes when attempting to examine the weld on the helium containment. Ultrasonci examination will be performed on the final closure weld joining the primary and the secondary vessels, and the helium containment weld made by ANC when joining the secondary tube closure, and the primary tube subassembly.

B. Testing

1. Prooftesting

Prooftesting or strength testing will be accomplished by either hydrostatic or pneumatic methods to pressure values which incorporate design pressures and temperatures as required by the Code and supplemented by RDT Standard E 15-2T and ANC 70008 and 70009 Design Requirements.

2. Leak Testing

Helium will be used for leak testing following the "Hood" method for total leakage, and supplemented by the "Probe" method if the total leakage exceeds prescribed limits to determine the location of the leak. Helium leak testing will utilize procedures prepared in accordance with requirements of the Code supplemented by RDT Standard E 15-2T that are approved by ANC to acceptance criteria per ANC 70008 and 70009 Design Requirements.

5.2.3 Loop Support Systems

5.2.3.1 Secondary Coolant (Helium) System

The functions of the Secondary Coolant (Helium) System and its design requirements are specified in the SDD,[1] Section 2.2.2.2.1.

The secondary coolant system is the heat-rejection system for the Fuel Element Failure Propagation Loop experiments via an intermediate heat exchanger that is located at the top and is integral with the loop. The primary coolant, to which heat developed in the experiment is rejected, is sodium. The sodium in the loop rejects its heat to the secondary coolant helium via the loop (intermediate) heat exchanger, which in turn rejects its heat to the tertiary coolant water external to the loop. The water coolant system is the ETR high-pressure, demineralized cooling water system (HDW) used as the heat sink for experiments using ETR. The design is for a heat rejection capability of at least 1.5 MW.

Figure 5.7 is a flow diagram illustrating the helium coolant system. Figures 5.8 and 5.9 show schematically the system location relative to the reactor and the placement of components.

During steady-state operation, helium at temperatures up to 1050°F emerges from the loop heat exchanger, passes first through a 2-μ filter, and then rejects its heat to the primary-heat-exchanger (M-7 of Fig. 5.7) cooling water. In order to maintain a constant inlet temperature to the gas circulators with changing helium outlet temperature of the loop heat exchanger, a three-way control valve regulates the amount of helium which bypasses the primary heat exchanger. The primary heat exchanger is a tube-in-shall type purchased for the ATR-GCL for use in a gas-gas heat exchanger system. This unit is qualified for use in this system as a gas-water (tube/shell) heat exchanger.

The gas circulators are operated in series to obtain sufficient ΔP at maximum required flow. The arrangement is similar to the ATR-GCL system for which the gas circulators were purchased. Figure 5.10 shows that gas-circulator performance curve expected for four circulators. Four circulators operated at 88% speed will supply the required 5750 lb/hr of helium at a system ΔP of 77 psi, with an inlet pressure and temperature of 190 psia and 200°F. With the loss of one gas circulator, the same flow rate and ΔP at the same inlet conditions will be attainable with three circulators operating at full speed. It should be noted that 5750 lb/hr is the extreme maximum flow required, and that for most of the operating time, the flow required will be lower, placing the operating point in the center of Zone I of Fig. 5-10. The circulator speed control accuracy and excess circulator capacity insures operation within Zone I at 5750 lb/hr of helium flow.

The helium leaving the gas circulators is water cooled in an after-cooler before entry into the loop heat exchanger. A bypass around the after-cooler is used to regulate the helium temperature at the inlet to the loop heat exchanger. Helium flow regulation is from 2000-6000 lb/hr for the temperature and pressure conditions given above. Total flow control is provided by varying the speed of the gas circulators.

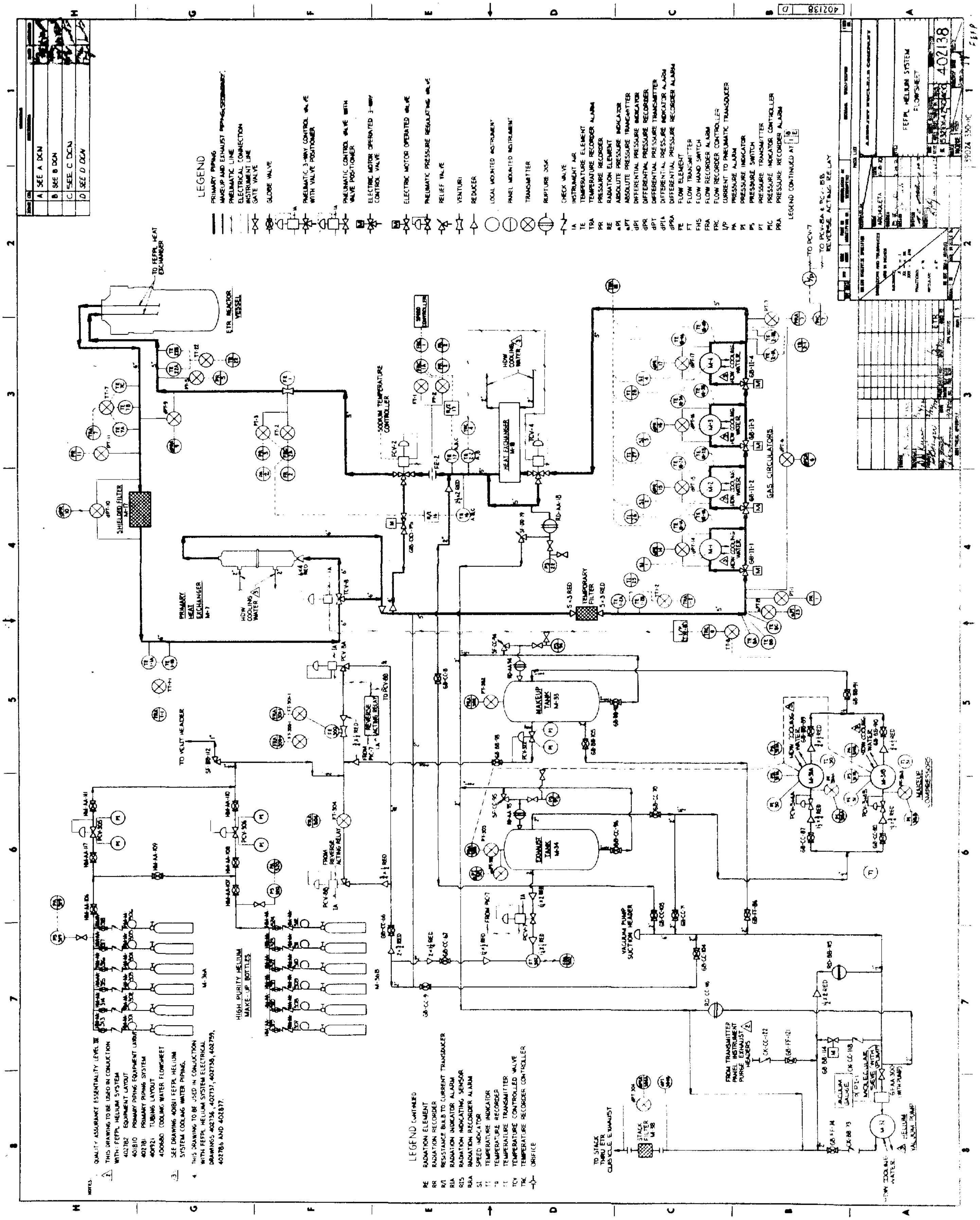

FIG. 5.7 - Flow Diagram Helium Secondary System

FIG. 5.8 - Layout of Heliu stem in Reactor

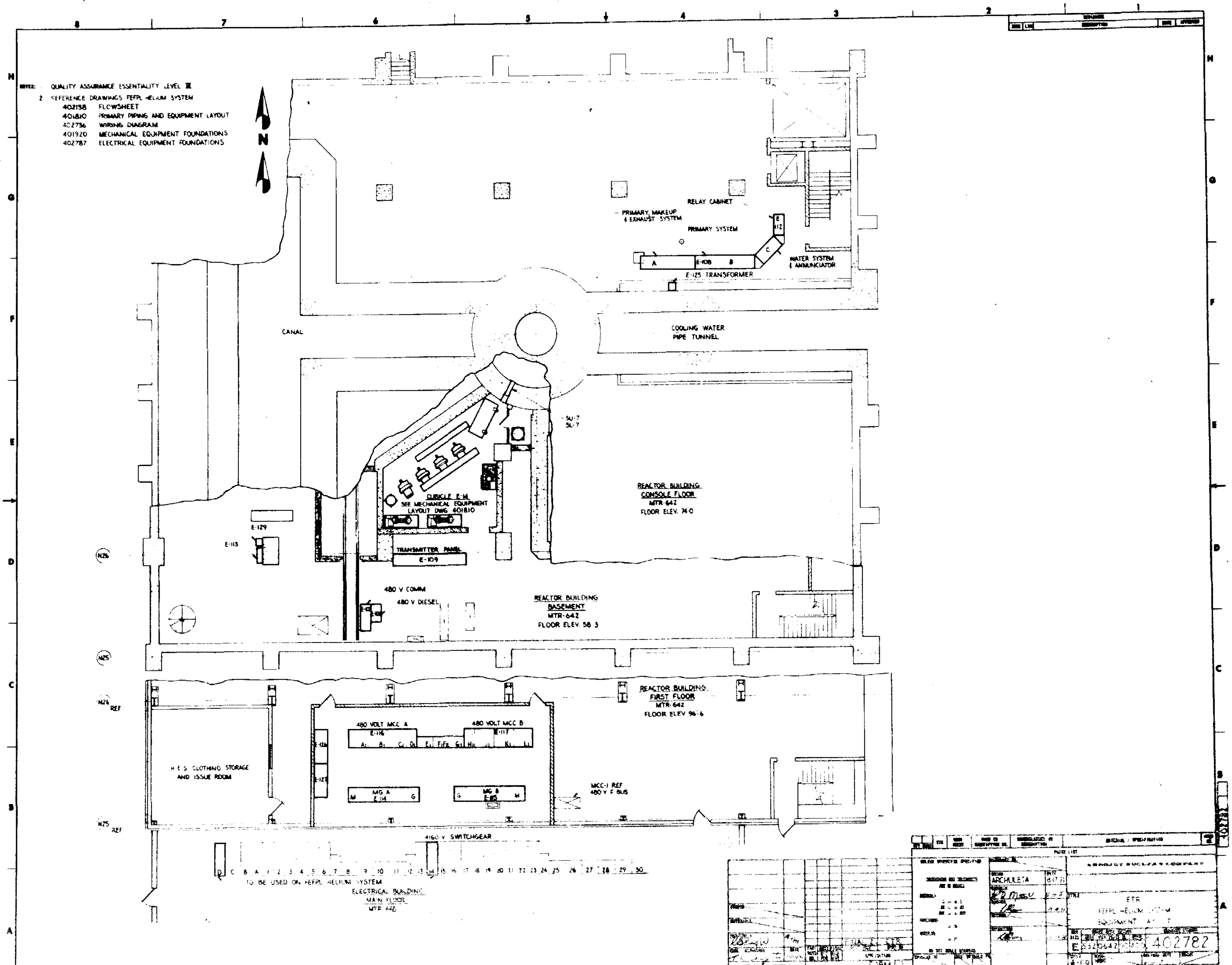

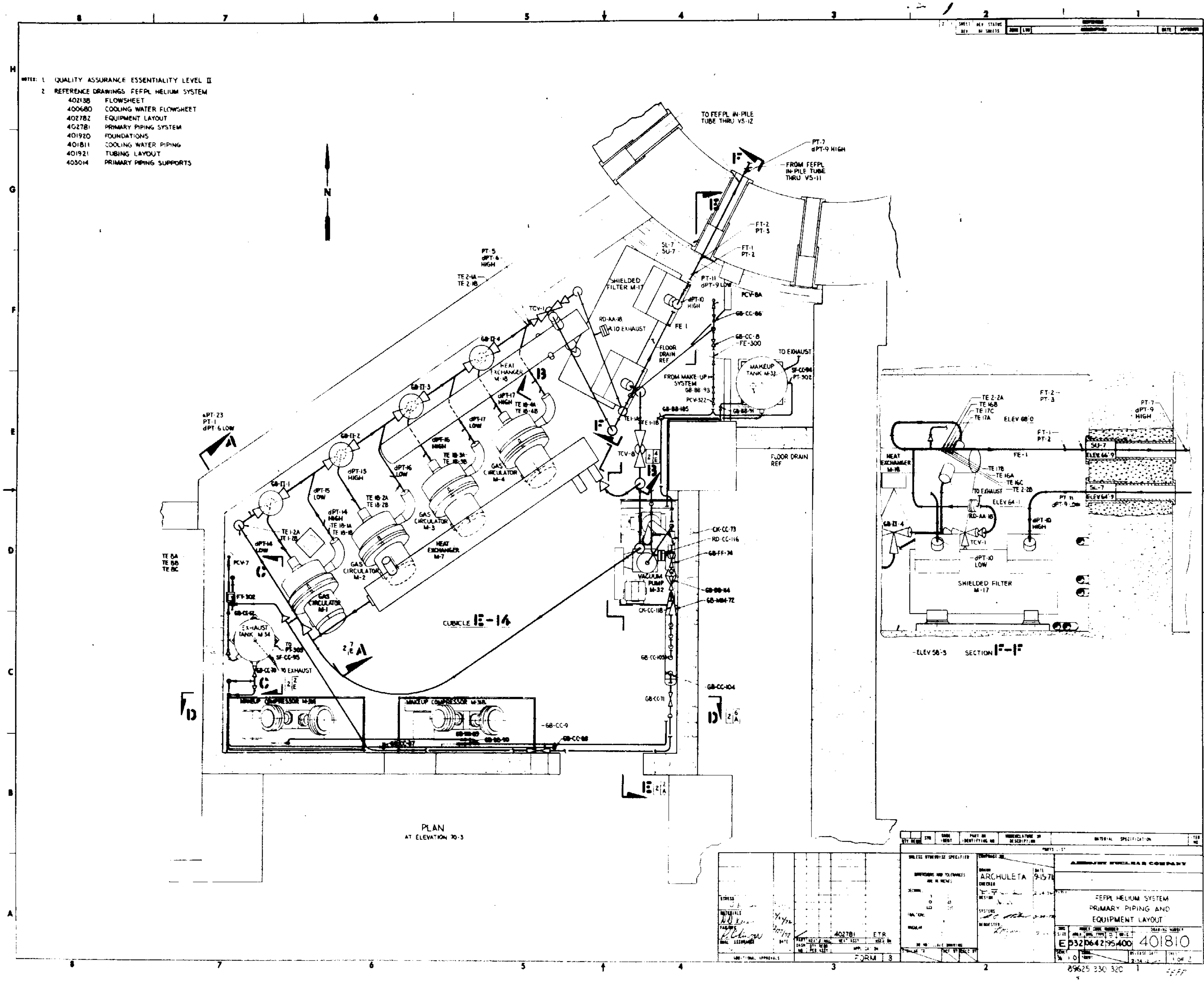

FIG. 5.9 - Layout of He[illegible] System in Cubicle

FOUR (4) CIRCULATOR OPERATION - UP TO T_o = 550°F

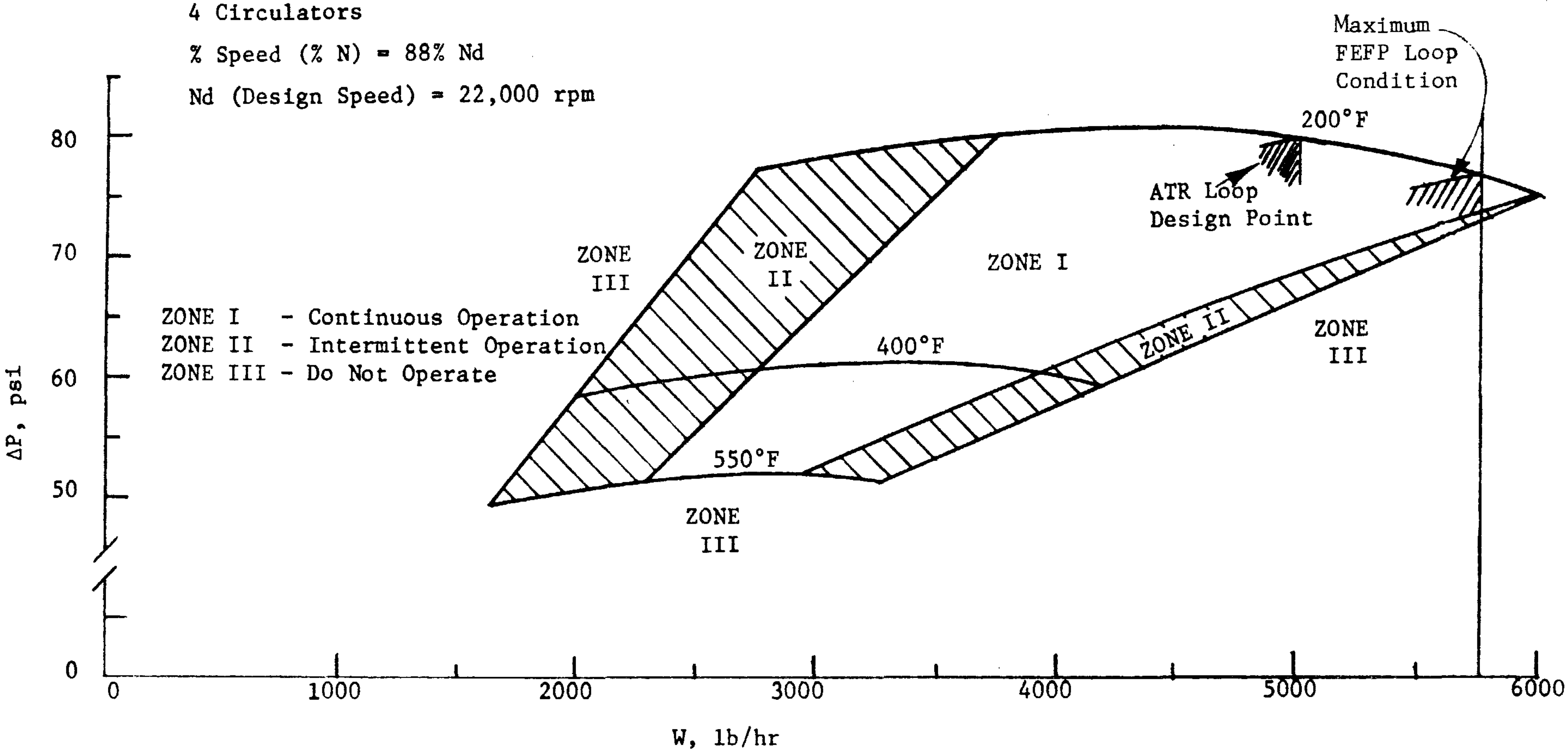

CURVE #1

FIG. 5.10 - Head-flow Curves for Helium System

Startup and shutdown of the system are manual. Steady-state operation is automatically controlled. The main piping of the helium system contains about 5 lb of helium equivalent to about 450 cu ft at STP. At 5750 lb/hr, the transit time is about 3 sec/cycle.

Banks of gas cylinders supply helium directly to the main piping as needed. The helium makeup and exhaust subsystem is basically an exhaust tank of 25 cu ft, to which the main piping vents excess helium, and a makeup tank of 40 cu ft, from which the main piping receives its makeup helium. The main piping requires a high volume of helium bleed-off to hold pressure constant at temperature increases and a high makeup volume to stabilize pressure as temperature decreases. The exhaust tank is normally operated at about 80 psi, receiving its helium from the exhaust tank via compressors having a capacity of 5 lb/hr at 1200 psi.

The helium coolant system can vent to the atmosphere, either directly through the ETR stack when at pressure or through a vacuum pump and molecular sieve if system evacuation is required.

The control console is located adjacent to the FEFP Loop control console and computer. The motor-generator sets and associated switchgear are located on the south side of the ETR main reactor floor in a fireproof and soundproof enclosure. Both commercial and diesel-generator power are used to operate the system, whereby loss of either source of power will allow the system to operate on three gas circulators. The electrical switchgear and instrumentation used were designed and purchased for the ATR-GCL.

5.2.3.2 Filling, Storage, and Remelt System

The functions and design requirements of this system are specified in the SDD,[1] Section 2.2.2.2.6.

After first evacuating the FEFP Loop and filling it with argon, the loop is filled with sodium after the test-train assembly is bolted in and the loop preheated. Two 3/8-in.-OD tubes are provided on the top of the test train for this purpose. A sodium-charging facility has been built to circulate and purify sodium when connected to a loop. Flanged connections are made between a new loop and the charging facility. Clean sodium is pumped into the FEFP Loop until the loop is completely filled and all gas has been vented out of the upper plenum. The ALIP is turned on at lower power to establish circulation in the loop. Sodium circulation is established through the charging facility connections and the purification system is used to reduce sodium oxides to <10 ppm. Loop temperature is increased while sodium purification continues, ultimately reaching 900°F at sodium oxide contents of <10 ppm. The loop cover gas (argon) is introduced through a smaller tube while the sodium is siphoned down to the level of the lower fill tube. The sodium tubes are blown clear with argon and are then cut by hand through ports on a glovebox around the top of the loop. Plugs are GTAW* welded into the tubes, and the cover gas line pressure is adjusted to a predetermined value. This line is then crimped, cut, and welded, accomplishing the final loop-closure seal. After isothermal checkouts and after the secondary containment is installed, a cover is welded over the bolts and tubes to provide a backup seal. The loop is now ready for transport or storage.

A vertical, shielded, electrically heated cylindrical oven will be used to remelt the sodium in a loop which has been inadvertently allowed to freeze. The oven will be constructed with nine separately controlled zones so that the loop can be heated sequentially downward from the top, sodium-free surface. The entire loop will be preheated to about 175°F uniformly, then the top zone raised to approximately 225°F. The second zone will be raised to 225°F when it is apparent that the first zone is molten by means of thermocouples on the loop and test train. In the above manner, each zone will be melted until all the sodium has been melted. The ALIP will then be powered and circulation established.

5.2.3.3 Annulus Gas System

The functions of the Annulus Gas System and its design requirements are specified in the SDD,[1] Section 2.2.2.2.7, and FDR-10 in Appendix F.

The Annulus Gas System consists of argon and helium gas storage tanks, gas tubing, valves, flow meters, control and indicating instrumentation providing controlled and monitored gas flow to the annular space between the primary and secondary tubes of the loop. During operation, the system can function in one of three modes; containment verification, meltdown cup cooling, or heat conduction control.

In the Containment Verification mode, the integrity of the primary and secondary containment vessels is monitored by a static pressure system. The annulus is maintained at a specified pressure, and any continuing flow above a background value indicates a breach of either primary or secondary containment. Periodic monitoring of the annulus gas for moisture and Na^{24} radioactivity is also provided. Normal operating conditions are indicated in Fig. 7-7.

*Gas Tungsten Arc Welded

In the Meltdown Cup Cooling mode, the Annulus Gas System Provides a flow of gas around the primary tube wall in the area adjacent to the fuel meltdown cup. Helium, from a storage tank, is delivered through tubes in the annular space between the primary and secondary vessels to the bottom of the loop, where it is released to the annular space. After flowing over the primary tube, the helium gas is exhausted from the annular space through a radiation monitoring station to the ETR Stock Vent System.

The Heat Conduction Control mode is utilized during loop transfer operations and at times when it is desired to minimize heat loss from the loop. The replacement of helium by argon in the annulus will reduce the heat loss rate to 1/5 the value with helium, and extend the time before sodium freezes in the loop during transfer operations when the ALIP pump is not working.

5.2.3.4 Mechanical Support System

The functions and design requirements of this system are specified in the SDD,[1] Section 2.2.2.2.8.

Supporting structures are located within the ETR (Fig. 1.2) to guide the loop during insertion and to hold the loop in position while the top closure is being mated and sealed to the top dome flange. A spring-loaded ring supported from arms hung on the experiment hangers provides a seat into which the loop is lowered. A shoulder at the top of the pump region (see Fig. 1.1) rests on the ring when the loop is fully inserted and during the time the seal is installed. However, as the seal ring flange bolts at the top of the loop are tightened, most of the loop weight is transferred to the support well. The travel of the springs in the seal ring is designed to accommodate the differential thermal expansion between the loop secondary and the ETR vessel during operation. The loop is restrained laterally at three points: (1) the guide tube and grid adaptor around the lower end of the loop in the core region; (2) the ring above the pump; and (3) the well in the ETR cover. The core filler piece and grid plate adaptor align the bottom of the loop in the L-8 hole.

The FEFP Loop is installed in the ETR by use of the ETR overhead crane and the loop handling machine (LHM). The LHM is positioned over the ETR and lowered to the shielding block from which a plug has been removed. The loop is lowered into the ETR by means of the LHM hoist. When seated, the hoist grapple is disengaged from the loop top flange by means of the offset tool through a small access port in the shield block alongside the

LIM. After the LIM grapple is raised, the LIM is secured and removed from the shield block V. The shield block V is now removed to give access for installing the removable top closure assembly. The loop top-seal ring is hung from the top closure and lowered into position by the ETR five-ton auxiliary crane. When mated, the shield block V is replaced and the clamps are installed on the seal ring by means of long-handled wrenches and hooks. The helium-manifold flanges are remotely actuated, as are loop instrumentation and pump power connectors. The extensive use of remotely actuated devices reduces the exposure of ETR personnel to radiation when removing a loop or replacing a loop at midcycle refueling.

5.2.4 Electronic Systems

The Data Acquisition System, Experiment Assurance System, and the Loop Control System are described in the following subsections. The FEFPL Plant Protection System, which is another major loop support system of a similar category, is described in considerable detail in Chapter 7.0 (see also the SDD,[1] Section 2.2.4.4).

5.2.4.1 Data Acquisition System

The functions of the Data Acquisition System and its design requirements are specified in the SDD,[1] Section 2.2.4.1, also FDR-02, "FEFPL Data Acquisition System Design Requirements". The Data Acquisition System is made up of subsystems described in the following paragraphs.

A Digital Computer System is used to acquire and record low-bandwidth experimental and operational measurements during normal operation and transient tests in the FEFP Loop, provide assistance for the control functions for the sodium loop, and display operational loop variables and certain engineering calculations to the loop operator. This system consists of a PDP-15-20 computer and associated peripherals. The computer hardware facilities include core memory, high-speed paper-tape facilities, and two magnetic-tape transports. Also included are a heavy-duty teleprinter and extended arithmetic unit, and high-speed nine-track digital magnetic-tape recorders.

An Analog Data Acquisition System is used to acquire and record broad-bandwidth experimental data, offer limited recording redundancy for channels being recorded on the Digital Computer System, and retain data signals that were recorded 10 sec before a planned or premature loop transient test.

A Timing System generates time-of-day information capable of being recorded on both the digital and analog data recorders.

An Event Logic System derives a rate signal from selected sensors, and triggers the digital and analog data recorders into a preprogrammed transient mode of operation.

An input patch facility is used to achieve manual program assignment of sensor signal inputs to both the digital and analog data recording systems.

5.2.4.2 Loop Control System

Loop Control System functions and detailed requirements are contained in the SDD,[1] Section 2.2.4.2, and ANC Document FDR-04 "FEFP Loop Control System Design Requirements". The bounds of this system have been carefully defined and in general relate to the direct control of the sodium loop parameters. Two subsystems have been designated: (A) Process Control System, and (B) ALIP Power System. These are discussed in the following paragraphs. The control system discussed in this section is not an all encompassing system that includes control aspects of the entire loop system. Other loop support systems (e.g., helium system, annulus gas system) have their associated instrumentation and controls that are considered part of the respective subsystem. There are, however, interfaces between the Loop Control System and the Helium System, and these interfaces as well as certain control features of the helium system are discussed in subsection A below under the Process Control System.

A. Process Control System

The FEFP Loop Control System maintains the loop sodium temperature and flow and test-section sodium flow at the conditions required for normal operation and for experiment test performance. The instrumentation also provides for operator surveillance of the controlled variables during the various operating phases--startup, isothermal, normal, abnormal, and shutdown. In the event of abnormal conditions, the control system must ensure correct control action.

The loop Heat Transfer System is composed of two flow loops, a sodium loop and a helium loop. These two are coupled through the loop heat exchanger which acts as an intermediate heat exchanger between the sodium and helium loops. Figure 5.11 is an In-pile Loop and Helium System Control Instrumentation Flow Plan showing these two loops with their major control system components. Loop control is on the left and Helium System on the right half

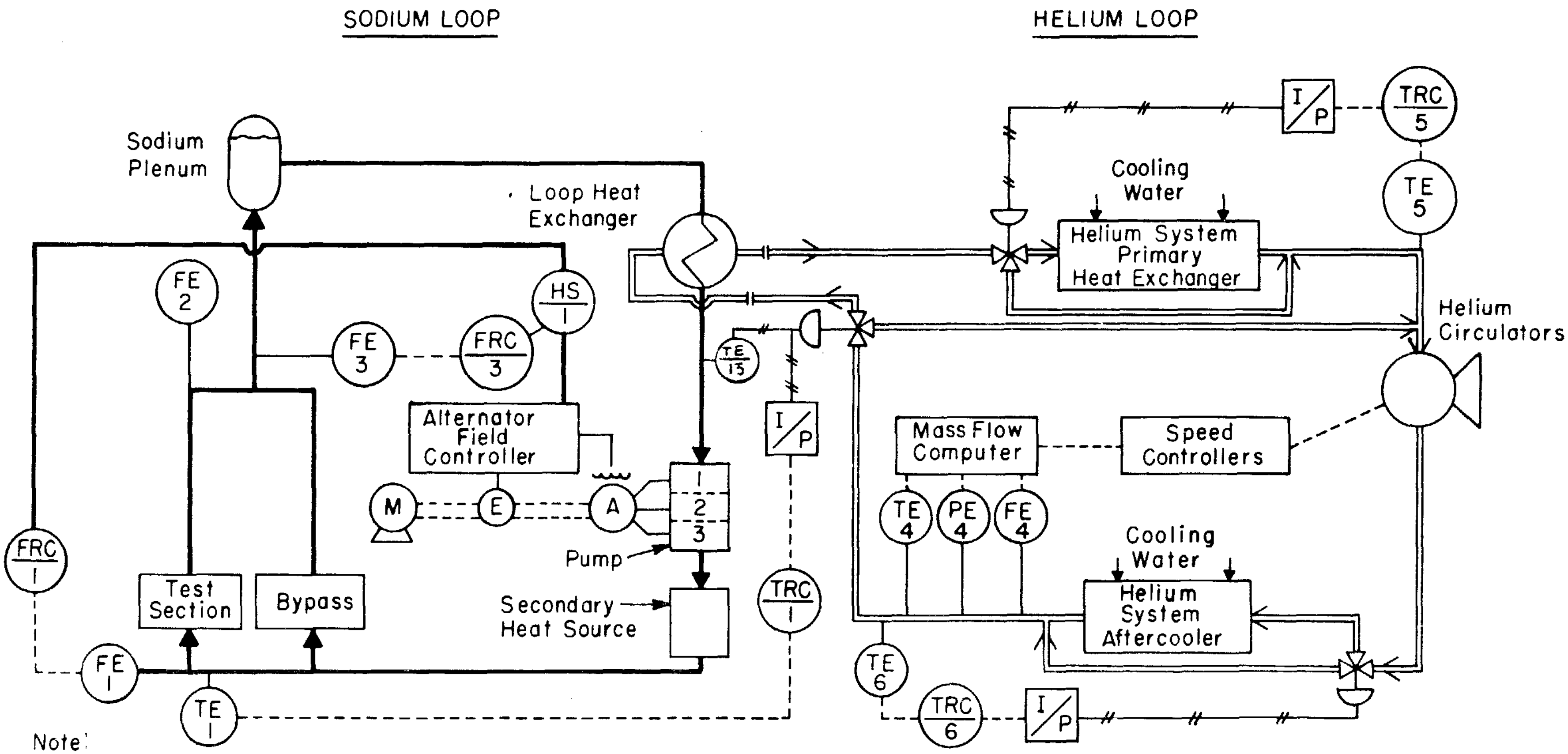

Note:
Controllers Shown do not Represent any Specific Piece of Hardware. They Show the Functions Performed by the Control System.

━ Sodium Flow Path
═ Helium Flow Path
M – AC Motor
A – Alternator
E – Exciter Generator

--- Electrical Inst Lead
-//- Pneumatic Inst Lead

FIG. 5.11 - In-pile Loop and Helium System Control Instrument Flow Plan

of the figure. Listed in Table 5.3 are the controlled variables for the sodium and helium control loops; sensors and controlling action (manipulated variable) are also indicated.

Loop Sodium Temperature Control

Loop Sodium Temperature Control is accomplished by regulating the loop heat rejection rate through the loop heat exchanger to the secondary (helium) coolant system. Heat generated in the loop is primarily due to the test fuel elements and gamma heating of loop components, and will vary greatly as a function of fuel content, number of fuel pins, and reactor power level. Removal of this heat requires varying the heat transfer rate in the heat exchanger over a wide range. Control is accomplished by regulating the helium mass flow through the loop heat exchanger.

The sodium temperature is measured at the test-section inlet by four thermocouples. The signal from the temperature element selected for control is conditioned to drive a current loop supplying a three-mode controller (TRC1), recorder and high-low alarm module. The controller compares the monitored temperature signal with the setpoint for the desired temperature and generates an output proportional to the error. The controller output, after conditioning, regulates a fast response, force-balance valve positioner, which positions a three-way valve in accordance with the controller output. The valve position regulates the helium mass flowrate through the loop heat exchanger as required to control the loop sodium temperature within the required limits. If the sodium temperature deviates from the normal control band, a high or low alarm alerts the operator of system malfunction.

Loop Sodium Flow Control

Control of total loop sodium flow is required to achieve specific loop operating requirements, such as sample temperature, test-section flow and total loop flow. To obtain the desired flow condition, the loop ALIP pump output is controlled by varying the pump input voltage. This voltage is supplied from a controlled output motor-alternator set. A special fast response, broad range field controller is provided for alternator field control. By controlling the alternator field voltage, the input voltage to the ALIP pump can be varied to control the pump output over the range required to achieve desired flow conditions. The alternator field excitor design prevents the control signal from driving the alternator output voltage below a value which would initiate transfer to the pump emergency power source (see subsystem B, below, for more detail on ALIP power system).

TABLE 5.3

Controlled Variables

Controlled Variable	Sensors	Controlling Action
Sodium Control Loop		
1. Sodium inlet temperature to test section	Inlet thermocouple (TE-1)	Helium flow to loop HX
2. Total loop sodium flow	Eddy current flow sensor (FE-3)	Pump voltage
3. Test-section sodium flow	Permanent magnet inlet flow sensor (FE-1)	Pump voltage
Helium Control Loop		
4. Helium system total mass flow	Helium inlet temperature (TE-4) Helium pressure (PE-4) Helium velocity (flow) (FE-4)	Helium circulators speed
5. Helium temperature at circulator inlet	Thermocouples (TE-4)	Bypass around helium primary heat exchanger
6. Helium temperature at inlet to loop HX	Thermocouples (TE-6)	Bypass around helium aftercooler

The control signal required for sodium flow control is derived from the loop total flow sensor (FE-3). The output signal from the selected flow sensor is conditioned to drive a current loop supplying a three-mode controller, recorder and high-low alarm module (FRC-3). The controller compares this output signal against a reference flow signal and generates an output proportional to the error. This output signal is used to drive the alternator field controller which varies the three-phase voltage to the pump to give required flow conditions. Deviation of the flow from the normal control band will actuate a high or low alarm to alert the operator of system malfunction. In steady-state operation, this flow will be set to give a desirable value of test-section outlet temperature. In transient situations, it is important that total flow be maintained in order to allow the temperature control loop to stay within allowed operating limits. Because of the secondary heat source due to gamma heating of the primary containment, a change in total flow (e.g., a sudden blockage in the test section) will cause a change in inlet temperature which the temperature control loop cannot correct for because of the sodium transport delay. The flow control loop will minimize the disturbances to the temperature control loop. Also, by maintaining total sodium flow, the temperature excursions at the inlet of the heat exchanger will be minimized.

Test-Section Flow Control

The capability of performing certain experiments involving flow coastdown is required. In order to match a test-section flow coastdown curve, the total flow control loop must be bypassed or modified. This will be accomplished by switching from total flow control and programming the pump voltage downward and using the test section inlet flowsensor as a control element.

The test-section flow is measured by a permanent magnet flow sensor (FE-1). The signal from this sensor is conditioned to (1) drive a current loop supplying a controller (FRC-1), recorder and high-low alarm module and (2) supply an input signal to the digital computer. The controller is capable of operating in an automatic analog, direct digital (DDC), or manual control mode. When the DDC mode is selected, the controller accepts a pulse output signal from the digital computer and generates an output proportional to a setpoint. This output is then conditioned to be used as an input to the ALIP voltage controller. The desired flow coastdown curve is achieved by programming the digital computer to obtain the required control characteristics.

If the computer signal fails, the controller will automatically return to either manual or automatic analog control as selected. The manual position will freeze the controller at the last output. In the automatic position, the controller will automatically ramp to a preselected position. The automatic analog mode also permits operating the controller as a standard three-mode controller. The high-low alarm unit permits monitoring the test-section flow and alerting the operator when it deviates from a selected control band.

Helium System Controls

A brief discussion on helium system controls (see Fig. 5.11) is presented here to clarify the overall heat transport system operation. Helium system mass flow will be controlled in order to maintain the helium circulators within the proper operating conditions. Helium mass flow will be computed from helium temperature (TE-4), pressure (PE-4), and velocity (FE-4) to control the speed of the helium circulators. Helium at temperatures as high as 1050°F will exit the loop heat exchanger and heat will be dumped to the ETR high pressure demineralized water cooling system through the helium system primary heat exchanger (see Section 5.2.3.1). Helium temperature (TE-5) to the circulators will be automatically controlled by bypassing helium around the helium system primary heat exchanger.

Helium temperature at the inlet to the loop heat exchanger (TE-6) will be automatically controlled by adjusting the helium bypass flow around the helium aftercooler. During normal operation, the aftercooler will remove the heat of compression generated in the circulators and maintain the helium inlet at ∿150°F. During isothermal operation of the loop, the inlet temperature to the loop heat exchanger can be maintained at a higher level (up to 400°F) in order to put heat back into the sodium and keep it from freezing

B. ALIP Power System

The flow of liquid sodium in the loop is accomplished with the use of an Annular Linear Induction Pump (ALIP). The pump contains three sections, each a complete three-phase pump capable of providing alone about one-third of the flow of the entire assembly. The rate of flow is governed by the amount of electrical power being supplied to the pump; thus, varying the three-phase voltage to all of the sections results in a proportionally-controlled sodium flow. The sectionalizing of the pump provides for redundancy, which in turn results in greater reliability. Each section is electrically isolated from the other two sections. These sections also have individual power supply feeders, making them completely independent in every respect. Should any section fail, the remaining two will provide sodium circulation at a proportionally reduced rate.

The above redundancy is continued in the power distribution system. Three separate three-phase feeders supply power to the ALIP pump. Each of the feeder systems is complete with the necessary fuse-backed air circuit breakers and fault sensing devices to protect against voltage problems, phase unbalances, and overcurrent difficulties. In addition to the electrical fault parameters, the distribution system includes the proper sensing devices and equipment required to transfer the entire pump to a preset reduced-voltage emergency power source, in event of commercial power failure.

To maintain redundancy, three separate transfer switches are used. The malfunction of one or two of the transfer switches will not cause a total interruption in the flow of sodium in the loop.

In order to prevent malfunctioning of the ALIP due to electrical phasing anomolies or inconsistencies, one controller will power all three sections simultaneously. If commercial power fails, the entire pump will be transferred to the emergency power source, since the emergency power is independent and not phase-synchronized with the commercial source.

The power sources, distribution system, and auxiliary protective appurtenances assure an uninterrupted flow of sodium. Although each of the devices is considered as very reliable, they in themselves cannot be regarded as absolutely failure-free. However, the combinations and duplication of these devices to provide redundancy provide a high level of confidence that an essentially failure-free power supply system is provided.

The total power source is a composite of the commercial power line, a diesel-driven alternator and a DC motor driven alternator to assure noninterruptable power for the ALIP. In this arrangement of power sources, the normal supply is the commercial power line. This is supplemented with the diesel-driven alternator running while a FEFPL experiment is in operation. The diesel is in an electrical standby status (i.e., machinery rotating with only partial electrical load). This avoids the possibility of any starting problems or loss of time in starting a cold engine and bringing it up to speed before switching the electrical load to this power source.

1. Normal Power

A detailed description of the ALIP normal power supply is as follows: Normal power is fed from the ETR double-bus feeder to the 4160 V commercial "D" bus, Fig. 5.12 (also see Section 7.2.10 for FEFPL/ETR Power Distribution System Schematic). The ALIP pump controller (motor-alternator) is connected

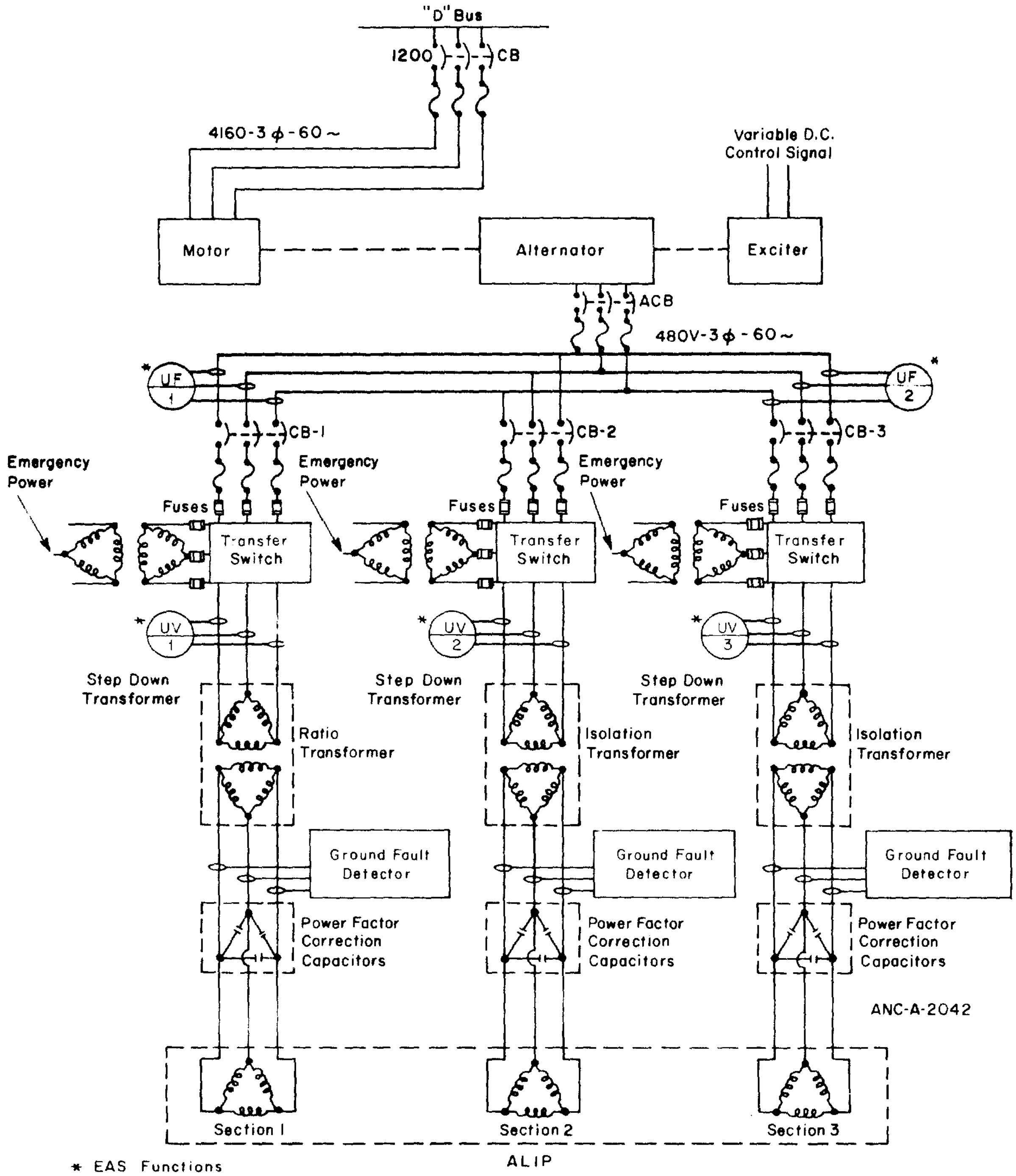

FIG. 5.12 - ALIP Power System Schematic

through a 1200 amp circuit breaker. This circuit breaker contains the interlocking and sensing devices that provide the motor with overcurrent, and ground-fault detection. The motor-alternator output voltage is controlled over a range of 20 to 100% by regulating the alternator field excitation with a special fast response, controllable exciter.

The motor-alternator output power is divided into three separate feeders, each supplying one of the three pump sections. Each of these pump section feeders is connected through pump circuit breakers CB-1, CB-2, and CB-3. Current limiting fuses are included in series with the breakers to reduce the possibility of fault current damage in the normal power mode. These circuit breakers, along with three remotely operated contactors in the emergency power feeders (not shown) permit remote isolation on the occurrence of overcurrent difficulties or ground faults in any pump section. The normal and emergency power feeders are connected to normal/emergency power transfer switches, the output of each feeding separate sections. These feeders include the ratio/isolation transformers to match the voltage to the particular impedance of each pump section. Section 1 of the ALIP is operated at a proportionally lower voltage because of the smaller coils necessary for the pump characteristics. For pump sections 2 and 3, isolation transformers provide limited current sources in event of a ground fault in the affected section.

Each feeder section contains relays to detect any ground faults. These sensors measure ALIP circuit impedance to ground. Any unbalance from the normal preset condition represents a fault condition and provides visual and audio alarm. The power feeders from the ratio transformers include the ground fault relays, and the power factor correction capacitors. These feeders are routed separately for each section, and run to individual and independent pump power connectors on the in-pile loop. These loop connectors are keyed to prevent incorrect connection of phase and pump sections. The under frequency and under voltage sensors shown in Fig. 5.12 are discussed in Section 5.2.4.3 in conjunction with the Experiment Assurance System (EAS).

2. Emergency Power

The ALIP emergency power is furnished from the ETR 480 V battery-backed diesel bus ("H" bus). This bus normally receives its power from the ETR 4160 V diesel power generating system. A diesel power failure initiates a disconnection of the "H" bus from the diesel generation system, and the "H" bus is transferred to a battery-backed inverting motor-generating set (MG-1) that is normally powered from the "H" bus to feed charging current to the battery bank. In the event of diesel power failure, the motor-generator set inverts and it is capable of supplying 120 kw of power for a 30 min period (∿55 kw allocated for ALIP emergency power). If diesel power is not restored prior to battery exhaustion, and commercial power becomes available, the diesel distribution system can be transferred to the commercial source. This condition is not satisfactory for continuing operation of the FEFPL in-pile. It is a condition that may be necessary for a limited time under some emergency conditions, such as when ETR is not at power. However, power is needed to keep sodium circulating at an isothermal condition in the loop under such circumstances.

Normally, emergency power is fed from the "H" bus to an experimenters failure-free power panel. This power is fed through three separate circuit breakers to step down transformers with secondary fuse protection where the voltage is reduced to a level required to maintain the minimum flow from any one of the three ALIP pump sections. The reduced power from these transformers is fed to the emergency side of the normal/emergency transfer switches.

Electrical power to the ALIP, when being supplied from the commercial source, is isolated from the power line by the fact that the commercial power supplies the energy to the motor of a motor-alternator set. The variable voltage required to drive the ALIP is supplied by the alternator. This variable voltage or the battery-backed source is fed to the ALIP via the three transfer switches. Whenever a FEFP experiment is in the reactor, both sources of power must be available at the transfer switches. The ALIP will be operated on normal power whenever the reactor is at power. A loss of commercial power will shut down ETR and initiate transfer to emergency power. Time of transfer, including sensing and transfer switch actuation, is 100 msec. The main breaker at the alternator output is tripped to open position when the transfer takes place, to further insure against feeding normal power to a pump section should a transfer switch fail in the normal position. Upon return of commercial power to its normal state, the transfer of ALIP to normal power must be initiated manually. Power operation of the reactor will not resume unless both the "emergency" and "normal" power are available and the ALIP connected to the "normal" power.

5.2.4.3 Experiment Assurance System (EAS)

Introduction

Experiment Assurance System detailed requirements are contained in ANC document FDR-16 "FEFPL Experiment Assurance System Requirements". ANC document FR-208 "FEFPL Experiment Assurance System Design Report" provides a complete system description. The primary function of the EAS is to prevent inadvertant damage during operations in the ETR to the test section and other loop components resulting from accidents not related to intentionally initiated experiment transients.

The presently identified malfunctions that must be guarded against lead to one or both of two off-design conditions defined by power-flow mismatch or malfunction of heat sink. The loop component that is most vulnerable to damage under these circumstances is the test train fuel because it is the major source of heat generation. Hence, under accident conditions, it is subject to direct and rapid overheating before other parts of the loop are affected. Consequently, if the fuel can be protected under off-design conditions, damage to other components will also be precluded.

Damage will occur when the fuel clad temperature exceeds a value that is a complicated, and not well understood function, of the design, irradiation history, and local environment. Because it is neither possible to predict accurately a damage threshold nor measure clad temperature, the EAS must sense and act on those initiating conditions that will lead to clad overheating if unchecked. This means, in most cases, that the ETR should scram rapidly upon confirmation of the malfunction that will result in overheating, or when a monitored parameter such as test section sodium outlet temperature, exceeds a given setpoint. Also, some accidents such as total loss of power to the ALIP, may result in temperature excursions that exceed 50°F in spite of prompt action by the EAS. This does not necessarily mean that the experiment must be terminated. A course of action will be determined by the experimenter based upon the nature of the test underway and its potential sensitivity to the degree of overheating that may have occurred.

The EAS will assure the integrity of the experiment, in particular the test train, prior to the initiation of an experimental transient. It is anticipated that the EAS protective function requirements may vary from experiment to experiment. The proposed system discussed below will form a basic part of the EAS for most experiments. It is further anticipated that some or all of the EAS protective functions may be bypassed at certain stages of an experiment in order to run planned experimental transients which may cause parameters to exceed protective channel setpoints. EAS function bypass switches are protected with a locked panel cover and a panel alarm provided to indicate a bypassed function. These features preclude unintentional or inadvertent bypass of an EAS function.

Relationship to FEFPL Plant Protection System (PPS)

It is important at this point to discuss the relationship between the EAS, the Loop Control System and the FEFPL Plant Protection System described in Chapter 7. The EAS has been classified as an independent in-reactor loop subsystem. It is not part of the FEFPL PPS, nor is it needed in order that the PPS meet its functional requirements. Many of the accidents which have been analyzed for the purpose of determining PPS protective-function requirements would cause the EAS to take protective action prior to the time when the PPS would be called on to take protective action. The EAS thus acts in a positive way to limit the severity of many postulated accidents. It is not considered a primary safety system, but acts to protect the results of the FEFP experimental program. However, it does form an additional line of defense in the overall safety scheme in the same sense that a typical control system is a line of defense. The EAS sets an envelope of operation for the loop control system.

The EAS is similar to the FEFP plant protection in many ways: electronic logic, protective action, detailed design requirements, equipment qualification, terminology, etc. EAS electrical power is supplied independently from the same source as the PPS. The PPS couples EAS-generated scram requests to the FTR PPS. Much of the description presented in this section concerning the EAS refers to figures or discussions in Chapter 7 in order to minimize repetition. The reader should bear in mind the distinction between the two systems, and that the EAS and FEFP PPS are functionally independent. Much of the terminology used to describe the EAS is the same as that used in describing the PPS; a complete glossary of terms is given in Section 7.1.2. These definitions are generally applicable to the EAS, unless specifically modified in this section.

EAS Protective Functions

Six EAS protective functions have been established. The six functions are:

(1) Detect loss of normal ALIP power
(2) Detect loss of test section coolant flow
(3) Detect test section coolant overheating
(4) Detect loss of heat sink
(5) Prevent sodium freezing
(6) Detect total flow blockage

The protective actions required are:

Scram and initiate transfer to emergency power for (1) and (6).

Scram for (2), (3) and (4).

Initiate reduction in helium flow to loop heat exchangers for (5).

EAS Requirements

In general, the design of the EAS shall conform to RDT Standard C 16-1T, "Supplementary Criteria and Requirements for RDT Reactor Plant Protection Systems", where applicable and practicable. The electronic logic system is structured similarly to that of the FEFPL PPS and will be designed to the same requirements. The main exceptions to RDT C 16-1T for the EAS are: (1) special sensors different from PPS sensors (i.e., ALIP voltage monitors) will not necessarily be fully qualified to the standard. However, the temperature sensors will be thermocouples purchased to RDT C 7-6T; (2) the protective actuators for actions other than scram will not necessarily be fully qualified to the standard; (3) exceptions to the cable isolation requirement on some parts of the system may be taken; (4) the system will have certain operational features which are not normally allowed for a plant protective system (see section on System Operation); and (5) exceptions to standards and modifications of the system shall be treated as part of the specific experiment requirements and reviewed and approved as part of the normal experiment review and approval procedure conducted by the FEFP Project.

System Description

The EAS protective functions were established in the preceding sections. Four of these functions relate to test-section fission power-flow mismatches, resulting from various postulated accidents. Two detect heat sink malfunctions.

Protective Function (1) monitors ALIP frequency and voltage input. Three under voltage sensors UV-1, -2, and -3 feed three instrument channels in a two-out-of-three logic protective channel and 2 under frequency sensors UF-1, and -2 feed two instrument channels in a one-out-of-two logic protective channel. Of the various accidents which could lead to high test-fuel clad temperatures, loss of commercial power is the most probable. This accident has relatively minor consequences with respect to the primary containment vessel, since the ETR PPS will respond to the commercial power loss; furthermore, the ALIP emergency power source will provide sufficient electrical power for adequate cooling of the primary vessel without protective action by the FEFPL PPS. However, the rate of rise of test-fuel clad temperature is large and this EAS function is needed to give maximum speed of response to loss of commercial power in order to minimize fuel damage.

Protective Function (2) monitors test-section sodium flow using the test-section inlet and outlet flowsensors (FE-1-1 and FE-2-1) in a one-out-of-two logic protective channel. These flowsensors are of the permanent magnet and eddy current type, respectively. This function is responsive to failures internal to the pump, flow blockages, and failure of the test section sodium flow-control system, if included in a given experiment

Protective Function (3) protects against all failures that relate to power-flow mismatch and loss of heat sink. Qualitatively, an EAS with this single function would provide adequate protection. The other functions are provided in general for rapid action in response to certain malfunctions in order to get as large a protective margin as practical. Three thermocouples (TE-2-1, -2, -3) mounted on the test train measure test-section outlet temperature and provide input signals to three instrument channels in a two-out-of-three logic protective channel.

Protective Function (4) protects against loss of loop heat sink. Four thermocouples (TE-13-1, -2, -3, -4) are located at the outlet of the heat exchanger and measure the wall temperature in contact with the outlet sodium. Three of these thermocouples provide the input signals to three high-level trip instrument channels in a two-out-of-three logic protective channel.

The primary purpose of Protective Function (5) is to protect against freezing of the sodium in the heat exchanger resulting from partial loop blockages in which the control system would call for maximum helium flow because of overheating of the sodium in the downcomer annulus between the outlet of the heat exchanger and the inlet of the test section where the temperature control thermcouples are located. This function utilizes the same thermocouples (TE-13-1, -2, -3) as protective function (4) for input to the low-level trip instrument channels in a two-out-of-three logic protective function.

Protective Function (6) acts to prevent pump damage in the event of a total or nearly total loop flow blockage (total flow reduced to less than 5% of its steady-state value) and to reduce the sodium pressure (hence, the saturation temperature) in the meltdown cup region. In the event of blockage resulting in a fuel meltdown or a fuel meltdown resulting in a blockage, it is desirable to maintain a minimum flow in order to cool the meltdown cup; however, it is also desirable to cut down the pump power (voltage) in order to reduce heating effects in the pump (ALIP). Sodium flow maintained above approximately 10% of steady-state is adequate to cool the pump at the steady state power input. In other words, to get into difficulty, it is necessary to have a very low flow situation with the control system calling for full pump power (voltage). This function will monitor total sodium flow and ALIP voltage for a low flow condition (approximately 10% of steady-state) coincident with pump voltage above the low value trip point of protective function 1. The protective action will initiate a scram and reduce pump voltage to a fixed value which prevents overheating of the pump and still provide adequate cooling of the fuel meltdown cup by switching the pump to the emergency power source. Monitoring of loop total flow only is not sufficient to provide protection in this case since certain experiments (p-2) may call for a total flow coastdown to approximately 10% of the steady-state value. This function utilizes the total flowsensors (FE-3, -1, -2) in two low-level trip instrument channels in a one-out-of-two logic protective subchannel in coincidence with ALIP under voltage monitors (UV-1, -2, and -3, protective function 1) in three instrument channels in a two-out-of-three protective subchannel.

Table 5.4 lists the EAS Protective Functions. It includes the function number, title, monitored variable, protective action, design basis accident, number of instrument channels, critical loop variable, instrument channel accuracy, and the sensor designation numbers.

The EAS protective functions will utilize a logic system whose basic components are similar to the FEFPL PPS logic system. The main differences result from the different number of protective and instrument channels, and ability to bypass logic outputs. A simplified block diagram of the EAS is shown in Figure 5.13.

System Operation

System setpoints, limits, etc. will be determined for each specific experiment and documented as part of each individual experiment plan. The EAS will be operated in various modes under the control of the FEFP experimenters. One mode might be with any or all of the protective channels bypassed during certain phases of the experiment. Also, the system setpoints may be adjusted to different values depending on nominal values of parameters during different phases of a planned experiment.

TABLE 5.4

Experiment Assurance System Protective Functions

EAS Protective Function Number	Protective Function Objective	Monitored Variable	Protective Action	Incident	Number of Instrument Channels	Critical Loop Variable	Instrument Accuracy***	Sensor Designation Numbers*
1.	Prevent Power-Flow Mismatch	ALIP Voltage & Frequency	Scram & Power Transfer	Loss of Pump Power	3 & 2	Clad Temperature	±5 vrms ±1.0 Hz	UV-1,-2,-3 UF-1,-2
2.	Prevent Power-Flow Mismatch	Test Section Sodium Flow	ETR Scram	Blockage-Control Failure	2	Clad Temperature	±5% of indicated	FE-1-1 FE-2-1
3.	Prevent Power-Flow Mismatch	Test Section Outlet Temperature	ETR Scram	Blockage-Control Failure	3	Clad Temperature	±3% of indicated	TE-2-1,-2,-3
4.	Detect Loss of Heat Sink	HX Outlet Temperature-High	ETR Scram	Loss of He Flow to HX	3	Clad Temperature	±3% of indicated	TE-13-1,-2,-3
5.	Prevent Sodium Freezing	HX Outlet Temperature-Low	Increase Loop HX Bypass Flow	Partial Loop Blockage	3	Sodium Temperature	±3% of indicated	TE-13-1,-2,-3
6.	Detect Total Flow Blockage	Total Sodium Flow & ALIP Voltage	Scram & Power Transfer**	Total Loop Blockage	2 & 3	Sodium Temperature	±5% of indicated ±5 vrms	FE-3-1,-2 UV-1,-2,-3

*These numbers are those assigned to the P-1 Experiment Test Train Sensor and Loop Sensors. This document establishes requirements for EAS sensors as indicated in the appropriate sections. The designation numbers themselves may vary from experiment to experiment.

**Protective action on low total loop flow and above under voltage setpoint.

***Instrument accuracy is % of indicated in the setpoint range.

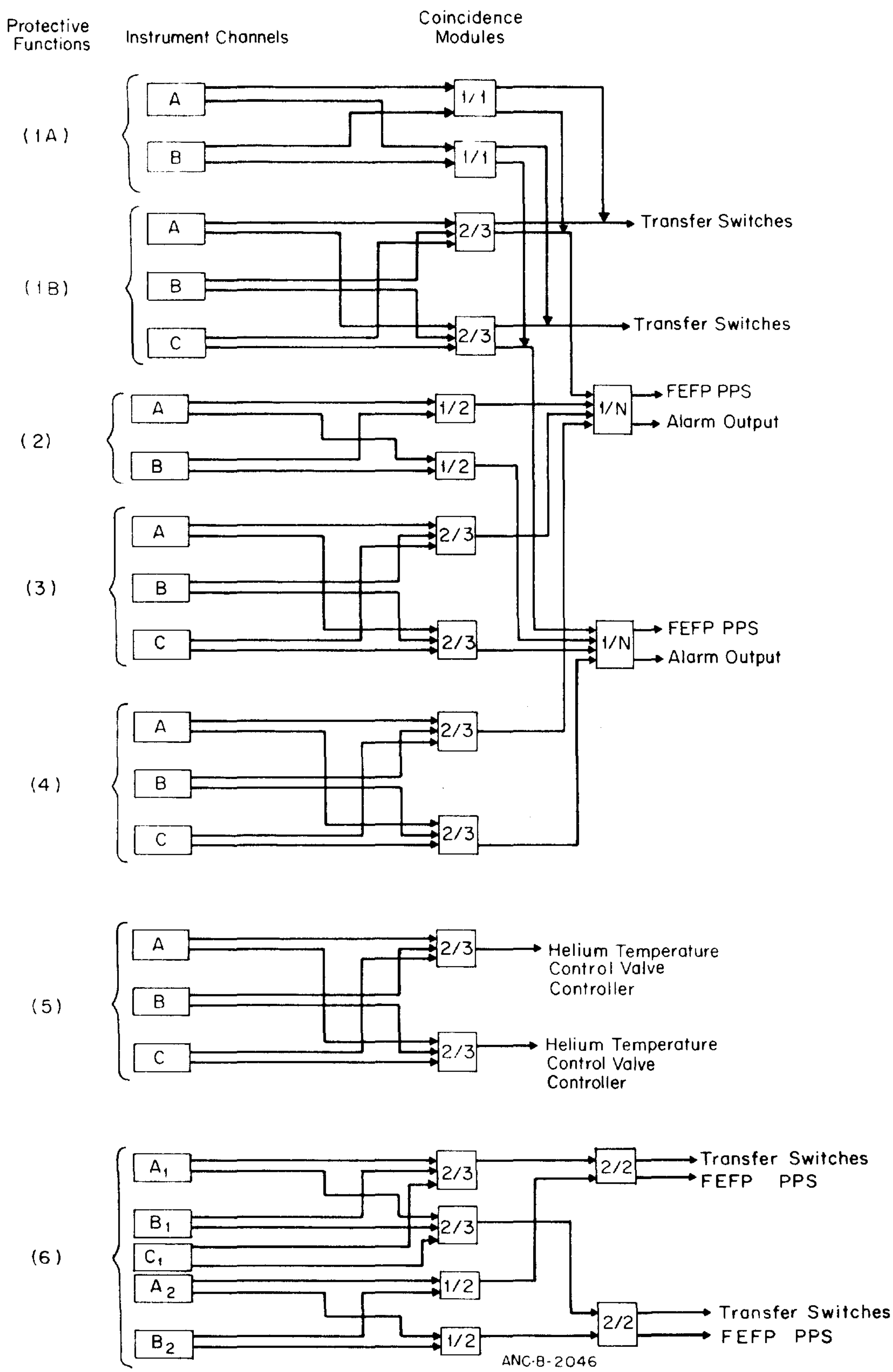

FIG. 5.13 - Experiment Assurance System Logic Diagram

5.3 Loop Handling System

Functions and design requirements for the Loop Handling System are specified in the SDD,[1] Section 2.3.

The loop handling system is capable of handling the FEFP in-pile loop at each of the interfacing facilities and transporting the loop between these facilities. The following items comprise the loop handling system:

Loop Handling Machine

Transporter (see Fig. 1.5)

Accessories:

HFEF Hook Spreader

Support Stand

The loop handling machine is basically a shielded hollow cylinder (see Fig. 5.14) with a 20-in. inside diameter. Its exterior shell is stepped with a 29.75-in. dia at the lower end and a 26.50-in. dia at the upper end. Depleted uranium, cast and machined as hollow cylinders, occupies the annular space between the outer and inner shells.

At the lower end of the machine is a nonsealing shield valve. The valve is powered by a commercial valve operator which contains limit and torque-cutout switches for the open and closed positions.

Penetrating the machine, just above the valve and again about one-third of the way up, are systems of motorized screw jacks which function as loop supports. Each such system consists of three supports spaced at 120° intervals around the periphery of the machine. The upper support jacks travel about 1 in., whereas the lower ones travel approximately 7 in. A nonmoving loop support is achieved at the very top by an insert which reduces the nominal 1/2-in. clearance between the 19-in. loop and the 20-in. inside body diameter to $\sim$1/16 in.

Affixed to the side of the machine is the grapple-drive mechanism. The drive provides hoisting capability through two, triple-stranded roller chains which are routed to the top of the machine where they are connected to the grapple. At the drive, the chains are reeved to individual idler sprockets which in turn are anchored to load cells external to the drive housing. The load cell-to-housing fasteners incorporate a spring device which provides some measure of impact protection to the hoist system. The chains extend from the load cell idlers to the drive sprockets and continue on to the spring-loaded takeup drums. The transmission to the drive sprockets

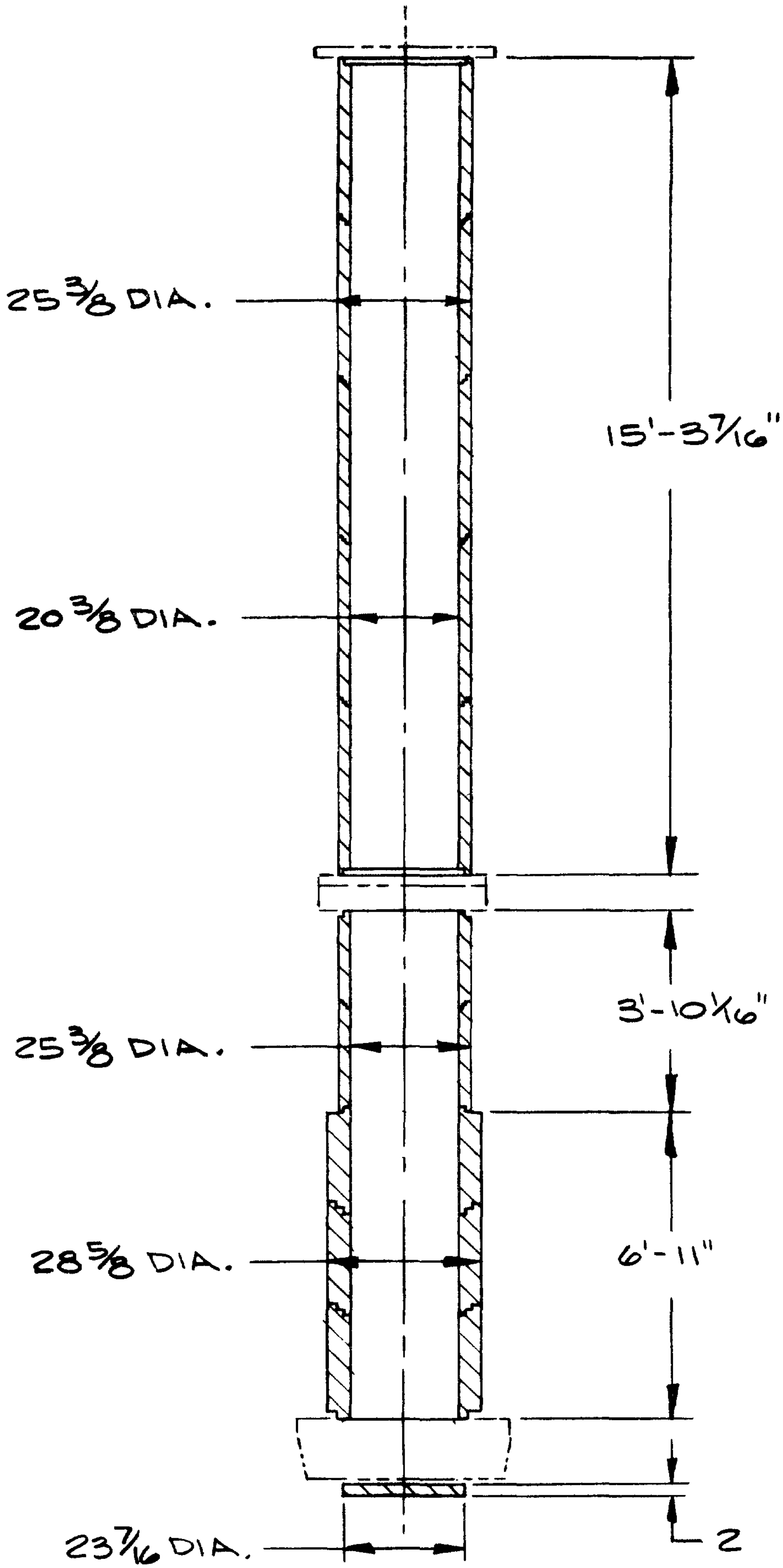

FIG. 5.14 - LHM Shielding Arrangement

includes a "No-Back" device, slip clutch, DC motor, and a manual override for motor backup. A mechanical counter, synchronized to numerically display chain payout (grapple position), is coupled to the transmission.

A thermocouple extension cable and pump power cable are rigidly wired to the top of the machine where they terminate in connectors. These connectors mate with the grapple connectors when the grapple is in its full-up position.

The transporter is a low bed trailer, jeep-rig combination, which serves as a mobile platform for the loop handling machine and its ancillary equipment. It contains a hydraulically powered cradle which can place the nested loop handling machine in either the vertical or near-horizontal positions. Hydraulically operated, overcenter clamps secure the loop handling machine to the cradle which can be secured by similar clamps to the frame of the transporter.

An engine-generator set together with the system power panel and three control consoles are packaged at the rear of the transporter. One console controls the transporter hydraulic system, the second controls power to the loop pump and heaters, and the third is used to control the loop-handling-machine hoist and support systems.

The general operational sequence for the handling system is depicted in Figs. 5.15a and b. Figure 5.15a illustrates the handling sequences during the loading and unloading of loops at the ETR. Figure 5.15b describes the handling sequences at the HFEF. In Fig. 5.15a, transit sightings and benchmarks are shown being established prior to loop irradiation to provide for the capability of remote LHM positionability at the ETR, should the need arise. The same technique can be used at the HFEF, if necessary.

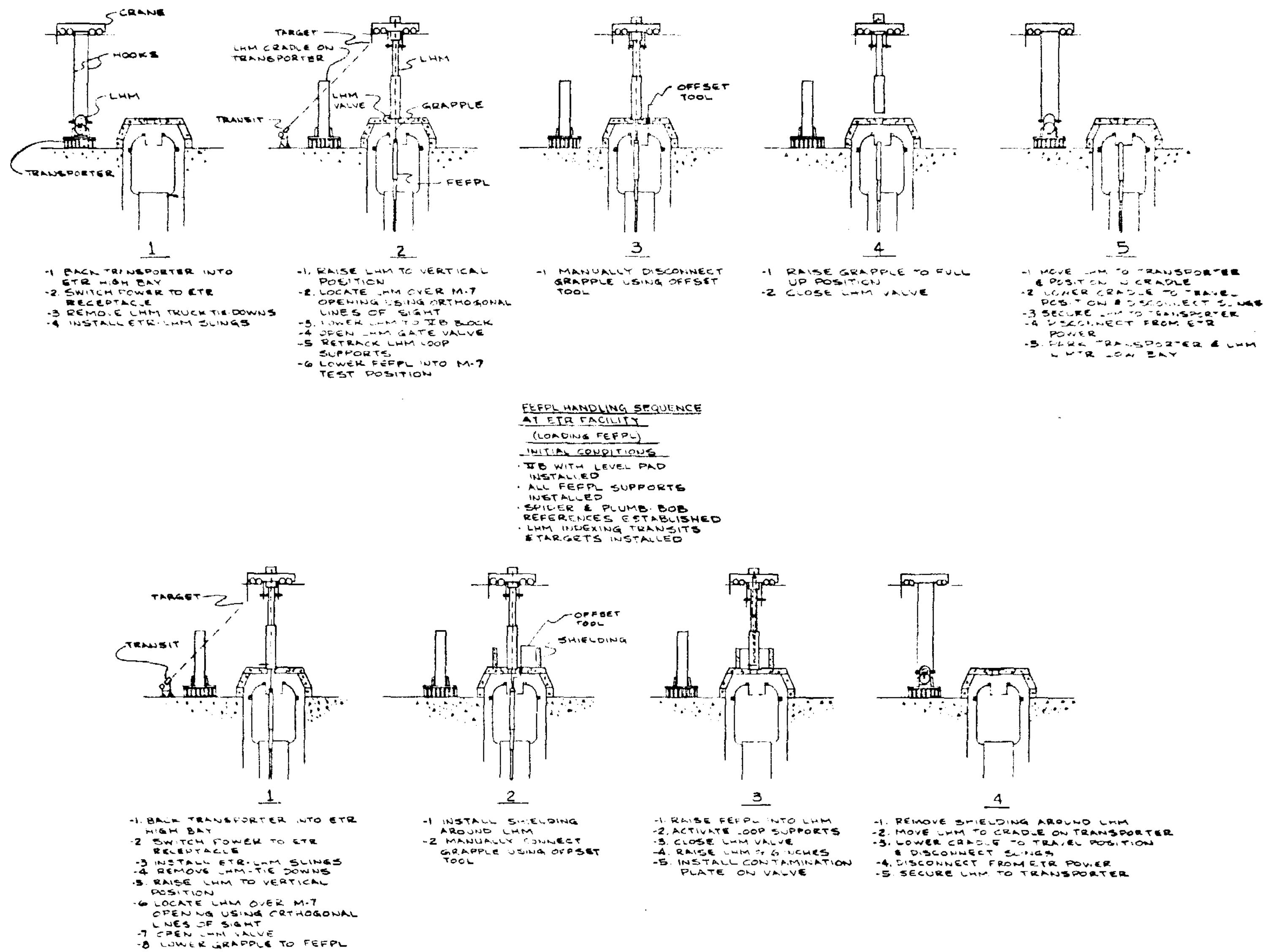

FIG. 5.15a - FEFPL Handling Sequence at ETR Facility

(UNLOADING FEFPL)
INITIAL CONDITIONS
· IIB WITH LEVEL PAD INSTALLED
· ALL FEFPL SUPPORTS INSTALLED
· SPIDER & PLUMB BOB REFERENCES ESTABLISHED

FIG. 5.15b - FEFPL Handling Sequence at HFEF

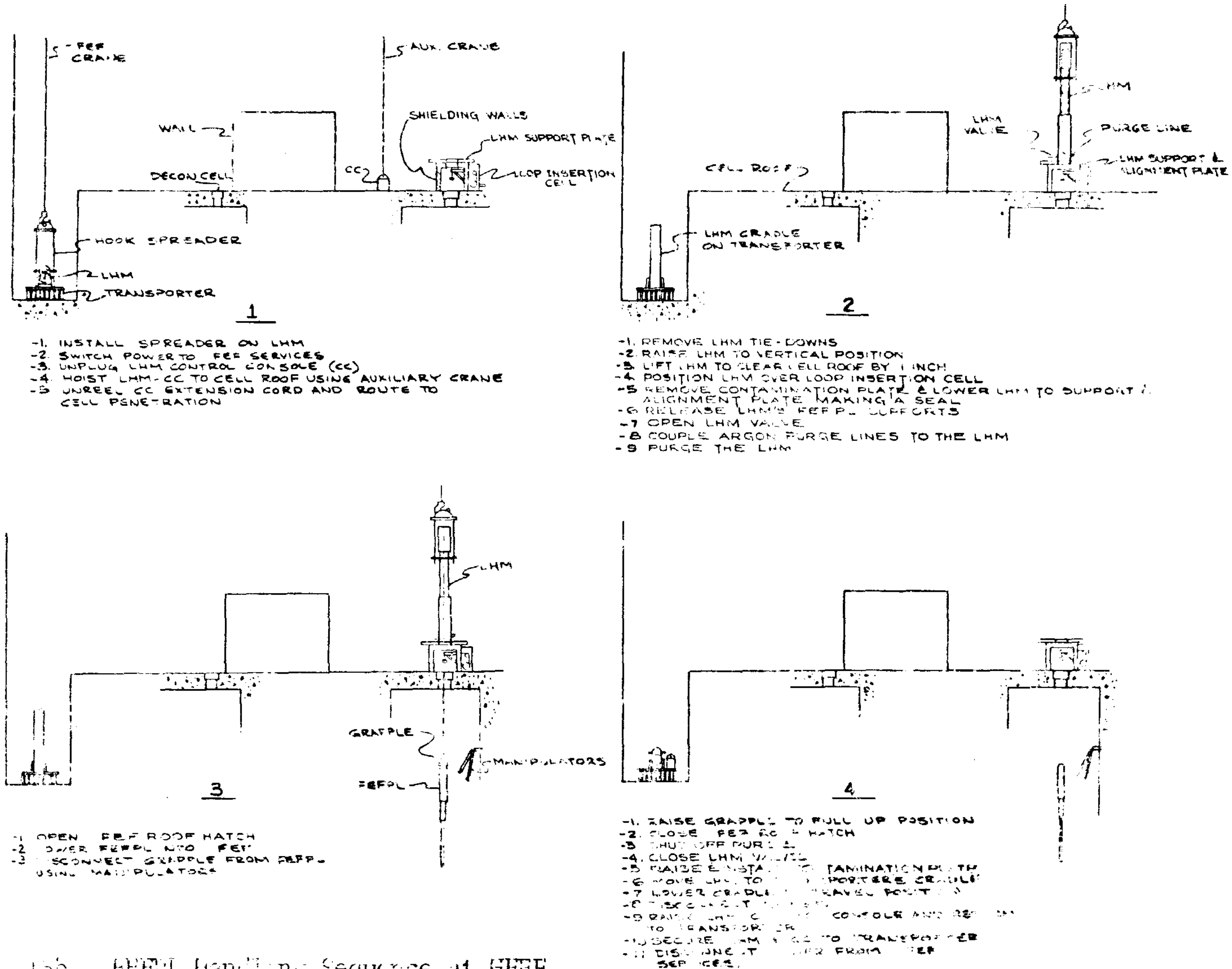

FIG. 5.15b FEFPL Handling Sequence at HFEF

5.4 Postirradiation Examination System

Functions and design requirements for the Postirradiation Examination System are specified in the SDD,[1] Section 2.4.

The Hot Fuel Examination Facilities (HFEF) has been selected as the remote-handling facility for disassembly and examination of the FEFPL. The HFEF consists of a four-cell complex. The cells to be utilized for the FEFPL are designated as HFEF-North (see Fig. 1.6). A pictorial representation of the loop in the HFEF is shown in Fig. 5.16.

The remote handling, disassembly, and examination system consists of various items which will be added to the remote handling facility to meet the requirements and functions stated above, including the following:

contamination control areas
experiment support devices
contamination control structures
cutting machines
furnaces
sampling devices
disposal systems
nondestructive and destructive testing devices

The safety aspects of these postirradiation examination procedures are outside the scope of this SAR and will be discussed in the addendum to Interim Facility Safety Report for HFEF-N, dated May 1972.

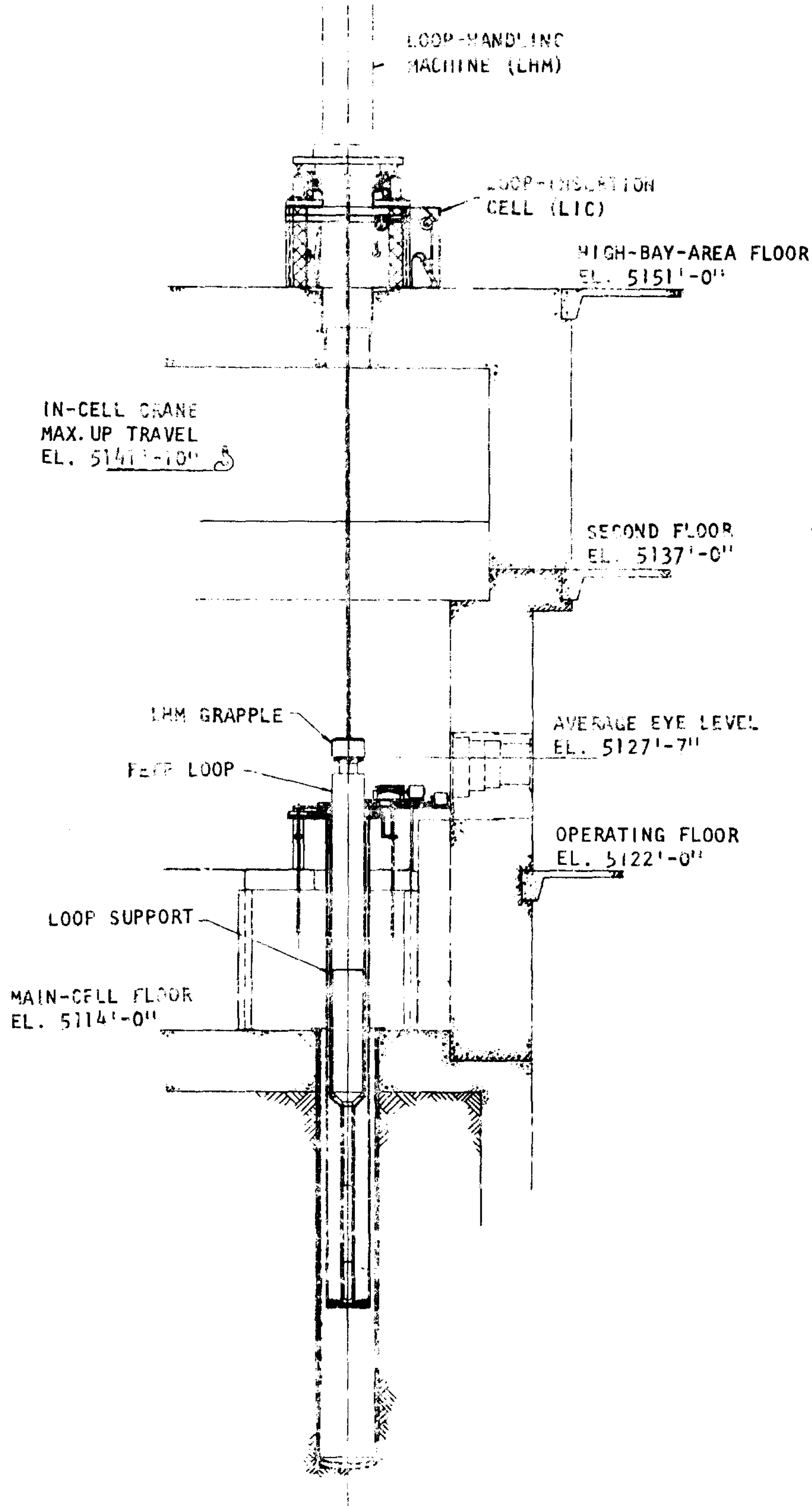

FIG. 5.16 - FEFPL in HFEF

References:

1. "System Design Description of the Fuel Element Failure Propagation In-pile Loop System," R1000-1001-SA (May 1972).

2. D. H. Lennox, et al., "In-pile Experiments for the Fuel Element Failure Propagation Loop," ANL/RAS 71-33 (October 1971).

3. W/FFTF "Engineering Test Plan for ANL FEFP Experiment P1 Fuel Pins", May 1972 - HEDL by M. K. Millhollen.

4. Guidance Statements Regarding Shipping Containers for Fissile and Other Radioactive Materials, AEC Immediate Action Directive IAD No. 0529-24 (March 23, 1971).

CHAPTER 6.0

TABLE OF CONTENTS

LIST OF TABLES

LIST OF FIGURES

6.0 Loop Operational Envelope

The EEFP Loop is designed both to meet specific performance objectives and to satisfy the ETR standards for in-reactor experiments. Within this framework, operational limits are established based upon the loop characteristics, with allowance made for an adequate safety margin plus control and measurement uncertainties. These limits define a normal operating envelope for all experiments which is independent of the design of a given test section.

Steady-state limits for loop temperature and pressure are two principal parameters fixed by the operational envelope. Upset transient events used in the design fatigue cycle analysis assume that the conditions initiate from within the operational envelope. These transient events are as specified in ANC-70008.

6.1 System Pressure Limits

6.1.1 Containment Limits

The major safety goals and safety design philosophy discussed in Chapter 3 depend in part for their implementation on the development of suitable system steady-state pressure limits. In order to insure no damage to the ETR core, systems, or structures, limits must be established beyond which the containment system must not be allowed to yield. Relation of these steady-state limits to the effects of dynamic loads is addressed in Chapters 10 and 11.

A number of approaches to the development of system pressure limits have been used. Figure 6.1 shows an idealized stress vs strain curve. The elastic portion of the curve is indicated by E_e and the inelastic (plastic) portion by E_p. The plastic portion of the curve illustrates effects of strain hardening. An alternative approach is to consider that the portion of the curve marked E_p is parallel to the strain axis, thereby taking no credit for strain hardening. To be conservative, the latter method is used here.

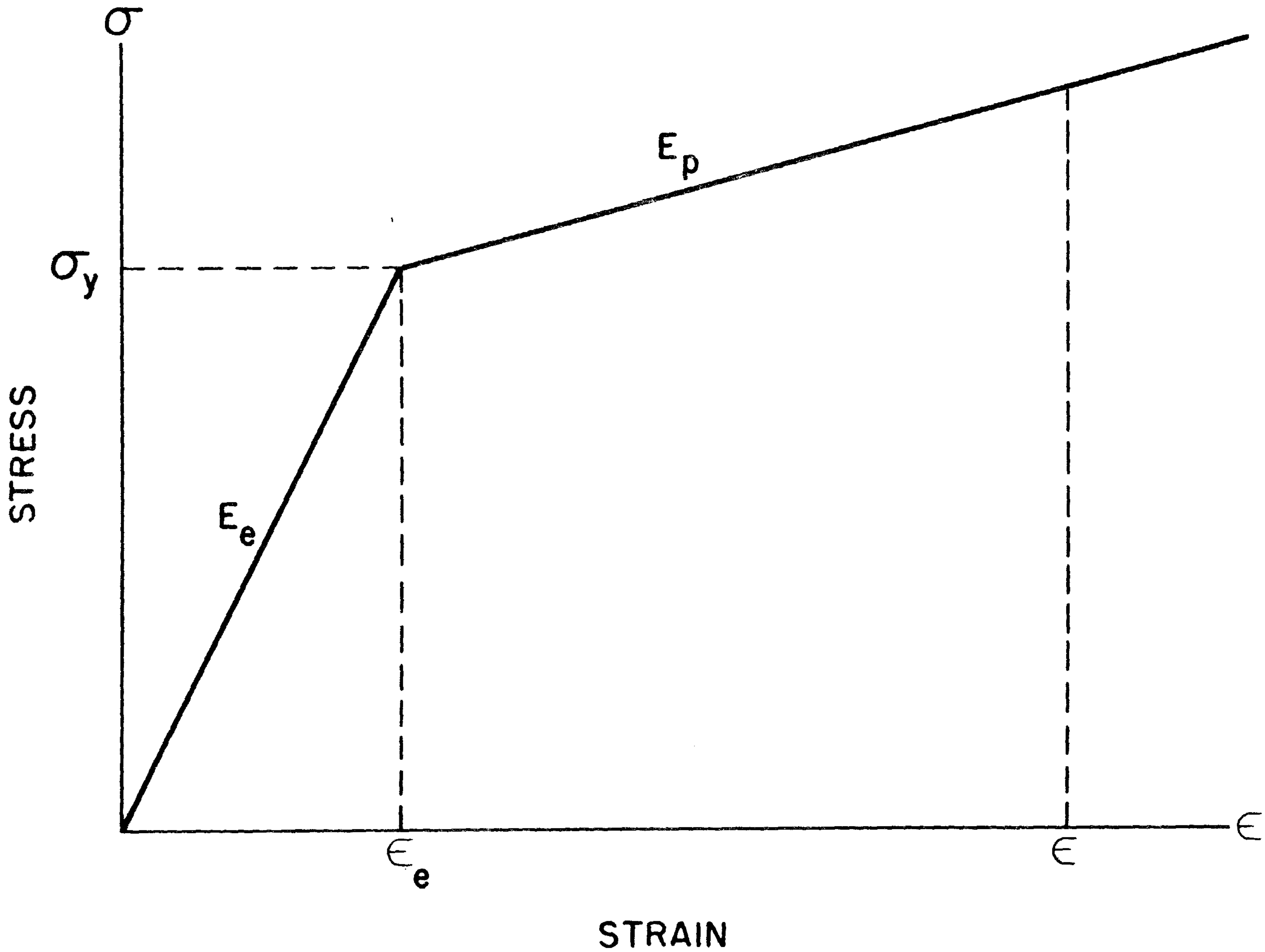

FIG. 6.1 - Idealized Stress Versus Strain Curve

The capabilities of the containment have been computed for the following cases:

a) The primary containment vessel is entirely in the elastic region and no load is transmitted to the secondary vessel.

b) The primary containment vessel is fully plastic, but no credit is taken for strain hardening and no load is transmitted to the secondary vessel.

c) The primary containment vessel deforms plastically and contacts the secondary vessel, but no load is transmitted to the secondary vessel.

d) The fully plastic primary containment vessel loads the secondary vessel but it remains entirely in the elastic region.

e) The primary containment vessel is plastically deformed and loads the secondary vessel until it is fully plastic (no strain hardening).

Although these calculations have been made assuming that the primary-secondary annulus contains only gas, assessments have been made of the potential effects of the gas flow tubes and the current concept for radial alignment pads. With respect to the former, analysis has shown that their crushing resistance is so small that associated stresses in the secondary vessel are insignificant in comparison to its yield stress. Also, the energy absorption capability of the system is essentially unaffected by the presence of the gas tubes.

The radial alignment pads locally reduce the gap dimension and could provide significant resistance to motion of the primary by stressing the secondary. However, the design is such as to minimize the possibility of gross deformation of the primary vessel occurring in that region. The pads are located at an elevation intermediate to the active fuel zone and the meltdown cup. This is an extremely unlikely MFCI reaction zone and a region of high internal strength, due to the presence of the large amounts of steel in the lower portion of the test train. Also, this additional structural material physically limits the amount of sodium locally available to quantities less than needed for an energetic MFCI. Nevertheless, it is a design requirement that this section of the loop, as well as others, meet the required energy absorption criterion without deformation of the secondary.

The capability of the loop containment system for each of the above cases is shown in Fig. 6.2 which plots allowable pressure as a function of

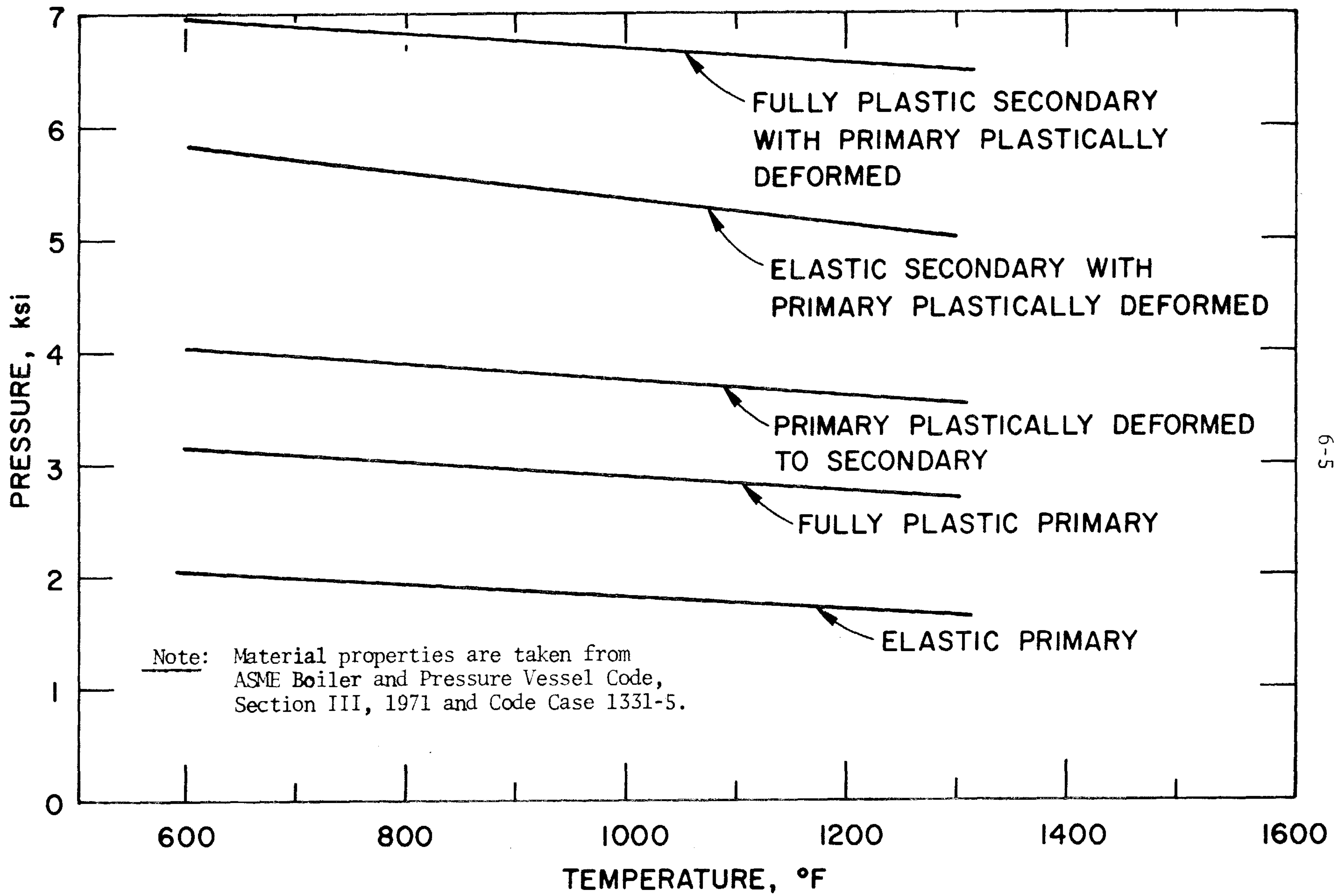

FIG. 6.2 - Capabilities of Pressure Vessel for Containment

temperature. For ease in use, key values from this curve are tabulated in Table 6.1

TABLE 6.1

Pressure Capability of Containment, psi

Temperature, °F	800°F	1100°F	1300°F
Case a	1920	1799	1670
Case b	2960	2830	2590
Case c	3890	3640	3550
Case d	5590	5220	5000
Case e	6840	6580	6500

The system pressure limits for the loop have been conservatively set, using Case b above, at 2960 psi for 800°F, 2830 psi for 1100°F, and 2590 psi for 1300°F primary vessel temperature. These values are well below the capability of the containment to prevent damage to ETR and even further below the pressures required for failure. Comparison of these limits with maximum experimental and accident conditions is discussed in detail in Chapters 10 and 11.

6.1.2 Calculational Methods

The material properties used for this study are from the following sources: The ASME Boiler and Pressure Vessel Code, Section III, 1971, and Code Case 1331-5.

NOTE: ASME Code Case 1331-5 was used in the initial FEFPL containment study as appropriate at that time and as specified in FEFPL SDD (Section 1.3.2.2). The current ASME Section III stress analysis on the in-pile loop is being performed in accordance with Code Case 1331-7 as supplemented by RDT Standard F 15-2T (see Loop Specification - ANC 70008 and SAR (Section 9.1.1.3)). Comparison of material data in the two code cases indicates equal or more conservative stress values for Case 1331-5 than Case 1331-7.

Primary Vessel

a) Elastic analysis

$$p = \frac{h}{R} \sigma_{all} \qquad (1)$$

where

p = pressure

h = wall thickness of the vessel

R = radius of the vessel

σ_{all} = allowable stress

b) Plastic analysis

The elastic-strain hardening curve is given schematically in Fig. 6.1, and the stress-strain relation beyond elastic limit is:

$$\sigma = \sigma_y + E_p (\varepsilon - \varepsilon_e) \tag{2}$$

where

E_p = hardening modulus, and
ε_e = strain corresponding to yield stress, σ_y

$$\sigma = pR/h \; ; \; \varepsilon = \Delta R/R \tag{3}$$

and ΔR is the radial displacement of the cylindrical vessel. Substituting Eq. 3 into Eq. 2, and specifying ΔR, we can compute

$$p = \frac{h}{R}\left\{\sigma_y + E_p\left(\frac{\Delta R}{R} - \varepsilon_e\right)\right\} \tag{4}$$

An alternative approach is to assume the vessel as a thick-walled cylinder of elasto-plastic material (without hardening).

When the vessel reaches full plasticity, the internal pressure is expressed as:[1]

$$p = \frac{2}{\sqrt{3}} \sigma_y \ln \frac{R_o}{R_i} \tag{5}$$

where R_o and R_i are the outer and inner radii of the cylindrical vessel.

Spherical Cap

a) Elastic analysis

$$p = \frac{2h}{R} \sigma_{all} \tag{6}$$

b) Plastic analysis

By specifying ΔR, we can obtain

$$\sigma_{\Delta R} = \sigma_y + E_p\left(\frac{\Delta R}{R} - \varepsilon_e\right) \tag{7}$$

The allowable pressures for the spherical cap in all cases exceed those for the cylindrical vessel; hence, the values in Table 6.1 are given for the cylindrical vessel only. Reduction in allowable stress at weldments in stainless steel is no greater than ten percent; in the FEFPL design this is compensated for by added material at weld locations that may experience high loads.

6.2 System Temperature Limits

6.2.1 Steady-state

The steady-state design temperature limits for the FEFP loop have been established, based upon (1) experimental requirements, (2) the performance capabilities of the heat exchanger, (3) the permissible thermal stresses, and (4) loss of strength with temperature.

It should be noted that the design limits exceed those for normal operation of the loop in order to provide an adequate margin for conduct of experiments. The experimental conditions will conform to the normal operating limits, as delineated in the SDD. However, for the purposes of safety analyses, loop design limits have been used to demonstrate that even under these most adverse limiting conditions safety is assured at all times. These steady-state design thermal limits are:

a) a minimum sodium outlet temperature from the heat exchanger of 450°F

b) a maximum sodium outlet temperature from the heat exchanger of 850°F

c) a maximum temperature differential between heat exchanger inlet and outlet sodium of 500°F

d) a maximum sodium inlet temperature to the heat exchanger of 1100°F.

The bases for establishing these temperature limits are presented below.

Minimum Sodium Temperature from Heat Exchanger

A sodium temperature of 450°F at the outlet of the heat exchanger has been selected as the minimum system operating temperature, based on heat exchanger and heat rejection characteristics and on sodium plugging conditions. Loop operation at this minimum 450°F sodium temperature will permit a maximum heat-rejection rate of 1.25 MW at a sodium inlet temperature to the heat exchanger of 950°F. This 1.25 MW heat rejection rate at the 500°F maximum sodium temperature difference in the heat exchanger exceeds the heat removal requirement for all currently planned experiments. During the loop filling procedure, the sodium will be circulated and purified to an oxide content of < 10 PPM at 900°F, perhaps reaching a plugging temperature as low as 260°F. The 450°F minimum system operating temperature is well above the 208°F sodium melting temperature, the 260°F plugging temperature or even the 388°F sodium plugging temperature corresponding to a 10 PPM oxide content. Operating at this minimum temperature presents no safety or operational problems from sodium freezing or plugging in the loop during normal operation, shutdown, or reactor scram. Vessel temperatures at this steady-state operating condition are low, with a primary vessel temperature of only 683°F.

Maximum Sodium Temperature from Heat Exchanger

The maximum sodium outlet temperature from the heat exchanger has been established as 850°F. This limit is set to keep the primary vessel temperature (with sufficient margin) below the 1300°F design temperature limit. Above 1300°F, the allowable stresses are not defined in Code Case 1331-5, but the strength of stainless steel decreases rapidly with increasing temperature. At this temperature, Fig. 6.2 indicates a pressure limit for the primary vessel of ∿ 2600 psi. At the highest temperature loop operating conditions (1100°F sodium inlet temperature to the heat exchanger; 850°F sodium outlet temperature from the heat exchanger) the maximum primary-vessel temperature is 1050°F at the core midplane. Even with an assumed 50°F uncertainty associated with this temperature value, this provides a 200°F temperature margin. This margin is sufficient to perform the experiments safely and to prevent excessive primary-vessel temperatures from occurring during accident situations.

Maximum Temperature Differential for Heat Exchanger

A maximum sodium temperature differential across the heat exchanger (inlet and outlet) of 500°F has been set to limit the thermal stresses within the heat exchanger. Detailed stress analyses will be provided to show that the thermal expansion and stresses for the heat exchanger are well within acceptable limits at this upper operating condition.

Maximum Sodium Inlet Temperature to Heat Exchanger

The maximum sodium inlet temperature to the heat exchanger has been established at 1100°F. This limit is set to insure a suitable operating margin below the 1300°F design limit. As the heat exchanger is far removed from the gamma field emanating from the core region, no internal hear generation will occur in the heat exchanger region. Metal temperatures in the heat exchanger will, therefore, be no higher than this 1100°F limit during steady-state operation with a 200°F temperature margin for transients.

6.2.2 Loop Operating Temperature Envelope

The loop is constrained to operate within a system temperature envelope defined by the design temperature limits described in the previous section and by the peak sodium and helium mass flowrates. Fig. 6.3 illustrates the system temperature envelope, presented as a function of the heat exchanger inlet and outlet temperatures, for steady-state loop operation at 1.0 MW. This envelope (enclosed within points A, B, C, D, E, and F) is formed as follows:

Bound	Limitation
A-B	500°F maximum sodium temperature difference for the heat exchanger
B-C	1100°F maximum sodium temperature into the heat exchanger
C-D	850°F maximum sodium temperature from the heat exchanger
D-E	150 gpm total loop flow
E-F	1.59 lb/sec maximum helium flow
F-A	450°F minimum sodium temperature from the heat exchanger

A helium inlet temperature of 150°F was assumed in developing this envelope.

The operating-temperature envelope shows that a wide range of helium and sodium flows is possible at the 1.0 MW operating condition. A similar latitude exists in the range of loop flows for other power levels, as illustrated in Fig. 6.4. The limitations forming the envelopes described in Fig. 6.4 are identical to those described above for loop operation at 1.0 MW. Operation of the loop from zero power to a maximum heat rejection capability of 1.65 MW (point G in Fig. 6.4) is allowable within the steady-state temperature design limits of the loop. Steady-state operation within the range of conditions described by the operating temperature envelopes in Fig. 6.4 is safe and provides a large margin to accommodate the transient temperature perturbations of experiments. These margins are discussed below.

6.2.3 Loop Operating Temperature Margins

The THYME-B computer code (Section B.1, Appendix B) was used to determine the peak primary and secondary vessel temperatures at various steady-state loop operating conditions. Vessel temperatures were evaluated at the operating conditions A, B, G, and C shown as the upper bounds for

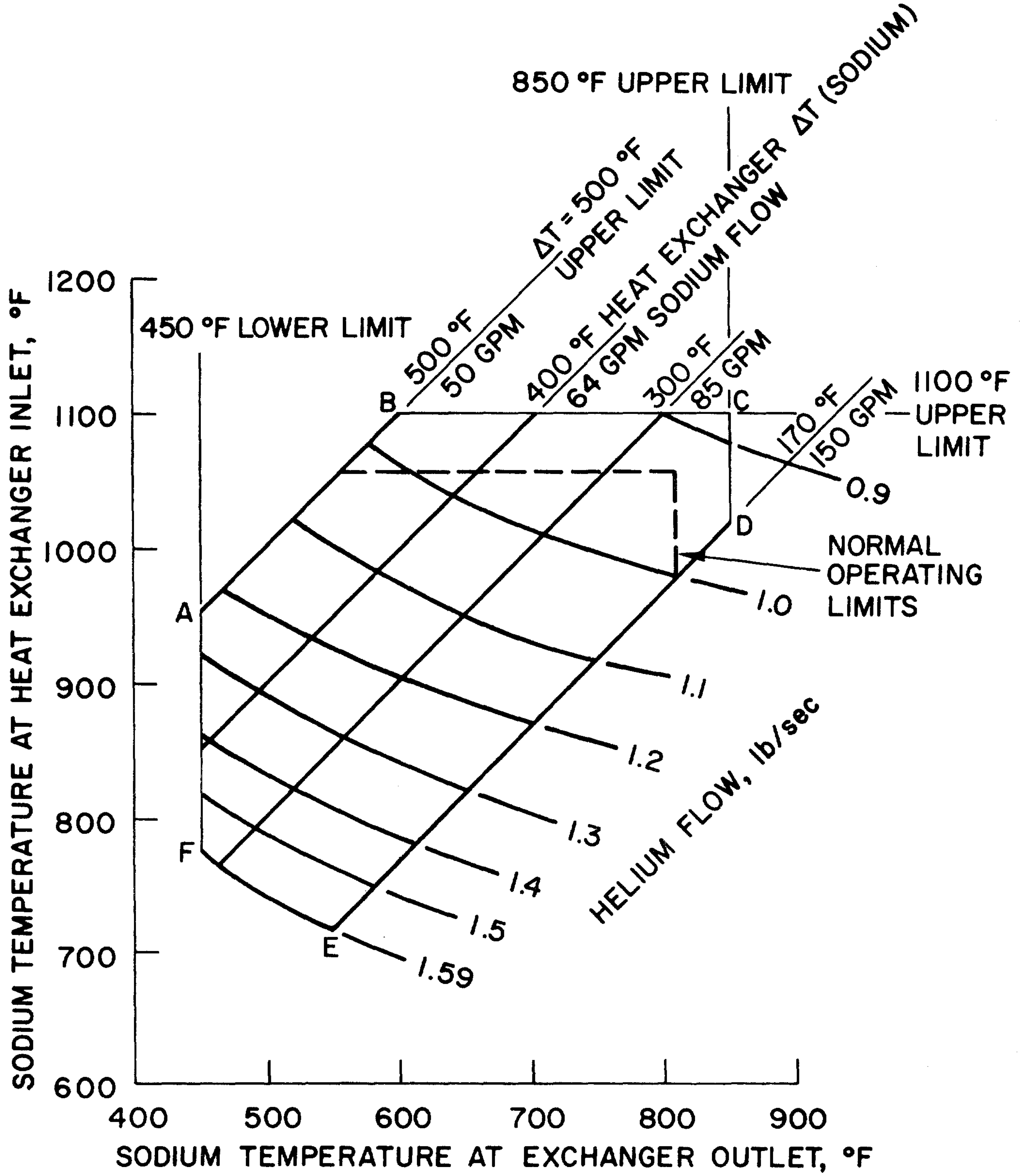

FIG. 6.3 - Heat-exchanger Inlet and Outlet Temperatures for Various Helium and Sodium Flow at a Total Loop Power of 1.0 MW

the system steady-state operating envelope in Fig. 6.4. Vessel temperatures at other loop power levels and operating conditions will be no higher than the temperature determined at this upper operating line. In this study, the maximum power levels possible for the test section at these conditions were used; the results are shown in Table 6.2. An assembly containing 37 full-length FTR fuel elements was used for the calculations. Smaller array sizes at equivalent sodium conditions would result in slightly lower vessel temperatures due to the smaller hex can. The test section bypass flowrate was adjusted in each instance to obtain the maximum steady-state loop thermal conditions of 1300°F from the test section and 1100°F at the heat exchanger inlet. The heat exchanger performance characteristics were also ajusted to obtain the maximum 500°F sodium temperature differential through the heat exchanger.

Recommended average gamma heating rates at the core midplane for loop design are 9.4 W/gm in the primary vessel and 11.5 W/gm in the secondary vessel for the ETR operating at 175 Mw and the FEFPL at 1.8 Mw.[2] For engineering design conservatism, these heating rates include a 25% margin above the calculated expected values. Since the gamma heating may vary slightly around maximum expected values due to possible flux tilting, reactor overpower or flux shift over the core lifetime, additional conservatism was used in the loop transient analysis and in the establishment of PPS trip point settings. The THYME-B calculations were therefore based upon equivalent average values at the core midplane of $\sim$ 18 W/gm in both vessels, thereby providing a generous margin of safety in calculating temperatures of the sodium and containment vessels.[3]

Figure 6.5 presents the FEFPL operating and safety temperature margins for the thermal conditions of the operating envelope. These margins are presented in terms of the average primary-vessel temperature versus the sodium temperature at the heat exchanger outlet.

The safety setpoint line has been established at a primary-vessel temperature of 1200°F with a temperature measurement uncertainty of ± 25°F (± 2% of reading). This provides a 75°F minimum safety margin before the design safety limit of 1300°F is reached. This 75°F minimum safety margin is more than adequate to prevent the primary vessel from exceeding the 1300°F design safety limit. At a peak, radial average gamma heating rate of 18 W/gm in the primary vessel, it would take about 1.3 sec for the vessel

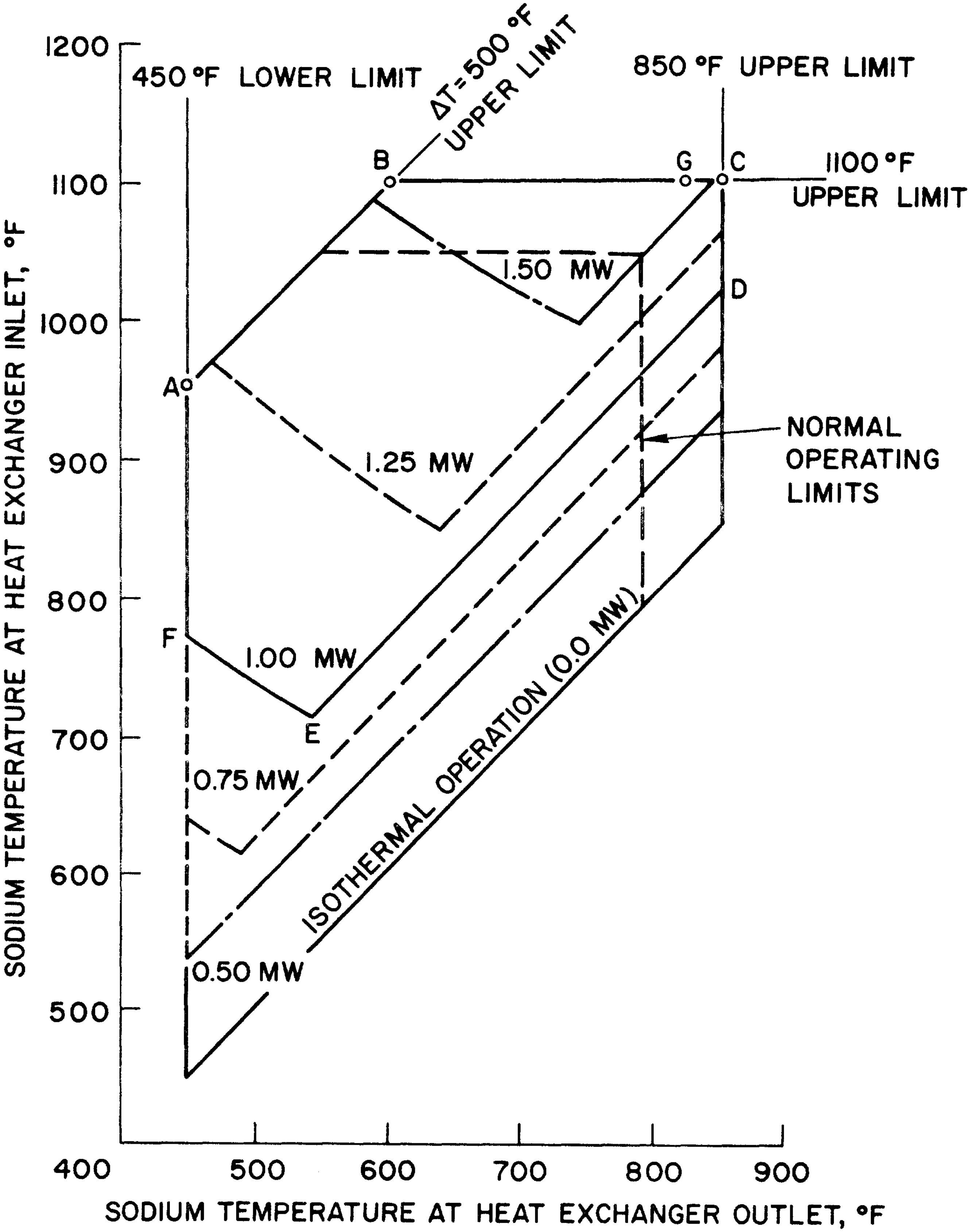

FIG. 6.4 - FEFP Loop System Steady-state Design Operating Temperature Envelope

TABLE 6.2

Summary of System Steady-state Operating Temperatures
at Upper-bound Operating Envelope Conditions *

	Heat-exchanger Conditions						Test-section Conditions				Max Vessel Temp	
	Heat Removal (kW)	He Flow (lb/sec)	Na Flow (lb/sec)	Na Inlet Temp (°F)	Na Outlet Temp (°F)	He Inlet Temp (°F)	Na Flow (lb/sec)	Assembly Power (kW)	Na Outlet Temp (°F)	Na Inlet Temp (°F)	Primary (°F)	Secondary (°F)
Point A	1235	1.59	7.56	950	450	150	3.86	935	1300	546	683	625
Point B	1552	1.59	9.51	1100	600	150	6.20	1230	1300	681	825	628
Point G	1652	1.59	18.28	1100	825	150	9.37	1277	1300	874	1029	631
Point C	1499	1.38	18.28	1100	850	150	8.90	1146	1300	897	1052	632

* Gamma heating in loop materials may vary slightly around the maximum expected values due to possible flux tilting, reactor overpower or flux shift over the core lifetime. A value of 18 watts/gm is used as an arbitrary value for calculations shown in this table in order to provide a generous margin of safety.

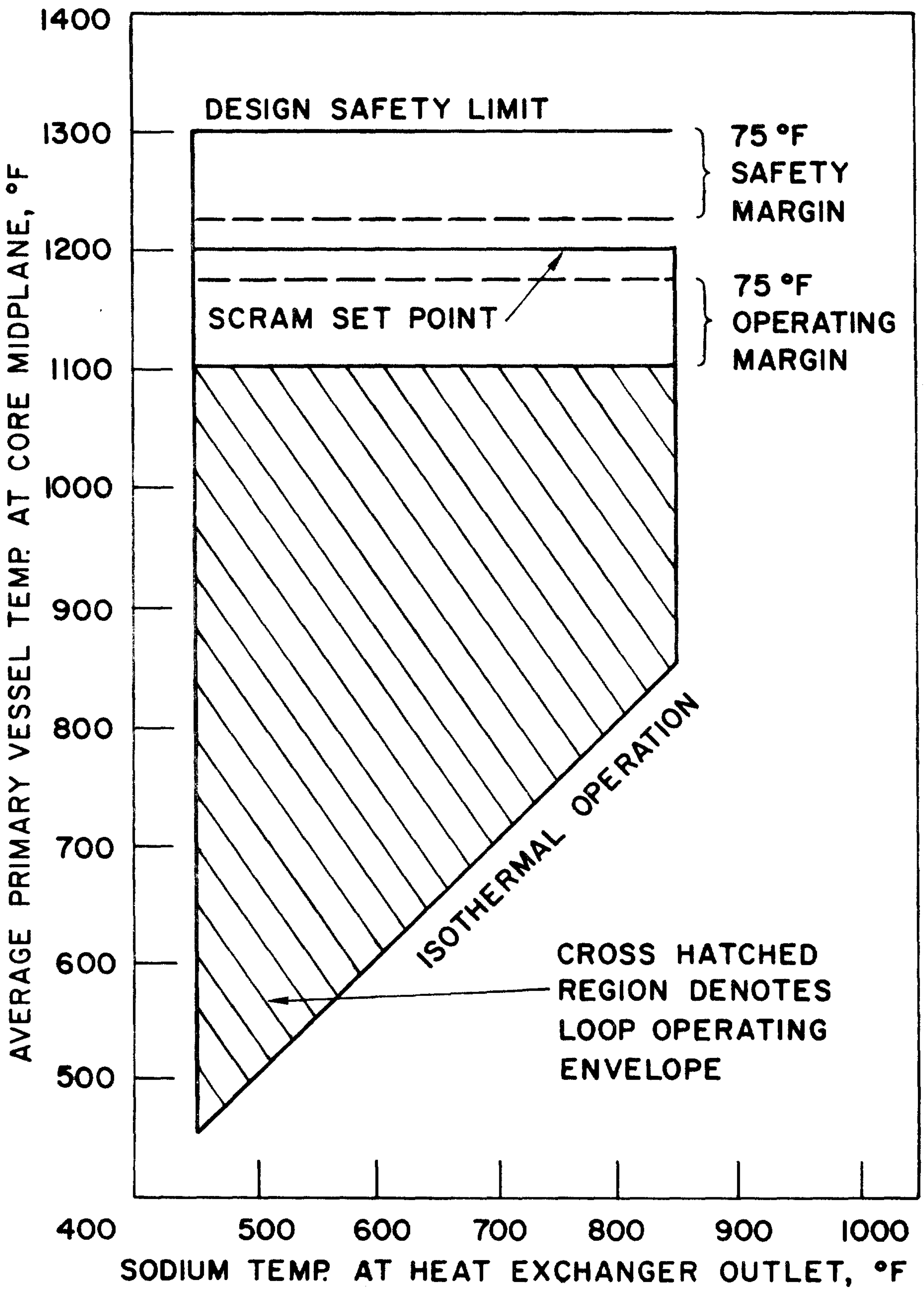

FIG. 6.5 - FEFPL Temperature Margins

temperature to increase 75°F, assuming that the vessel heating is adiabatic. As the ETR scram time is approximately 0.3 sec, the reactor would have been shut down well before this 1300°F safety temperature limit is reached. The adiabatic heating rate overstates the actual vessel temperature rise because the primary vessel is in direct contact with the loop sodium and thus would be cooled.

As Fig. 6.5 indicates, a minimum operating margin of about 75°F is present in the design. This minimum margin occurs at the highest outlet sodium temperature from the heat exchanger and should be sufficient to perform the high-temperature experiments without premature reactor scram.

The design basis for a PPS protective function which monitors vessel temperature is discussed in Section 7.1.3.3. This function is based on the outside wall temperature (the monitored variable) and takes into account worst case gamma heating effects. The diagram presented above is based on average wall temperature (critical plant variable), and the numbers presented are derived from the protective function design basis.

6.3 ETR Experimental Standards

Experimental standards have been established within which experiments may be operated in the ETR.[4] These standards are reproduced below with an additional paragraph discussing the capability of the FEFP loop design and operation (compliance) to meet each specification.

6.3.1 Void Reactivity Limits

Objective: The objective in limiting experiment void reactivity is to prevent power excursions beyond the limits determined as safe in the analysis of neutron level subsystem. This objective applies to initiation of an excursion and to aggravation of an excursion already in progress.

Throughout the ETR Technical Specifications,[4] administrative controls have been imposed to limit potential sources for accidental reactivity additions. These limitations have been established such that allowance has been made for potential positive reactivity feedback from loop experiments during an accident excursion. The maximum positive-feedback value permitted has been set at 0.15% $\Delta k/k$, instantaneously applied. However, additional analyses were performed to identify those ramp or delayed ramp feedbacks which are equivalent to the instantaneously applied value. The feedback equivalences, determined from analyses of ramp and step accidents and applied when the power first exceeded 1.5 times full power, are stated in Subsection 3.2 of the ETR Technical Specifications.[4] It is only necessary that one of the requirements be met, to establish that all equivalent kinetic responses are consistent with the limits of these specifications.

Specifications: All experiments must meet the following specifications:

The maximum reactivity worth of removing all coolant from an experiment shall not be greater than 0.75% $\Delta k/k$.

The maximum positive reactivity feedback during a reactor excursion of 124 MW/sec (above 1.5 times full power) shall meet one or more of the following requirements for all loop experiments considered together:

(1) The instantaneous positive feedback during the stated excursion shall not exceed +0.15% $\Delta k/k$.

(2) The positive feedback during the stated excursion shall not exceed 1.125% $\Delta k/k$ entered at a rate of 3.75% $\Delta k/k$/sec beginning when the reactor power reaches 1.5 times full power.

(3) The positive feedback during the stated excursion shall not exceed 1.125% $\Delta k/k$ entered at a rate of 15% $\Delta k/k$/sec beginning 48 msec after the reactor power reaches 1.5 times full power.

Compliance: In this SAR, the intent of the specifications is met by broadly interpreting the specifications to mean all potential sources of positive reactivity feedback. These potential sources of positive feedback are examined in Section 10.5; they include loss of sodium coolant, fuel compaction radially outward, and fuel meltdown. The calculations indicate that the specification is met. In addition, the effects of the postulated reactivity excursion on the loop cadmium filter, containment vessel, and experimental fuel elements are shown in Section 11.6.1 to be acceptable.

In addition, studies were made to determine the effect of reduced initial ETR power levels on transient conditions. These parametric studies were performed in support of the ETR Technical Specifications[4] and they conclude that the total energy release always decreases as the initial power decreases; therefore, the damage potential of a step reactivity accident also decreases as the initial power decreases.

6.3.2 Heat Transfer Limits

Objective: The objective of the experiment heat transfer technical specification is to identify limiting heat-transfer conditions for safe and reliable operation of experiments in the ETR which depend upon the ETR primary coolant system for cooling.

Specifications: These specifications apply only to those experiments to be inserted in the ETR which are in contact with and depend upon the ETR primary coolant for heat transfer.

For each of the following abnormal reactor conditions, the heat transfer specifications below shall be met.

Abnormal Conditions:

. 0.48 times normal flow; power and pressure are normal

. 1.25 times full power; flow and pressure are normal

. 140 psig inlet pressure; power and flow are normal

Heat Transfer Specifications:

The hot spot heat flux shall be three standard deviations or more (a probability less than 0.14%) away from the departure from nucleate boiling (DNB), or the hot spot DNB ratio (ratio of DNB heat flux to hot spot heat flux) shall not be less than two.

The hot track coolant exit temperature shall be three standard deviations or more away from flow instability, or the ratio of temperature rise for flow instability at the channel exit over the hot track coolant exit temperature rise shall not be less than two.

Compliance: The primary sodium coolant of the FEFP in-reactor loop is not in direct thermal contact with the ETR primary coolant and is at all times doubly contained. The loop depends upon the ETR primary coolant for heat transfer from the secondary or outermost containment vessel and cadmium filter, due principally to the gamma heating in the secondary vessel over the three foot active axial section. For this situation an analysis was made of DNB and flow instability ratios. The DNB calculation was made using the correlation of Gambill.[5] The results were as follows: The hot spot (axial center of the active section) DNB ratio (ratio of DNB heat flux to actual hot spot heat flux) was 11, and thus complies with the specifications. For flow instability, the ratio of the temperature rise which would produce flow instability (based on a coolant temperature rise 80% of the way to saturation) to the actual water temperature rise was 214/13.4, or a ratio of

16, and so complies with the specifications.

In addition, a statistical heat transfer analysis was performed to further demonstrate compliance with the specifications.[6] The following assumptions were employed in the calculations:

1) Gamma heating as outlined in Ref. 2.
2) All of the heat generated in the secondary vessel and 42% of the heat generated in the aluminum core filler piece flows into the cooling water annulus. The 42% value was arrived at by assuming that heat generated in the core filler piece would split in proportion to inside and outside surface areas,
3) The loop is located eccentrically in the core filler piece so as to be touching the top and bottom centering spline on one side thereby generating the hot track or strip,
4) The hot spot is located 3 inches below the core centerline and coincident with that point both the loop and the filler piece have dimensions based on the worst combination of machine tolerances,
5) There is no cross flow mixing along the hot stripe as pertaining to heat transfer, but there would be circumferential equalization of pressure since the total differential pressure must conform to the reactor differential pressure.

Based upon current design of the core filler piece, results of the analysis demonstrates compliance with the specifications as shown in Table 6.3.

TABLE 6.3

Statistical Burnout and Flow Instability Data for the FEFP Loop

Reactor Conditions	Standard Deviations to Critical Heat Flux	Standard Deviations to Flow Instability
Normal Power, Flow and Pressure	3.9	15.0
48% of Flow, Normal Power and Pressure	3.6	7.3
125% of Full Power, Normal Flow and Pressure	3.7	12.0
140 psig Inlet Pressure, Normal Power and Flow	3.7	13.1

6.3.3 Containment Requirements

Objective: The objective of the ETR experiment containment requirements technical specifications is to assure safe and reliable operation of experiments in the ETR.

Specifications: If the ETR primary coolant system can reasonably be expected to be radioactively contaminated to more than 200 μCi/ml by breaching of an experiment, double containment shall be required.

If an experiment contains corrosive, reactive, or explosive materials, sufficient safety analysis shall be provided to the proper ANC review groups to show that the safety and reliability of the ETR are not compromised.

Compliance: The FEFPL provides double containment to meet the requirements of this specification.

6.3.4 Gas Leakage Limits

Objective: The objective of this specification is to define the gas leak rate that can be tolerated without compromising the ETR fuel element heat transfer or without causing unacceptable reactivity effects.

Specifications: Leak monitoring and protective subsystems shall be provided for experiments with a potential gas leakage rate into the reactor vessel of more than 80 standard cubic feet per minute. The reactor shall be shut down if the leakage of gas into the reactor vessel and through the core from any experiment in the ETR exceeds 2.2 standard cubic feet per minute, which is equivalent to a rate of one 220 standard cubic foot gas bottle every 100 minutes.

Compliance: The Annulus Gas System (AGS) performs three basic functions which are, to monitor the integrity of the primary and secondary tubes and the helium heat exchanger, to provide backup cooling if required for the lower 10 in. of the primary tube when the fuel meltdown cup contains molten fuel, and to provide a method of reducing the heat loss from the loop during periods when the pump is unpowered (transfer operations).

The containment is verified by a static pressure system. Gas flow into and out of the system occurs during temperature and pressure changes. Leaks through either the secondary or primary vessel are indicated by a continuing flow of gas required to maintain a constant pressure in the annulus. The gas flow will be continuously monitored and cause reactor scram at a trip level set well below 2.2 SCFM. For further discussion of the AGS and associated PPS design and functions, see Sections 5.2.3.3 and 7.1.3, respectively.

6.3.5 Reactivity Standards

Objective: It is postulated that the sudden shift of an experiment or a part thereof can result in a reactivity accident. The reason for the setting of experiment reactivity standards is to prevent accidental reactivity additions beyond the limits determined as safe in the analysis of neutron level subsystems.

Specifications: Except as specified below, the absolute reactivity worth for any movable experiment or movable experiment holder and its contained experiments shall not exceed 0.75% $\Delta k/k$ (1\$). Experiments with greater reactivity worth may be inserted provided that positive seating is assured and proper positioning of the experiment is verified consistent with the requirements specified for fuel elements (see Specification 2.1 of Ref. 4).

Compliance: The loop has a reactivity worth greater than 0.75% $\Delta k/k$, the maximum allowable for a movable experiment. The bulk of it is negative reactivity contained in the cadmium filter, which extends 0.5 ft above and below the core. Hence, a method to insure positive seating and proper positioning of the loop is required.

Supporting structures are located within the ETR to guide the loop during insertion and to hold the loop in position while the top closure is being mated and sealed to the recessed head or well. A spring-loaded ring supported from arms hung on the experiment hangers provides a seat into which the loop is lowered. A shoulder at the top of the pump region (see Fig. 1.1) rests on the ring when the loop is fully inserted and during the time the seal is installed. However, as the seal-ring bolts at the top of the loop are tightened, most of the loop weight is transferred to the support well. The travel of the springs in the seat ring is designed to accommodate the differential thermal expansion between the loop secondary vessel and the ETR vessel during operation. The loop is restrained laterally at three points: (1) the guide tube and grid adapter around the lower end of the loop in the core region; (2) the ring above the pump; and (3) the well in the ETR core.

A procedure consistent with specification 2.1.4 of Ref. 4 requires that prior to startup, two elevation measurements shall be performed for the express purpose of identifying that the experiment is properly positioned and seated. These measurements must be independent of one another, and shall be exclusive of the initial insertion and visual verification of seating. Of course, no repositioning will occur during reactor operation.

Loss of cadmium filter is not considered credible. The cadmium filter design is discussed in Chapter 5. The temperature of the filter is always less than the melting point of the cadmium. This is guaranteed by meeting the design specification for heat transfer from the FEFPL secondary vessel.

6.4 Compliance with System Pressure and Temperature Limits

Loop steady-state pressure and temperature limits, defined in Section 6.1 and 6.2, respectively, and in the SDD were established to develop an operational envelope that provides an adequate margin of safety for all conceivable operating conditions. In Chapters 10 and 11, loop safety is demonstrated for specific transient conditions that may be caused by either planned experiments or accidental events, particularly those of such severity that will cause activation of the EAS and/or PPS system.

The desired steady-state experimental conditions will conform to the loop normal operating limits, as delineated in the SDD. In addition to providing input to the control system, the EAS and PPS, loop instrumentation will monitor and provide information to the operator needed to assure that the desired conditions are being maintained.

6.4.1 Compliance with System Temperature Limits

In the event that significant temperature deviations occur, the control system is designed to automatically restore the set point value. If the control system is unable to provide the desired corrective action, either automatically or by manual adjustment, a scram will be effected. The scram may be automatic, caused by exceeding trip point settings for the EAS or PPS, or manual. If any of these measures prevent all system temperature limits from being exceeded, power operation of the loop may be continued or resumed since its functional and containment capability has been preserved. A decision to continue the experiment will be based upon studies to determine the cause of the abnormality, feasibility of preventing re-occurrence and/or assessment of consequences should it reoccur.

If corrective actions fail to prevent one or more design temperature limits from being exceeded, power operation will not be permitted, pending results of a detailed investigation focused upon determining the safety status of the loop. If the results are positive, i.e., all critical system components are functional, the cause of the abnormality is identified and its re-occurrence eliminated, and the containment margin is preserved, reactor startup and power operation of the loop will resume. If these conditions are not met, return to power will not be permitted and the planned experiment terminated.

6.4.2 Compliance with System Pressure Limits

Protection against exceeding the loop design pressure limits is assured through PPS action, with trip points set well below limiting values. As specified in the SDD, the loop internal pressure limit is 300 psi for normal steady-state operation, which is well above the expected value. Nevertheless, an automatic scram will occur should there be an indication of a significant pressure rise above the desired experimental value. This is accomplished through Protective Function (E), described in detail in Section 7.2.6. of Chapter 7.

The system pressure limits cited in Section 6.1.1 of this Chapter are static equivalents that are related to dynamic loads that may be caused by fuel-coolant interactions during planned or inadvertent transients. These limits are well above the best assessment of MFCI values, described in Section 10.2.1 of Chapter 10. However, in the unlikely event that pressure levels should approach these design limits, an automatic scram will occur. This is accomplished through Protective Function (D), described in Section 7.2.5 of Chapter 7.

If a scram occurs through activation of either of the above cited protective functions, and it is desired to return to power operation, the shutdown state must be maintained until it can be demonstrated that the containment margin is preserved. This will involve an investigation to determine the cause of scram, including an assessment of whether it was spurious as might result from a high level pressure spike of negligible energy, or the occurrence of instrument noise sufficient to effect a trip. The investigation would also involve a detailed study to determine the functional state of critical components and the state of the containment, viz., that integrity is preserved and no permanent deformation occurred. If the results of the investigation provides assured safety for continued operation, power operation may be resumed. Otherwise the experiment will be terminated.

References:

1. O. Hoffman and G. Sacks, Introduction to the Theory of Plasticity for Engineers, McGraw-Hill Book Co., Inc., New York, (1953).

2. R. C. Young, J. K. Kunze, T. E. Young, and A. W. Brown, "Recommended Nuclear Specifications for FEFPL,"Aerojet Nuclear Co., Internal Report - CI-1246, (October 1972).

3. ANL Internal Memorandum, "Review of Containment Vessel Temperatures," W. A. Bezella, (July 13, 1972).

*4. "ETR Technical Specifications," Aerojet Nuclear Co., CI-1233, (February 1972).

5. "Generalized Prediction of Burnout Heat Flux for Flowing, Subcooled, Wetting Liquids," Ch. Eng. Prog. Symp. Series, 59 (41): 71-87, W. R. Gambill, (1963).

6. ANC, EDF No. 833 Supplement 1, "Asymmetric Cooling Water Effects Analysis," F.O. Haroldsen, (July 13, 1973).

*Under Revision

CHAPTER 7.0
TABLE OF CONTENTS

LIST OF TABLES

LIST OF FIGURES

7.0 FEFPL Plant Protection System

7.1 Functions and Requirements

7.1.1 System Function

The FEFP loop is designed to operate safely in the ETR without endangering the reactor, reactor operating personnel, or the general public. The basic approach to assuring FEFPL safety is detailed in Chapter 3, Safety Philosophy. The loop design establishes multiple lines of defense which include:

- Double Containment System
- FEFPL Plant Protection System (PPS)
- Experiment Assurance System (EAS)
- Loop Control System

A primary line of defense for the protection of the public and the plant is the FEFP loop double containment system. It is a redundant vessel system which provides passive protection for the public and the plant that provides an additional margin of safety over and above the other lines of defense. The FEFPL Plant Protection System interfaces with the ETR PPS and acts to terminate or prevent reactor operation unless the integrity of the loop double containment is assured. This system is designed in accordance with AEC Plant Protection System Standard C 16-1T[1].

The basic objective of the FEFP Loop Plant Protection System is to ensure the continued existence of the containment system safety margin by: (1) monitoring the primary and the secondary containment vessel integrity, and (2) automatically terminating operation if the containment safety margin is reduced. In order to establish the specific functional requirements for the FEFPL-PPS, a systematic identification is made with the aid of safety fault trees (Appendix A) of all accidents that might challenge the loop containment system. These postulated accidents are evaluated to determine their consequences and to establish what protective action is required to preserve the specified safety margins (Chapter 10 and 11).

All of the identified accidents or malfunctions that may adversely affect the containment system integrity to a significant degree must ultimately lead to at least one of the three following abnormal conditions:

(1) leaks in either vessel which, depending on magnitude, require immediate remedial action,

(2) excessive temperature in either vessel, and

(3) excessive internal pressure.

Thus, it is concluded that the containment system integrity can be verified and maintained by protective action that is a function of seven principal parameters:

A. Primary containment temperature in fuel zone.

B. Primary containment temperature in meltdown cup region.

C. Secondary containment temperature in fuel zone.

D. Internal pressure pulse.

E. Primary containment integrity.

F. Secondary containment integrity.

G. Annulus gas system pressure. only one addressed in ETR fuel spec.

Detection of loss of integrity of either primary or secondary loop containment shall result in a ETR scram and, upon subsequent verification, removal of the FEFP loop before further power operation of the ETR. Detection of a reduction in the containment safety margin from excessive vessel deformation (pressure pulse) or high vessel temperature also will initiate a ETR scram. However, ETR and normal loop operation may resume when it has been determined that an adequate safety margin has been reestablished.

The protective function associated with each of the seven parameters listed is discussed in detail within the remainder of this chapter.

7.1.2 Definition of Terms

For the purposes of this document, the definitions in this section apply. Additional definitions related to PPS equipment are presented in RDT C16-1T.[1] A number of these terms which are related to protective functions are illustrated in an example in Section 7.1.3.1.

7.1.2.1 Accuracy

A number defining the specified, allowable, or observed limit of error (maximum error throughout the instrument span) in:

- instrument scale units
- units of the measured variable
- the ratio (expressed as percent) of error to the instrument range, span, or full scale, or

- the ratio (expressed as percent) of the error to the observed (indicated) value

7.1.2.2 Accuracy, Instrument Channel

The accuracy of an instrument channel includes errors introduced by the sensor, signal conditioning and trip logic.

7.1.2.3 Comparator

A component having a logical output which is a function of the reference reference setpoint and monitored variable inputs. The logical output has two, and only two, discrete stable output states defined as "reset" and "tripped".

7.1.2.4 Excursion, Maximum or Minimum Predicted

The magnitude of an excursion is expressed in terms of the maximum or minimum predicted value of a monitored or critical plant variable during an incident. This term is particularly applicable in determining the protective margin when the PPS acts to prevent (in accordance with some limiting criteria) a plant variable from exceeding a permissible limit.

7.1.2.5 Instrument Channel

All the components and interconnections from sensor(s) to comparator(s) inclusive, necessary to monitor a plant variable or condition and to initiate an instrument trip when the variable or condition deviates beyond a set limit. An instrument channel terminates at the output of the comparator.

7.1.2.6 Limit, Permissible Variable

Permissible limit is a value of a chosen variable at which it can be said with confidence that if the value of the variable were to be at the limit and all other variables were at the least safe bounds of their operating range, and if all uncertainties in technical knowledge of the process were resolved unfavorably, the public and the plant would not be endangered. This term may be applied to monitored or critical plant variables.

7.1.2.7 Logic Train

An independent, electrically isolated, logic matrix containing the logic switching elements required by the PPS protective subsystems. Each logic train drives one or more final trip device(s).

7.1.2.8 Operating Range, Normal

The range of values for a variable expected during normal operating conditions.

7.1.2.9 Protective Action

The operation of a sufficient number of actuators to effect a protective function.

Examples:

- reactor automatic shutdown
- containment isolation
- actuation of the emergency core cooling system

7.1.2.10 Protective Channel

A distinguishable, related group of devices, usually not containing redundant elements, which when taken together are capable of implementing a protective function, either alone or in coincidence with other channels. A protective channel may include instrument channel(s), logic, and actuators.

7.1.2.11 Protective Function

The monitoring of one or more plant variables associated with a particular plant condition and the initiation and completion of a particular protective action at values of the variables established in the design basis. Protective action is considered complete when the condition initiating the action is brought to a status at which the consequences of terminating the protective action are considered to be acceptable.

7.1.2.12 Protective Logic

The equipment necessary to initiate a protective action based on the specified combination of the logic outputs from the comparators. This equipment includes at least two logic trains, each of which contains the necessary electronic circuitry, mechanical mounting equipment, wiring, and terminals.

7.1.2.13 Protective Margin

The difference between the most severe predicted level (maximum or minimum predicted excursion) or a plant variable and its permissible limit during an accident. This term may be applied to monitored or critical plant variables.

7.1.2.14 Setpoint

The selected value of a monitored variable at which a comparator is set to trip.

7.1.2.15 Setpoint, Nominal (Range of)

The value or range of values selected for a monitored variable setpoint during normal operation.

7.1.2.16 Setpoint, Worst Case

The maximum or minimum value of a setpoint allowed in order to prevent exceeding a permissible variable limit during the most severe predicted incident. It is the limiting protection system setting.

7.1.2.17 Time, Maximum Allowed for Completion of Protective Action

The maximum allowed value of the time interval between the instant the actual value of a monitored variable exceeds the worst case trip point and the instant a protective action is completed for the most severe predicted incident (see Section 7.1.3.2 for discussion of scram completion). This value is determined from analysis of the most severe predicted excursion with the setpoint at its worst case value.

7.1.2.18 Trip Point

The value of a monitored variable at which a comparator actually trips.

7.1.2.19 Trip Point, Worst Case

The value of a trip point with the setpoint at its worst case value which gives the minimum protective margin during an incident

7.1.2.20 Variable, Critical Plant

A plant variable for which a limit(s) have been established. It is not necessarily the variable monitored in implementing a plant protective function.

7.1.2.21 Variable, Monitored

A variable which is continuously observed with an automatic device which provides a signal or trip if the variable departs from set limits. The output of monitoring a go/no-go, two valued signal.

7.1.3 FEFPL PPS Protective Functions

The FEFPL PPS protective functions, based on the system functional requirements (Section 7.1.1), are:

A. Primary containment temperature in fuel zone
B. Primary containment temperature in meltdown cup region
C. Secondary containment temperature in fuel zone
D. Sodium pressure pulse
E. Primary containment integrity
F. Secondary containment integrity
G. Annulus gas system pressure

It is the purpose of this section to present the required protective function documentation and essential design basis information for each of the above-listed functions.

7.1.3.1 Types of Protective Functions

These protective functions can be classified into three types; preventive, detective, and secondary. A preventive function acts to prevent plant variables or conditions from reaching their respective permissible variable limits. A detective function detects an existing undesirable condition and acts to mitigate its consequences. A secondary function provides a diverse protective subsystem which ensures automatic initiation of appropriate protective action upon the occurrence of a credible single event which would prevent another protective function from taking its proper protective action. Functions A, B, and C are of the preventive type. Functions D, E, and F are of the detective type and function G is a secondary protective function. In general, the terms defined in Section 7.1.2 referring to protective functions are most applicable to the preventive type function. Terms which are not applicable or need to be redefined for the other type functions are indicated in the appropriate function descriptions.

An Example:

It is meaningful at this point to give an example of a preventive function in order to illustrate the definitions of the various terms used. Assume that the following function is part of a fictitious reactor plant protection system:

Protective Function: core coolant outlet temperature

Incident: loss of core coolant flow due to primary pump failure

Monitored Variable: mixed-mean core coolant outlet temperature

Critical Plant Variable: fuel pin cladding temperature

Analyses have shown that by monitoring mixed-mean core outlet coolant temperature as a plant protective function and ensuring it does not exceed 1200°F (permissible variable limit) during a coolant flow coastdown and scramming the reactor at the appropriate point, the fuel pin clad temperature will not exceed 1600°F (fuel clad failure criterion).

Figure 7.1 illustrates the various terms used to establish specific protective function requirements. After a study of the various accident conditions, the most severe incident was selected in order to determine the

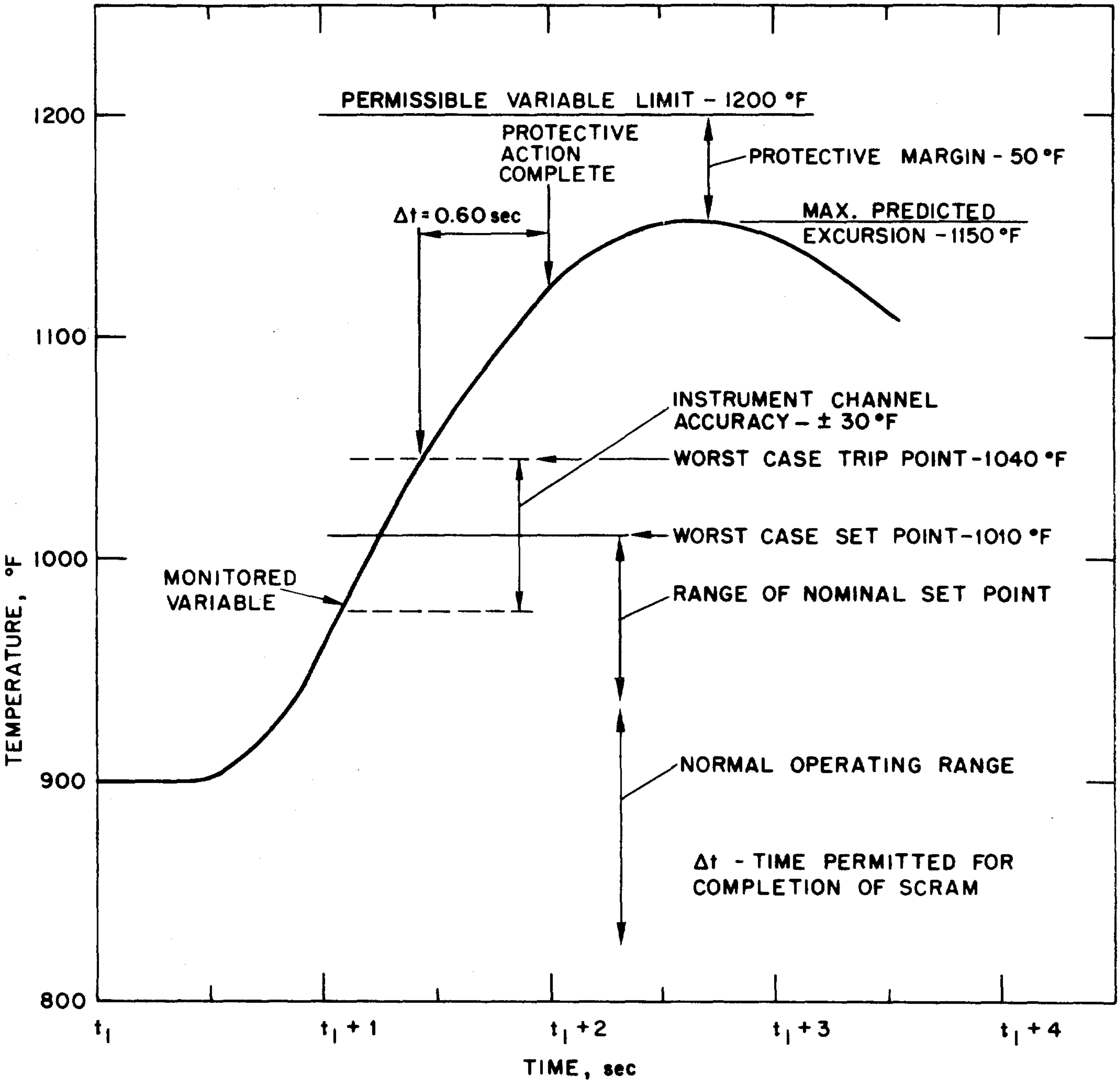

Fig. 7.1 Example Illustrating Protective Function Terminology

setpoint, accuracies, time intervals, etc. for the protective function. The predicted value of the monitored variable is shown assuming that the scram action was completed at t_1 + 2.0 sec. This prevents the variable from exceeding the permissible variable limit of 1200°F with a protective margin with respect to the monitored variable of 50°F. A worst case setpoint and maximum time for completion of the scram can be determined from the transient and the requirement of completing the scram by t_1 + 2.0 sec. The instrument channel accuracy (± 30°F) is indicated as a band around the worst case setpoint with the worst case trip point at the upper end. The time (Δt) permitted for completion of scram is the interval between the instant the value of the variable exceeds the worst case trip point and the instant the protective action must be completed. This time interval includes analog measuring system response time, logic delay times and actuator response time.

7.1.3.2 Protective Action

The required protective action for each protective function is an ETR scram. Figure 7.2 shows the reactor power (neutron flux) reduction versus time for an ETR scram.[2] The zero point of the time axis shown corresponds to that instant of time when rod motion begins. Completion of a scram from full power (100%) is defined as reduction of the power below 5%. The time interval from start of rod motion to completion of scram is approximately 170 milliseconds. The time delay prior to an ETR scram is defined as the time interval between reception of a signal at the ETR PPS interface and the start of rod motion. This delay is less than 25 milliseconds. These time intervals do not include time delays in the FEFP PPS intrument channels or logic trains.

7.1.3.3 Design Basis

A summary of the design basis for each protective function is presented in this section. Specific protective function information is tabulated in Table 7.1, parts (A) through (G).

A. Primary Containment Temperature in Fuel Zone

Although the system can tolerate higher temperatures safely, 1300°F has been established as the upper limit of the primary vessel for continued operation to be consistent with code requirements. The results of studies of various accidents (Chapter 11) indicate the need for monitoring the primary vessel temperature in the region of the fuel zone as a PPS protective function.

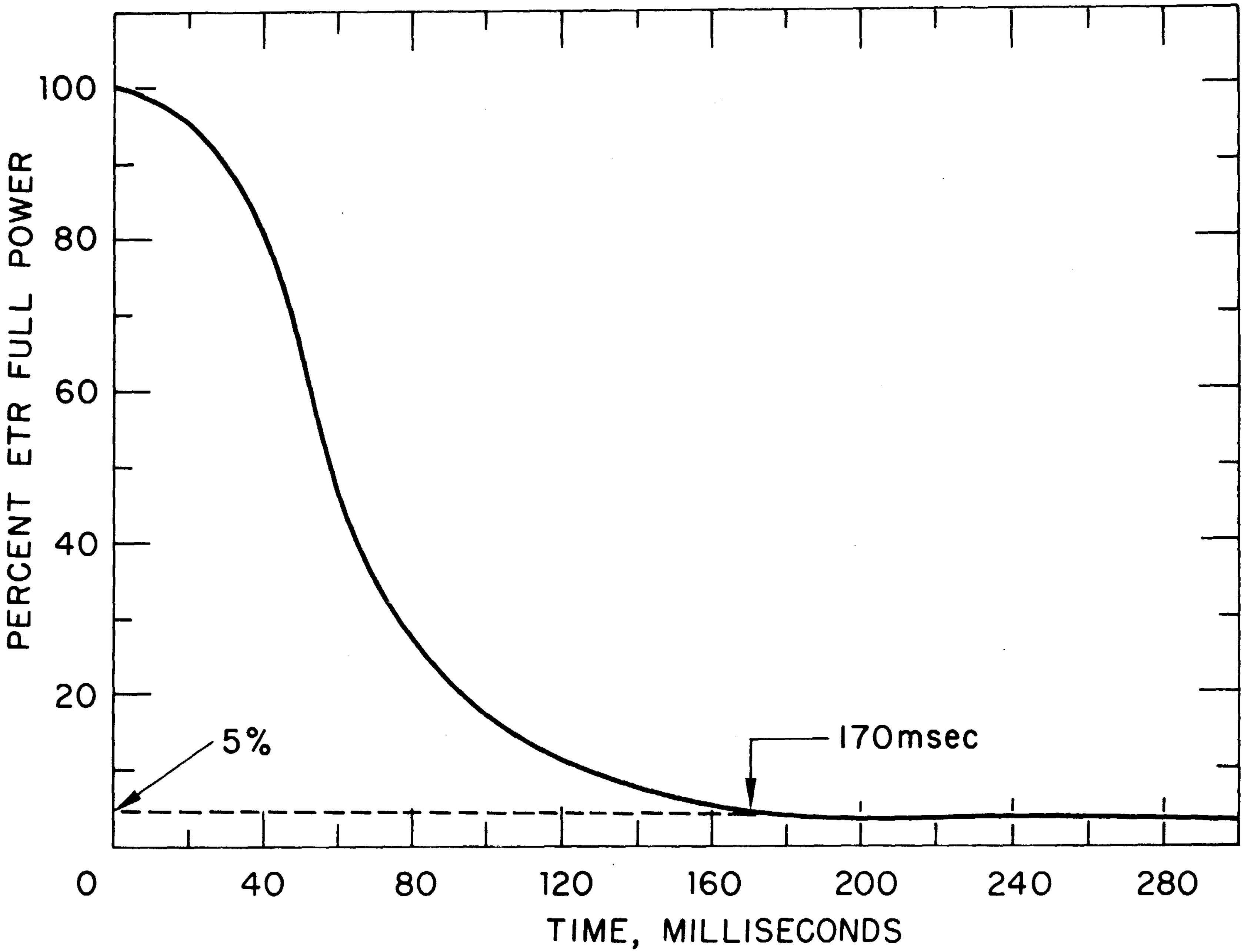

Fig. 7.2 Approximate ETR Power (Neutron Flux) vs Time for ETR Scram

In general, all accidents considered relate to loss of cooling capability of the primary vessel in that region. Due to the gamma heat generated in the primary vessel wall, the temperature would continue to rise after the cooling is lost. Scramming the reactor removes the major heat source and minimizes the possibility of a molten fuel-coolant interaction occurring with the wall temperature above 1300°F. The most severe accident condition would be generated by a total loss of ALIP electrical power (Section 11.2.2). The monitored variable for this protective function is the temperature of the outside surface of the primary vessel at a location 3 in. below the core centerline which is the location of the peak gamma flux.[3] The critical plant variable is the primary wall temperature, averaged radially. There is a significant temperature differential across the wall, since the outside is in contact with helium from the annulus gas system, and the inner surface is cooled by sodium flowing in the downcomer annulus. Therefore, the monitored variable is significantly different from the critical plant variable, and the analysis must compensate for this difference.

The permissible variable limit for the monitored variable must be determined. The limit for the average wall temperature is 1300°F, as stated above. In order to determine the permissible variable limit on the outside wall temperature, a gamma heating rate of 5.4 Watts/gram* is assumed (Note: gamma heat causes a temperature differential across the wall and the minimum gamma heating rate gives the minimum value for the permissible variable limit). The temperature differential calculated for this case is 78°F;[4] thus, the permissible limit is 1300°F plus 39°F or 1339°F.

A system operating limit for the sodium outlet temperature from the heat exchanger is 850°F (Section 6.2, System Temperature Limits). This corresponds to a maximum average wall temperature of 1062°F.[6] The maximum temperature differential across the wall with a gamma heating rate of 18 Watts/gram* is 260°F. The most severe predicted steady-state outside wall temperature is: 1062°F, plus half of the temperature differential (130°F),[4] plus an additional temperature increment of 40°F due to a postulated offset of the flow divider with respect to the primary vessel, for a total of 1232°F.

---

* The maximum expected value for gamma heating is 9.5 watts/gm. In order to provide a generous margin of safety values of 5.4 watts/gm and 18 watts/gm are selected arbitrarily to bound the minor ETR flux variations that may occur over the test period.

(If an offset of as much as 0.180 in. occurs, a local temperature rise of 40°F at the worst case point could result.[5] This is due to the reduced cooling effect as a result of lower sodium flow in the localized region. The gap between the flow divider and the primary vessel would be 0.100 in. This is the postulated worst case offset.) Calculations[5] have shown that in order for at least two sensors to be sensitive to an offset (assuming the failure of any single thermocouple is a credible single event), thermocouples should be placed at 45° intervals around the primary vessel, for a total of eight. A systematic error of 25°F maximum can be introduced if an offset occurs 45° away from one thermocouple, while no error is introduced in the measurement in line with the offset.

Figure 7.3 shows plots of the outside surface wall temperature in line radially with an offset for the total loss of ALIP power accident, (Section 11.2.2)[6] both with and without an ETR scram. Also plotted is the monitored variable 45° away from the offset. This plot is used to determine the worst case setpoint for all thermocouples. This truly represents a worst case situation since if the offset is radially directed in line with any sensor then the two adjacent sensors each 45° away will respond to the transient and scram the reactor before the surface temperature in line with the offset exceeds the permissible variable limit. The initial value of the outside wall temperature is taken as 1232°F, (assuming the maximum gamma heating rate) and the permissible variable limit as 1339°F (assuming the minimum gamma heating rate). It can be seen that without an ETR scram, the temperature rises to over 1500°F in 30 sec. However, with an ETR scram completed at approximately 7.5 sec after the start of the accident, the temperature will not exceed 1339°F with a protective margin with respect to the monitored variable of at least 25°F. Note that for this variable, there is very little overshoot after the scram is initiated and the variable decreases as soon as the scram is completed. A worst case setpoint of 1247°F has been selected for this protective action. Allowing a ± 25°F instrument channel accuracy, a time interval of 0.7 sec is permitted for completion of the protective action.

Table 7.1 - (A) lists essential protective function information. See Section 7.2.4 for instrument channel description.

B. <u>Primary Containment Temperature in Meltdown Cup Region</u>

A meltdown cup (Section 10.4.2) has been provided as part of the test train to prevent overheating of the primary vessel wall due to accumulated fuel debris or molten fuel. The major consideration in the design of the

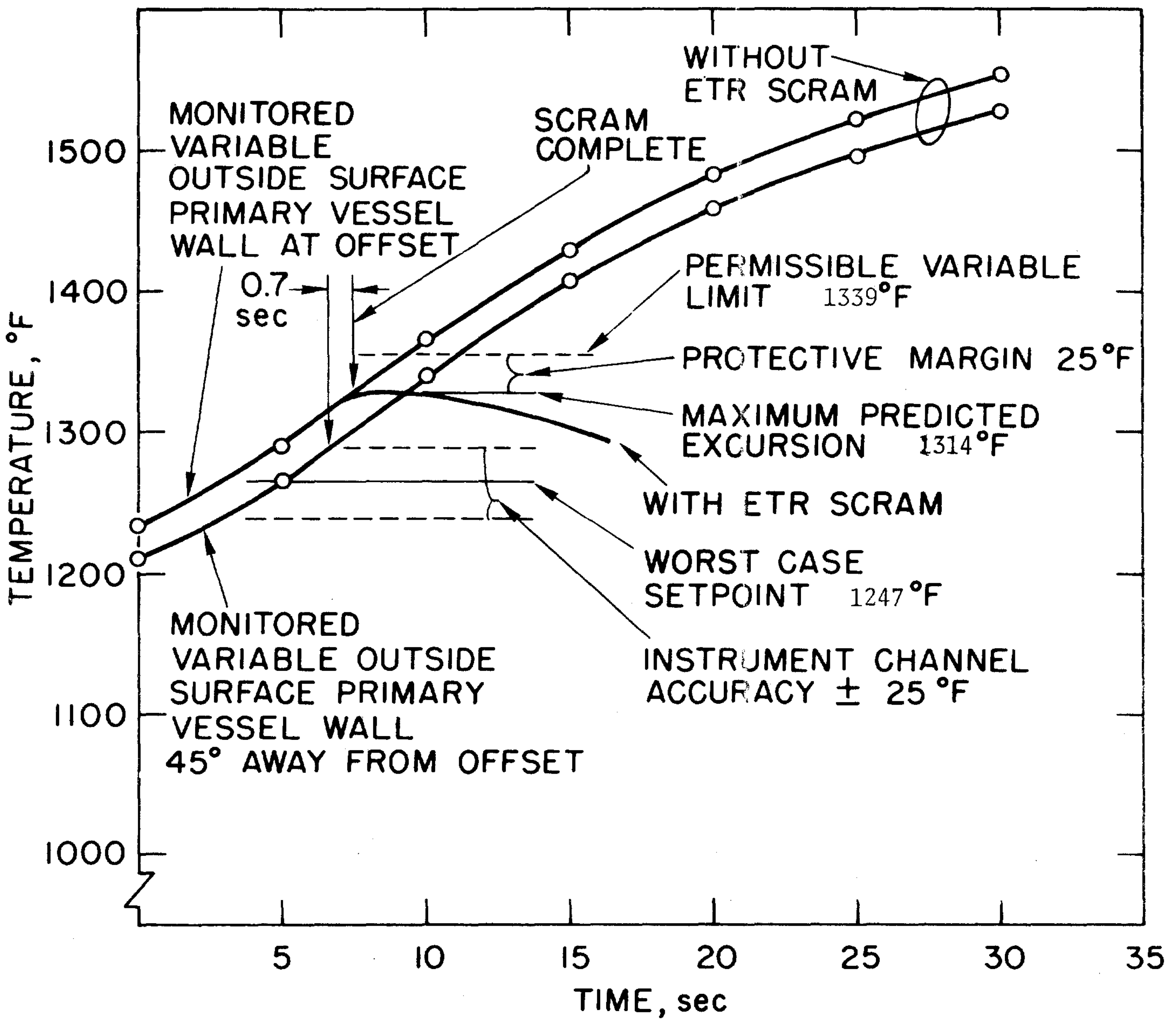

Fig. 7.3 Design Basis Excursion (Protective Function (A))

Data obtained from Ref. 6 as modified by ANL memorandum, J. J. English to D. H. Lennox, "FEFP PPS Data for Protective Function (A)," July 17, 1973 (ENG-PT-RAS-0209).

TABLE 7.1 - (A)

FEFP Loop Protective Function

Protective Function (A)

Title: Primary Containment Temperature in Fuel Zone

Incident(s) Requiring Protective Action:

Total Loss of ALIP Electrical Power (Design Basis)
Loop Flow Blockage
Loss of Helium Flow
High Helium Inlet Temperature

Reference to Design Basis Documentation:

Section 6.2 - System Temperature Limits
Section 10.3.4 - Compliance with Safety Design Requirements
Section 11.0 - Accidents

Monitored Variable: Outside Surface of Primary Vessel Wall

Protective Action: ETR Scram

Maximum Time Permitted for Protective Action Completion: 0.7 sec

Critical Plant Variable: Primary Vessel Temperature (averaged radially)

Permissible Variable Limit: 1339°F for the monitored variable. This corresponds to 1300°F for the critical plant variable.

Protective Margin: 25°F (with respect to the monitored variable)

Worst Case Setpoint: 1247°F

Required Instrument Channel Accuracy: ± 25°F

Nominal Setpoint: 900 to 1247°F

Normal Steady-State Operating Condition: 1192°F maximum (without an offset of the flow divider with respect to the primary vessel).

Maximum Predicted Excursion: 1314°F

Remarks:

a) Measurements at 45° intervals around the primary vessel at the elevation of the maximum gamma heating rate are provided.

b)"Two out of eight" logic is provided for this function. A minimum of four instrument channels, uniformly spaced around the primary vessel with adjacent channels independent, are required for normal operation. With less than eight channels the function will operate with "one out of N" logic, where N is the number of remaining channels.

meltdown cup has been to provide adequate heat-removal capacity for all possible circumstances. The most severe heat removal case would result from the rapid introduction of molten fuel and steel into the cup without any interaction with sodium in or above the cup. The cup must accept the latent and sensible heat of the fuel and accompanying steel as well as provide for removal of the decay heat generated in the fuel. The cup is in a region of low neutron flux; therefore, significant fissioning will not occur in the collected fuel even if an ETR scram were delayed.

Heat transfer from the loop to the ETR water is hindered by the gas gap between the primary and secondary vessels. The sodium surrounding the meltdown cup may rise to its boiling temperature (about 1900°F at the existing pressure) if a significant amount of molten fuel and steel enter the cup. A protective function which prevents the primary vessel in the region of the meltdown cup from exceeding 1300°F is required, during the time when the possibility of a molten fuel-coolant interaction (MFCI) exists. The protection system can provide this feature by ensuring that the reactor is scrammed sufficiently early to anticipate the time interval during which an MFCI might occur, and so that the vessel temperature will not exceed 1300°F. If half the available fuel melts and fills the cup, the primary temperature will increase at the maximum rate shown in Fig. 7.4. The primary vessel temperature setpoint of 1050°F, provides a sufficient time interval <u>before</u> 1300°F is reached for a crust to form on the fuel in the cup and preclude an MFCI. With less fuel in the cup, the time between scram and 1300°F lengthens proportionately to give greater margin. This PPS requirement is generated by the meltdown cup design basis discussion (Section 10.4.2) where it is shown that the primary vessel wall temperature varies inversely with the fraction of fuel in the meltdown cup that is molten, and, hence, available for MFCI. The fuel freezes as it losses its heat to the surroundings, including the primary vessel.

The monitored variable for this protective function is the outside surface temperature of the primary vessel in the cup region (see Fig. 7.11 for locations). The critical plant variable is the primary wall temperature, averaged across the wall. In the region of the fuel cup, the gamma heating rate in the primary wall is insignificant; thus, for steady-state operation the primary wall is at the temperature of the inlet sodium to the test train, with a negligible temperature differential across the wall. However, when fuel is deposited in the cup, heat flows through the wall and a temperature differential will exist, with the inside surface at a higher value. The permissible variable limit for the monitored variable must account for this temperature differential. For the design-basis quantity of fuel deposited in the meltdown cup, an outside wall temperature of 1245°F corresponds to an average wall temperature of 1300°F. No significant circumferential or axial temperature gradients are expected due to the presence of a good conductor (sodium) between the meltdown cup and the primary vessel wall during the transient. The absence of gamma heating in this region, which could introduce temperature asymmetries, makes the stated protective margin valid for the minimum channel requirements of 1 out of 2 logic. Figure 7.4 shows a temperature versus time plot of the value of the monitored variable for the design basis case.

Fig. 7.4 Design Basis Excursion (Protective Function (B))
(Data taken from curves presented in Chapter 10)

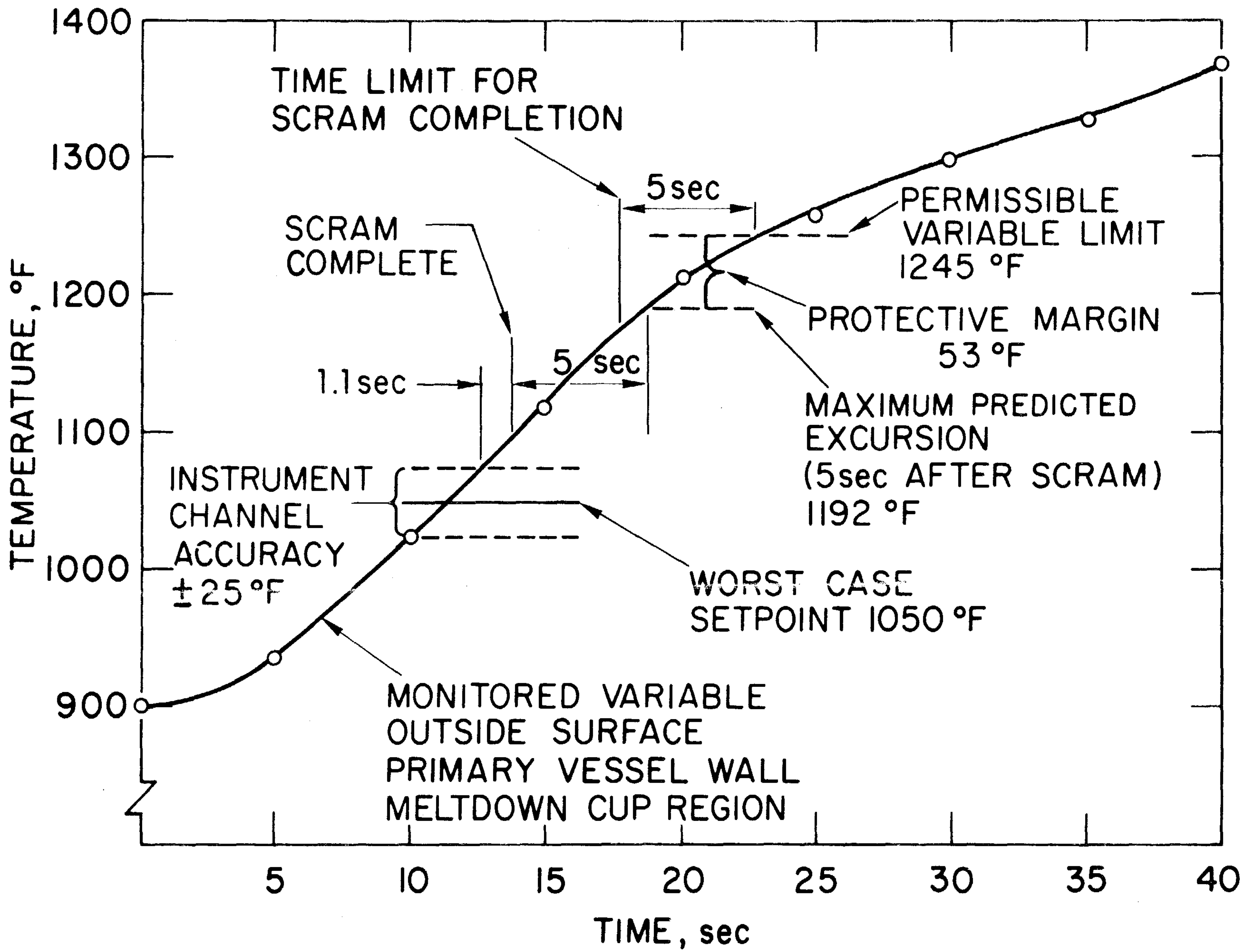

The initial temperature is the maximum operating sodium temperature at the test train inlet. It can be seen that the temperature increases to over 1350°F in 40 sec after it is no longer possible for an MFCI. The longer-term temperature profile of the primary vessel, which may reach higher values before dropping is discussed in Section 10.4.2. The protective channel will scram the reactor at least 5 sec prior to the time the variable exceeds 1245°F (at approximately 22.5 sec). The time limit for scram completion is 17.75 sec after the start of the accident. A worst case setpoint of 1050°F has been selected for this protective action. A scram would be completed by 13.75 sec allowing 1.1 seconds for the completion of the protective action. The protective margin needs to be interpreted in a slightly different manner than explained in the example previously given; because now the system does not act to limit the variable, it acts to terminate full power operation 5 sec prior to the variable exceeding a design limit. In this case, the protective margin with respect to the monitored variable is determined as the difference between the permissible limit and the value (maximum predicted excursion) attained 5 sec after the scram is complete. This occurs at 18.75 sec and the value of the protective margin is 53°F. The maximum predicted excursion is taken as the value at this instant.

Table 7.1 - (B) lists essential protective function information.

C. Secondary Containment Temperature in Fuel Zone

The maximum permissible temperature of the secondary vessel in the fuel zone is determined by the structural limitations of the vessel and by the melting temperature of the cadmium filter. Analysis of postulated incidents which would result in an over-temperature of the secondary vessel established that the limiting temperature is the cadmium filter. The melting temperature of cadmium is 609°F which has been established as the permissible variable limit for the critical loop variable. The only significant heat source to the secondary vessel and cadmium filter in the fuel zone is from gamma heating. The ETR coolant removes this heat at the flow annulus located between the loop and the core filler piece (see Figure 7.5). Only accidents which either increase the heat input or reduce the cooling have been considered. The protective action required is an ETR scram which will immediately reduce gamma heating and result in a temperature decline.

The following transients were considered as the most severe accidents to establish the design basis for this protective function[7]: (1) ETR overpower (131% of rated power of 175 MW), and (2) 80% coolant water flow blockage in the annulus. The power increase of Case (1) was assumed

TABLE 7.1 - (B)

FEFP Loop Protective Function

Protective Function (B)

Title: Primary Containment Temperature in Meltdown Cup Region

Incident(s) Requiring Protective Action: Meltdown Cup Design Basis Meltdown

Reference to Design Basis Documentation:

Section 10.4.2 - Meltdown Cup

Section 6.2 - System Temperature Limits

Monitored Variable: Outside Surface Temperature of Primary Vessel Wall

Protective Action: ETR Scram

Maximum Time Permitted for Protective Action Completion: 1.1 sec

Critical Plant Variable: Primary Vessel Temperature (averaged across wall)

Permissible Variable Limit: 1245°F for the monitored variable (ETR scram to occur 5 sec prior to reaching this limit). This corresponds to 1300°F for the critical plant variable.

Protective Margin: 53°F (determined as the difference between the permissible limit and the monitored variable 5 sec after the scram is complete)

Worst Case Setpoint: 1050°F

Required Instrument Channel Accuracy: ± 25°F

Nominal Setpoint: In the range 700 to 1050°F

Normal Steady-State Operating Condition: In the range 550 to 900°F

Maximum Predicted Excursion: 1192°F (the value of the monitored variable 5 sec after the scram is complete)

Remarks:

a) See text for discussion of definitions.

b) "Two out of four" logic is provided for this protective function. A minimum of two independent instrument channels shall be required for normal operation. With less than four channels the function will operate with "one out of N" logic, where N is the number of remaining channels.

c) See Fig. 7.11 for TC locations.[9]

d) A logic output from this function's coincidence module is used to initiate the cup cooling mode of the Annulus Gas System.

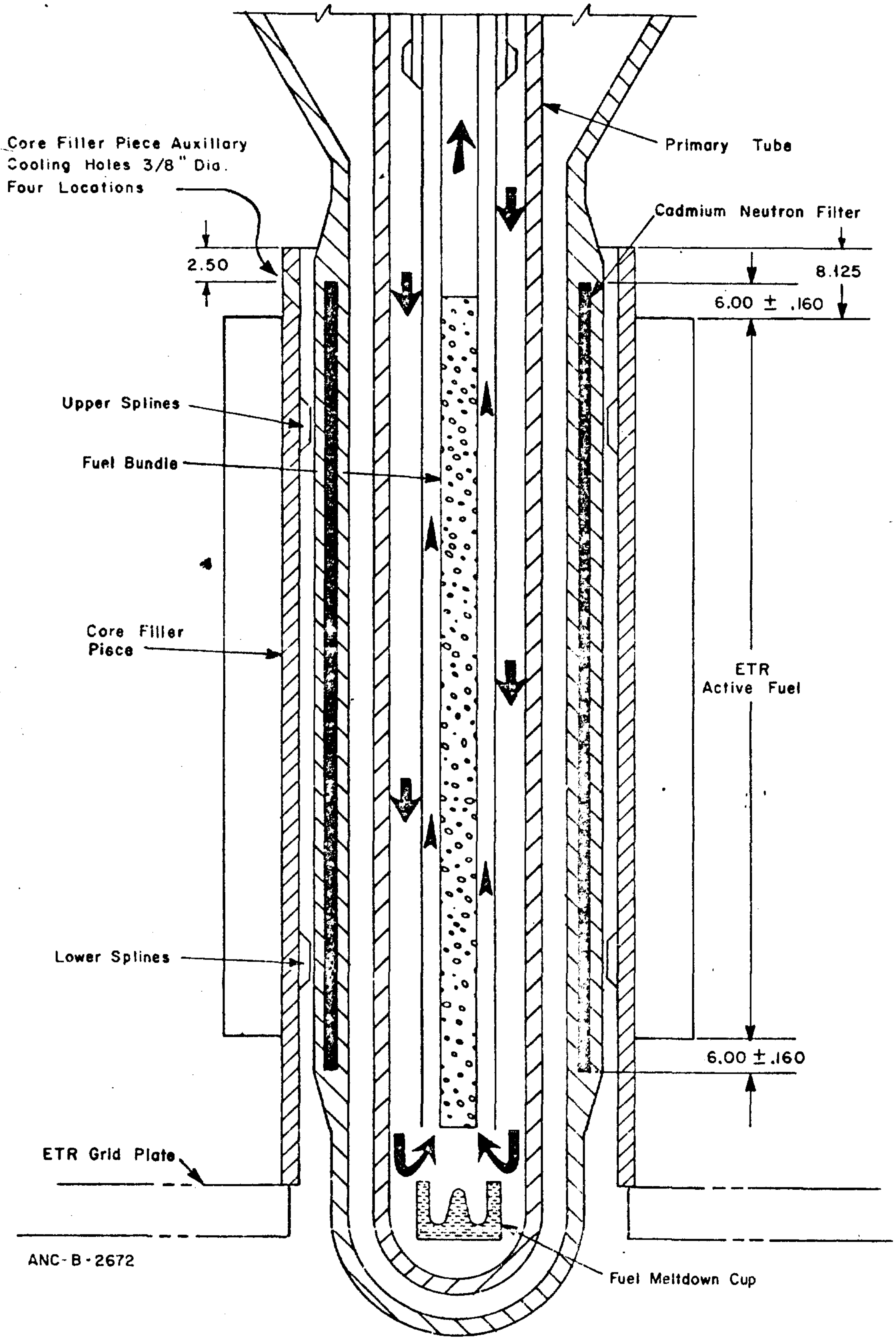

FIG. 7.5 - ETR/HEFPL Inpile Tube, Neutron Filter and Core Filler Piece Schematic

to hold at the threshold of the worst case trip by the ETR PPS level and coolant high delta temperature detection subsystems. In Case (2), it was assumed that the flow at the annulus inlet between the loop and the core filler piece was completely blocked and two of the four bypass coolant water passages in the core filler piece were also blocked. As an initial condition for both accident cases, it was assumed that a ±20% power tilt accident condition was undetected at the time.

Thermal analysis of the filter hot spot showed the following maximum cadmium temperatures without detection[8]:

Accident	Maximum Cd Temp	Margin to Melting (unprotected)
a) 131% step overpower with ±20% power tilt	412°F	197°F
b) 80% annulus water blockage with ±20% power tilt	472°F	137°F

The operating margin without protective action is significant. It is noteworthy that these results were based on worst case thermal analysis:

1) Design gamma heating rates: Apply at reactor power of 175 MW, includes 25% factor applied to calculated rates for engineering uncertainties.

2) Minimum core delta pressure (38 psid) for flow calculations.

3) Eccentric positioning of the loop within the core filler piece to provide minimum water channel thickness (54 mils).

4) Peak of power tilt assumed to be oriented to coincide with the minimum water channel.

To provide a relationship between threshold cadmium melting and the monitored variable, a thermal analysis was performed to simulate a more severe condition. Due to the number of independent failures already assumed for the 80% blockage accident (3), it was decided that further flow reduction is extremely unlikely and was therefore discarded from consideration (however, the accident condition is discussed in Chapter 13). The approach taken was to increase the gamma heating. In the simulation, it was found that cadmium melting could be produced for accident Case (2) if the gamma heating rates were 150% of design[8]. The unprotected temperature response at the cadmium hot spot (3 in. below core centerline) is shown in Fig. 7.6. Maximum temperature was shown to be 622°F.

Protective action for this simulation case is also shown in the figure and was based on a minimum operating trip logic of 1 of 2 channels. The worst case trip point (660°F, setpoint 635°F) was based on providing an

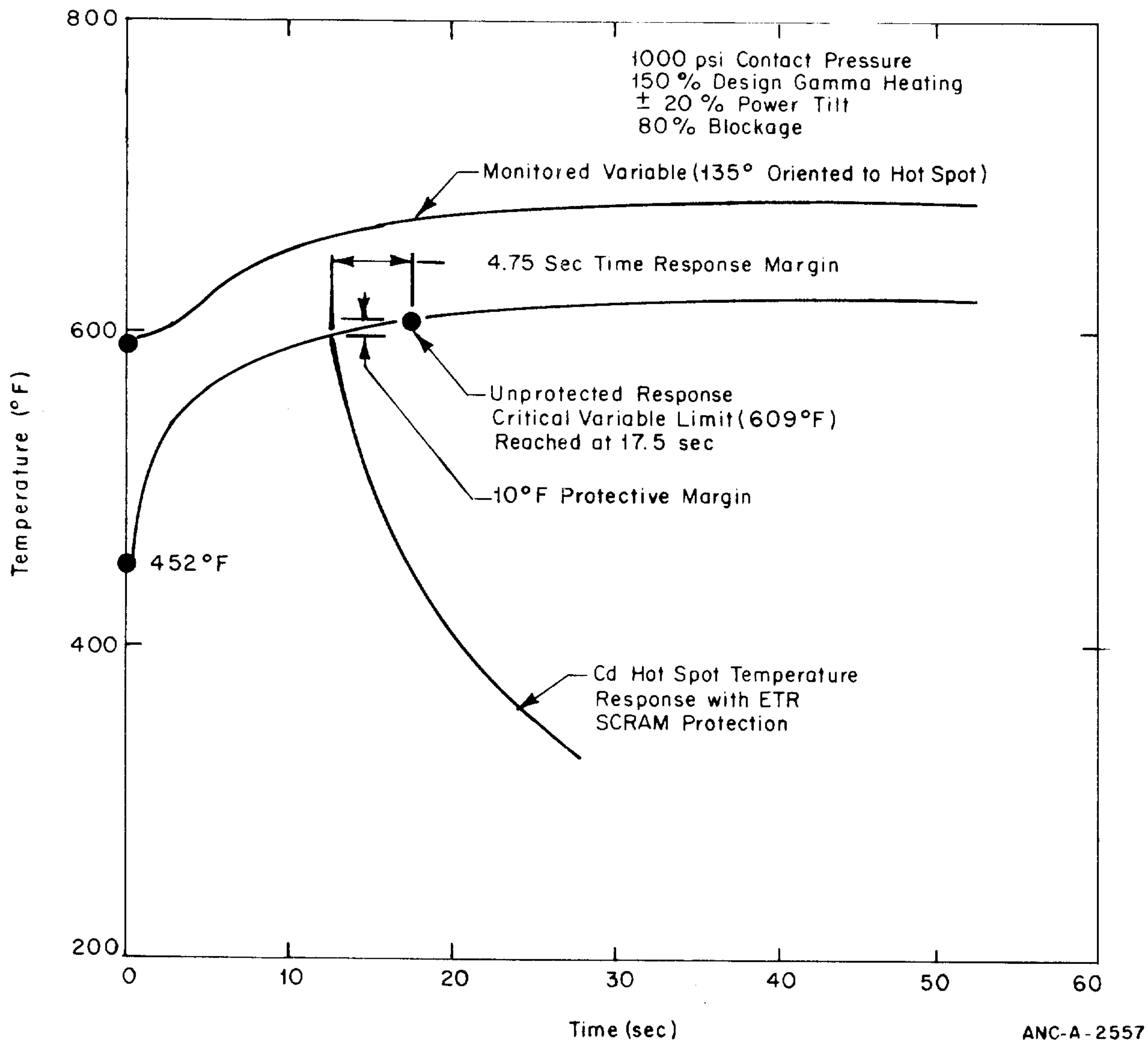

FIG. 7.6 - Worst Case Critical Variable Response for Protected Simulation DBA - Minimum Channels Operating

indicated 10°F protective margin. The monitored variable was oriented 135° with respect to the hot spot to provide worst possible means of detection; however, the monitored variable was assumed to coincide axially with the hot spot. To compensate for shift of the power density relative to the monitored variable (3 in. below core centerline), a 30°F allocation was provided for this uncertainty[7]. Hence, the adjusted worst case setpoint was determined to be 605°F.

All of the thermal analysis discussed so far on this protective function was based on a contact pressure of 1000 psi between the cadmium filter and the secondary tube. In the single bonded cadmium filter concept, this contact pressure was assumed as the upper bound for full power operation[7]. The basis for this assumption is that the heat transfer from the secondary tube to the cadmium increases with greater contact pressure. Hence, for a given operating power, the monitored variable will be at a higher temperature with respect to the critical variable than for lower contact pressures. Therefore, the lower contact pressure supplies operating margin under normal conditions which may lead to spurious scrams.

Based on worst case monitored variable and thermal conditions at an assumed lower bound contact pressure (100 psi) for full power operation, the minimum operating margin was found to be very small ($\sim$1°F). Minimum trip logic of 1 of 2 channels was assumed with one monitored variable aligned at the hot spot. Also, a maximum normal power tilt of ±7.5% was assumed. The resulting monitored variable was found to be 564°F. The remaining difference between this temperature and the setpoint was a 40°F provision for channel accuracy. About 25°F of this allowance is related to sensor cooling effects due to the gamma heating and primary tube radiative heat transfer operating environment. Fortunately, the FEFPL experiments are expected to require less power density than available at the reactor full power rating; hence, the lower power operation will reduce the heat generated in the secondary containment. For example, the 564°F temperature shown for 175 MW operation reduces to 438°F at 120 MW.[7] In this case, the operating margin could increase to 132°F with the 605°F setpoint.

A compilation of the essential performance requirements for this protective function is given in Table 7.1-(C). Section 7.2.4 gives a description of the instrumentation channels.

D. Sodium Pressure Pulse

Potentially the most energetic events for the FEFPL inpile loop are planned experiments that involve molten-fuel coolant interaction. During

TABLE 7.1 - (C)

FEFP Loop Protective Function

Protective Function (C)

Title: Secondary Containment Temperature in Fuel Zone

Incident(s) Requiring Protective Action: Partial blockage (80%) of ETR coolant flow adjacent to FEFPL combined with 150% design gamma heating rate and ±20% flux tilt (see Remark a)

Reference to Design Basis Documentation: ANC Report EDF-1312, "Design Basis Analysis for FEFPL PPS Protective Function (C) Requirements".

Protective Action: Alarm and ETR scram

Maximum Time Permitted for Protective Action Completion: 700 msec (see Remark b)

Critical Loop Variable: Cadmium filter temperature

Critical Variable Limit: 609°F

Monitored Variable: Temperature of secondary vessel inside surface in the core midplane region.

Permissible Monitored Variable Limit: Not applicable

Protective Margins (see Remark c):

a)	80% water coolant blockage:	137°F (unprotected)
b)	131% reactor overpower (230 MW max):	197°F (unprotected)
c)	Case (a) at 150% design gamma heating rates (simulated for design basis):	10°F

Worst Case Setpoint: 605°F

Required Instrument Channel Accuracy:

a) Maximum positive: +40°F

b) Maximum negative: -25°F

Nominal Setpoint: In the range 475°F to 605°F (see Remark d)

Normal Steady-state Operating Condition: <565°F (at full reactor power)

Maximum Predicted Excursion (see Remark c):

a)	80% water coolant blockage	472°F (unprotected)
b)	121% reactor overpower (230 MW):	412°F (unprotected)
c)	Case (a) at 150% design gamma heating rates (simulated for design basis):	599°F

Remarks:

a) Represents a simulated accident condition in which the critical variable limit threshold was reached when not protected by a reactor scram. Most severe postulated accident cases were shown to not require protective action.

Remarks (Contd.):

b) This response time represents that time interval between the instant the actual value of the monitored variable exceeds the setpoint and the reactor control rods are seated.

c) Accident cases (a) and (b) represent initial conditions of 100% design gamma heating rates, ±20% flux tilt, minimum core delta P, minimum water channel aligned with peak power tilt.

d) At full reactor power (175 MW) the setpoint is 605°F. The range minimum possible of 475°F represents reactor power of 120 MW.

e) "Two-out-of-four" logic is provided for this protective function. A minimum of two independent instrument channels shall be required for normal operation. With less than four channels the function will operate with "one-out-of-N" logic, where N is the number of remaining channels.

normal operation, the rate of energy production in the fuel equals the rate of energy removal by the coolant; if, however, a condition arises that causes the energy production rate to exceed the rate of heat removal, the fuel temperatures can increase rapidly, causing the clad to fail. Then the hot, and probably molten, fuel will be expelled and will eventually come into contact with the sodium coolant. The resulting sodium vaporization is theoretically capable of performing a considerable amount of work and possibly producing extensive structural damage; therefore, this process has received considerable experimental as well as analytical study. One of the major objectives of the FEFP in-pile loop program is to obtain information and insight as regards this process in prototypical FFTF fuel-rod arrays. Because the objective is to study fuel failure, the loop must withstand safely the most energetic MFCI that is credible. For these reasons a comprehensive study has been conducted to establish the margin of safety needed to withstand an MFCI greater than the maximum expected within the FEFP loop system.[10]

Chapter 10 contains a discussion covering the most probable MFCI that is expected based on current experimental evidence plus analyses for two additional, more severe, MFCI's used to fix protective criteria. These represent: (1) the "upper limit" pressure considered to be possible, and (2) the pressure postulated for a hypothetical MFCI not obtainable in a realistic experiment. Figure 7.7 illustrates the loop pressure containment capability with both of these cases indicated. These values are 70 atmospheres and 190 atmospheres, respectively. Also indicated are values where permanent deformation of the primary vessel occurs (340 atmospheres) and where the primary vessel deforms to the secondary vessel (680 atmospheres).

The FEFPL plant protection system provides a protective function which monitors the magnitude of pressure pulses in the sodium. This function is to detect a pressure pulse larger than the permissible limit and terminate power operation of the reactor. This function does not prevent an excessive pressure pulse but acts to prevent additional pulses after a single excessive pulse has occurred. For this function the standard definitions for terms in Section 7.1.2 have been somewhat modified or interpreted in a different light. The permissible variable limit with respect to the monitored variable is established as the Design Envelope MFCI (190 atm or 2800 psi). This is the design limit for pulses after which steady-state operation is not allowed. The worst

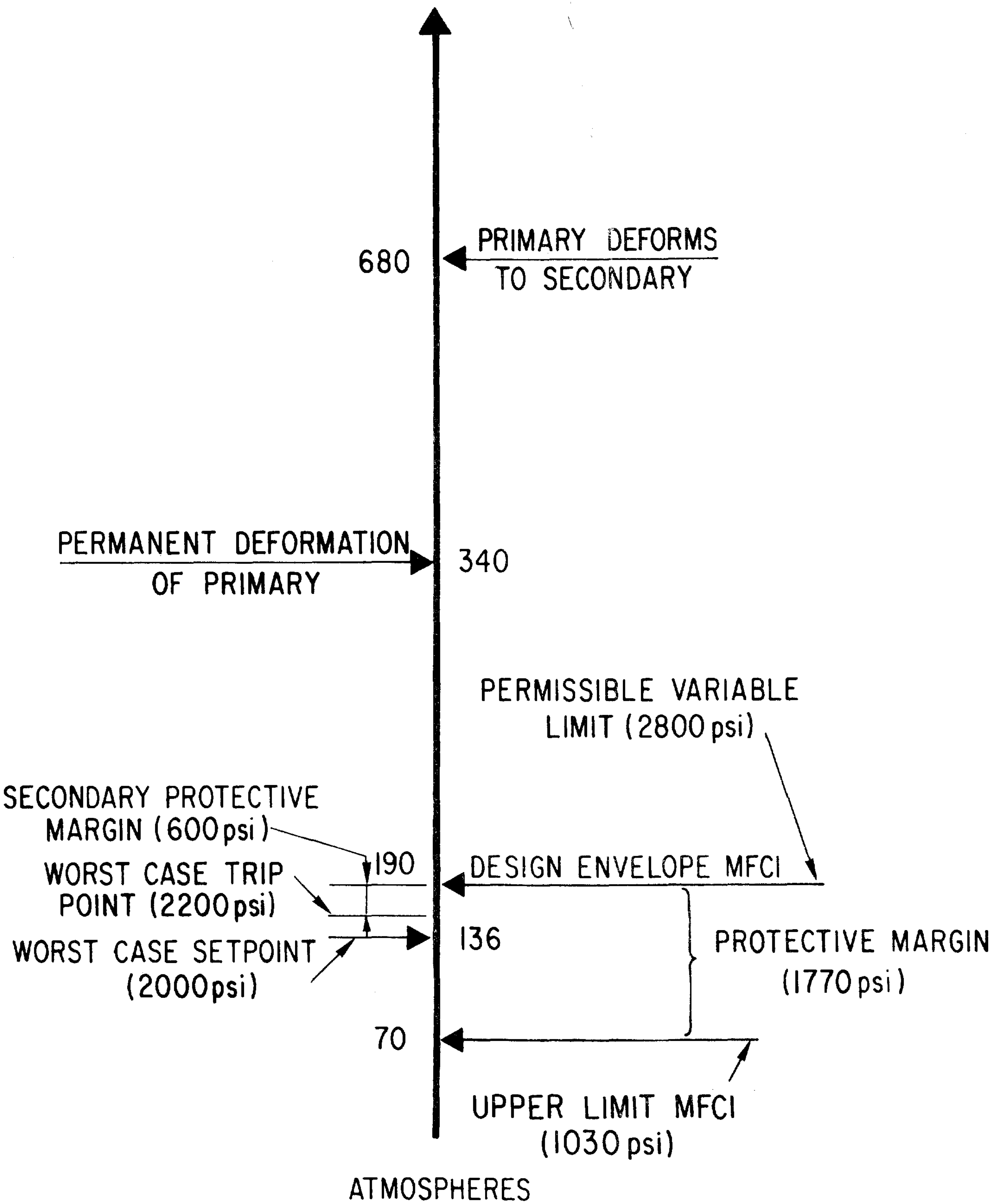

FIG. 7.7 PROTECTIVE FUNCTION (D) - LIMITS AND MARGINS

case setpoint is 2000 psi (136 atm). The instrument channel accuracy has been taken as ± 10% of full scale (2000 psi). The worst case trip point would be 2200 psi. The time allowed for completion of the scram is 0.75 sec. For this function the time is defined as the interval between the instant the monitored variable causes the instrument channel to be tripped and the instant the scram is completed. This value is based on the required time for the ETR shutdown system to operate ($\sim$ 0.19 sec) and allowing approximately 0.5 seconds for FEFPL-PPS system delays. This time is sufficiently short so that very little additional fuel has time to melt for a potential MFCI. The protective margin in this case is taken as the difference between the "upper limit" MFCI and the design envelope MFCI, 1770 psi (120 atm). This is indicated as "Protective Margin" on Figure 7.7. Because this protective function does not limit the pressure, the protective function setpoint is not directly related to this protective margin. A secondary protective margin is indicated. This value is 600 psi (41 atm) and may be interpreted as the margin with respect to continued operation after a pulse, it is the difference between the worst case setpoint and the permissible variable limit. Table 7.1 - (D) lists essential protective function information.

The primary purpose of this protective funciton is to prevent continued operation of the loop if an excessive pressure pulse actually has been generated by a molten fuel-coolant interaction. This function provides a backup for the very extensive analyses performed to determine the results of postulated reactions. Nevertheless, these analyses and the containment system design are extremely conservative; consequently, it should be possible to continue operation whenever it can be shown that insufficient energy had been released to deform the primary vessel. One mode of operation which would provide adequate protection would be to operate the loop without this function as long as there was no other indication that even a small MFCI had occurred. As soon as such indication occured, the operator would immediately manually scram the reactor and terminate the experiment before significant quantities of additional fuel could melt.

A second acceptable mode would be to operate without this protection function after an indicated MFCI if no leaks have occurred and all supporting

TABLE 7.1 - (D)

FEFP Loop Protective Function

Protective Function (D)

Title: Sodium Pressure Pulse

Incident(s) Requiring Protective Action: Molten Fuel-Coolant Interaction generating excessive energy release.

Reference To Design Basis Documentation:

Section 10.2.2 - Molten Fuel-Coolant Interaction

D. H. Lennox, et.al., Containment Study for the FEFP In-Pile Loop, ANL/RAS 71-36 (Nov. 1971).

Monitored Variable: Transient Sodium Pressure

Protective Action: ETR Scram

Maximum Time Permitted for Protective Action Completion: 0.75 sec.

Critical Plant Variable: Strength of the primary vessel

Permissible Variable Limit: 190 atm (1300°F max. average primary wall temperature) design limit for pulses, after which operation is not allowed.

Protective Margin: See discussion

Worst Case Setpoint: 2000 psi (136 atm)

Required Instrument Channel Accuracy: ± 10% full scale or (± 200 psi)

Nominal Setpoint: In the range 1180 psi (80 atm) to 2000 psi (136 atm)

Normal Steady-State Operating Condition: Does not apply.

Maximum Predicted Excursion: 1030 psi (70 atm)

Remarks:

a) See text for discussion of definitions.

b) "Two out of four" logic is provided for this protective function. A minimum of two independent instrument channels shall be required for normal operation. With less than four channels the function will operate with "one out of N" logic, where N is the number of remaining channels.

evidence indicates that the MFCI was below the maximum expected. This function is provided as a fast acting automatic aid to the operator and is included as part of the PPS in order to assure that it is designed to the highest level of standards and performance.

NOTE: The setpoints, protective margins, etc., for this protective function which have been established here are considered to be very conservative, first with respect to the analyses performed and second with respect to having large protective margins. The setpoints and protective margins indicated in Table 7.1 - (D) are considered worst case for all experiments, and it is expected that if less restrictive values are established for future experiments these values will be submitted as an addendum to this SAR prior to the appropriate experiment.

E. Primary Containment Integrity

The requirement for double containment of the FEFPL experiment during ETR operations establishes a need for a monitoring system which will detect if primary containment is not maintained. There is no time response requirement stated in the ETR Technical Specifications[11] for protective action upon detection; therefore, any normal means of reactor shutdown by the operator complies with the requirement. It was felt prudent in the design basis analysis, however, that an automatic scram action capability be provided to back up the operator in event he fails to initiate a scram upon a pre-trip alarm[12].

The Annulus Gas System (AGS) allows the FEFPL-PPS to continuously and automatically monitor the primary containment below the heat exchanger lower tube sheet for leaks. This capability applies when the loop is in the reactor (prior to startup and when the reactor is in operation) and the leak exceeds the setpoint (protective function (F)). Leaks in the primary containment tube might lead to sodium entering the annulus gas space but the secondary containment would prevent if from coming into contact with the reactor coolant water. Also, the AGS pressure is regulated within limits and monitored by the FEFPL PPS (protective function G)) so that in event of a leak, the flow would be helium into the loop primary system.

This function has been established to detect primary containment leaks smaller than that detectable by protective function (F). As discussed in Section 7.1.3.3-F, the worst case trip point for this function is 1.1 SCFM of helium flow from the annulus through either containment.

Loss of integrity of the primary vessel will be detected by protective function (E) sensing a pressure increase in the primary system. All boundaries of the primary system are exposed to gas systems with pressures higher than corresponding operating pressures in the primary containment. Annulus Gas System pressure is monitored by protective function (G) for low pressure. Loss of helium system pressure would result in a loss of loop cooling capability which would lead to increased primary vessel temperature causing a scram by protective function (A). Any leakage of the primary containment will permit the higher pressure gas to enter the primary system and rise to the cover gas space. Any significant leakage of sodium will be prevented until pressure equilibrium is reached across the breach. The protective action, an ETR scram, will occur when the cover gas pressure reaches the protective function trip point. This protective function does not act to prevent an unacceptable operating condition, primary containment leakage, but only to detect a condition and to terminate or prevent ETR operation.

Loop cover gas pressure will be between 10 and 50 psia with a maximum anticipated operating pressure in the sodium of 211 psia (50 psia cover gas, 158 psi pump head and 3 psi sodium head). During ETR operation, the gas annulus pressure will be normally maintained between 260 and 270 psia. A leak in the primary containment will permit gas to continue to enter the loop until the cover gas pressure exceeds setpoint trip (70 psia). The worst case trip point (instrument channel accuracy equals ±10 psi) is 80 psia which is 5 psi less than the steady-state pressure (85 psia) attained in the loop plenum assuming a leak in the primary at a point of maximum operating sodium pressure (211 psia) and the worst case trip point for low AGS pressure (246 psia). A helium leak rate of 1.1 SCFM was postulated to occur under these conditions in the design basis analysis for this function. The following time response results were obtained for an initial leak driving head of 35 psi[12]:

Pressure	Time Response
a) Time to reach 70 psia setpoint (20 psi pressure rise)	40.5 sec
b) Time to reach 80 psia worst case trip point (30 psi pressure rise)	92.0 sec

These results indicate that the pressure buildup is relatively slow and operator action based on pre-trip alarm can be anticipated in many cases prior to the backup automatic action. Under normal AGS pressure conditions and lower sodium pump pressure rise operation, the response will be faster for the same leak rate. Also, the margin will increase as the cover gas pressure rise limit is set by the magnitude of the initial driving head at the point of the leak.

A compilation of the essential performance requirements for this protective function is given in Table 7.1 - (E).

TABLE 7.1 - (E)

FEFP Loop Protective Function

Protective Function (E)

Title: Primary Containment Integrity

Incident(s) Requiring Protective Action: Failure of primary containment resulting in leakage of annulus gas into primary system.

Reference to Design Basis Documentation: EDF-1342, "Design Basis Analysis for FEFPL Protective Function (E): Primary Containment Integrity", May , 1974.

Protective Action: Alarm and ETR scram

Maximum Time Permitted for Protective Action Completion: 500 msec (see Remark a)

Critical Loop Variable: Primary containment integrity

Critical Variable Limit: Detection of a leak

Monitored Variable: 1) Primary containment cover gas static pressure
2) Annulus gas makeup flow rate (see Remark b)

Permissible Monitored Variable Limit: 35 psi static pressure rise (see Remark c)

Protective Margin: 5 psi (see Remark d)

Worst Case Setpoint: 20 psi above cover gas operating pressure at experiment test conditions

Required Instrument Channel Accuracy: ±10 psi

Nominal Setpoint: In the range 30 psia to 70 psia depending on normal steady-state operating condition

Normal Steady-state Operating Condition: In the range 10 psia to 50 psia

Maximum Predicted Excursion: Not applicable

Remarks:

a) This response time represents that time interval between the instant the actual value of the monitored variable exceeds the setpoint and the reactor control rods are seated.

b) Protective function (F) which utilizes Annulus Gas System makeup flow rate from the accumulator to detect leakage from the annulus would detect primary vessel leakage if of sufficient size (setpoints established by function (F) requirements).

c) The permissible limit has been defined as the minimum initial condition driving head across a postulated primary containment leak assuming the annulus gas pressure at the protective function (G) worst case trip (246 psia) and the maximum anticipated normal operating primary coolant pressure (211 psia) for any experiment.

Remarks: (Contd.)

d) Protective margin for this function is defined as the difference between the worst case trip point (80 psia) and the permissible monitored variable limit (85 psia).

e) "Two-out-of-four" logic is provided for this protective function. A minimum of two independent instrument channels shall be required for normal operation. With less than four channels, the function will operate with "one-out-of-N" logic, where N is the number of remaining channels.

F. Secondary Containment Integrity

The requirement for double containment of the FEFPL experiment during ETR operations establishes a need for a monitoring system which will detect if secondary containment is not maintained. There is no time response requirement stated in the ETR Technical Specifications[11] for protective action upon detection; therefore, any normal means of reactor shutdown by the operator complies with the requirement. There is a need to scram the reactor, if during a loss of secondary containment, there should occur a gross gas leak which (1) violates the limits of the ETR Technical Specifications relating to experiment gas leakage, or (2) allows gas flow in the water annulus channel between the loop and the core filler piece of a magnitude which would impede cooling enough to cause threshold cadmium melting of the thermal neutron filter.

The Annulus Gas System (AGS) allows the FEFPL PPS to continuously and automatically monitor the secondary containment for leaks. This capability applies when the loop is in the reactor (prior to startup and when the reactor is in operation).

This protective function has been established to monitor the secondary containment for leaks and initiate an automatic reactor scram when the leaks exceed the logic setpoint. It also detects leaks in the primary containment below the heat exchanger lower tube sheet which are large enough to allow annulus gas flow to exceed the setpoint for this protective function. The monitoring is accomplished by pressurizing the annulus between the primary and secondary containments with helium gas. The gas is maintained at a pressure higher than either the ETR coolant water pressure or the maximum anticipated normal sodium coolant pressure (see discussion in Paragraph 7.1.3.3-E). Protection against a low annulus pressure is provided by protective function (G) (see Paragraph 7.1.3.3-G). Any leakage through the secondary containment will result in escape of the gas from the annulus to the ETR coolant water. Leakage of gas from the annulus will be replaced by the AGS accumulator which is used as a static pressure reference. In effect, a gas leak initiates a double blowdown (e.g., the annulus and accumulator). Gas flow in the connecting line from the accumulator to the annulus is monitored, and if the flowrate exceeds the setpoint, a reactor scram is initiated (a description of these flow channels is given in Section 7.2.7).

An AGS pressure between 260 and 270 psia during this protective function is required (containment verification mode, CVM). A control dead band is permitted between 263 and 267 psia. At the lower bound a controlled makeup supply (0.1 - 0.2 SCFM) is initiated and maintained until the pressure increases to 265 psia. At the upper bound, a controlled exhausting (0.2 - 0.3 SCFM) is initiated and maintained until the pressure decreases to 265 psia. The controls provide long-term pressure correction due to changes in loop operation. The flow rates were kept low to minimize the impact on this protective function[13, 14].

A new extermely unlikely (EU) probability of occurrence gas leakage requirement has been determined for experiments as a result of the ETR Technical Specifications upgrading activity. The new requirement is: "if system design will allow transient gas leakage rates in excess of 15 SCFM, the PPS must initiate safety rod release within 0.350 seconds"[15]. The previously used requirement of 2.2 SCFM (steady-state limit) applied for leaks of an anticipated probability of occurrence. Since the FEFPL secondary containment is a Class 1 nuclear vessel designed and constructed to Section III requirements of the ASME Code[16], it was concluded that the EU classification for a gross gas leak was appropriate.

New FEFPL gas leak leakage requirements have been determined related to the reduced cooling for the thermal neutron filter. First, analysis showed that a gas-water flow mixture would occur in event of a leak[17]. Previously, it was conservatively assumed that a gas blanket occurred on the outside of the loop. Second, a two phase flow thermal analysis was performed to improve upon the earlier 0.106 SCFM steady-state limit. The critical condition was found to be homogeneous flow at a high void fraction. The results yielded a steady-state limit of 6.0 SCFM and a transient response whose time limits vary with higher leak rates. For example, a 9.6 SCFM leak rate requires a rod release by 4.8 seconds[18]. As can be seen, the FEFPL requirements are less demanding compared to the ETR gas leakage requirement.

An ETR-FEFPL composite rod release response time requirement curve has been plotted in Fig. 7.8 for leak rates greater than 6 SCFM. As indicated by the diagonal line area, a 1.0 SCFM adjustment (reduction) in the gas leak rate requirement was made[13]. When the FEFP primary loop undergoes a change in operating condition, the annulus gas located below the sodium level changes temperature, which affects the AGS operating pressure. For example, during a temperature rise, the pressure increase in the annulus causes some gas flow towards the accumulator (opposite to the flow direction to monitor a leak). Rapid changes in reactor power due to either a fast recovery startup to override xenon buildup or a scram were considered to be the dominant effect. From loop model thermal analysis, it was found that a 1.0 SCFM adjustment envelopes the startup transient while the reactor is at power[13, 19]. During

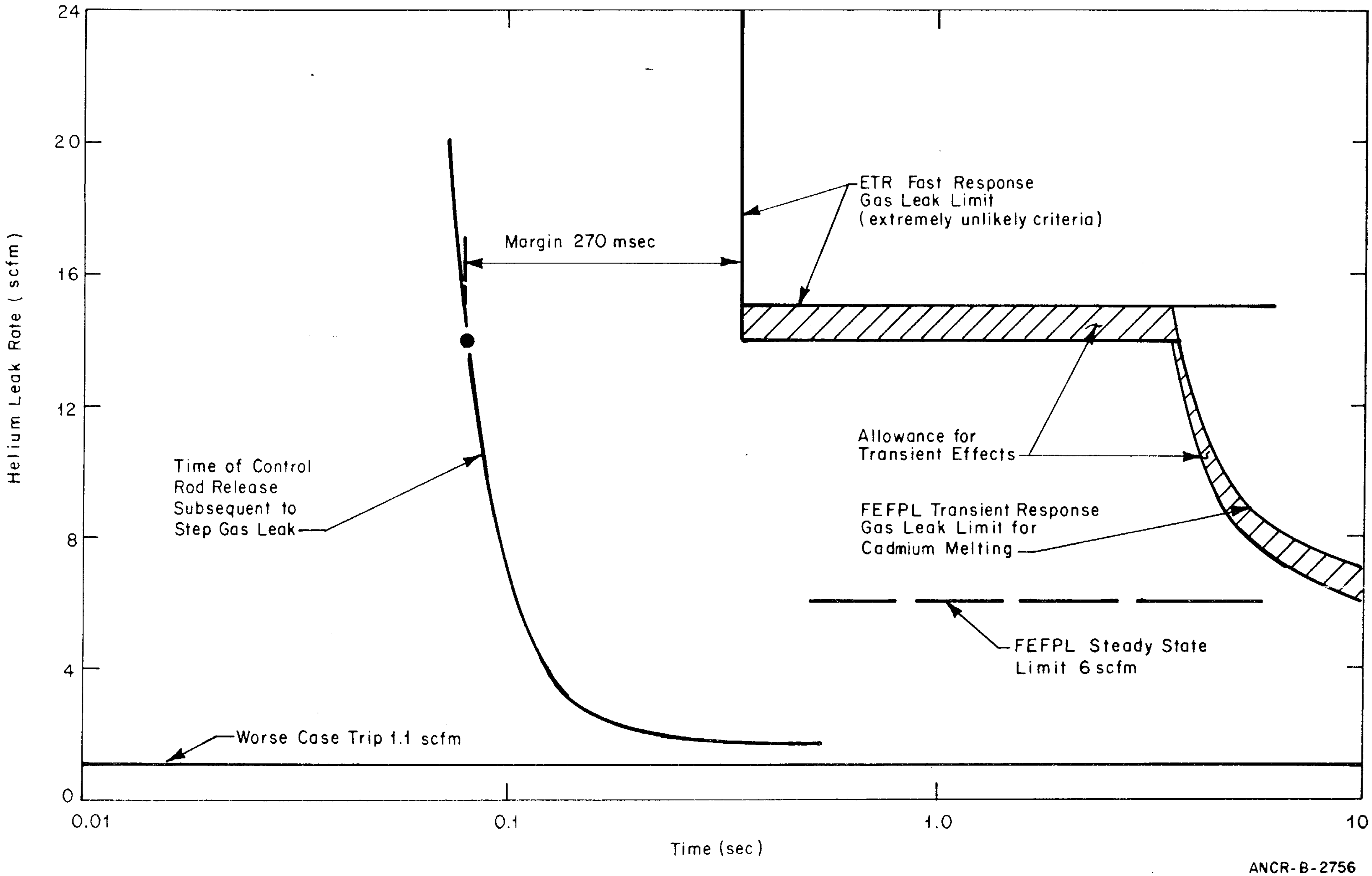

FIG. 7.8 - PPS (F) Time Response Release of Control Rods for Step Leaks

reactor scrams, the pressure condition occurs subsequent to when the reactor returns to a safe condition.

A computer code was developed to model the annulus and accumulator volumes with a line connection[20]. A double blowdown analysis was performed for gas leak rates ranging from 1.7 to 20 SCRM. The response time curve for reactor safety rod release is shown in Figure 7.8 for comparison with the gas leak requirements. A margin of 0.270 sec was obtained for a gas leak rate of 14 SCFM,representing the adjusted ETR gas leak requirement. The time response is shown to be satisfactory for all other leak rates exceeding 6 SCFM where transient requirements were specified. The analysis was based on the following parameters:

a) a worst case trip point of 1.1 SCFM which is related to a 1.0 ±0.1 SCFM setpoint.

b) flow sensor time constant of 100 msec.

c) signal processing by FEFPL PPS and ETR PPS leading to rod release of 30 msec.

The blowdown analysis data represents system parameters of 265 psia pressure, 660^{O}F gas temperature in the annulus, and an accumulator volume of 10 cu ft. A sensitivity analysis of varying each of these parameters over their likely range showed either greater time response margin of a margin reduction of only 10 msec for the worst case[13, 20].

Loop model thermal analysis indicated that for extreme loop operating and reactor recovery startup conditions, there is a possibility of spurious scrams with a 1.0 setpoint. However, at typical operating conditions, it should be more remote as the pressure change sensitivity in the annulus reduces[13].

Due to the severe sensitivity of certain combinations of reactor scrams and loop operating conditions, some trips by this protective function are likely to occur after the reactor is in a safe condition. The most significant accident producing this effect is the "loss of instrument air to ETR". Thermal analysis has indicated a possible flowrate of 2.3 SCFM over a minute after the scram has occurred. The loop sodium undergoes a severe chilling transient which reduces the annulus gas temperature; hence, a flow is created from the accumulator to the annulus to make up the reduced pressure in the latter.

A compilation of the essential performance requirements for this protective function is given in Table 7.1 - (F).

TABLE 7.1 - (F)

FEFP Loop Protective Function

Protective Function (F)

Title: Secondary Containment Integrity

Incident(s) Requiring Protective Action: Failure of secondary containment resulting in leakage of annulus gas into primary system.

Reference to Design Basis Documentation: EDF-1343, "Design Basis Analysis for FEFPL Protective Function (F): Secondary Containment Integrity", May , 1974.

Protective Action: Alarm and ETR scram

Maximum Time Permitted for Protective Action Completion: 410 msec (see Remark a)

Critical Loop Variable: Secondary containment integrity

Critical Variable Limit: Detection of a leak

Monitored Variable: Annulus Gas System makeup flowrate from the accumulator to the annulus gas space.

Permissible Monitored Variable Limit: (see Remark b)

a)	Steady state:	5.0 SCFM
b)	14.0 SCFM gas leak:	350 msec
c)	8.6 SCFM gas leak:	4.8 sec

Protective Margin: (see Remark c)

a)	14.0 SCFM gas leak	270 msec
b)	8.6 SCFM gas leak	4.7 sec

Worst Case Setpoint: 1.0 SCFM (see Remark d)

Required Instrument Channel Accuracy: ±0.1 SCFM

Nominal Setpoint: 0.5 SCFM to 1.0 SCFM

Normal Steady-state Operating Condition: Less than 0.9 SCFM during reactor power operations (see Remark e).

Maximum Predicted Excursion: Not applicable

Remarks:

a) This response time represents that time interval between the instant the actual value of the monitored variable exceeds the setpoint and the reactor control rods are seated. Requires sensor time constant (τ) $\leq$100 msec

Remarks: (Contd.)

b) Gas leak limits shown represent ETR and FEFPL gas leak rate limits adjusted downward 1.0 SCFM to account for uncertainties in pressure changes resulting from loop transients and AGS controlled makeup - exhaust operation.

c) Protective margin for this function represents the time interval between the actual and the required safety rod release time.

d) This setpoint was established to provide automatic scram protection for the ETR 2.2 SCFM steady state limit for anticipated probability of occurrence gas leaks (design goal, not a requirement).

e) Indicated flow rates up to 2.3 SCFM may occur subsequent to some reactor scrams due to the uncertainties arising in pressure changes from loop transients and possible concurrent AGS controlled makeup-exhaust operation.

f) "One-out-of-two" logic is provided for this protective function.

G. Annulus Gas System Pressure

Annulus gas pressure must be maintained above the pressure of the primary sodium, the pressure of the ETR water, and the helium system pressure to assure proper performance of protective functions (E) and (F). A secondary protective function has been provided which will scram the ETR if the AGS pressure is less than 35 psi above the maximum anticipated normal operating high pressure in the loop sodium or less than 33 psi above the nominal ETR water pressure and alarm the loop operator if the AGS pressure drops below the Helium System maximum operating pressure at the inpile loop heat exchanger, the maximum ETR system pressure above the core or the maximum faulted primary sodium pressure.

Pressures in the adjacent systems are maintained within the following controls:

ETR System Pressure Above Core[11]:

Nominal	200 psig (213 psia)	
Maximum	238 psig (250 psia)	ETR PPS worst case trip point for scram on high water pressure.

FEFPL Primary Sodium Operating Pressure:

Maximum anticipated normal operating[12]

Maximum	211 psia
Cover gas	50 psia
Pump head	158 psid[21] (restricted orifice case)
Hydraulic head	3 psid

Faulted[22]:

Maximums	250 psia
Cover gas	50 psia maximum
Pump (stalled)	190 psid
Hydraulic head	10 psid

Helium System Pressure[22]:

Nominal	260 psia supply (max to the IPL heat exchanger)
Faulted	300 psia

This protective function will provide an alarm if the AGS pressure falls below 260 psia and will scram the ETR if the pressure falls below 246 psia which is 35 psi greater than the maximum anticipated normal sodium pressure during operations. This is sufficient margin to assure operation of functions (E) and (F) during all normal loop operations and to assure an alarm if the annulus pressure drops below a level which under extreme loop conditions may limit the operation of function (E).

Figure 7.9 shows the relationship between the AGS pressure limits and setpoints. Criteria for the alarm and scram setpoints are listed in the brackets.

Two criteria have been used to establish the scram setpoint for AGS pressure at 250 psia:

1) The AGS pressure should be at least 35 psi greater than the maximum anticipated operating pressure in the sodium system (196 psia) allowing an instrument channel accuracy of ±4 psi and a worst case trip point of 246 psia. This ensures that for all expected operating conditions, a pressure differential of at least 35 psi would cause the inward flow of AGS helium through a leak in the primary containment, and is a design basis condition for protective function (E) (Primary Vessel Integrity). This is the principal criterion for the establishment of the scram setpoint.

2) The AGS pressure should be greater than the anticipated ETR water pressure in order that in the event of a secondary containment leak, water would not leak into the space between the primary and secondary containments. The nominal ETR water pressure is 213 psia. By using the scram setpoint established by criterion (1) above, a margin of 33 psi over the nominal ETR pressure is provided in order to meet the criteria stated in the previous sentence.

Three criteria have been used to establish the alarm setpoint for AGS pressure at 260 psia:

1) The AGS pressure should be greater than the maximum ETR water pressure. The ETR PPS worst case trip point for scram on high water pressure is 250 psia. If the AGS pressure drops below 260, the alarm would alert the operator that the pressure differential across the secondary containment could be close to zero if the ETR water pressure were up near its worst case trip point. If a secondary containment leak occurred, water could leak into the annulus gas space. An alarm is satisfactory since this can only occur if a leak existed along with two independent abnormal conditions, namely, low AGS pressure and high ETR water pressure. This condition would not prevent protective function (F) from meeting its design basis requirement for detecting gas flow into the reactor water[15].

2) The AGS pressure should be greater than the maximum faulted primary sodium pressure. This would prevent sodium from entering the annulus gas space under faulted conditions. If the primary sodium pressure were at its faulted maximum, protective function (E) would not necessarily rapidly detect a leak in the primary containment if the AGS pressure was abnormally low, near 250 psia.

FIG. 7.9 - Annulus Gas System Pressures - Limits and Setpoints

Pressure (psia)	
270	Annulus Gas System Maximum Operation Pressure (CVM)
267	Controls Deadband for AGS Makeup-Exhaust Operations
265	Annulus Gas System Nominal Operating Pressure (CVM)
263	
260	Annulus Gas System Minimum Operation Pressure (CVM) and AGS Low Pressure Alarm Setpoint Greater than Maximum ETR System Pressure Above Core Greater than Maximum Faulted Primary Sodium Pressure Greater than Maximum Helium System Operating Pressure
254	Instrument Channel Accuracy (±4 psi)
250	AGS Low Pressure Scram Setpoint
246	Worst Case Trip Point
	33 psi - Difference Between Worst Case Trip Point and Nominal ETR Pressure
	35 psi - Difference Between Worst Case Trip Point and Maximum Anticipated Sodium Operation Pressure
213	Nominal ETR System Pressure Above Core
211	Maximum Anticipated Sodium Operating Pressure

AGS 39 psi Greater than Maximum Sodium Operating Pressure
AGS 37 psi Greater than Nominal ETR System Pressure Above Core

3) The AGS pressure should be greater than the Helium System maximum operating pressure at the IPL heat exchanger. Meeting this criterion ensures that if a leak occurred in the heat exchanger shroud and the helium system were at its maximum operating pressure, protective function (F) would not be compromised because makeup flow to the annulus gas space would still be supplied from the AGS rather than the helium system thus indicating a leak.

The difference between the scram and alarm setpoints is small and one might suggest that the scram setpoint be raised to 260 psia at which point all five criteria indicated above could be applied to the scram setpoint. It has been set at 250 psia in order to provide additional operating margin and prevent spurious scrams. It should be noted that the criteria used for the alarm setpoint all guard against multiple failure situations and abnormal conditions.

A compilation of the essential performance requirements for this protective function is given in Table 7.1 - (G).

TABLE 7.1 - (G)

FEFP Loop Protective Function

Protective Function (G)

Title: Annulus Gas System Pressure

Incident(s) Requiring Protective Action: Low gas pressure in the annulus between the primary and secondary containments

Reference to Design Basis Documentation: EDF-1345[22,23,24,25,26], "Design Basis Analysis for FEFPL Protective Function (G): Annulus Gas System Pressure", May , 1974.

Protective Action: Alarm and ETR scram

Maximum Time Permitted for Protective Action Completion: 1.13 sec (see Remark a)

Critical Plant Variable: Annulus gas pressure

Permissible Variable Limit: Pressure must be greater than 246 psia

Monitored Variable: Annulus gas pressure

Protective Margin: Not applicable

Worst Case Setpoint: 250 psia

Required Instrument Channel Accuracy: ±4 psi

Nominal Setpoint:

a) Alarm: 260 psia

b) Reactor scram: 250-256 psia

Normal Steady-state Operating Condition: 260-270 psia

Maximum Predicted Excursion: Not applicable

Remarks:

a) This response time represents that time interval between the instant the actual value of the monitored variable exceeds the setpoint and the reactor safety rods are seated.

b) This is a secondary protective function which detects a condition which may limit the operation of protective functions (E) and (F). No transient is considered for this action. In the event of a malfunction in the Annulus Gas System which would prevent helium flow, this function will scram the reactor upon the occurrence of a secondary containment leak when the pressure drops below the setpoint.

c) "One-out-of-two" logic is provided for this protective function.

7.1.4 ETR Plant Protection System

The Engineering Test Reactor presently operates with a plant protection system (the ETR PPS) which allows experiments to be performed within its operating envelope. This system has provided satisfactory operation over a period of years. In addition, it is planned that as part of the reactor modifications needed for operation of the FEFP Loop in ETR that the ETR PPS will be upgraded. The system will be upgraded using RDT C 16-1T as a guideline. Specific requirements for the upgraded system are presently in preparation and not available at the time of completion of this document.

The purpose of this section is to establish some general requirements imposed on the ETR PPS and to identify ETR PPS/FEFP PPS interface requirements. These requirements are given in the following section and are briefly stated to indicate their existence, not necessarily to completely define each one.

7.1.4.1 System Upgrade

The system shall be upgraded, as committed in Ref. 27, to the requirements set forth in the ETR PPS Protective Subsystem SDD's.[28]

7.1.4.2 ETR Accidents

The ETR PPS shall limit the consequences of ETR accidents to the envelope as defined in the ETR Technical Specifications.[11]

7.1.4.3 Commercial Power

The system shall be designed to provide for reactor scram upon loss of commercial power. A protective function which indirectly responds to loss of commercial power is satisfactory for this requirement. The upgraded system will include a protective function which monitors reactor-core differential water pressure. The primary water pumps will lose power on loss of commercial power, the water flow will coast down and cause a trip on the core differential pressure protective function. The requirements as established in Ref. 28 for this protective function are satisfactory for the FEFP Loop. The purpose of the FEFPL requirement is to ensure that the reactor would not continue to operate for extended periods of time (scram shall be initiated within 3.5 sec after loss of commercial power). This requirement is established in Section 11.2.1, Loss of Commercial Power.

7.1.4.4 ETR PPS/FEFP PPS Functional Interface

The ETR PPS shall provide two inputs for FEFPL PPS generated scram signals. The detailed interface requirements (logic levels, impedance, etc.) shall be established by the ETR PPS responsible system designer. FEFP PPS/FAS interface requirements shall be established by the FEFPL PPS responsible system designer.

7.1.4.5 Manual Scram

The ETR PPS shall provide for the manual scram feature of the FEFPL PPS. The FEFPL PPS does not directly include the loop operator in implementing a protective function. However, manual control devices for manual initiation of each and every protective action (scram only for the FEFPL) are required by RDT C 16-1T for defense against unanticipated events. These manual control devices are considered part of the PPS and will be provided by the ETR PPS. The detailed interface requirements (electrical and mechanical) shall be established by the ETR PPS responsible system -esigner.

7.1.4.6 Electrical Power

The ETR PPS shall make provision for FEFPL PPS electrical power supply as part of its electrical power system. The ETR PPS responsible system designer shall establish the detailed interface requirements. This system shall meet the requirements established in Ref. 28.

7.1.5 System Design Guidelines

This section establishes guidelines used for the FEFPL Plant Protection System design. The FEFPL Plant Protection System includes all sensors, cable assemblies, signal conditioning, electronic trip modules, buffer amplifiers and logic modules necessary to provide the required FEFPL protective functions. Detailed requirements are covered in Ref's. 29, 30.

7.1.5.1 Applicable Documents

Unless otherwise specified, the following documents shall form a part of this document to the extent specified herein.

Government Documents

RDT C 1-1T	Instrumentation and Control Equipment Grounding and Shielding Practices (1/73)
RDT C 16-1T	Supplementary Criteria and Requirements for RDT Reactor Plant Protection Systems (12/69)
RDT C 16-2T	Protection System Logic (4/72)
RDT C 16-3T	PPS Buffers (10/71) Amendment 1 (12/71)
RDT C 16-4T	Protection System Comparator (4/72)
RDT C 17-4T	General Instrumentation (2/72)
RDT F 4-20T	Operation and Maintenance Manuals (10/71)

RDT F 7-2T Preparation for Sealing, Packaging, Packing and Marking of Components for Shipment and Storage (2/69)
Amendment 1 (10/21) Amendment 2 (9/72)

AEC Appendix 0500-1
Standard Health and Safety Requirements

IDO-12044 Health and Safety Design Criteria Manual

U. S. Government, Department of Labor, Occupational Safety and Health Act (OSHA), 29CFR 1910.

Non-Government Documents

NFPA No. 70 National Electric Code

Aerojet Nuclear Company Documents

FDR-08 FEFPL Instrumentation Integration System Design Requirements.

FDR-09 FEFPL PPS Design Requirements.

QAPP-1-2 FEFP Quality Assurance Program Plan.

CI-1233 ETR Technical Specifications.

Argonne National Laboratory Documents

R-1000-1001-SA
Fuel Element Failure Propagation Loop System Design Description.

7.1.5.2 Specific Requirements

The FEFPL Plant Protection System shall be designed in accordance with RDT C 16-1T "Supplementary Criteria and Requirements for RDT Reactor Plant Protection Systems". The FEFPL protective functions are documented in Table 7-1 as required by C 16-1T. The system shall implement these functions as indicated.

The following requirements shall apply:

Grounding and Shielding

The FEFPL PPS shall be designed in accordance with the draft standard RDT C 1-1T, "Instrumentation and Control Equipment Ground and Shielding Practices".

Logic Requirements

The FEFPL PPS logic system shall meet the requirements of RDT C 16-1T, and shall use RDT C 16-2T "Protective System Logic".

Buffers

All FEFPL PPS buffers shall meet the requirements of RDT C 16-1T, and shall use RDT C 16-3T "PPS Buffers".

Comparators

All FEFPL PPS comparators shall meet the requirements of RDT C16-1T, and shall use RDT C16-4T "Protection System Comparators".

Interface

The FEFPL PPS logic output signals shall interface with the ETR PPS. The interface shall meet the requirements of appropriate sections of the ETR PPS System Design Description*.

The FEFPL PPS channels shall provide a suitable buffered analog signal to the FEFPL Instrumentation Integration System (see FDR-08).

Location

System instrument panels shall be located at the FEFPL console area in the northeast corner of the ETR console floor. Instrument racks, cables, and sensors shall be separated to provide adequate isolation between redundant channels.

Panel Layout

The system instrument panel layout shall provide visibility and accessibility of controls, setpoints, calibration, and monitoring points, etc., required to maintain efficiency, reliability, and safety of operation.

Design Life

In-pile loop sensors shall have a design life exceeding 70 days full-power ETR irradiation time plus out-of-pile isothermal operation at 900°F and 450°F for 30 days and 180 days respectively. System subassemblies external to the FEFP loop shall have a design life of five years.

Environment

Environmental conditions for sensors internal to the FEFP loop shall be as specified in R-1000-1001-SA. External loop instrumentation and cable assemblies shall be designed to meet the following ETR environmental conditions:

	Console Floor	Nozzle Trench
Temperature	- 40°F - 120°F	80°F - 180°F
Humidity	- 0-95% RH	0-98% RH
γ -Radiation	NA	10^7 R (5 year total dose)

* This document is presently in preparation and specific references are not yet available.

Calibration

Design provisions shall be made for calibration of each instrument channel, exclusive of the channel sensor. Provisions for on-line functional checkout of the sensors will be provided where loop design permits.

Maintenance

The system shall be designed so that it can be maintained with normal plant maintenance practices. This requires that the design include provisions for recognition, removal, replacement, repair or adjustment of components or modules with the minimum interference with other equipment.

Commonalty

To the maximum extent possible, like modules shall be utilized in the design of the instrument channels to minimize spare parts requirements and facilitate maintenance.

Safety

The system shall be designed to comply with all applicable health and safety requirements specified in AEC Appendix 0500-1, IDO-12044, and U.S. Government, Department of Labor, Occupational Safety and Health Act.

Electrical Design

The electrical design of the FEFPL PPS shall meet the requirements of RDT C17-4T, "General Instrumentation," Section 3.6.

Mechanical Design

The mechanical design shall meet the requirements of RDT C17-4T, "General Instrumentation," Section 3.7.

Power Supplies

FEFPL PPS shall utilize the ETR-PPS Failure Free power supplies.

Identification

The FEFPL PPS shall be identified in accordance with IDO-12044, page 69A and RDT C16-1T, paragraph 4.9.

Features to Implement Administrative Control

Controlled access to the FEFPL PPS to implement administrative control shall meet the requirements of RDT C16-1T, paragraph 4.8.3.

7.1.5.3 Quality Assurance Provisions

Quality Assurance

System hardware shall be purchased, documented, inspected and tested in accordance with QAPP-1-2, FEFP Quality Assurance Program Plan.

Documentation

Operating and maintenance manuals will be provided in accordance with RDT F4-20T, "Operation and Maintenance Manuals".

Performance Verification

Verification that the FEFPL PPS design meets the requirements of this document shall be made prior to FEFPL operation. The successful performance of system operating tests to approved procedures will provide the basis for acceptance of system hardware.

7.1.5.4 Component Packing and Marking

Components and parts procedure after the issue date of this document shall be packaged and marked for shipment and storage in accordancd with RDT F7-2T, "Preparation for Sealing, Packaging, Packing and Marking of Components for Shipment and Storage," and ordering data as required for each component or part.

7.2 System Description

7.2.1 Summary

The containment safety margin is monitored by measuring: (A) loop primary vessel temperature in the fuel region; (B) loop primary vessel temperature around the meltdown cup; (C) secondary vessel temperature in the fuel region; and (D) primary vessel transient pressure. These measurements are made using 8 independent instrument channels for function (A) , and 4 independent channels each for (B), (C), and (D), utilizing redundant 2 out of 8 (2/8) and 2 out of 4 (2/4) logic, respectively, to initiate a scram signal.

The integrity of both the primary and secondary vessel is monitored by establishing a static helium pressure in the annulus between the containment vessels. The static pressure will be maintained above both the loop primary coolant pressure and ETR primary coolant pressure. A leak in either the secondary vessel or the primary vessel, in common with the annulus gas system, will be detected if helium flows into the annulus at a rate above that needed to compensate for temperature changes. A leak in the primary vessel from the annulus gas system, or from the secondary coolant (helium) system through a heat exchanger tube, will cause an increase of the loop static pressure as measured by pressure sensors in the sodium plenum. The annulus gas system is designed to limit the helium flow rate into the annulus to a value less than the maximum allowed by the ETR Technical Specifications[11] for leakage into the ETR vessel.

The primary containment static pressure is monitored by 4 independent channels utilizing 2/4 logic. The annulus gas system helium flow and pressure are monitored by 2 channels of instrumentation for each measurement and 1/2 logic is utilized for each protective channel. A summary of the essential performance requirements of the instrument channels is given in Table 7.2.

The choices for protective channel redundancy as indicated above were based on RDT C16-1T requirements and FEFPL system configuration and requirements. RDT C 16-1T requires:

1) Two or more protective channels shall be used to implement each protective function.

2) The PPS shall be designed so that the failure of any one instrument channel to a safe state will not unduly reduce plant availability.

3) The PPS shall be designed with defenses against protective subsystem failures caused by internal random failures and credible single events. Further, it recommends instrument channels be used in coincidence, M out of N, where $N > M \geq 2$.

For FEFPL PPS instrument channels whose sensors are located on or in the in-reactor loop structure, the corresponding protective functions are implemented using two out of four or two out of eight logic. This choice was made based on the following considerations:

a) At least 2 out of 3 is needed to minimize loss of loop availability due to random failure of a sensor. It is very difficult to repair or replace failed sensors on the in-reactor loop structure. This complies with (2) above by implementing at least a 2 out of 3 system as recommended. However,

b) At least 2 out of 4 is needed since there are two isolated routes for PPS cables, assuming an undetected failure in a cable route is a credible single event. This complies with (3) above.

For FEFPL PPS instrument channels whose sensors are located external to the ETR vessel, 1 out of 2 logic will be used. These sensors are relatively easy to repair or replace, and isolated cable routes will be provided. See Section 7.2.9 for additional discussion on system cabling.

TABLE 7.2

SUMMARY OF INSTRUMENT CHANNEL ESSENTIAL PERFORMANCE REQUIREMENTS

Protective Function	Monitored Variable	DBA Time Permitted for Scram Completion	Number of Channels	Minimum Required Instrument Range	Instrument Channel Accuracy	Primary Sensor Designation Numbers*	Backup Sensor Designation Numbers
A	Primary wall (OD) temperature in fuel zone	0.7 sec	8	400-1400°F	± 25°F	TE-14-1,2,3, 4,5,6,7,8	------
B	Primary wall (OD) temperature around meltdown cup	1.1 sec	4	400-1400°F	±25°F	TE-15-1,2,3, 4	------
C	Secondary wall (ID) temperature in fuel zone	0.7 sec	4	200-1000°F	+40°F -25°F	TE-16-1,2,3, 4	------
D	Transient sodium pressure	0.75 sec	4	0-2000 psi	±200 psi	PE-1-1,2; PE-3-1; PE-6-1	PE-3-2; PE-6-2
E	Primary Containment cover gas static pressure	0.5 sec	4	1-100 psia	±10 psi	PE-7-1,2,3, 4	PE-2-1,2 PE-4-1,2
F	Annulus gas makeup flowrate	0.41 sec	2	0-3.0 SCFM	±0.1 SCFM	FT-1,2	------
G	Annulus gas static pressure	1.13 sec	2	150-300 psia	±4 psi	PSL-1,2	------

* These numbers are those assigned to the P-1 experiment test train sensors (see Table 5.1). This document establishes requirements for PPS sensors as indicated in the appropriate sections. The designation numbers themselves may vary from experiment to experiment.

Figure 7.10 shows a typical protective function utilizing four redundant instrument channels to monitor a single loop variable. Signals A, B, C and D are four redundant analog variables corresponding to a single loop variable. These signals are amplified by the signal conditioner to provide a standard 0 to 10 volt output signal to the comparator and buffer inputs. The buffer output, which is isolated from the signal conditioner output, is available for non-PPS use (i.e., data acquisition, indicating, etc.). The comparator compares the signal conditioner output level with its integral setpoint (which is manually set) and outputs two logic signals and an isolated relay contact closure, the status of which depends on the relative magnitude of the input signal and setpoint level.

The two logic signals are buffered through optical couplers at the logic train inputs. The logic train performs the necessary logic functions and outputs a logic signal and a relay contact closure. The logic output signal goes to the ETR PPS and the relay contact closure is used for annunciator and alarm service. Optical couplers are used to provide complete electrical isolation at strategic points throughout the protection system logic. There is no electrical connection between the comparator output and logic train, or logic train and ETR PPS. Consequently, an electrical fault in a single instrument channel cannot propagate through the other channels. Each logic system is isolated from the others so that any one can initiate protective action regardless of an internal electrical fault in any other logic system. With optically coupled signals, common grounds are eliminated between the various subsystems. This assures that common mode ground line noise will be minimized thereby reducing the number of spurious trips.

7.2.2 Comparator

The comparator (see Fig. 7.11) is fabricated totally of solid state circuitry. The input signal is compared with the setpoint signal by the comparator circuit which generates a logic signal, the state of which depends upon the relative magnitude of the input signal and setpoint level. The comparator output drives two optical isolators, one located in each logic train. A relay output is also provided for annunciator and alarm service. The input signal level is monitored with indicator lamps located on the comparator front panel. This allows the operator to immediately determine the status of each channel. The setpoint generator can be manually set for

FIG. 7.10 - TYPICAL PROTECTIVE FUNCTION BLOCK DIAGRAM (2/4 FUNCTION)

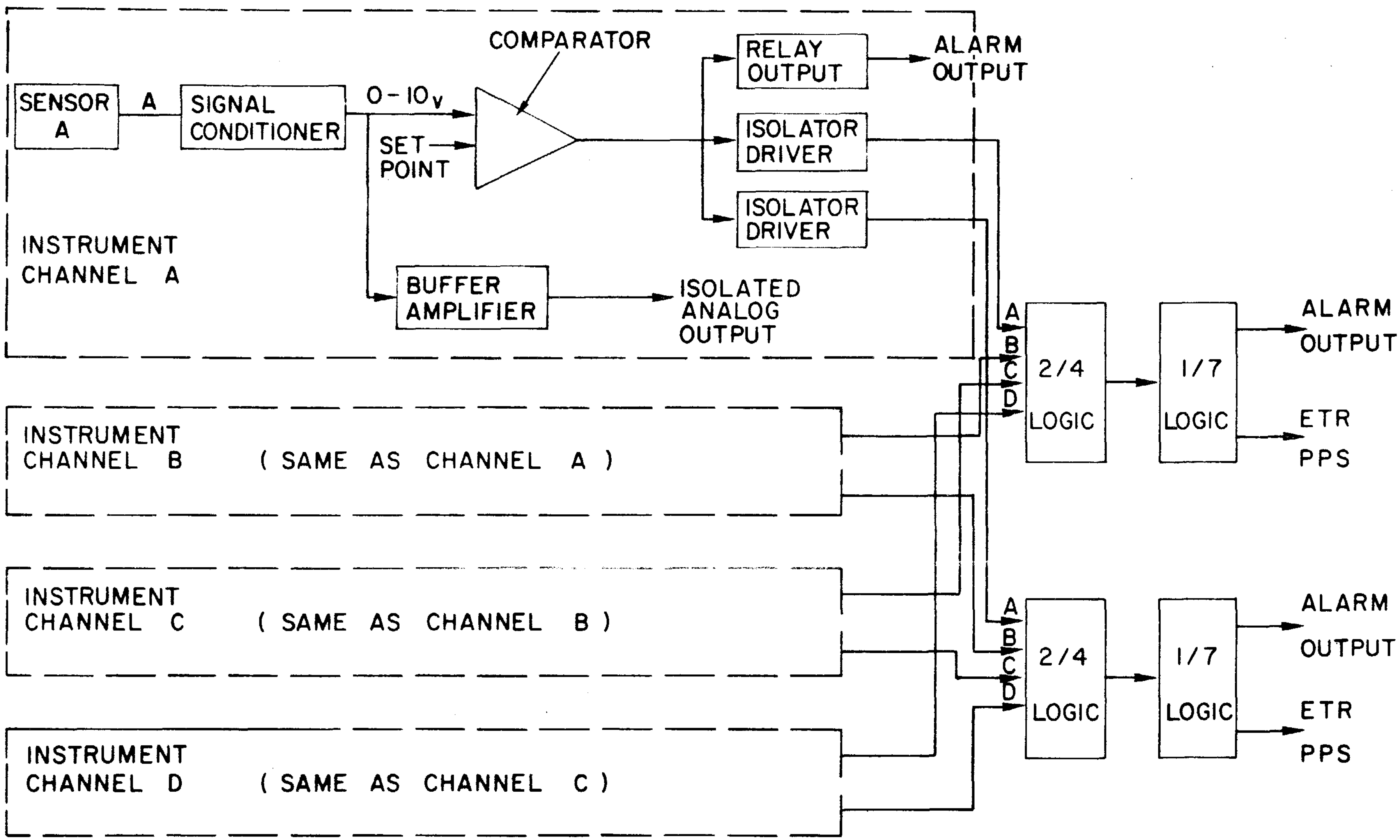

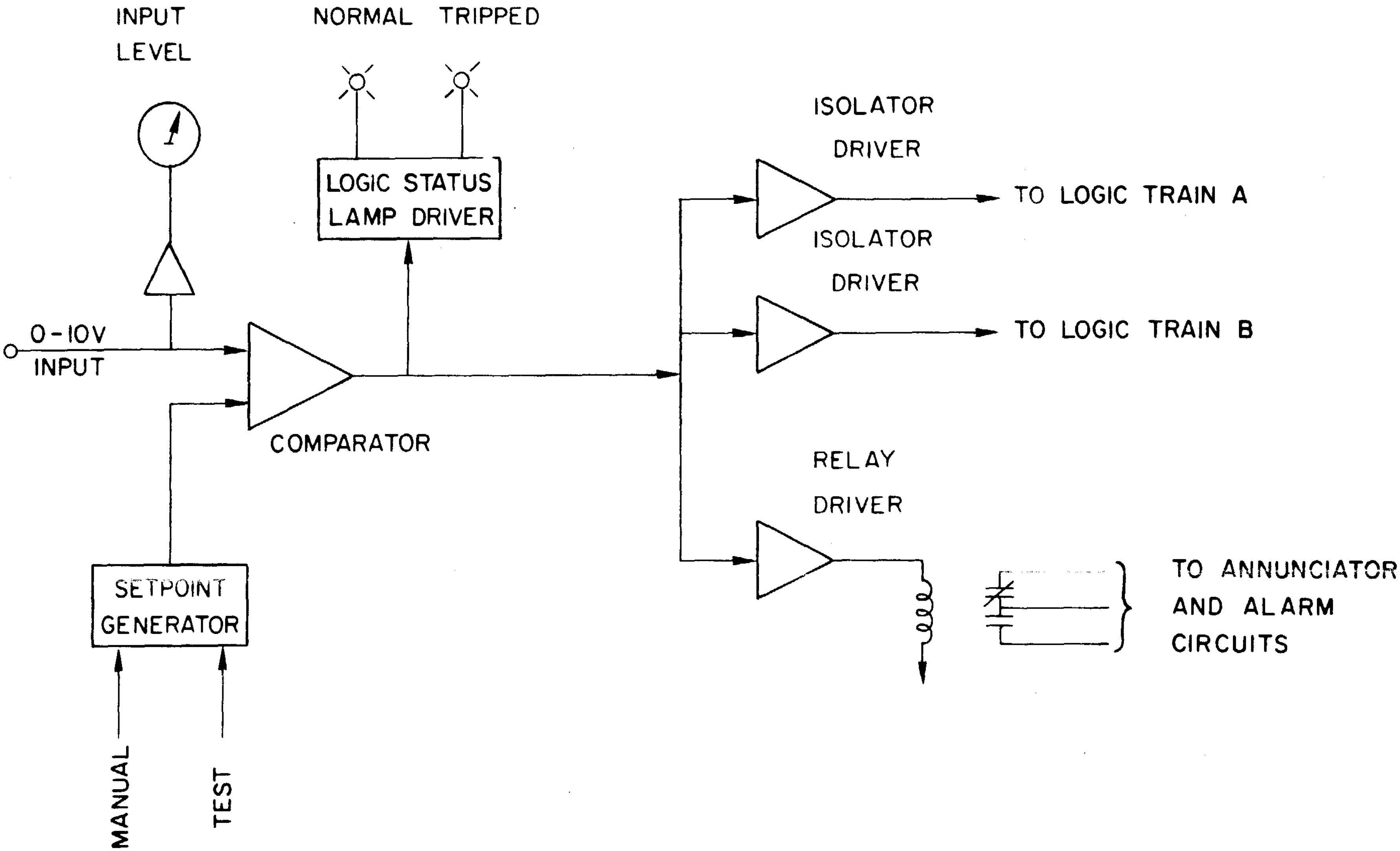

FIG. 7.11 - PROTECTION SYSTEM COMPARATOR

any setpoint over the input range of the comparator (0 to 10 volts). A test input provides for on-line testing of the comparators and logic circuitry for "two out of four" or "two out of eight" channels. All logic levels will be high (nominal + 15 volts) during normal operating conditions. When the input signal level exceeds the setpoint, the logic level will switch to a low (at or near zero volts) state. This gives added protection against: 1) logic cable shorts to ground, 2) logic cable breaks, 3) removal of a comparator module, and 4) power supply failure. If any of these occur, the logic train will go to the tripped or safe condition. All the comparator circuits used in the FEFP Plant Protection System will be identical.

7.2.3 Logic Train

The two logic trains (see Figure 7.12) are identical and utilize all solid-state high level logic. The input circuits are optical isolators and accept the logic signals from the comparators. These provide the necessary isolation between the instrument channels and logic train. The logic train performs the necessary 2/4, 2/8 and 1/2 logic functions as required by the protective channels and outputs a logic signal to a one out of seven logic gate. This gate is tripped when any one of the seven required protective channels is tripped. The 1/7 logic function outputs a signal to the ETR PPS. Two independent logic trains provide inputs to two ETR PPS channels. Each logic train provides an isolated relay output for alarm annunciator service, for operator surveillance and to facilitate maintenance and testing.

7.2.4 Temperature Channels (Protective Functions A, B, C)

Temperature measurements are made for three protective functions on the loop, (see Figure 7.13). Thermocouples for protective function (A) are designated TE-14-1 through TE-14-8, and are used in a 2 out of 8 protective channel. Thermocouples for protective functions (B) and (C) are designated TE-15-1 through TE-15-4 and TE-16-1 through TE-16-4, respectively, and are used in 2/4 protective channels. Each channel consists of a thermocouple (type K), transmitter, comparator, buffer amplifier, and interconnecting wiring. The transmitter is sized to provide a 0-10 volt signal into the comparator and buffer amplifier over a full temperature range. The buffer amplifier has unity gain and provides a 0 to 10 volt output to the data system.

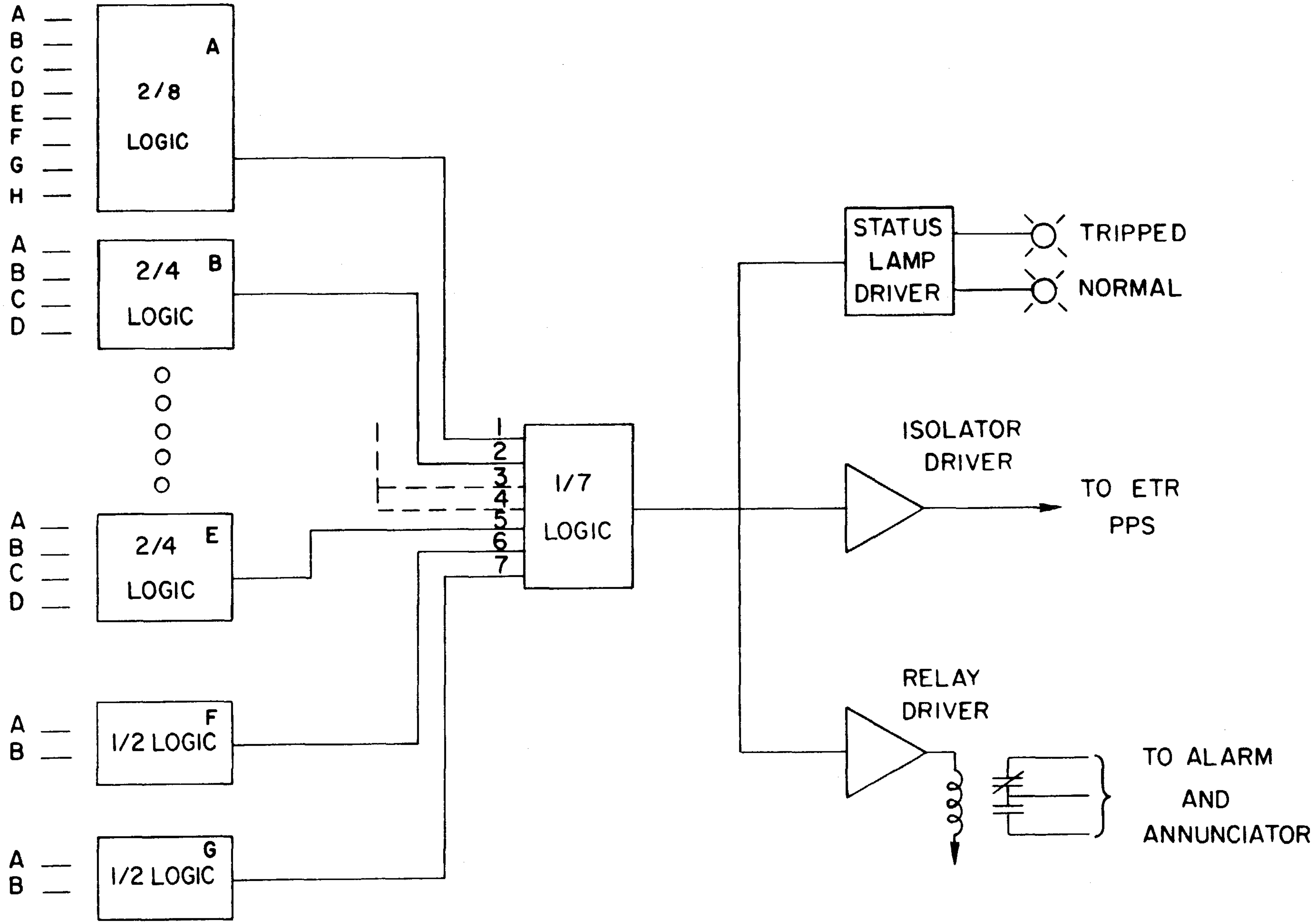

FIG. 7.12 PROTECTION SYSTEM LOGIC TRAIN

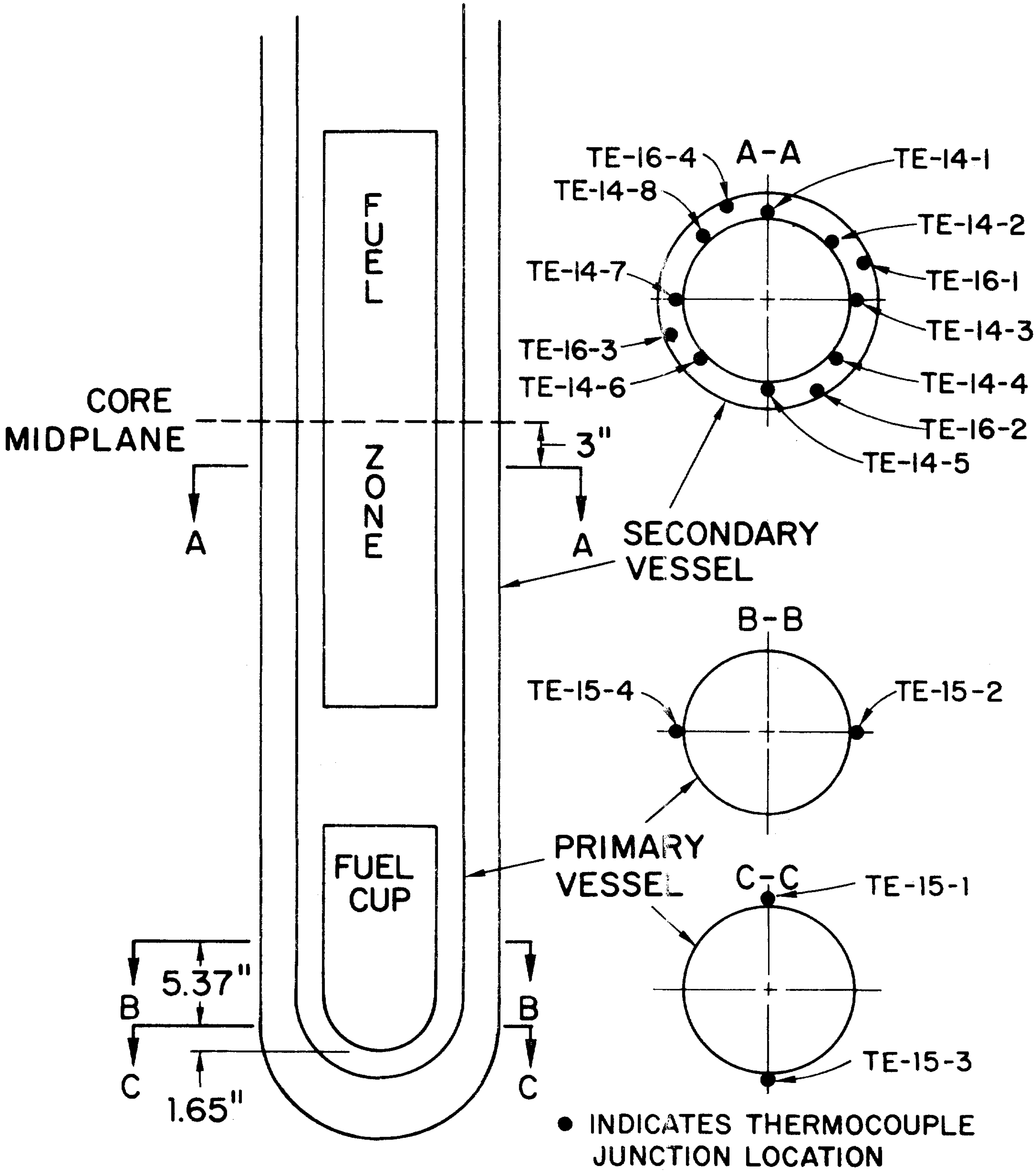

FIG. 7.13 THERMOCOUPLE LOCATIONS

Conventional Type K metal-sheathed magnesia insulated thermocouples are used with a standard 0.062 in. diameter sheath and a grounded junction. These thermocouples meet the requirements of RDT C7-6T "Thermocouple Assembly, Nuclear Grade, Chromel-P vs. Alumel, Stainless Steel Sheathed, Magnesium Oxide Insulated."

Some general requirements for the thermocouples are listed below:

Type:	Chromel (P)-Alumel, ISA Type K (grounded)
Range:	0°F to 2200°F
Thermocouple Alloy Accuracy:	Special Limits of Error* (± 2°F from 32° to 530°F, ± 3/8% from 530°F to 2300°F)
Response Time:	100 milliseconds time constant design goal for grounded
Neutron Flux:	3.3×10^{14} n/cm^2-sec thermal, maximum 1.5×10^{15} n/cm^2-sec fast, maximum
Gamma Flux:	1.5×10^{9} R/hr maximum
Sheath Material:	304 Stainless Steel

Specific locations and mounting techniques are shown on drawing ANC 402984 "FEFPL In-Pile Tube Instrumentation Locations".

7.2.5 Sodium Loop Transient Pressure Channels (Protective Function (D))

The primary containment transient sodium pressure is monitored with strain gage pressure sensors within the test train. Locations are indicated in Figure 7.14. The sensor signal conditioning provides a 0 to 10 volt signal for the comparator and buffer amplifier. Four independent channels supply signals to the 2/4 logic train.

The Type II pressure sensors PE-1-1 and PE-1-2 in the test train inlet pressure sensor holder above the inlet flow sensor, and PE-3-1 and PE-6-1 located at the fuel bundle outlet and at elevation of the heat exchanger outlet plenum, respectively, are bonded-strain-gage-type pressure sensors. Sensors PE-3-2 and PE-6-2 are backup sensors for this protective

---

* This definition is in accordance with ASTM E 230 "Temperature-Electromotive Force (EMF) Tables for Thermocouples". It essentially specifies a special grade of alloys and not necessarily the measurement accuracy of a thermocouple assembly.

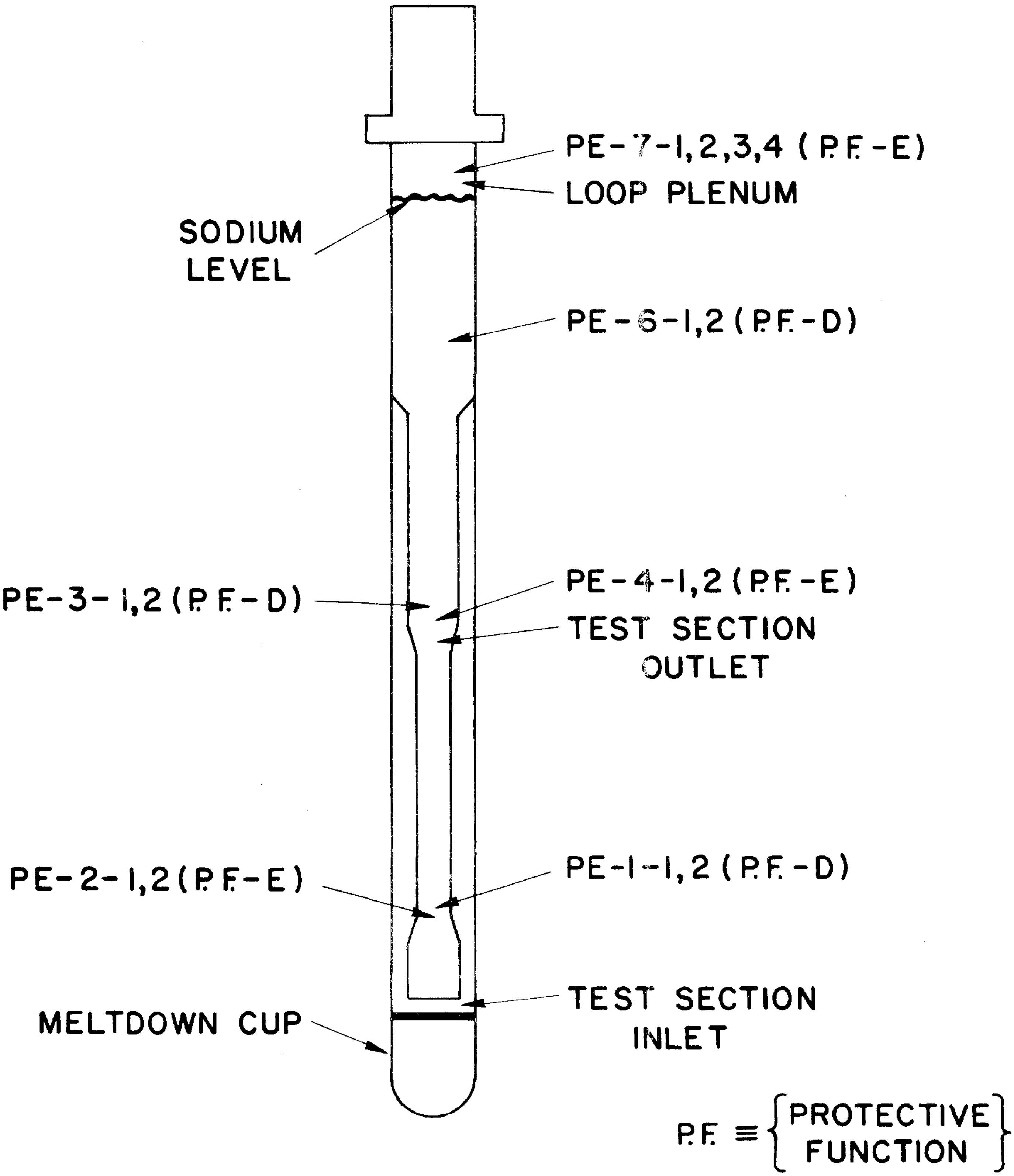

See ANL Drawing R1012-0002-DE-01
"FEFP Test Train P1 Layout Drawing"
for specific locations.

FIG. 7.14 TEST TRAIN PRESSURE SENSOR (PRIMARY AND BACKUP) LOCATIONS function. These sensors measure fast transient pressure pulses that may be generated by a molten fuel-coolant interaction. Each sensor is a cylinder housing a rectangular type 316 stainless steel post with two strain gages mounted on each side of the post. The strain gages are applied by flame spray techniques. The post is set into one end of the cylinder (non-sensing end) and the other end of the post is set into a diaphragm support and post centering disk (sensing end). A diaphragm is placed over the sensing end and welded to the cylindrical housing. All welds on the sensor are tungsten inert gas welds. The case material and other metal parts are 316 stainless steel. The strain gages are used in a fully active four arm bridge requiring four wires.

The electrical signal is obtained from the change in resistance of the gages when their lengths are changed. Two metal sheathed, two conductor cables terminate in the non-sensing end of the sensor providing the four sensor wires.

Type II Transient Pressure Sensor Characteristics:

Ranges: Local ambient to 2000 (Primary) and 10,000 (Backup) psi

Accuracy: ± 10% of full scale required; design goal ± 5% of full scale

Signal to Noise Ratio: Greater than 10:1 required; design goal greater than 20:1

Rise Time: 10% to 90% of full scale in 35 microseconds

Low Frequency Cut-Off: 2Hz

Environment: Sodium liquid or vapor, argon on helium gas

Operating Temperature: 400°F to 1300°F

Neutron Flux: $< 2 \times 10^{10}$ n/cm^2-sec thermal maximum
$< 2 \times 10^{6}$ n/cm^2-sec fast maximum

Gamma Flux: $< 10^{8}$ R/hr maximum

Static Operating Pressure: 0-200 psia

Envelope: As per ANL Drawing R-1040-0004-DA, Transient Pressure Sensor Case Configuration Control Drawing

Since these transient pressure sensors are developmental sensors they will be extensively tested in sensor qualification tests to assure their reliability before they are used in the first nuclear tests. If sufficient reliability cannot be demonstrated in qualification tests, the following changes will be implemented: 1) The primary PPS sensor PE-3-1 will be relocated to the PE-6-2 location. This will reduce the required upper operating temperature from 1300°F to approximately 1050°F for all primary sensors; 2) The transient pressure sensors will be qualified to these reduced requirements, or 3) Eddy current pressure sensors available to RDT Standard C6-3T "Liquid Metal Pressure Measurement System, Flush-mounted, Eddy Current-type, Inductive, Absolute or Gage" will be procured, qualified and used to replace the strain gage sensors. Eddy current sensors are commercially available for operating temperatures to 1050°F, with satisfactory time response characteristics.

7.2.6 Sodium Loop Static Pressure Channels (Protective Function (E))

Eddy current pressure sensors located in the primary containment monitor sodium static pressure. Locations on the test train are indicated in Figure 7.14. The sensor signal conditioning provides a 0 to 10 volt signal for the comparator and buffer amplifier. Four channels supply signals to the 2/4 logic train.

The Type I static pressure sensors PE-7-1,2,3,4 are slow response and measure the loop plenum pressure. Sensors PE-2-1,2 and PE-4-1,2 are backup sensors for this protective function. These eddy-current sensors are housed in type 316 stainless steel cylinders. The cables are 1/16 in. OD, magnesia insulation, stainless steel sheath with stainless wires.

Type I Static Pressure Sensor Characteristics:

Range: 0 - 100 psia*, 0 - 200 psia (backup)

Accuracy: ± 10% of full scale required, design goal ± 5% of full scale.

Signal to Noise Ratio: Greater than 10:1 required; design goal greater than 20:1

Rise Time: 10% to 90% of full scale in 100 milliseconds

Environment: Same as Type II, except for Envelope which is per ANL drawing R-1040-0003-DA, Static Pressure Sensor Case Configuration Control Drawing.

These static pressure sensors are developmental sensors and will be extensively tested in approved qualification tests to assure their reliability before they are used in the first nuclear test. If sufficient reliabil-

* This is a nominal value, these sensors have at least a 50% over-range capability.

ity cannot be demonstrated, the following changes will be implemented: 1) The backup sensors PE-4-1, -2 are required to operate to 1300°F, however, the primary PPS sensors PE-7-1, -2, -3, -4 are in the gas plenum and will never exceed 1050°F operating temperatures. These primary sensors will, therefore, be qualified to the lower temperature requirements, 2) if qualification cannot be demonstrated to the reduced temperature requirement, these sensors will be replaced with sensors commercially available to RDT Standard C 6-3T, which are rated for 1050°F operation.

7.2.7 Annulus Gas Flow Channels (Protective Function (F))

The PPS will provide continuous monitoring of the FEFPL containment vessels for any leakage which is of sufficient magnitude to require prompt action. The Annulus Gas Flow Channels provide instrument channels for plant protective function (F) which monitors for containment leakage. The Annulus Gas Flow Channels utilize gas flow transmitters in the Annulus Gas System (AGS). These two flow transmitters are identified as FT-1 and FT-2 in Figure 7.15.

A brief description of the Annulus Gas System as it operates with the Plant Protection System will aid in explaining the operation of these flow channels.

Prior to ETR startup, the annulus gas (helium) pressure is increased to the 265 psia nominal pressure for the AGS containment verification mode (CVM) (see Fig. 7.9). Solenoid operated block valves, used for the Fuel Meltdown Cup Cooling Mode (FMCCM) or system blowdown (due to Helium System depressurization to atmosphere), are closed to restrict the CVM gas volume and minimize out leakage. During the meltdown cup cooling operation, these valves open to permit helium flow from the FMCCM gas system to the bottom of the loop and, thence, to the ETR exhaust stack. However, this mode occurs only during reactor shutdown, as it is initiated by a buffered FEFPL PPS protective function (B) trip signal.

During CVM operation, the gas pressure is allowed to float within a dead band region of 263-267 psia. Some change in the static pressure is expected due to sodium loop heat transfer disturbances. To provide long-term correction in pressure due to major changes in the sodium loop status, a makeup-exhaust control capability has been provided (see Fig 7.15). The accumulator provides a static reference pressure for the loop annulus gas space. Whenever one of the following events occurs, the flow transmitters will indicate a gas flow movement from the accumulator towards the annulus.

a) gas leak in secondary containment

PR - Pressure Regulator
SV - Solenoid Valve
FCV - Flow Control Valve
PS - Pressure Switch
FT - Flow Transmitter
DPS - Differential Pressure Switch
MRV - Mechanical Relief Valve
CV - Check Valve

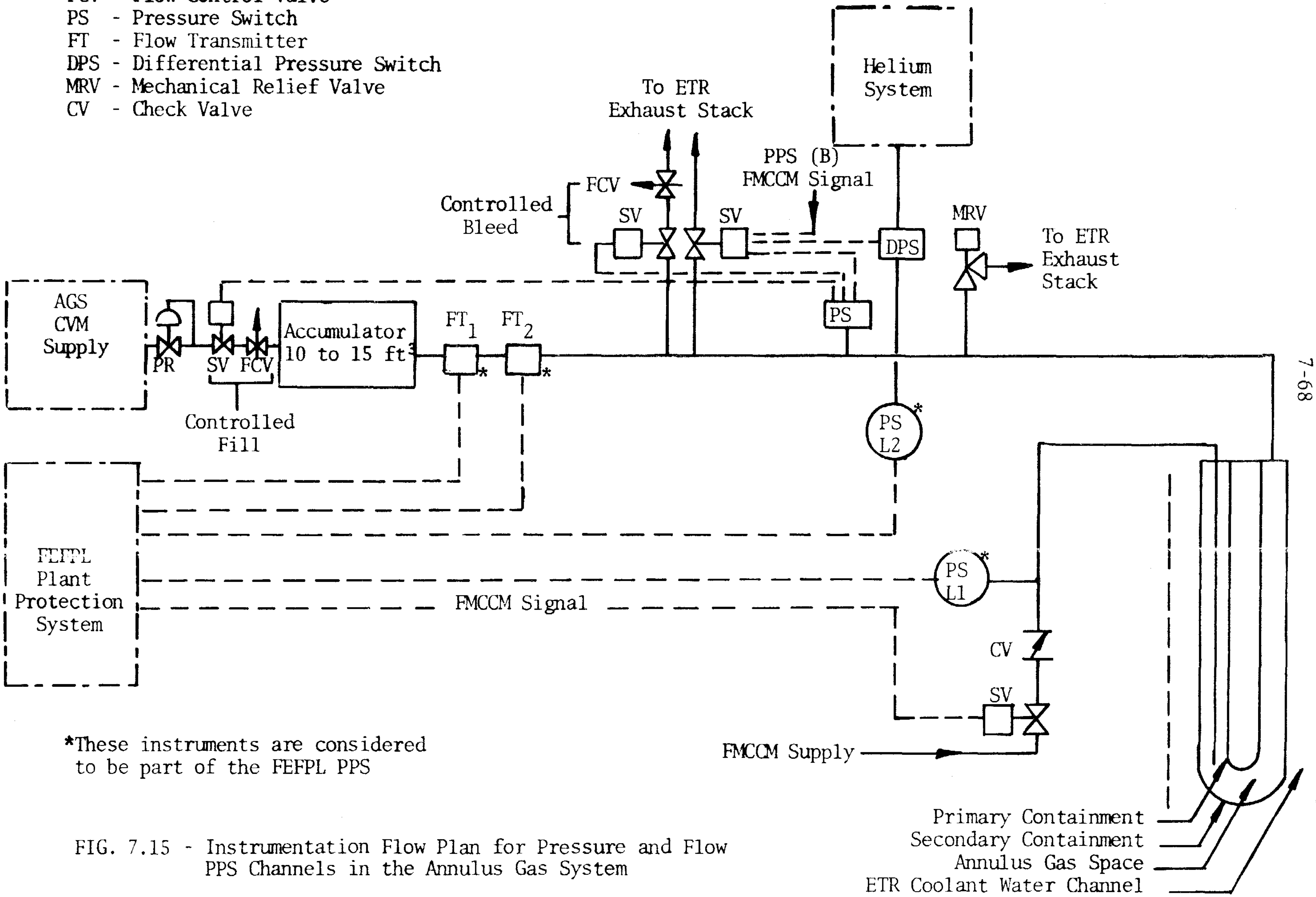

*These instruments are considered
to be part of the FEFPL PPS

FIG. 7.15 - Instrumentation Flow Plan for Pressure and Flow PPS Channels in the Annulus Gas System

b) gas leak in primary containment below heat exchanger lower tube sheet

c) gas leak in heat exchanger outer shell

d) annulus gas temperature decrease from loop transient

e) AGS controlled makeup or exhaust operations.

This "makeup flow" is indication of a leak if the setpoint for protective function (F) is exceeded. Items (d) and (e) combined are not expected to initiate trips while the reactor is at power. An annulus gas temperature increase from a loop transient causes flow in reverse (e.g., towards the accumulator). This effect has been compensated in gas leak limit requirements.

Gas flow through both FT-1 and FT-2 is detected by the FEFPL PPS comparators. If the flow exceeds the comparator setpoints as established by protective function (F), Table 7.1 - (F), the PPS is tripped thereby initiating a signal to the ETR PPS which scrams the reactor. A scram alarm indicates to the operator that the double containment integrity has been lost. The PPS setpoints are set above any normal gas flows which will occur during temperature transients or due to minor leakage through valves or instruments external to the annulus.

Two flow transmitters and associated cables, comparators and logic are provided for redundancy and shall be physically separated to prevent failure of both channels by any single credible event. Provisions shall be provided to permit end-to-end testing of these PPS channels prior to ETR startup.

All signal conditioning, comparators and logic for these flow channels will be installed in the FEFPL PPS equipment racks. A flow indicator will be provided for each channel to permit operator monitoring of the channel status. The protective channels will utilize "one-out-of-two" protective logic, therefore, testing must be performed during ETR shutdown conditions.

7.2.8 Annulus Gas Pressure Channels (Protective Function (G))

The annulus gas pressure is monitored with two pressure switches. One switch (PSL-1) monitors AGS pressure on the FMCCM supply side of the annulus, the second switch (PSL-2) senses the gas pressure on the FMCCM exhaust side of the annulus (Fig. 7.15). This provides for physical separation of the two channels including the lines which couple to the annulus. Each pressure switch will be in a closed contact state during normal operation with the annulus pressurized above the required setpoint. Each switch will have contacts energized by a logic voltage power supply to drive input optical couplers to both FEFPL-PPS logic trains. On drop of pressure below the setpoint, the contacts will open. Contacts opening on either switch will result in trip signals to both logic trains and an ETR scram. Monitor lights will be provided on the PPS instrument panels to provide easy operator observation of the status of each switch. An analog monitor will also be provided to indicate the actual annulus pressure. This monitor will have no PPS functions. Annulus pressure is maintained above both ETR primary system pressure and the FEFPL sodium loop maximum operating pressure. The pressure switches are adjusted to trip at a pressure corresponding with the desired setpoint as established in the design basis. These channels operate with "one-of-two" logic, therefore, testing must be performed during ETR shutdown. PSL-1 and PSL-2 provide both the alarm and scram trip points for this protective function.

7.2.9 Interconnecting Cables and Equipment Layout

Thermocouple cables for each protective function located on the in-pile tube are physically isolated from each other by uniform spacing around the outside and inside diameters of the primary and secondary vessels, respectively. These cables are brought through two connectors (Figure 7.16, Connectors 3 and 4) at the top of the loop. Cables from each of protective functions (A), (B), and (C) (2/8, 2/4 and 2/4) are split sequentially between these two isolated connectors. Cables from pressure sensors, protective functions (D) and (E) (2/4 and 2/4), pass through a single connector at the top of the test train (see Section 7.2.12 for exceptions to isolation requirements) and are routed to two isolated connectors (Figure 7.16, Connectors 1 and 2) in the removable top closure with cables from each protective function split between these connectors.

The system interconnecting cables from the removable top closure (see Figure 7.16) are routed in such a way as to maintain PPS channel isolation. Four cables originating at the loop connectors (1,2,3,4) go through the nozzle trench and cable access (CA) holes to two junction boxes at the north balcony. In these junction boxes the Data Acquisition System signal cables are separated from the PPS cables and the PPS cables are separated into the four isolated routes each connecting to one of four PPS instrument racks. Two cables connect each PPS instrument rack to the logic trains. Two independent cables go from the annulus gas system to the PPS instrument racks. Two independent cable routes also run from the logic trains to the ETR PPS. Figure 7.17 shows the locations of these cables.

For FEFPL PPS instrument channels whose sensors are located on or in the in-reactor loop structure, the corresponding protective functions are implemented using "two out of four" or "two out of eight" logic. RDT C16-1T requires that the PPS shall be designed with defenses against protective subsystem failures caused by internal random failures and credible single events. Further, it recommends instrument channels should be used in coincidence M out of N, where $N > M \geq 2$, to reduce the number of spurious trips causing the initiation of a protective action. A minimum of two isolated cable routes (with exception as noted above) are provided for each protective function, and assuming that an undetected failure of instrument channels in

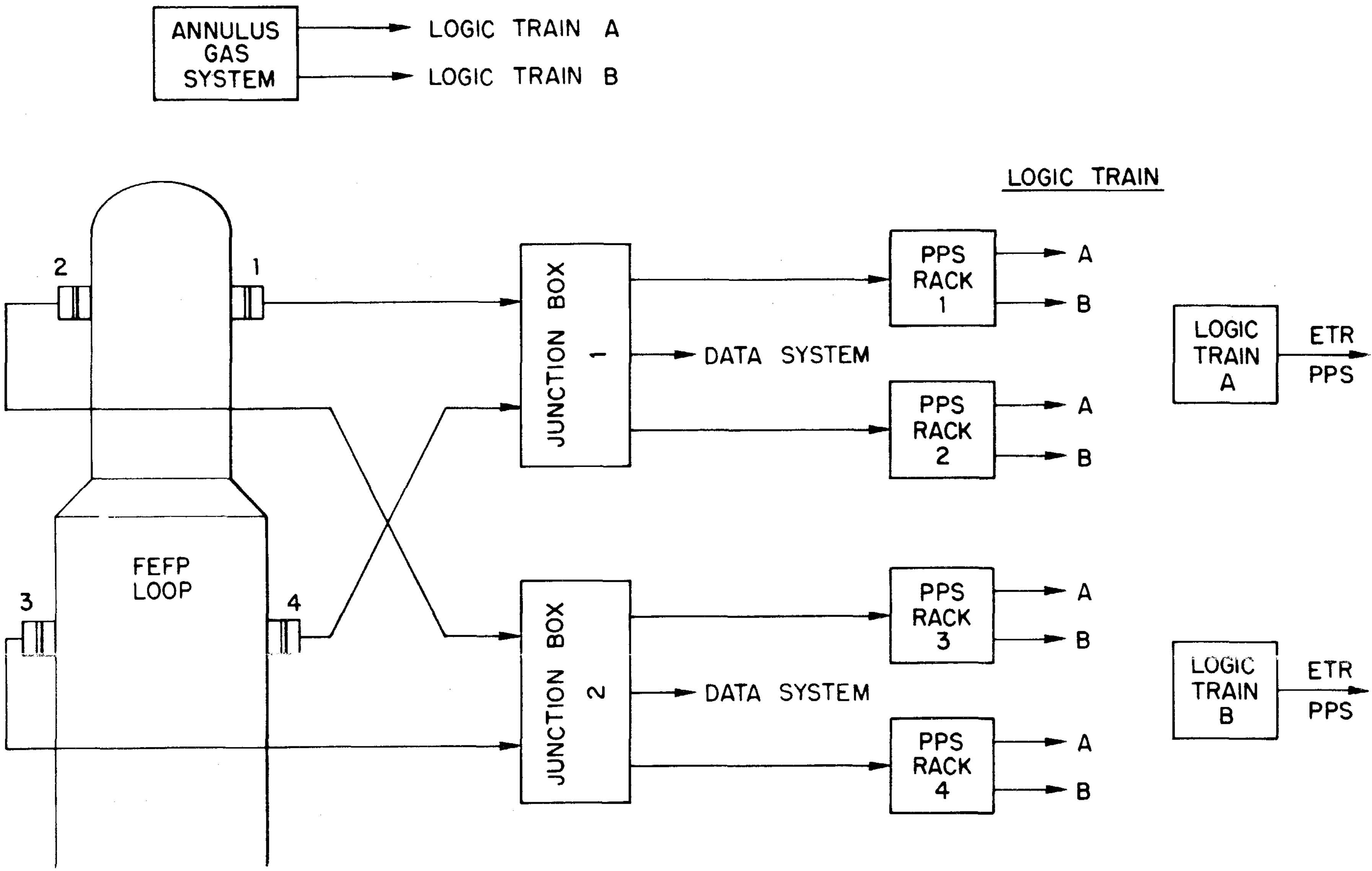

FIG. 7.16 BLOCK DIAGRAM - INTERCONNECTING CABLING SYSTEM

FIG. 7.17 FEFPL CONSOLE LAYOUT AND CABLE ROUTING

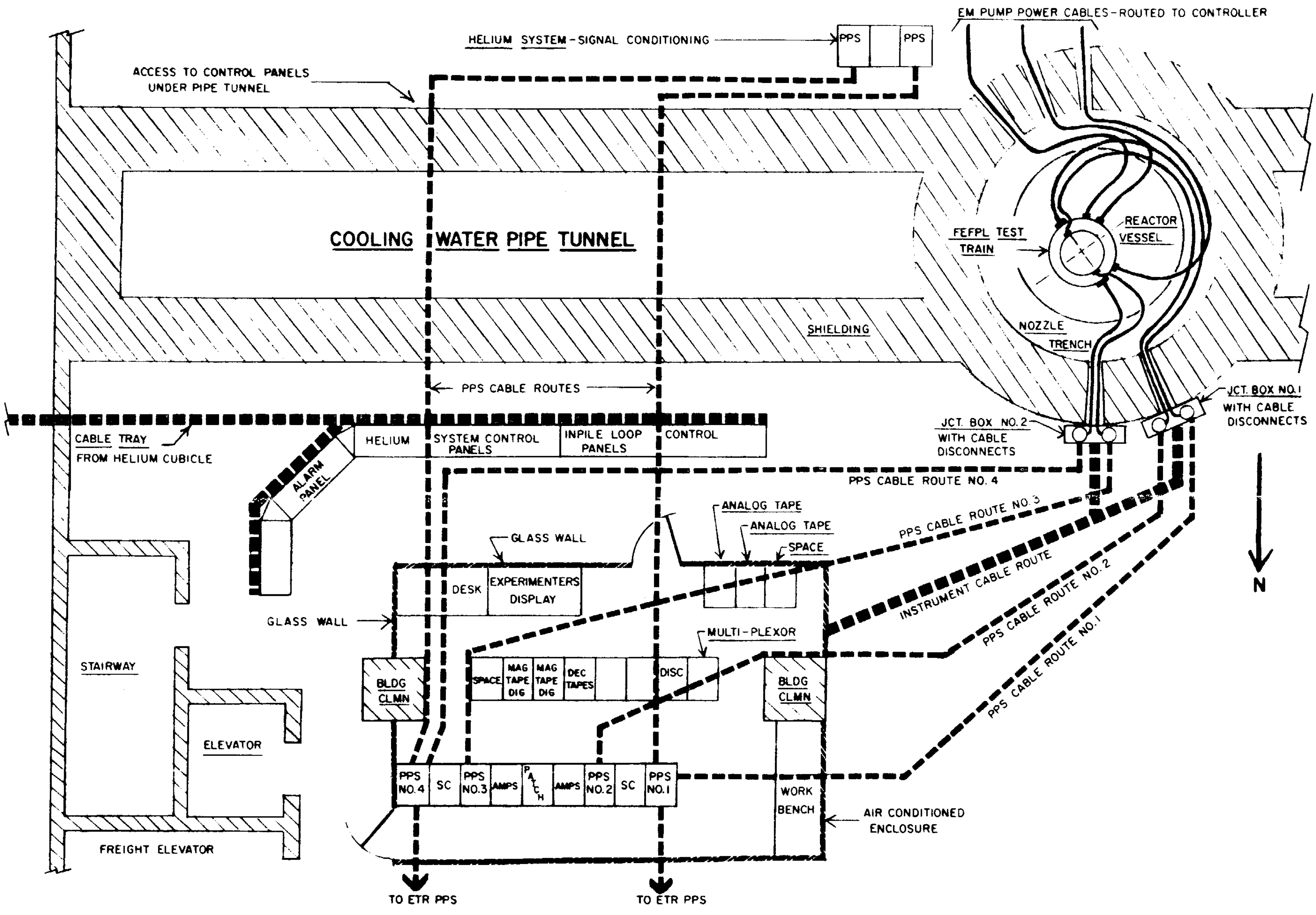

a given cable due to a failure in the cable is a credible single event, then a system using a "two-out-of-four" or "two-out-of-eight" logic for protective channels is needed. FEFPL PPS instrument channels whose sensors are external to the ETR vessel, use 1-out-of-2 logic. Two isolated cable routes are provided. Operation with detected instrument channel failures is discussed in Section 7.3.2.

Four racks of PPS equipment are located in the FEFPL Data Acquisition System Enclosure. These racks indicated in Figure 7.16 and 7.17 include PPS equipment (instrument channels less sensor, logic trains, etc.,), and equipment for spare PPS channels which may be connected to the PPS upon failure of loop PPS sensors. A description of the EAS is included in Chapter 5.0 of this document. Figures 7.18, 7.19, 7.20, 7.21 are FEFPL PPS Functional Diagrams with System Interfaces for racks 1, 2, 3, and 4, respectively. Spare instrument channel sensors are indicated as Data Acquisition System (DAS) inputs on the left of each figure. Each instrument channel of a protective function is in a different rack, except for function (A) (2/8) which has two channels in each rack. The two logic trains are in Rack 1 and Rack 4, respectively.

7.2.10 Power Sources

The FEFPL Plant Protection System utilizes the same power source as the ETR PPS. The ETR PPS direct power source is a battery-backed motor-generator system. Redundant power systems for the ETR PPS are unnecessary because the ETR rods are fail-safe (i.e., a loss of power drops the safety rods and scrams the reactor). However, auxiliary sources of power are provided by a second battery-backed motor-generator set and battery, and by a direct tie to diesel power. Either of these sources may be manually transferred to power the plant protection system for prolonged periods. Figure 7.22 shows an electrical schematic of the FEFPL/ETR power distribution system. The system, from the FEFPL PPS equipment racks to the diesel power source, is described in this section.

Power is supplied to the FEFPL PPS equipment racks through four separate breakers (PPS-CB-1, PPS-CB-2, PPS-CB-3, PPS-CB-4) for isolation and over-current protection of each rack. Undervoltage (UV) protection trips scram the reactor on loss of PPS power. Two transformers (PPS-T-1 and PPS-T-2) and breakers (PPS-CB-5, PPS-CB-6) isolate the FEFPL PPS power source

FIG. 7.18 FEFPL PPS FUNCTIONAL DIAGRAM WITH SYSTEM INTERFACES (RACK 1)

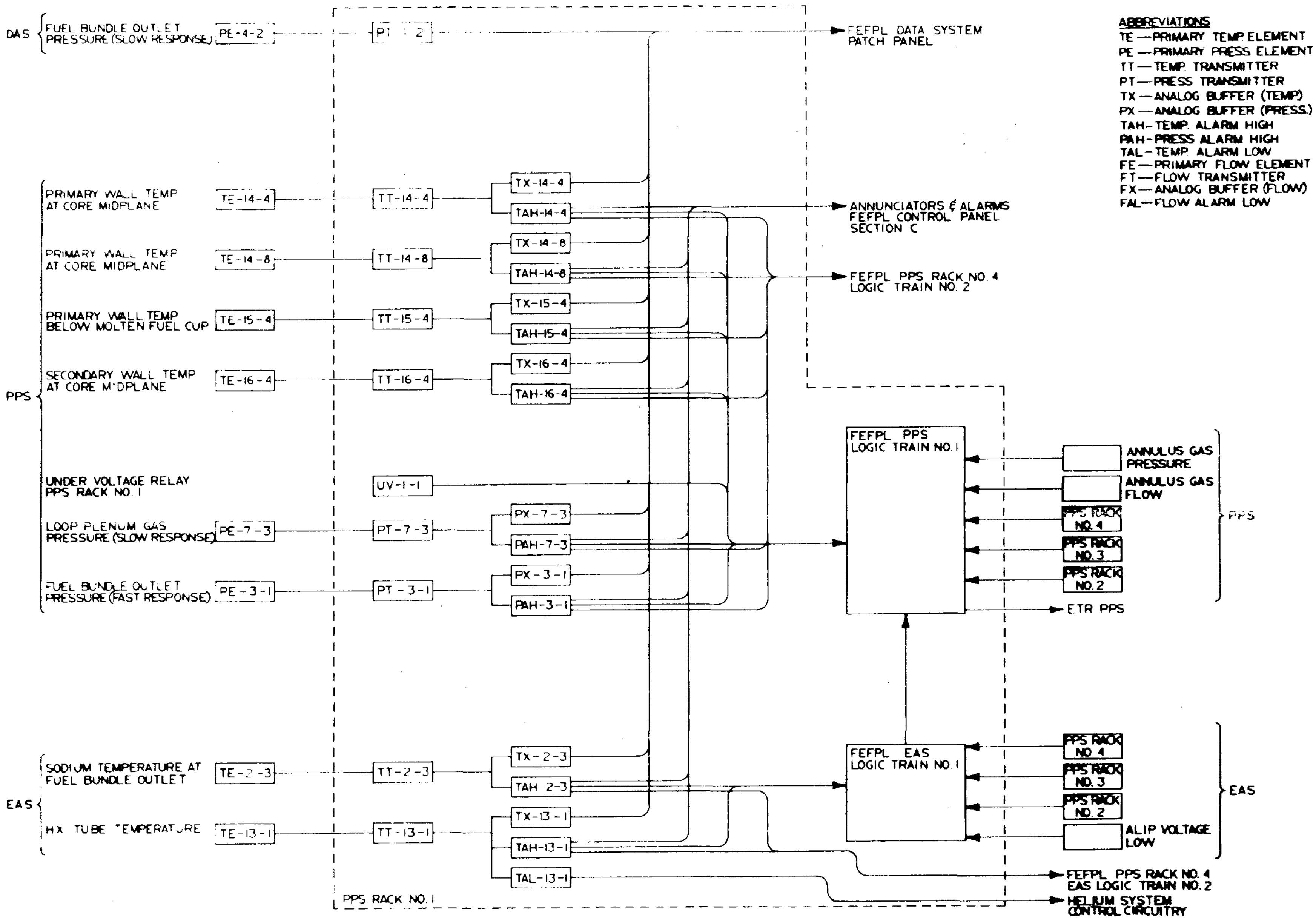

7-75

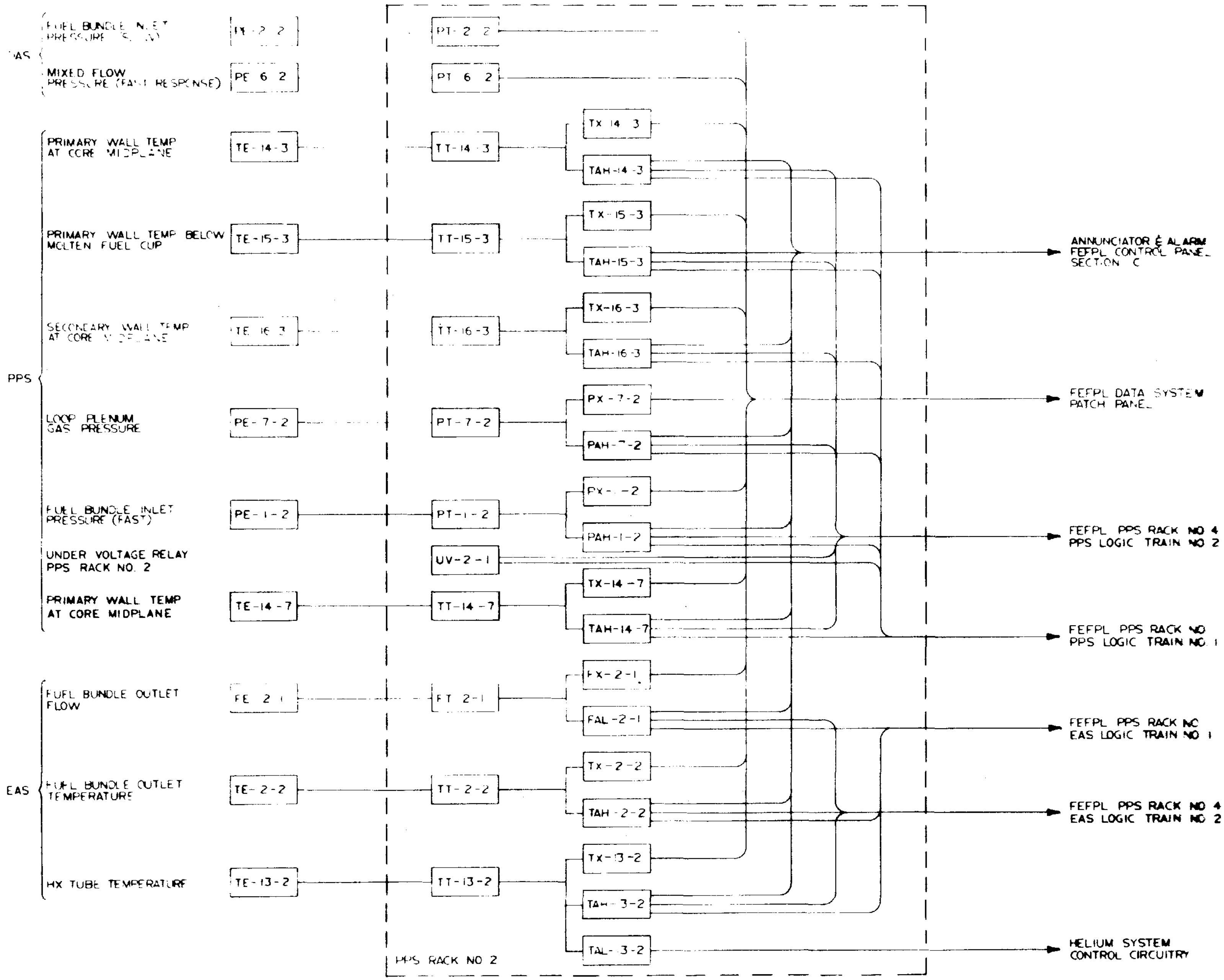

FIG. 7.19 FEFPL PPS FUNCTIONAL DIAGRAM WITH SYSTEM INTERFACES (RACK 2)

FIG. 7.20 FEFPL PPS FUNCTIONAL DIAGRAM WITH SYSTEM INTERFACES (RACK 3)

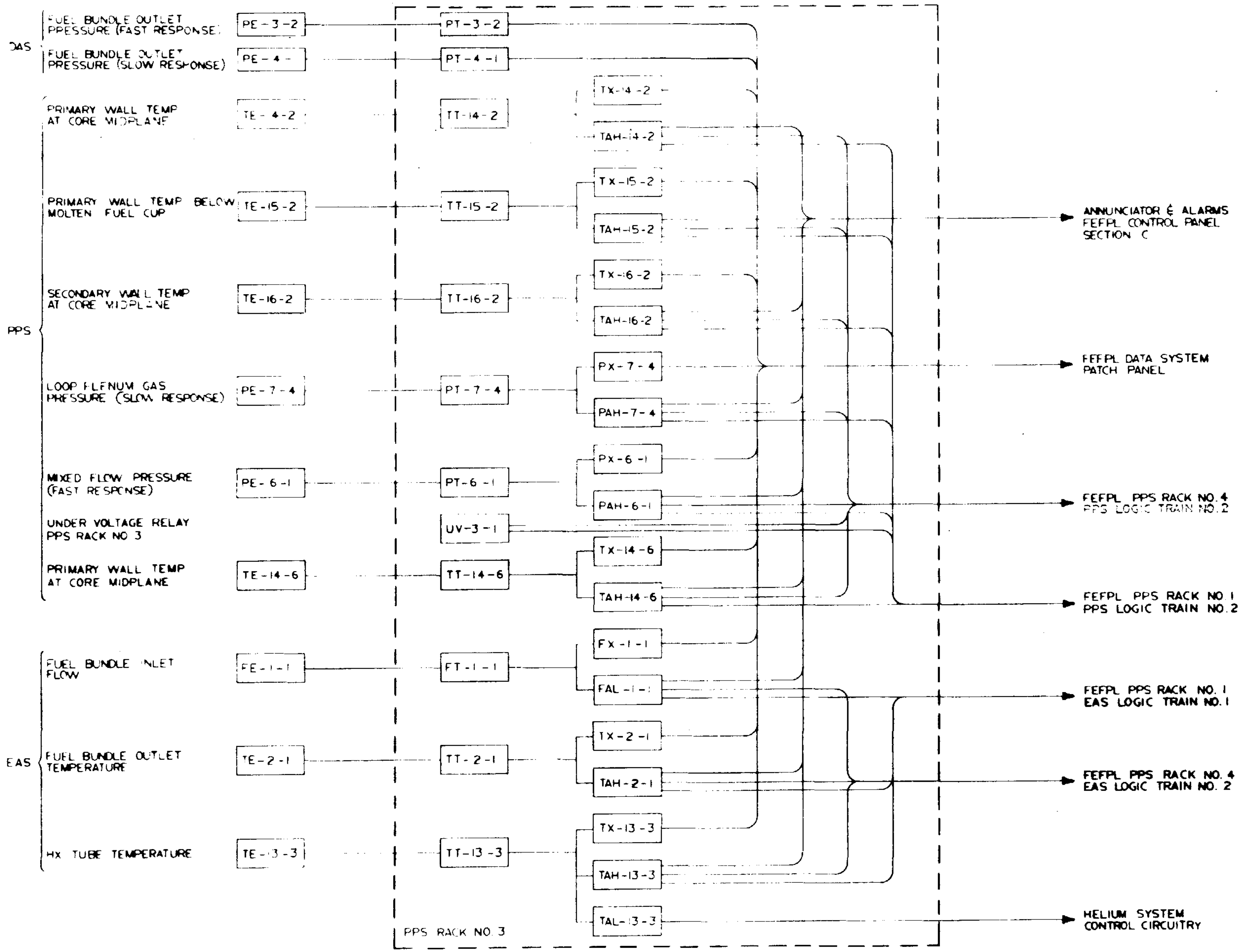

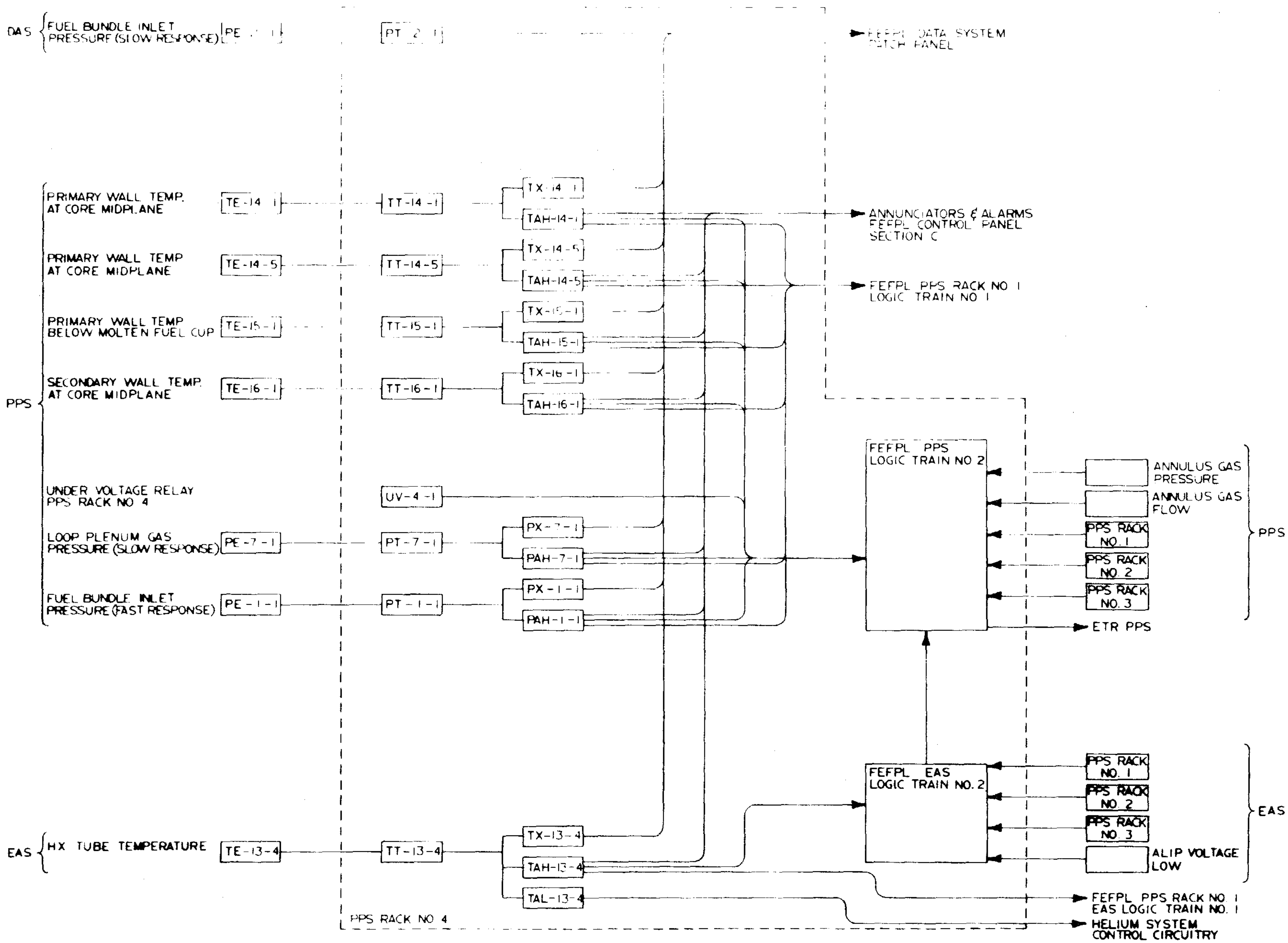

FIG. 7.21 FEFPL PPS FUNCTIONAL DIAGRAM WITH SYSTEM INTERFACES (RACK 4)

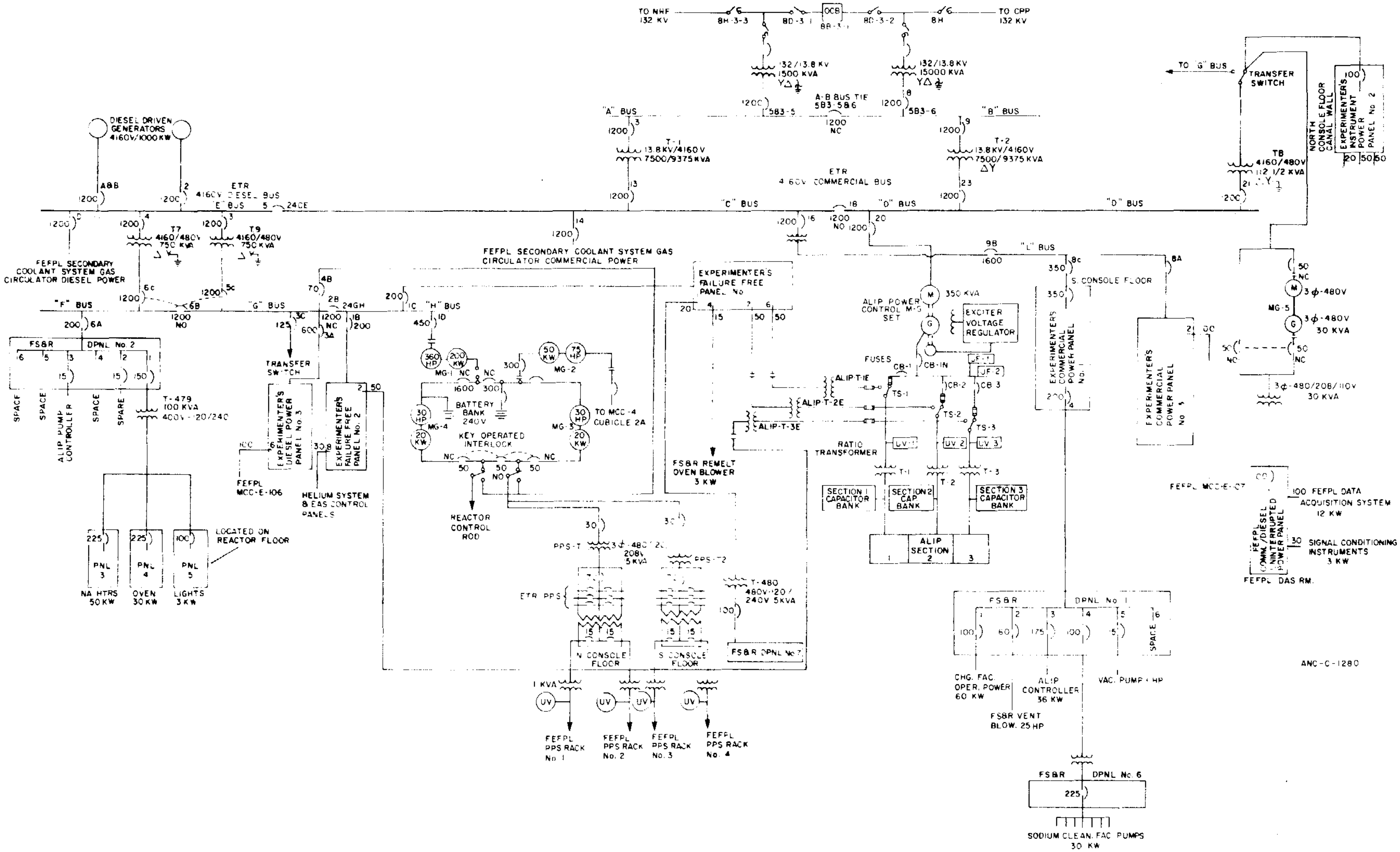

FIG. 7.22 - FEFPL/ETR Power Distribution System

equipment from the ETR PPS. A single breaker and transformer can satisfy protection system requirements; however, redundant units are provided to ensure surveillance capability of PPS protective functions after a reactor shutdown in spite of a single failure in a breaker or isolation transformer. The ETR PPS and FEFPL PPS power is provided through a manual transfer switch (FF-TS-1) which provides direct energizing of the PPS equipment from diesel power on the "G" bus if desired. The principal power source (MG-3) is a 30 HP dc motor driving a 20 KW ac generator. Power for the motor goes through a breaker (1FF) from a dc bus connected to a 240 volt battery bank (#1) which is normally charged by motor-generator set MG-2. This motor-generator set is comprised of a 50 kW dc generator and a 75 HP ac motor driven from the diesel "G" bus. The output frequency of MG-3 is monitored by the ETR PPS system which initiates a scram on low frequency.

The PPS systems can be manually switched from MG-3 to MG-4 using key operated interlock breakers. MG-4 is similar to MG-3 and is powered from a separate dc bus (#2). This bus is charged by MG-1, a 360 HP ac/200 KW dc inverting motor-generator set. Normally the ac machine is driven from the "H" bus, and the dc machine charges the battery bank. The two battery banks may be connected in parallel through a cross-tie breaker (2FF). The "H" and "G" busses are normally connected through the GH tie breaker (24GH). The "G" bus is driven from the "E" bus through a setpdown transformer (T9) and breaker (5C). The "E" bus is energized by the diesel driven generators. Only a single diesel driven generator is on line at any given time. Upon loss of diesel power the GH tie breaker is automatically disconnected. The breaker and dc bus voltage are monitored by the ETR PPS which initiates an alarm on an open breaker or low voltage. Also, MG-1 inverts and energizes the "H" bus which supplies power to the Experimenter's Failure Free Panel Number (1). It serves as the emergency power source to the Annular Linear Induction Pump. (See Section 5.2.4.2 for additional discussion on the ALIP power system).

Two system features not directly related to PPS operation are worthy of note. The "E" bus (diesel power) may be manually tied (breaker 5) to the "C" bus (commercial power) on loss of diesel power in order to power systems normally powered by diesel power. Also, the "E" and "G" busses may be manually tied together through breaker (6B). This breaker is interlocked with breakers (5C) and (6C) and can be closed only if either (5C) or (6C) is open. Table 7.3 lists various power system failures with the resulting

TABLE 7.3

PPS POWER SYSTEM FAILURES

Incident(s)	ETR PPS Action	FEFPL PPS Action *	Power System Automatic Action	Remarks
1. Power failure in a single FEFPL PPS rack (rack breaker failure, shorted or open wiring).	-----	Trip of instrument channels in rack. Scram if 1/2 Protective channel tripped or rack includes a logic train.	-----	FEFPL PPS (three racks) available for surveillance.
2. Failure of ETR/FEFPL PPS power isolation components (breaker failure, transformer failure, shorted or open wiring).	-----	Scram on undervoltage trips.	-----	FEFPL PPS (two racks) available for surveillance.
3. Failure of MG-3, output breaker, input breaker or feeder lines to PPS system.	Scram on MG-3 frequency. Scram on ETR PPS power undervoltage.	Scram on undervoltage.	-----	Manual transfer to MG-4 available on MG-3 failure to power PPS Systems.
4. Overcurrent on battery bank breaker.	Alarm on breaker trip.	Scram on subsequent PPS undervoltage.	-----	Manual transfer to MG-4 available to power PPS Systems.
5. Failure of MG-2, failure of MG-2 breakers or feeder lines, battery bus low voltage.	Alarm on low bus voltage.	Scram on subsequent PPS undervoltage.	Drive MG-3 from battery bank.	Bank capable of driving MG-3 for at least 30 minutes.
6. Failure of Diesel power or "G" bus feeder lines.	Alarm on GH tie breaker disconnect.	Scram on subsequent PPS undervoltage.	GH tie breaker opens. MG-1 energizes "H" bus.	This bus provides power to experimental equipment, i.e., ALIP sodium pump at reduced power to maintain circulation.

* These actions are initiated by design features of FEFPL-PPS that are incorporated to eliminate single failure vulnerability.

ETR PPS, FEFPL PPS and power system responses indicated.

7.2.11 System Defenses Against Failure

The FEFP Loop double containment system is a redundant vessel system which provides a passive protection for the public and reactor plant. Safety analyses have shown that no credible event or sequence of events exists which can lead to the failure of both vessels. The FEFPL PPS is an electronic system which provides diversity to the containment system by monitoring the integrity of each of the vessels and automatically terminating reactor operation if the containment safety margin is reduced.

As required by RDT Standards, the design of the FEFPL PPS has been subjected to analyses to assure adequate defense upon the occurrence of credible single or common mode failures. Generally, defenses are provided in the form of redundancy, isolation, and/or self-shutdown features to prevent single or common mode failures. However, where shown to exist, all credible single or common mode failures are acceptably integrated by detector and/or reactor shutdown as demonstrated in the previously mentioned analysis[30].

7.2.12 Loop Subsystem Requirements

The operation of the loop in the ETR involves three major systems. These are: 1) the ETR reactor, 2) the ETR plan, and 3) the in-reactor loop system. The FEFPL Plant Protection System is a subsystem of (3). The FEFPL PPS interacts with the various subsystems of these three major systems. Detailed definition of subsystem requirements are documented in Ref. 25. It is the purpose of this section to indicate the interaction of requirements imposed on or generated by the various subsystems on or by the FEFPL PPS. The following sections are titled by the system names, with the requirements given relating to the FEFPL PPS.

7.2.12.1 ETR Plant Protection System

See Section 7.1.4.

7.2.12.2 Test Train

A) The test train shall provide transient pressure sensors to implement protective function (D) (Sodium Pressure Pulse) as discussed in Sections 7.1.3.3 and 7.2.5.

B) The test train shall provide static pressure sensors to implement protective function (E) (Primary Containment Integrity) as discussed in Sections 7.1.3.3-E and 7.2.6.

7.2.12.3 In-pile Tube

The in-pile tube shall provide thermocouples to implement protective functions (A) (Primary Containment Temperature in Fuel Zone), (B) (Primary Containment Temperature in the Meltdown Cup Region), and (C) (Secondary Containment Temperature in Fuel Zone) as discussed in Sections 7.3.3.3-A, B, C, and 7.2.4.

7.2.12.4 Experiment Assurance System

The FEFPL PPS shall receive EAS generated logic signals requesting reactor scram and generate ETR scram signals through the FEFPL PPS logic trains.

7.2.12.5 Annulus Gas System

A) The Annulus Gas System shall make provision for FEFP PPS flow sensors to implement protective function (F) as discussed in Sections 7.1.3.3-F and 7.2.7.

B) The Annulus Gas System shall make provisions for FEFP PPS pressure sensors to implement protective function (G) as discussed in Sections 7.1.3.3-G and 7.2.8.

C) The FEFPL PPS shall provide a logic output to the annulus gas system to initiate the system's meltdown cup cooling mode of operation upon trip of protective channel B (Primary Temperatures in the Meltdown Cup Region).

7.2.12.6 Data Acquisition System

Each FEFPL PPS instrument channel shall provide a buffered analog output for data recording purposes.

7.2.12.7 Helium System

The helium system alarm panel shall provide annunciators for each of the FEFPL protective channels.

7.2.12.8 Instrumentation Integration System

The instrumentation integration system shall provide cabling of PPS signals from the loop and the removable top closure to PPS equipment racks.

7.3 Principles of Operation

The brief principles of operation discussed in this section pertain to general system operation; specific complete details will be provided in the FEFPL PPS System Design Report and in the FEFPL PPS Operation and Maintenance Manual. This will include references to appropriate documentation provided by the system manufacturer as required by applicable RDT Standards. The FEFPL will be subjected to and operate under various conditions while it is installed in the ETR. All loop conditions with respect to PPS operation are considered to fall under one of three categories: Isothermal operation (ETR shutdown), Normal operation (ETR startup and power operation) and Post-power operation (after ETR shutdown and before isothermal conditions are established).

The FEFPL PPS will normally be in operation for the time interval following insertion of the in-pile loop into the reactor and electrical connection has been completed, and prior to the electrical disconnection and removal of the in-pile loop from the reactor. Normal operation of the PPS protective functions shall be in accordance with minimum requirements specified below and as may be additionally specified in the experiment test plan.

7.3.1 Isothermal Operation (ETR Shutdown)

Isothermal operation with the reactor shut down represents a normal operational mode for the FEFPL. Prior to ETR startup and during periods when ETR is shut down, FEFPL will be required to maintain sodium coolant circulation and to control the sodium temperature (nominally at 450°F) to prevent freezing the sodium. During this mode of operation, vessel temperatures are well below their design maximums and no energy source exists which could induce significant pressure pulses in the sodium coolant. An examination of the FEFPL Fault Tree (Appendix A), considering that ETR is shut down, indicates no credible event or accident which can cause failure of the FEFPL double containment system. For isothermal operation (ETR shutdown) subsequent to in-pile loop insertion and completion of electrical connections, the following PPS operational requirements shall be met:

a)* Containment integrity verification shall be made a minimum of once each operating shift. This may be accomplished by the use of at least one instrument channel each of FEFPL PPS functions E, F, and G in conjunction with the containment verification mode of the Annulus Gas System (AGS). Also, it may be accomplished by containment integrity monitoring features (radiation and moisture detectors) of the AGS in the fuel meltdown cup cooling mode or the heat conduction mode.

b) The loop operator shall be provided with a continuous temperature indication representative of loop sodium temperature. This may be provided by FEFPL PPS analog outputs from protective functions A and B, temperatures from EAS protective functions (test section outlet temperature or heat exchanger outlet temperature), control system parameters (test section inlet temperature) or various test train thermocouple readings normally recorded by the data acquisition system.

7.3.2 Normal Operation

Normal operation shall include all periods of operation of the FEFPL while it is in the ETR and the ETR is not shut down. This mode shall also include the period just prior to ETR startup when conditions must be established and verified for ETR operation. Since it is required that the ETR not be operated without verified double containment on the FEFPL, the FEFPL PPS will be operational (in accordance with the general requirements below and the specific requirements for each function given in FDR-09) sufficient time prior to beginning ETR startup to permit containment verification and temperature monitoring.

The seven FEFPL PPS protective functions and their essential performance requirements are tabulated in Table 7.1 (A through G). A summary of the instrument channel requirements for the monitored variable of each function are tabulated in Table 7.2. As Table 7.2 indicates, there are eight channels for protective function (A), four channels for functions (B), (C), (D), and (E), and two channels for functions (F) and (G). The PPS logic utilizes "two-out-of-eight" logic for the eight channel system, "two-out-of-four" logic for four channel systems and "one-out-of-two" logic for two channel systems.

*The FEFP PPS shall meet this requirement within one shift after insertion of loop in reactor.

The minimum PPS capability during normal operation shall be two independent channels for each monitored variable except protective function (A) shall require at least four channels which must be uniformly spaced around the circumference of the primary vessel, and adjacent channels must be independent. PPS operation with less than the full number of channels for any protective function shall utilize "one-out of N" logic, when N is the number of operational instrument channels equal to or greater than the minimum independent channels required. That is, any operating channel which trips will cause an ETR scram.

As explained in Section 7.2.9, only two signal connectors are available from the removable top closure for the test train sensors and only two signal connectors are available for the in-pile tube sensors. The cabling has therefore been arranged so that instrument channels in Racks 1 and 2 share common in-pile tube and removable top closure connectors and channels in Racks 3 and 4 share the other in-pile tube and removable top closure connectors. Thus, to assure channel independence when operating with only two channels on a four channel system one channel must be located in Rack 1 or 2 and the second channel in Rack 3 or 4.

7.3.3 Post Power Operation

Post power operation is loop operation after ETR has been shut down and before near isothermal conditions are established. This period of operation is the short transient period following ETR shutdown. Minimum requirements are provided for the following categorical situations:

a) For ETR shutdown due to ETR PPS or FEFPL PPS power system failure, electrical power recovery for continuous FEFPL PPS operation shall be completed within one hour.

b) For ETR shutdown due to ETR PPS or FEFPL PPS power system failure where requirement a) is not met, the loop operator shall be provided with continuous representative indications for the following parameters:

(1) Loop sodium temperature

(2) Annulus gas flowrate and pressure.

The former may be provided by any thermocouple readings either on or within the primary containment barrier. The latter may be provided by either special battery hookup to the applicable PPS instruments or the AGS instrumentation, as may be available.

c) For ETR shutdown due to a planned operation or to a reactor scram in which loop parameter have stabilized (within ±25°F of the expected steady-state value, nominally 450°F) containment integrity verification and temperature monitoring shall be available in accordance with the requirements (a & b) of 7.3.1.

d) For ETR shutdown due to an experiment transient or accident condition in which the loop parameters do not stabilize continuous FEFPL PPS operation shall be required until the loop parameters do stabilize then containment integrity verification and temperature monitoring shall be available in accordance with the requirements (a and b) of 7.3.1.

If an ETR PPS or FEFPL PPS power failure should occur during the continuous PPS operation phase, revert to the requirements of a) until power is restored.

e) For ETR shutdown due to a FEFPL PPS induced scram or if a FEFPL PPS trip is subsequently indicated, continuous FEFPL PPS operation shall be required until it can be shown that conditions for reactor restart have been satisfied in accordance with the experiment plan or that the decision has been made to remove the loop from the reactor. If an ETR or FEFPL power system failure should occur, revert to the requirements of (a) until power is restored.

7.3.4 PPS Startup

It is assumed that the FEFPL Plant Protection System has been operationally checked and that all instrument channels were tested during vendor acceptance, construction, component and system operation tests. This startup refers to PPS operation prior to loop normal operation.

7.3.4.1 Equipment Warmup

Equipment will be solid state, and approximately 15 minutes will be required for temperature stabilization. Power will be applied to the instruments by closing circuit breakers in the respective distribution panels and by closing "Power On" switches, where provided, on the instrument panels.

7.3.4.2 Calibration

Once the equipment is warmed up, calibration will be performed on each instrument channel including adjustment of scram setpoints. Whenever possible, end-to-end calibration will be performed to improve calibration accuracy. Setpoints will be adjusted at steady-state conditions, but will be approached in the increasing or decreasing direction similar to the expected parameter change.

7.3.4.3 Testing

On systems where it is possible to activate the process to check functional performance of the instrument channel, logic and actuator, the process will be activated. Readouts, setpoints, annunciator alarms, actuator action, and overall performance of the system will be checked to ascertain that calibrated equipment has been restored to its normal operating mode and the overall system reacts as expected. When it is not possible to activate the process, techniques will be used to simulate actual conditions by inserting a signal simulating the detector output.

On line calibration of (2/4) or (2/8) channels in the FEFP Loop PPS circuitry will be possible while the reactor is in operation. The testing feature of the 2/4 and 2/8 logic element shall be used to test these elements. On-line testing of 1/2 protective functions will be performed during normal operation. This testing will be performed during shutdown periods. On-line testing is not required, since the operating periods are very short compared with the required maintenance intervals.

7.4 Maintenance Principles

The PPS is designed for easy and accurate testing, maintenance, and equipment replacement. On-line maintenance is expected to be performed routinely, and the layout of redundant channels reflects the need for test and repair on a signal channel without affecting any other redundant instrument channel. The use of redundancy in the design allows any one channel (for 2/4 or 2/8 functions) to be tripped without causing a protective action, and allows one channel to be removed and replaced as necessary.

7.4.1 Objectives

Since the maximum expected FEFP experiment run without scheduled shutdown is an ETR cycle, the preventive maintenance program should be scheduled on such a basis. This provision bypasses the need for preventive maintenance during plant operation.

7.4.2 Lists of Special Maintenance Considerations

7.4.2.1 Maintainability Check List

a) Design should be such that equipment can be removed or readily accessible for personnel, and tools required for the performance of normal maintenance should be readily available.

b) Since the removal of a component is possible during plant operation (due to 2/4 or 2/8 coincidence logic*), provision shall be made to insure the removal of components is acknowledged both visually and audibly. This will be accomplished through the annunciator system.

c) Test points will be internally available to check all power supply, analog, and logic voltage levels.

d) Trip test controls will be internally accessible. The trip test function is to be used only for checkout and maintenance operations.

*This is not true for the 1/2 protective channels. However, the provision shall still be required.

References:

1. RDT Standard C 16-1T, "Supplementary Criteria and Requirements for RDT Reactor Plant Protection Systems", Division of Reactor Development and Technology, U.S.A.E.C. (December 1969).

2. M. J. Neder (ANC), letter to J. J. English (ANL), "FEFPL-ETR Scram Delay Time", NeD-1-71, (January 4, 1971).

3. ANC Report CI-1247, "ETRC-FEFPL Mockup Experiment and Calculation", (Table XI), (November 1972).

4. ANL Internal Memorandum, W. A. Bezella to D. H. Lennox, "Review of Containment Vessel Temperatures", (Table II), July 13, 1973).

5. ANL Internal Memorandum, J. H. Tessier to D. H. Lennox, "Effects of Misalignment of FEFPL Flow Divider", (November 7, 1972).

6. ANL Internal Memorandum, W. A. Bezella to D. H. Lennox, "Loss of ALIP Accident Study", (Table I), (August 23, 1972).

7. R. W. Thomas, "Design Basis Analysis for PPS Function "C" Secondary Containment Temperature in Fuel Zone", ANC EDF-1312 (May 1974).

8. ANC EDF-1344, R. A. Wells, "Thermal Analysis of Cadmium Filter at Reduced Flow and High Gamma Heat for PPS Function "C"," (May 1974).

9. ANL Internal Memorandum, C. A. Bloomquist to D. H. Lennox, "Loop T.C. Locations Adjacent to Meltdown Cup", (May 10, 1973)

10. D. H. Lennox, et al., "Containment Study for the FEFP In-pile Loop ANL/RAS-71-36", (November 1971).

*11. ANC Report CI-1233, "ETR Technical Specifications", (February 1972).

12. R. W. Thomas, ANC Report EDF-1342, "Design Basis for PPS Protective Function "E" Primary Containment Integrity", (May 1974).

13. ANC Report EDF 1343, R. W. Thomas, "Design Basis Analysis for FEFPL PPS Protective Function (F): Secondary Containment Integrity", (May 1974).

14. ANC Report FDR-10, "Annulus Gas System Design Requirements".

15. R. G. Ambrosek, AMB-14-74, "ETR Gas Leakage Limits - Extremely Unlikely Fault", ANC Memo, (April 11, 1974).

16. ANC-70008A, "Design Specification for the Fuel Element Failure Propagation In-pile Loop System".

17. ANC Report EDF 1213, B. J. Merrill, "Consideration of Blanketing by FEFPL Annulus Gas Subsequent to a Break in the Secondary Vessel", (January 7, 1974).

*These titles indicate analyses presently being revised or completed.

18. ANC Report 1275, R. A. Wells, "Analysis to Determine the Maximum Helium Leak Rate without Melting of the Cadmium Filter", (March 7, 1974).

19. ANC Report TR-495, (in preparation), K. H. Liebelt, "FEFPL Thermal-Hydraulic Analysis of Selected Upset Conditions and Recovery Transients with the Revised Loop Model A1".

20. ANC Report TR-496, (in preparation), W. Madsen, "Double Blowdown Analysis of FEFPL Annulus Gas System Due to a Secondary Containment Leak".

21. ANL Report ANL/RAS 72-22, "Test Requirements for Fuel Element Failure Propagation In-reactor Experiment P-2", (Revision, January 1973).

22. ANC Report EDF 1345, R. W. Thomas, "Design Basis Analysis for FEFPL PPS Protective Function (G): Annulus Gas System Pressure", (May 1974).

23. ANL/RAS 72-9, Rev. 1, "Test Requirements for Fuel Element Failure Propagation In-reactor Experiment P-1", (November 1972).

24. ANC Report, EDF-597, "Steady-state Pressure Drop and Sodium Temperature Data for 19-A and 37-A Pin SINDA Models", (December 8, 1972).

25. ANL Internal Memo, D. H. Thompson to M. J. McDaniels, "Interim and Advance Pumps for the FEFP Loop", (December 9, 1971).

26. ANC Report, FDR 01, "FEFPL Helium System Design Requirements", (4/3/73).

27. ANL/RAS M-118, Meeting Report, "ETR Operating and Modification Requirements", AEC Headquarters, Germantown, Md., February 17 & 18, 1972.

28. ANC Memo, F. L. McMillan to V. A. Walker, "ETR PPS Design Agreements", FMc-453-73, (July 3, 1973).

29. ANL R-1000-1001-SA, "System Design Description of the Fuel Element Failure Propagation In-pile Loop System", (May 1, 1972).

*30. ANC Report, FR-217, "FEFPL PPS Single Failure Analysis, (April 1974).

---

*This report currently under review (May 1974).

CHAPTER 8.0

TABLE OF CONTENTS

LIST OF TABLES

LIST OF FIGURES

8.0 Administrative and Procedural Safeguards

Operation of the Test Reactor Area (TRA), of which the ETR/FEFPL is a part, is governed by a rigorous and visible management control system. Features of the system are:

1. A well-defined interface between AEC and Aerojet Nuclear Company to assure a high degree of responsiveness to AEC requirements.

2. A document structure that defines discrete levels of ETR/FEFPL control and accomplishes:

   a) a "handoff" of responsibilities and authority from one management level to the next;

   b) consistent and uniform operational policy concerning ETR/FEFPL routine and nonroutine operations;

   c) step-by-step procedural control of ETR/FEFPL operations where significant safety or programmatic risk is involved.

3. An organizational unit to control all documentation used in the ETR/FEFPL reactor operation.

8.1 Organization

General - Figure 8.1 shows the documentation interface with AEC and the discrete levels of documentation including interrelationships that comprise the management control system. The figure identifies the contractual agreements and technical limitations, and factors them into the control documentation; also, the delegation of authority and assignment of responsibility by Aerojet Nuclear Policies & Procedures (ANPP)[1] and Company Management Directives (MD's) through the Test Reactor Facilities Division Manager (Standard Practices (SP))[2] to the operational procedures used in performing the work (Detailed Operating Procedures) is delineated. Under the control of the shift supervisor, the Reactor Cycle Control Document (RCCD) is used for plant operation from one cycle shutdown to the beginning of the next cycle shutdown. The RCCD contains reference to procedures required and instructions and approvals necessary for the operation of the ETR/FEFPL reactor cycle.

The organizational unit in the Test Reactor Facilities Division that controls the documentation system from the Standard Practice level on down is the Administrative Control Group (see Fig. 8.2). This group provides system for document control, long-range planning and property control.

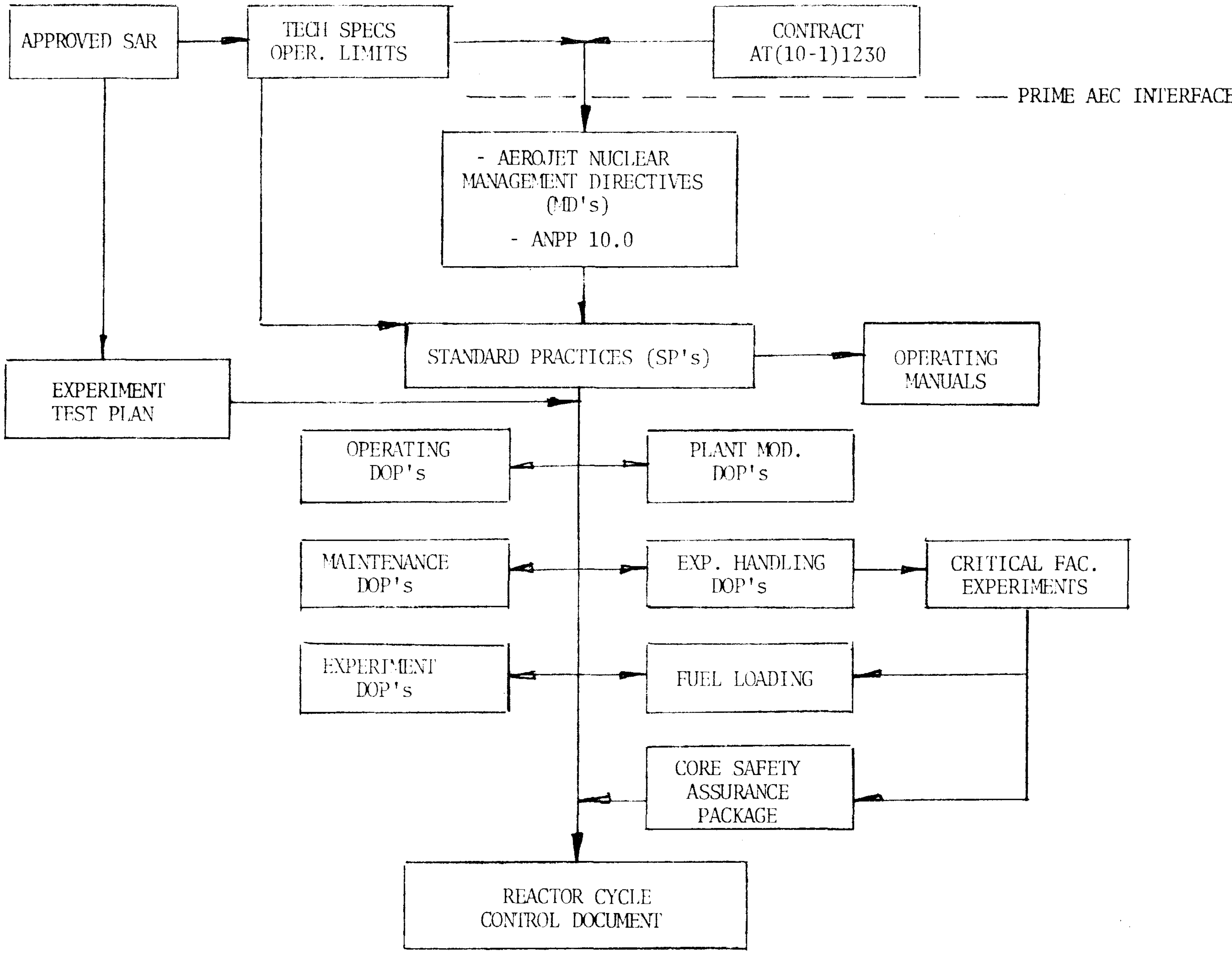

FIG. 8.1 - Framework for Document Control

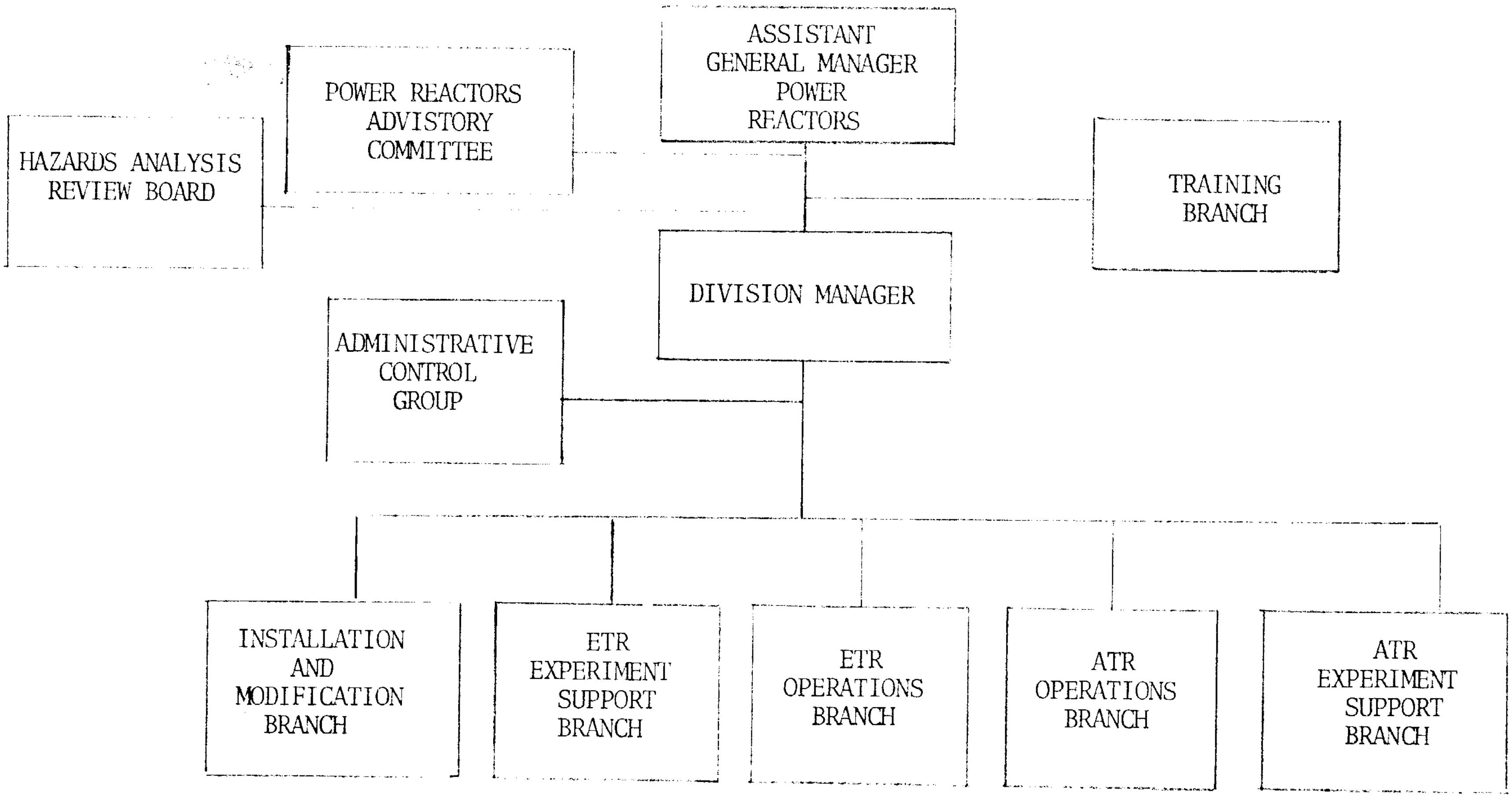

FIG. 8.2 - Simplified Organization of Test Reactor Facilities

Administrative Control Group

Administrative Control Group Manager - The Group Manager provides services necessary to perform audits of other branches and their activities in the Test Reactor Facilities Division.

Configuration and Document Control Section - The Configuration and Document Control Section writes and processes Division Standard Practices, and processes experiment, operating, maintenance, and modification procedures, operating manuals and division forms for the ETR/FEFPL facility. Standard Practices, Detailed Operating Procedures, and division forms, whenever applicable, are reviewed with other branches and divisions. As specified by division management, schedules Procedure Review Board (PRB) review of Standard Practices and Detailed Operating Procedures coordinating PRB requirements with division personnel, obtaining PRB approvals and other approvals as required.

A Reactor Cycle Control Document (RCCD) covering ETR/FEFPL operation will be prepared by ETR Operations Branch for each reactor cycle. This document references the following and contains signoff steps for Operations upon completion of specified items:

- All plant and FEFPL experiment modifications to be installed during a shutdown period,
- all periodic checks, shutdown tests, calibrations, maintenance, or repair to be performed on the plant during shutdown,
- FEFPL experiment and reactor loading and verification of the reactor loading prior to startup,
- shutdown schedule for all FEFPL experiment and fuel movements
- reactor and system shutdown surveillance requirements to assure that plant and FEFPL experiments are maintained in the required conditions during the shutdown period,
- all procedures to be used for pre-startup, startup, operating, shutdown, and post-shutdown actions for the plant, FEFPL experiments, and related equipment,
- core approval letters and forms and technical information pursuant for reactor operation,
- division manager approval for reactor startup and operation.

In addition, the Administrative Control Group section receives and processes all Document Revision Requests and all proposals for new or modified Standard Practices and detailed Operating Procedures. The required number of copies of all procedures, Standard Practices, manuals, etc., are distributed and the control of such documents is maintained by an established record system. A master file and records on all documentation is maintained in the control documents structure. Records of the FEFPL experiment loadings in the ETR are kept to permit a controlled system for distribution of irradiation costs to sponsoring organizations. An adequate inventory of all approved procedures is maintained for use in the field. Operational Documentary Photographs are also on file.

8.2 Independent Review and Approval of Test Reactor Facilities Documentation and Activities

Reactor Facilities Procedures Review Board (PRB) - The PRB is composed of representatives from the Engineering Division (chairman), the Test Reactor Facilities Division, Quality Division, the Safety Division, and the Nuclear Technology Division. The board is appointed by the General Manager, Aerojet Nuclear Company, and is solely responsible to him for its activities.[3]

The board reviews and approves Standard Practices and Detailed Operating Procedures (Experiment Procedures, Standard Operating Procedures, and all DOPs and those SPs that concern maintenance) when such documents are:

- related to reactor safety
- of significance due to their particular or special potential for an industrial safety hazard
- of importance due to their effect on plant or equipment safety
- significantly related to safety in handling or operating experiment systems or equipment

Power Reactors Advisory Committee (PRAC) - The PRAC is a permanent review committee chartered to review all matters with nuclear safety implications. The committee is appointed by the Assistant General Manager, Aerojet Nuclear Company, and is solely responsible to him for its activities.[3]

The committee reviews and makes recommendations to the AGM relative to modifications to the reactors, associated facilities, and experiment systems having a safety significance.

Approval of these items by the committee is required prior to operation of the reactor and/or performance of the experiment. The committee assures itself that the risk level of reactor operations is not increased beyond the level that has been established by the safety analyses associated with the particular reactor involved, and shall identify those cases where risk level is considered to exceed that encountered in normal operation.

Test Reactor Facilities Standards Technical Change Board - This board is composed of representatives from the Engineering Division (chairman), the Test Reactor Facilities Division, and the Quality Division. The board is appointed by the General Manager, Aerojet Nuclear Company, and is solely responsible to him for its activities.[3]

The board reviews and approves deviations from the applicable industrial and RDT codes and standards. Requests are backed up by analyses and justification prepared by the Engineering Division. The board also reviews and approves codes and standards which will be used to modify experimental equipment that has been procured.

Safeguard and Accident Review Boards - All Aerojet Nuclear Company activities and facilities are subject to periodic safety review by interdisciplinary safeguard review boards composed of individuals not directly associated with the activity or facility under review. Facilities are reviewed on an annual basis. Review of subjects related to nuclear and operational safety are performed as required. These reviews are not related to the continuing day-to-day review and approval activities of the Test Reactor Facilities Procedures Review Board and the Power Reactors Advisory Committee.[3]

Accident Review Boards are convened as required to review certain accidents and incidents occurring in connection with Aerojet Nuclear Company activities.

If the review boards recommend corrective actions, upgrading, etc., the manager of the applicable division(s) is responsible to submit to the board within a specified time limit his means of compliance, with time schedule for implementation of the recommendations, or he shall reject the recommendation with cause. The board submits a final report to the General Manager indicating whether responses fulfill the intent of the board recommendations.

Safety Division Review - The Safety Division of Aerojet Nuclear Company reviews and approves hazardous and potentially hazardous activities engaged in by the Company. Examples of subjects for review are: Design work performed by outside contractors, the Engineering Division, the Construction Engineering Division, and experiment sponsors; existing and proposed hazardous and potentially hazardous activities; proposed facility or systems acquisitions.[3]

FEFPL Hazards Analysis Review Board (HARB) - This board is composed of representatives from Engineering, Quality, Nuclear Technology, and Test Reactor Facilities Divisions. The board is appointed by the General Manager, Aerojet Nuclear Company.[3]

The board will review the FEFPL SAR and any other phases of the FEFPL Project that are required before the SAR is approved or that are not covered by the SAR and that may have significant and unusual problems associated with nuclear operation. The board will determine that the safety-related conclusions presented are supported by facts and that all risks are properly identified and described.

8.3 Management Safety Appraisal Boards

Management Safety Appraisal Boards are periodically appointed by and are responsible to the General Manager, Aerojet Nuclear Company. The purpose of these boards is to appraise the Company's internal safety-review system for adequacy of performance and to review significant or unusual problems associated with nuclear operations. Review of the internal safety system is conducted every three years, more often if necessary.[3]

8.4 Surveillance and Audit of Test Reactor Facilities Operations

In addition to periodic internal audit by the Test Reactor Facilities Division Administrative Control Group, there is continuing surveillance and audit performed by the Quality Division (QD) and the Safety Division (SD). QD audits procedures, controls, inspections, tests, certifications, modifications, fabrication, etc. Safety Division concerns itself with surveillance and review of nuclear and industrial safety activities, the Training and Qualification Program, etc.

Deficiencies and noncompliances are reported on a regular schedule to the Test Reactor Facilities Division Manager as well as to the Aerojet Nuclear Company General Manager.

8.5 Management Audit of Test Reactor Facilities

The General Manager, Aerojet Nuclear Company, has selected a management audit pool from the various company divisions. A three-member team (including a chairman) is selected from the pool and performs an audit quarterly to assure that reactors are operated in accordance with approved procedures, and that such procedures comply with managerial and contractual requirements. In addition, the General Manager conducts his own inspections of reactor operations at least once every two months to assess the performance, efficiency, and effectiveness of any activity related to reactor operations.

8.6 Power Reactors Training and Qualification

Introduction - The personnel charged with operating and maintaining the test reactors at TRA participate in a comprehensive training and qualification program. This program is administered by the Reactor Training Branch (see Fig. 8.2). The basic objectives of the Test Reactor Facilities Division Training and Qualification Program are in order of importance:

- to assure that employees in the Test Reactor Facilities Division are aware of and properly trained to perform their assignments in a safe and adequate manner.
- to assure the test reactors are operated and maintained in accordance with AEC requirements and guidelines
- to provide a coordinated method for the on-shift dissemination and implementation of management directives and other information of value in upgrading the TRA operational ability
- to assure that formal documentation is made of training conducted

In order to implement these basic objectives, a formal and uniform program for personnel training and qualification is established. A program for the formal training and qualification of personnel in the following operational positions is provided:

ETR or ATR

Plant Manager
Shift Supervisor (SS)
Assistant Shift Supervisor (AS)
Senior Reactor Engineer (SRE)
Reactor Engineer/Reactor Technician (RE/RT)
Experiment Engineer/Experiment Technician (EE/ET)
Reactor Instrument Technician (RIT)
Process Operator (PO)

TRA

Reactor Instrument Supervisor (RIS)
Maintenance Foreman (MF)
Utility Area Operator (UAO)
Utility Area Coordinator (UAC)

The TRA Qualification Review Board has the responsibility for approving the qualifications of candidates for every operational position. This board is established and maintained by the Test Reactor Facilities Division Manager in accordance with Test Reactor Facilities Division Standard Practices.

Makeup of a particular board for routine qualification examinations other than Plant Manager, is chosen as shown in Table 8.1. Board membership will be modified for FEFPL qualifications as applicable. Specific responsibilities of the TRA Qualification Review Board are:

- review individual candidate's training and qualification records and administer oral examinations as part of the formal qualification process
- make evaluations, suggestions, and recommendations to the Test Reactor Facilities Division Manager concerning the applicability and effectiveness of the training program

Organizational Relationships and Responsibility Summaries - Figure 8.3 shows the informational flow paths for the Test Reactor Facilities Training and Qualification Program. The line and staff relationships and responsibilities as detailed in introduction, are briefly summarized below:

- Test Reactor Facilities Division Management - The Test Reactor Facilities Division Manager is responsible to the Aerojet Nuclear Company Assistant General Manager for all aspects of safe and efficient reactor operation. He provides the basic policy and overall direction for the training and qualification program.

TABLE 8.1

Membership of TRA Qualification Review Committee

Operational Position	Principal Member	Alternate Member(s)
a. All	Reactor Training Branch Manager (Chairman)	Operations or Maintenance Training Supervisor (Alternate Chairmen). A Shift Supervisor from the plant will replace this member if the candidate is in the Reactor Training Branch.
b. All	Operations Branch Manager from the candidate's plant (for TRA positions, this may be either Operations Branch Manager).	Assistant Operations Branch Manager from the candidate's plant. (A shift supervisor from the candidate's plant but from a different shift may represent his branch for all operational positions except Shift Supervisor, Reactor Instrument Supervisor, Utility Area Coordinator and Maintenance Foreman).
c. All	Safety Division Representative (Individual(s) to be appointed by Test Reactor Facilities Division Manager's letter)	
d. (One as follows)		
SS/AS	Any other Test Reactor Facilities Division Branch Manager	
SRE; RE/RT; EE/ET	ETR Experiments Support Branch Manager	Loop Senior Project Engineer for the candidate's plant
PO/UAO	Senior Operator certified in the candidate's plant (Individual(s) to be appointed by the bargaining unit)	
MF	TRA Maintenance Branch Manager	Instrument/Electrical or Mechanical Section Supervisor
RIT;RIS	Nuclear Technology Division representative (Individual(s) to be appointed by Test Reactor Facilities Division Manager's letter)	
UAC	Any ATR Shift Supervisor	

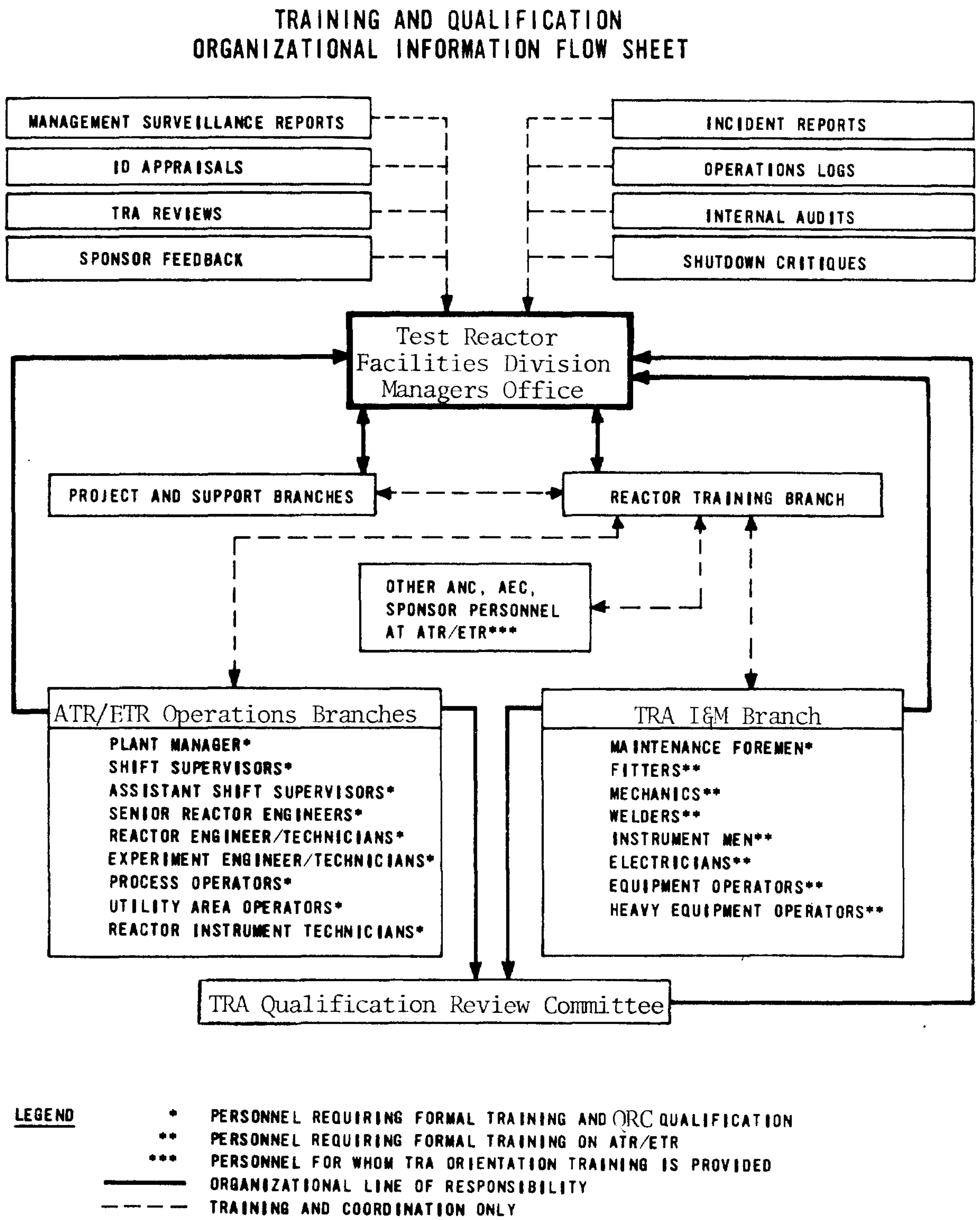

FIG. 8.3 - Training and Qualification Organizational Information Flow Sheet

. Reactor Training Branch - The Reactor Training Branch Manager is responsible to the Assistant General Manager Power Reactors for the coordination and documentation of the training program. The following specific training is administered through the Reactor Training Branch.

formal classroom training courses (reactor training school)
reactor simulator training programs
experiment loop simulator training programs
reactor tank mockup training programs
shift briefings

The Reactor Training Branch also maintains training and qualification records for individuals in Test Reactor Facilities Division.

. ATR Operations, ETR Operations, and TRA Installation and Modification Branch -

ATR and ETR Operations Branch Managers and the TRA Installation and Modification Branch Manager are responsible for the training and performance of each employee in their respective branches. They provide inputs to the Reactor Training Branch Manager to assure that the training program is evaluated and upgraded to keep it current, applicable, and in harmony with Test Reactor Facilities' objectives.

Each Shift Supervisor and Maintenance General Foreman is responsible for the day-to-day training and performance of each man assigned to him. Each assures that the on-the-job training is carried out for his personnel in accordance with approved training programs. Each personally examines and then formally recommends his candidates for qualification to the TRA Qualification Review Board.

Each Maintenance Foreman is responsible for the day-to-day training and performance of TRA Installation and Modification Branch craftsmen assigned to him. He assures that the on-the-job training is carried out for his personnel in accordance with approved programs.

. Other Test Reactor Facilities Division Branches - Each branch manager provides inputs and suggestions concerning phases of reactor operation over which he has cognizance. Instructors for various briefings are obtained from the branches as deemed appropriate.

. Safety Division (SD) - Safety Division Manager provides support to the training programs by providing instructors upon request and by providing a representative to the TRA Qualification Review Board.

ETR and ATR Health Physics Technicians, members of the Health & Safety Branch in the Safety Division, receive formal training on plant systems, policies and procedures important to them in carrying out their duties.

. Nuclear Technology Division - The reactor simulators are constructed, maintained, and modified as necessary by Nuclear Technology Division personnel. The division provides instructors as requested for various briefings to Test Reactor Facilities Division personnel and provides a representative to the TRA Qualification Review Board.

. TRA Qualification Review Committee - The TRA Qualification Review Committee has the responsibility for approving the qualification of candidates for every operational position. This includes the formal review of training records and the administration of comprehensive oral examination of each candidate. The committee membership is as specified in Table 8.1.

. Aerojet Nuclear Company Education and Training Branch - The training and qualification program is reviewed periodically by the Aerojet Nuclear Company Education and Training Branch, and an annual evaluation is submitted to the Aerojet Nuclear Company General Manager.

Each Test Reactor Facilities Division Employee is responsible for working toward and maintaining proficient knowledge and ability commensurate with his assignment. Each has the privilege and responsibility to make constructive suggestions concerning the upgrading of the training program.

. FEFPL Training Program

.. Training Summary

... ETR Operations Personnel - An individual systems approach will be used to train and qualify ETR Operations personnel for FEFPL. This approach allows personnel to be trained as the Project progresses and will provide qualified personnel prior to initiation of operational testing on each system.

A system study guide will be prepared for ETR Operations employees on each FEFPL system, containing the following items as a minimum:

applicable Operating Manual section, DOPs and prints and other pertinent information

a detailed Initial System Training Checklist to be completed on an individual basis

An open book exam will be provided for the system, upon completion of the Initial System Checklist. This exam will provide a mechanism for each individual to compare his knowledge level with an established standard prior to qualification.

Additional training will be provided in the form of formal lectures, videotapes, or handouts on an as-needed basis for each system.

... Maintenance Personnel - Maintenance foremen and craftsmen will participate in formal training sessions detailing the pertinent aspects of FEFPL associated maintenance tasks. A full-size dummy loop of correct weight will be used during loop handling training sessions. Training will be conducted to insure familiarity of maintenance personnel with both the applicable DOPs and the mechanical aspects of the following:

All IPT loop handling operation
Loop handling machine
Applicable FS&R facility tasks

.. Qualification Summary

... ETR Operations Personnel - ETR Operations employees will be qualified on each individual system prior to initiation of operational tests on that system. Prior to reactor operation for FEFPL, each employee will be qualified for integrated FEFPL operation.

.... System Qualification - To be qualified for system operational (SO) testing, each ETR Operations' employee must satisfactorily complete the following for each system:

initial system training including system checklist and open book examination

comprehensive written examination on that system to be prepared and administered by the Reactor Training Branch

an oral system walkthrough conducted by a knowledgeable individual selected by the ETR Branch Manager

.... FEFPL - To be qualified for integrated FEFPL operation, each ETR Operations' employee satisfactorily completes the following:

qualification on each system as applicable

comprehensive written examination on all applicable aspects of FEFPL, plant, and reactor operation. Examination to be prepared and administered by the Reactor Training Branch

an oral examination conducted by a specially designated FEFPL Qualification Review Committee

... Maintenance Personnel - Critical maintenance work performed for FEFPL will be under the direction of trained and qualified Maintenance Foremen who have completed formal certification by the TRA

Qualification Review Board. These foremen will act as job supervisor for critical maintenance jobs. Craftsmen participating in critical maintenance work will be selected on the basis of their participation in formal training sessions and documented on-the-job training by the supervisor responsible for the task. Pre-job briefings will be conducted for critical maintenance work.

8.7 Administrative Controls

Codes and Standards - Revisions, modifications, and additions to the ETR facility and its experiments shall be consistent with current industrial and RDT codes and standards.

Deviations from applicable codes and standards shall be subjected to an appropriate engineering analysis and approved by the Aerojet Nuclear Company Standards Technical Change Board (STCB).

Drawing Control - Control of FEFPL drawings is maintained by the Experiment Systems Configuration Control as defined by ROD Standard Practice 10.3.1.5. Key drawings are placed on a Master Facility Drawing List (MFDL). Drawing control for all work performed at TRA is maintained by ROD SP 10.1.2.2, Maintenance Job Release (MJR), and by ROD SP 10.3.1.1, Design Change Control. All maintenance work is performed in accordance with work instructions on an MJR, which is supplemented by the necessary procedures, inspection instructions and drawings. Changes to drawings are documented by the use of Form ANC-1435, Document Change Notice (DCN) which becomes an attachment to the drawing, or the drawing is revised if it is on the MFDL.

Violation of Technical Specifications - All violations shall be reported immediately to the Aerojet Nuclear Company General Manager. A written report of each violation shall be submitted to the Aerojet Nuclear Company General Manager for transmittal within two (2) working days to AEC. If reactor shutdown is specified by the General Manager or the Technical Specification, the reactor shall remain shut down until approval for further operation is received from the Aerojet Nuclear Company General Manager.

Technical Specifications Changes and Review of Adequacy - The technical specifications shall be reviewed at intervals not to exceed 13 months by

ETR Operations Branch and the appropriate Aerojet Nuclear Company Review Board and/or Committees to determine their adequacy. The responsibility for proposing additions to the Technical Specifications resides with the Power Reactors Technical Support Division (TRTSD).

Any change(s) to the facility or procedures which involve safety considerations not described or implied in the Technical Specifications require a documented supplementary safety evaluation, and shall be approved by Test Reactor Facilities Division Manager and the appropriate Aerojet Nuclear Company Review Committee. Documentation of such changes shall bear the signatures or initials of the internal approving signatories. When fully approved, a copy shall become a part of the ETR Official Documentation. All planned deviations from the specifications subsections of the ETR Technical Specifications require final written approval of the appropriate Aerojet Nuclear Company Review Board and/or Committee, Test Reactor Facilities Manager (TRTSD Manager), Aerojet Nuclear Company General Manager, and the AEC.

Approved permanent changes shall be documented by reissuance of the appropriate sections of the Technical Specifications. Temporary changes shall be approved as noted above, for a specified time interval or through a specified series of tests. They will be documented by fixing a change sheet, describing the change, the initials of the internal approval signatories, and the expiration limit, at the appropriate place in the master copy of the Technical Specifications document. Upon expiration, the temporary change sheet shall be removed from the document. No changes from or modifications to the Technical Specifications shall be applied until the prescribed approval and documentation chain is complete. Deviations and changes to specifications subsections require AEC approval in addition to the above Aerojet Nuclear Company approvals. Specific reference to the AEC approval shall be included in the Official Documentation.

8.8 Quality Assurance

The FEFP Project Quality Assurance Program Manual[6] describes the quality assurance elements and methods to be used in all FEFP Project activities. This QA program provides:

- assignment of responsibility for activities affecting quality
- requirements for performance of work in a planned, systematic manner
- control of specifications

- procedures for prevention and prompt detection of discrepancies
- procedures for timely and positive correction action
- procedures for controlled inspection and testing to ensure compliance with requirements
- provisions for objective documentary evidence of adequate QA
- provisions for audits

Included in the scope of the manual is a description of the intent and provisions of the QA program, the objectives of the Project, and the Project organization. Job descriptions and responsibilities for all major positions on the Project are provided and a responsibility and authority matrix for designated functions established. The quality assurance requirements, policies, and procedures are the method for verification and assurance that the hardware is consistent with design and operation in accordance with approved procedures. The objective of this document is to assure that the experiments and analyses are accomplished and the facilities are designed and constructed in compliance with established criteria. To achieve this objective, quality assurance controls are established and implemented for all phases of the Project so that necessary action can be taken to prevent, detect, and correct any deficiencies.

The Aerojet Nuclear Company Quality Assurance Program for the FEFP conforms to the requirements of Ref. 6 and requires that materials, parts, and assemblies have been procured, fabricated, tested, and conform to the design, as required on specifications and drawings. It is the responsibility of the Project Manager to insure that these requirements are met.

8.9 Codes and Standards

Components for the FEFP Loop shall be fabricated to RDT Material, Process and Product Standards in accordance with FEFP Loop System Specification Tree.[7]

8.10 FEFPL Safety Approval Chain

In order to assure compliance with the administrative and procedural safeguards described in the previous sections for all phases of the FEFPL Project in the ETR, a preliminary approval chain has been established for use by the Test Reactor Facilities Division. This demonstrates that the same level of safety review and approval is obtained for all systems prior to operation if a potential hazard exists. Certain FEFPL tasks will be performed before the loop is inserted into the reactor, and before the SAR is approved. These include the operation of the helium system circulators, operation of the Filling, Storage, and Remelt sodium system, and checkout of the Loop Handling Machine. Aerojet Nuclear Company approval of the SAR will be given by the FEFPL Hazards Analysis Review Board (HARB), in accordance with ANPP 14.11, and with an Independent Safety Review in accordance with Management Directive No. 6.

The FEFPL SAR approval will form the operating limits of the complete FEFPL experiment program at ETR. Each test beginning with the P-1 test will have a Test Plan. Aerojet Nuclear Company approval will be given by the AGM based on recommendation by PRAC before the loop is inserted into the reactor. The necessary Detailed Operating Procedures and operating instructions will then be issued to ETR Operations.

8.11 FEFPL Design Basis and Accident Analysis Verification

Programmatic considerations dictate that the FEFPL Safety Assessment Report accident analysis proceed in parallel with major systems and component design and analysis.

Thus, at a given time, one or the other of these efforts leads or lags the other. It is then necessary to identify the means by which at a given time, prior to approval for each FEFPL experiment, that the then current hardware and system designs can be compared with the SAR accident analysis to insure that the design changes are adequately bounded by the SAR or to identify that additional analysis and addenda to the SAR required.

Such a comparison will be accomplished by means of a document now under the cognizance of the FEFPL Project and titled the "SAR Source Reference List".

This document is updated on a periodic basis and includes a reference index system by SAR chapter and, as such, provides reference source control and retrieval capability for SAR reference documents. The document has two indexes. The first classifies reference documents by categories (e.g., project reports, EDF's, memoranda, ANC policy and government documents, etc.), the second classifies reference documents by general functional categories (e.g., Specifications, thermal-hydraulic analysis, stress analysis, etc.).
This document then provides the vehicle by which, prior to request for experiment approval, design or system changes and modification can be compared against the SAR envelope to insure changes have not invalidated safety analyses.

8.12 Loop Integrity Limits and Control for Pre-Insertion Testing

Loop system testing will be conducted prior to insertion of the loop for irradiation. It is necessary that these tests be conducted in a manner and under a system that identifies the limits for loop conditions such as to insure loop integrity is not compromised prior to insertion.

The bounding conditions are established by the Section III faulted casualty events although Test Plan requirements may dictate specific, more restrictive criteria.

The FEFPL PPS and EAS systems will provide the means by which loop conditions can be monitored and annunciated during FS&R testing although not providing automatic control functions or mitigating action such as during reactor operation.

The mechanism of surveillance, i.e., minimum instrument channels, diagnostic intervals, etc., to insure Section III faulted casualty criteria are not exceeded prior to reactor operation, is being developed in conjunction with the Experiment Test Plan and Experiment Operating Instructions and control documentation.

References

1. Aerojet Nuclear Policy Procedures (ANPP) 10.00 Series, Test Reactor Facilities.

2. Test Reactor Facilities Division Standard Practices.

3. Policy Manual (PM) 2.7.1.

4. ANPP 14.00 Series, Committees and Boards.

5. TRF Training and Qualification Program Booklet.

6. ETR Technical Specifications, Aerojet Nuclear Company, Report CI-1233, (February 1972).

7. "Fuel Element Failure Propagation Project Quality Assurance Program", R1000-1000-SA-00, (August 4, 1971).

8. "Specification Tree for the Fuel Element Failure Propagation Loop", R1001-1000-SA-00, (October 12, 1971).

CHAPTER 9.0

TABLE OF CONTENTS

LIST OF TABLES

LIST OF FIGURES

LIST OF FIGURES (Contd.)

9.0 Normal Loop Operation

The primary objective of this chapter is to present information about normal operation of the FEFP loop. This knowledge then serves as a foundation on which expanded discussion presented in subsequent chapters on experiments (Chapter 10) and accidents (Chapter 11) can be based. An additional objective is to provide adequate assurance that these normal operations are safe.

The operation and conditions presented in this chapter are classified as normally defined by the ASME Code, Section III.[1] (The one exception is the ETR scram case which is an upset condition.) Therefore, all of the Section III criteria pertaining to normal operating conditions apply to the FEFPL operations discussed in this section. The normal ETR operating procedures also apply to the FEFP in-pile loop as they do to all other in-pile experiments. Normal operation above 1% ETR power will be controlled automatically. Manual control will be available for backup or override as required for safety or special experimental needs and for a fast recovery following a reactor scram.

Figure 9.1 presents a histogram of normal operating conditions. Parameters shown are: sodium flow, reactor power, helium system pressure, annulus gas pressure, and reactor coolant flow rate. Under conditions which are not the result of an accident (see Chapter 11), an ETR scram is considered as a normal loop condition. A window in the histogram is shown in which the FEFPL experiment is performed. Experiment-related transients are discussed in Chapter 10.

This chapter is arranged to discuss normal loop conditions as: steady state (at initiation of experimental transients), pre- and post-experiment standby, and transients between these two operating levels. Description, function, and requirements for components of the loop have been presented in Chapter 5.

9.1 Steady State

In the FEFPL a wide range of steady-state operating conditions are possible, and operating set points will be selected to satisfy the objectives and conditions required for each experiment.[2] These conditions, however, must be within the loop safety and performance envelopes identified in

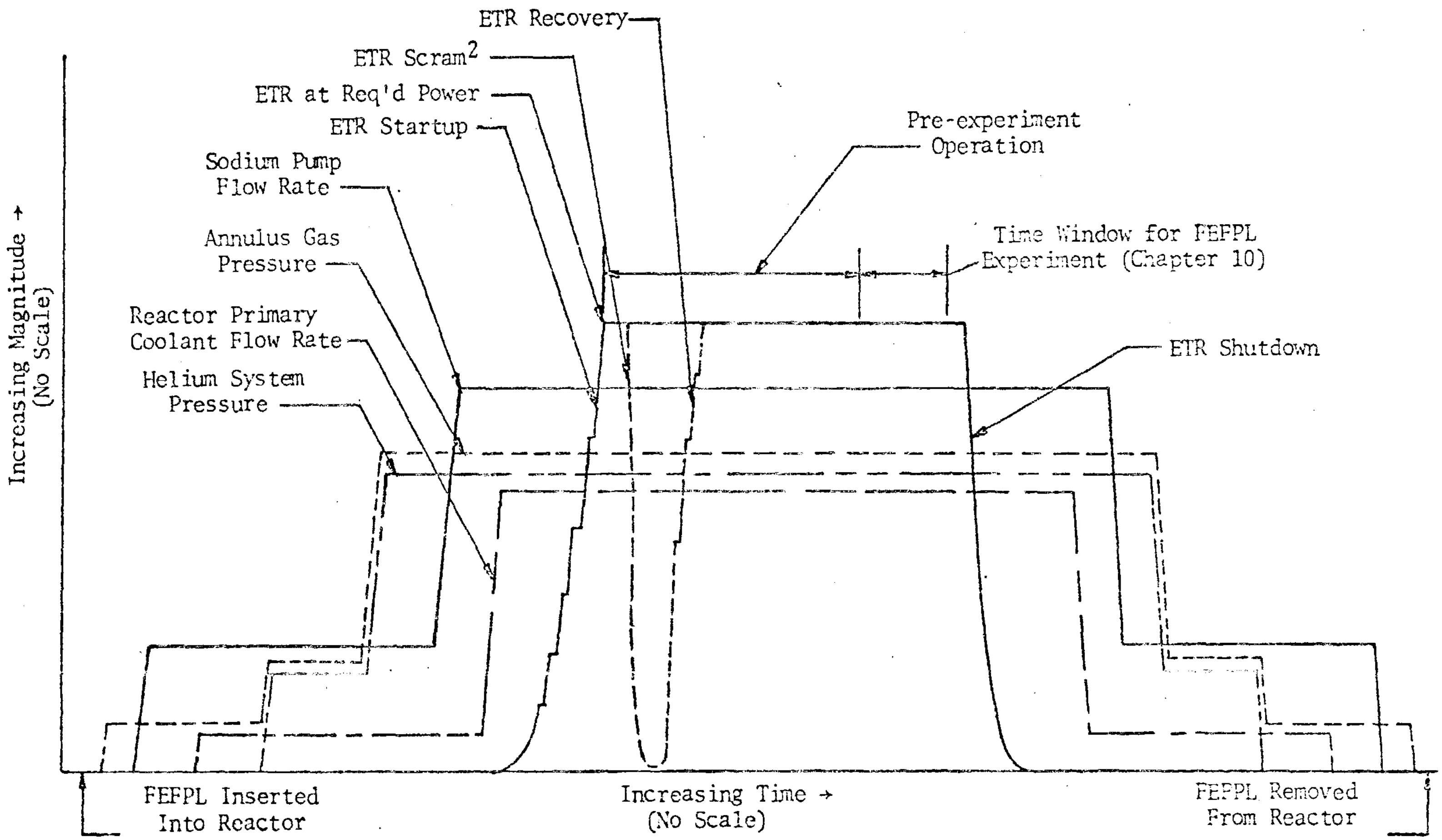

NOTES:

1. Histogram shows a general sequence of key events. Detail steps are omitted for clarity.
2. ETR scram is considered as an unplanned (or abnormal) event. Although scram may occur at any time, its occurrence during an experiment is extremely unlikely because of the small time span of the experiment.

FIG. 9.1 - Simplified Histogram of Various Major Parameters During Normal Loop Operations

Chapter 6. An Experiment Safety Analysis report will be generated prior to each experiment to demonstrate the fulfillment of this criterion.

The basic steady-state operating characteristics of the loop are presented in the following two subsections. The first pertains to the loop as a whole with emphasis on the portion outside of the test section. The second pertains to the normal operating conditions within the test section, which are designed to simulate FTR conditions. Due to the nature of the experimental program, loop operating conditions and test-section design will vary from experiment to experiment.

9.1.1 Loop Conditions

9.1.1.1 Loop Power

Calculated net loop power levels for the 19- and 37-pin test bundle configurations are shown in Table 9.1. The values shown for the fission power are based on achieving a uniform power per pin of 35.1 kW and 32.1 kW, respectively.

Gamma heat in FEFPL comes from two sources: the ETR core and the test fuel in the loop. Calculations indicate that the dominant source of gamma heating for the in-pile loop containment components is the ETR. The minimum design axisymmetric gamma-heating rates used for design of the in-pile loop components are shown on Fig. 9.2. A factor of 1.25 was applied to the gamma heat-rate calculations to account for uncertainties (e.g., basic nuclear data, model approximation, flux peaking).[4] Table 9.2 shows calculated typical gamma heating in various regions of the FEFPL for the specified materials. Gamma-heat data will be verified from critical facility experiments and actual operation in ETR.

The maximum gamma heating variation across the loop due to reactor flux tilting during steady-state operation has been determined to be 15% (± 7.5%) of the design axisymmetric gamma heating value.[5] Asymmetric gamma heating tends to cause the loop to bow in the ETR core region. The loop is centered in the core filler piece by splines on the core filler piece located just above and below the ETR core. Between these splines the core filler piece is relieved to a larger diameter providing an annulus for ETR coolant water flow. The loop is free to bow within the annulus between the secondary tube and the core filler piece; however, more than 15% flux tilting is required for contact.

Nodal model simulation of the test train flow divider, primary vessel and secondary vessel was used to analyse the asymmetric heating using the STRAP-S Computer Code (see Appendix B.9 for discussion of this code) to determine the deformed shape, internal moments and reaction forces. This modeling assumed fixed support of the loop at the ETR top head and lateral support at the in-vessel support interface. The core filler piece was assumed to be rigidly supported by the reactor. Computer results[35] for the critical case were found to be:

1. Maximum primary and secondary tube stresses (asymmetric portion only) were 3,180 psi and 3,840 psi, respectively (core midplane region),

2. Clearance was provided between the loop and the core filler piece within the core region,

3. Maximum reaction force at the lower spline interface was 73 lbs.

The reaction force is further traced to the ETR at the grid plate support interface with the core filler piece.

As shown in Table 9.1, the EM pump also adds heat to the sodium circulating in the loop. The higher power shown for the 19-pin case, as compared to the 37-pin case, is due to greater impedance required to provide experiment simulation. For either configuration, 150 kW is the maximum heat input available from the pump.[6]

TABLE 9.1

Calculated Net Loop Power (kW) Removed
by the Heat Exchanger for Two Test-Bundles

Power (with Cd Filter)	Number of Pins in Test-Bundle	
	19	37
Fission[1]	673	1197
	(35.1 kW/pin)	(32.1 kW/pin)
Gamma[2]	315	302
Pump[3]	114	68
Loop Loss[4]	-74	-72
Net Power	1028	1495

Notes:

1. Enrichments in each pin row are varied to make all fuel pins operate at the same power levels.
2. Does not include power generated in the secondary vessel.
3. Calculated amount of heat generated in pump.
4. Calculated heat loss from sodium loop to the secondary vessel (thence ETR water)
5. Data generated from SINDA loop model steady-state analysis (Ref. 3).

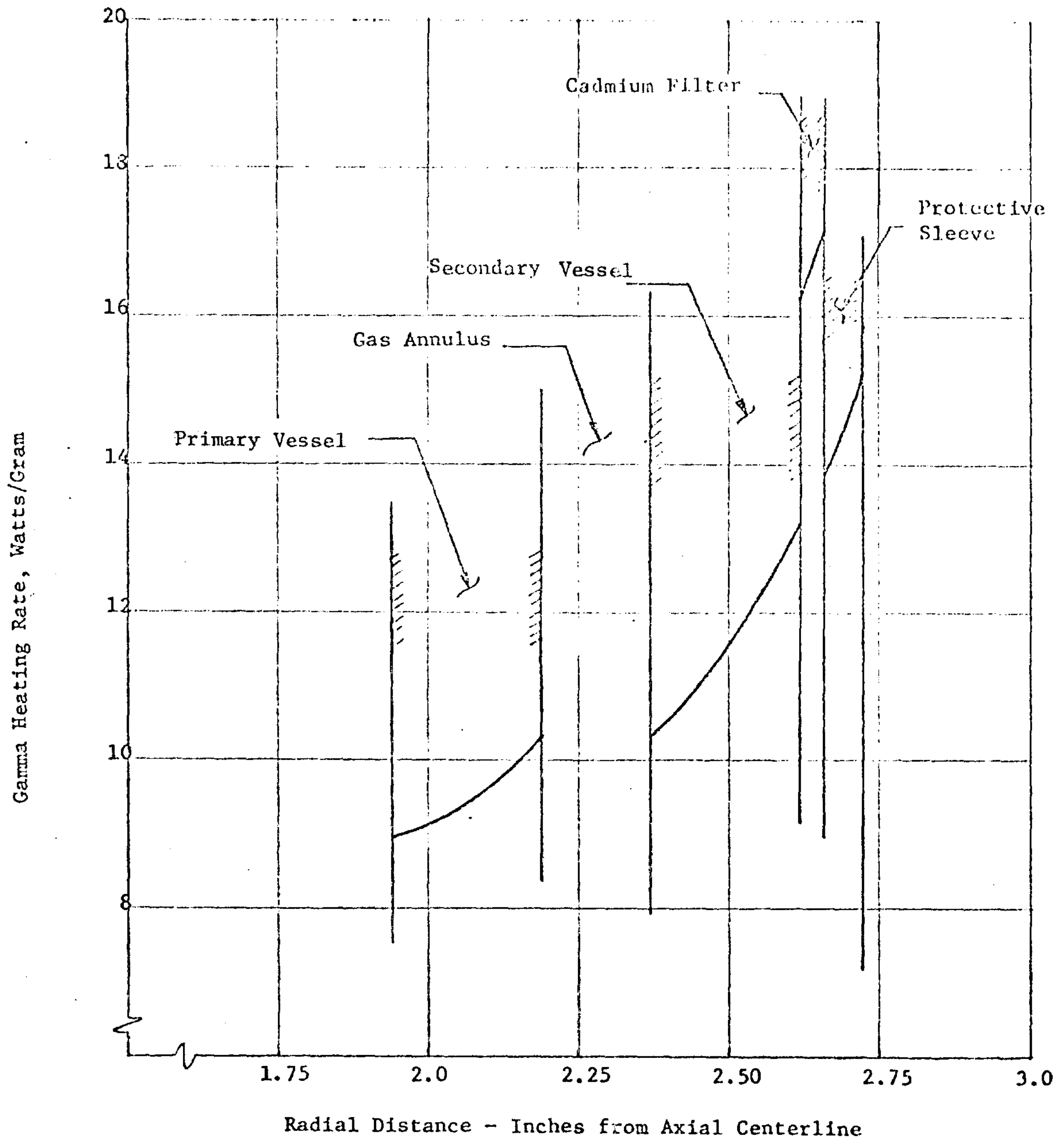

NOTES: 1. Curves for 316 SS Material (Exception - Filter)

2. Curves based on Gamma Heating Analysis discussed in Reference 4.

FIG. 9.2 - Design Gamma Heating Rates at Core Midplane for FEFPL Primary and Secondary Tubes

TABLE 9.2

Calculated Gamma Power Distribution in FEFPL Contributing to the Heat Exchanger Load[1]

A.	Inside Hex Shroud	
	1. Fuel	79.1 kW
	2. Fuel-element cladding and spacer wires	6.9
	3. Sodium	2.0
	4. Inner hex shroud wall	2.2
		90.2 kW Subtotal[2]
B.	Bypass	
	1. Outer hex shroud wall	19.6 kW
	2. Sodium	16.0
	3. Inner flow-divider	32.7
		68.3 kW Subtotal
C.	Downcomer	
	1. Outer flow-divider wall	33.7 kW
	2. Sodium	16.3
	3. Primary vessel	183.8
		233.8 KW Subtotal
		302.1 kW Total (excluding gamma heat within hex shroud)

Notes:

1. Data represents the 37-pin test-bundle configuration at 32.1 kW/pin. See Table 9.1 and Fig. 9.7.
2. Included with fission power in the test section power total.
3. Data generated from SINDA loop model steady-state analysis (Ref. 3).

Loop heat losses, other than the heat removal by the heat exchanger, are small (Table 9.1). These are primarily due to conduction through the pump stator to the secondary vessel and heat transfer across the helium-filled annulus between the primary and secondary vessels.

9.1.1.2 Loop Hydraulics

The sodium loop model used for hydraulic calculations is shown schematically in Fig. 9.3. The loop is a closed loop with one free surface which interfaces with a pressurized cover gas. As will be discussed in more detail in the next subsection, a controlled amount of the total loop flow passes up through the fuel bundle to simulate FTR conditions. The remainder of the flow is bypassed around the test section and is then recombined with the test-section flow.

Thermal-hydraulics calculations made in support of the ASME Code Section III stress analysis were obtained from the FEFP loop model using the ANC SINDA 3G computer code.[7] To determine steady-state pressure drops (or rises, in some regions), the sodium loop is divided into numerous regions, each with a specific length of flow area, equivalent diameter, and flow expansion/contraction loss coefficient. Net sodium circulation head due to the changing sodium temperature (or density) and net pump head rise are also calculated. The required pump power input for the specified loop operating conditions is then obtained from pump parametric power operating curves expressed in terms of pressure rise versus flow rate.

Pressure drop calculations based on the loop model shown on Fig. 9.3 use over 168 regions to describe the loop and test train. Individual region pressure drops within the loop for test trains containing 19- and 37-pin fuel bundles are shown on Figs. 9.4 and 9.5, for several loop flowrates. The net pump pressure rises for various mass flow rates are summarized as follows:

Steady State FEFPL Net Pump Pressure Rise as a Function of Bundle Size and Mass Flow Rate[3]

Loop Mass Rate Flow lbs/sec	Pressure drop, psi 19-pin bundle	Pressure drop, psi 37-pin bundle
6.58 (∿54 gpm)	138.7	---
12.19 (∿100 gpm)	143.2	76.1
17.60 (∿150 gpm)	---	82.4

FIG. 9.3 - FEFP Loop Model for Hydraulic Calculations

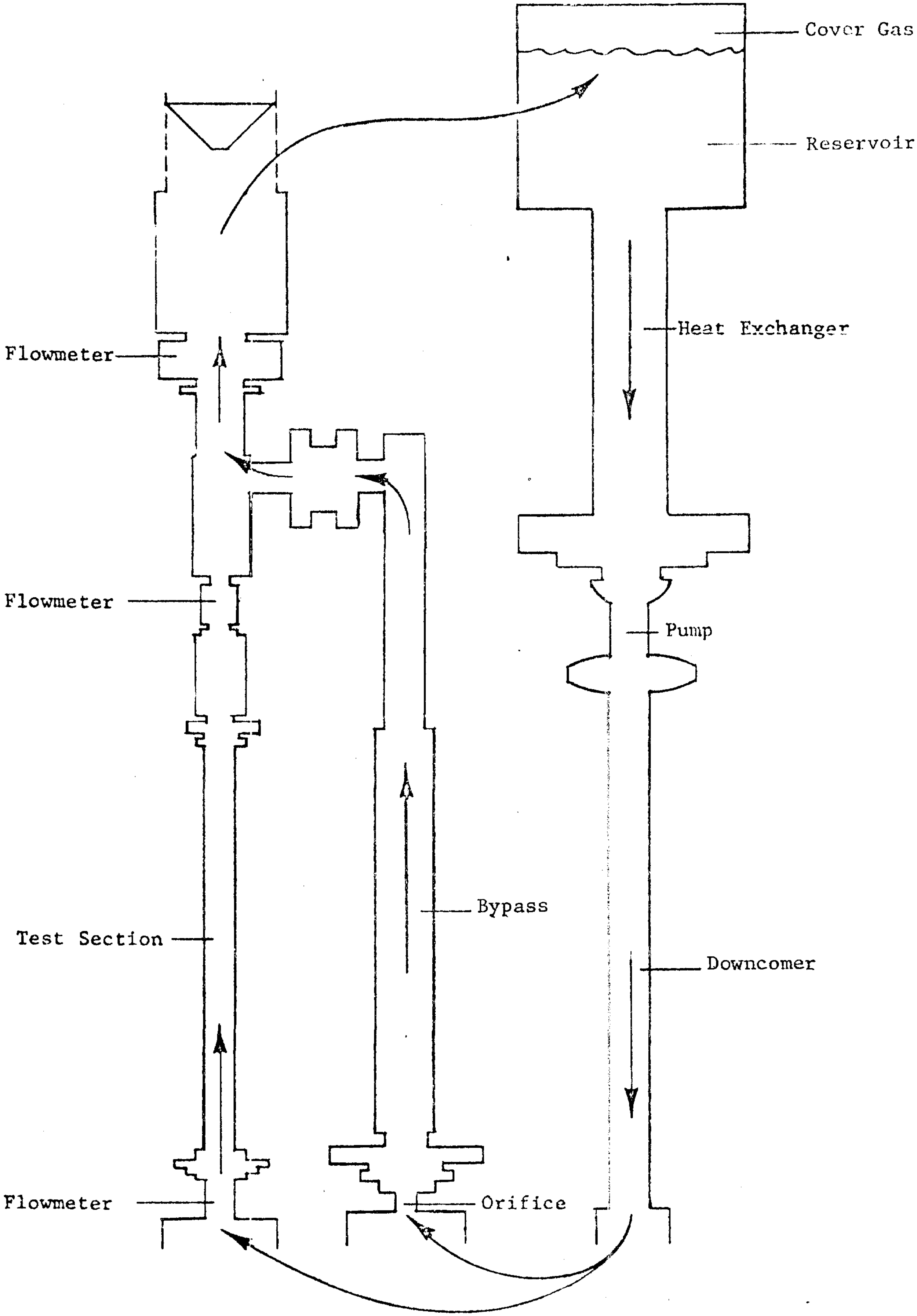

Note: ● Indicates location of pressure calculations for indicated values (psi).

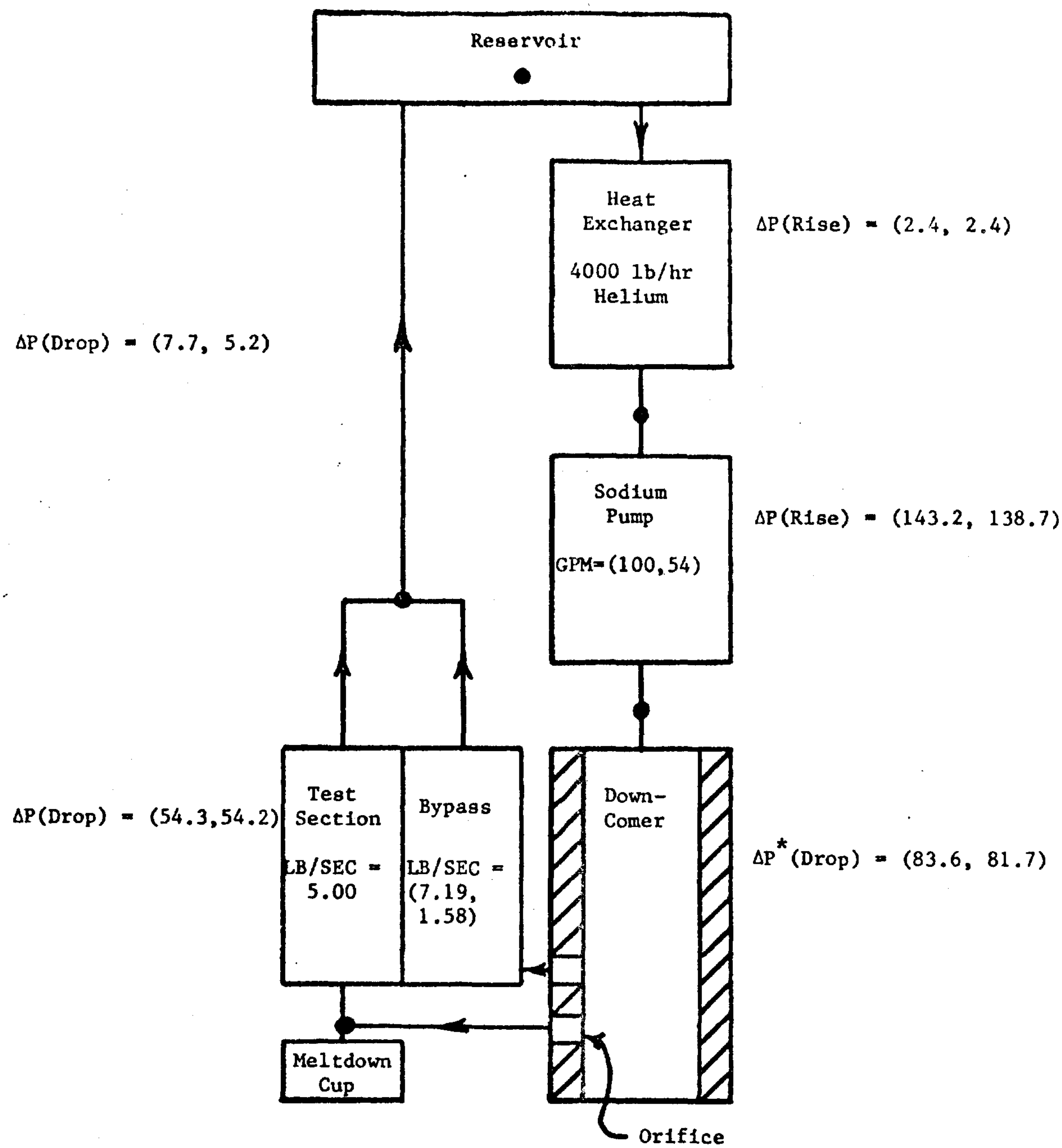

*Essentially all pressure drop due to orifice.
Data generated from SINDA Loop Model Steady State Analysis (Reference 3)

FIG. 9.4 - Schematic of FEFPL Model for 19-pin Test Section with Steady-state Total Pressure Drop for Indicated Flowrates

Note: O Indicates location of pressure calculations for indicated values (psi).

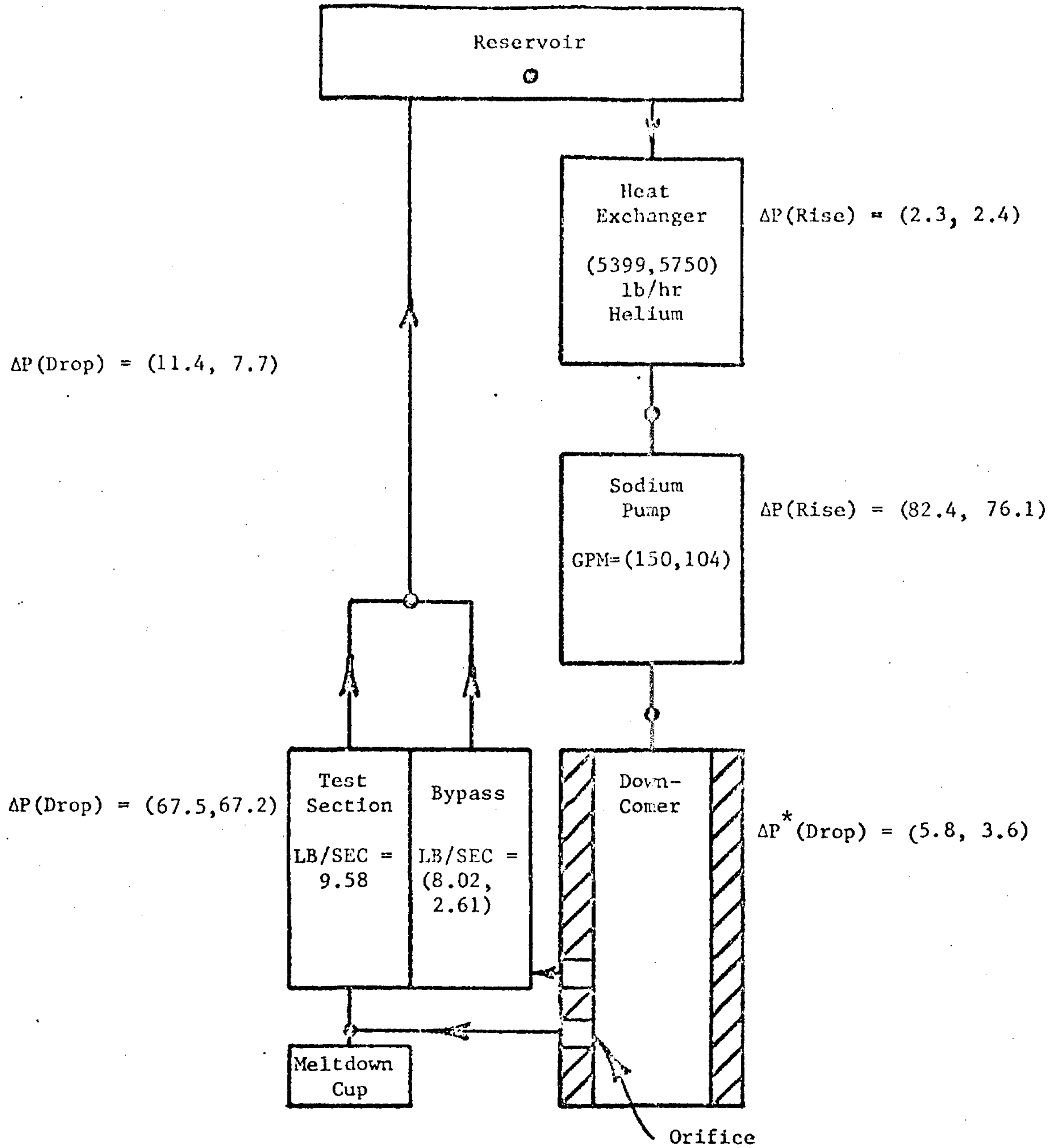

*Essentially all pressure drop due to orifice.

Data generated from SINDA Loop Model Steady State Analysis (Reference 3)

FIG. 9.5 - Schematic of FEFPL Model for 37-pin Test Section with Steady-state Total Pressure Drop for Indicated Flowrates

The above total pressure drops include losses at the bottom of the loop due to the change in flow direction, and losses at the flow combiner slots and the slots in the reservoir area adjacent to the flow diverter. For additional discussion on the computer code model, see Appendix B.9.

9.1.1.3 Loop Temperatures

Steady-state temperatures in the sodium loop at ETR power are controlled by the sodium temperature control valve, which regulates loop secondary (helium) coolant flow to the shell side of the loop sodium-to-helium heat exchanger. This is a three-way valve which is used to split the mass flow from the constant mass flow supply of the helium system according to demand. See Section 9.1.1.4 for a discussion of the heat exchanger.

Figures 9.6 and 9.7 show sodium temperatures in various regions of the loop for selected sodium mass flowrates. As with the pressure drop calculations, these temperatures were obtained using the SINDA loop model for preparation of the steady-state operating map. This model was used for thermal analysis data as input for the Section III stress analysis.

From Figs. 9.6 and 9.7, it is seen that some loop temperatures exceed 800°F, which is the maximum temperature covered by the ASME Code Section III.[1] For temperatures between 800 and 1300°F, material-allowables and properties are used from ASME Interpretation Case 1331-7, "Nuclear Vessels at High Temperature Service."[8]

As previously discussed and shown in Table 9.1, most of the primary loop gamma-heating and pump-power-generated-heating are removed by the heat exchanger. The small loop losses are transferred across the helium gas annulus to the secondary vessel. This heat, in addition to its gamma heating, is removed from the secondary vessel by the reactor primary coolant water passing downward through the ETR core.

To minimize regenerative heat transfer within the loop between the downcomer and bypass flows, and to provide thermal isolation in the pump and heat exchanger regions, the flow divider design incorporates a double walled construction with the gap filled with argon gas. Preliminary tests indicate that at 1000°F, overall heat transfer coefficients as low as 15 to 20 Btu/hr-ft^2-°F can be obtained.[9]

Note: ○ Indicates location of indicated temperatures (°F).

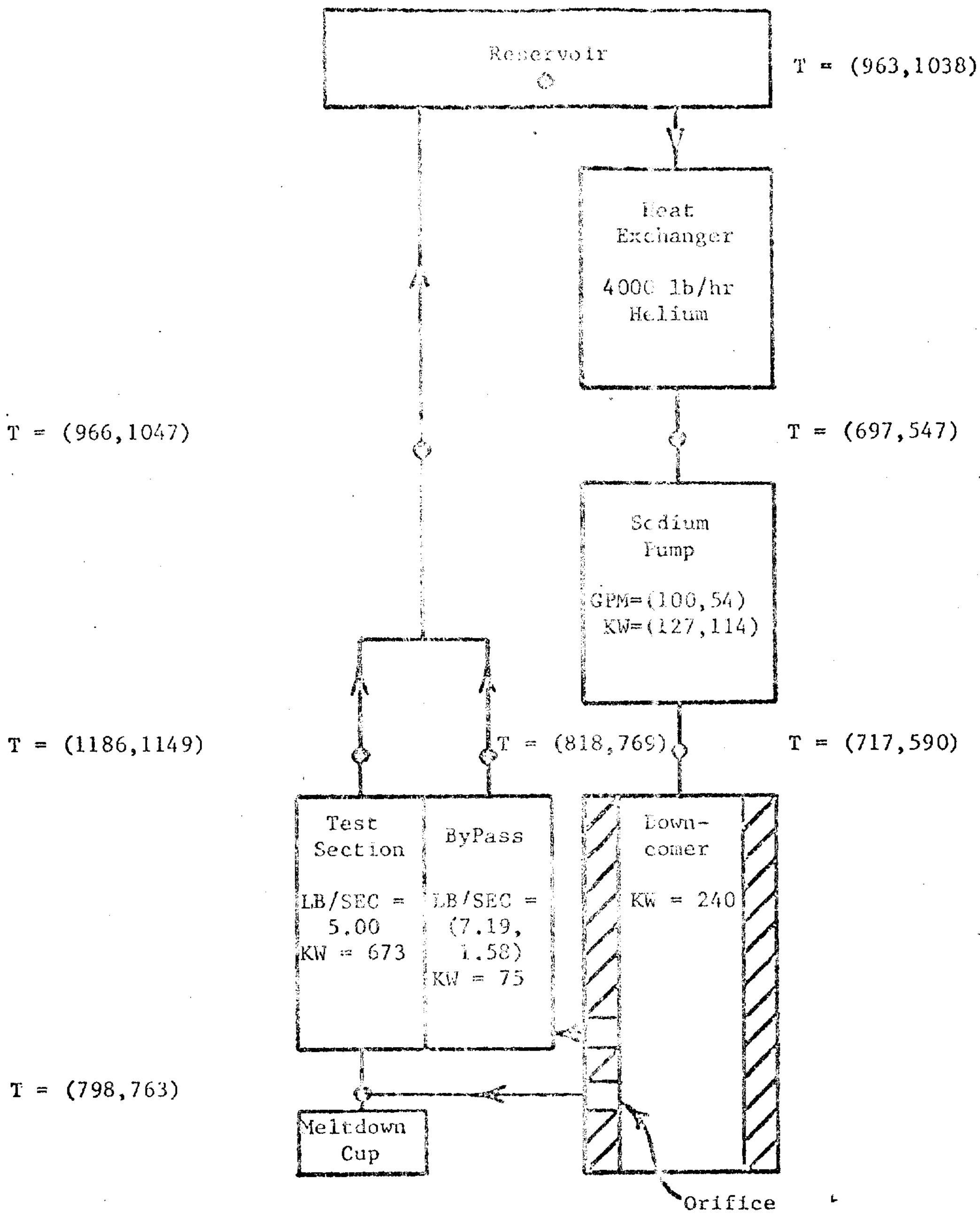

Data generated from SINDA Loop Model Steady State Analysis (Reference 3)

FIG. 9.6 - Schematic of FEFPL Model for 19-pin Test Section with Steady-state Temperatures at 35.1 kW/pin for Indicated Flowrates

Note: ○ Indicates location of indicated temperatures (°F)

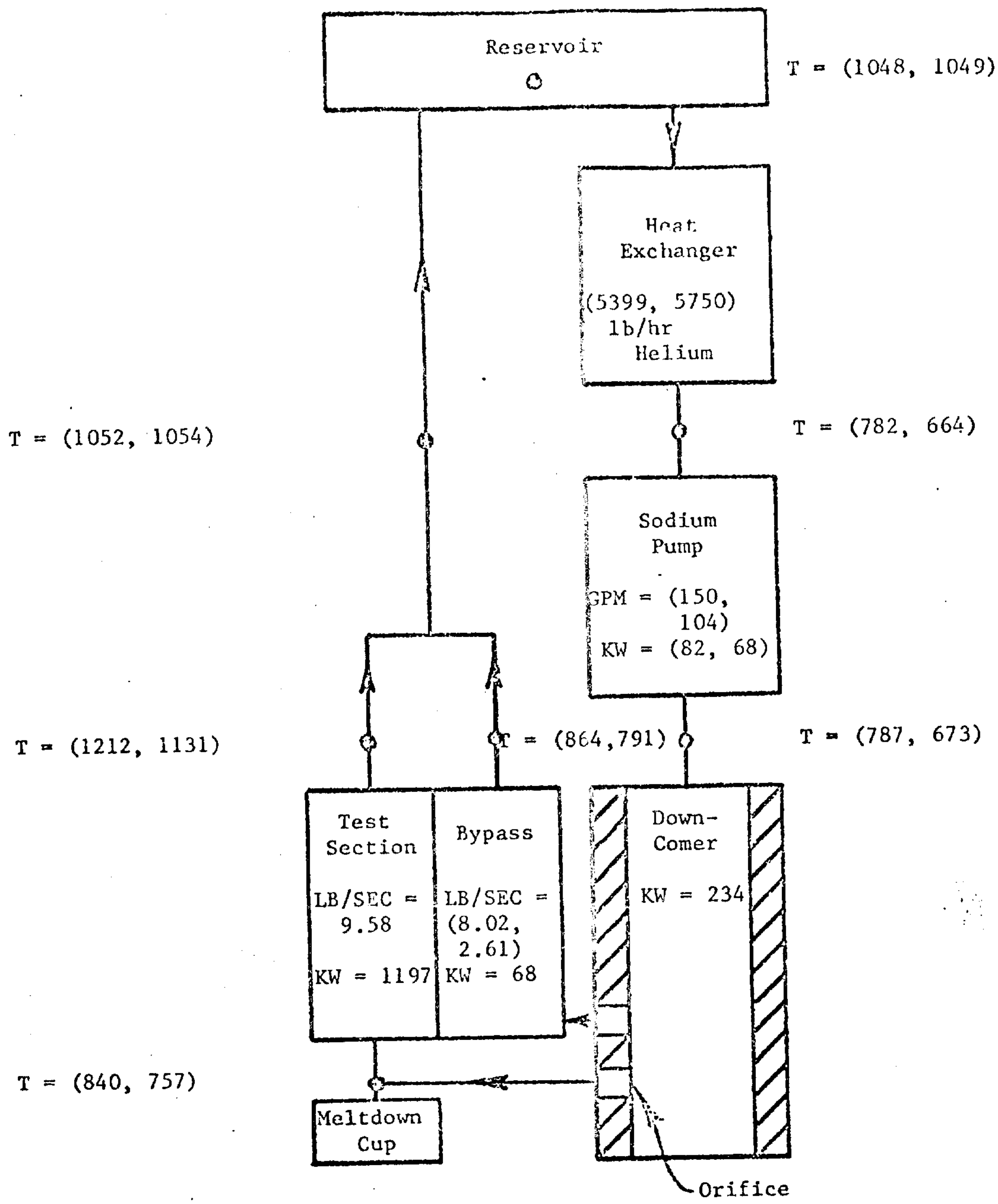

Data generated from SINDA Loop Model Steady State Analysis (Reference 3)

FIG. 9.7 - Schematic of FEFPL Model for 37-pin Test Section with Steady-state Temperatures at 32.1 kW/pin for Indicated Flowrates

9.1.1.4 Heat Exchanger

The basic means of heat removal from the sodium loop is with a heat exchanger in which the secondary coolant is helium gas. The heat exchanger is a tube-and-shell, counter current, once through, cross-flow type. The sodium and helium flow in the tube and shell sides, respectively. Eight baffles are located in the shell side to improve heat transfer performance.

The helium inlet temperature is maintained at 150°F through automatic control. Under normal operation, the helium system is to provide a constant 5750 lb/hr (1.59 lb/sec) mass flow to the sodium temperature control valve. Helium system pressure drop, excluding the sodium loop heat exchanger, is about 13 psi.[10] The heat exchanger pressure drop at a maximum flowrate of 5750 lbs/hr is 20 psi.[11] The total head requirement for this flow case is then about 33 psi, which can be satisfied by any two of the four available circulators.[12] If three or four circulators are operating, reduced speeds may be maintained accordingly.

Heat exchanger performance showing UA versus helium mass flowrate and required UA versus heat removal are shown on Figs. 9.8 and 9.9, respectively. Figure 9.9 curves A and B show the influence of sodium inlet temperature on heat exchanger performance. The cross lines in Figs. 9.8 and 9.9 show the heat exchanger design basis.[13]

The design maximum heat removal by the heat exchanger is 1.5 MW.[14] This is based on heat transfer area and maximum helium mass flow. An upper limit on test-fuel bundle power will be based on this maximum heat removal capability. The 500°F limit on ΔT (the temperature difference at the heat exchanger between inlet and outlet sodium) establishes a lower limit on sodium flow for any given power, i.e.,

$$\text{Sodium Flow} > \frac{\text{kW}}{20}\ \text{gpm}.$$

Table 9.3 summarizes heat exchanger data for the heat loads and sodium flowrates shown on Figs. 9.6 and 9.7. Helium demand is shown to be within the 5750 lb/hr (1.59 lbs/sec) limit.

9.1.1.5 Vibrations

Certain vibrations of the in-pile loop assembly are possible during normal operations. Likely forcing functions are sodium pump flow oscillations, secondary coolant flow disturbances to the loop heat exchanger, and

FIG. 9.8 - UA vs Helium Mass Flowrate for FEFPL Heat Exchanger

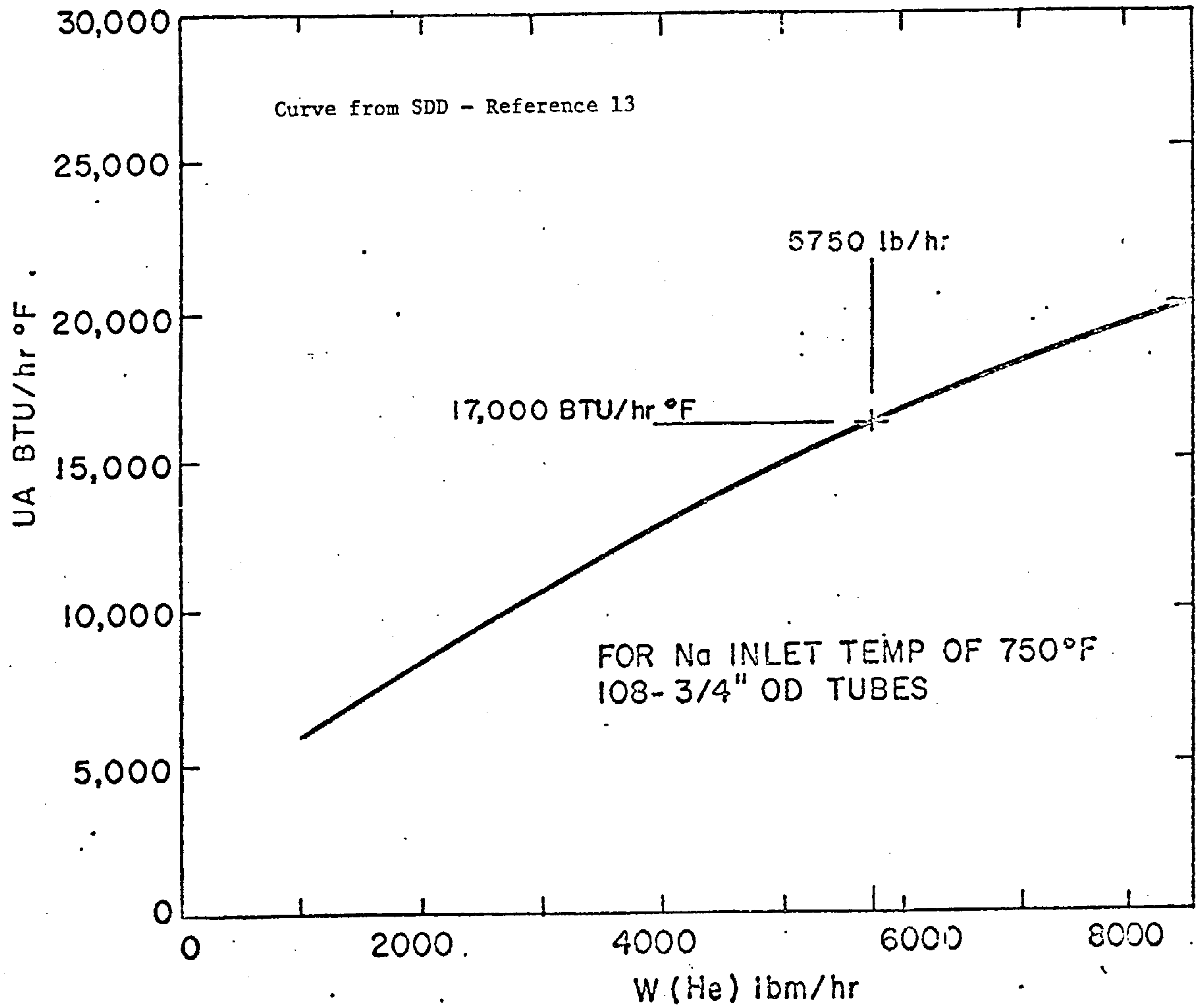

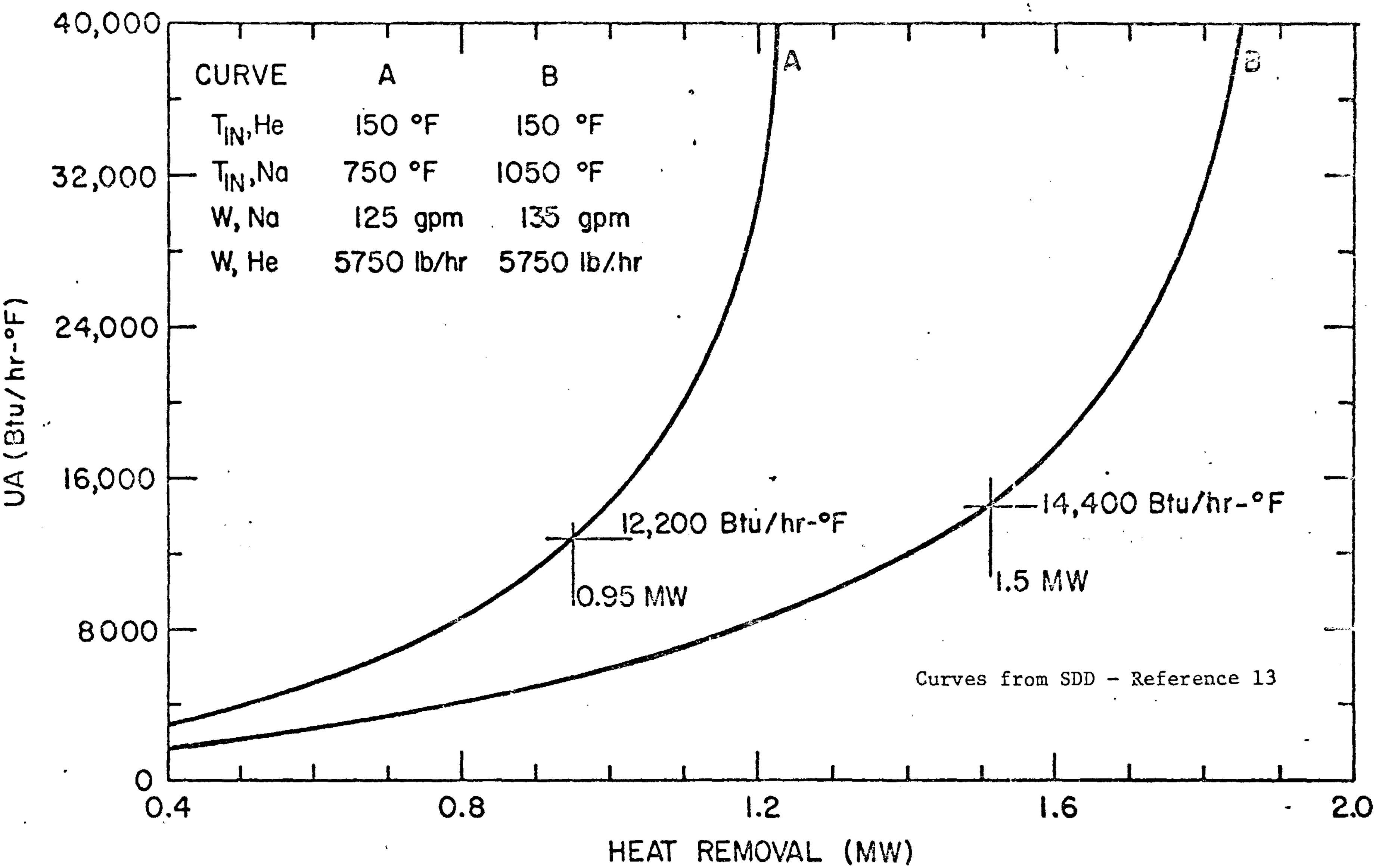

FIG. 9.9 - Required UA vs. Heat Removal for FEFPL Heat Exchanger

TABLE 9.3

Heat Exchanger Conditions for Loop Operation Shown in Figures 9.6 and 9.7

No. Fuel Pins	Element Power (kW/pin)	Net Loop[1] Power (kW)	Loop Sodium Flowrate (lb/sec)	Sodium Temperature at HX Inlet (°F)	Sodium Temperature at HX Outlet (°F)	HX Sodium ΔT (°F)	Approximate Helium Flowrate (lb/sec)
19	35.1	1028	6.58	1038	547	491	1.11
		1028	12.19	963	697	266	1.11
37	32.1	1481	12.19	1049	664	385	1.59
		1495	17.60	1048	782	266	1.50

Notes:

1. Represents loop power removed by heat exchanger.
2. Data obtained from SINDA loop model steady state analysis (Ref. 3).

reactor primary coolant flow disturbances. Table 9.4 provides a summary description on these forcing functions: magnitude, frequency region, and probable cause. Seismic and accident dynamic effects are discussed in Chapter 11.

For small disturbances, the first vertical and horizontal natural frequencies of the loop are 2.5 Hz and 4.5 Hz, respectively. For the several forcing functions below 1 Hz, it is readily seen that the excitation is sufficiently frequency isolated from the fundamental frequencies so as to preclude concern for loop response. Sodium loop analog results for the Helium System oscillations support this conclusion.[33]

The nearest natural frequency to the 60 Hz pump oscillation is 65.3 Hz (vertical); however, the resulting ±0.26 psi pressure oscillation has a small effect.[37] It was found that this pressure pulse amplitude and the associated EM pump loads were about 0.1% the magnitude of the static design conditions. Although a ±6 kW power oscillation of the ALIP input could occur under maximum conditions, the influence of the sodium inertia at frequencies of 60 Hz and higher significantly attenuate the response amplitude.

Due to the baffling within the heat exchanger, the secondary coolant provides a crossflow excitation to the sodium tubes. Dynamic analysis for this condition has been performed for the helix and straight tube sections.[38] The fundamental frequency for each configuration was determined to be within the operating range of the secondary coolant flow to the heat exchanger inlet. Amplitude of motion for operation at resonance in each was determined considering damping at 2% of critical. In comparing resultant vibration stresses with the high temperature ASME code case 1331-7, it was found that the stress ranges were below the limit of material sensitivity to cycle fatigue.[39]

The reactor water coolant causes two possible disturbances. The first is due to the crossflow from the primary coolant pipe impinging on that portion of the loop assembly which is above the core. The second is due to the turbulent flow downward through the core between the core filler piece and the loop secondary vessel. In both cases, the vibrations were found to have a very small effect because of a wide difference between the frequency due to the forcing function and the natural frequencies of the loop, or because the forcing function magnitude produced very small deflections. The resultant stresses were found to be small when compared to stresses due to normal operating conditions.[16]

TABLE 9.4

Loop Vibration Forcing Functions During Normal Operating Conditions

Disturbance	Magnitude[1]	Frequency	Probable Cause
1. Pump Flow Oscillation	±1.0 psi	<0.7 Hz	Sodium flow controller
	<0.26 psi	60 Hz	MG set voltage variation (±2%
2. Helium Flowrate Oscillation to Heat Exchanger	±111 lbs/hr	<0.3 Hz	Helium system pressure oscillation of ±5 psi
	±45 lbs/hr	<0.2 Hz	Helium system temperature oscillation of ±5°F
	Turbulent Flow	90 Hz	Helium crossflow to the helix wound HX tubes
	Turbulent Flow	665 Hz	Helium crossflow to the straight HX tubes
3. Reactor Primary Coolant Water Flow	Note 2	0.29 Hz	Cross flow to upper part of the loop
	Turbulent Flow	Random	Axial flow along in-pile tube

Notes:

1. Magnitudes shown represent upper bounds and do not indicate typical condition.
2. Magnitude was not determined since the calculated upper loop natural frequency of 202.5 Hz was considerably higher than the vortex shredding frequency shown.
3. Data obtained from References 16, 33, 37, and 38.

The preceding discussion summarizes the results of vibration analysis conducted to date on the loop vessel and heat exchanger for the three forcing functions identified in Table 9.4. Additional vibration analysis on the test train is in progress, but remains to be completed.
The results of this analysis will dictate the extent of and approach used in additional vibration work (i.e., analysis, vibration instrumentation and/or model test train post-test examination) to insure acceptable vibration stress levels prior to P-1 operation.

9.1.2 Experimental Simulation

The FEFP Program will be required to simulate a variety of FTR accidents; therefore, the test conditions and requirements differ for each experiment. In the following paragraphs, the major loop operational variables used to effect the simulation of experiments are discussed.

9.1.2.1 Test Section Power

Fuel enrichment specifications for the 19- and 37-pin test bundles are shown in Table 9.5. The purpose of varying the enrichments (by test bundle row) is to develop equal power for all pins in the test bundle.

In determining these specifications, an additional objective was to ensure that adequate FEFPL experiment pin-powers could be achieved within the ETR full power capability. Maximum required FFTF experiment pin-power for the test bundle configurations is 35.4 kW/pin.[17]

In the analysis to ensure adequate pin-power margin, an estimate for the ETR core configuration was made.[4] Results from the FEFPL mockup flux

TABLE 9.5

Fuel Enrichment (% ^{235}U) Specifications for 19- and 37-pin Test Bundle Configurations

Pin Position	19-pin All UO_2	19-pin 22 w/o PuO_2 Mixed Oxide	37-pin 22 w/o PuO_2 Mixed Oxide
Center pin	93	93	93
6 pin ring	86	86	89
12 pin ring	73	65	79
18 pin ring	N.A.	N.A.	58

Notes:

1. Specifications are based on developing equal power in all pins of the test bundle.
2. Data obtained from Ref. 4 and Ref. 36.

mapping experiment in the ETR Critical (ETRC) facility were used as a guide.[18] Predicted pin-power capabilities for a condition of ETR at full power are shown in Table 9.6. The calculations were based on a normal ETR axial cosine flux distribution with a peak/average factor of 1.4. Thermal neutron filtering due to the .040-in.-thick cadmium (located in-core around the loop secondary vessel) was included; however, further axial flux flattening to a 1.24 peak/average factor for FTR was not included.

Further ETRC flux mapping and analysis is planned to determine the final core configuration for experiment P1, which may alter some of the results shown in Table 9.6. However, the margin that exists appears adequate to provide the desired pin power. Operation of the loop will be dependent upon loop conditions, in particular the test bundle power, and this is related to the fission density produced by ETR. Therefore, ETR will be controlled at a condition less than its rated capability to provide the FEFPL requirements. As discussed in paragraph 9.1.1.4 (Heat Exchanger), the upper limit power will be based on the maximum heat removal capability of the loop heat exchanger (1.5 MW).

9.1.2.2 Fuel Bundle Radial Temperature Profile

It has been shown[19] that the radial temperature distribution in the test assembly is affected by sodium flow streaming at the fuel-bundle boundary and by heat loss to the bypass coolant. A typical radial coolant temperature distribution for an FTR subassembly is shown in Fig. 9.10. As can be seen, the central portion of the temperature profile is essentially flat.

To simulate the radial temperature profile in the center portion of the FTR subassembly, a thermally insulated shroud will be used to reduce the heat loss from the test fuel coolant to the bypass coolant and one-half normal diameter spacer wires will be used at contact points between the outer row pins and the hex can to minimize overcooling due to flow streaming. The shroud is in the form of a double-walled hex can, with the gap filled with helium gas.[13] Heat losses through the shroud have been calculated to be about 2 kW.[21] Hence, the radial temperatures do not drop sharply at the fuel boundary due to the combined effects of low heat loss and flow streaming.

9.1.2.3 Fuel Bundle Mass Flowrate

Size (OD) and spacing (pitch) of the pins within the FEFPL fuel bundle has been set identical to the FTR subassembly to provide mass-flowrate-simulation

TABLE 9.6

Calculated Pin Powers Based on Assumed ETR Core Operated at Full Power (for fuel specified in Table 9.5)

	19-pin	37-pin
FEFPL fuel pin[1] full length (3 ft) with 1.4 peak to average axial factor	57 kW (±5%)	44 kW (±5%)
Peak axial power developed in pin	26 kW/ft (±7%)	20 kW/ft (±7%)
Power developed by hottest of surrounding 12 ETR elements	4.1 MW (±5%)	4.3 MW (±5%)

Notes:

1. All fuel pins are assumed to give equal powers, as a result of enrichment variations as given in Table 9.5. Also, the values quoted in line 1 are for the normal ETR axial flux cosine distribution, which gives a peak/average longitudinal factor of approximately 1.41.
2. Calculations were obtained for an assumed core based on preliminary flux mapping at ETRC and analysis. Magnitudes are subject to change depending on the final core selection.
3. Reference 4 for analysis.
4. The conditions listed for the 19-pin bundle apply to both all UO_2 and mixed oxide fuel.

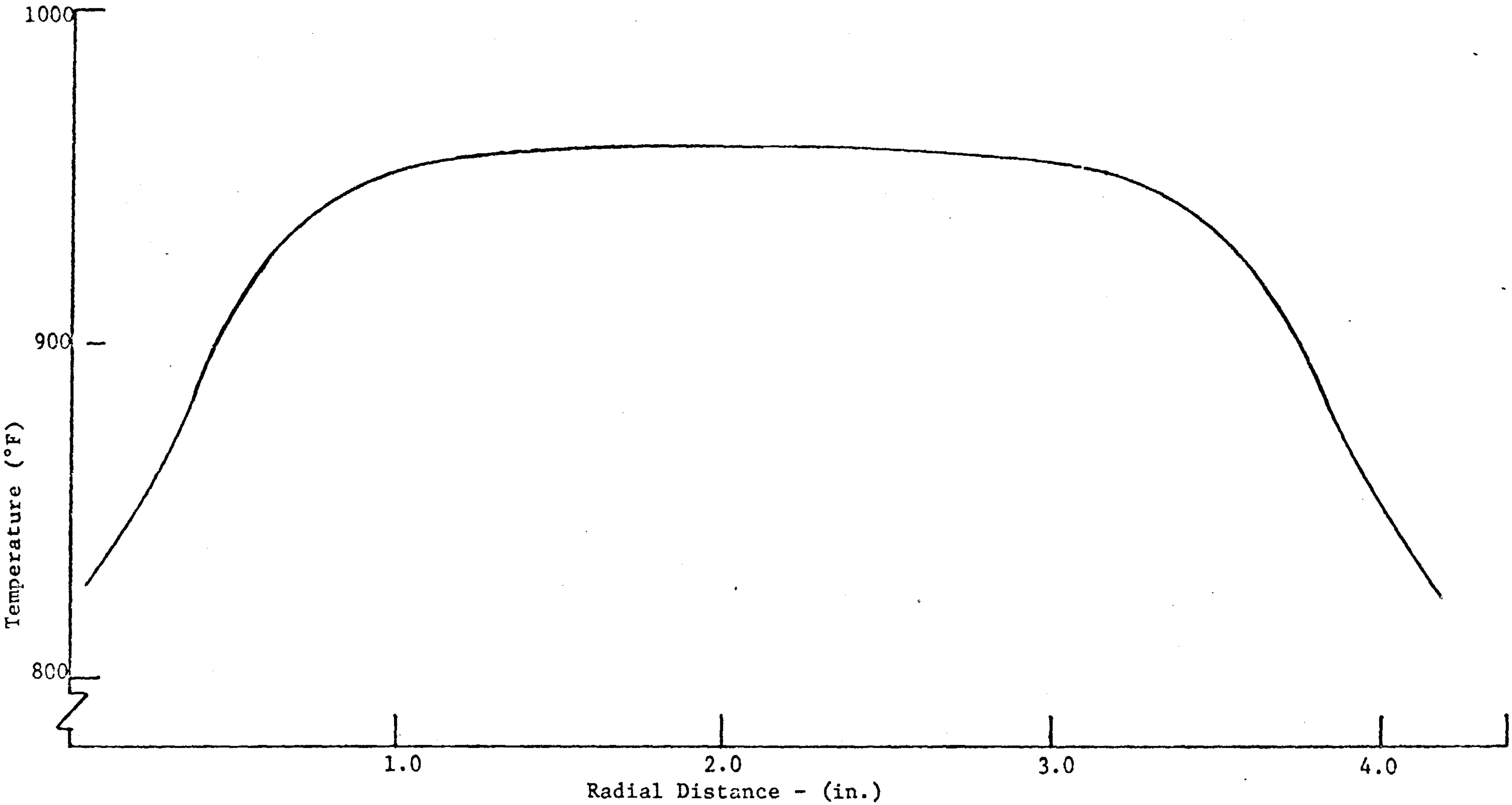

Curve from BNWL - 1064 Reference 20

FIG. 9.10 - Radial Temperature of Subassembly at Top of Active Core in FTR

control for the experiments. Test-section mass flowrates equivalent to FTR rated power conditions are 4.9 and 9.5 lb/sec for the 19- and 37-pin configurations, respectively.[22] However, the flowrates may be run below these values depending on the experiment.

Distribution of the flow within the test section is controlled to a lesser degree. A comparison of center, edge, corner, and average pin-coolant flow between the FTR central subassembly and FEFPL is shown in Table 9.7.[22]

As shown in Fig. 9.3, total flow is divided between the test section and the bypass. During experiment P1, a constant relationship will be used. An orifice in the bypass will be sized to give the desired test-section flowrate. In later experiments, a bypass valve controlled from test-section mass flow will maintain the proper flow split. As will be discussed in Chapter 10 (Experimental Transients), certain experiments will be conducted where variable test-section mass flowrates are programmed to simulate FTR safety conditions.

9.1.2.4 Absolute Pressure

The current FTR design has a head of sodium approximately 25 ft above the active fuel.[17] The constraint on total loop length within ETR permits only approximately 18 ft of sodium head.[23] Simulation of the absolute pressure is important whenever sodium boiling is anticipated and to properly model conditions for the occurrence of sodium expulsion and reentry phenomena. To compensate for this difference in head, adjustment in the cover gas pressure is made. The present design range is 10 to 50 psia,[23] with the actual value predetermined to fit the particular experiment conditions.

Minimum requirements for the volume of cover gas includes consideration of the potential effects on sodium expulsion behavior and multiple-shot fission gas release experiments. In a single experiment, expulsion and reentry characteristics of the FEFPL could be adversely affected if significant changes in cover gas pressure occurred due to changes in the sodium content of the reservoir. In an analysis in which voiding of the 19-pin fuel bundle was assumed, it was found that compression of the cover gas with an initial volume of 20 liters causes a pressure increase of less than 5%. In a fission gas release experiment study of the 19-pin configuration, it was found that following gas release from 5 pins there would be a cumulative increase of 2 psi in pressure (30 liters volume), or 11 to 12% of the initial value planned. These increases have been considered as tolerable.[24] Hence, the

TABLE 9.7

Flowrate Distribution Comparison of FEFPL Fuel Bundle with FTR Central Subassembly

Description	Coolant Flow Area (in.^{2})	Total Coolant Flowrate (lb/sec)	Pin Coolant Flow, lb/sec Center	Edge	Corner	Average	Maldistribution Factor[1]
1. FTR central subassembly	6.722	58.89	0.236	0.390	0.428	0.269	0.88
2. 19-pin test bundle	0.606	4.87	0.236	0.275	0.262	0.256	0.92
3. 37-pin test bundle	1.132	9.35	0.236	0.275	0.262	0.253	0.93

Notes:

1. Maldistribution factor = $\frac{\text{Center-pin coolant flowrate}}{\text{Average-pin coolant flowrate}}$

cover gas plenum volume has been specified to be a minimum of 1 cu ft ($\sim$ 30ℓ).[13]

9.2 Pre-experiment Standby Operations

Standby operation represents a normal operational mode for the FEFPL prior to reactor startup (also after shutdown, see 9.4), in which the FEFPL facility will be operated at essentially isothermal conditions.

The sodium temperature will be maintained at 450°F using power lost from the sodium pump (ALIP). For a reactor primary coolant flowrate of 2000 gpm at a temperature of 70°F, with helium gas in the annulus gap, approximately 15 kW total pump power is required to maintain this steady-state condition.[25] This power level is well within the 150 kW rated capability of the pump. This temperature (450°F) was selected to provide an adequate margin against freezing or plugging in the event of loss of pump heating power and to provide adequate time for loop transfer operations. For loss of normal power to the pump, 15 kW emergency (battery) power is available. Also, the helium system three-way valves can be positioned so that helium flow will bypass the primary and after cooler heat exchangers to provide helium at 400°F to the loop heat exchanger if additional heat is required.

Figure 9.1 shows the relative phasing of various supporting system operations during this mode: helium system, gas annulus, and sodium pump. Once the loop has been inserted into the ETR, the argon gas in the annulus between the loop primary and secondary vessels will be purged and replaced with helium gas. If it is desired to reduce heat losses to ETR during an unusually long standby period, there is the option of replacing the helium with argon.

9.3 Operational Transients

During normal operations, the following transients will occur at least once during a particular FEFPL experiment: transition between standby to reactor startup, reactor startup, reactor normal shutdown and transition to post-experiment standby. Other possible transients are an ETR scram for situations other than those discussed in Chapter 11, (Operational Accidents) followed by a fast recovery to power.

9.3.1 Standby to ETR Startup Transition

This transient represents (1) changing the sodium mass flowrate from the standby value to that required for the specific experiment, and (2) in creasing the reactor primary coolant water flowrate to the level required for powered operation (Fig. 9.1). The increased electrical power to the EM pump will raise the loop temperatures. The subsequent ETR primary coolant flow change will require a minimal adjustment to reach a stable loop flow and temperature, or hot standby conditions, prior to reactor startup. The magnitude of the flow ramps will be controlled so that induced thermal gradients are less than those experienced during a normal reactor startup.

For those experiments which incorporate a bypass control valve, the test-section flowrate will be adjusted to the required set point value. Sodium temperature control will be in operation to maintain inlet temperature to the test section at the set point required for the experiment.

This time period will be used for final FEFPL system instrumentation and control checkout before startup is initiated. Detailed checkout procedures for the FEFPL will be contained in the FEFPL test document which will be issued for each experiment.

9.3.2 ETR Startup

In general, the normal ETR startup and operating procedures will apply during the startup of the FEFPL. Normal ETR operation will be automatic in the power range, although manual control is provided. The loop and reactor protective systems will be operative during this operational phase.

Procedures similar to the existing ETR Standard Operating Procedures[26] required during startup will apply. Manual operation is used to take the reactor critical and up to a power level, N_L (nominally equal to 1% full power), but less than 3 N_L. From N_L, power is increased stepwise by operator action in automatic control. The rate of power increase is dependent on mode selection by the operator: fast (stable period $\sim$ 20 sec) and slow (stable period $\sim$ 108 sec).[27] At each power level increment, a power hold is maintained until instrumentation readings are checked. Extensive measurements will also be made on the FEFPL behavior during startup. The reactor will be limited to the ETR startup power levels until it is determined that the loop and associated equipment are functioning as expected.

The ETR power level during the startup will be limited to $\leq$ 175 MW by any of the following FEFPL conditions:

(1) Power required to provide the experiment operating conditions (Chapter 10, Experimental Transients).

(2) Heat removal capability of the loop heat exchanger.

(3) Special low power tests (e.g., natural circulation during P1).

Thermal conditions within the loop and thermal gradients across the loop vessel walls will be less severe than expected for a fast recovery from a scram (Section 9.3.5).

9.3.3 ETR Normal Shutdown

A normal shutdown represents a controlled reactor power reduction. From full (or operating) power to generally N_L ($\sim$1%), the reduction is by automatic operation using either fast or slow speed modes. The stable periods for these two shutdown modes are the same as for the two automatic startup modes (Section 9.3.2). At N_L the control rods are scrammed to their respective limits. In some instances, this step is initiated at a higher value to check certain protection system parameters.[28]

Loop control set points will be maintained during shutdown; however, the loop temperatures will stabilize at a lower level which is determined by pump power, decay heat, and heat losses to the reactor primary coolant. Thermal gradients will be less severe than obtained during an ETR scram, discussed below.

9.3.4 ETR Scram

During normal operation, conditions other than those discussed in Chapter 11 (Operational Accidents) may arise which would initiate a reactor scram (e.g., high differential coolant temperature). This transient represents the most severe thermal condition during normal operating conditions due to the sudden changes in the power level. As shown in Fig. 9.11, the neutron flux reduces to $\sim$10% (normalized) within 150 msec. Normalized decay heat attenuation with time is shown in Fig. 9.12. These data have been used in thermal analyses which are being conducted in support of Section III stress analysis of loop components.

Figures 9.13, 9.14, and 9.15 are presented to show general loop responses for an ETR scram from full power, using the SINDA-19A thermal analysis model.[7,29] Loop temperature control is effected by helium mass flow control (see Fig. 9.13) as determined by a system analog.[30] For the most part, loop

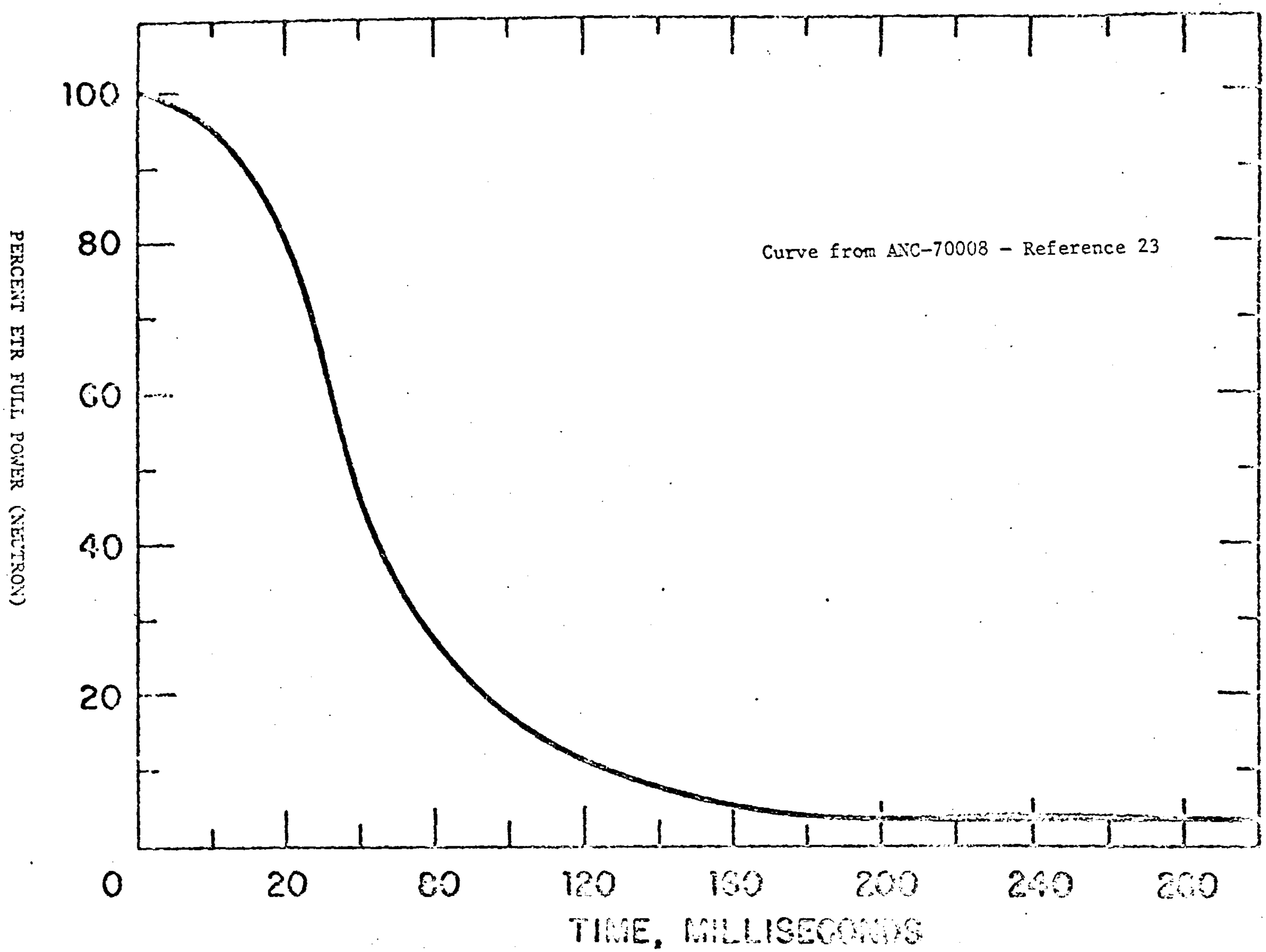

FIG. 9.11 - Approximate ETR Power (Neutron) vs Time for ETR Scram

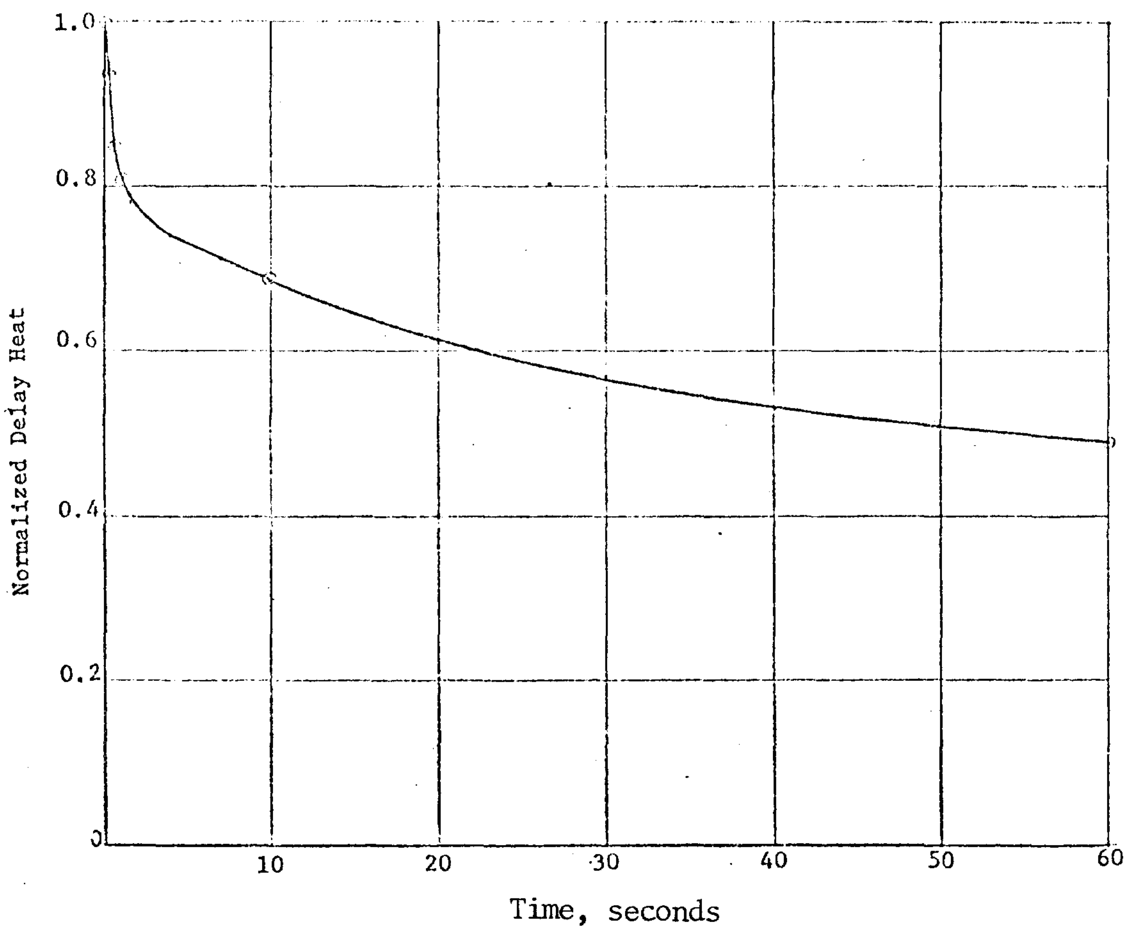

Data points shown from SINDA Loop Model-Reference 7. Decay heat is based upon shutdown after 34 days of full power operation. Thermal model interpolates between circled data points.

FIG. 9.12 - Normalized Decay Heat vs Time Following an ETR Scram

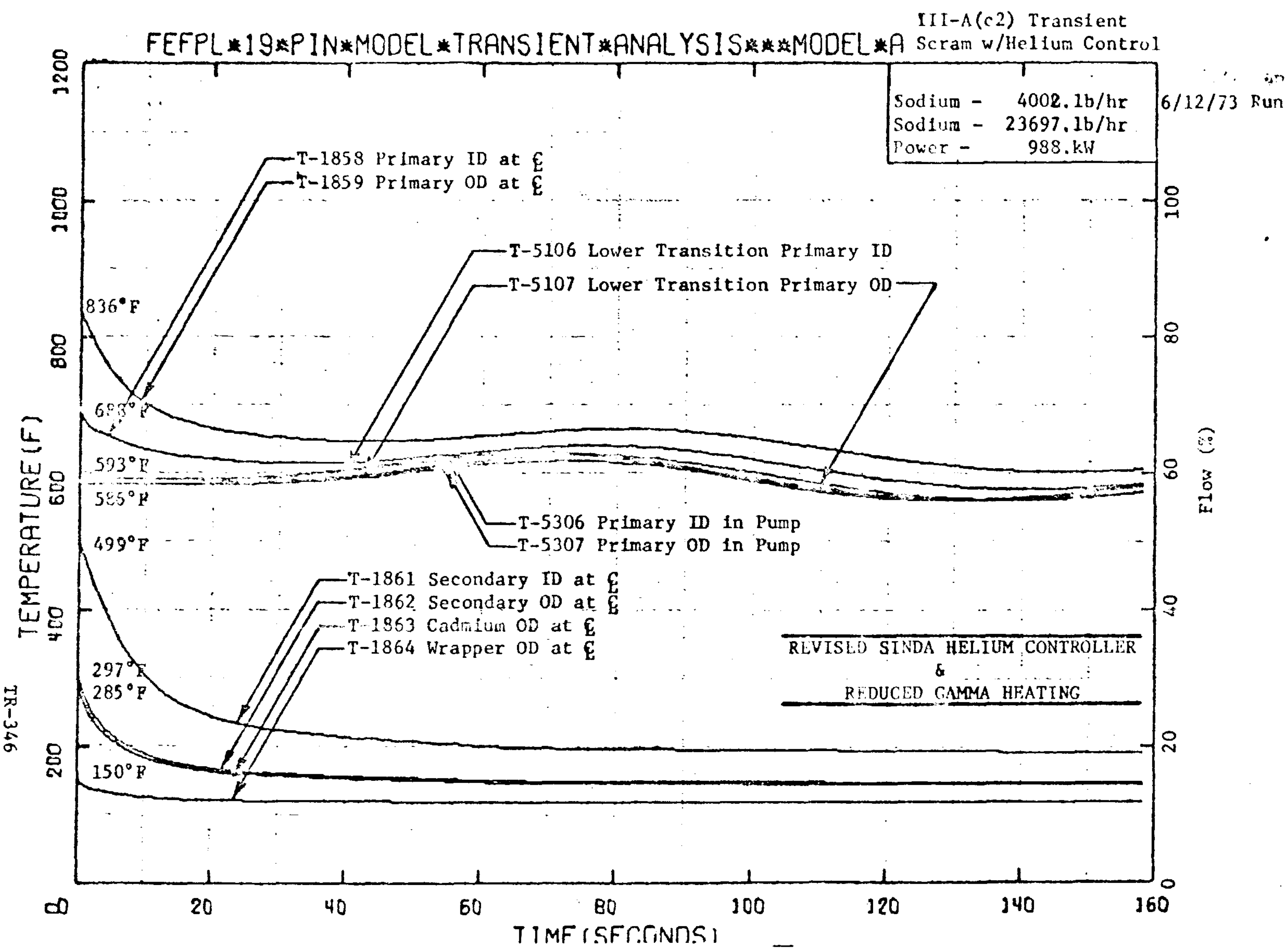

FIG. 9.13 - Loop Thermal Responses During an ETR Scram

FIG. 9.14 - Loop Thermal Responses During an ETR Scram

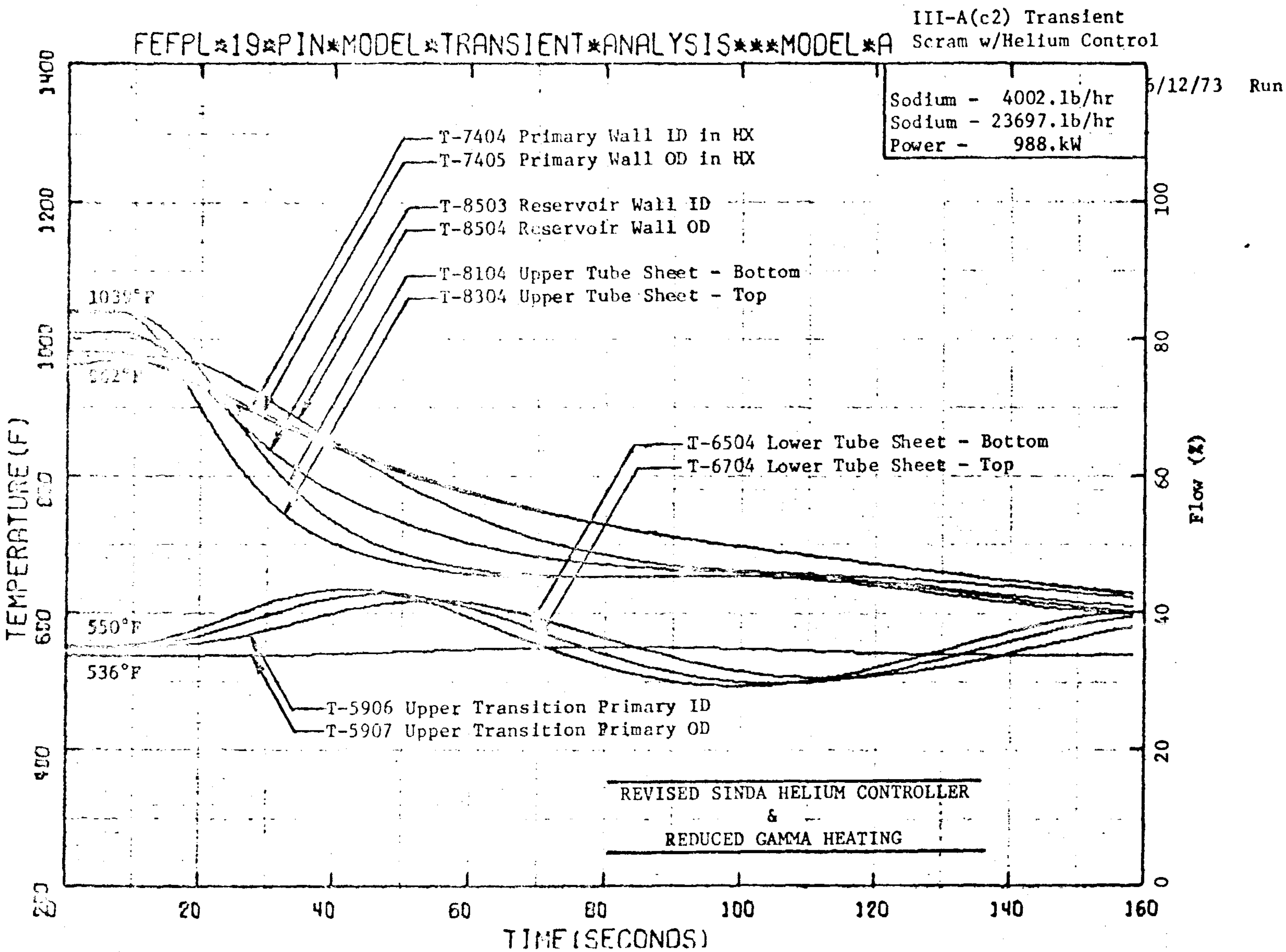

TR-346

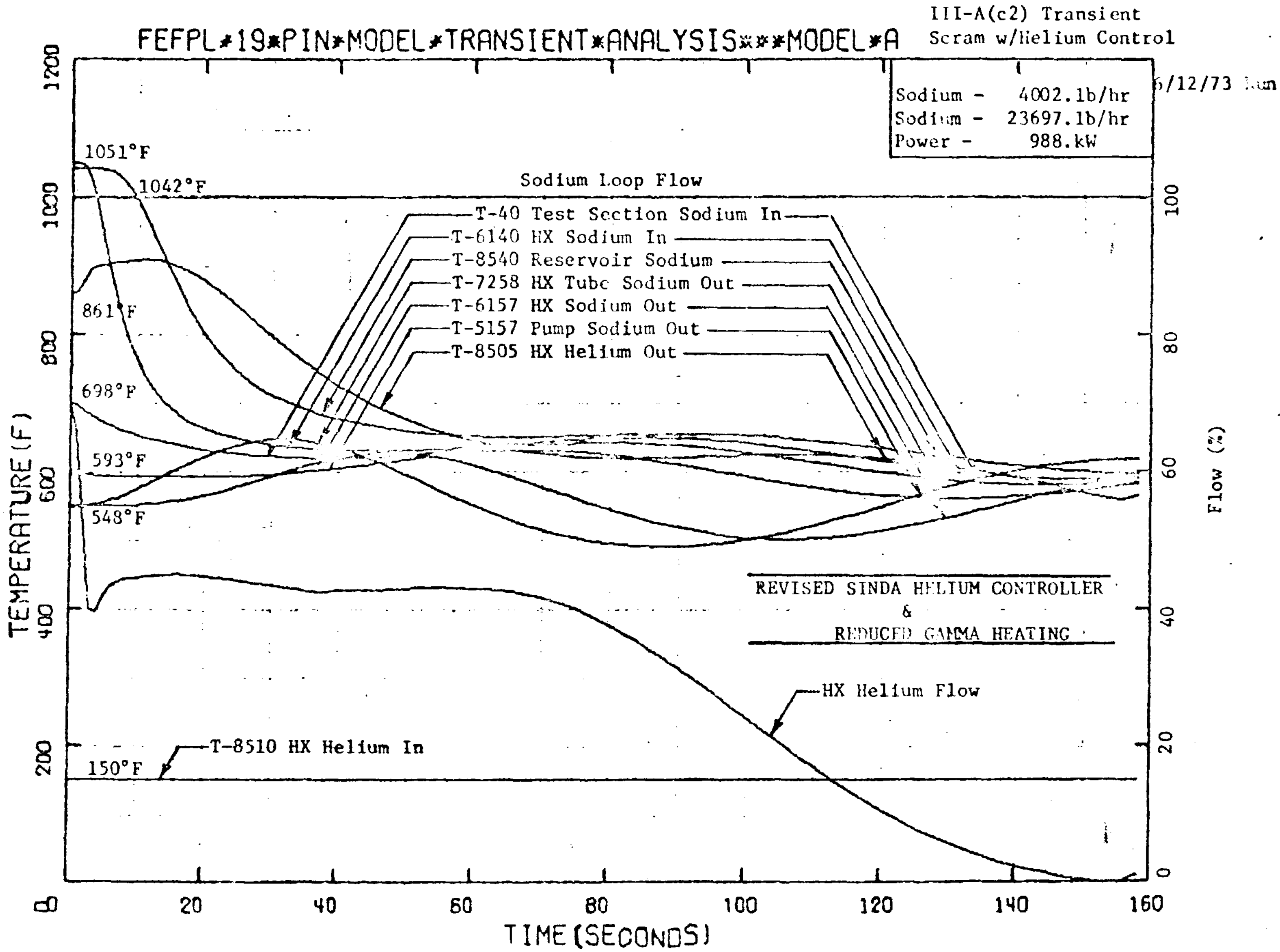

FIG. 9.15 - Loop Thermal Responses During an ETR Scram

TR-346

temperatures tend to decay; the increasing temperatures shown in Figs. 9.14 and 9.15 are not severe and are well within the acceptable envelope. Thermal gradients have been evaluated and found acceptable.[31]

9.3.5 ETR Recovery to Power

In the event of an ETR scram that can be quickly resolved, it is desirable to return to power quickly to preclude a xenon shutdown. The existing ETR Standard Operating Procedures[32] permit a 7 sec stable period if time is of the essence.[28] Although more severe than a normal startup, the resulting thermal conditions for this transient are considered less severe than for the ETR scram condition (Section 9.3.4). Control system analysis has shown that all controlled variables remain stable under such a 7 sec stable period recovery.[33]

9.3.6 ETR Shutdown to Standby Transition

From a shutdown following completion of an experiment, this transient represents the reverse of the transition to startup (Section 9.3.1). It may also be necessary if considerable time is required for investigative purposes following a scram; if so, Sections 9.3.1 and 9.3.2 then apply for the return power.

As shown in Fig. 9.1, the reactor coolant flowrate is reduced and loop conditions are reasonably stabilized. Then the sodium pump flowrate is ramped down to a power level required to maintain the 450°F isothermal condition. This rate will be selected to ensure that thermal gradients are less severe than those obtained during a normal reactor shutdown. Prior to the pump ramp, a decrease in loop temperatures for a constant flowrate is expected due to decay of the gamma heat source.

9.4 Post-experiment Standby Operation

Following the experiment and the subsequent operational modes discussed in Sections 9.3.3 (or 9.3.4) and 9.3.6, the loop will be returned to the 450°F isothermal standby condition using procedures (but in reverse order) discussed in Section 9.3.1. However, a higher sodium flowrate than previously mentioned may be necessary for a period to remove residual decay heat. During this phase, temperatures of the primary and secondary vessel walls will be well below the at-power operating point; hence, stress levels are acceptable. Eventually, the 450°F isothermal condition will be stabilized and procedures for loop removal from the reactor can be initiated (Fig. 9.1).

9.4.1 Long-term Heat Removal

Following an experiment in which a significant fuel meltdown occurs, increased duration of heat removal is to be anticipated. Experiments involving gross fuel melting are discussed in detail in Chapter 10. Depending on the severity of the meltdown, a redistribution of heat sources may occur that would lead to local loop temperatures that are higher than normal levels. This is the result of fuel being retained either in the meltdown cup at the bottom of the loop or at the filter located at the heat exchanger inlet (see Section 9.4.2 for further discussion on fuel transport and deposition).

A 50% meltdown of the test fuel bundle (37-pin full-length configuration) has been specified as a faulted condition for the loop design. Although it has been conceived that an event of such a magnitude could occur from a planned experiment, a lesser magnitude is expected and considered as a normal post-experiment recovery. Hence, the effect is expected to be less severe than for the faulted case considered in detail in Chapter 11.

9.4.2 Fuel Transport and Deposition

As discussed briefly in Section 9.4.1, experiments are planned that will purposely fail fuel pins in the test fuel bundle. Discussion within this chapter on fuel transport and deposition pertains to the post-experiment conditions in which the magnitude of fuel meltdown is less than the faulted case (Chapter 11).

Provision has been made in the loop design to collect fuel and/or debris that might be transported by the coolant. There are two major collection points in the loop where fuel deposition may occur:

(1) The molten fuel cup located below the test section in the lower loop region.

(2) The filter located in the inlet to the heat exchanger in the upper plenum region.

Significant amounts of fuel deposition in other areas of the loop, especially in-core, are highly unlikely, due to loop design. Flow regions, other than for the two considered, do not have large changes in sodium velocity.

Both collecting points are located in areas outside the ETR active core region; hence, the resultant heat generation from the fuel collected in these regions will be due to fission product decay heat. Collection in the molten fuel cup is the more severe of the two locations from a fuel quantity consideration.

The molten fuel cup located in the lower region of the loop has been sized and designed to contain ∿ 3400 gm of molten fuel (19 full-length FFTF fuel rods) safely. The decay heat from the fuel will be dissipated directly to the loop sodium and indirectly to the ETR cooling water. The behavior of the meltdown cup is discussed in detail in Section 10.4.2.

The filter provided at the entrance to the heat exchanger is designed to catch fuel and debris particles with diameters larger than 1/16 in. This greatly reduces the possibility of flow blockages in other portions of the loop. The safety aspects associated with the collection of large quantities of fuel in the filter were assessed.

Results from a simple Stokes-law analysis indicate that sodium flowing at test-section conditions is capable of sweeping fairly large fuel particles into the region of the fuel filter. For sodium velocities ranging from 5 to 10 ft/sec in the test train, spherical fuel particles with a maximum diameter of 1/4 to 1 in. could be entrained. With the present vertical filter design, a maximum annular bed thickness of less than 0.5 in. conceivably could be formed from all the fuel in a 37-pin bundle. Calculations based upon the work of Hesson[34] indicate that the decay heat from a bed with a depth of 2.37 ft could be adequately cooled by the flowing sodium. Therefore, no adverse thermal situations in the area of the fuel filter are expected (see discussion in Chapter 10).

Several means are available to detect fuel deposition in the filter region. The delayed-neutron monitor (to be installed after P1) mounted external to the loop will be focused on this filter region. In addition, any impedance will be detected by monitoring the thermal-hydraulic conditions with the loop instrumentation.

References:

1. American Society for Mechanical Engineers, "Boiler and Pressure Vessel Code, Section III - Rules for Construction of Nuclear Power Plant Components," (July 1, 1971).

2. D. Lennox, et.al., "In-pile Experiments for the Fuel Element Failure Propagation Loop," Argonne National Laboratory Report, ANL/RAS 71-33 (October 1971).

3. K. H. Liebelt, "Steady-State Pressure Drop and Sodium Temperature Data for 19-A and 37-A Pin SINDA Loop Models," Aerojet Nuclear Company FEFPL Report EDF-597, (December 8, 1972).

4. J. F. Kunze, et.al., "Recommended Nuclear Specifications for FEFPL," Aerojet Nuclear Company Internal Report, CI-1246, (October 1972).

5. A. L. Bowman, "Power Gradients Across the FEFPL Loop," Aerojet Nuclear Company Memorandum, Bowm-29-72, (December 7, 1972).

6. T. A. Ciarlariello, et.al., "Annular Linear Induction Pump Interim Design Report," MSA Research Corporation Report, MSAR-72-111, (May 1972).

7. K. H. Liebelt, "Revised Thermal-hydraulic Loop Model for the Fuel Element Failure Propagation Loop," Aerojet Nuclear Company Engineering Report, TR-337, (November 16, 1972).

8. American Society of Mechanical Engineers, "Interpretation of the ASME Boiler and Pressure Vessel Code (1971)," Case 1331-5, "Nuclear Vessels at High Temperature Service", (August 4, 1971 - replaced by Case 1331-7, August 14, 1972).

9. P. L. Zaleski, "Flow Divider - Thermal Tests," Argonne National Laboratory Intra-laboratory Memorandum, (November 8, 1972).

10. J. D. Reed, "FEFPL Helium System Pressure Drop Data," Aerojet Nuclear Company Memorandum, JDR-11-71, (December 1, 1971).

11. R. E. Craig and E. M. Mouradian, "Final Report: Analysis of Thermal Performance of FEFPL Heat Exchanger," Atomics International Report TI-542-320-008, (September 11, 1972).

12. General Electric Company, "Instruction Manul, Gas Bearing Circulators with Adjustment Frequency Power Supply for ATR Gas Loop," (March 1970).

13. Argonne National Laboratory, "System Design Description of the Fuel Element Failure Propagation In-pile Loop System," R-1000-1001-SA, (May 1, 1972).

14. Aeroject Nuclear Company, "Design Specification and Ordering Data for the Fuel Element Failure Propagation Loop Heat Exchanger," ANC-70009, (June 20, 1972 - as revised August 17, 1972).

15. Superseded by References 33 and 37.

16. B. L. Harris, "Flow Induced Vibration of FEFPL," Aerojet Nuclear Company FEFPL Report EDF-515, (October 27, 1972).

17. Westinghouse Electric Corporation - Advanced Reactors Division, "Fast Flux Test Facility System Design Description for Reactor System," SDD 31.

18. A. L. Bowman, et al., "ETRC-FEFPL Mockup Experiment and Calculations," Aerojet Nuclear Company Internal Report CI-1247, (November 1972).

19. R. C. Ivins, et al., "Thermal-hydraulic Simulation in the FEFPL," Argonne National Laboratory Report ANL/RAS 71-17, (April 1971).

20. E. G. Stevens, et al., "FFTF Fuel Pin and Subassembly Conceptual Design Methods and Data," Battelle Northwest Laboratory Report BNWL-1064, (June 1970).

21. J. H. Tessier, "FEFPL Test Section Heat Loss to Bypass Coolant," ANL Intra-Laboratory Memo, (August 2, 1973).

22. D. H. Thompson, "Coolant Distribution in FEFP In-reactor Test Subassemblies," ANL Intra-Laboratory Memo, (August 9, 1973).

23. Aerojet Nuclear Company, "Design Specification for the Fuel Element Failure Propagation In-pile Loop," ANC-70008, (June 2, 1972).

24. J. H. Tessier, "Experimental Design Requirements for FEFPL: Sodium Head and Cover Gas Volume," Argonne National Laboratory Intra-laboratory Memorandum, (June 29, 1971).

25. G. Nielsen," Isothermal Analysis of FEFP Loop with Stagnant Helium in Purge Annulus," ANC FEFPL Report EDF-661, (January 21, 1973).

26. Aerojet Nuclear Company, "ETR Startup and Power Approach Checklist," ETR-DOP 6.2.1, (October 27, 1972).

27. Idaho Nuclear Corporation, "Engineering Test Reactor Operating Manual, Volume VIII, Reactor Console and Tank Operation," CI-1065, (December 1967).

28. R. Rider, "ETR Normal Operations," Aerojet Nuclear Company FEFPL Report EDF-610, (December 21, 1972).

29. K. H. Liebelt, "Thermal-hydraulic Analysis of the FEFPL Upset Conditions," Aerojet Nuclear Company Engineering Report TR-346, (January 10,1973) (Addendum 2 June 15, 1973).

30. R. W. Keller, "19-A and 37-A Model Sodium Temperature Controls," Aerojet Nuclear Company FEFPL Report EDF-582, (November 29, 1972).

31. (ANC Section III Stress Analysis Report - to be published).

32. Aerojet Nuclear Company, "Full Scram Recovery Checklist," ETR-DOP 6.2.3, (January 25, 1972).

33. S. R. Gossmann, "Flow Induced Vibration of FEFPL," Aerojet Nuclear Performance Verification Study," ANC Report FR-186, (July 1973).

34. J. C. Hesson, et al., "Post Accident Heat Removal in LMFBR's," ANL-7859, (September 1971).

35. B. L. Harris, "Asymmetric Bowing of FEFP Loop for 10% and 15% Flux Tilt Cases," ANL FEFPL Project Report EDF-648, (February 23, 1973).

36. D. H. Thompson, et al., "Test Requirements for Fuel Element Failure Propagation In-reactor Experiment P2," ANL/RAS 72-22 (Rev. 1), (June 1973).

37. R. W. Thomas, "FEFPL Pump Vibration Due to Electrical Characteristics", ANC FEFPL Project EDF 12-03, (December 20, 1973).

38. H. M. Minami, et al, "FEFPL Heat Exchanger Stress Report", Atomics International Report TI-542-320-009, (November 13, 1972).

39. B. V. Winkel, "Vibration Stresses in FEFPL Heat Exchanger Tubes", ANC Memorandum BVW-8-73, (November 13, 1973).

CHAPTER 10.0

TABLE OF CONTENTS

LIST OF TABLES

LIST OF FIGURES

10.0 Experimental Transients

The safety-related consequences of the transients that stem from planned experiments are discussed in this chapter. The reference experiment represents the maximum challenge to the loop integrity among all tests now visualized which will contain up to 37 full-length pins.

The effects of rapid fuel melting and the interaction that may follow with coolant and structure are assessed for the reference experiment as a function of the postulated degree of conservatism in the analyses. It is shown that the loop can contain, with a sizeable margin of safety, this upper-limit experiment which, in turn, establishes an envelope for the current FEFP experimental program.

10.1 Classification of Transients

In the FEFP experimental program the types of transient tests that are planned generally involve undercooling fuel pins while they are operating at power. The general nature and objectives of the first ten near-term tests scheduled for FFTF studies are identified in Section 1.3; specific details will be included in subsequent test plans as they are developed for each experiment. Sufficient studies have been made now, however, to assess the safety of these experiments within the FEFP loop limits.

Four general types of transient experiments are planned to evaluate the following FTR phenomena:

- gas release
- flow decay
- flow blockage
- molten-fuel release

The characteristic behavior of the FEFPL during these transients is examined for conditions typical of planned experiments. Loop transients during operational accidents are presented in Chapter 11.

10.1.1 Gas Release

The gas-release tests are designed primarily to determine thresholds for fuel-element failure, mode of fuel-element failure, and the possibility of propagation of fuel-element failure caused by the release of fission gas in an FTR-type geometry.

Typical results to be expected for FEFPL gas-release test with a 37-element test subassembly have been developed and compared to those expected for FTR. The smaller FEFP test subassembly exhibits a similar voiding behavior with a slightly faster response. The amount of sodium contained in the test section (the smaller flow area requires less change in coolant flow rate to produce the same displacement as in a large subassembly) accounts for this difference. Data obtained from out-of-pile experiments are being used to verify these analyses.

Although the final gas-release test plan is not complete, the procedure would be basically as follows:

(1) establish nominal steady-state loop operating conditions,

(2) inject gas into the test section by triggering a special gas-release device,

(3) continue to run loop at full power to determine whether fuel failure has occurred or will propagate (unless the ETR is shutdown deliberately by the experimenter or by the automatic FEFPL Plant Protection System (PPS) upon detection of abnormal conditions),

(4) repeat the above procedure for the next scheduled gas-burst test if fuel-rod failure has not occurred.

The inert gas will be released at various mass flow rates and velocities. Injection of the gas into the coolant will be designed either to (1) provide gas-jet impingement on a neighboring fuel element, or (2) form a two-phase flow mixture, thereby causing a local flow reduction. These could lead to a substantial reduction in nominal heat transfer with resultant rise of cladding temperature. In either case, significant flow reduction is expected to occur in only a few flow channels, and the resulting thermal transient experienced by the total system will be small. Coolant that flows through the outer fuel-element channels and the bypass coolant around the fuel bundle will combine with the two-phase mixture, and the entrained gas will be trapped in the loop reservoir (plenum).

Should the consequences of the experiment exceed those anticipated, the loop will be protected by terminating the experiment before significant amounts of fuel become molten. The failure of cladding on one or more of the prepressurized test elements would result in gas and possibly fuel release into the coolant channels. If gross cladding failure occurs the resulting flow perturbation will be detected by instrumentation and the experiment will be continued to determine the potential for this failure to propagate. During this period the FEFP PPS provides safety assurance for the loop and the reactor against any adverse thermal or mechanical effects that might have the potential to reduce the loop containment margin.

10.1.2 Flow Decay

FEFPL simulation of a postulated, unprotected loss-of flow accident for the FFTF is an important experimental objective. Duplication of anticipated reactor conditions in the FEFP loop, especially before boiling occurs, requires a control strategy that provides the proper transient-thermal-hydraulic behavior in the test section.

Analysis indicates that it will not be possible to perform the test by simply reducing total loop flow to match the reactor coastdown. This is because the significant gamma heating of the sodium between heat exchanger outlet and test-section inlet causes the temperature at the inlet to the active test zone to vary inversely with flow, which is atypical of FFTF.

As a result, a control strategy will be used to hold total loop flow (and therefore inlet temperature) constant, while flow through the test section duplicates that for reactor loss of flow. This involves simultaneous control of total loop flow and flow through the test-section.

Figure 10.1 depicts the required time-dependent behavior of the relevant loop variables needed to simulate flow coastdown in the test section for a constant total loop flowrate of 100 gpm. The indicated control continues into the anticipated range for boiling inception; when boiling is detected, a different control mode is initiated to continue the simulation in this regime. The major design considerations that arise for conducting this experiment are:

(1) control of pump power within speed and accuracy limits
(2) provision for low pressure-drop bypass-flow path
(3) incorporation of a bypass-flow control valve with speed and accuracy sufficient to yield the desired test-section flow.

Although all of the above are currently under development, their present status indicates they can be achieved successfully so that the experiments can be conducted as planned.

The safety of loss-of-flow tests will be well within the loop design limits as defined in Chapter 6. The loop will be operated at a steady-state until the transient starts with a programmed change both in the operation of

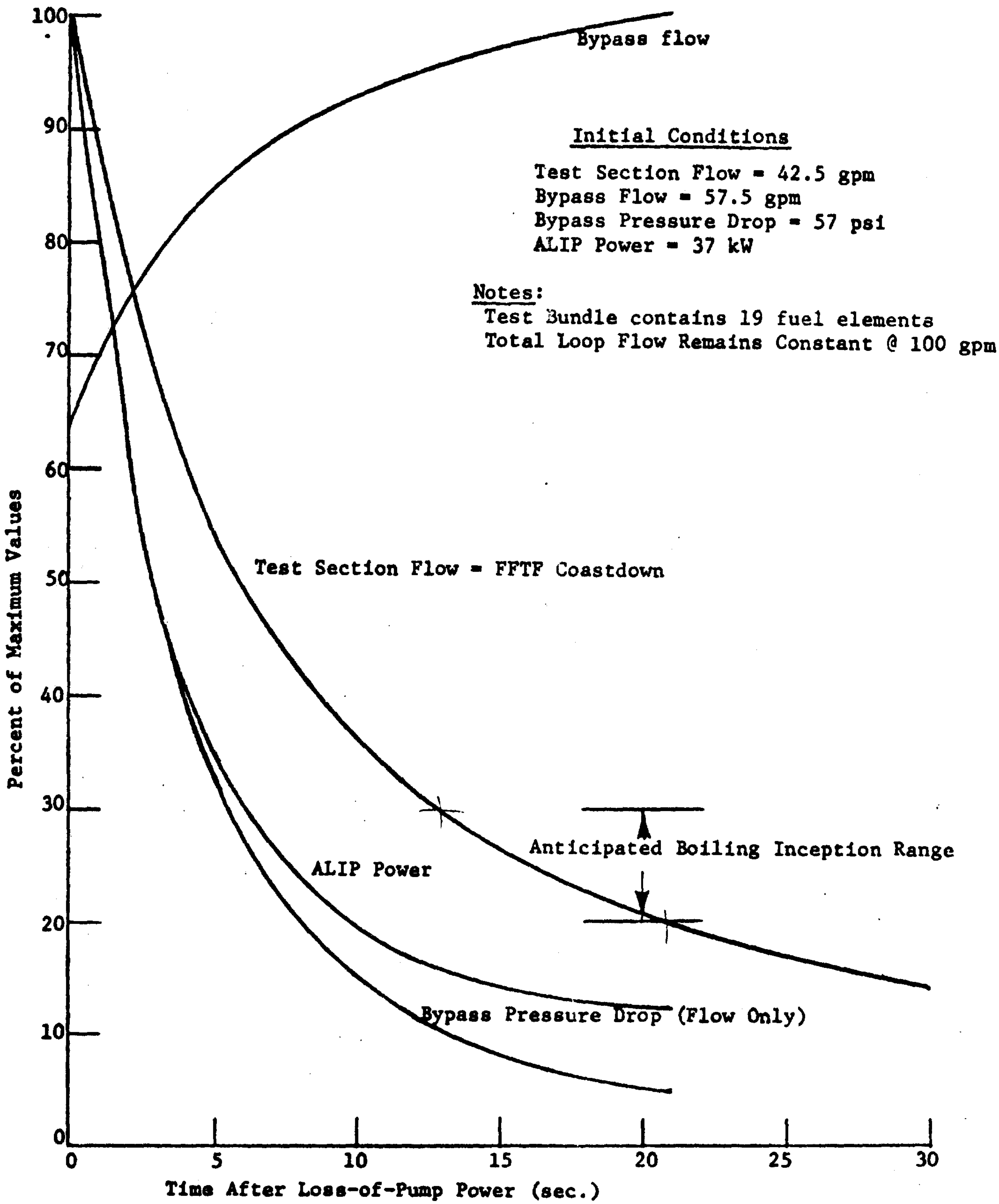

FIG. 10.1 Loop Conditions for Simulation of FFTF Loss of Flow

the ALIP and bypass-flow resistance. The program will be designed to give a time-dependent decay of coolant flow through the test bundle that matches the coastdown flow upon loss of power to the FTR pumps.

It may be desirable to terminate some flow decay experiments long before possible safety limits are reached in order to either limit the amount of molten fuel produced or to "freeze" the test at a given point to preserve specific information for the post-mortem examination. For this action, reactor shutdown would be effected by the FEFPL-Control System at a preset time after loss-of-flow starts or after the test section coolant reaches a fixed temperature, and the PPS will not be challenged.

10.1.3 Flow Blockage

Two types of flow blockage experiments are planned. The first involves a blockage within the fuel region that may perturb a limited number of flow channels. The second is a gross flow reduction to the entire test section effected by an impedance, such as a valve, at the inlet. In the former, local boiling followed by fuel pin failure may occur. The latter, however, will produce widespread fuel melting in order to study experimentally: a) the coolant expulsion and reentry, b) the work-energy release from a molten fuel-coolant interaction, and c) the movement and disposition of fuel and clad.

For the fixed internal partial blockage tests, the loop would be operated at full flow but with progressively greater ETR power until the desired FFTF linear power is reached in the fuel. Experiments that utilize an inlet blockage will be at maximum operating power and flow when the flow reduction device is actuated.

The FEFPL inlet flow-blockage experiment has the potential to generate the most molten fuel, therefore, it is the reference experiment that establishes the loop limits (see Section 10.2.2). This type experiment, with 37 pins, will follow several mild experiments which will provide prior experience to substantiate safe operating conditions and procedures. The detailed analysis, which will identify the margin of safety (i.e., conservatism in the analysis), will be provided in the Test Plan for each experiment.

10.1.4 Molten Fuel Release

One purpose of the first experiment is to study the effects of the release of a small amount of molten fuel. It is designed to observe the associated effects occurring over several minutes in a cluster of fuel elements, particularly to determine whether propagation of a fuel element failure occurs. Based upon calculations, results of out-of-pile tests, and results of TREAT and MARK-II fuel failure tests, it is expected that this experiment will demonstrate that failure will not propagate through the subassembly.

This type of experiment will provide data needed to analyze the consequences of the release of a small amount of molten fuel and insight into short-term effects of operation with failed fuel. The objective of this first experiment is to attain sufficient test temperature to breach the fuel cladding and release fuel, while localizing failure. This will be achieved by means of a protective partial flow reduction or reactor flux skew.

The experiment will be conducted in a stepwise fashion, commencing with the ETR startup. During the initial increases in ETR power, the FEFPL instrumentation will be monitored closely for detection of any evidence of boiling or premature fuel failure. Upon reaching the specified ETR power level required for the experiment with no evidence of fuel failure, the loop conditions will be stabilized at rated flow.

This type of experiment may result in a small molten-fuel coolant interaction. However, the resultant potential pressure generation is well below the conservatively calculated pressure pulse as specified for the reference experiment. The small amount of molten fuel available for damage can be safely contained within the FEFPL system.

10.2 Molten Fuel Coolant Interactions (MFCI)

As presented in the previous sections, the proposed experiments in FEFPL all involve various heat generation-to-heat removal mismatches in a fuel bundle. Based upon previous theories, the subsequent creation of molten fuel has the potential for thermally interacting with the sodium coolant with the resulting sodium vaporization being capable of performing a considerable amount of work and producing extensive structural damage.

In this section, the molten fuel-coolant interaction phenomena is discussed as it relates to the FEFP experimental program. A heat transfer assessment of the MFCI situation in FEFPL is presented based upon recent experimental and analytical information. From this evaluation, it is concluded that an energetic MFCI is very unlikely in the FEFP Loop. Also discussed, is the very conservative analysis approach employed in the design of FEFPL based upon results from a bounding reference experiment an an earlier conservative MFCI calculational model. Summarized are the predictions for two hypothetical source terms: An Upper Limit MFCI Source Term and Design Envelope Source Term (see Appendix D for definitions). Long term thermal effects resulting from an MFCI are also discussed. Supporting MFCI information is presented in Appendix C.

10.2.1 Best Assessment of MFCI in FEFPL

The first MFCI calculations made to establish the loop design indicated - based on very conservative assumptions - that the complete flow blockage event, gave the maximum molten fuel and also gave the maximum pressure pulse.

Recent, more realistic analysis, show however that this reference event grossly over-estimates the pressure that the loop containment system might actually experience from either a flow blockage or any other situation of which molten fuel is generated, such as an over-enrichment error. Hence, to provide additional safety margin, the original flow blockage model is retained as the basis for establishing the design envelope pressure pulse.

Accident simulation tests to be carried out in the Fuel Element Failure Propagation Loop will cover situations where molten fuel will be generated with both sodium-out (loss-of-flow-simulation) and sodium-in (local over-enrichment error). While the sodium-out case involves considerably more molten fuel than the sodium-in case, current understanding and experimental facts (for detailed discussion see Appendix C.1) indicate that this does not imply that the case with more molten fuel is necessarily the worst case. In terms of pressure generation, the local over-enrichment error simulation may result in larger pressure generation (yet much smaller than the design envelope pressure pulse) than a complete flow blockage case, since in the latter case, liquid sodium, may not be present to interact coherently with the fuel. The point here is that the conditions and amounts of fuel are not the only important factors. The conditions and whereabouts of liquid sodium at the time molten fuel is being generated are equally important. Therefore, in order to illustrate margin of safety of the planned FEFPL experiments, cases involving both sodium-out and sodium-in will be discussed below:

a. Loss-of-flow Experiment

Since the axial-coolant temperature profile and the test section hydraulic resistance closely simulate FFTF conditions, the voiding characteristics (e.g., see Fig. 10.4 in Section 10.3.2) represent a reasonable estimate of the time scale for voiding of the heated fuel zone. Voiding will proceed more rapidly depending upon the fission-gas plenum pressure which may breach the clad and increase the rate of sodium voiding[1]. In any case, the heated test fuel zone will be completely voided of sodium directly with no reentry with a time scale of approximately 1 second.

Local clad dryout may occur immediately (within 20 msec) after flow reversal[2]. However, massive clad melting will occur only after the liquid film associated with sodium voiding is evaporated or blown out of the heated zone. Clad relocation is uncertain. Initial motion in the direction of vapor flow is expected. However, gross relocation and plug formation are not well established. It may require approximately an additional 1/2 to 1 second for fuel cladding to melt away and an additional 2 to 4 seconds to produce large amounts of molten fuel.* The important consideration is that molten fuel is produced at a time when sodium is out of the fuel zone and not likely to reenter because of a combination of clad plugging and sodium vaporization from hot steel at the axial extremes of the test section. The most likely sequence of events is that molten fuel will not contact liquid sodium within the test fuel zone and the large fraction of fuel will fall downward out of the fuel zone. Fuel falling out of the fuel zone will be partially quenched by intermittent contact (nucleate boiling) with sodium and the steel. Under steady power, fuel cannot remain in the flux zone long enough to melt through the container wall. Any fuel that is held up in the flux zone for more than 1 second at full power after reaching its melting temperature and has a characteristic thickness of more than 1/4 in. will be dispersed by vaporization of the fuel itself. Depending upon prior clad motion, which is quite uncertain, molten fuel will either fall out of the test fuel zone due to gravity, or redistribute itself because of the above mentioned upper limit on critical dimensions of uncooled fuel at full power. The relative distribution is difficult to assess and passive protection is provided against meltthrough as described in Section 10.5 of this report.

Fuel-sodium interactions within the loss-of-flow sequence are presently anticipated to be extremely mild insofar as a potential means for doing mechanical damage. Since no large external forces are available, saturated liquid sodium is unable to reenter the fuel zone coherently. Local contact will occur, however, between liquid and molten fuel based upon the best assessment of the minimum temperature for film boiling. This will lead to nucleate boiling which will provide sufficient vaporization and therefore

* This time scale may be considerably lengthened if molten clad is not dispersed out of the fuel zone. See Appendix C for clad-sodium interaction discussion.

prevent coherent mixing between the fuel and the liquid sodium. The resulting slow quenching of the molten fuel by nucleate boiling produces heat transfer rates sufficiently slow so that heat losses and condensation effects will prevent any significant pressurization. This picture is consistent with current TREAT L-series experiments. No fuel-coolant interaction could be identified in these experiments. It is particularly important to note that large quantities of sodium were found in the fuel region during postmortem examination of the L-2 sample. One can only conclude that liquid sodium was available to interact with the fuel, however, no explosive fuel-coolant interaction occurred. Explosive boiling is further prevented by the presence of nucleation sites. For most practical sodium systems, cavities in solid surfaces, entrained gas, or especially in in-reactor environment, the radiation field will limit the superheat in liquid sodium to levels well below those required for spontaneous nucleation. The presence of gas, solid surfaces, and the radiation field in FEFPL experiments will provide abundant nucleation sites and prevent vapor explosions between UO_2 and sodium in the proposed loss-of-flow experiments. Therefore, the margins to reach the stability limit of liquid sodium in the FEFPL experiments would appear to be very large, since fuel temperatures of 5000°C and above would be required to cause contact temperatures to exceed the stability limit.* Furthermore, at these fuel temperatures, the fuel would be in a two-phase state and the UO_2 vapor pressure would prevent direct liquid-liquid contact as indicated by the TREAT S-series experiments. In this case, the liquid sodium would act as an energy dissipating fluid. It should also be noted here that fuel temperatures much above the nominal boiling point (3400°C) would be very unlikely in the FEFPL experiments since overpower transient simulations are not involved. Finally, it is recognized that an order of magnitude more molten fuel will be available in the FEFPL experiments than previously tested. However, the important characteristics associated with the loss-of-flow sequence and possible fuel-coolant interactions (saturated sodium-out conditions, availability of nucleation sites and contact temperatures much less than the stability limit of the more volatile liquid) are the same in both the TREAT L-series and the forthcoming FEFPL experiments, and therefore no difference in results is expected. This conclusion is further substantiated by recent experiments involving several kilograms of molten fuel dropped into liquid sodium,[3] which resulted in very

---

* The stability limit temperature, T_s, is the temperature at which the liquid undergoes spontaneous homogeneous nucleation. For the molten UO_2-sodium system with UO_2 at 3000°C, the interfacial temperature, T_i, is ~1200°C, T_s is ~2050°C, while the minimum temperature of the hot surface necessary to support film boiling of sodium is ~5000°C. This significance of this criterion for MFCI is discussed in Appendix C.

mild interactions similar to earlier tests involving only a few grams of molten UO_2 dropped into liquid sodium.[4]

b. Overenrichment Error

Incorrect fuel composition could result in the release of small amounts of molten fuel and fuel-pin-failure propagation. However, two recent in-pile experiments at Argonne (D1 and D1A),[5] with the objective of studying pre-and postfailure effects of a small overenriched fuel section and release of molten fuel therefrom, have demonstrated that clad failure is very unlikely under conditions approximating normal flow and temperature in the coolant.

The test pins were 30-7/8 in. long, with 13.5 in. high fuel columns. The cladding material and dimensions, the pellet shape, diameter, and length, and the spacer-wire material, pitch, and diameter all conformed to the current FFTF designs. Six peripheral pins having 20%-enriched UO_2 fuel were used, along with a central pin having 12 in. of 26%-enriched UO_2 fuel, with a 1.5 in. long fully-enriched section at the middle of the column. This "hot" section had a power density about 2.1 times the average in the balance of the cluster.

Breach of the cladding and release of fuel into the coolant did not occur in either test. Posttest destructive examination of the central pin from Test D1 showed that some melting did occur at the centerline of the hot section, although it was not clearly indicated in the radiographs. No melting was observed in the normal-enrichment pellets. Considerable cracking of both fully-enriched and normal-enrichment pellets was noted. Radiographic evidence from the D1A test indicates extensive melting in the hot section and some melting in the normal section. The observations are in general agreement with pretest calculations that indicated approximately 50% mass fraction molten fuel in the hot section for Test D1A. Generally, the molten fuel in the hot section tended to move axially rather than radially toward the cladding.

On the other hand, if one assumes that molten fuel is ejected into coolant, best assessment shows that heat losses and condensation will prevent any significant pressure generation and void propagation and therefore the possibility of additional failures. This is illustrated by using an approach similar to that used to interpret the data of the H2 TREAT experiment.[6] However, the model has been extended to account for spherical void growth in a rod bundle, by obtaining a coupled solution to the energy and the momentum equations of a single bubble that grows and collapses within a subassembly containing coolant and intact pins, and molten fuel released from the failed pin.[7]

Figure 10.2 shows the extent of spherical bubble growth and pressure buildup caused by 8 g of molten fuel (this is believed to represent a conservative upper limit of possible fuel ejected in the planned experiment) interacting with sodium in the pin bundle otherwise operating at normal conditions. The choice of the initial mixing zone and its properties is based on the Test H2 voiding history: initial fuel temperature of 2800°C, particle diameter of 500 μ, volume of mixing zone 2.5 cm^3, and volume fractions of fuel, liquid, and vapor 10, 40 and 50%, respectively. Condensation coefficient is taken to be 1.5 cal/sec cm^2°C. The pressure pulse generated is approximately 10 atm and with a pulse width of several msec. Furthermore, because the bubble only grows to a maximum size of 2.1 cm, uncovering only 19 pins, and because of the short bubble lifetime, local dryout as well as flow instability can be considered highly unlikely events in the case of release of small amounts of molten fuel in the FEFPL subassembly. As demonstrated by laboratory experiments, molten UO_2 readily fragments when introduced into subcooled sodium. This can be explained by the fact that the minimum temperature for film boiling of the UO_2-Na system is considerably above the melting temperature of UO_2 (see Appendix C for theoretical details). The released fuel is therefore more likely to be carried along as small particles by the coolant rather than causing an increased blockage. Finally, formation of shock waves due to released fuel is considered very unlikely in view of current understanding of the cause for the vapor explosion with LMFBR materials, as discussed previously.

In summary, on the basis of recent analytical and experimental results, it is concluded that energetic interactions between molten UO_2 and sodium within the FEFPL experiments will not occur, and that sustained pressure pulses larger than the order of 10 atm are very unlikely. The following statements summarize these conclusions:

1) Current understanding of vapor explosion phenomena as discussed in Appendix C indicates that liquid-liquid contact and contact temperatures substantially above the nominal boiling point of the volatile liquid are required to produce coherent vapor explosions. Furthermore, sufficient nucleation sites provided by solid

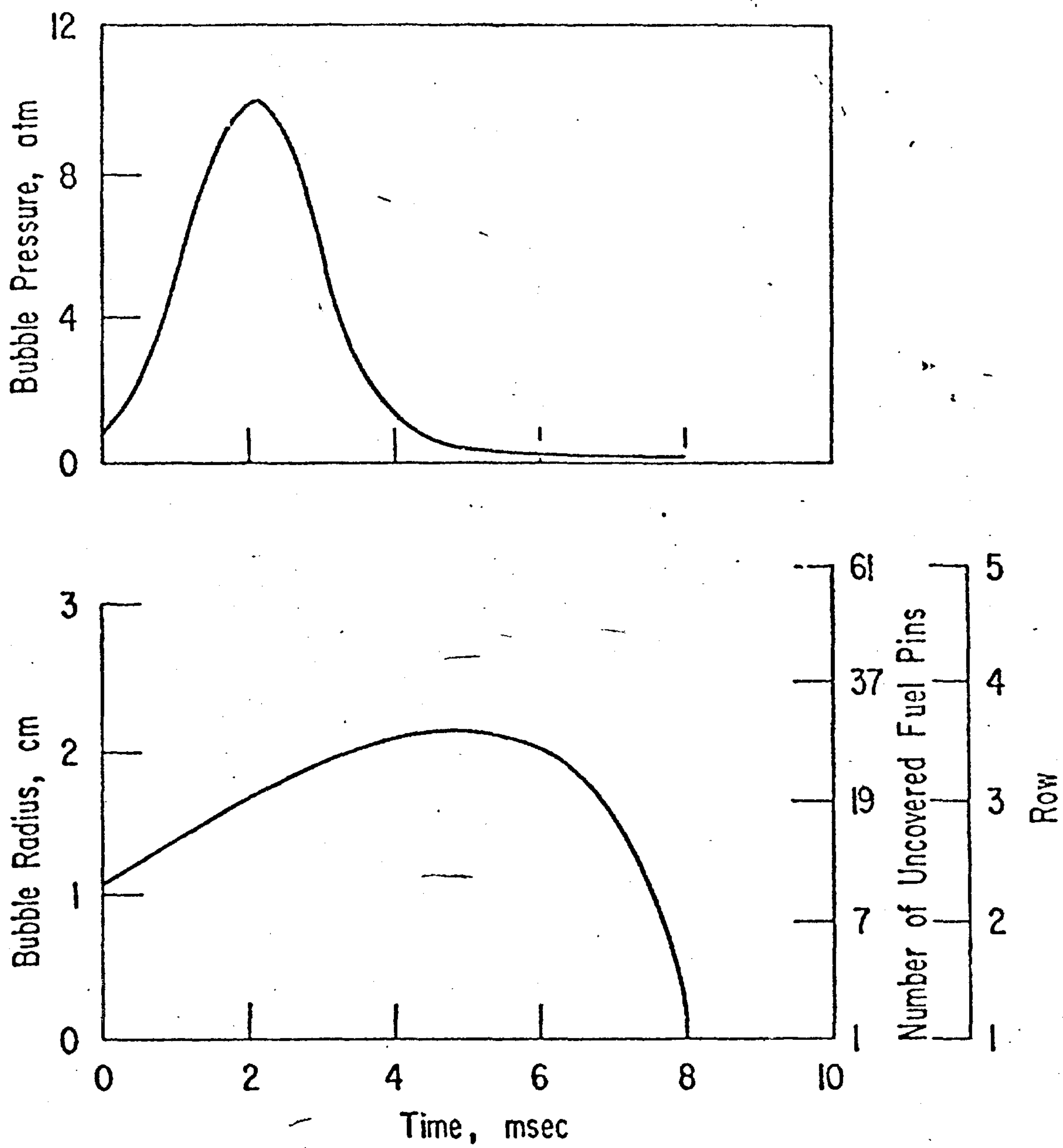

Fig. 10.2 Bubble Growth and Collapse in an FFTF Subassembly due to Release of Molten Fuel.

surface, gas, and radiation field will be present in the FEFPL tests to provide for continued sodium boiling at low superheat thus quenching the liquid UO_2 in a non-explosive manner with resultant low heat transfer rates such that heat losses and condensation will prevent any significant pressurization.

2) The loss-of-flow sequence provides for saturated sodium-out conditions which precludes mixing in a manner conducive to providing efficient conversion of thermal-to-mechanical energy.

3) Prior experiments including over some 20 interactions involving molten fuel contacting liquid sodium (loss-of-flow as well as overpower transient simulations) have shown results consistent with the present conclusions.

Design Basis for Containment of Molten Fuel and Liquid-sodium Interactions

Recent experimental and analytical information summarized above demonstrated that in the experimental sequence energetic interactions of fuel and sodium on a large scale are not possible. However, the loop containment capability, which can accommodate the consequences of even hypothetical events, is consistent with earlier information available when the design started. A very conservative analytical approach was employed in evaluating the initial conditions for the fuel-coolant interaction from a postulated reference flow-blockage experiment. This early conservative analysis upon which the FEFPL design is based is summarized in terms of two source terms: Upper Limit MFCI Source Term and Design Envelope MFCI Source Term. A discussion of these analyses is presented in the next sections.

10.2.2 Reference Experiment

To establish the initial conditions for use as an upper limit for loop safety evaluations, a rapid flow blockage of the test section at full ETR power was assumed. Also, an ETR scram was deliberately avoided. The initial steady-state test conditions were deliberately selected to envelope the initial series of ten FEFPL tests planned. This type of experiment has the potential for creating the largest amount of molten fuel, and when conservatively analyzed, represents the most adverse situation for a MFCI. The situation of a localized MFCI during an over-enrichment test is bounded by the conservative parameters used in the MFCI analytical model. Coincidental large power increases from either an ETR malfunction or loop reactivity feedback are prevented by the loop design safeguards as well as the operating characteristics of the ETR. The steady-state operating conditions for this postulated test are:

Average Fuel-element linear power	13.1 kW/ft*
Peak Fuel-element Linear Power	15.7 kW/ft
Sodium Inlet Tempeature	800°F
Sodium Outlet Temperature	1230°F
Average Sodium Velocity	26 ft/sec
Plenum Pressure	2.6 psig

These conditions are assumed to apply to a full 3-ft-length 37-pin bundle, although the required total power exceeds the present requirements for the loop heat-exchanger design. Nevertheless, to establish an upper bound on the stored energy available within the fuel, and melting times, it was assumed that these linear powers apply. The 1.25 P/A axial power shape prototypical of FTR is used as a reference for this experiment. If an axial flux shape with a peak to average of 1.40 (ETR expected shape with no axial flux modification) is used, then it will take longer to melt significant quantities of fuel, assuming both shapes have the same peak heat flux.

To analyze the initial sequence of events associated with rapid flow blockage and to estimate conditions for calculating a potential MFCI, a single-channel SAS2A computer model was used (the details of the SAS application to the FEFPL are presented in Appendix B). As the radial power profile across the FEFPL fuel bundle will be flattened by variable enrichment, the analysis for this channel would be typical of all the fuel rods because the radial peak/average is about 1.10.

The calculated test section flow reduction with time is shown in Fig. 10.3 for the sudden blockage postulated. This sudden flow reduction was obtained from SAS by introducing a very large hydraulic resistance ($L/De = 10^7$) at the inlet of the test section. The blockage was assumed to be complete within 0.10 seconds resulting in essentially zero flow through the test section after 80 msec. If it were physically possible to effect total blockage faster, the time sequence of events postulated to lead to an MFCI would not change significantly, because the blockage time is already short in comparison with the period required to melt fuel. Results of test section conditions predicted for this transient are summarized in Table 10.1 and Figs. 10.4 through 10.6. The significance of these SAS results, pertinent to the MFCI phenomena, is discussed below.

* This value is approximately 10% greater than the FTR linear power rating of 11.8 kW/ft.

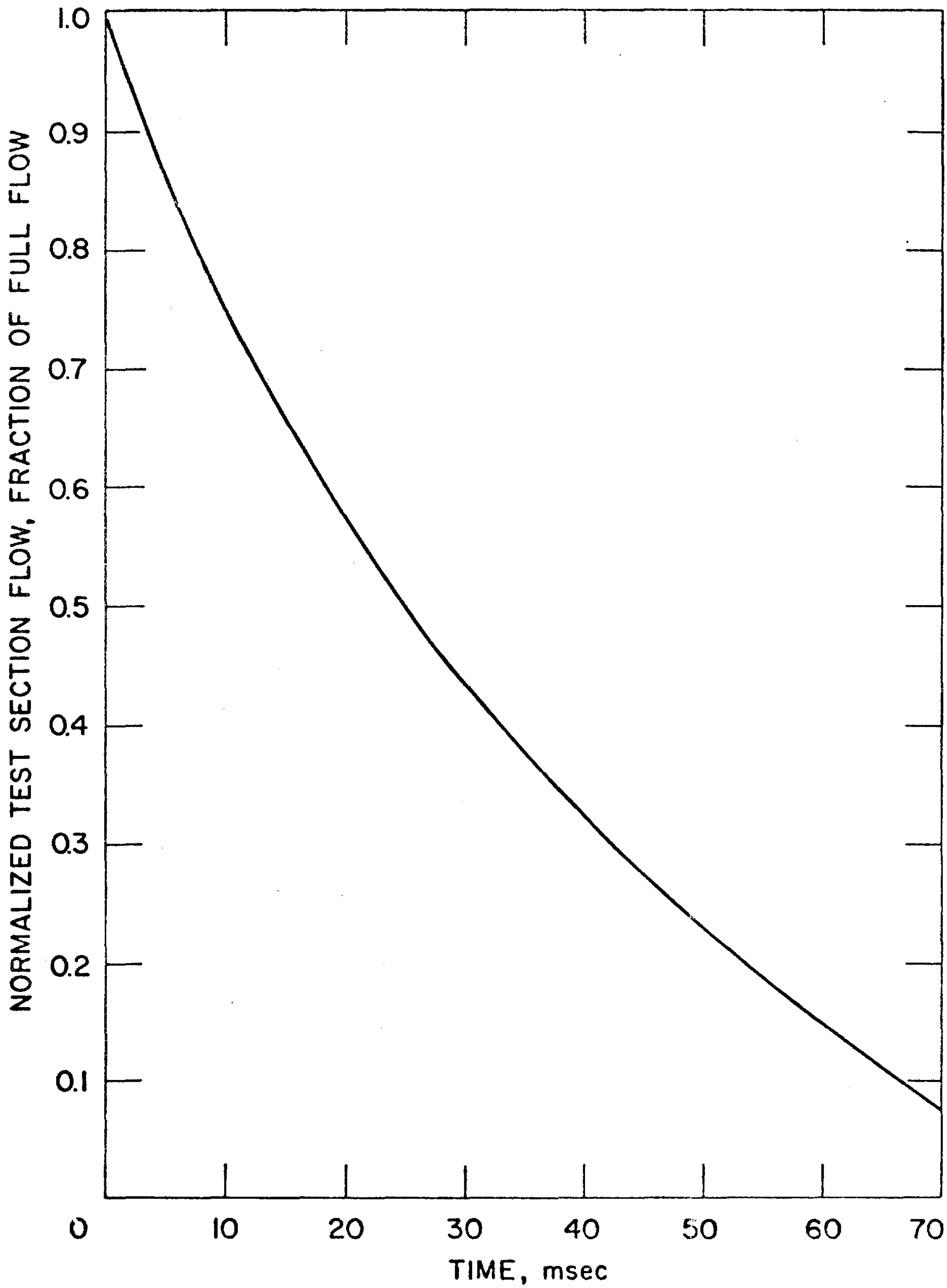

FIG. 10.3 - Normalized Test Section Flow Rate vs Time
After Total Test Section Inlet Flow Blockage

a. Presence of Sodium Vapor

The SAS model of sudden flow blockage voiding (see Fig. 10.4) shows the upper and lower liquid leg interface locations during the voiding process. The active fuel region is entirely voided for the period of time that fuel failure would be expected to occur (see Table 10.1). There does not appear to be a viable mechanism to cause this sodium vapor to recondense completely. It appears for this type of coolant activated power flow mismatch transient that the generation of large quantities of molten fuel guarantees the presence of sodium vapor. Therefore it is clear that at the initiation of the MFCI, sodium vapor will be present in significant quantities.

b. Quantity of Molten Fuel

The test section molten fuel and cladding fractions as a function of time after a sudden flow blockage are presented in Fig. 10.5. The test fuel cladding begins to melt after 0.88 sec into the transient and melts quite quickly (see Table 10.1) as shown in Fig. 10.5. At 2.75 sec, all of the cladding has completely melted, at which time only 15% of the test fuel has melted. The total fuel inventory is estimated to require about 10 sec to completely melt from the initiation of the transient.

In these calculations a flat radial power distribution is assumed within the test section. A radial power gradient no more than 15% across the fuel region is a design objective. Fuel melting can cause, at the very most, a reactivity increase of 0.12% (see discussion in Section 10.5). This reactivity addition corresponds to a power increase of about 20%. This underprediction of melting rate caused by the assumption of constant power is balanced by assuming no heat loss from the test section.

To establish the amount of fuel that can be available for the MFCI, the time required to transport molten fuel in the test section to the liquid sodium located below the fuel was estimated.[8] The results from this analysis suggest that the time for fuel to be transported to the MFCI reaction zone is short (0.1 to 4 sec) compared to the melting time interval (8 sec). It appears that molten fuel can arrive at the liquid-sodium interface region and be available for interaction before significant quantities of fuel have melted. If, however, sodium reenters the molten-fuel zone of the test section, reaction could occur sooner and involve less fuel (see calculations presented in Appendix C.3) Based upon the above time comparison, a molten-fuel inventory of 50% of the total fuel inventory was conservatively selected

TABLE 10.1

SEQUENCE OF FUEL ROD FAILURE EVENTS FOR REFERENCE DESIGN BASIS EXPERIMENT

Clad Reaches 1600°F	.21 sec
Sodium Boiling Initiation	.41 sec
Clad Film Dryout Completed	.71 sec
Clad Melt Inception	.88 sec
Significant Fuel Melt Begins*	1.9 sec
Clad Completely Melted	2.7 sec
Fuel Becomes 50% Molten	3.8 sec

* Fuel initially was 3.7% molten at steady-state.

FIGURE 10.4

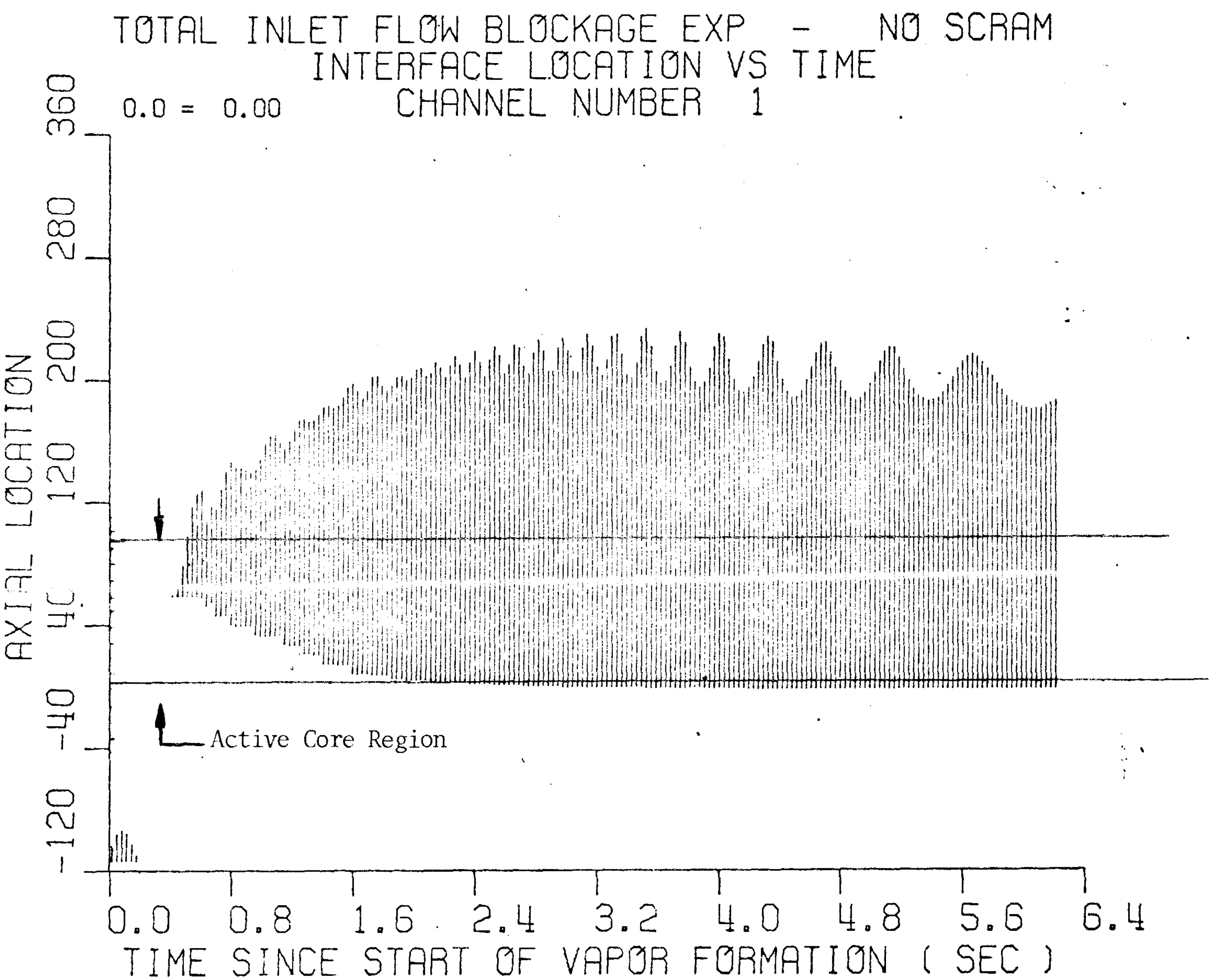
TOTAL INLET FLOW BLOCKAGE EXP - NO SCRAM
INTERFACE LOCATION VS TIME
CHANNEL NUMBER 1
0.0 = 0.00
AXIAL LOCATION
-120
-40
40
120
200
280
360
Active Core Region
0.0
0.8
1.6
2.4
3.2
4.0
4.8
5.6
6.4
TIME SINCE START OF VAPOR FORMATION (SEC)

FIG. 10.5 - Test Section Molten Fractions During Reference Design Basic Experiment

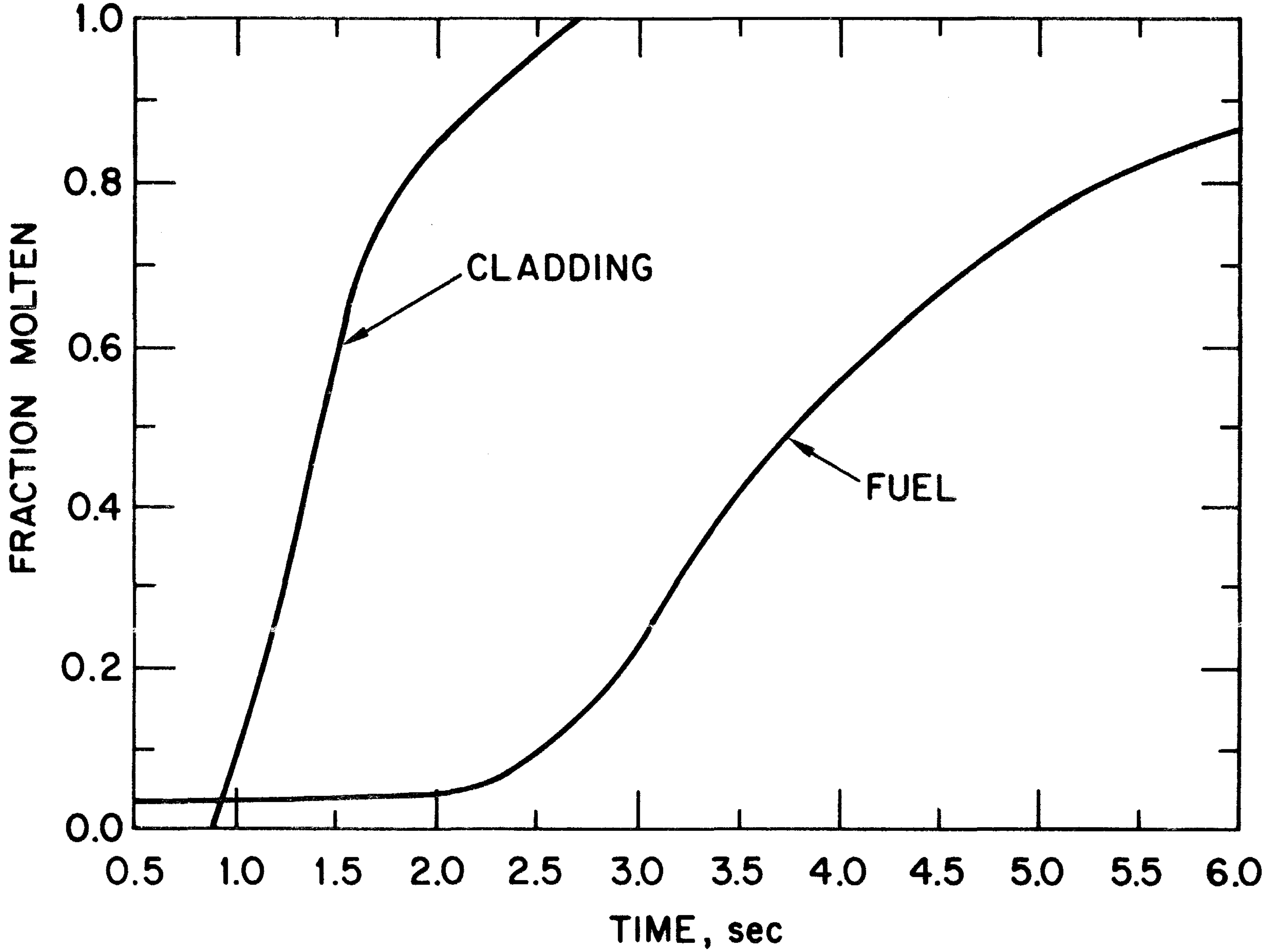

to be the amount of fuel participating in the MFCI. From Fig. 10.5 the time required to melt 50% of the fuel is about 4 sec.

The justification for a limit of the amount of molten fuel equal to 50% of the total fuel inventory is further substantiated by consideration of the time it takes fuel to vaporize. In Fig. 10.6, a plot of average molten fuel temperature versus time is presented for the total inlet flow blockage experiment without scram. As this figure indicates, at the inception of fuel vaporization (temperature of 3425°C occurs at 3.9 sec), 52.5% of the total amount of test section fuel would be molten. This condition of fuel vaporization sets an upper limit to the molten fuel inventory for sudden MFCI participation. Without a prior MFCI, which would be a reasonable expectation before this time, the increased fuel vapor pressure would begin to drive the molten fuel and sodium together. Therefore, a 50% molten fuel quantity seems conservative for use as an upper limit design value for instantaneous participation in an MFCI.

c. Molten Fuel Temperature

Figure 10.6 shows the SAS2A prediction for the average molten fuel temperature as a function of time. In the MFCI FEFPL studies an initial fuel temperature of 3661°K is employed (assumed melting temperature of 2827°C plus 561°C heat of fusion temperature equivalent). The SAS2A average molten fuel temperature at the time of 50% molten fuel generation is 2920°C (see Fig. 10.6 @ 3.8 sec). This roughly 100°C difference in molten fuel temperature is well within the accuracy of the MFCI calculational model. In addition, these molten fuel temperature predictions are the result of a highly idealized calculation in which heat losses have been neglected. Therefore, a 2827°C molten fuel temperature is not too unrealistic a value for MFCI use when interacting the large quantity of fuel (50%) assumed in this study (higher fuel temperatures have been used in the reactant transport limited MFCI evaluations presented in Appendix C).

10.2.3 Upper Limit MFCI Source Term

In the MFCI analysis, the ANL-FCI parametric model based upon early information was employed with input parameters selected to give a realistic, upper-limit value for an MFCI source appropriate to the FEFPL geometry and reference experiment discussed in the previous section. A conservative modeling approach was employed using the ANL Parametric Model described in Appendix B.4, in which the reaction zone constitutes a "closed" system in which

FIG. 10.6 - Molten Fuel Temperature Prediction for Reference Design Basis Experiment

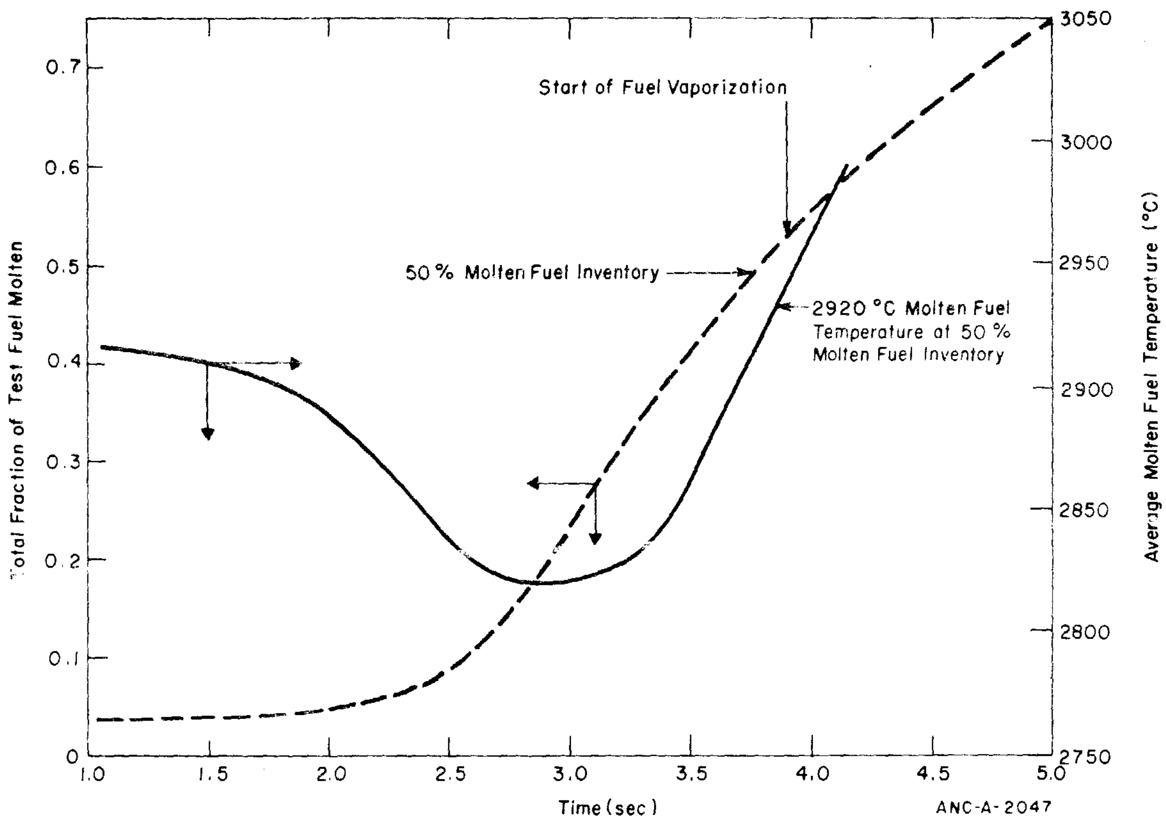

reactants are assumed to be initially present in a homogeneous mixture (see Appendix C). The amount of fuel participating was fixed at 50% of the total fuel inventory, for a full-length 37-pin test section as discussed previously. Therefore, these results are equivalent to 100% of the fuel in a 19-pin test section available instantaneously. The fuel was considered initially to be molten at an equivalent temperature of 3661°K, with the coolant temperature taken as 1100°K. All molten fuel particles were assumed to have a radius of 200 μ, (the mean value found after TREAT tests with pressurized pins). A thermal cutoff time of 5.7 msec was employed that is consistent with the acoustic roundtrip time to the gas interface in the loop plenum. A mixing and fragmentation time of 5.7 msec also was postulated - in essence, this permits enough heat in the particle to be transferred to reach a peak pressure before two-phase cutoff occurs. The characteristic heat-transfer time of the fuel particle is conservatively determined to be 0.0186 sec.

Partial credit was taken for the gas and vapor present initially in the FEFPL test section near the reaction zone; this corresponds to a gas-to-liquid volume ratio of 2.75. This is about 70% of the compliance volume potentially available as identified in Appendix C. The parameters used in the calculations are summarized in Table 10.2. The detailed evaluations conducted in support of these MFCI parameters are contained in Appendix C.

The characteristic pressures for the upper limit MFCI are summarized in Table 10.3. Figures 10.7 and 10.8 are the pressure-time and the pressure-volume relationships that are obtained for this upper limit MFCI source.

The peak pressure is 68.9 atm at the thermal cutoff time of 5.7 msec. At this time, the mixture quality is already about 8%; the mixture void fraction expected is about 50%, sufficient to gas blanket the fuel particles. Both the pressure-time history of Fig. 10.7 and the pressure-volume relationship of Fig. 10.8 represent fuel-coolant interactions significantly more energetic (approximately an order of magnitude) than the expected based upon recent understanding of fuel-coolant interaction phenomena.

10.2.4 Design Envelope MFCI Source Term

In this MFCI analysis conservative parameters were chosen to put a reasonable upper limit on the energy releases and containment loads when the design started. The criterion for this analysis was that each parameter chosen be representative of the "worst case" for the reference FEFPL experiment conditions within the existing experimental MFCI data and understanding

TABLE 10.2

PARAMETERS USED FOR THE UPPER LIMIT MFCI SOURCE TERM

Model Description

Equivalent Length of Molten Fuel Interaction (ft)	1.5
Equivalent Length of Liquid Sodium (ft)	3.0
Fuel-to-liquid Sodium Mass Ratio (1/2 opt)	5.55
Fuel-particle Radius (μ)	200
Mixing and Fragmentation Time Constant (msec)	5.7
Vapor-gas to Liquid Volume Ratio	2.75
Thermal Cutoff Time (msec)	5.7
Initial Fuel Temperature (molten) (°K)	3661
Initial Coolant Temperature (°K)	1100

ANL Parametric Model Values

Flow Area Per Gram Heated Sodium, S (cm^2/gm)	0.029
Acoustic Impedance AI (sec-atm-gm/cc)	5.5
Specific Heat of UO_2 X Mass Ratio, C_fW (cal/gm-°C)	0.5305
Initial Volume of Gas per g Na, V_{go} (cc/g)	2.6536
Characteristic Heat-trasnfer Time of Fuel Particle, $R^2/3\alpha_f$, (sec)	0.0186
Length of Unheated Sodium Column, L (cm)	609.6
Density of Unheated Sodium Column, ρ_o(g/cc)	0.7537
Cover Gas Pressure, P_∞ (atm)	1.18
Initial Reaction Zone Pressure, P_o (atm)	1.6

TABLE 10.3

UPPER LIMIT MFCI SOURCE RESULTS

Peak Pressure Results

Time at Peak Pressure	5.7 msec
Peak Pressure	68.87 atm
Sodium Temperature	1964°K
Fuel Temperature	3021°k
Work Generated	0.526 J/g UO_2
Thermal-to mechanical Conversion Efficiency	0.04%
Total Work Generated (37-element full-length array)	1750 J

Results When Reaction Zone Interface Leaves Fueled Region[a]

Time	41.3 msec
Pressure	56.6 atm
Sodium Temperature	1902°K
Fuel Temperature	3021°K
Work Generated	3.482 J/g UO_2
Thermal-to-mechanical Conversion Efficiency	0.3%
Total Work Generated (37-element full-length array)	11,600 J

[a] Upper liquid column has moved approximately 92 cm.

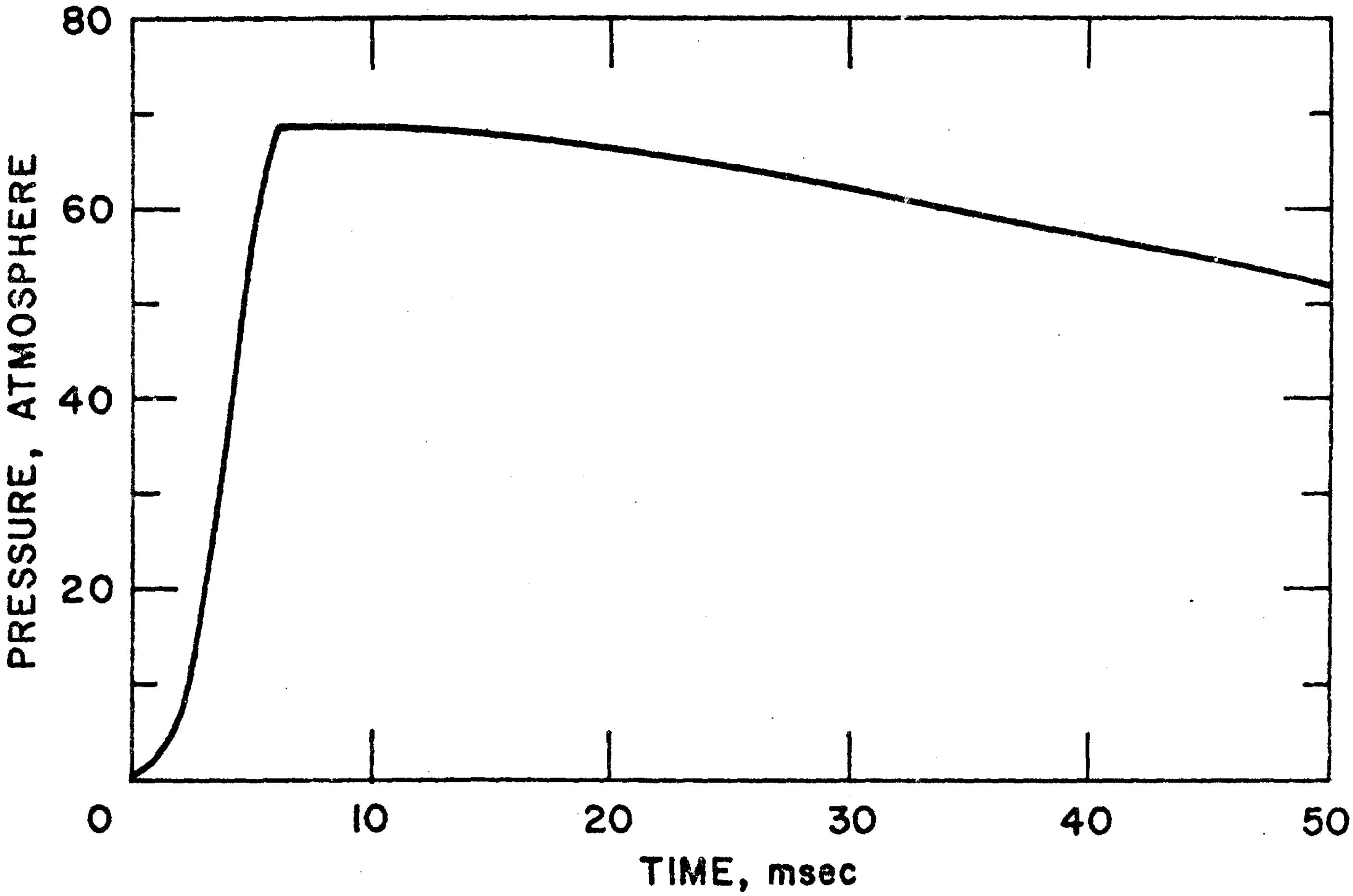

FIG. 10.7 - Pressure vs Time for Upper Limit MFCI

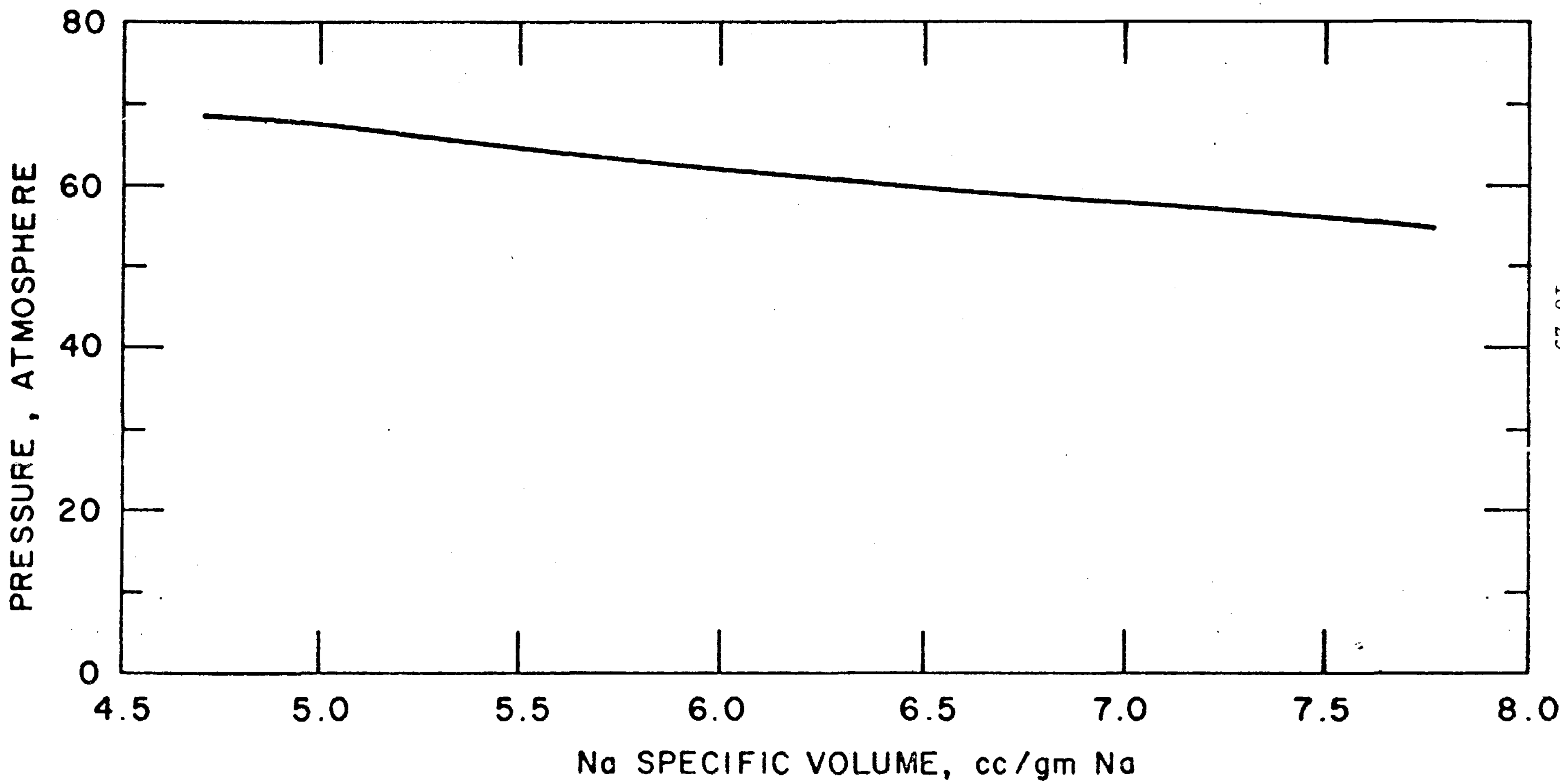

FIG. 10.8 - Pressure vs Volume for Upper Limit MFCI

at the time.

The design envelope MFCI source term was also calculated using the conservative ANL Parametric Model described in Appendix B.4. The input parameters used are presented in Table 10.4. They are identical to those for the upper limit source evaluation presented in the above section with the following exceptions made in order to establish an upper bound:

1) the fuel particle radius is decreased to 117 μ, with the characteristic heat transfer time constant reduced to 0.0064 sec;
2) the mixing and fragmentation time constant is decreased to 3 msec.
3) the volume ratio of vapor-gas to liquid is decreased to a value of 1.0.

Detailed discussions of these parameters are contained in Appendix C.

The results of the design envelope MFCI calculation are summarized in Table 10.5 and Figs. 10.9 and 10.10. The results given in Table 10.5 are for three times: the time at peak pressure, the time that the reaction zone leaves the active fueled region, and the time that the reaction zone reaches the upper plenum region. As can be seen in Table 10.5, a peak pressure of 194 atm is obtained. This occurs at the thermal cutoff time of 5.7 msec; however, by then there is a high mixture quality (about 9.5%). Consequently, gas blanketing of the fuel particles seems fairly certain before this time. The total work generated at the time of the peak pressure is 1818 J for the 37-element full-length bundle. This translates into a thermal-to-mechanical efficiency of about 0.04%.

The effect of the thermal cutoff time of the resulting peak system pressure and energy conversion is somewhat different than found for the upper limit MFCI source. The 3-msec mixing and fragmentation time postulated gives slightly more heat transfer to the coolant prior to 5.7 msec. At the 3-msec cutoff time, only a 300°K temperature differential exists between the fuel (at about 2600°K) and the coolant (at about 2300°K). If no retardation in heat transfer by the large amount of sodium vapor present in the reaction zone is hypothesized, then the peak pressure would increase 10%.

By the time the reaction zone interface leaves the active fuel region, estimated at 26 msec, the pressure has dropped to 143 atm. As Fig. 10.9 shows, this decrease is considerably more rapid than indicated in Fig. 10.7.

TABLE 10.4

PARAMETERS USED FOR THE DESIGN ENVELOPE MFCI SOURCE TERM

Model Description

Equivalent Length of Molten Fuel Interacting	1.5 ft.
Equivalent Length of Liquid Sodium	3.0 ft.
Sodium Mass Ratio of Fuel to Liquid, (1/2 optimum)	5.55
Fuel-particle Radius	117 μ
Mixing and Fragmentation Time Constant	3.0 msec
Volume Ratio of Vapor-Gas to Liquid	1.0
Thermal Cutoff Time	5.7 msec
Initial Fuel Temperature (molten)	3661°K
Initial Coolant Temperature	1100°K

ANL Parametric Model Values

Flow Area per Gram Heated Sodium	0.029 cm^2/gm
Acoustic Impedance	5.5 sec-atm-gm/cc
Specific Heat of UO_2 X Mass Ratio	0.5305 cal/gm-°C
Initial Volume of Gas per Gram Sodium	1.3268 cc/gm
Characteristic Heat-transfer Time of Fuel Particle	0.0064 sec
Length of Unheated Sodium Column	609.6 cm
Density of Unheated Sodium Column	0.7537 gm/cc
Cover-gas Pressure	1.18 atm
Initial Reaction-zone Pressure	1.6 atm

TABLE 10.5

DESIGN ENVELOPE MFCI SOURCE CHARACTERISTICS

Peak Pressure

Time at Peak Pressure	5.7 msec
Peak Pressure	194.2 atm
Sodium Temperature	2389°K
Fuel Temperature	2613°K
Work Generated	0.546 J/gm UO_2
Thermal-to-mechanical Conversion Efficiency	0.0406%
Total Work Generated (37-element full-length array)	1818 J

Reaction Zone Interface Leaves Fueled Region

Time	26.0 msec
Pressure	143.0 atm
Solid Temperature	2246°K
Fuel Temperature	2613°K
Work Generated	7.6 J/gm UO_2
Thermal-to-mechanical Conversion Efficiency	0.6%
Total Work Generated (37-element full-length array)	25,300 J

Reaction Zone Interface Reaches Upper Reservoir

Time	71 msec
Pressure	59 atm
Sodium Temperature	1913.4°K
Fuel Temperature	2613°K
Work Generated	33.8 J/gm UO_2
Thermal-to-mechanical Conversion Efficiency	2.5%
Total Work Generated (37-element full-length array)	112,600 J

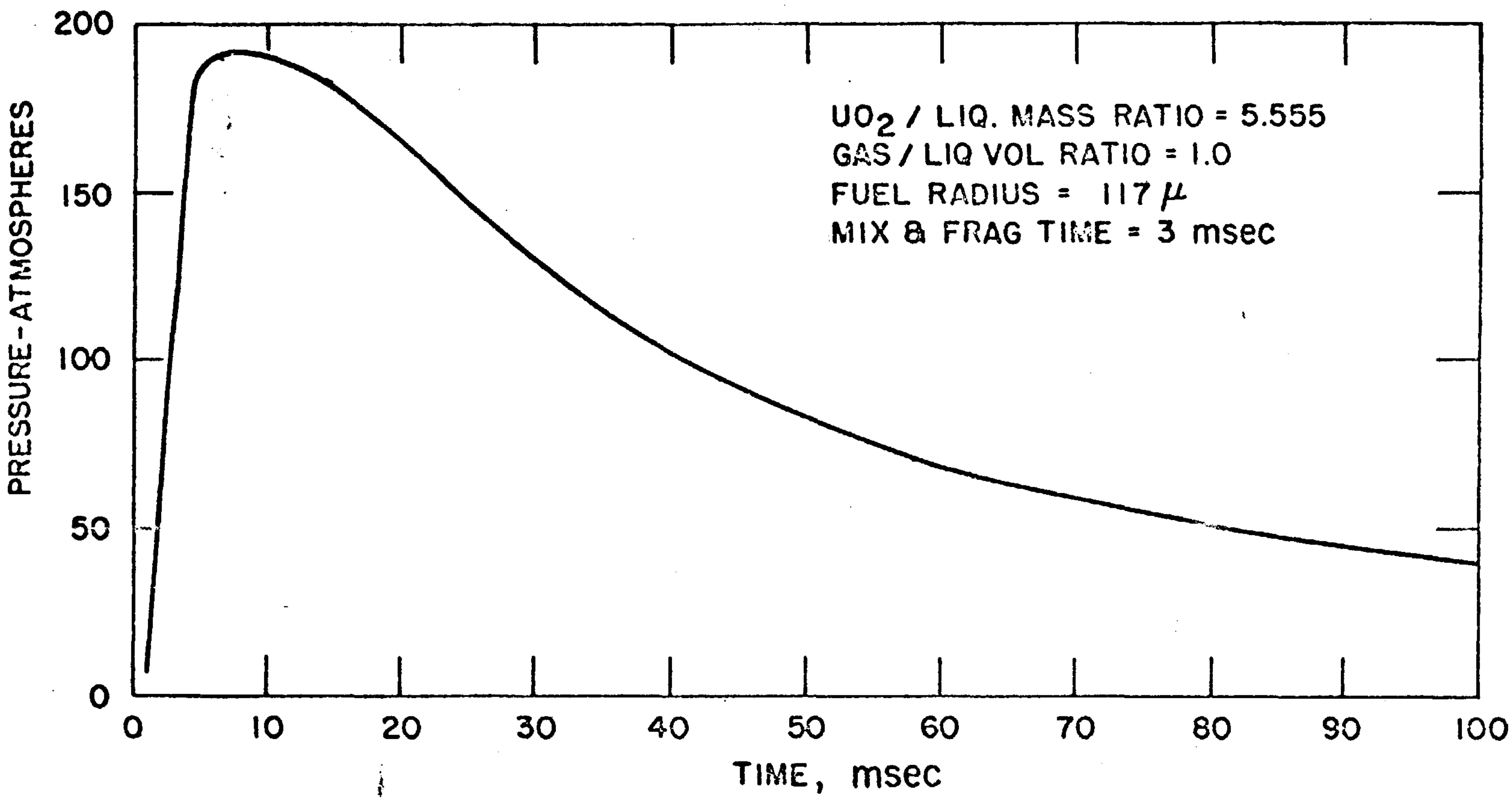

FIG. 10.9 - Pressure vs Time for Design Envelope MFCI

FIG. 10.10 - Pressure vs Volume for Design Envelope MFCI

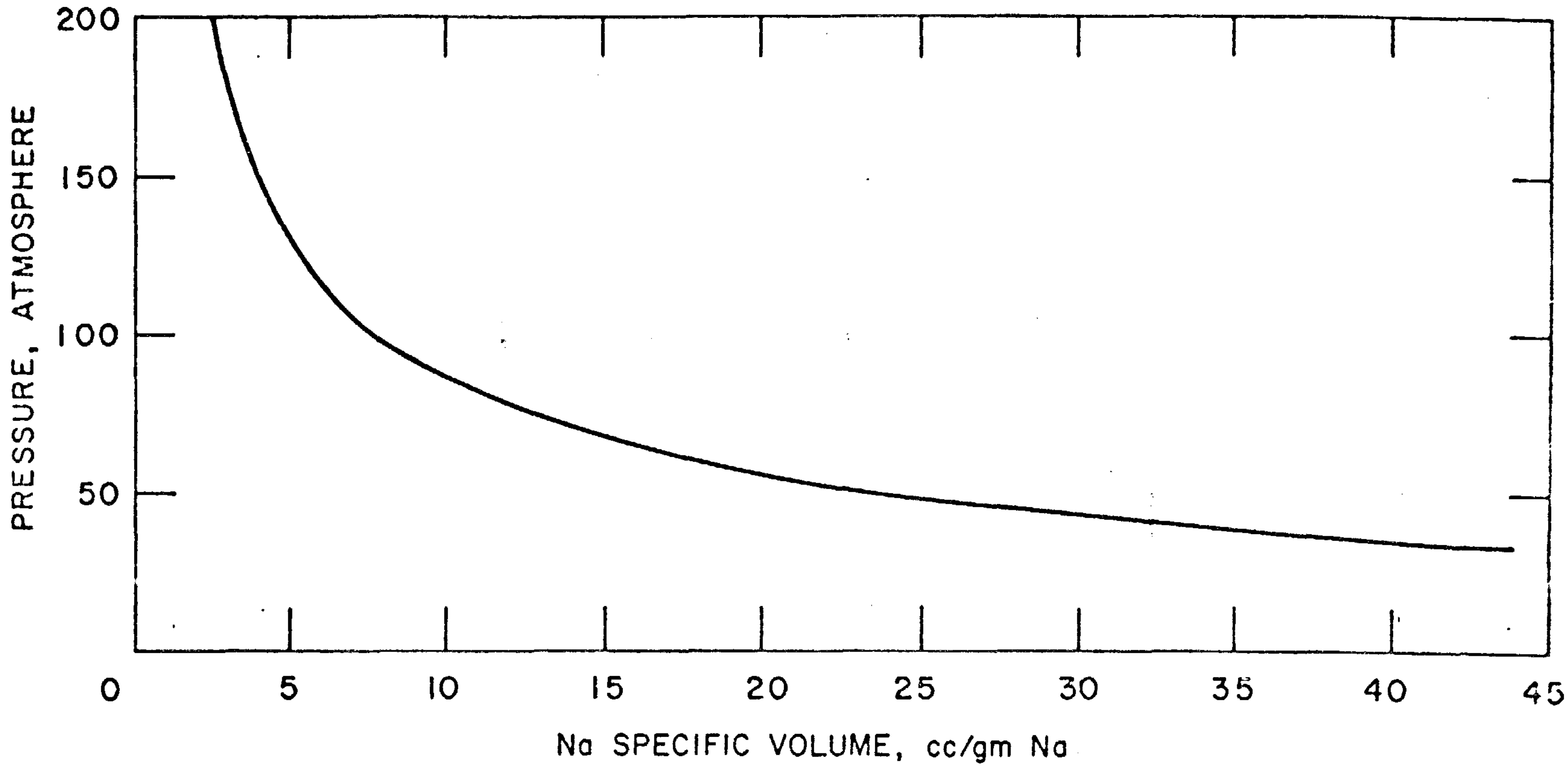

The faster inertial relief of the higher pressure explains most of this difference. As the expansion continues, the pressure falls to 50 atm at the loop upper reservoir. The integrated mechanical or pdv work amounts to 112,600 J, giving energy conversion efficiency of 2.5%. Based upon current understanding of the experiment sequence, this energy conversion efficiency is considered extremely improbable, and provides for a very conservative estimate of the fuel-coolant interaction for design purposes and assurance of loop integrity.

10.2.5 Long-term Effects

For a complete safety analysis, the MFCI sequence and loop response must be determined until a steady-state condition is reached. The two major post-MFCI conditions to be considered are the possible recurrence of an MFCI and the long-term heat removal of this MFCI energy by the FEFPL system.

Multi-MFCI Pressure Pulses

If it is postulated that the loop experience the design envelope MFCI, one resulting from the reaction of 50% of the test-section fuel inventory, a further hypothetical situation would be to postulate a second MFCI involving all of the remaining fuel. If we consider, however, the chaotic nature of the first postulated MFCI and the availability of large heat sinks in the loop, it is not likely that the remaining fuel will be molten. Further, it is unlikely that this remaining fuel would reassemble in a way so that it could all react simultaneously. Nevertheless, if this hypothetical sequence of events were to occur, the loop primary containment vessel still would not undergo any significant deformation.

The fact that fuel melting is an incoherent and relatively lengthy process suggests that there would be an appreciable delay between the two MFCIs. This delay time need only be long enough to permit the structures to recover elastically from the initial impulse. Because the rate of fuel melting is long in comparison with the MFCI pressure decay time, such recovery is a reasonable expectation. For the design envelope MFCI, the pressures are below the primary-vessel elastic limits; consequently, the structure can be expected to contain a second impulse (of magnitude equal to the first) safely. Based upon TREAT experience, a series of several pressure pulses of amplitude much smaller than the FEFPL upper limit source term may be expected. Multiple pressure pulses that fall within the loop design envelope (Chapter 6) can be safely tolerated. Indeed, from an experimental standpoint, the major problem may be to prevent a spurious scram after a pressure spike and thus terminate the opportunity to obtain information of value regarding possible subsequent events.

MFCI Heat Losses

Heat losses from the sodium vapor and subsequent condensation of the sodium vapor will control to a large extent the long-term effects of the MFCI. Based upon the MFCI calculations, estimates were made which indicate that complete vapor recondensation will occur before the upper-mixture interface leaves the FEFPL fuel bundle. The relatively large amount of steel, about 8 lbs at 1230°F, in the upper fuel-assembly plenum region, will remove approximately 500 BTU of heat during the 15 msec time interval that it takes the upper-mixture interface to move through this region. This energy loss is larger by a factor of twenty than the expansion work experienced by the mixture if heat losses are ignored.

A conservative estimate of the effect on primary vessel temperature of the energy from an MFCI shows that the containment temperature safety margin is not compromised. It is assumed, conservatively, that all the thermal energy from the design envelope MFCI is distributed uniformly to the bypass sodium, flow divider, downcomer sodium, and primary vessel located only within the 3 ft active test section region. A resulting equilibrium temperature of about 1350°F is calculated. This primary vessel temperature is 50°F outside the loop temperature envelope; however, based upon the conservatism of the calculation it suggests that no gross loss of vessel strength will result and the loop can safely contain a second MFCI pressure pulse equal in magnitude to the first if such an event were postulated.

An extension of the MFCI calculational model to obtain a more quantitative description of loop conditions following an interaction requires incorporation of heat losses and consideration of the large inherent heat capacity of the loop and loop components. This would reduce the source pressure to a lower value than used in these safety analyses.

An energy balance for the loop indicates that all the energy contained in the reaction mixture could raise the in-pile portions of the loop test train only about 20°K. In this calculation, the large mass of steel in the primary and secondary vessels as well as the sodium and steel in the heat exchanger were neglected. Only the mass of sodium (about 14 gals) and steel (about 500 lbs) within the flow divider were considered.

Long term thermal effects when no MFCI is postulated but, instead, molten fuel collects in the meltdown cup, are considered in Section 10.4.

10.3 Consequences of a Molten Fuel-Coolant Interaction

The analyses presented in this section have as their basis the conditions postulated in Section 10.2 for the reference experiment. Presented herein are the consequences of the MFCI source terms discussed in the previous sections along with other longer term effects produced by the reference transient.

The upper limit MFCI source term described in Section 10.2 is well within the pressure capability limits of the FEFP Loop primary containment. The peak pressure of 1000 psia (68.8 atm) is well below the loop static design limit (see Chapter 6.0). The sodium slug energy from this event can easily be absorbed in the loop upper plenum without damage. In addition, the thermal loads on the loop components from an MFCI will not present any excessive problems of long-term heat removal (see Section 10.2.5). Missiles or debris from a MFCI present no major threat to the safety of the loop. Reactivity insertions due to the reference transient also are acceptable. Loop design features are adequate to contain molten fuel, and a comfortable safety margin exists between the maximum expected consequences of the reference trasient and the loop design capability.

10.3.1 Pressure Pulse Propagation

Starting with the design envelope MFCI source pressures (and energies) obtained using and ANL parametric model given in Section 10.2, this analysis assumed a reaction volume free to expand axially but surrounded radially by rigid walls. The pressure (and energy) with respect to time is valid only within the hex-can region. Important, however, in the appraisal of loop containment capability is an assessment of how this pressure (and energy) is transmitted throughout the loop. To obtain this information in the radial and axial directions of the multi-vessel FEFP Loop, the studies described below were conducted.

The evaluations described below have, therefore, focused on the design envelope source to show that the loop can safely contain this most energetic event.

A. Radial Pressure Distribution

The radial pressure distribution throughout the test section region of the loop after the design envelope MFCI is determined from analysis using the REXCO-H code. A brief description of the REXCO code is presented in Appendix B.3, along with the physical model of the loop that is used. The design envelope source term is used as input.

Investigations are made using REXCO-H for two types of loop conditions; normal and abnormal. Both types use as a basis the design envelope source term MFCI. The normal case represents the conditions within the loop which are expected at the time of an MFCI. The possibility of off-normal conditions existing in the loop just prior to an MFCI are recognized, however, and therefore are also considered. The results of these evaluations are presented in the following sections.

Normal Loop Conditions

This REXCO analysis is based upon the expected conditions within the regions of the loop surrounding the test section just prior to an MFCI event. Figure 10.11 illustrates these conditions. Liquid sodium is present in both the bypass region and downcomer region outside of the interaction zone contained within the hex can. Furthermore, as monitored by the FEFPL-PPS, the gap between the two containment vessels is occupied by helium gas.

The radial pressures at various loop locations at the axial test section location, as predicted by REXCO-H, are plotted in Fig. 10.11 for the design envelope source term. Figure 10.11 shows that inside the hex can the pressure remained constant at approximately 200 atms. Over the 1-msec REXCO-H calculation, it was found that the hex can deforms very little. A maximum radial hex can deformation of about 0.034 cm is indicated. Therefore, for all practical purposes, no pressure relief of the source pressure occurs during the short time range of interest.

As seen in Fig. 10.11, significant radial pressure attenuation is predicted at the flow divider and primary-vessel regions. The maximum pressures in each region do not necessarily occur at the same axial location at each time step; thus, the curves represent a greatest upper bound for pressure. They indicate that the 190-atm pressure within the hex can is reduced to about 125 atm in the flow-divider region and to about 90 atm at the primary vessel. Only very minor movement of the primary vessel occurs - a deformation of about 0.005 cm, which is in the elastic range.

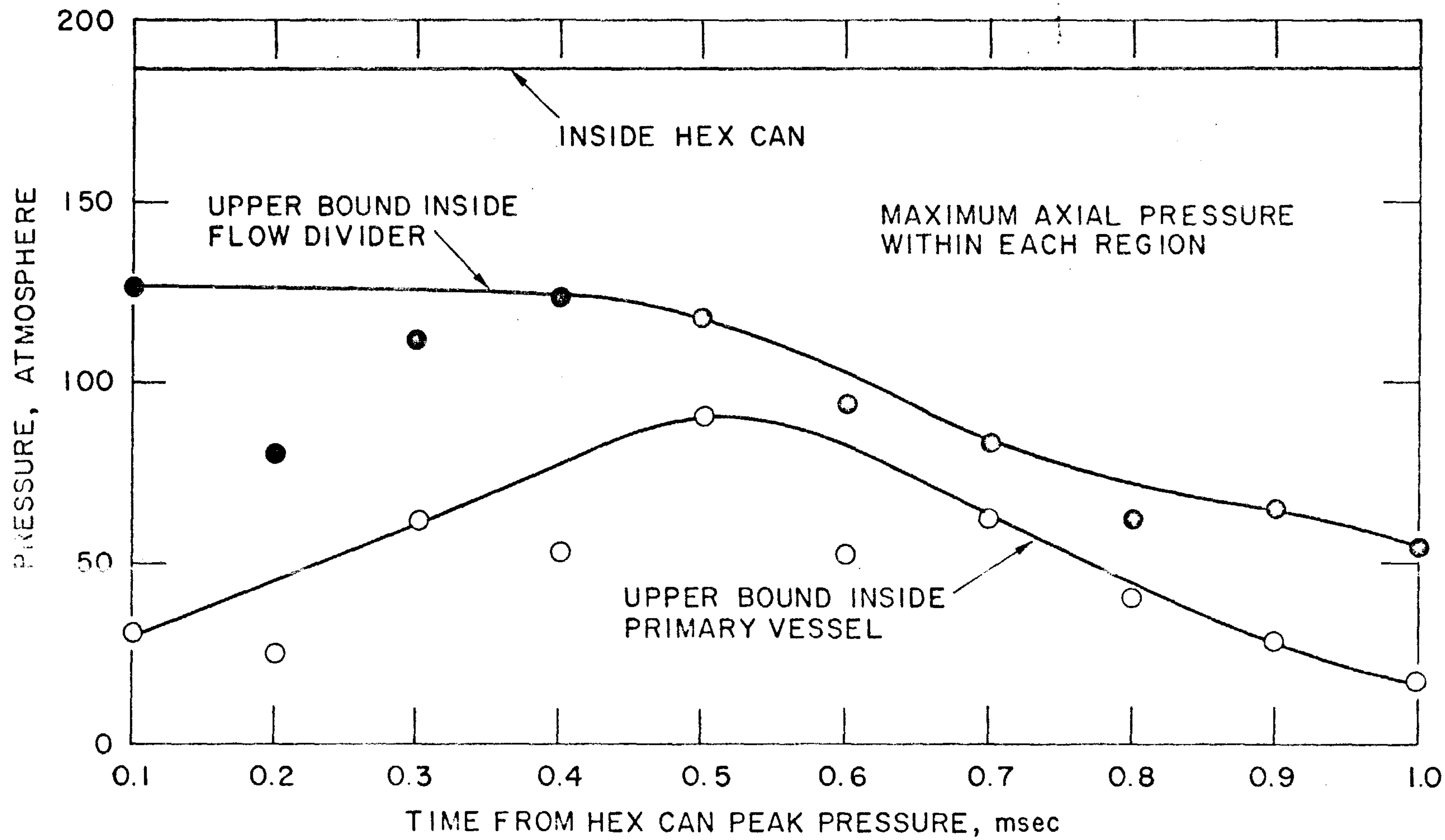

FIG. 10.11 - Attenuation of Radial Pressure Pulse by REXCO Analysis

To calculate the dynamic response of the loop, the maximum radial pressures shown in Fig. 10.11 are extrapolated back to the initiation of the transient. Figure 10.12 shows this estimated radial pressure distribution across the three most important regions which are used to determine the axial pressure propagation throughout the loop. The equivalent static pressure method along with classic elastic and plastic stress solutions are employed to evaluate the structural capability of the containment system. The dynamic REXCO-H predicted deformations, however, have been used to check the reasonableness of this essentially static analytical approach.

Abnormal Loop Conditions

The effect of off-normal loop conditions just prior to and during an MFCI event have been investigated as to their influence on the results predicted in the previous section for the normal loop conditions. Two abnormal situations are explored: 1) an MFCI occurring with the gap between containment vessels filled with liquid (either Na or water), and 2) an MFCI occurring with the loop bypass and downcomer regions filled with sodium vapor. Both situations are extremely unlikely, but have nevertheless been studied using the basic REXCO-H model of Fig. B.11 of Appendix B (using appropriate material modifications).

The possibility of an MFCI occurring, either during a planned experiment or resulting as a consequence of an accident, with a liquid filled contianment gap is quite remote. Failure of the FEFPL-PPS leak detection subsystem is necessary before this condition can develop. Even loss of this protective action does not imply that the containment compliance volume is lost. The high annular gas system pressure will prevent inleakage of either loop sodium or ETR water. Nevertheless, in order to determine the containment margin of safety, it is postulated that an MFCI pressure pulse occurs with the annulus between vessels filled with a liquid.

The results of a REXCO-H calculation indicate no appreciable change in containment capability from that for normal loop conditions. Although there now is some transfer of energy to ETR, the deformations in the loop secondary vessel and ETR core filler piece are still in the elastic range. Increases in the deformations over the normal case are observed in the hex can and flow divider. The primary vessel, however, remains in the elastic range. The predicted secondary vessel deformation of 0.001 cm is also well within the elastic range. No damage to ETR should result from this hypothetical event because the ETR core filler piece deflection is also minimal,

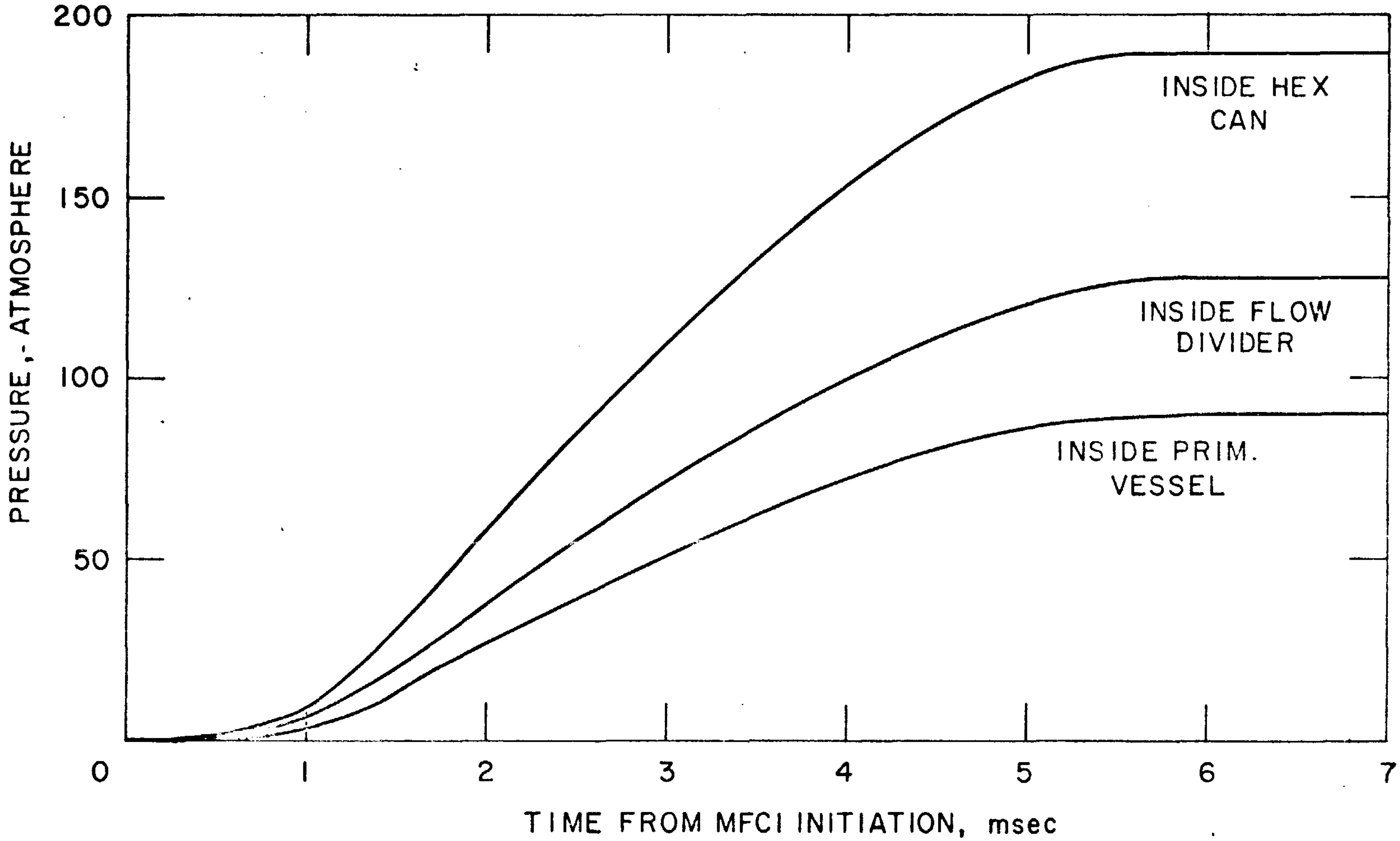

FIG. 10.12 - Extrapolation of REXCO Pressure-pulse Data to Zero Time

(0.0025 cm).

A severe MFCI occurring in the test section with voided bypass and downcomer regions also appears extremely remote. The THYME-B analysis of the loop conditions just prior to voiding in the test section indicate a large degree of liquid subcooling in these areas. Expulsion of sodium from these areas during any possible MFCI also does not appear possible due to the characteristics of the loop. The large hydraulic resistance in the lower regions of the loop favors a preferential upward expulsion in the test train. Heat losses to the relatively large structural metal heat sinks in lower regions, flow divider, and primary vessel also will prevent the reaction zone from penetrating very far into these regions. Extensive voiding in regions other than the test section, therefore, is not expected. Nevertheless, the consequences of this condition are studied to determine the containment margin for this postulated off-design condition.

As expected, the results of the REXCO-H run with the bypass and downcomer regions voided (see Fig. B.11) indicate a less severe challenge to loop containment than the liquid-filled, normal case. The primary vessel is effectively shielded from the design envelope pressure occurring within the hex can by the compliance volume in the voided bypass and downcomer regions. Essentially no pressure loading is felt on the flow divider or primary vessel until the hex can ruptures. The rupture of the hex can is predicted to occur at about 0.3 msec. The REXCO-H analysis presently does not consider mass transport between zones. The calculational results after 0.3 msec are therefore not valid for this situation. It is clear, however, that the rupture of the hex can will introduce a large expansion volume (voided bypass region) which will greatly reduce the 190 atms source pressure. Failure of the flow divider is not expected and, therefore, essentially no pressure loading on the primary vessel in the vicinity of the core midplane is expected.

B. Axial Pressure Distribution

Computer programs NAHAMMER and TRANSEP were used to study the axial pressure pulse transmission in the FEFP loop for the design envelope MFCI pressure source described in the previous sections. Both NAHAMMER and TRANSEP are based on waterhammer theory, i.e., that a pressure perturbation in the system travels away from the source at sonic velocity, and changes in magnitude as it is transmitted and reflected through the system. NAHAMMER, described in Appendix B, Section B.8, uses a superposition method to solve simplified one-dimensional equations of mass and momentum for friction-free pressure transmission in a rigid system containing a single pressure source. TRANSEP, a proprietary code owned by Atomics International, is based on general one-dimensional equations of mass and momentum solved by the method of characteristics for pressure transmission in a rigid or elastic system having single or multiple pressure sources.

The TRANSEP analysis of axial pressure pulse transmission in the FEFP loop was performed by Atomics International under contract to Argonne National Laboratory. The TRANSEP model of the FEFP loop is shown in Fig. 10.13 Both NAHAMMER and TRANSEP calculations were performed for isentropic transmission of MFCI pressure perturbations through compressible single-phase sodium in the loop. NAHAMMER and TRANSEP results for a single pressure source in a rigid loop are in excellent agreement, as illustrated in Fig. 10.14 Both indicate peak pressures at the bottom of the loop and at the pump of 1900 psi and 950 psi, respectively, for a design envelope MFCI producing a peak pressure of $\sim$ 2855 psi in the test section.

Single-source calculations assume only axial transmission of pressure waves from the test section. This underestimates the radial pressure loading of the flow divider and primary vessel. MFCI-induced radial movement of the test subassembly hex can and flow divider will produce a flow divider and primary vessel pressure loading that is larger and occurs sooner than that due to acoustic reflection from the bottom of the loop or the sodium-helium interface at the top of the loop.

REXCO calculations, described previously, were made to determine the radial pressure transmission of the flow divider and the primary vessel. This analysis predicted the radial pressure in three zones in the core region: 1) the hex can of the test subassembly; 2) the bypass flow area between the hex can and the flow divider; and 3) the downcomer flow area between the flow divider and the primary vessel. Structural response due to the design envelope MFCI in the test section will produce peak pressures of 125 atm and 90 atm acting against the flow divider and primary vessel, respectively. This radial attenuation of the source pressure is illustrated in Fig. 10.11.

Multiple-source TRANSEP calculations were made to determine the effect of radial, structural transmission of the source pressure on the system pressure levels. The three pressure vs time sources in Fig. 10.12 were used as simultaneous inputs for the multiple-source TRANSEP analysis; the source

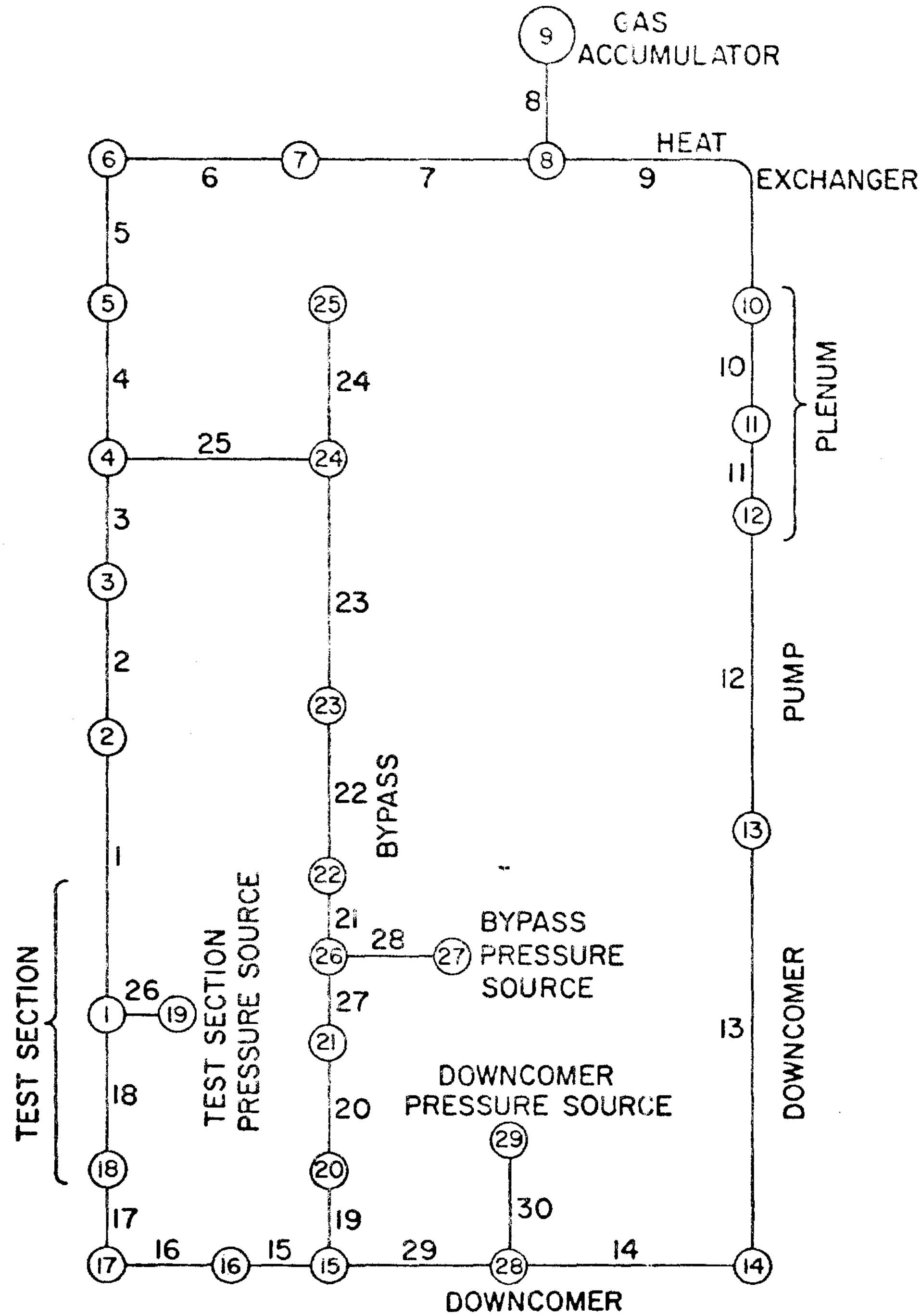

FIG. 10.13 - Model of FEFP Loop for TRANSEP Analysis

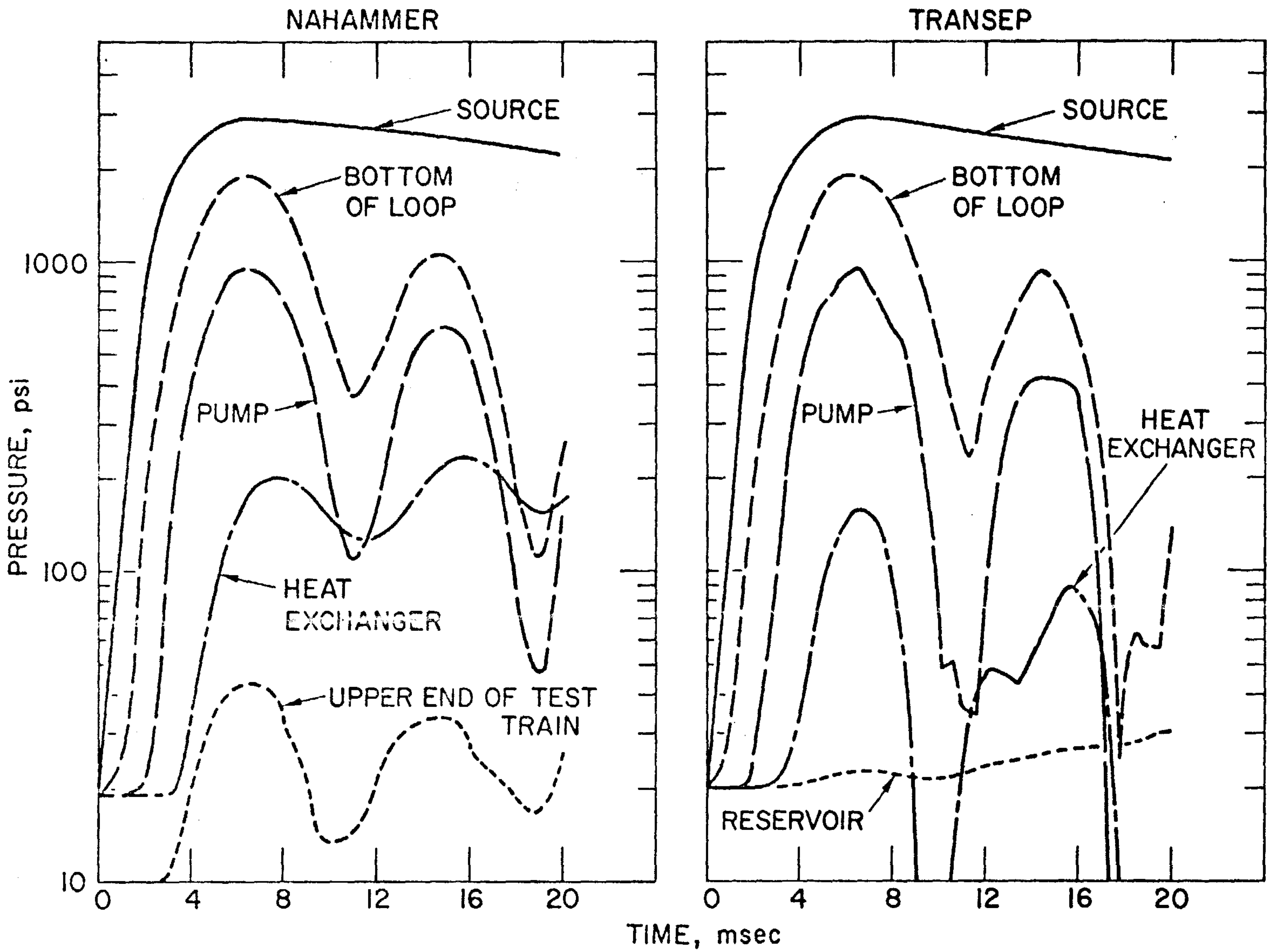

FIG. 10.14 - Pressure History in Rigid FEFP Loop for Design Envelope Source in Test Section

pressures were held constant after 6 msec. Results of these calculations are shown in Fig. 10.15. The magnitude of the peak pressure at the various loop components of interest is only slightly higher than that for a single pressure source. Results of other calculations comparing rigid vs elastic system and friction vs friction-free fluid flow indicate that these considerations have little effect on the acoustic transmission of pressure waves in the FEFP loop.

Attenuation of acoustic pressure waves in the FEFP loop, due to the numerous geometry changes, etc., is sufficiently high that the peak pressures at the bottom of the loop and throughout the downcomer are well below the design envelope MFCI source pressure. Peak pressure levels at various locations in the FEFP loop, from the NAHAMMER/TRANSEP calculations, are as follows:

Location or Component	Peak Acoustic Pressure, psi
Lower spherical cap of the primary vessel	1968
Primary vessel at the elevation corresponding to the midplane of test fuel elements	1520
Pump, lower end	1026
Lower tube sheet heat exchanger	200

These results form the basis of the containment structure analysis presented in Section 10.3.4.

10.3.2 Analysis of Sodium Slug

Pressure perturbations in the loop may force sodium out of the test section and the energy of the displaced sodium may have potential for containment damage. Computer program FEFPSLUG, described in Appendix B, Section B.6, was used to simulate the hydraulic behavior of the sodium coolant in the FEFP loop. As the MFCI proceeds coolant flow reverses first in the test section below the location of the MFCI and is followed by reversal in the direction of coolant flow through the downcomer.

Sodium responding to the design envelope MFCI will void the 3-foot fueled region of the test subassembly in 14 msec. The coolant velocities in the test subassembly are shown in Table 10.6 to reach $\sim$ 230 ft/sec as the sodium is displaced from the heated region of the test subassembly, but the corresponding coolant velocities in the other, larger flow area regions of the the loop are much smaller. These results assumed an initially liquid-

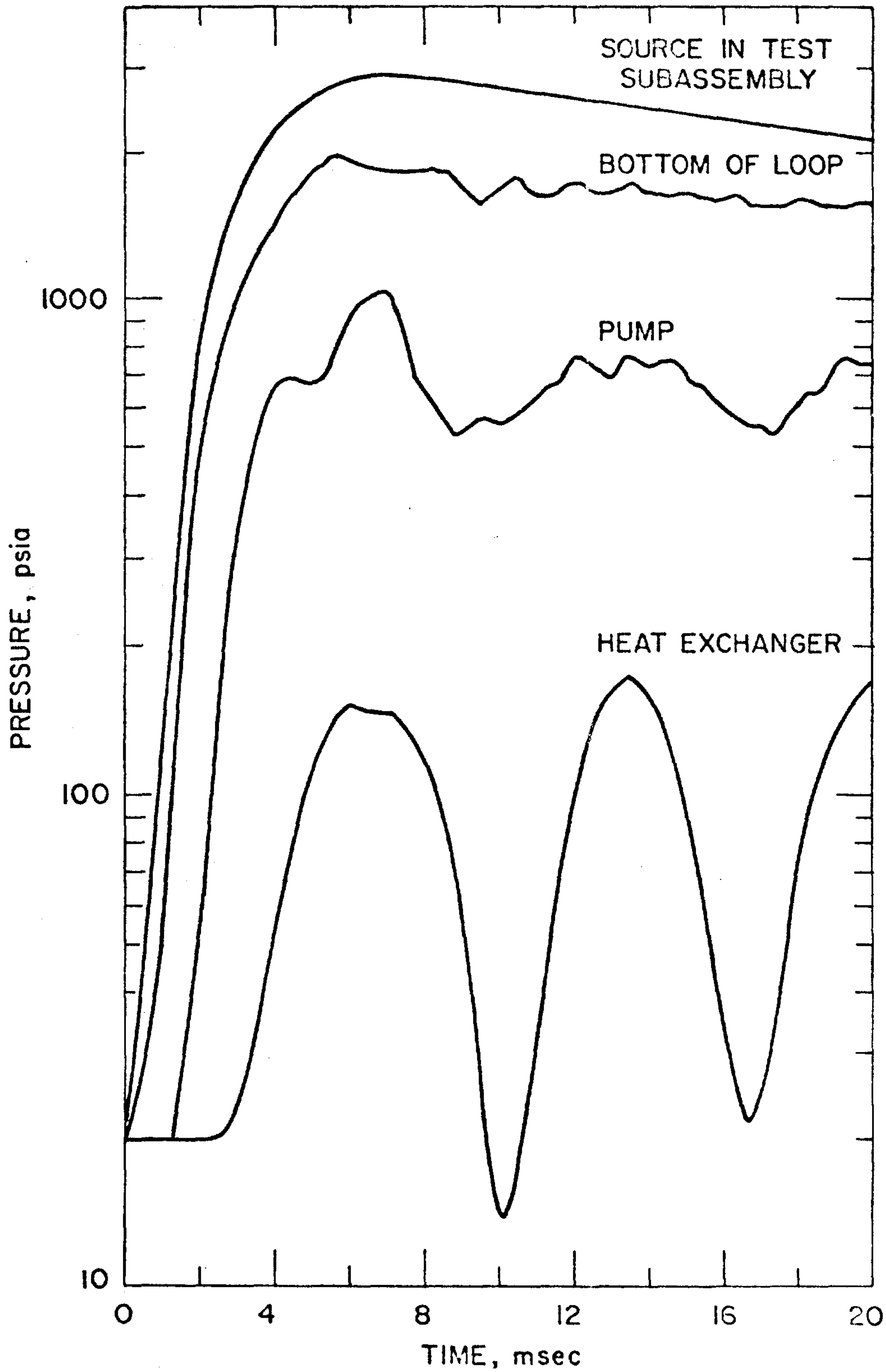

FIG. 10.15 - Pressure History in Elastic FEFP Loop for Multiple Pressure Sources Within Loop

Table 10.6

Coolant Response to a Design Envelope MFCI in the FEFP Loop

Time, sec	Coolant Velocity in Test Section: Above Fuel Centerline, ft/sec	Coolant Velocity in Test Section: Below Fuel Centerline, ft/sec	Volume of Coolant Displaced from the Test Section, liters	Coolant Velocity in Plenum Region: Riser, ft/sec	Coolant Velocity in Plenum Region: Downcomer, ft/sec
0.000	8.0	7.4	0.00	7.7	0.41
0.001	8.6	6.7	0.00	7.9	0.41
0.002	12.9	1.6	0.00	8.8	0.38
0.003	25.4	-13.4[a]	0.01	11.6	0.29
0.004	44.8	-36.7	0.02	15.9	0.15
0.005	68.4	-65.1	0.04	21.2	-0.02[a]
0.006	93.6	-95.3	0.08	26.7	-0.20
0.007	117.7	-123.7	0.13	32.0	-0.38
0.008	139.4	-148.7	0.18	36.6	-0.54
0.009	158.9	-170.4	0.25	40.6	-0.68
0.010	176.1	-189.2	0.33	44.1	-0.80
0.011	191.2	-205.2	0.41	47.0	-0.92
0.012	204.3	-218.9	0.50	49.5	-1.01
0.013	215.7	-230.7	0.60	51.6	-1.10
0.014	225.6	-240.7	0.70	53.4	-1.18

[a]Sign convention: negative sign indicates flow reversal.

filled test section without pressure relief from structural movement. The geometry of the loop flow channels and test subassembly is assumed to be unchanged by the molten fuel-coolant interaction.

The FEFP loop originally was designed with two plenum regions, one a large-area ($\sim$ 120 in.^{2}) region above the upper tube sheet of the heat exchanger and the other a small-area ($\sim$ 6 in.^{2}) extension of the flow divider to the loop top closure. Communication of cover gas between the two plenums contributed to a potential sodium-impact problem by permitting the gas in the small-area plenum to escape into the other plenum as the sodium level in the flow divider increased, thereby offering little resistance to sodium being expelled upward against the loop top closure. The current loop design utilizes a flow diverter near the top of the loop to direct the upward-moving sodium through two changes in flow direction and into the single, large-area plenum above the heat exchanger. Use of a single plenum insures the continual maintenance of a cover-gas atmosphere to cushion the loop top closure against sodium-slug impact.

10.3.3 Missiles and Debris

Missiles and debris may be formed during an experiment, particularly those experiments in which molten fuel is present in sufficient quantity to cause a MFCI. A fuel-element failure in which the clad tube is melted or broken may also release fuel fragments into the coolant. If a fuel element were severed into two separate pieces, the bottom portion would continue to be held in place by the lower support grid, but the top part would be restrained by only its weight and the lateral loading from neighboring fuel elements, via the spacer wires. During a design envelope MFCI a fuel element broken at the center of the fueled region could experience a peak lifting force of 120 lbs on the top part and a maximum downward force of 36 lbs on the bottom part. However, these different forces that result from unequal ejection velocities in the axial direction exist only momentarily. It takes only 14 msec to completely void the fueled-region of the test subassembly during a design envelope MFCI and the hydraulic forces rapidly decrease as coolant is expelled from the test subassembly.

Outside the test subassembly the coolant flow areas in the loop are considerably larger and the ability of the coolant to produce missiles or to continue carrying fuel fragments is much reduced because of the lower coolant velocity. In the downward direction, the fuel elements, lower support grid, small-diameter throat of the lower test section flowmeter, and meltdown cup are all barriers to passage of other than particulate matter. Barriers between the test subassembly and the primary vessel in the upper axial direction include the three probe-type flowmeters and their supports, the filter, the flow diverter, and the numerous instrument leads. Radially, the test elements and primary vessel are separated by two barriers; inner-outer hex can assembly, and flow divider wall. REXCO analysis indicates that maximum radial deformation of the hex can during a design envelope MFCI is less than 0.1 cm; hence, both radial barriers remain intact to protect the primary vessel.

Total loop sodium volume is about 113 liters and the gas plenum volume is 30 liters. This gas plenum volume is equal to the volume of sodium contained within the flow divider, i.e., the test section, bypass, and combined-flow regions of the loop, a substantial fraction of the loop sodium inventory. At the moment the full 36-inch fueled region of a 37-element test subassembly is voided of coolant, 0.7 liters of sodium will have been displaced into the plenum. This change in plenum gas volume will cause a pressure increase of less than 1 psi. Although the coolant velocities reach $\sim$ 230 ft/ sec as sodium is voided from the heated region of the test subassembly, the upward velocities in the combined flow region of the flow divider and the tubesheet area of the heat exchanger are 53.4 and 1.2 ft/sec, respectively. The corresponding upward velocity of the gas-liquid interface in the plenum is only 4 ft/sec.

Kinetic energy of all sodium in the loop at the time the fueled region is voided is 6 Btu. If this kinetic energy is assumed not to be diminished by the appreciable frictional forces or by sodium-vapor condensation against system heat sinks outside the test-subassembly heated zone, the slug-energy compression of the loop cover gas would increase the gas pressure to a maximum of 110 psia (isothermal compression) or 125 psia (adiabatic compression). These pressures and associated system response to a design envelope MFCI appear to minimize sodium impact and to have little potential for damaging the loop primary vessel.

In Fig. 10.16, the axial pressure distribution predictions from FEFP-SLUG are shown for the design envelope source. These results exhibit characteristics similar to the NAHAMMER/TRANSEP predictions of Section 10.3.1.2. Although the inertial pressure levels are generally lower, the distance- and time-attenuation behavior are quite similar for the two types of pressure constraint. The acoustic-pressure predictions, therefore, provide an upper

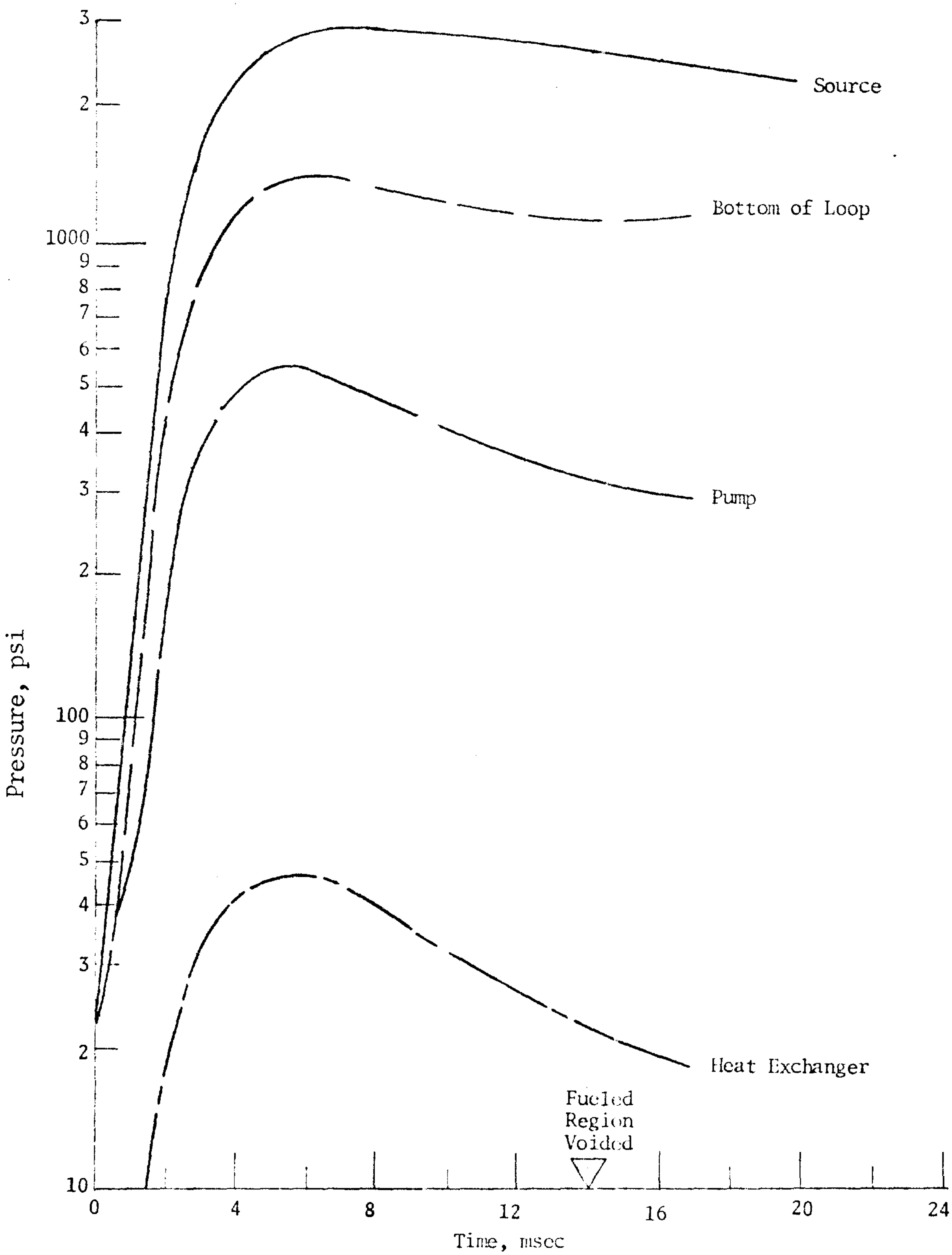

FIG. 10.16 - Pressure History in Rigid FEFP Loop for Design Envelope MFCI In Test Section (Inertial Response)

estimate of the pressures throughout the system.

10.3.4 Structural Analysis

To determine the response of a multivessel system to a large transient pressure pulse with the degree of accuracy necessary to meet the intention of the ASME Boiler and Pressure Vessel Code, the analysis must include the following:

- definition of the source term
- computation of the dynamic loads resulting from the source term - (pressure vs time) on each component of the loop.
- the response of each component to the dynamic loads

There exists no single analytical model which considers all three aspects of the problem in sufficient detail for a system as complex as the FEFP loop. The two-dimensional hydrodynamic code REXCO and others which include structural response capability are by necessity limited in the axial detail achievable in the long slender FEFP loop. Detailed calculations are possible and have been made for small sections of the loop (i.e., test section region), but a complete and consistent simulation of the entire loop is not possible. The analytical method of Proctor and Wise[9] based upon the NOL explosive tests also has similar geometric limitations in its application to FEFPL. In addition, uncertainties exist in the application of this semi-empirical method based upon high explosive TNT tests in a single-vessel water system to this FEFPL situation. Both of these methods, however, have been utilized to check the method which is employed in this study as described below.

The approach taken in the analysis of the FEFPL containment system is to utilize the ANL-FCI parametric model in the determination of the pressure source term. Using these pressure-volume results for the hex can region, the radial dynamic pressures in the vicinity of the core region are obtained from REXCO-H. These pressure histories are then used in the one-dimensional NAHAMMER and TRANSEP codes to generate the pressure-time acoustic pulse histories axially throughout the loop. A discussion of these methods is presented in previous sections of this report.

Given the pressure-time curves, the third part of the problem is the calculation of the dynamic response of the containment shells. As already observed, REXCO nodal models could be developed which describe the various loop regions of interest using as input the pressure-volume relationships for each axial location. This represents an extensive modeling effort which is not warranted at this time. Youngdahl's dynamic analysis[10] is valid only for the separable cases where $p = R(r)T(t)$ and considers plastic deformation only. Both assumptions are not necessarily valid for the MFCI pressure loadings expected in FEFPL.

Thus, in view of the approximations that must be made and the resources available, it appears appropriate to use a simplified engineering approach developed by Newmark[11] and Alvy.[12] Their method, which has been used in the design of PBF loops, essentially calculates a static load which will result in an effect on a structure equivalent to that imposed by the dynamic load of the shock wave in the structure. These equivalent static pressures are then compared to the allowable pressures of the primary vessel using the classic elastic and plastic solutions presented in Section 6.0.

10.3.4.1 Equivalent Static Pressure

Following Newmark and Alvy's work, we have

$$q = \frac{p_{sw}}{K} + p_e , \qquad (1)$$

where

q = equivalent static pressure, psi

p_{sw} = shock wave pressure, psi

p_e = equilibrium pressure

and

$$K = \frac{(2\mu - 1)^{0.5}T}{\pi t_1} + \frac{1 - \left(\frac{0.5}{\mu}\right)}{1 + \left(\frac{0.7T}{t_1}\right)}$$

where

μ = ductility of material, $40 < \mu < 100$ for steel piping

t_1 = area of pressure - time curve/p_{sw}

T = $(2R\pi\frac{m}{Eg})$ natural period of vibration, sec*

R = average radius, in.

* It is conservative to ignore the added mass due to fluid for the calculation of q.

m = density of material, $lb/in.^3$

E = modulus of elasticity, $lb/in.^2$

g = gravitational constant - 384 in/sec^2

Note that the factor of 2 which represents the reflection factor of the shock wave as it strikes a surface has been dropped in Equation 1. This factor is included in the source pressure-time curves as generated by the REXCO and NAHAMMER.

10.3.4.2 Compliance with Safety Design Requirements

The assessment of the ability of the FEFP in-pile loop to contain the design envelope pressures is based upon the equivalent static method described in the previous section. The pressures in three regions of the primary vessel (the test section region, the lower spherical cap region, and the pump region) were analyzed and compared to the loop design safety limits presented previously in Section 6.0. Ongoing analyses show that loop components such as the heat exchanger and pump will tolerate these loads. They will be presented in the ASME Section III Stress Analysis Report now in the final stages of completion (see Ref. 13 for interim analysis).

Containment Capability

The source term used in the design envelope MFCI source. The equivalent static pressures for this source, generated by NAHAMMER are compared in Table 10.7 to the static solutions of the fully plastic thick-walled design safety limits developed for the primary vessel in Section 6.0. The values of μ in Table 10.7 represent the degree of ductility, the higher value representing greater ductility. The test-section pressure represents the pressure in the in-pile cylindrical portion of the primary vessel, whereas the spherical-cap results represent the axial pressure conditions in the lower primary-vessel region of the loop. The pump pressure depicts the pressure on the primary vessel in the lower region of the pump (location closest to MFCI source). Based on values for the propagation of the pressure pulse throughout the loop as determined from the NAHAMMER analysis, these three regions see the highest loads, and, consequently, establish the containment capability of the system.

A comparison of the results in Table 10.7 indicate that the consequences of the design envelope can be safely contained. In the four major loop regions of concern (in-pile region, lower spherical cap, pump region, and heat exchanger) the primary vessel is below the fully plastic design limit. As indicated, the primary vessel can elastically contain the predicted

TABLE 10.7

COMPARISON OF DESIGN ENVELOPE PRESSURES WITH DESIGN CONDITIONS

Primary Vessel Region	Primary Vessel Design Conditions*		Design Envelope MFCI Source Term Results			
			Degree of Ductility Assumed			
			μ = 40		μ = 100	
	Elastic Pressure (psi)	Fully Plastic Pressure (psi)	Equivalent Static Pressure (psi)	Calc. Strain (%)	Equivalent Static Pressure (psi)	Calc. Strain (%)
Test Section Midplane	1670	2590	1516	0.062	1500	0.061
Lower Spherical Cap	3340	4490	1963	0.083	1913	0.080
Loop Pump Exit Region	1670	2590	1013	0.042	1002	0.041
Heat Exchanger Lower Flange	1020	Not Applicable	188	0.013	185	0.013

*Based upon 1300°F wall temperature limits of Section 6.0

pressures. These levels are well below the loop safety limits outlined in Section 6.0.

Top Dome Flange

The attenuated load-time history was obtained using the dynamic pressure pulse results of WHAM (report in TR-A-150, TR-240), corresponding to the design envelope source term of 194 atmosphere maximum amplitude, and the dynamic analysis results of SHOCK computer program (report in EDF-391). The structure was analyzed for this vertical loading at the top using the NASTRAN computer program. The results indicate that the stresses are within the Nuclear Vessel Section III emergency condition requirements.[14]

Meltdown Cup

The stress analysis of the meltdown cup, due to the application of the static equivalent pressure of 2570 psi corresponding to the design envelope source term, was performed. The material properties were chosen at 950°F corresponding to the initiation of pressure pulse. The stresses under this condition are less than the yields. The thermal stress analysis for post thermal shock situation is underway. It should be noted, that from the pressure calculations considerable margin with the allowable stress exists. If the final superimposed results of thermal and pressure loadings exceed the allowable limit (Section III guidlines will be used to lead to reliable design) then the upgrading of the material of the meltdown cup will be explored. Finite element axysymmetric computer code AGN-14063 is being used for the subject analysis.

10.3.4.3 Evaluation of Structural Response Calculational Method

Newmark considers his static equivalent analysis to be adequate for sizing purposes only; consequently, these computations are not expected to give the exact values that may occur, instead, they provide a reasonable envelope for a design evaluation. It has been chosen because of the lack of any rigorous method presently available which can predict the response for the entire FEFPL system. This rather simplified equivalent static pressure method along with the classical elastic and plastic stress methods, then, provides an approach which is well suited to the analysis of a loop system as complex as FEFPL. In light of the recognized uncertainties, a comparison of this calculational method with the previously discussed REXCO-H computer results and the empirical NOL method of Proctor and Wise[9] is valuable. These analyses and comparison results are presented below.

Empirical NOL Structure Response Method

Several tests were performed at NOL to study the vessel response to TNT explosions. On the basis of these tests, Proctor and Wise developed an empirical correlation for the quantity of TNT required to induce a given vessel deformation. The application of the method is valuable because it provides a measure of the containment margin that is based on experimental data. However, there are significant differences between the Proctor and Wise-TNT system and the FEFPL-MFCI system that should be recognized to assure that the comparison is properly interpreted.

The first major difference is in the nature of the sodium vapor expansion as compared with TNT expansions. TNT expansions typically start with initial pressures on the order of hundreds of thousands of psi, and, as a result, roughly 50% of the energy is shock energy. Sodium vapor expansion, on the other hand, start with much lower pressures and may, in some cases, have essentially no shock energy. Because of this difference, the partitioning of the energy into surrounding structures may not be the same for each system.

It is also difficult to determine if the TNT comparison is conservative or not. In the Proctor and Wise tests, with charge to vessel diameter ratios greater than three, it has been estimated that roughly half of the shock energy was dissipated as heat into the water. In addition, where the blast pressures, the residual pressure following the shock, were below the resistive force of the vessel, no vessel deformation occurred after the shock. Thus, in some cases, only 25% of the energy available theoretically was effective in doing damage.

On the other hand, the sodium vapor expansion is available for doing damage only during that portion where the pressure is greater than the resistive force of the vessel. When MFCI work equivalents are quoted, they usually refer to vapor expansions down to one atmosphere. Since the vessel resistive force can support pressure much greater than one atmosphere, only some fraction of the work theoretically available from the sodium vapor expansion would be effective in doing work.

There is a second problem in using the Proctor and Wise correlation for the FEFPL. Proctor recommends that the correlation be restricted to water-filled right-cylindrical vessels with the following characteristics (only the restrictions of significance here are quoted):

1. Charge radius, R_c, and vessel radius, R, are related by $R > 3R_c$
2. Only single vessel systems

3. The explosive charge is compact, i.e., length of charge $\sim$ diameter.

For the FEFPL, the radius of the primary vessel is 2.3 times larger than the radius of the MFCI mixing zone. This would indicate that more energy could be deposited in the vessel wall (since there would be less dissipation). Similarly, because the source is not compact, there is less capability to relieve the forces by axial expansion and vessel deformations could be greater than predicted for the FEFPL system.

On the other hand, the FEFPL has multiple cylinders - both the hex can and the flow divider are between the MFCI source and the primary vessel. Since both of these barriers are capable of absorbing energy, the actual deformation of the primary vessel would tend to be less than predicted. It is probable that this would more than compensate for the above effects.

The conclusion from this is that TNT-MFCI comparisons should be made with care. However, because extensive testing has been done with TNT and essentially no testing has been done with the MFCI, there is some qualitative value in determining the damage potential from a TNT explosion with the energy equivalent of a reference MFCI. With these reservations, an analysis is made of the FEFP loop's primary vessel energy absorption capability using the empirical Proctor and Wise correlation presented in Ref. 9.

The results using the Proctor and Wise correlation indicate that between 190 and 200 kjoules are required to produce the design safety limit strain in the primary vessel (deformation of primary vessel to secondary). Mechanical property data used in this analysis were identical to those utilized in Ref. 8. These energy values correspond to a vessel temperature of from 800 to 1100°F. Comparing this energy containment capability with the 112.6 kjoule design envelope MFCI source term suggest a safety margin of about 80 kjoules between the upper limit of the credible MFCI source potential and the containment capability. These results are in basic agreement with the equivalent static prediction of no contact between the primary and secondary vessels for this design envelope MFCI source term.

REXCO-H Deformation Predictions

Analyses using the REXCO-H code (see Appendix B.3 for description) were made to predict the pressure distribution radially across the loop in Section 10.3.1.1. By necessity, only the loop area in the vicinity of the core midplane could be described in detail due to nodal restrictions required in modeling the long slender FEFP loop. Structure deformations are predicted by REXCO-H and, therefore, some comparison can be made with the results obtained by the equivalent static method in the core midplane region.

The REXCO-H structure analysis results obtained for the design envelope source pressure predicted an elastic condition for the primary vessel over the 1 msec REXCO-H calculational range studied. A peak deformation of about 0.005 cm is predicted. The majority of strain energy was absorbed in the hex can with the flow divider also exhibiting only very minor deflections of about 0.007 cm. Essentially, no pressure loading of the secondary vessel is indicated for the design envelope MFCI event with helium present in the containment gap.

The prediction of the elastic primary vessel condition is consistent with the elastic prediction (see Table 10.7) obtained using the equivalent static method. Thus, some correlation is indicated.

Based upon these comparison studies, it is concluded that the equivalent static method provides a conservative appraisal of the containment capability of the loop. In view of the uncertainties associated with the characterization of the MFCI event, it appears prudent to employ this procedure. At this time, the more detailed and comprehensive dynamic analyses required to take advantage of the inherent conservatism in the design are not warranted.

10.4 Loop Meltthrough Protection

An analysis was made of molten fuel and molten steel as they might affect the survival of the primary vessel. As illustrated in Fig. 5.1, the fuel is normally surrounded by a hex can, sodium in the bypass region, the flow divider, sodium in the downcomer, the primary vessel, the helium annulus, and the secondary vessel. Beneath the fuel are the grid structure, instrumentation, a double-walled meltdown cup which is filled with and surrounded by sodium, and the primary and secondary vessels.

Several fuel failure modes were postulated to cover various conditions that might exist following a loss of cooling accident or test. These conditions include:

1. Plugging of the subassembly bottom with steel,
2. Failure of the hex can,
3. Loss of pumping,
4. Rapid injection of molten fuel and steel into the meltcup region:
    a. without a violent interaction
    b. with a violent molten fuel sodium interaction.

10.4.1 Test Section

In a loss of cooling event, the cladding melts soon after sodium voiding. Based on the early L-series loss-of-coolant tests, the molten cladding may freeze and plug the lower end of an accident subassembly. The FEFPL test train has a massive, sodium-cooled entrance to the subassembly that will quench molten materials that fall from the subassembly and will promote plugging.

Additional molten steel may fill the subchannels around the fuel. Calculations were made for the bottom of a subassembly with the following initial conditions:

Fuel power of 11.8 kW/ft (196 W/g) (average)
Fuel average temperature 3500°F
Fuel surrounded by molten steel at 2451°F (mp taken as 2450°F)
Subassembly plugged with frozen steel beneath the fueled region
Inner hex-can melted and gone
Outer hex-can at 800°F
Sodium entering bypass region at 800°F (h=3540 Btu/hr-ft^2-°F)

The results indicated a temperature in the hex-can wall of 1200°F at the time the fuel melted and the configuration changed. Melting of the inner surface of the fuel elements, boiling in the center of the center elements, and boiling of steel near the surface of the elements all were calculated to begin between 6 and 7 seconds following the start of the hypothetical situation.

Once the fuel is molten, the molten steel and fuel will separate. A second calculation was made for the resultant separated phases. The initial conditions assumed are:

A frozen steel blockage below the originally fueled region,
A 10 in deep column of molten fuel above the blockage (at 5300°F),
Heat generation in fuel 196 W/g,
Hex-can wall 1200°F,
Inlet sodium 800°F,
Frozen steel adjacent to hex-can (from results of calculation above) at 2449°F.

Fuel boiling began in 1.1 seconds. At this time the heat flux into the sodium was 9×10^5 Btu/hr-ft^2. A meltthrough rate of 0.04 in./sec existed for the steel beneath the fuel. As molten steel floated into the fuel, it would remove additional heat by boiling (not considered).

The hex-can wall became coated with a film of frozen fuel near the wall. J. C. Hesson, of the Post Accident Heat Removal Section, ANL, estimated, based on his experiments with electrically heated aqueous salt solutions, the convection coefficient between boiling fuel and the frozen fuel as 880 Btu/hr-ft^2. Using this value for the present case, the calculated steady-state heat flux to the sodium was 1.4×10^6 Btu/hr-ft^2 and the inside temperature of the hex can wall was 1900°F.

If the pump is not operating, the natural circulation required to prevent meltthrough of the hex can at full power would be achieved when the loop plenum temperature reached 1900°F (50 psia) if the heat exchanger could cool the sodium to 500°F. Since these conditions far exceed the design limits for the heat exchanger, forced convection is needed to preserve the hex can; however, natural circulation will prevent duct meltthrough due to decay heating.

Because of the internal heat generation, accumulations of fuel cannot long persist. In the core region with the ETR at power, accumulations of fuel larger than the equivalent of a 0.8 cm sphere will boil internally, even if submerged in sodium. An accumulation equivalent to a 3 cm sphere will boil from decay heat alone. Fuel and steel that boil will condense in the upper regions of the subssembly or loop. In the core region, condensed material can collect on the hex can as a solid layer of heat generating fuel to a depth of 0.1 in. (Outside the ETR flux much greater thickness can collect). For greater thicknesses in the core region, the excess fuel will flow downward. Fuel boiling may be important in redistributing fuel and can spread the fuel to a coolable geometry if sodium reentry does not occur first.

Mixtures of fuel and steel in which the steel phase is interconnected (continuous) can melt through barriers more readily than fuel alone, because of the enhanced effective thermal conductivity. However, from investigations of mixtures of fuel and steel,[15,16,17] it is concluded that the phases separate readily and the fuel is the continuous phase for mixtures; therefore, enhanced effective fuel conductivity will not be encountered at normal power levels ($\sim$ 200 W/g).

It is postulated that thermal interactions between molten fuel and liquid sodium may rupture the hex can or that the vapor pressure of steel or sodium may fail the hex can if the top and bottom are plugged. Fuel might be introduced into the bypass region following hex can failure. Even if molten fuel and steel are injected against the flow divider, it will survive the thermal shock and the fuel will spread to a coolable geometry. The flow divider will not be damaged significantly by conceivable molten fuel-sodium interaction. Although some fuel debris may be deposited in the bypass region, the quantity and distribution will not promote blockage of the bypass flow. Either forced or natural convection of sodium will be maintained down the downcomer and up the bypass following a meltdown event. This flow will prevent accumulation of molten fuel in the bypass region.

If the bottom of the test section does not plug, a thermal interaction of molten fuel and sodium might temporarily force liquid sodium out of the bypass and downcomer regions adjacent to the fuel. Because of the short duration of the pressure pulses and the pressure that would be developed in the loop plenum, the liquid will quickly "spring back" into the bypass and the downcomer. If voided, the primary duct in the pump will heat only at about 5-1/2°F/sec; and if uncooled and exposed to molten fuel, the hex can and flow divider would survive for about 1.2 and 3 sec, respectively. Molten steel at the melting temperature of fuel could breach these uncooled walls in about 0.3 and 0.8 sec, respectively. Sodium reentry to these regions is expected to occur within one second.

It appears unlikely that any significant amount of molten fuel will escape the test subassembly; however, fuel debris may spread throughout the loop. A thermal interaction between fuel and sodium would produce a great many small particles. The normal sodium velocity is adequate to lift any particle, that is not physically restrained, up to the filter region. Particles smaller than 0.05 in. may pass through the filter and recirculate in the loop. A portion of any circulating particles may accumulate outside the meltdown cup. If the pump is off, particles cannot reach the region outside the cup, but if the pump is on, particles might fill the annulus up to the inlet to the bypass. The high velocity through the bypass orifices will prevent plugging of these orifices by the small particles (<0.05 in.).

The particles on the screen will be out of the neutron flux and easily coolable by the surrounding sodium. The effect of particles outside the meltdown cup has been analyzed. The tubes provided for sodium circulation around the cup will be designed to avoid plugging (e.g., many small side openings only at the top and several side exits plus the end exit at the bottom). Normally, when the pump is operating, the flow through these tubes will be >5 ft/sec. This velocity also will avoid plugging due to debris.

If no significant heat source exists in the cup, debris outside the cup can be cooled by either the sodium flow down the tubes and through the bed, or by the helium flow outside the primary vessel. In either case, the peak primary vessel temperature will be less than 1350°F. If, however, debris collects outside the meltdown cup when it contains fuel, the forced circulation provided by the loop pump around the cup (5 lb/min) is sufficient to cool the cup plus a postulated bed of debris 12 in. deep composed of 0.005 in. particles with a porosity of 0.5. In this event, the sodium temperature may reach a maximum of about 1400°F. Even without forced circulation, the required cooling can be provided by natural convection of sodium, which may boil within the debris, plus helium cooling in the annulus between loop primary and secondary vessels.

10.4.2 Meltdown Cup

A meltdown cup (see Fig. 5.2) has been provided to prevent overheating of the primary vessel wall due to accumulated fuel debris or molten fuel.[18] The cup has been designed to contain 3.6 kg of molten fuel, plus 3 kg of molten steel. This quantity of fuel corresponds to half of the fuel from 37 full-length elements and all the fuel from 19 full-length elements, but much less than half of the fuel from a test subassembly is expected to reach the meltcup. This conclusion will be verified further by the tests involving only 19 elements. The cladding and hex can surrounding the fuel and instrumentation at the lower end of the test train contain about 6 kg of steel. Because of sodium cooling of the external wall of the hex can and the outer portions of the bottom section, less than 3 kg of steel may melt.

The cup can only contain a total of about 2 kg of fuel and cladding as solid debris, because of the lower bulk density for particles.

The meltdown cup has been designed to afford adequate heat removal during any possible circumstance while protecting the primary vessel from failure due to overheating. The most severe heat removal case would result from the rapid introduction of molten fuel and steel into the cup without any interaction with sodium in or above the cup. With the exception of melting temperature, the important thermal properties of UO_2 and mixed UO_2-PuO_2 are indistinguishable within the accuracy of available data. The higher melting point of UO_2 was used as more conservative for analyzing effects of molten fuel.

The cup must accept the latent and sensible heat of the fuel and accompanying steel as well as provide for removal of the decay heat generated in the fuel. The cup region is exposed to a low neutron flux; fission heating will be less than 0.6 kW in the collected fuel, even if ETR scram were delayed. (The fuel from 37 FEFP fully enriched elements, if accumulated in a sphere and surrounded by water, would be 1/10 of a critical mass.[19]) Gamma ray heating in the cup region with fuel present would be about 2.8 kW when the ETR is at power. Many of the fission products are too volatile to remain in molten fuel. Hesson[20] has calculated that for the first 15 minutes the beta-gamma heat generation will be lowered more than 35% because of vaporized elements and compounds. The delayed-neutron emitters are all volatile.

The heat generation rate used for calculations is based on the American Nuclear Society's proposed standard[21] ANS-5.1. These values were modified as follows:

1) increased 20% to the top of the uncertainty band,
2) increased 5% to allow for uncertainty for plutonium fissions,
3) decreased 35% for volatilized elements,
4) decreased 15% for escaping gamma rays,
5) decreased 10% for finite irradiation time
6) increased 2-1/2% for U-239 and Np-239 decay,
7) increased 1.0 kW/kg fuel to account for fissioning and gamma heating from ETR for first 7 sec (assuming ETR scram at 7 sec after fuel falls to cup due to detection of primary vessel temperature >1025°F).
8) increased by $0.55/t^{0.18}$ kW/kg for times greater than 7 sec to allow for gamma heating from the ETR.

The resulting heat source* is summarized in Fig. 10.17 for an average operating specific power of 11.8 kW/ft ($196\ \frac{kW}{kg}$) for the FEFP fuel prior to the meltdown.

The meltdown cup is designed to prevent boiling of molten fuel. This requires that the thickness of collected fuel be restricted; the central core of the cup (see Fig. 5.2) is provided for that purpose. (The core also increases the heat capacity of the cup and assists in quenching molten fuel.) The cup is located away from the primary vessel wall to allow sodium cooling between the cup and the wall. If molten fuel falls into the cup, the fuel surface temperature will drop quickly because of rapid heat loss to the cooler cup, sodium and steel. This quenching reduces the immediate requirements for heat removal from the system; however, within about 2 minutes "steady-state" heat removal must be established.

---

* Determined by: (ANS 5.1 value) x (1.0 + 0.2 + 0.05) x (0.65 × 0.85 × 0.9 + 0.025) + (ETR γ's + fission) = (ANS 5.1) × 0.65 + (ETR γ's + fission)

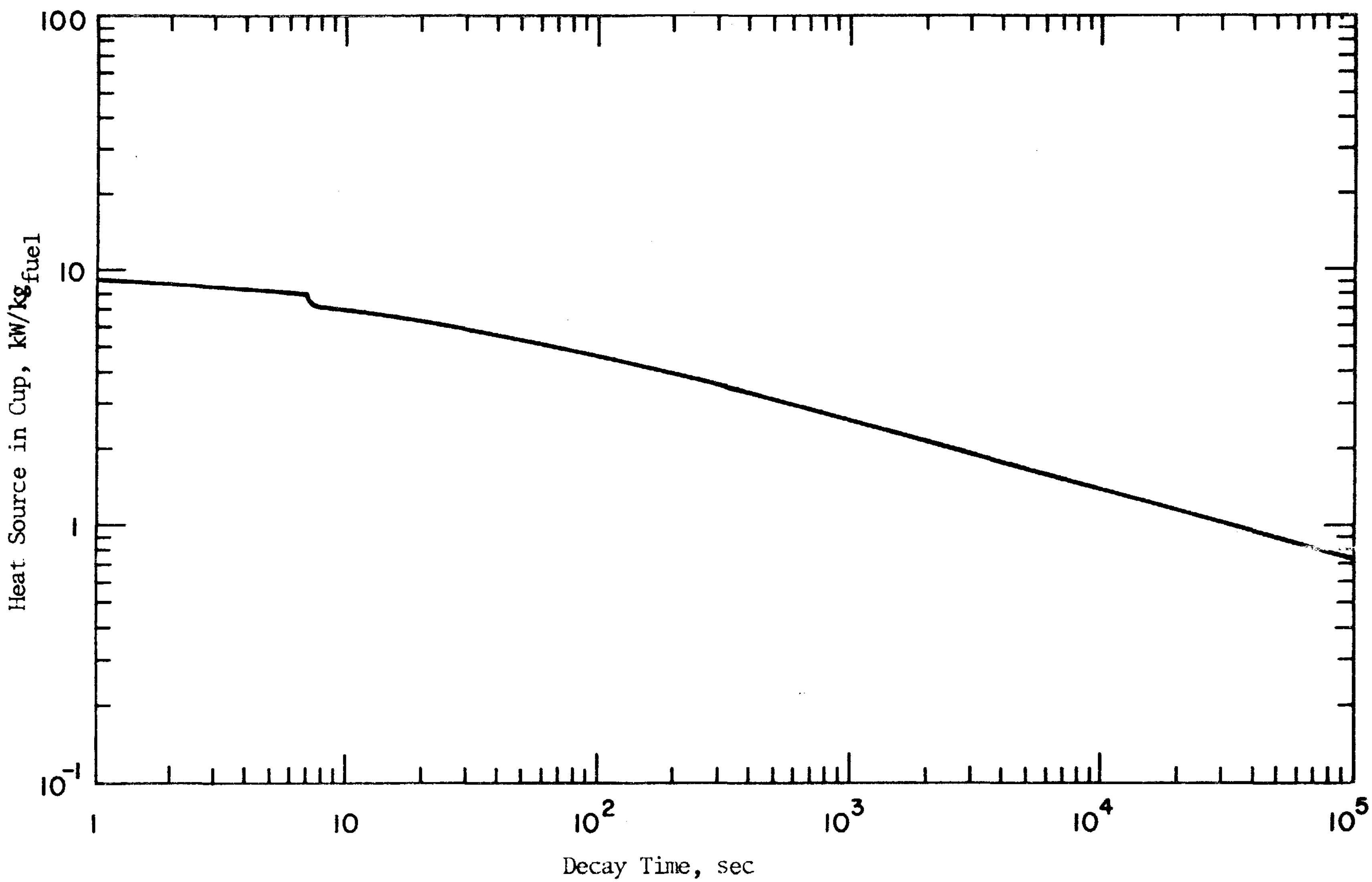

FIG. 10.17 - Meltdown Cup Heat Source

There is no satisfactory material of construction for the cup that is compatible with both molten fuel and molten steel, but, if adequate heat removal is provided, the molten phases will be contained in a frozen wall of fuel and steel on the cup surfaces. Tungsten has been selected as a cup material because of its high melting point, low coefficient of thermal expansion, and high-temperature strength. Although the brittle-to-ductile transition temperature is above room temperature, it is below the temperature of the sodium in the lower portion of the loop. Tungsten is generally used to contain molten UO_2 and $(U,Pu)O_2$ in experimental programs (e.g., studies of high temperature properties[22]). The melting temperature for UO_2 is about 5160°F,[22] and the solidus temperature of $(0.8U, 0.2Pu)O_2$ is 5050°.[23] The melting point of tungsten is 6170°F,[24] and the atmospheric-pressure boiling temperature of UO_2 is about 6200°F.[22]

The cup is designed as a double-walled vessel with the tungsten inner vessel supported in an Inconel outer vessel. The Inconel vessel is hung from the flow divider as illustrated in Fig. 5.1 . The Inconel vessel is designed to meet the strength requirements of the cup. Thermal shock and pressure pulses from molten fuel-sodium interactions were both considered.[18] As shown, the tungsten and Inconel may be thermally bonded by liquid sodium, while the gap between the vessels remains below the sodium boiling temperature; however, the sodium would boil out at higher temperatures and a major heat transfer resistance would be provided by the sodium-vapor in that gap. The increased resistance reduces the heat flux to the system outside the Inconel and lengthens the time for the initial quenching of the hot fuel and steel. A room temperature gas gap of 0.02 in has been calculated to be optimum to delay the heat transferred to the primary while not causing boiling in fuel collected in the cup. (The gap reduces to about 0.005 in during a meltdown event.) It is a design requirement that a resistance equivalent to such a gap be provided between the Inconel and tungsten walls either as a gap or as an insulating solid.

Two codes were used for the heat transfer calculations for the meltcup region of the loop; a modified version of THTB a general heat transfer code, and MELTCUP[18] an explicit code for the present application. Cylindrical symmetry was assumed for all calculations; two-dimensional calculations were made using THTB.

Heat transfer by conduction and radiation through the annulus between the primary and secondary vessels would be about 3 kW in the local region adjacent to the meltdown cup with stagnant sodium outside the cup at a temperature just below boiling. Forced helium flow at 2 lb/min in the annulus will increase the heat removal from this region of the primary vessel to about 10 kW. If the heat load from the cup is larger, the sodium around the cup will boil to remove the balance of the heat over a greater area. Even without forced helium circulation, boiling is calculated to remove at least 12 kW. Calculations were made to verify that this boiling rate would be stable, that is, that liquid sodium could flow down the annular region past the rising sodium vapors. Several gas-liquid flooding correlations were considered and boiling rates up to 20 kW appear stable.[18] However, as an added protection, three tubes are located in the downcomer region of the loop, from below the pump to below the meltdown cup, to provide a path for return of liquid sodium that does not contact the rising vapors. These tubes have the added feature that they provide a path for forced sodium circulation past the cup under normal conditions when the sodium pump is operating (approximately 1% of the loop sodium flow will go through the tubes and past the cup).

At a loop sodium circulation rate of 100 gpm, the flow past the cup will be 0.9 gpm which is sufficient to prevent sodium boiling and limit the primary vessel temperature to less than 1300°F. If the pump is not operating, boiling will occur and establish thermal convection. Sodium vapor will flow up the loop, lose heat, and condense over a distance of several feet.

Figure 10.18 summarizes calculated temperatures of the inside of the primary vessel wall adjacent to a meltdown cup following the collection of a large amount of molten fuel at 5300°F. For these calculations, the initial temperature in the cup region was taken as 900°F. It was assumed that the gap between the tungsten and Inconel was 0.02 in. at room temperature and was filled with sodium vapor. If a solid insulation is substituted for this gap, the heating rate for the primary vessel will be lower because thermal radiation will be prevented. From these calculations, it is concluded that the primary will not exceed 1300°F, if the normal sodium flow is maintained in the loop. If the sodium flow drops below about 10% of normal, the sodium outside the cup may boil. For the cases presented, the maximum heat removed by boiling is 4 kW for Case 2 (with forced He cooling) and 12 kW for Case 3 (no He cooling).

Normally, it is expected that heat will be removed from the meltdown cup by forced convection because the loop pump and heat exchanger are designed to operate continuously during an experiment. Nevertheless, should cooling by natural convection be required, the primary vessel temperature may reach 1800 to 1900°F. Under these conditions, with no pressure head from the ALIP,

Temperature of Inside Surface
Of Primary Vessel
Adjacent to Meltdown Cup
Following Collection of Fuel at 5300°F

Case	Loop Sodium Flow, gpm	Helium Flow, lb/min
1	100	2
2	0	2
3	0	0
4	100	0
5	10	2

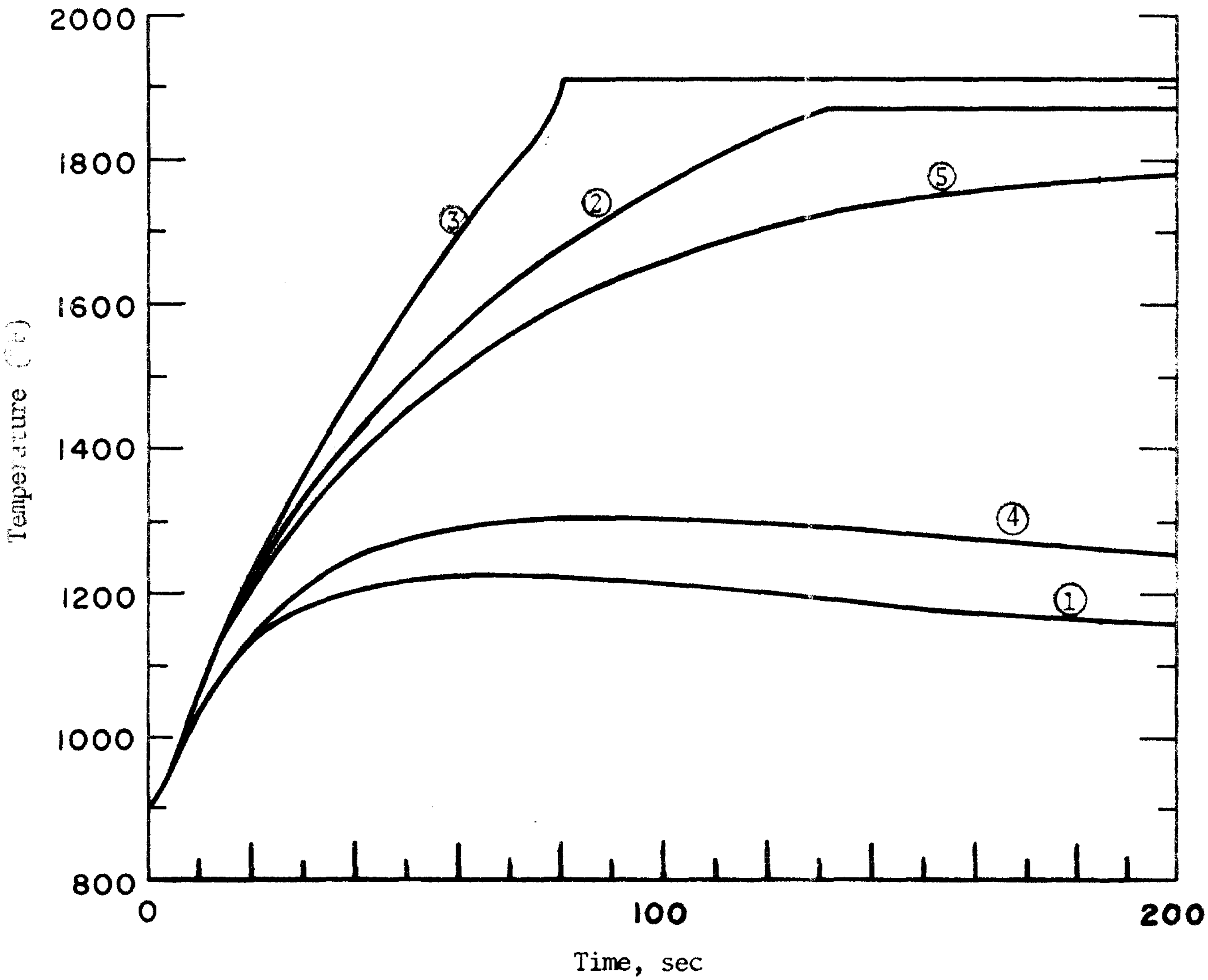

FIG. 10.18

the pressure within the primary vessel will be about 50 psia, whereas the normal annulus gas pressure is 275 psia. Thus, there is a 225 psia differential buckling load across the wall that must be considered. Using a yield strength for 316 stainless steel of 4500 psi at 1900°F, the calculated buckling pressure is 510 psi.[25] Therefore, in the very remote event that forced circulation were not available, the primary vessel would not buckle at the temperature that may be reached during natural convection cooling.

The Inconel cup has been analyzed for thermal stresses due to molten fuel and steel collecting in the cup. The results of these calculations indicate that the cup will survive the thermal shock. An experiment involving dropping 3 kg of a mixture of molten UO_2 and a Cr-Mo alloy into a simulated meltdown cup produced no detectable thermal stress damage to the cup.[18]

Because of its higher thermal conductivity, molten steel can lose latent and sensible heat more rapidly than fuel. Thus, molten steel may cause rapid heating of the cup region, but since there is no heat generation, high temperatures will not persist around the steel. Figure 10.19 compared primary vessel temperatures for two calculated cases for molten steel in the meltdown cup with a comparable case for molten fuel at 5300°F (Case 2, Fig. 10.18). These results indicate that unless the steel were about 4500°F (2000°F over its melting range) that even the short-term effect on the primary vessel is less than that for fuel at 5300°F.

Peak fuel temperatures are presented in Table 10.8 for conditions with and without helium and sodium flow. Two maxima are observed for each case. The first occurs in the middle of the fuel, while the cup and its core are acting as heat sinks. The final maximum temperature occurs adjacent to the tungsten core before the outside of the fuel had cooled sufficiently and the heat generation rate has become low enough to allow all of the decay heat to be removed. The fuel temperature is relatively insensitive to the heat removal scheme because of the fuels low conductivity ($\sim$1.3 Btu/hr-ft-°F). The maximum temperature rise calculated was 800°F for fuel initially at 5300°F. At the pressure in the bottom of the loop (>50 psia), the boiling temperature of the fuel will be >6700°F. If fuel at 6200°F entered the cup, the peak fuel temperature was calculated to be 6465°F. Because of the cooling by sodium and by melting and boiling steel, there appears to be no way to get fuel with an average temperature as hot as 6200°F down to the meltcup.

The insulating effect of the gap between the tungsten and Inconel walls of the meltcup may cause molten steel to be against the tungsten wall for several minutes. Since the solubility of tungsten in the steel constituents

Primary Vessel Inside Temperature
Following Collection of Molten
Material in the Meltdown Cup

Basis No Na Flow, He at 2 lb/min

Case 6 - Steel in cup at 3500°F
Case 7 - Steel in cup at 5000°F
Case 2 - Fuel in cup at 5300°F

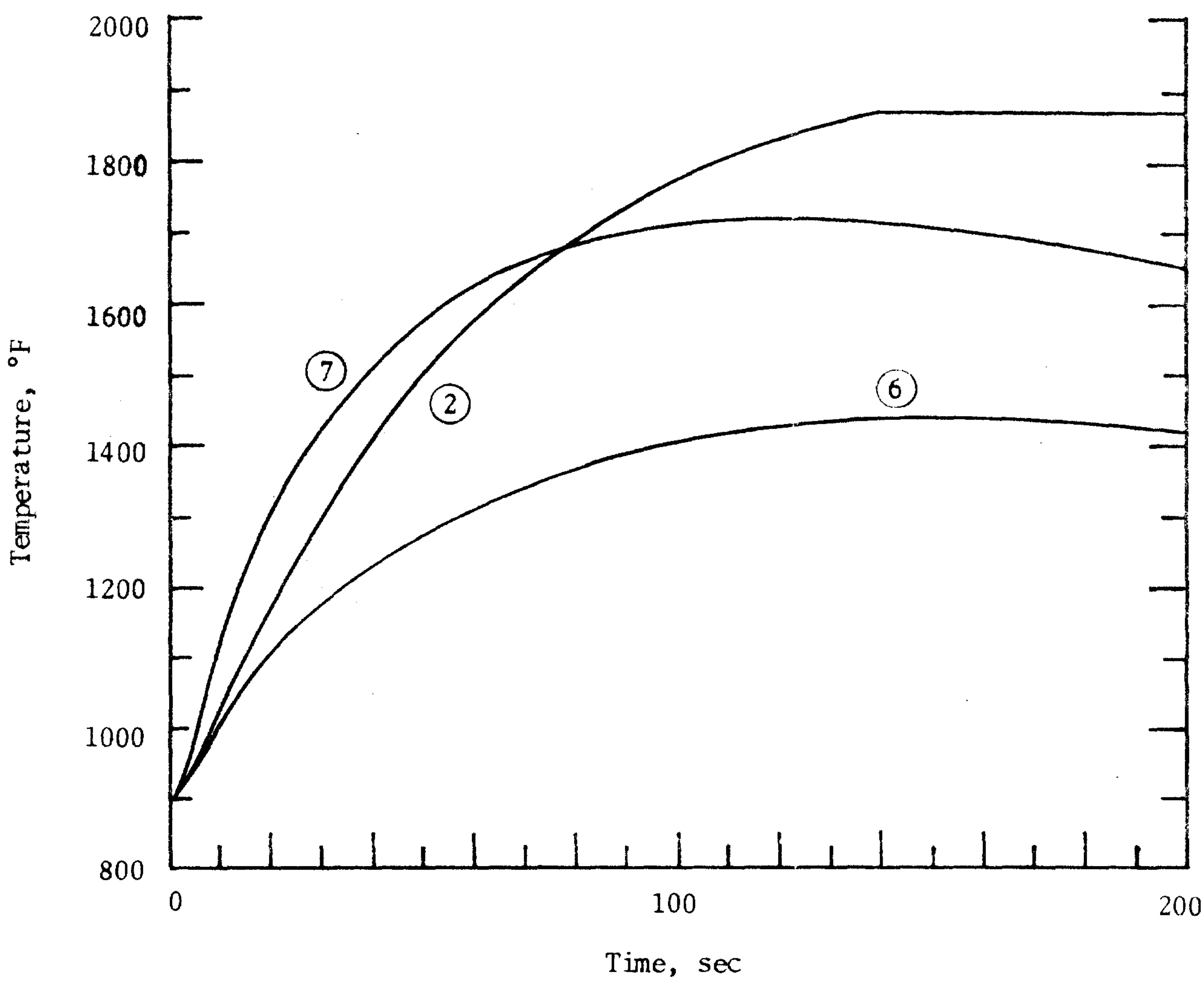

FIG. 10.19

TABLE 10.8

Calculated Peak Fuel Temperatures in the Meltdown Cup

Initial Fuel Temperature, °F	5300	5300	5300	6200
Sodium Flow in Loop, gpm	100	0	0	0
Helium Flow in Secondary, lb/min	2	2	0	2
First Peak				
Time, sec	26	25	25	16
Temperature, °F	5685	5680	5680	6465
Second Peak				
Time, sec	420	525	533	440
Temperature, °F	5895	6100	6100	6330

is high (~30 wt% at melting temperatures[26]), some dissolution of tungsten that is adjacent to molten steel is expected. The quantity of steel necessary to dissolve through the tungsten is fairly large (equivalent to a 1/2 in. thick layer), and corrosion through the tungsten appears possible only in a region of the cup above the fuel. If the tungsten inner vessel is breached, the liquid steel (or fuel) solution will freeze instantly on the well-cooled Inconel surface. Direct steel contact with the Inconel vessel will increase heat transfer to the sodium outside the cup, but the delay that is inherent in the tungsten dissolution (minute or more)[18] and the absence of heat generation in the steel result in heat transfer requirements that are less than those for the unfailed region of the cup that contains fuel.

As discussed in Chapter 7, the scram will be initiated and helium flow started when the temperature on the outside of the primary vessel reaches 1025°F. If there is a large amount of fuel in the meltdown cup, the primary vessel temperature will continue to rise. For the case where there is no sodium flow (Case 2), the temperature will reach 1300°F (average) in an additional 18 sec. This case was used in the Chapter 7 analysis. After scram, the heat generation in the test train will drop to about 10% of its full power value. The fuel and steel that already passed through the test section entrance will either have plugged or nearly plugged the bottom of the test section; at the reduced power, any additional fuel or steel that drains into the entrance region will freeze and plug the bottom of the test section.

Two-dimensional calculations using THTB for a large amount of molten fuel and steel in the meltdown cup indicate that at the time the primary vessel wall reaches 1300°F (at the midpoint), the fuel and steel will have cooled such that the fuel has a frozen crust 0.2 in. thick on the top surface. A thin crust also will cover the molten steel sitting above the fuel. These frozen barriers will prevent the intermixing with sodium that would be necessary for a fuel-coolant thermal interaction.

An assessment was made of the effect of the concentrated decay heat source that may exist in the meltdown cup on removal of the loop from the ETR.[18] The loop may be removed from the ETR water after about 2 days cooling. If the loop were hung in the LHM without sodium circulating, the sodium near the cup will boil and spread the heat over sufficient surface of the loop (about 2 linear feet) so that natural convection will remove all the heat that is generated. When the sodium pump is operating, the sodium around the cup will remain below its boiling temperature.

10.4.3 Secondary Vessel

It has been concluded that the flow divider and meltdown cup will protect the primary vessel from meltthrough. However, if these defenses fail and a large quantity of molten fuel collects against the primary vessel wall, the primary may also fail and introduce fuel into the secondary vessel. Calculations were made for hypothetical cases in which molten fuel or molten steel entered the gap between the primary and secondary vessels. Secondary temperatures and heat fluxes to the ETR water that were calculated for fuel at 5300°F and for steel at 3000°F are presented in Figure 10.20[18].

These heat fluxes are not excessive into the subcooled ETR water. The peak flux is about 1/2 the burnout limit to a pool of water at its saturation temperature[18, 27].

10.4.4 Loop Sodium Filter

A filter screen, located about 16.5 ft above the test section in the test train (see Fig. 5.1), is provided to prevent the fuel and other debris generated in an experiment from interferring with the continuation of an experiment. Of major concern is the continual circulation within the loop of large solid particles that could conceivably accumulate in the heat exchanger, clog the ALIP (annulus ∿ 0.180 in), or collect in the inlet regions of the fuel section. These effects might possibly distort or disturb the required test conditions and, therefore, mask the experimental results.

The filter screen design represents a compromise between the desirability of having a screen with large openings to reduce the potential pressure drop when loaded, and the desirability of having small openings to maximize the retention of fuel and debris. The final design of the filter is an annular 30-in. long and 2 in. in diameter, consisting of 20 mil stainless steel wires. The mesh spacing is 14 x 14 wires to the inch resulting in a 0.051 in. opening. All loop flow areas have at least a 0.1 in. minimum flow diameter. Therefore, the possiblity of a large flow blockage in the heat exchanger and other loop regions (pump, downcomer, etc.) from particles less than 0.050 in. in diameter is remote. Collection of these small particles (∿ 1250 μ) will present no cooling problem in the flowing sodium system outside the high neutron flux region.

The safety aspects of fuel accumulation at this filter screen are assessed and summarized herein. The basic considerations are the potential for:

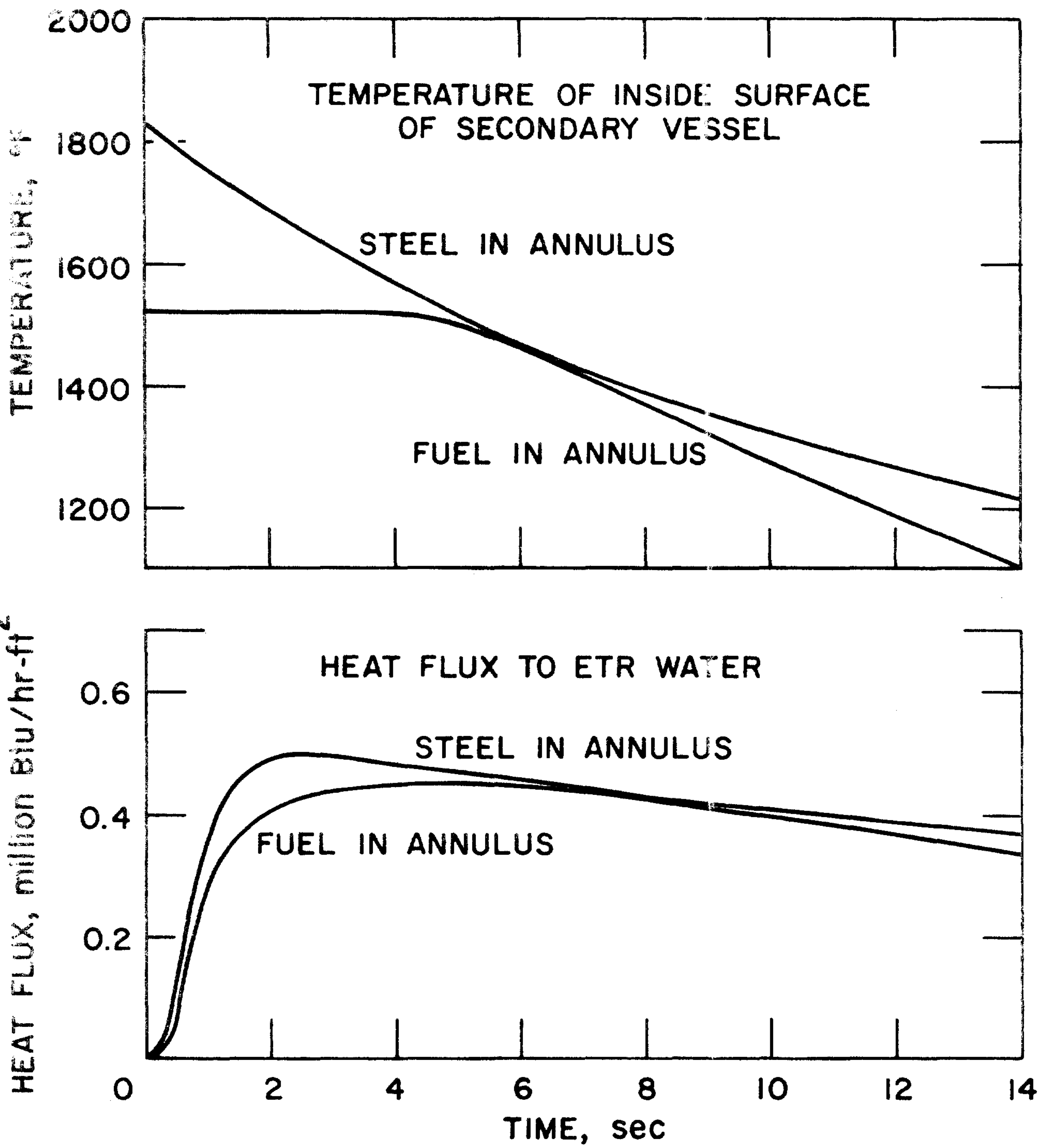

Fig. 10.20 Fuel at 5300°F or Steel at 3000°F in the Annulus Between the Primary and Secondary Vessels

1) transporting fuel and debris to the filter
2) debris to clog the filter
3) melting through the filter
4) filter damage and failure

Each of these potential problem areas is discussed.

Fuel and Debris Transport to Filter

In evaluating the modes of transport for the fuel-debris, it is necessary to consider the potential driving forces. Basically, there are two: the pressure differential created by the ALIP, and the possible fuel-coolant interactions in the test section. Molten fuel coolant interactions (MFCI) capable of driving large quantities of fuel to the filter ($\sim$ 16.5 ft above the test section) would necessarily be large - of the order of the design envelope MFCI source intensity. Because pressure pulses of this magnitude are not considered possible, attention is turned to more realistic fuel and debris motion under less severe operating conditions where loop flow is the major driving force. Therefore, the analyses are focused on this driving force.

The potential for fuel transport to the filter region is analyzed using the pressure driving forces and hydraulic characteristics of the loop, along with a simple Stokes Law type force analysis for the particles. Assuming creation of a bed of fuel particles within the test section, from fluidized flow theory, the minimum pressure drop and loop conditions required to fluidize the bed are calculated. In this idealized analysis, liquid sodium driving forces at flow conditions around the full flow loop point (9.5 lbs/sec through test section) are evaluated and compared to the terminal velocity of the fuel particles. (If the superficial velocity is larger than the terminal velocity, the particles will be carried to the filter.)

There are two major observations from these simplified calculations. First, even for pump pressures as low as 20 psi ($\sim$ 80 psi is the rated 150 gpm full flow condition), particles less than 5000 μ in diameter could be carried to the filter. Particles much smaller than these are expected to be created during fuel-coolant interactions (i.e., on the order of 30-500 μ). Typical experimental particle size distributions, presented in Fig. C.3 of Appendix C, indicate that essentially 100% of the fuel particles will be less than 5000 μ in diameter.

The second observation is that the results are not affected by the quantity of fuel-debris in the bed. The reason for this is that the pressure drop across the bed is only a small fraction of the total pressure drop in the test section leg in the highly idealized calculational model.

Without conducting an extensive prototype testing program, it must be concluded that all fuel debris formed in the test section could ultimately be relocated at the filter. It should be recognized that this conclusion is based upon the results of a highly idealized analysis. In actual practice, debris in irregular shapes could become clogged and jammed in the fuel section thus reducing the quantity of fuel-debris transport to the filter. In addition, the many instrument leads between the test section and the filter provide sites for fuel and debris collection not considered in this idealized analysis.

The Potential to Clog the Filter

Given that fuel and other debris can be carried to the filter screen, the potential for clogging and significantly reducing loop flow is assessed. This clogging potential is, of course, dependent upon the quantity of the particles, size, and porosity of the bed created. Parametric studies were, therefore, conducted with the major results summarized below.

If all of the fuel (37 pin full length bundle) were packed against the screen to form a cylindrical shell with a minimum porosity of 35%, the thickness would be 0.271 in. The pressure drop (based upon packed bed theory) is a function then solely of the particle size. The calculations at 150 gpm loop flow indicate that the pressure drop could not exceed 10 psi unless the particles are less than 60 μ in diameter. This translates into a loop flow reduction of about 7% based upon the normal 80 psi pressure drop at 150 gpm flow through the loop. Assuming the particles are all ∿ 2150 μ in diameter (equal to the 0.051 in screen opening at 150 gpm loop flow), the pressure drop across the bed is less than 1 psi. A 5 psi bed pressure drop is indicated for particles of the ∿ 100 μ diameter. This 100 μ size represents the average of the experimental fuel particle distribution data observed in previous fuel failure tests (see Fig. C.3 in Appendix C).

The above results are obtained based upon conservative conditions. If less than 100% of the fuel were present, or if the bed porosity were increased, the pressure drop would be even less. Realistically, particles would preferentially collect at the end of the screen leaving smaller amounts at the inlet. This bed configuration would also reduce the resultant loop pressure drop. Thus, it is clear that under expected conditions, large quantities of fuel debris (up to and including the total amount from a 37 pin test bundle) could accumulate at the screen without resulting in an adverse loop flow rate reduction.

The Potential for Melting Through the Filter

The filter screen is located about 16.5 ft above the active ETR core region; therefore, decay heating is the principal heat generating source in the fuel bed created in this loop region. As discussed in the previous sections, with the present vertical filter screen design, a maximum annular bed thickness of only about 0.271 in could conceivably be formed from all of the fuel in a 37 pin test bundle. Calculations based upon the work of Hesson[19] indicate that the decay heat from a bed with a thickness of several feet could be adequately cooled by the flowing sodium without boiling of the sodium. Therefore, a considerable thermal margin exists using the expected conditions in the filter region.

However, even assuming a complete flow stoppage through the filter, no adverse safety problem is anticipated. The small particle size along with the voidage in the bed suggests that local sodium boiling will maintain a sodium filter temperature well below the melting temperature of steel. This condition, along with the large heat sinks available in the upper loop regions provide additional assurance that fuel debris can be safely retained in the loop filter region.

Potential for Filter Damage and Failure

The physical location of the filter screen, far removed from the test section and shielded by the instrument leads, reduces it susceptibility to damage from missiles or shockwaves from an MFCI event. The annular screen design also minimizes the threat of direct frontal attack by events in the test section. Material transported within the rapidly expanding reaction zone during an MFCI are not expected to reach the filter region. Collapse of the MFCI reaction zone is expected well before it reaches the filter.

Although total loss of the filter screen is not likely, the safety implications of this occurrence do not appear to be very severe. A suspension of these fine fuel particles circulating in the sodium will reduce the reactivity of the coupled FEFPL/ETR system, because $\sim$ 90% of the loop sodium inventory is outside the active region. The FEFPL design which consists primarily of annular flow paths also precludes the possibility of a complete flow blockage due to debris collection. The efficient heat removal capability of the sodium will maintain the temperature in the vicinity of a local collection of fuel debris well below the level which could conceivably affect containment integrity. Sodium boiling at 1800 to 2000°F provides a heat removal mechanism which precludes the local melting of loop structure components.

10.5 Reactivity Effects

10.5.1 General

The nominal fission power in a 37-pin test section in FEFPL is about 1300 kW. This amounts to less than 1% of the total coupled system with the loop in ETR at 175 MWt. To assess the potential feedback from the loop to the ETR core during the reference transient presented in Section 10.2, a number of events were examined including:

1) loss of sodium coolant
2) fuel compaction outward
3) meltdown of fuel

Other reactivity effects between the loop and ETR (i.e., loss of water in annulus outside of secondary and water flooding of FEFPL test bundle) are discussed in the appropriate accident sections in this report. Calculations of reactivity were made using the one-dimensional diffusion-theory code MONA.[28] A pointwise flux-convergence level of 0.00001 was attained in all calculations. A 26-group spectral structure was used. Cross sections for the three highest lethargy (smallest energy) groups were calculated using the INCITE code. Cross sections for the remainder of the groups were generated by the fast spectrum code PHROG.[29] Since PHROG calculates cross sections corrected for resonance self-shielding, separate PHROG runs were made for the different fuel configurations involved in the postulated incidents.

10.5.2 Loss of Sodium Coolant

For investigating loss of coolant, the sodium was replaced with a void having a diffusion coefficient of 1.0 in all groups and having zero absorption. This treatment of the void ignored a possible increase in neutron leakage out the end of the test section; however, this is in the direction of conservatism and greater reactor safety. The change in reactivity accompanying the loss of sodium was 0.015%. This corresponds to a stable reactor transient period of about 600 sec, well above the 5 sec period for which the reactor begins automatic shutdown, or the period of 1 sec which triggers an electronic scram. The prompt jump power level increase for this reactivity insertion will be only about 2%. Thus, experiments in which the sodium coolant is expelled from the test section should not present a reactivity problem.

10.5.3 Fuel Compaction Outward

In this case, it was assumed that the hexagonal can would deform into a right circular cylinder with the inner wall in contact with the outer wall. The fuel elements were uniformly compacted against this wall with the ratio of fuel to clad materials unchanged. The calculation shows that the ETR reactivity increased by 0.019% by this accident. This reactivity results in a asymptotic reactor period of about 470 sec; as with the previous case, the consequences are well within the capability of the reactor to control. A maximum ETR power level increase of about 2.5% would result.

10.5.4 Meltdown of Fuel

The meltdown accident was postulated to proceed as follows: the top two-thirds of the fuel melts and fills the hexagonal can for the middle third of its length. Attainment of this compaction would be very remote in actual practice. Above this melted-down lump is void or sodium, while below it is the normal fuel configuration. A combination of the results for several one-dimensional cases indicates that the increases of reactivity for the postulated incident would be small enough so that a more precise two-dimensional calculation is not necessary.

With melted, high-density fuel extending the full test section length, the calculations show that the ETR reactivity change would be +0.58% relative to the normal fuel configuration; however, only the middle 12 in. contain this material in this postulated accident. With sodium completely filling the test section (no test fuel), the ETR reactivity change is -0.79% relative to the normal fuel configuration; however, only the upper 12 in. would contain only sodium in this postulated accident. For this accident, the lower 12 in. are filled with normal fuel. The actual ETR reactivity change that would result from this postulated meltdown accident is a combination of the two maximum reactivity changes as computed by MONA (+0.58% and -0.79%). These reactivities were combined by assuming that the ETR axial and adjoint fluxes at the surface of the loop followed a cosine distribution, and therefore a cosine weighting function was used.

Assuming a 3.0 in. reflector savings, the effective half-length of ETR is 21.0 in. By letting the neutron flux go to zero at the extrapolated length, the cosine distribution of the flux is

$$\phi(\ell) = \cos \frac{\pi}{2} \cdot \frac{\ell}{21.0}$$

where ℓ is the distance in inches from the reactor center. This quantity squared is the weighting function used to combine the reactivity changes associated with the two extremes. The weighting factor for the +0.58% reactivity change was obtained by integrating from ℓ = -6.0 to +6.0 in., and the factor for the -0.79% change was obtained for ℓ = -6.0 to 21.0 in. These integrations gave weighting factors of 0.54 and 0.23, respectively.

The combined reactivities lead to a predicted ETR reactivity change of +0.12% for this postulated accident. In such an accident, there would be an increase in the leakage from the loop that would cause a small reactivity reduction. An additional calculation in which the melted fuel was replaced by void rather than sodium gave a difference in reactivity less than 0.01%; therefore, it makes very little difference whether or not the sodium is expelled in this meltdown accident. The reactivity increase of 0.12% corresponds to an asymptotic period of about 50 sec. For this conservative fuel compaction reactivity insertion, a prompt jump ETR power level increase of about 20% is indicated. Although this is well within the capability of the reactor control system, it is possible that a rapid compaction may cause short-term transients in local neutron density which could trigger a reactor scram. If it were desirable to continue the test at power through this incident, a detailed analysis would be needed to determine the proper settings for the reactor safety signals (such information will be included in the detailed plan issued prior to each experiment in which a meltdown of this type is possible).

References

1. W. Bohl, et al., "A Preliminary Study of the FFTF Flow Coastdown Accident," ANL/RAS 71-39 (Rev.1),(April 1972).

2. H. K. Fauske, Procedures from International Seminar on Heat Transfer in Liquid Metals, Tragir, Yugoslavia, (September 1971).

3. T. Johnson, Argonne National Laboratory, Personal Communication, (June 1973).

4. D. R. Armstrong, F. J. Testa and D. Raridan, Jr., "Interaction of Sodium with Molten UO_2 and Stainless Steel," ANL-7890, (December 1971).

5. L. W. Deitrich, Trans. Amer. Nucl. Soc., 15, 816, "TREAT Mark-II Loop Experiments on FFTF-like Pins Having Local Overenrichment, (1972).

6. A. W. Cronenberg, H. K. Fauske and D. T. Eggen, Nuclear Science and Engineering, 50, 53-62,"Analysis of Coolant Behavior Following Fuel Failure in Molten Fuel Sodium Interaction in a Fast Nuclear Reactor," (1973).

7. H. K. Fauske and A. W. Cronenberg, Trans. Amer. Nucl. Soc., 15, 344, "The Behavior of Small Amounts of Released Molten Fuel in an LMFBR".

8. D. H. Lennox, et al., "Containment Study for the FEFP In-pile Loop," ANL/RAS 71-36, (November 1971).

9. W. R. Wise, Jr. and J. F. Proctor, "Explosion Containment Laws for Nuclear Reactor Vessels," NOLTR 63-140,(August 1965).

10. C. K. Youngdahl, "Correlating the Dynamic Plastic Deformation of a Circular Cylinderical Shell Loaded by an Axially Varying Pressure," ANL-7738, (October 1970).

11. N. M. Newmark, "An Engineering Approach to Blast Resistant Design," Pro. Amer. Soc. Civil Engrs., (October 1953).

12. R. R. Alvy, "Design of Pressure Vessels and Piping Containing Explosive Mixtures," Holmes and Narver, Inc., Los Angeles, Cal., NP-6516, (1957).

13. H. M. Minami, "FEFPL-HX Interim Design Report Stress Analysis," AI Report TI-542-320-007, (July 28, 1972).

14. T. K. Burr, "ETR-FEFPL Top Dome Flange Section III Design Stress Analysis Final Report," ANC Report TR-304,(September 14, 1972).

15. J. Fisher, J. Schilb, "Reactor Materials Fuel Phase Studies at High Temperatures," in Chemical Engineering Division Annual Report-1970, ANL-7775, P. 78, (1971)

16. J. Schilb, ANL, Personal Communication, (September 1972).

17. D. R. Pedersen, et al., "Support Studies for In-pile Program - Meltdown Cup," ANL-RDP-18, (July 1973).

18. R. D. Pierce, C. A. Blomquist, D. R. Pedersen, "Design Criteria and Evaluation of a Meltdown Cup for Fuel Element Failure Propagation in In-pile Loops," ANL/RAS 73-31, March 1974.

19. ANL Memorandum, R. T. Curtis to W. A. Kaspic, "Consideration of Inadvertent Criticality during Loop Handling Operations", January 4, 1974.

20. J. C. Hesson, R. H. Sevy, and T. J. Marciniak, "Pestaccident Heat Removal in LMFBRs: In-vessel Considerations," ANL-7859, (September 1971).

21. Amer. Nucl. Soc., "Proposed ANS Standard Decay Energy Release Rates Following Shutdown of Uranium Fueled Thermal Reactors," ANS-5.1, draft, (November 1971).

22. M. Chasanov, et al., "Reactor Safety and Physical Properties Studies," in Chemical Engineering Division Annual Report-1970, ANL-7775, pp. 71-79.

23. J. L. Krankota and C. N. Craig, "The Melting Point of Plutonia-Urania Mixed Oxides Irradiated to High Burnup," GEAP-13515, (July 1969).

24. E. Geghardt and R. Rothenbacker, "Physical Properties of Refractory Metals", in the Science and Technology of W. Ta, Mo, Nb, and Their Alloys, N. E. Promisel, Ed., Pergamon Press and MacMillan, (1964).

25. ANL Memorandum, P. Wang to D. H. Lennox, (June 28, 1973).

26. M. Hansen and K. Anderko, "Constitution of Binary Alloys," pp. 571-734 and 1058, McGraw-Hill Book Co., New York, N.Y., (1958).

27. J. P. Holman, "Heat Transfer," McGraw-Hill Book Co., Inc., New York, N.Y. (2nd Edition) p. 288.

28. G. E. Putnam, "Multigroup One-dimensional Neutronics Analysis Code, IDO-17225.

29. PHROG, Phillips Petroleum Co., Program Library File, No. 400134.

30. Proceedings ANS Topical Meeting on Fast Reactor Safety, R. K. Fauske, "Some Aspects of Liquid - Liquid Heat Transfer and Explosive Boiling", (April 2-4, 1974).

CHAPTER 11.0

TABLE OF CONTENTS

LIST OF TABLES

LIST OF FIGURES

11.0 Operational Accidents

11.1 General

In this chapter, various accidents including loop system malfunctions or failures, plus in-reactor accidents that may be initiated within the loop, or external to it, are evaluated to ensure that the multiple levels of defense effectively prevent damage to the ETR and protect personnel. As described in Chapter 3, under the first level of safety, extensive safety precautions and procedures will be invoked during the design, construction and operation of the loop and loop systems to prevent accidents. However, it is recognized that in spite of these safety precautions and controls, the possibility of operational abnormalities cannot be completely ruled out. Therefore, consistent with the second and third levels of safety specified in Chapter 3, a wide range of low-probability events have been studied to make an assessment of their safety implications and consequences.

Treated in this chapter, then, are postulated accidents which are assumed to occur when the loop is at power in the ETR. Accident consequences are assessed for various degrees of loop control system intervention. A wide accident spectrum was investigated ranging from expected conditions where all loop systems perform as designed to various degrees of unprotected situations where it is postulated that some of the control and/or protection systems fail. Some of the latter accidents are hypothetical and belong more properly in Chapter 13 (Hypothetical Events); however, for continuity of presentation,they are discussed along with the expected conditions of accidents having the same generic origin that are arrested by successful control and/or safety system action. Other types of in-reactor hypothetical accidents (i.e., a condition having no credible sequence of initiating events) are presented in Chapter 13. Potential accidents associated with the various phases of handling the loop or during operation in the FS&R facility are discussed in Chapter 12.

11.1.1 Accident Analysis Approach

The approach to accident analysis is consistent with the safety philosophy as outlined in Chapter 3, and is summarized in Section 11.1.1.1. In Section 11.1.4 the FEFPL Safety Fault Tree which was used to identify the accident initiating faults and malfunctions is briefly discussed. The loop conditions and calculational bases used in these accident analyses are contained in Section 11.1.3. The evaluations and studies of specific malfunctions and abnormal operating conditions are categorized and presented in subsequent sections. In general these categories pertain to off-normal major loop parameters (e.g., loss of loop sodium flow) with the discussions focusing on various accidents which can lead to these perturbations.

11.1.1.1 Safety Philosophy

As described in Chapter 3, the FEFPL SAR philosophy is based upon three levels of safety summarized as follows:

1) The FEFPL system, as designed and as it will be constructed, tested, operated and maintained, provides a highly assured capability for reliable and predictable operation and an inherent capability to prevent the occurance of accidents.

2) The system is designed so that in the event of errors, malfunctions or off-normal conditions, protective systems and other features will arrest the event or limit its consequences to defined and acceptable levels.

3) The system design provides considerable margin for containment of extremely low probability or arbitrary postulated hypothetical events without exceeding accepted guideline values for the protection of public health and safety. (A detailed discussion of these three levels of safety is presented in Section 3.3 of Chapter 3).

As seen above, a major element of this approach is the systematic evaluation and analysis of accidents to insure that the operation of the FEFPL system in the ETR does not endanger the reactor, reactor personnel, or the general public. Therefore, accidents occurring while the loop is operated in ETR will be discussed within the general context of these three levels of safety. The evaluation of a specific malfunction or abnormal event will start with a discussion of the design and safety features provided to prevent the accident (Level 1). Next, the evaluation will focus on the accident consequences, assuming that in spite of these safety precautions the accident nevertheless does occur. The loop behavior will be analyzed for the realistic situation expected in which the loop control and/or loop protective systems function as designed to mitigate the accident consequences (Level 2). Finally, the safety margin will be assessed for accidents which require postulating partial failure of the protective systems in conjunction with an independent malfunction, recognizing that some of these accidents are presented in this chapter for continuity instead of in Chapter 13 where other hypothetical events are considered.

11.1.1.2 Calculational Methods

Many of the accidents were analyzed using a revised version of the THYME-B computer program to predict the overall loop thermal-hydraulic behavior. A brief description of this program is presented in Appendix B.1. Additional input was obtained for several of the more severe accidents (i.e., those resulting in sodium boiling or having the potential for generating molten test fuel) with the SAS2A computer program. The application of SAS2A to the FEFPL geometry and loop conditions is also discussed in Appendix B.2.

Representative accidental transients have been selected to meet the structural requirements of the July 1971 ASME Section III Boiler and Pressure Vessel Code for Nuclear Vessels. In these studies, the loop thermal-hydraulic behavior was predicted using the SINDA-3G Code (for description see Appendix B-10). These Section III transients are enveloped by the safety analyses presented in this chapter and therefore are not repeated herein. Results of some of these thermal-hydraulic studies have recently been published;[1] the complete Section III structural analysis report is expected in January 1974.

11.1.2 FEFPL Protection Systems

In addition to the safety action provided by the ETR Plant Protection System, two separate and distinct protective systems; the FEFPL Experiment Assurance System (EAS) and the FEFPL Plant Protective System (PPS), have been designed for the FEFP loop. These are briefly discussed below as they relate to the accident evaluations presented in this chapter. Further details of these systems can be found in Chapters 5 and 7.

11.1.2.1 Experiment Assurance System

An additional subsystem is provided as part of the loop control system to implement the tripartite safety approach that prevents accidents in FEFPL or mitigates their consequences. This system, called Experiment Assurance System (EAS), described in Chapter 5, is designed using RDT Standard C16-1T as a guide, protects the test train and other loop components such as the heat exchanger from inadvertent and costly damage should abnormal loop conditions occur prior to an experiment. This FEFPL-EAS system is part of the first level of safety in the defense against operational accidents evaluated in this chapter. It should be recognized that this system acts in a manner analogous to a nuclear reactor control system that would terminate an accident before clad damage or fuel failure could occur. Because the FEFPL program is designed to study fuel failure and the loop is designed to tolerate planned loop transients, the FEFPL-EAS is not essential to guarantee the safety of the FEFPL facility. Therefore, certain EAS functions may be bypassed (e.g., test section outlet temperature) during the experiment transient phase of a FEFPL test. However, all of the EAS functions will be in operation during normal steady state loop operation.

Features of the FEFPL-Control System pertinent to the accidents analyzed are shown in Table 11.1. Typical values are indicated for control action and scram set points. Final selection of these parameters will be made upon completion of the detailed loop control evaluations. These values may also change or be different for each experiment based upon the particular requirements of the test. Details of the major features of the FEFPL Control System are presented in Chapter 5.

11.1.2.2 FEFPL Plant Protection System

The overall safety margin of the FEFP loop will be guaranteed by the FEFPL Plant Protection System (PPS) discussed in Chapter 7. It must be recognized that the FEFP loop is a high performance test vehicle designed specifically for safety experiments; therefore the experiments planned will be made to purposely simulate LMFBR accident situations. Fuel failure and some test train damage are expected and represent a normal condition for the reference experiment to be used as the benchmark for evaluating all abnormal loop conditions including accidents. In Chapter 10, the conditions and safety evaluations of this reference experiment are discussed.

The FEFPL-PPS is designed to preserve the loop safety margin by sensing and taking preventative action on parameter variations which may lead to a possible reduction of the as-designed loop containment margin. When the loop is at power, the FEFPL-PPS monitors continuously the FEFPL containment vessel temperature and FEFPL systems pressures and initiates an ETR scram when excessive overpressures or overtemperature conditions are sensed. In addition, the FEFPL-PPS monitors for leaks in either containment vessel and automatically scrams ETR when a violation of double containment is observed.

TABLE 11.1

FEFPL Control System Parameters Employed in Accident Analyses*

A. LOOP CONTROL VARIABLES

Controlled Variable	Sensor Designation	Controlling Action	Initiation** of Action	Control Time** Constant
1. Sodium inlet temperature to test section sodium	TE 1	Helium flow to loop HX	+25°F	3.30 sec
2. Total sodium loop flow	FE 3	Pump voltage	-10% of full scale	1.00 sec
3. Test section sodium flow	FE 1	Bypass flow resistance	-10% of full scale	
Helium Control Loops				
4. Helium system total mass flow	TE 4, PE 4, FE 4	Helium circulators speed	-10% of full scale	3.30 sec
5. Helium temperature at circulator inlet	TE 5	Bypass around helium primary HX	+25°F	1.67 sec
6. Helium temperature at inlet loop HX	TE 6	Bypass around helium aftercooler	+25°F	1.67 sec

B. EXPERIMENT ASSURANCE SYSTEM

	Protective Function	Monitored Variable(s)	Protective Action	Number of Instrument Channels	Instrument Channel+ Accuracy	Sensor Designation Numbers*	Scram Setpoint**	Scram Delay***
1.	Detect Loss of ALIP Power	ALIP Voltage & Frequency	ETR Scram & Transfer to Emergency Power	3 & 2	±5 vrms ±1.0 Hz	UV-1,-2,-3 UF-1,-2	75% of Normal Power (57.5KW)	250 msec 100 msec
2.	Detect Loss of Test Section Coolant Flow	Test Section Sodium Flow	ETR Scram	2	±5% of indicated	FE-1-1 FE-2-1	80% of Normal Flow (7.5 lbs/sec)	500 msec
3.	Detect Test Section Coolant Overheating	Test Section Outlet Temp.	ETR Scram	3	±3% of indicated	TE-2-1,-2,-3	+100°F of Normal (1300°F)	500 msec
4.	Detect Loss of Heat Sink	HX Outlet Temp. High	ETR Scram	3	±3% of indicated	TE-13-1,-2,-3	+100°F of Normal (837°F)	500 msec
5.	Prevent Sodium Freezing	HX Outlet Temp. Low	Increase Loop HX Bypass Flow	3	±3% of indicated	TE-13-1,-2,-3	-100°F of Normal (637°F)	500 msec
6.	Detect Total Flow Blockage	Total Sodium Flow (low) & ALIP Voltage	Scram & Power Transfer****	2 & 3	±5% of indicated ±5 vrms	FE-3-1,-2 UV-1,-2,-3	80% of Normal Flow (12.7 lbs/sec)	500 msec

*The values and sensor designation numbers are typical parameters for the P-1 Experiment Test Train and loop sensors, and may vary from experiment to experiment.
**Values are only illustrative. Finalized values await completion of detailed control studies and checkout tests.
***Defined from the time the setpoint is reached until ETR scram is initiated.
****Protective action on low loop flow and above under voltage setpoint.
+Instrument accuracy is % of indicated in the setpoint range.

Therefore, the FEFPL-PPS is not needed to prevent cr mitigate those operational accidents which produce loop conditions within the safe operating envelope of the loop. (In fact, the FEFPL-PPS will be unable to differentiate between a planned experiment and an operational accident.) It will, however, monitor loop conditions throughout the operational period in ETR and ensure that severe accidents (or experiments) will not reduce the loop safety margin. Details of this FEFPL-PPS are provided in Chapter 7; the loop operational envelope and safety limits upon which the system is based are discussed in Chapter 6.

11.1.3 Accident Analysis Conditions

11.1.3.1 Initial Loop Conditions

There exists a wide range of safe, steady-state operating conditions for conducting transient experiments in the FEFP loop. Therefore, the accident studies concentrate on upper limit conditions within the design capability of the loop as identified in Section 6.2 in order to establish a safety envelope for all possible experiments. These points represent conditions more severe than the normal loop operating conditions and are conservative starting points. In addition, transient calculations have been performed using P-1 experiment conditions which are representative of a typical set of loop parameters which will be employed during the currently planned FEFPL program. Although a 37-pin bundle was assumed rather than the P-1 19-pin bundle and the conditions for P-1 are not necesarily the most adverse planned for the FEFPL program, these calculations nevertheless illustrate the margin between realistic and upper limit events. Typical loop parameters at these steady-state points are summarized in Table 11.2.

To present a realistic appraisal of the safety consequences of various postulated accident situations, studies are presented for various cases starting at loop conditions identified for the P-1 experiment.[2] However, for comparison with the upper limit operating envelope, a 37-pin FTR test fuel assembly was studied rather than the reference 19-pin P-1 fuel bundle. In general, the evaluations for this set of loop conditions concentrated on the expected accident sequence (i.e., an accident with successful control system intervention). A comparison of these results with an accident starting at the upper limit operating conditions provides the basis for determining

TABLE 11.2

FEFP Loop Steady-State Conditions Considered in Accident Analyses

	Operating Envelope Limits* Point C	Point G	Point B	P-1 Type Experiment Conditions**
Loop and Heat Exchanger (HX) Conditions				
Total heat removal, kW	1499	1652	1552	1596
ALIP power, kW	71.7	90.6	37.0	76.7
Helium flowrate, lbs/sec	1.38	1.59	1.59	1.59
Inlet sodium temperature to HX, °F	1100	1100	1100	1043
Total loop sodium flowrate, lbs/sec	18.28	18.28	9.51	15.83
Outlet sodium temperature from HX, °F	850	825	600	737
Helium inlet temperature, °F	150	150	150	150
Primary vessel temperature, °F	1052	1029	825	946
Test Section Conditions				
Number of fuel rods (FFTF type)	37	37	37	37
Test section sodium flowrate, lbs/sec	8.90	9.37	6.20	9.35
Total assembly power, kW	1146	1277	1230	1230
Maximum heat flux, kW/ft	12.8	14.3	13.7	13.7
Inlet sodium temperature, °F	897	874	681	792
Outlet sodium temperature, °F	1317	1318	1337	1205
Axial peak/average power factor	1.25	1.25	1.25	1.25

* See Section 6.2.2 of Chapter 6.

** Conditions for a 37-pin assembly at 19-pin P-1 conditions presented in Ref. 2.

how sensitive the consequences are to initial steady-state operating conditions and also for judging the inherent safety features of the FEFP system.

For all of the upper limit type loop operational accidents (i.e., those where failure of protective systems are also assumed) reported in this study, the loop was assumed to be operating initially at steady-state Point C of Table 11.2. As discussed in Section 6.1 of Chapter 6 and seen in Table 11.2, at this limiting operating point the loop steady-state conditions result in the highest loop containment vessel temperature (primary vessel temperature of 1052°F) presently allowable in the FEFP loop. Therefore, this loop operating point provides thermal conditions which reflect the minimum allowable loop operating margin before containment thermal safety limits are exceeded. (It should be noted that all of the steady-state points shown in Table 11.2 have test section power levels below the reference experiment value of 15.7 kW/ft.) By assuming the loop is initially at this point, then the resultant loop transients produced by various accident events provides the sternest test of the loop safety system ability to cope with them due to the minimum time interval for protective action. However, in addition, the consequences of an accident occurring in the loop when it is operating at both Point G and Point B on the operating envelope limit curve has also been evaluated for the loss of pump power accident.

11.1.3.2 Reference Experiment

The severity level of all postulated accidents presented in this chapter has been evaluated and compared to the reference experiment presented in Chapter 10. The loop conditions for this reference experiment (a sudden and complete test section flow blockage) have been conservatively selected to bound any conceivable experiment or accident which results in test fuel melting. The safety consequences of this reference experiment have been extensively studied with details of the assumptions and approximations provided in Sections 10.2 and 10.3 of Chapter 10. The supporting molten fuel coolant interaction (MFCI) analyses are provided in Appendix C.

11.1.4 Accident Delineation

11.1.4.1 FEFPL Safety Fault Tree

The fault trees, shown in Appendix A.1, provide the framework for identifying areas requiring the safety studies presented in this section, and for assessing the requirements and features of the safety protection system for the loop. The trees were prepared to provide added insight to the overall safety problems considered.

The fault trees were developed starting from the "ultimate" undesired event" which is identified and placed at the top of the tree. For the FEFP Loop the event is: "a failure of FEFPL which results in damage to the ETR vessel, or which presents a hazard to the public or operating personnel." This statement sets both the requirements and restraints on the performance of the FEFPL experiment assurance system (EAS), on the FEFPL plant protection system (PPS), on the loop design, and on the test conditions. The remainder of the fault tree outlines events and conditions which could conceivably lead to this final event. For brevity, these initiating events represent in some instances only major categories of faults or malfunctions. It should be noted that additional accidents falling within these general categories, which are of safety concern, have also been studied and are discussed in this report. The progression and sequence of accident events up the tree to levels of increasing severity as depicted on the tree represent in most instances the "worst" case of the several alternate paths an accident can take. These paths ignore loop safety instrumentation which will effectively terminate an accident path well below damage threshold levels.

The tree then is basically an orderly display of the relationship between the major conceivable events that might occur, if no remedial action is taken, that might lead to ETR damage or release of radioactive material. Some of these events are obviously trivial, while others need considerable study to evaluate their likelihood and the controls needed to prevent their occurrence. Included also in Appendix A is an Accident Summary Table A.1.1 based on the formalism outlined in RDT Standard C 16-1T which requires identification of fault events, classifications as to likelihood and comparison with consequences. Table A.1.1 combines fault events described in the SAR text, the previous SAR Accident Summary Table, the fault trees and additional events logically related to events identified in the text. The detailed discussion of many of the more severe accidents identified in Table A.1.1, along with supporting analysis evidence which resolve satisfactorily their safety implications, are presented in the following sections. Other faults or malfunctions shown in Table A.1.1 have been identified as clearly hypothetical are discussed in Chapter 13.

11.1.4.2 Accident Severity Classes

To aid in the assessment of the safety consequences of FEFPL operational accidents, the various faults, malfunctions, and abnormal operating conditions evaluated in this chapter have been categorized into three rather broad classes. These three accident classes are related to the resultant severity level or consequences of each incident in terms of its ultimate safety effect on FEFPL and are defined as follows:

Class I - No test train or FEFPL test section clad damage, fuel melting or sodium boiling with no loss in FEFP loop or component effective lifetime.

Class II - Only minor test section damage, some localized loss in cladding integrity possible, small amounts of fuel melting (less than 10%), good possibility of sodium boiling but with no loss in FEFP loop or component effective lifetime other than FEFP test train.

Class III - Major test train and test fuel damage, extensive and prolonged sodium boiling with gross test fuel melting likely. Possibility of some loss in effective lifetime of FEFPL components but no reduction in loop containment capability or creation of a safety hazard.

In Table 11.3 the major operational accidents studied in this chapter have been tabulated in terms of the above three accident classes. Clearly shown in Table 11.3 is the beneficial influence of the various protective systems in reducing the accident severity level. For the majority of accidents successful FEFPL control (e.g., increase power to ALIP or helium flow to the HX) and FEFPL-EAS action (see Table 11.1) will limit the resultant severity level to the Class I category. Only a few of the low probability events (e.g., instantaneous ALIP power reversal) fall into Class II in spite of FEFPL control and EAS intervention. No accidents have been identified which reach a Class III condition with successful FEFPL control and/or EAS action.

As shown in Table 11.3, the safety and FEFPL containment protection systems (ETR-PPS and FEFPL-PPS) will limit all accidents to a Class III incident. It should be noted that for this to occur requires the improbable

TABLE 11.3

Severity Level of FEFPL Operational Accidents as Limited by Protective Action

Accidents		Normal	EAS or Control System Failure		EAS and Control System Failure	
					Protective Action	
			FEFPL Test Fuel Damage Protection		Safety and FEFPL Containment Protection	
		FEFPL Control and EAS Action	FEFPL Control Action Only	FEFPL-EAS Action Only	ETR-PPS Action Only	FEFPL-PPS Action Only
A. Loss of Commercial Power						
1. To loop and ETR	A	Class I	Class II	Class II	Class II	Class III
2. To only loop	A	Class I	Class II	Class II	N.A.	Class III
B. Loss of All Electrical Power						
1. To loop and ETR	EU	Class II	Ineffective	Class II	Class II	Class III
2. To only loop	EU	Class II	Ineffective	Class II	N.A.	Class III
C. ALIP Accidents						
1. Loss of 1 section	A	Class I	Class I	Class I	N.A.	N.R.
2. Loss of 2 sections	U	Class I	Class I	Class I	N.A.	N.R.
3. Loss of 3 sections	EU	Class II	Ineffective	Class II	N.A.	Class III
4. Total loss of commercial power	A	Class I	Class II	Class II	N.A.	Class III
5. Instantaneous power reversal	EU	Class II	Ineffective	Class II	N.A.	Class III
D. Sodium Flow Blockage						
1. Partial test section	A	Class I	Class I	Class I	N.A.	N.R.
2. Total test section	U	Class II	Ineffective	Class II	N.A.	Class III
3. Partial loop	A	Class I	Class I	Class I	N.A.	N.R.
4. Total loop	EU - H	Class II	Ineffective	Class II	N.A.	Class III
E. Helium Flow Blockage						
1. Partial blockage	A	Class I	Class I	Class I	N.A.	N.R.
2. Total blockage	A	Class I	Ineffective	Class I	N.A.	Class II
F. Helium Circulator Accidents						
1. Loss of 1 circulator	A	Class I	Class I	Class I	N.A.	N.R.
2. Loss of 2 circulators	A	Class I	Class I	Class I	N.A.	Class I
3. Loss of 3 circulators	U	Class I	Class I	Class I	N.A.	Class II
4. Loss of all circulators	U	Class I	Class I	Class I	N.A.	Class II
G. Loss of HDW Flowrate						
1. Loss to aftercooler	A	Class I	Class I	Class I	N.A.	Class I
2. Loss of primary HX	A	Class I	Class I	Class I	N.A.	Class II
3. Total loss of HDW flow	A	Class I	Class I	Class I	N.A.	Class II
H. Loss of HDW Coolant						
1. Loss to aftercooler	A	Class I	Class I	Class I	N.A.	Class I
2. Loss to primary HX	A	Class I	Class I	Class I	N.A.	Class II
3. Total loss of HDW	A	Class I	Class I	Class I	N.A.	Class II
I. Failure of Control System						
1. Failure of auto control	A	Class I	Ineffective	Class I	N.A.	Class II
J. ETR Design Basis Accidents						
1. Reactivity accident	EU	Class II	Class II	Class II	Class II	N.R.
2. Loss of cooling	H	N.R.	N.R.	N.R.	Class I	Class II

N.A. = not applicable
N.R. = not required

A = Anticipated
U = Unlikely
EU = Extremely unlikely

H = Hypothetical
(see Appendix D for definitions)

Severity Level Definitions

Class I - No test train or FEFPL test section clad damage, fuel melting, or sodium boiling with no loss in FEFPL loop or component effective lifetime.

Class II - Minor test section damage, loss in cladding integrity possible, small amount of fuel melting (less than 10%), good possibility of sodium boiling but with no loss in FEFP loop or component effective lifetime, other than FEFPL test train.

Class III - Major test train and test fuel damage, extensive and prolonged sodium boiling with gross test fuel melting likely. Possibility of some loss in effective lifetime of FEFPL components, but no reduction in loop containment capability or creation of a safety hazard. Conditions no worse than Reference Experiment (Section 10.2.2).

failure of the first line of defense; namely, the FEFPL control and EAS systems which prevent damage to test fuel. For most accidents (with the exception of those that are ETR initiated) the FEFPL control and EAS system will terminate an accident well before loop conditions develop which challenge the FEFPL-PPS.

The evaluations and analyses which support the accident severity levels identified in Table 11.3 are discussed in the following sections.

11.2 Loss of Electrical Power

In this section, the loop safety implications of the total and instantaneous loss of power accidents are discussed. Two types of accident situations are postulated and considered:

- Loss of commercial power
- Loss of all electrical power

Power failures to individual loop components (i.e., ALIP, helium circulators) are discussed in detail later in the accident sections which consider failures in these specific loop components.

11.2.1 Loss of Commercial Power

NRTS power-system records show the occurrence of 14 commercial power outages in the period from January 1966 to December 1971. The following table shows frequency and duration of outages during this period.

Date	Number of Outages	Duration
10/66	1	15 min
6/67	1	0.3 sec
12/67	1	63 min
2/68	1	2 min
5/68	1	7 min
6/68	1	5 sec
6/69	1	4 min
12/69	1	1 min
6/70	1	2 min
6/70	1	5 sec
12/71	1	1 min
12/71	1	1 min
12/71	1	4 min
12/71	1	0.3 sec

Maximum Outage Duration - 1 hr 3 min

Minimum Outage Duration - 0.3 sec

Average Outage Duration - 6.7 min

Frequency - 3 per year

Reliable power is required for both the helium circulators and for the ALIP. Power will be normally supplied from the ETR commercial power-distribution system. Based on the frequency of past outages, the probability of an outage occurring during any given 5 min FEFPL test phase period is of the order of 3×10^{-5}. It is therefore not expected that a commercial power outage would occur during a FEFPL test transient. However, in the event that this condition did occur, the safety consequences would be no more severe than the reference experiment discussed in Chapter 10. Of course, the loss of commercial power superimposed upon an experimental transient might seriously affect the quality and usefulness of the test results.

The power-supply system for both helium circulators and the ALIP include backup sources should the commercial power system fail. A full discussion of these systems is given in the later sections describing the helium circulator and ALIP accident studies.

Three potential loss of commercial power situations can be postulated:

- Loss of commercial power to ETR and loop
- Loss of commercial power to only the loop
- Loss of commercial power to only ETR

Of these three cases, the first - namely the loss of commercial power simutaneously to ETR and the loop - is the most probable. An electrical power outage initiated in the commercial distribution system is an ETR anticipated fault, based upon the power outage experience presented previously. Loss of power to only ETR or to only the FEFP loop requires a failure in the individual power busses or circuitbreakers.

Thermal conditions in the loop for the loss of commercial power accident to only ETR are not discussed. This accident produces only a very minor change in internal loop conditions (inside the FEFPL primary vessel) after 50 seconds into the accident. The thermal effect on the loop secondary containment vessel due to the reduction in ETR water flow for this accident event is almost identical to that presented for the complete loss of commercial power accident (loss to ETR and loop). The reason for the agreement between the two accident cases is because of the poor thermal communication between the FEFPL containment vessels created by the helium filled insulating gap.

11.2.1.1 Loss of Commercial Power to ETR and Loop

Loss of commercial power to ETR has been classified as an anticipated fault, and has been analyzed in detail for its potential ETR safety consequences in Ref. 4. ETR protection against this accident is provided by the ETR-PPS (Plant Protection System) through the action of the following protective subsystems:

- Tank differential pressure (low)
- Reactor core differential temperature (high)
- Reactor core outlet temperature (high)

To limit the ETR severity level of this anticipated fault to a condition below DNB (departure from nucleate boiling) at the ETR hot spot and to prevent an ETR flow instability with no core damage, the total ETR protective response time requirement is a maximum of 3.5 sec from loss of power to the ETR pumps until scram.[8] The suggested ETR protective margin for this case is 3 standard deviations from DNB with the ETR reactor vessel differential pressure protective subsystem providing the initial scram request.

In addition to the safety afforded by the ETR-PPS, two FEFPL systems:

- FEFPL control system
- FEFPL plant protection system

provide loop protection against the consequences of this accident. The FEFPL control system provides the necessary action to prevent test section and loop component damage. The FEFPL-EAS (Experiment Assurance System) provides the rapid ETR scram via the ALIP low voltage protective channel and transfers the ALIP to emergency power within 100 msec after loss of power. The low voltage scram initiation is expected to occur within 80 msec after the fault. A conservative 250 msec scram delay has been used as a design value (see Table 11.1). Delay times up to 500 msec have been used in these safety analyses without any appreciable difference in the results. Backup FEFPL-EAS protection is provided by an ETR scram initiated from any one of the following three subsystems: 1) test section sodium flowrate, 2) test section sodium outlet temperature, and 3) sodium outlet temperature from the heat exchanger. Typical set points for the FEFPL-EAS system are presented in Table 11.1, with details of the design provided in Chapter 5.

For this accident, the primary and secondary containment vessel temperature subsystems provide the major pre-MFCI loop protection. An ETR scram is the required FEFPL-PPS action when the containment temperature becomes excessive. The details of this FEFPL-PPS design are presented in Chapter 7. The following transient conditions apply for the loss of commercial power accident:

- Loss of ALIP power with resultant drop in loop sodium flowrate
- Loss of two out of four FEFPL helium circulators
- Loss of ETR water flow in ETR core filler piece surrounding the FEFPL, but with emergency ETR pump assistance.

Figure 11.1 shows the decay of the total loop sodium flow after the abrupt loss of ALIP electrical power. In Fig. 11.1 the total loss of commercial power accident loop sodium flow reduction curve assumes successful transfer to emergency power after 100 msec resulting in a loop flowrate to prevent boiling in the test section of $\sim$50% of full flow. The ALIP emergency power requirements are $\sim$45 kW, or about 15 kW per pump section. This will normally give more than the 50% of full flow required. Nevertheless, for the analysis represented by Fig. 11.1, it is assumed that one section is inoperative in order to demonstrate additional safety margin. As Figure 11.1 indicates the reduction of loop flowrate for the loss of all electrical power accident (no emergency power assist) is rapid, reaching an almost constant natural-circulation flowrate ($\sim$4% of full flow) after 5 seconds.

The loss of commercial power to the helium circulator system results in only the loss of power to two out of the four helium circulators, since two circulators are connected to the diesel power system which is operated continuously. As seen in Fig. 11.2, this can cause a maximum helium flow reduction of about 30% of full flow, assuming no increase in the speed of the remaining two circulators or increase in helium flow to the loop via reduction in helium bypass flow. Increasing the speed to the remaining two circulators results in only about a 20% helium flowrate reduction (see Fig. 11.2). For successful helium system control action, it was assumed control action commenced at 90% of rated flow with the helium flow controller having the 3.3 sec time constant as specified in Ref. 3. Both flow curves shown in Fig. 11.2 assumed a circulator speed coastdown of 60 sec (100% full speed to 1% speed).

FIG. 11.1 - Loop Sodium Flowrate for Loss of Electrical Power Accident

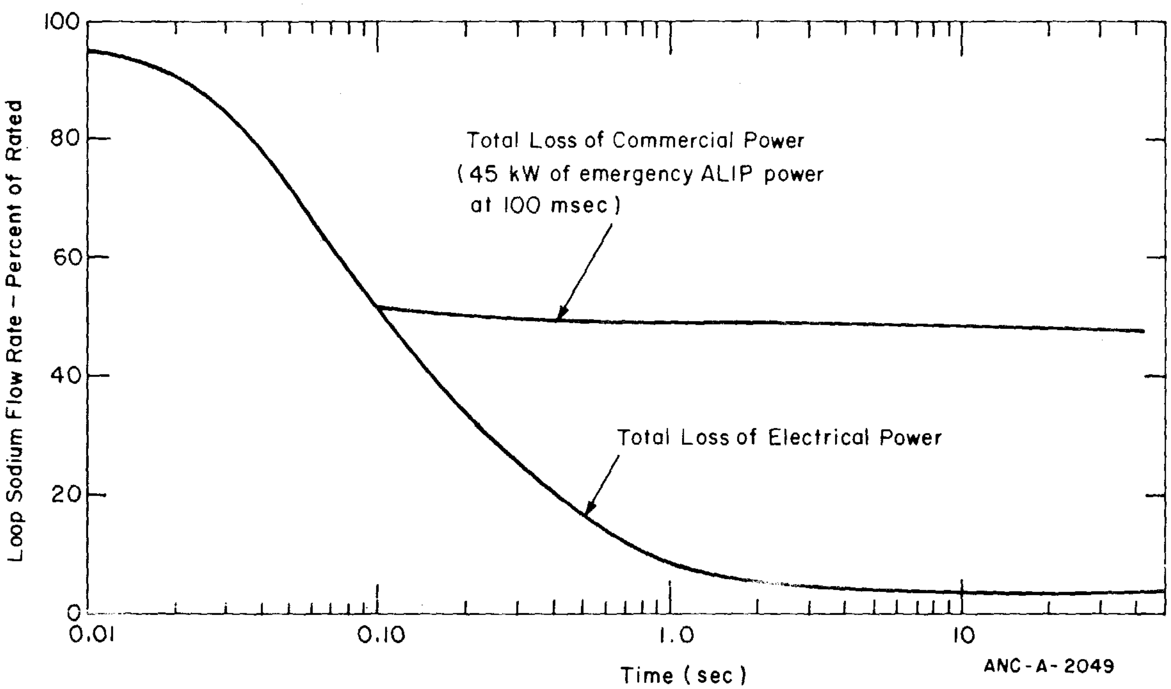

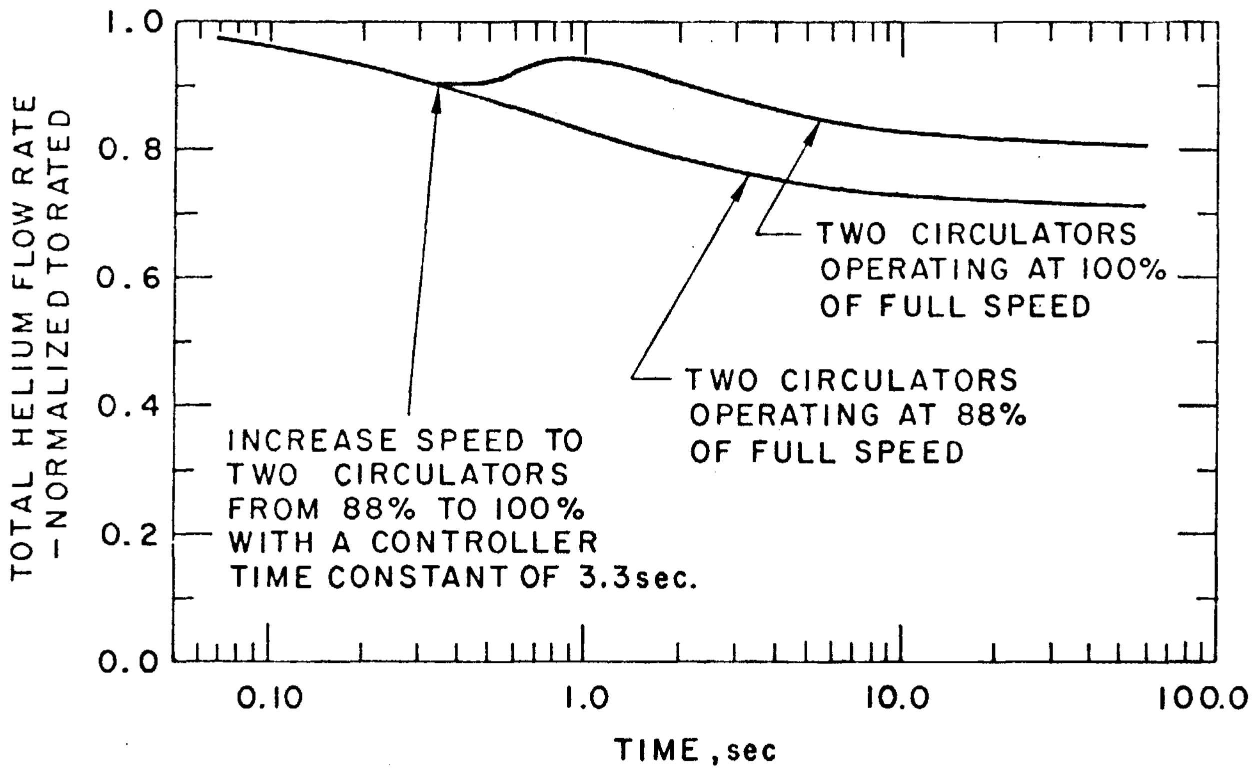

FIG. 11.2. Helium Flowrate for Loss of Commercial Power Accident

FIG. 11.3. ETR Core Flow Coastdown for
Total Loss of Commercial Power

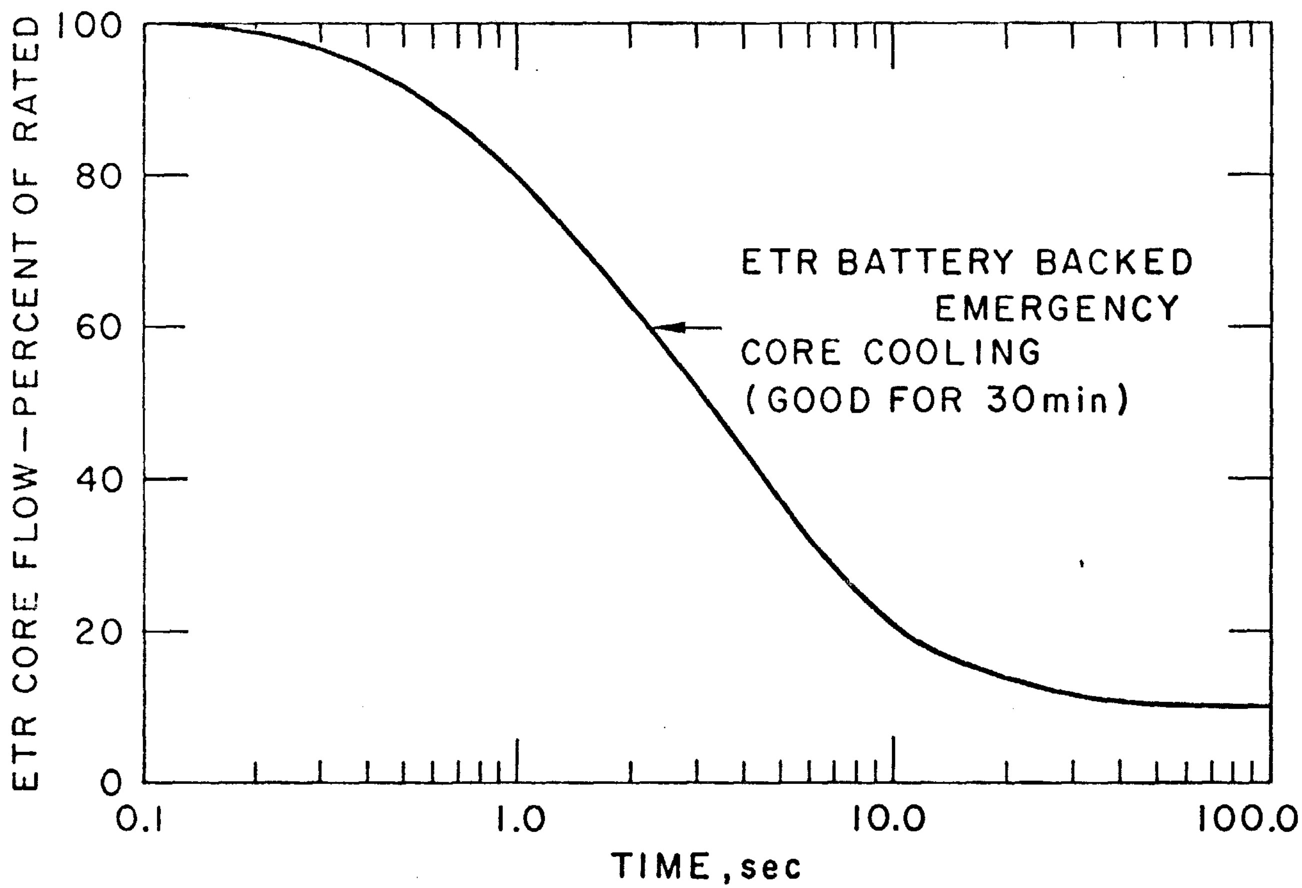

Loss of ETR cooling water flow on the outside of the FEFPL secondary containment will follow the flow reduction calculated for the ETR core. Fig. 11.3 shows this normalized ETR water flowrate as estimated for the loss of commercial power accident (see Ref. 4). As indicated, the ETR battery backed 2000 GPM emergency flow system guarantees an ETR water flowrate which is 3 standard deviations away from an ETR flow instability.

Loop thermal-hydraulic results for this loss of commercial power accident to both ETR and the FEFP loop are discussed below including the loop protection system failures that must be postulated in order to permit an accident to reach a given class of severity as defined in Section 11.1.4.2.

Class I Accident - No Test Section Damage

FEFPL protective action (ETR scram initiated from FEFPL-EAS low ALIP voltage after 80 msec delay), along with transfer to 45 kW of emergency ALIP electrical power and increase in speed of the remaining two helium circulators from 88 to 100%, terminate this accident without damage to loop components or test fuel. Calculations using the THYME-B Code (see Appendix B.1 for description) for the loop initially at P-1 experiment conditions with a 37-pin test section (see Table 11.2 for steady-state parameters) indicate sodium boiling will not occur. With scram after 80 msec, the maximum test section sodium temperature reached was 1471°F (T_{sat} = 1780°F) approximately one second into the transient. This saturation temperature is the lowest value envisioned for FTR simulation experiments; it is the minimum sodium temperature that could lead to boiling, dryout and fuel damage. Smaller thermal perturbations at other loop locations leveled off after about one minute.

For this accident, the emergency ALIP power had the major influence in minimizing potential adverse accident consequences. An ETR scram delay of 500 msec gave no appreciable change in loop thermal conditions over those predicted with the expected 80 msec scram delay. (This 500 msec delay would be representative of scram action initiated by the EAS sodium flowrate sensor). The peak sodium temperature of 1550°F for this case is still well below saturation. Furthermore, one minute after the accident, loop temperatures are within 2°F of those indicated for the shorter 80 msec scram delay case.

Evaluation of this accident, assuming the loop is initially at the upper limit of the loop operating envelope (Point C in Table 11.2), also indicates consequences which do not threaten the safety of ETR. For this analysis, it was conservatively assumed that the helium flow loss was instantaneous (30% reduction) with no speedup of the remaining two helium circulators. A SAS2A analysis (see Appendix B.2 for code description) of the FEFPL test section showed that the sodium would not boil during this accident. The sodium reached a peak temperature of about 1560°F after ∿0.8 sec into the transient (∿200°F below saturation) and then decreased rapidly. A peak test section cladding temperature of 1580°F was obtained (also after ∿0.8 sec into the accident). This relatively high cladding temperature existed for only a short time, however, decreasing to ∿1440°F after 2 sec.

Other loop locations exhibit similar decreasing temperatures reflecting the reduced loop power to flow ratio. THYME-B total loop simulation results for the EAS protected accident revealed that after 50 sec into the accident, the temperature of sodium into the small tubes in the loop heat exchanger was down to 900°F from its original 1110°F value. The sodium temperature at the exit of the HX was 694°F (at 50 sec), down 169°F from its initial 861°F steady-state value. Metal temperatures were also greatly reduced by the FEFPL control system during this transient. After 50 sec, the primary temperature at the core midplane was reduced to 825°F and the secondary vessel to 282°F.

It is concluded from this that the FEFPL-control system and EAS can effectively cope with the consequences of this loss of commercial power to ETR and the loop accident. Sodium boiling within the loop is prevented, and the resultant temperatures in the test fuel cladding are low enough to suggest that significant test section damage will not be realized. Temperatures at the other loop locations do not increase significantly, hence no loss in component lifetime or effectiveness should be incurred.

Class II Accident - Minor Test Section Damage

In the improbable event that the FEFPL-EAS scram does not occur successfully, FEFPL-control system action (i.e., transfer to ALIP emergency power and increase speed of remaining two helium circulators) will be sufficient to limit loop damage to the Class II category. (It should be noted that this accident event is very remote but is provided for illustration purposes. As the most likely reason for no scram is a failure to detect the undervoltage condition, the transfer of the ALIP to emergency power will also not occur. The analysis of this delayed scram accident without transfer to emergency power is presented below.) Without any ETR scram for the loop initially at P-1 type initial conditions, calculations indicate that no immediate safety hazard due to this accident exists. For this unlikely eventuality, the loop thermal conditions will reestablish at a higher level but still well within acceptable safety limits. The maximum sodium test section temperature peaks at ∿10 sec at 1621°F (T_{sat} = 1780°F) dropping to 1504°F after 60 sec. Therefore, some clad damage may result. The average primary vessel temperature at the core midplane peaks at about 960°F at 8.5 sec then drops to 840°F after 60 sec into the accident due to improved heat removal in the heat exchanger caused by the elevated temperatures. The tube temperature increases in the heat exchanger are not severe and will remain less than about 200°F after 60 sec into the transient. The secondary vessel temperature undergoes a gradual increase reaching 672°F after 60 sec (about 42°F increase from steady state). The analysis illustrates the effectiveness of the FEFPL control features which are provided to mitigate this accident's consequence on the loop. Ample time for scramming ETR is indicated.

Minor fuel damage (Class II severity level) can also be obtained for this loss of commercial power accident to the loop and ETR if it is postulated that both the FEFPL control and EAS do not take preventative action. For such an event, the next line of defense will be an ETR-PPS scram. The bounding case for this delayed scram would be to assume that the scram is initiated from an ETR primary coolant subsystem. This scram action will occur after about 3.5 sec into the accident. The ETR tank differential pressure subsystem set point at 20 psi provides one malfunction indication.

For this delayed scram situation with no emergency ALIP power assistance sodium boiling, test section clad damage and initially some test fuel melting will no doubt occur. SAS2A results obtained with the loop at the upper operating limit Point C (see Table 11.2) indicate that sodium void initiation will occur at ∿0.6 sec into the accident. Clad and fuel melt will occur shortly thereafter at ∿1.2 sec and ∿2.4 sec, respectively. However, at the 3.5 sec time of scram, the total amount of molten fuel generation will be only about 8% of the total test fuel inventory (37-pin bundle). This is well within the 50% molten fuel value used in the design envelope MFCI source term evaluation for the design basis experiment discussed in Chapter 10.

THYME-B predicted loop conditions for this ETR initiated scram loss of commercial power accident indicated that containment vessel temperature will be well within the loop's safety envelope values at 3.5 sec. The primary vessel temperature at the core midplane will be only 1096°F (up from steady-state 1062°F value). The secondary vessel temperature at the core midplane would have increased only 0.4°F at the time of the ETR-PPS scram.

These results suggest that an ETR-PPS initiated scram at 3.5 sec may be too late to preclude the occurrence of an MFCI within the FEFPL test section. However, the amount of molten fuel (∿8%) and thermal conditions of the containment vessel (primary ∿1100°F) are such that the MFCI consequences will be well within the design capabilities of the loop (Loop can tolerate an MFCI involving 50% of the 37-pin fuel inventory with a primary vessel temperature at the core midplane of 1300°F). Therefore, for this situation, the safety of the loop is not threatened.

Class III Accident - Major Test Section Damage

In the extremely unlikely event that both the FEFPL-EAS and the ETR-PPS do not take preventative action, the FEFPL-PPS provides assurance that loop conditions will not exceed loop safety limits. For this situation in the accident analysis, it was assumed that the transient proceeded unchecked until a FEFPL-PPS set point was exceeded. This case, therefore, represents an extension of the previous analysis further into the fuel failure propagation regime.

The THYME-B loop thermal predictions for this FEFPL-PPS protected commercial power accident indicate that the primary vessel temperature at the core midplane will reach its 1265°F set point after ∿6 sec into the transient. The primary temperature at the bottom of the loop at this time (6 sec) would be less than about 986°F, and wouldn't reach its set point (1050°F) until after almost 13 sec into the accident. The secondary vessel temperature at the core midplane after 6 sec had increased only about 5°F from its steady-state 632°F value. After 50 sec, this secondary vessel temperature was still only 675°F, or 25°F below its 700°F set point value. This very low secondary vessel temperature rise indicates that melting of the cadmium filter would not occur.

The test section conditions pertinent to the MFCI phenomenon for this accident are identical to those calculated by SAS2A for the total loss of ALIP power accident and are presented in Section 11.3.1.2. Molten test section fuel generation rates and other MFCI conditions are less severe than the conditions assumed in the reference MFCI design envelope analysis. These conditions along with the fact that containment temperatures are within the acceptable range during the time that an MFCI would be reasonably expected, produce an acceptable safety margin for this accident event.

11.2.1.2 Loss of Commercial Power to Loop Only

The loss of commercial power to only the loop, and not ETR, was also considered. As the electrical power supply diagram indicates (see Fig. 7.20 in Section 7.0), to produce a total loss of commercial power to the loop only would require the failure of the experimenter's "C" and "D" bus power. The more probable mode of commercial power failure (i.e., loss of power at source) would also affect ETR as was discussed in Section 11.2.1.1.

Nevertheless, this accident has also been analyzed with the THYME-B program. For this accident, the loops steady-state conditions were again at the limiting operating envelope point (Point C of Table 11.2). The loop sodium and heat exchanger helium flow rate reductions are identical to those used for the loss of commercial power accident to the ETR and loop. The only difference between this loss of power to only the loop accident and the loss of power to ETR and the loop accident, is that for this situation no water flow reduction occurs in the ETR. Therefore, the cooling water on the outside of the FEFPL secondary vessel was held constant at its steady-state value.

Upper limit (loop initially at Point C of Table 11.2) THYME-B calculations for this accident were performed and are discussed below for the various severity classes defined in Section 11.1.4.2.

Class I - No Test Section Damage

For the FEFPL control system and EAS protected accident, an ETR scram is initiated by the FEFPL-EAS which is expected after 80 msec (low ALIP voltage indication). Automatic transfer to 45 kW of emergency power occurs after a 100 msec delay securing loop sodium flow at about 50% of that initially.

The helium flow rate is conservatively assumed to drop 30% instantaneously without corrective action by the other two helium circulators. For this accident full ETR water flow on outside of the FEFPL secondary vessel will be present. The THYME-B analyses conducted for this transient assumed the loop to be initially at the upper limit of the loop operating envelope (Point C of Table 11.2).

As expected, the thermal conditions inside the loop for this accident are almost identical to those obtained for the total loss of commercial power to both ETR and the loop accident discussed previously (Section 11.2.1.1). Loop sodium and metal temperatures inside the primary vessel agree almost exactly, or differ at the most by about 1°F (lower temperature for this loss of loop power only accident) after 50 seconds into the transient. The secondary vessel temperature for this accident shows the largest deviation from the total loss of commercial power case. After 50 seconds the continuing ETR core filler piece water cooling has reduced the secondary temperature to 270°F versus 282°F for the accident when commercial power is lost to both ETR and the loop.

The consequences of this loss of commercial power accident to only the loop, therefore, is almost identical to the consequences of the FEFPL-Control System and EAS protected total loss of commercial power accident discussed previously. No sodium boiling, fuel melting, or clad damage are expected. A reduced secondary vessel temperature for this case due to continued constant ETR water flow is the only major thermal difference between the two protected loss of commercial power cases.

Class II Accident - Minor Test Section Damage

Partial failures in the FEFPL EAS system yield consequences quite similar to those discussed for the Class II severity level of the previous loss of commercial power accident to the loop and ETR (see Section 11.2.1.1). However, two major differences exist between these two accident cases as discussed below.

The rated ETR water flow rate on the outside of the loop secondary vessel provides continued cooling of the secondary vessel and cadmium filter. Therefore, successful FEFPL-Control System action in the event of a failure of the FEFPL-EAS to scram limits this accident to a severity level no greater than Class II. The emergency power supplied to the ALIP and helium circulators is sufficient to prevent major test section damage. The good thermal insulation provided by the helium gap between the loop containment vessels makes the secondary vessel (and cadmium filter) rather insensitive to the internal loop conditions with continued ETR water flow.

For this loss of commercial power to the loop only, the intermediate ETR scram protection provided by the ETR-PPS system will be unavailable. This action is not of critical importance, as it would require failure of three and possibly four (HX sodium outlet temperature) FEFPL-EAS scram subsystems (see Table 11.1) before the ETR-PPS would be challenged.

Class III Accident - Major Test Fuel Damage

Again, the assumed accident situation where it is postulated that a complete failure of the FEFPL control system and EAS occurs, results in loop conditions for this loss of commercial loop power accident almost identical to the FEFPL-PPS protected total loss of commercial power accident of Section 11.2.1.1. At the 6 sec time that a FEFPL-PPS initiated scram would occur, only the secondary vessel temperature shows any appreciable temperature difference between the two cases (~4°F lower for the case of loss of loop power only). Therefore, the discussion of the consequences of the total loss of commercial power accident situation for the Class III severity level as discussed in Section 11.2.1.1 apply directly to this situation as well.

11.2.2 Loss of All Electrical Power

The complete loss of all electrical power accident required that three power sources must be lost for this to occur: 1) commercial power, 2) diesel power, and 3) battery power. For this situation to develop, it would require either a series of unrelated multiple failures to occur simultaneously or a common mode failure such as water filling up the ETR top dome flange or a fire in the nozzle trench, both of which are extremely unlikely. The ETR diesels are operated continuously whenever ETR is at power. Undervoltage relays on the power source to the ETR PPS will scram the reactor on loss of diesel power and subsequent failure of the MG Set to provide emergency power. As discussed in Section 11.2.1, loss of commercial power will also result in an ETR shutdown. As the FEFPL-PPS cables are also physically located in the top dome flange and nozzle trench regions, a common mode event which would disrupt the FEFPL power would also short the PPS circuits which fail safe (initiates a scram). Therefore, the occurrence of this total loss of electrical power is improbable, but has been studied because of its potential severity level and presented in this chapter for continuity of presentation.

As was the case with the loss of commercial power accident, three possibilities exist:

- Loss of all electrical power to ETR and the loop
- Loss of all electrical power to only the loop
- Loss of all electrical power to only ETR

For the same reasons as given for the loss of commercial power accident, only the thermal results of the first two cases will be discussed.

11.2.2.1 Loss of All Electrical Power to ETR and Loop

The initial phase of this accident is identical to the loss of the commercial power accident since in both instances the loss of commercial power will initiate an ETR primary coolant pump coastdown. However, with the loss of diesel power, the electric power to the ETR pressurizing pumps and gland seal pumps also stops. Therefore, all forced flow drives become inactive and the flow coastdown continues until the buoyant forces in the core create a flow reversal into a natural convection cooling regime. This phenomenon occurs in ETR after about 23.8 sec into the transient.

The ETR protective action for this accident will be a scram initiated from undervoltage relays on the power supply to the ETR-PPS (estimated to occur .125 sec after the accident). In addition to ETR-PPS protection against the consequences of this accident, the FEFPL EAS and FEFPL PPS are provided for loop protection. All power to the loop ALIP and helium circulators is lost in this accident, with the emergency power to the ALIP and two out of four circulators unavailable. The first loop level of protection will again be a FEFPL-EAS scram initiation expected within 80 msec from a low ALIP voltage signal. In addition, the FEFPL-PPS continuously monitors both loop vessels to protect against possible overtemperature in order to preserve the containment safety margin.

A discussion of the consequences of this accident for the various severity levels is provided below. The expected mode of protective action against the consequences of this extremely unlikely accident will be insufficient, for the loop initial conditions investigated, to prevent the occurrence of some test section damage. Without the emergency power provided to the ALIP by the FEFPL control system action, it will be impossible to limit the accident consequences to a Class I severity level. However, the Class II severity level (minor test fuel damage) expected for this accident is acceptable from a safety standpoint because of its low probability of occurrence plus the fact that the presence of the FEFPL will not add to the consequences of an ETR loss-of-power accident.

Class II Accident - Minor Test Section Damage

For a realistic appraisal of the consequences of the total loss in electrical power to the loop and ETR, the loop is assumed to be initially at P-1 type conditions (see Table 11.2). The loop sodium flow coastdown relationship used for this accident is the total loss of power curve shown in Fig. 11.1 (no emergency ALIP power assistance). The helium flowrate reduction assumed is shown in Fig. 11.4 and is based upon a speed reduction in all four circulators to 1% of full speed in one minute. The ETR cooling water flow on the outside of the loop's secondary vessel is assumed to follow the ETR core flow coastdown relationship presented in Fig. 11.5. As noted in Fig. 11.5, the transition to a natural circulation up-flowrate occurs at 23.8 sec after the loss of all electrical power and stabilizes at about 2.6% of rated full flow.

The THYME-B analysis of the loop thermal behavior during the total loss of all electrical power to ETR and the loop studied under the above conditions indicate that some test section damage will occur. Although FEFPL EAS action (i.e., transfer ALIP to emergency power) will be ineffective, the expected FEFPL-EAS scram on low ALIP voltage after 80 msec will prevent test fuel melting. However, due to the high power to flow ratio caused by the decay heating, test section sodium boiling will occur within the test section during a time period extending between about 1 sec to approximately 25 sec into the accident. The resultant redistribution in heat within the test fuel elements (during this period of retarded heat transfer) will cause some local clad melting. Also, the overall loop thermal conditions will generally increase due to the loss of HX heat sink. The large inherent heat capacity of the loop internals and the natural circulation sodium head are sufficient, however, to keep the loop temperature within acceptable limits. After 60 sec into the accident, the test section sodium outlet temperature would be about 1370°F (T_{sat} = 1780°F). The inlet sodium temperature to the test section has increased at this time (60 sec) about 200°F (from its steady-state value) to 994°F.

FIG. 11.4. Helium Flowrate for Loss of All Electrical Power

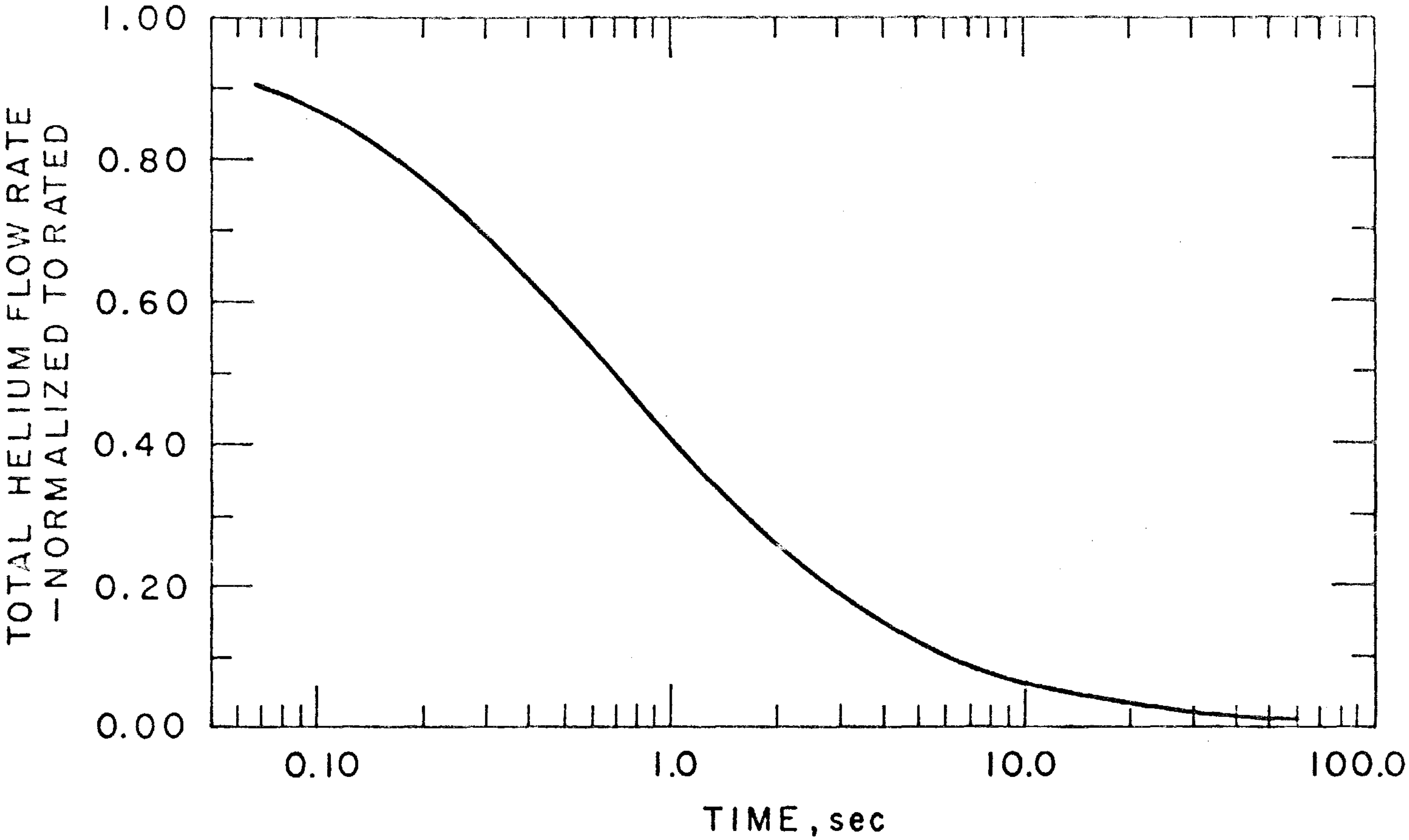

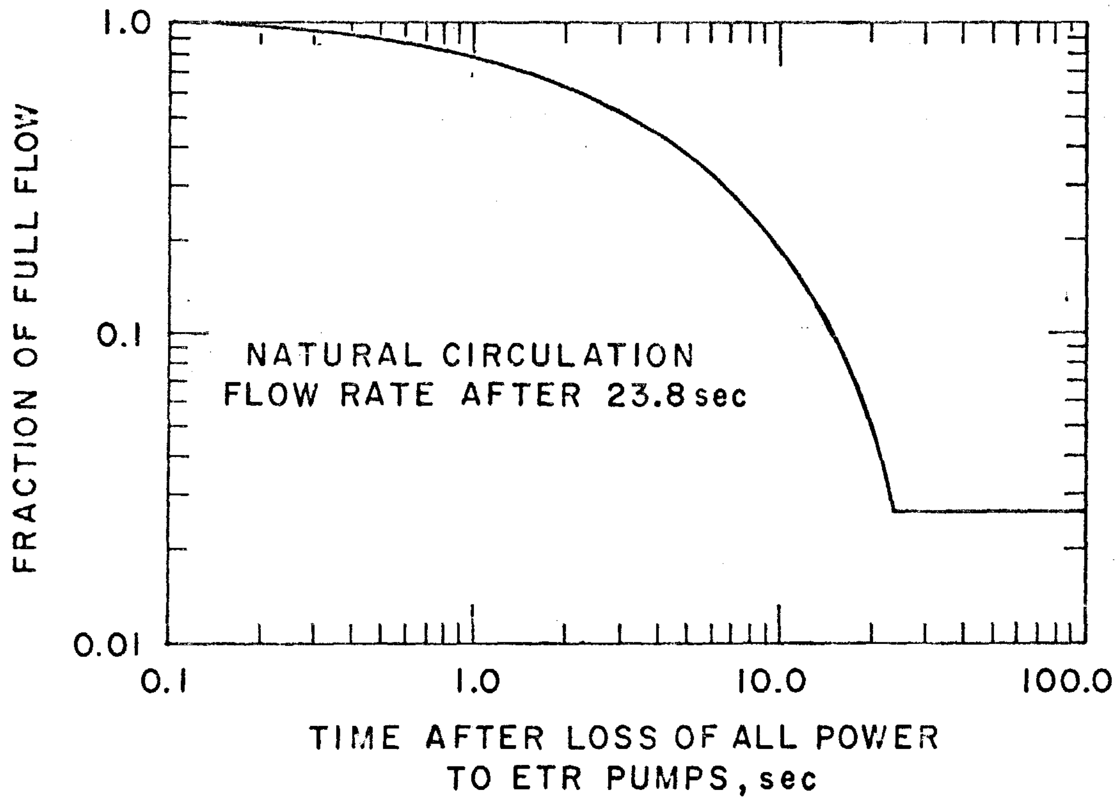

FIG. 11.5. ETR Cooling Water Flow Coastdown for Total Loss of All Electrical Power

Loop containment temperatures remain at acceptable levels throughout the accident being about 940°F for the primary at the core midplane and 312°F for the secondary also at the core midplane after 60 seconds. A maximum primary vessel temperature (i.e., volume average value at core midplane) of 975°F occurs at 163 seconds into the accident. Provided no additional heat loads are placed on the loop from ETR (e.g., large heat input into the loop from ETR fuel melting) a gradual cooling of the loop via heat rejection to ETR is expected. These THYME-B calculations indicate that boiling of ETR water will not occur in the ETR core filler piece annulus surrounding the loop. A gradual cooling of the secondary containment vessel throughout the entire transient is predicted and hence melting of the cadmium filter is not likely.

Calculations indicate that a delay in ETR scram (i.e., due to failure of the expected EAS scram sensor signal at 80 msec) of 500 msec had only a minor influence on the course of the accident described previously with the loop initially at P-1 type conditions. This 500 msec time delay would be a typical delay for a scram initiated from the sodium flowrate EAS protection sensor (see Table 11.1). A slightly longer sodium boiling time interval results ($\sim$ 1 sec to 30 sec) along with somewhat higher loop temperature. After 60 sec into the accident a test section sodium outlet temperature of 1416°F, test section sodium inlet temperature of 907°F, primary vessel temperature at the core midplane of 940°F and secondary vessel temperature of 313°F are predicted. Therefore, no adverse safety consequences are indicated for a 500 msec delay in scraming ETR.

Calculations performed assuming the loop initially at the upper limit of the operating envelope (Point C of Table 11.2) indicate accident conditions for this accident similar to those predicted for the loop initially at P-1 type conditions. However, as expected, thermal conditions within the loop are more severe than those obtained for the corresponding FEFPL-Control System protected loss of commercial power accident presented in Section 11.2.1.1. Again, the loss of all helium flow to the loop's heat exchanger and the unavailability of the emergency ALIP power account for these temperature increases.

Sodium boiling within the test section cannot be prevented by the FEFPL-EAS scram which occurs at 80 msec into the accident. SAS2A results indicate that boiling will commence at $\sim$ 0.7 sec. In addition, test clad melting will also occur soon thereafter at $\sim$ 1.8 seconds. However, the beneficial FEFPL-EAS scram is sufficient to prevent the generation of molten test fuel. Therefore, although test section damage might be excessive for this accident, no molten fuel coolant interactions are possible.

Containment temperatures predicted for this event remain within the acceptable limits by the FEFPL-EAS scram. After 50 seconds into the transient, the primary vessel temperature at the core midplane will have decreased about 15°F to 1046°F. The secondary containment temperature will have decreased over 300°F down to 320°F. No boiling of ETR coolant on the outside of the secondary containment nor melting of the cadmium filter will occur during this transient.

Based upon these results, it is concluded that the consequences of this EAS protected accident will not threaten the safety of the loop. An economic penalty may be incurred however due to the extensive test section damage which is predicted.

Upon failure of the FEFP-EAS the next level of defense is a ETR-PPS intiated scram occuring at 0.125 seconds. This protective action is provided considerably earlier than the 3.5 seconds ETR-PPS scram action assumed for the corresponding loss of commercial power accident. The loop consequences, therefore, will be less severe. Although sodium voiding and clad melting would be expected, the 0.275 sec scram time is sufficient to prevent test fuel melting. Loop temperatures would be slightly higher than the previous FEFPL-EAS protected case - but containment temperatures would decrease well before the attainment of an unacceptable level. No ETR core filler piece annulus boiling nor cadmium filter melting would be realized. Thus, even pessimistically assuming failure of the first level of defense - namely a FEFPL-EAS scram - will not allow an unsafe loop condition to develop.

Class III Accident - Major Test Section Damage

In the event of failure of the FEFPL-EAS and ETR-PPS protective shutdown, successful FEFPL-PPS action will limit accident conditions to a Class III severity level. The THYME-B temperature predictions in the test section region for this accident (conducted at Point C operating limit of Table 11.2) are in general agreement with the comparable results from the loss of all commercial power accident. Slightly higher temperatures occur primarily in the secondary vessel and heat exchanger region. The more retarded ETR water flow rate and lack of any helium cooling to the heat exchanger account for these temperature increases.

As was the case for the FEFPL-PPS protected loss of all commercial power accident, the primary vessel would exceed its PPS set point at ∿ 10 seconds into the accident. This occurs well after an MFCI would be reasonably expected. The loop thermal conditions during the pre-MFCI period are expected to be identical to those for the loss of all commercial power case. Therefore, as was the case with the loss of commercial power accident a potential MFCI will be less severe than the reference design envelope source term (see discussion in Section 11.3.1.2 for loss of ALIP power accidents).

At the time of the FEFPL-PPS scram (∿ 6 sec), the secondary containment vessel temperature would have increased only about 4°F. At this time, no boiling of ETR cooling water would have occurred. Furthermore, the cadmium filter is well below the melting point when scram occurs.

Based upon these thermal analyses, it is concluded that the consequences of this event are no worse than the loss of all commercial power accident. Although an MFCI may well occur, the conditions are such that it would be less severe than the MFCI predicted for the reference experiment which permits continued melting of test section fuel without intervention by the ETR-PPS.

11.2.2.2 Loss of All Electrical Power to Loop Only

The initial conditions for this accident are identical to those assumed previously in Section 11.2.2.1 for the loss of all electrical power to ETR and the loop, with the exception of the ETR cooling water flow rate. For this case with no power interruption to ETR, the ETR cooling water on the outside of the secondary vessel remained constant. The probability of occurrence of this event during the FEFPL program is so low as to be extremely unlikely.

THYME-B loop thermal predictions for this accident are also almost identical to the total loss of all electrical power accident results discussed in the previous section. Only the loop's secondary vessel temperature predictions for this accident differ markedly from the total loss of all electrical power to the loop and ETR accident. For this accident, the constant ETR water flow ensures the continued cooling of the secondary vessel and hence secondary vessel temperatures are 10°F to 50°F lower.

The loop safety implications of this accident for the two classes of accident severity level are in general the same as discussed in the previous section (Section 11.2.2.1). However, for this loss of all electrical power accident to only the loop the additional ETR scram protection provided by the ETR-PPS malfunction indication may be unavailable. This extra protection is not considered to be essential in view of the extremely unlikely nature of this accident and the resultant acceptable severity level.

11.3 Loss of Loop Sodium Flow

11.3.1 ALIP Failures

This section presents the safety evaluations associated with the ALIP system of the FEFP in-pile loop. The study treats the consequences of failure in the ALIP power supply as well as failures of the ALIP itself. The failures treated are as follows: 1) the total, or partial failure of the ALIP power system, 2) other malfunctions within the ALIP, or before the transfer switch for emergency power.

The effect on the loop performance of accidents which result in total or partial pump failure is analyzed. The ability of the loop to cope with these accidents as well as the "worst case" incident (the instantaneous loss of total ALIP power accident) is demonstrated.

11.3.1.1 Description of the ALIP and Power System

The function of the pump is to circulate primary coolant sodium at required pressure and flow during isothermal operation out-of-pile, and during in-pile experiments.

The pump is a concentric, counterflow, annular linear induction pump described in Section 5.2.2.1.3. The present pump is designed for the requirements of 150 gpm of 900°F sodium at 150 psi head.

The ALIP is a three-section pump, and divided electrically into three parallel sections. The three equivalent sections of the pump provide fail-safe redundancy in design in the event of failure of a portion of the pump. Loss of any section of the pump can be tolerated without endangering the experiment or the loop, and thus, an adequate safety margin with respect to loop temperature can be maintained.

The pump power control will consist of a single 3-phase line, supplied by the commercial grid bus, and with a single motor-alternator for variable voltage output to the whole pump. Through appropriate distribution, individual 3-phase leads furnish power to each of the three sections of the ALIP.

See Section 5.2.2.2.3 for description of the ALIP power system.

Potential malfunctions of the ALIP are two types: 1) loss of power to the pump, and 2) failures inside the pump. Corrective actions which are available either singly or in combination are as follows: 1) transfer to alternate power supply, 2) increase power to pump, 3) cut faulted section out of circuit, 4) control Na temperature by means of other loop parameters, such as bypass valve and heat exchanger, and 5) scram the reactor as dictated by either the FEFPL-EAS or FEFPL-PPS requirements. The effect on loop performance of several ALIP malfunctions has been analyzed and is discussed below.

11.3.1.2 ALIP Power System Failures

The ALIP power system must be capable of continuously supplying the pump with power required to maintain a minimum loop flow. The pump is sectionally divided into three sections with each pump section having the capacity to supply a required minimum flow of 50% to protect the experiment. For the FEFPL cases reported herein, this flowrate translates into an emergency ALIP power requirement of 45 kW. Design of the power system, therefore, requires that at no time will a system failure prevent power to at least one pump-stator section. The pump-power system provides for supplying the pump from two independent power sources. Separation of the pump-power feeders to each pump section is maintained. The analysis of power system failure (see fault tree presented in Appendix A3) verified independence of the pump power sources. The analysis also identifies areas where particular design attention must be exercised to maintain a fail-safe power system.

Power is supplied to each pump section from separate transfer switches in the ALIP power system. The power cables for the pump sections are separately routed and terminated at the in-pile tube pump-power connectors to prevent a common failure from disrupting power to the entire pump. Correct phasing of the pump power is necessary to prevent reverse loop flow. Verification of power phasing at each connector for the two independent power sources will be required prior to connector hookup to the loop. The connector design incorporates mechanical interlocks to prevent incorrect hookup of phase and pump section. Instrumentation is provided to monitor voltage and current in the individual cables. A simultaneous undetected failure of the three power leads from the ALIP controller and the loop connectors is very unlikely.

The design of the transfer switches and their control interlocks is extremely important from the standpoint of a single failure. The two independent power sources are fed through these switches to the associated pump sections. A simultaneous failure of the three switches which could prevent power to at least one pump section must be prevented from occurring. Under normal conditions, the transfer switches will supply commercial power to the pump. A failure of commercial power will initiate transfer to the battery-backed power source and initiate reactor shutdown. The transfer switches are electrically interlocked in such a way that when one switch transfers, the other switches are forced to transfer. Physical separation of the selector switches within the ALIP power system is provided to prevent simultaneous mechanical damage to the three switches. To prevent inadvertent repowering of a pump section with commercial power in case of switch failure in the normal position, interlocks open the commercial power contactors of the pump. The transfer switches do not automatically transfer back to the commercial power position when commercial power returns to normal. Prior to a FEFPL test, a complete functional checkout of the transfer switches will be performed to ensure their reliability.

The pump commercial power is fed from the ETR experimenter's power bus. Loss of this power can occur if the ETR commercial power distribution system fails, or a failure of site-power voltage occurs. Redundancy in the ETR power distribution system makes the commercial power source relatively reliable, with only a few power interruptions per year occurring. An isolation transformer provides isolation of the loop pump-power system from the ETR commercial power system. The commercial power level to the pump is established by a single power controller. Any commercial power failure to the pumps will be detected and a power source transfer will be made.

The pump emergency power feeds from the ETR failure-free power system. This system is powered from the ETR diesel-power bus. In addition, a battery-backed motor-generator set will supply power to this bus if a diesel power failure should occur. The emergency power is fed from the battery-backed distribution panel through separate stepdown power transformers and circuit breakers to each transfer switch. A power fault in one section of the pump is thus isolated from the other two sections.

The evaluations of the consequences of various ALIP power system failures are discussed in terms of the three accident severity classes discussed in Section 11.1.4.2. Studies have been made for the realistic or expected accident situation in which protective action is completely successful and occurs as planned. For that realistic analyses the loop is assumed to be initially at P-1 type conditions prior to the accident (see Table 11.2 for details). In addition, results are reported for upper bound accident cases in which partial failures of the FEFPL protection system are postulated. For these limiting cases the loop is assumed to be initially at the upper limit of the loop operating envelope (Point C conditions shown in Table 11.2).

Class I Accident - No Test Section Damage

The consequences of all potential types of ALIP power failures are limited to a Class I accident severity level by successful action of the FEFPL-EAS. These accident results are discussed in terms of specific malfunctions.

a) Loss of Power to One Section of ALIP

The loss of power to one section of pump will result in the loss of that section and a reduction in loop flow. This type of fault can only occur in the pump circuit between the triple output of the ALIP controller and the input connectors of the pump. For the proposed loop experiments, sufficient sodium flow can be maintained by increasing power input to the remaining two-thirds of the pump. Detection and protective action for this accident is the responsibility of the FEFPL-EAS, which is part of the loop control system. The ALIP voltage and test section flow subsystems provide the primary malfunction indication. An instantaneous loss of power to one section of the ALIP will cause only a minor perturbation in loop thermal conditions. This condition will be only temporary with the FEFPL-Control System quickly restoring the initial loop conditions by increasing power to the remaining two ALIP sections.

THYME-B calculations based upon the loop initially at P-1 type parameters (see Table 11.2 for conditions) were conducted assuming a 500 msec delay in control system action. With a 1 sec controller time constant, the 16% initial test section flow reduction can be restored to full flow after about 1 sec into the accident. The 33% power reduction to the ALIP due to the loss of one section would be sufficient to initiate an ETR scram (see Table 11.2). However, even with no scram action the maximum sodium temperature increase within the loop was only about 50°F in the test section with metal temperature increases of the order of only 10°F. After about one minute the FEFPL-Control System action would have returned the loop conditions to those present initially prior to the accident.

However, even without any corrective action (i.e., increase power to other ALIP sections and ETR scram) the loss of one section of the ALIP does not constitute a loop safety problem. THYME-B temperature results at various loop locations for this accident are shown in Figs. 11.6 through 11.11. This analysis assumes the loop is initially operating at the upper limit of the loop performance envelope (Point C of Table 11.2). Details of the THYME-B modeling are presented in Appendix B.1. For this accident, the loop sodium flow rate drops to 88% of full flow. As with the previous analysis at P-1 type conditions, sodium temperature increases within the loop are also less than 50°F as evident in Figs. 11.6 through 11.10. However, without FEFPL-Control action these temperature changes are permanent. Metal temperatures throughout the loop also exhibit very minor temperature perturbations as typified by the primary vessel temperature response as presented in Fig. 11.11. The relatively small sodium flow rate decrease, along with continued heat removal in the heat exchanger, explains the lack of any large thermal changes in the system.

b) Loss of Power to Two Sections of the ALIP

The loss of power to two-thirds of the pump will result in the loss of two-thirds of the pump and a reduction in loop flow of about 40%. Increasing the power input to the remaining one-third of the pump is not likely to permit continuation of an experiment. Although the ALIP is designed for a capacity considerably greater than required for the first loop experiments, one section of the pump is probably not capable of maintaining the desired experiment sodium flow. However, the resulting 60% loop sodium flow is sufficient to adequately cool the test section from a safety consideration standpoint.

Successful protective action by FEFPL control system will terminate this instantaneous loss of two sections of the ALIP accident without resulting in test section damage. An ETR scram, although it will be invoked via the low voltage FEFPL-EAS subsystem, is not essential to prevent test section damage. The increase in electrical power to the remaining operable ALIP section will return the loop sodium flow to about 85% of that prior to the accident. The increase of ALIP power to the one pump section of 50 KW is at the limit of the present pump's capability.

THYME-B calculations conducted assuming the loop to be initially at P-1 type conditions indicate that the pump power increase control action is more than adequate to prevent test section damage. Assuming a 500 msec controller action delay and a 1 sec controller time constant, the maximum sodium temperature increase within the test section will be on the order of 180°F. The peak sodium test section exit temperature of 1362°F is some 420°F below the corresponding saturation temperature. The minor thermal perturbations introduced by this accident are completely damped out after 60 sec. Steady-state is re-established at slightly higher test section sodium temperatures ($\sim$ 50°F). However, without any helium system flow correction due to the reduced loop sodium flow, some loop temperatures will be lower than their initial level (e.g. inlet sodium temperature to the test section is reduced $\sim$ 30°F). For this accident, loop conditions will not be severe enough to challenge the FEFPL-PPS.

An upper bound type investigation of this loss of two ALIP section accident also indicated no test train damage would be incurred. THYME-B predictions of the loop thermal behavior in the remote event of no corrective action (i.e., no FEFPL Control System or FEFPL-EAS action) also yielded acceptable temperature changes within the loop. Even with the loop assumed to be initially at the upper limit of the loop operating envelope (Point C of Table 11.2) the sodium temperatures within the loop increased only 100°F to 175°F (see Fig. 11.6-11.10). The corresponding loop metal temperatures also show maximum increase of at most $\sim$ 100°F after 50 sec into the accident. In fact, as Fig. 11.11 indicates, for the temperature trace of the primary vessel the continued heat exchanger operation with the reduced loop sodium flow tends to reduce temperature in some areas of the loop.

Therefore, as was the case for previous loss of one ALIP section accident, the loop has ample operating margin to tolerate safely the loss of two sections without incurring test train damage. Even without a reactor scram, a single ALIP section is more than sufficient to maintain the required sodium flow to protect the loop and experiment against overheating.

c) Loss of Commercial Power to All Three Sections of the ALIP

The loss of commercial power from the main electric line to all sections of the pump will result in the temporary loss of all pumping action. This first corrective action would consist of transferring through the Transfer Switch to the Emergency Diesel Supply under direction of the FEFPL-Control System. This action coupled with a FEFPL-EAS scram from the low ALIP voltage subsystem will be sufficient to prevent test train damage.

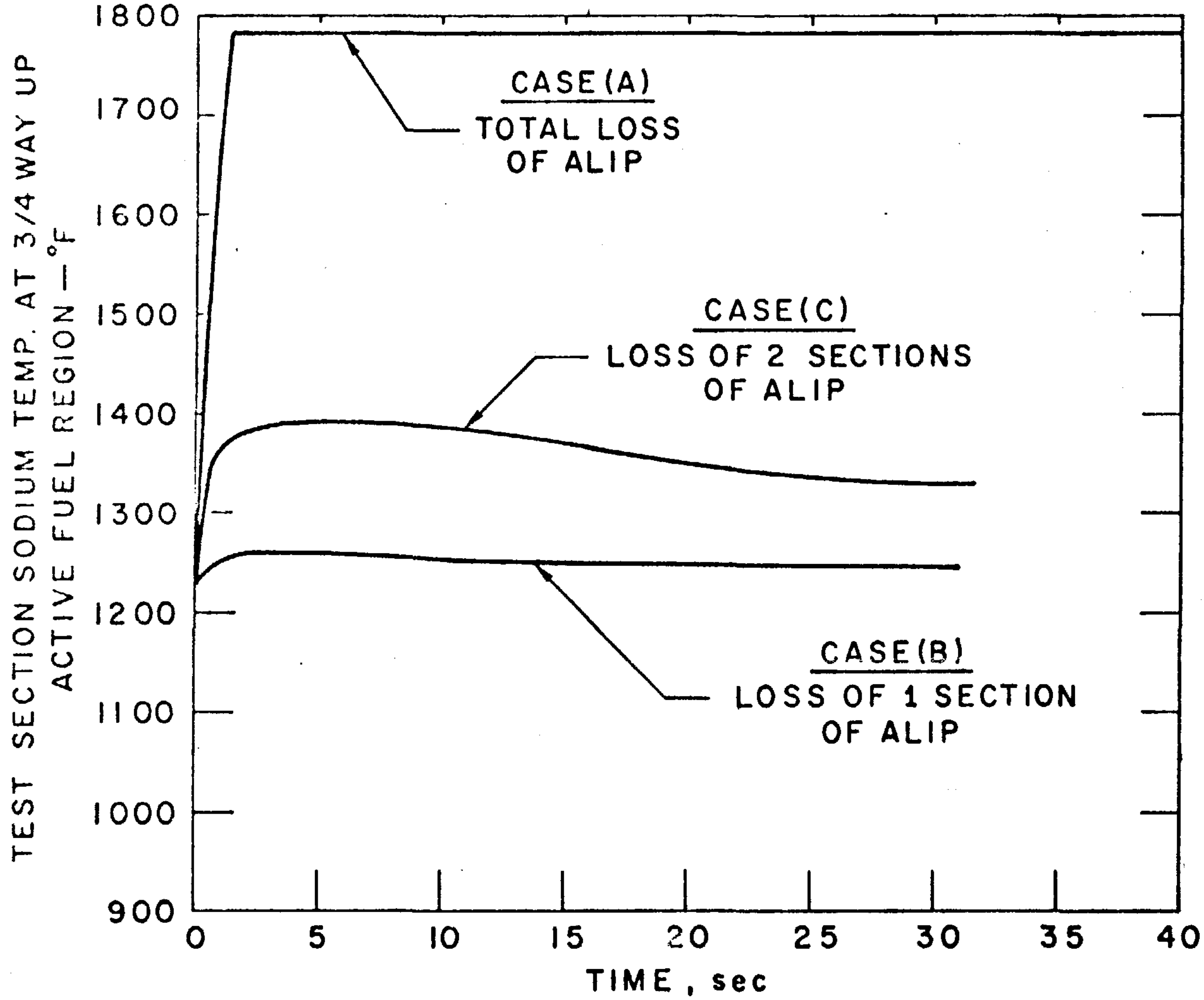

FIG. 11.6. Upper Limit Loss of ALIP Accident Plot of Sodium Temperature at 3/4 Location Up Active Fuel

FIG. 11.7. Upper Limit Loss of ALIP Accident Plot of Sodium Temperature at Exit from Test Section after Mixing with Bypass

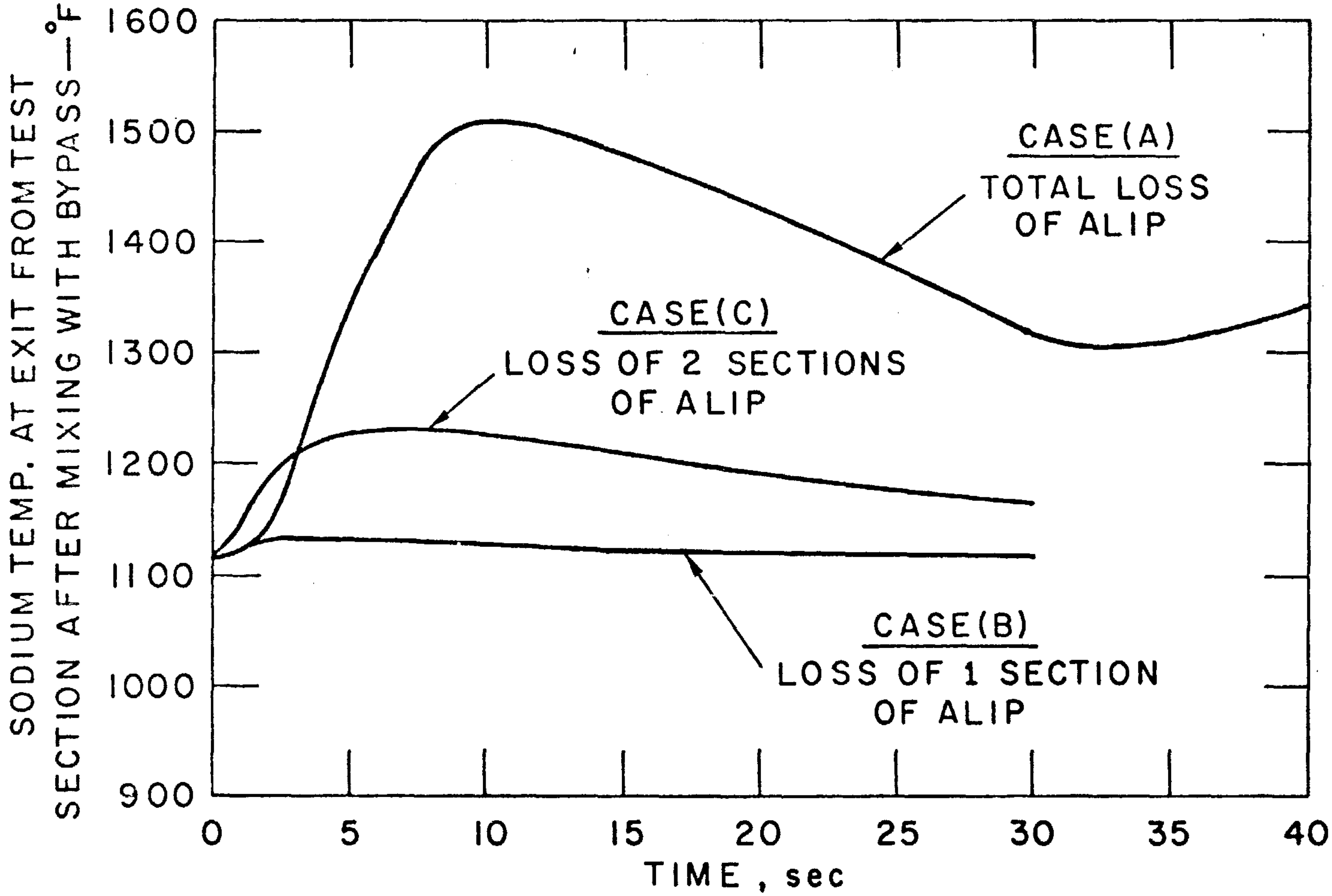

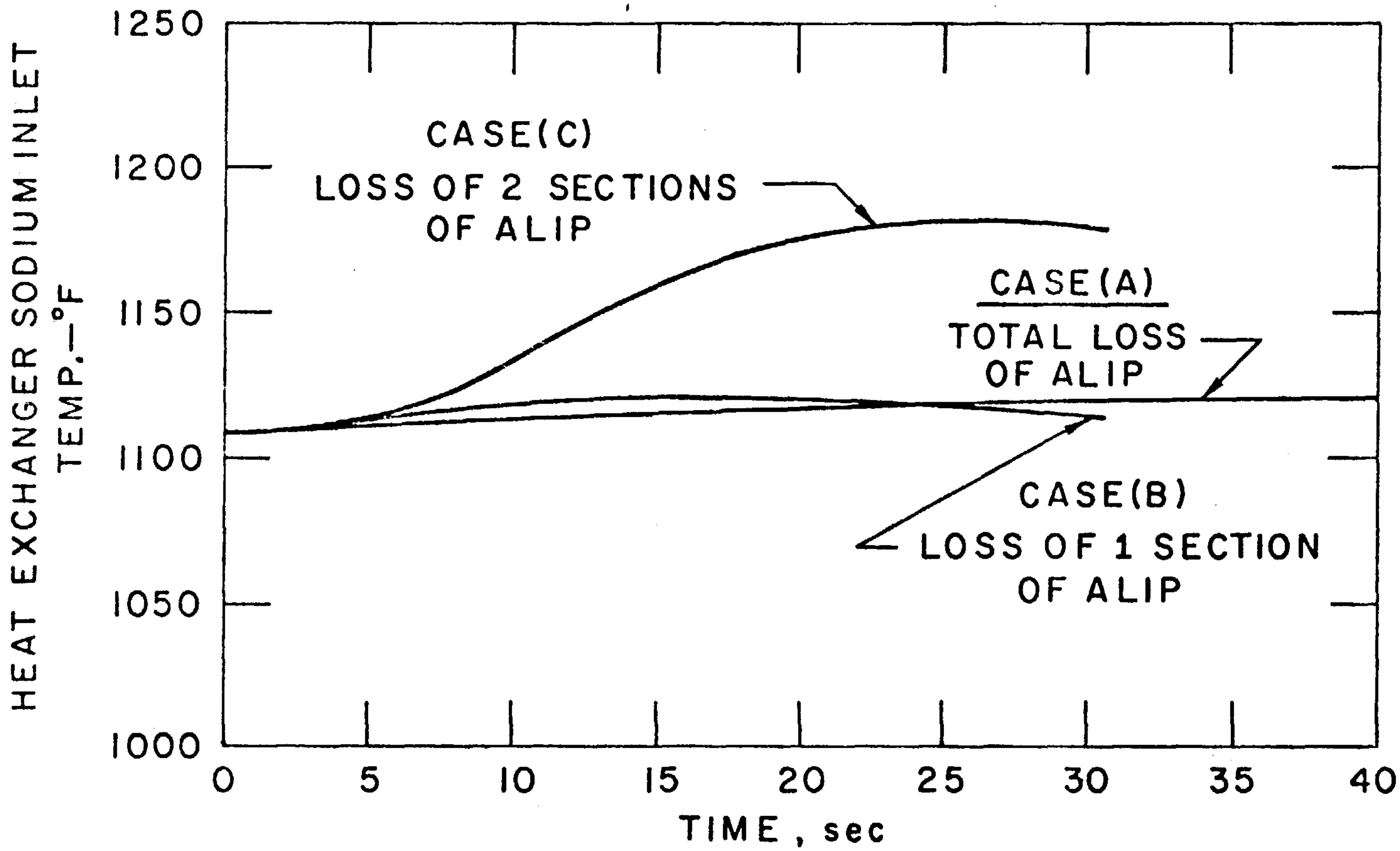

FIG. 11.8. Upper Limit Loss of ALIP Accident Plot of Heat Exchanger Sodium Inlet Temperature

FIG. 11.9. Upper Limit Loss of ALIP Accident Plot of Heat Exchanger Sodium Outlet Temperature

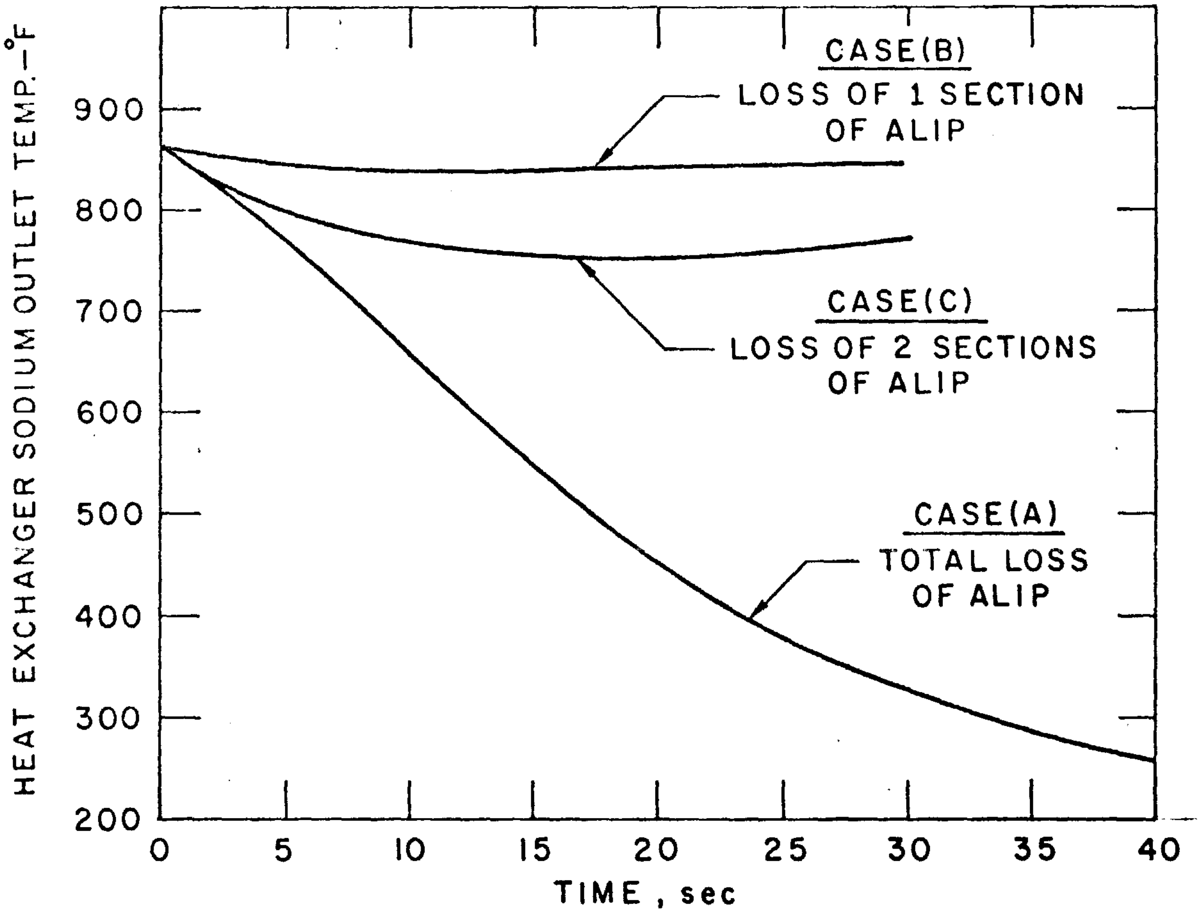

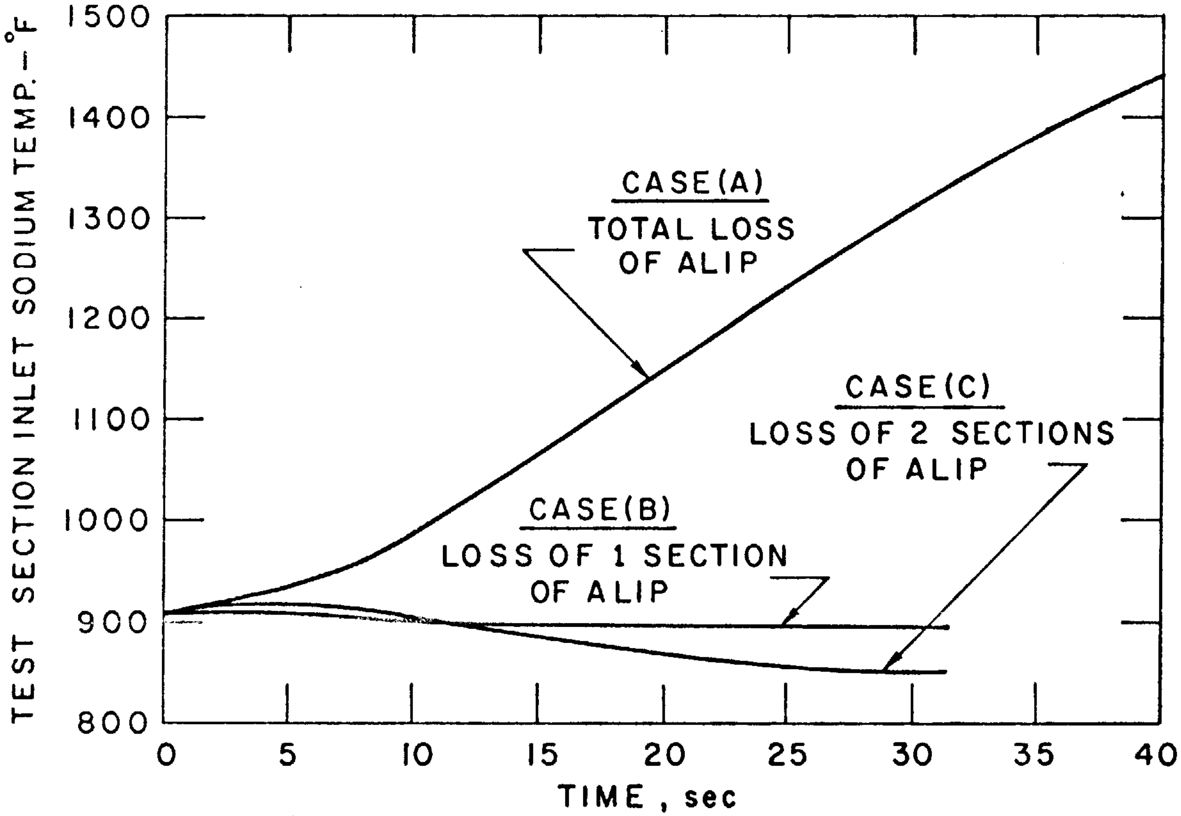

FIG. 11.10. Upper Limit Loss of ALIP Accident Plot of
Test Section Inlet Sodium Temperature

FIG. 11.11. Upper Limit Loss of ALIP Accident Plot of Primary Vessel Temperature

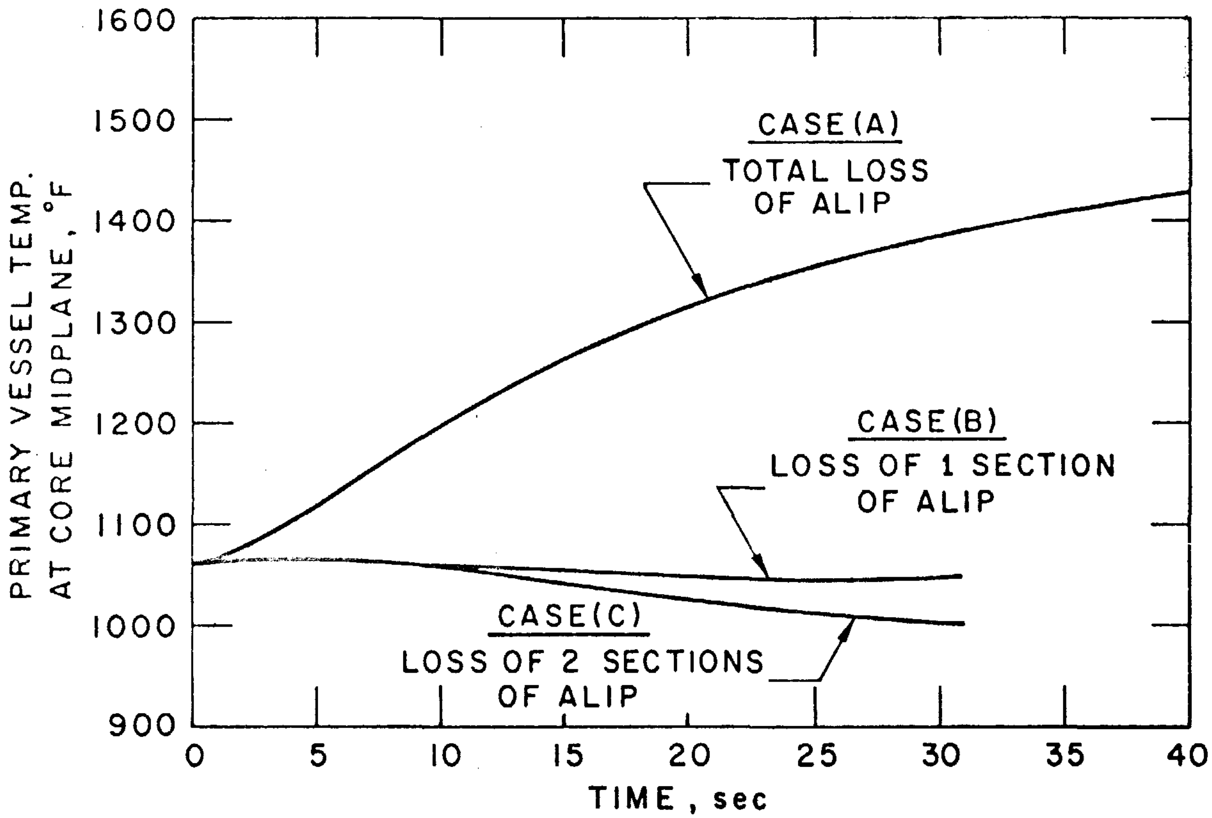

The FEFPL test section thermal behavior for this accident is quite similar to that for the Class I severity level loss of commercial power accident to the loop (see Section 11.2.1.2). With the greatly reduced loop sodium flow (see Fig. 11.1), the continued full helium flowrate has only a minor influence on the test section thermal conditions. Therefore, the conclusions reached for the loss of commercial power to the loop accident are also applicable to the ALIP loss of commercial power accident. However, for this specific ALIP accident, a detailed SAS2A calculation was performed to assess the potential test section damage effects.

This total loss of pump power accident case assumes that only 15 kW out of 45 kW total emergency power is available after a maximum delay of 100 msec (see Fig. 11.1 for flow coastdown). ETR shutdown initiation was studied for three assumed FEFPL-EAS low ALIP voltage scram delay times: 1) the design maximum 250 msec delay, 2) a 180 msec delay, and 3) expected 80 msec delay. The test section sodium flow rate was again calculated by SAS2A for this case, using the expected pump head versus time relationship described in Appendix B.2.

The results for these studies are summarized in Figs. 11.12 and 11.13. With the 15 kW of emergency power, the test section flowrate leveled off at approximately 45% of full flow after ∿200 msec into the accident. In Fig. 11.12, the local inner clad temperature is presented. For a 250 msec scram delay, a peak cladding temperature of ∿1630°F was obtained at the top of the active fuel region ∿0.7 sec after initiation of the accident. With the expected 80 msec scram delay, Fig. 11.12 shows a peak cladding temperature of only ∿1580°F. As Fig. 11.13 indicates, no fuel melting was obtained for this accident as the emergency flow was sufficient to resume rapid fuel cooling.

It is concluded from the results of this case that the delayed emergency pump power assistance coupled with an ETR shutdown will be sufficient to assure the safety of the FEFP Loop. For the occurrence of the loss of power at the FEFP operating conditions assumed in this evaluation (sodium inlet temperature of ∿900°F and outlet of 1300°F with a peak heat flux of 12.8 kW/ft), the peak clad temperature exceeded ∿1600°F (peak of ∿1630°F) for less than 1/2 second, assuming the maximum 250 msec design delay in ETR scram initiation. A more reasonable 80 msec scram delay results in a peak cladding temperature of 1580°F, which is below the FTR clad damage 1600°F threshold temperature[5]. (For fuel containing an end-of-life plenum pressure

FIG. 11.12 - FEFPL Control System Protected Total Loss of ALIP
Accident Inner Cladding Surface Temperature vs Time

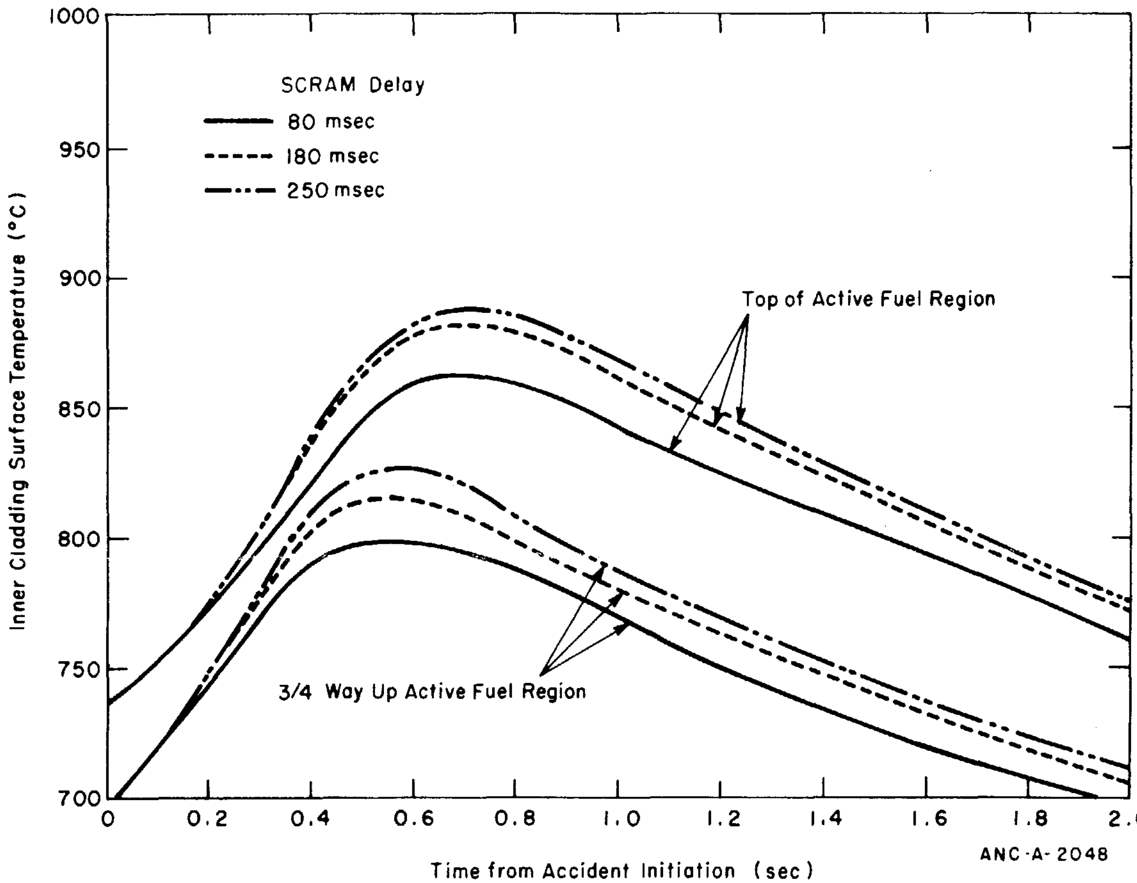

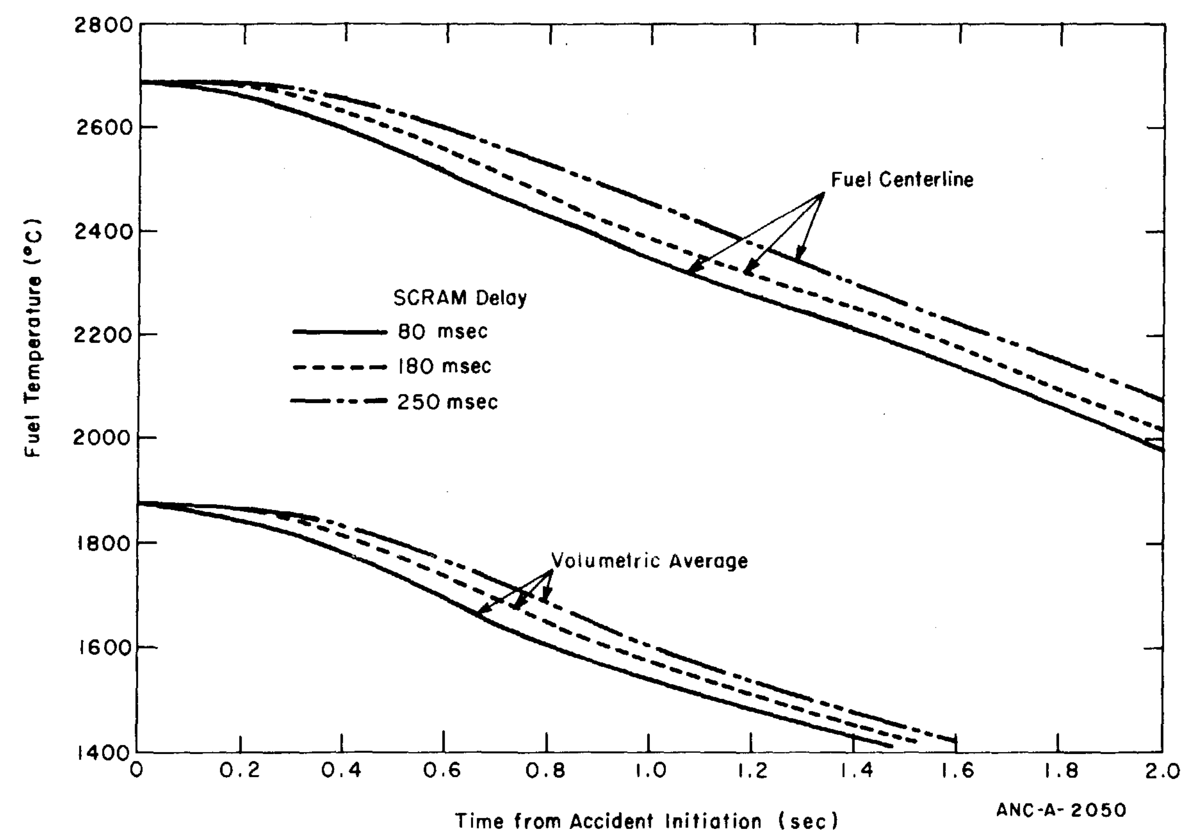

FIG. 11.13 - FEFPL Control System Protected Total Loss of ALIP Accident Axial Core Midplane Test Fuel Temperature vs Time

of 800 psi, the steady state stress equals the clad ultimate tensile strength at about 1725°F).

Class II Accident - Minor Test Section Damage

Potential ALIP malfunctions that may result in some test section damage (see Section 11.1.4.2 for definition) are accidents that require the simultaneous failure of some FEFPL protective systems. As discussed in the previous Class I Accident Section, no FEFPL corrective action is required to prevent test damage for partial pump power losses involving loss to one or two ALIP sections. The ALIP accidents which will result in a Class II accident severity level are discussed below. All analyses have been conducted assuming the loop to be initially at the upper limit of the loop operating envelope (Point C).

a) Loss of Commercial Power to ALIP

Failure of either one of the two FEFPL EAS functions (ETR scram or transfer to emergency power) is required to create some test fuel damage. As discussed in the previous section, successful action by this system will prevent test section damage. The loop thermal behavior for this ALIP accident is about identical to those for the Class II severity level loss of commercial power to the loop accident. Therefore, the details of the effectiveness of the FEFPL protection systems presented in Section 11.2.1.2 apply as well to this loss of commercial ALIP power accident.

In addition, however, SAS2A calculations were performed for this ALIP power accident where the failure of the FEFPL control system (transfer to emergency power) is postulated. For this case, assuming that an ETR shutdown was successfully initiated after a 180 msec delay, no test section fuel melting was realized. The FEFPL test section power decrease, however, (rapid reduction to ∿10% of full power after ∿.25 sec following shutdown initiation) is not sufficient to preclude sodium boiling nor clad melting. A void initiation time of ∿0.69 sec, a clad sodium liquid film dryout at ∿1.24 sec and clad melt inception time of ∿1.84 sec are predicted. The positions of the liquid vapor interfaces during sodium voiding due to the colder fuel obtained for this reactor shutdown case, remain deeper in the test section (upper interface oscillated in the fission gas plenum region around the 130 cm axial elevation with the lower liquid leg remaining near the 20 cm axial elevation relative to the bottom of the active fuel region).

Additional SAS2A calculations were made investigating the influence of an assumed ETR scram time delay on the total loss of ALIP power accident without emergency ALIP power. In this study, a total time scram delay of 80 msec and 250 msec were used. The 80 msec value assumes there is no time delay in detecting the loss of power nor time lag in transmitting the scram signal to the experiment amphenol. The 250 msec delay is the maximum design value.

The SAS2A predictions for this accident are summarized in Table 11.4

TABLE 11.4

INFLUENCE OF SCRAM DELAY ON TOTAL LOSS OF ALIP POWER ACCIDENT WITHOUT EMERGENCY POWER ASSISTANCE

	80 msec Scram Delay (sec)	180 msec Scram Delay (sec)	250 msec Scram Delay (sec)
Time clad temp reaches 1600°F	∿0.4	∿0.4	∿0.4
Void initiation time	0.73	0.69	0.67
Clad film dryout time	1.22	1.20	1.12
Clad melt inception time	2.05	1.84	1.75
Fuel melt inception time	never	never	never

Void initiation assumed at a 70°C sodium liquid superheat.

These results indicate that significant test section damage will occur even with a 80 msec scram delay. Conditions predicted for the maximum 250 msec scram delay are not appreciably different than the shorter delay times with the maximum amount of clad melting predicted to be 4%. However, the lack of molten fuel generation suggest that the possibility of a violent MFCI is quide remote and the safety of the loop is not threatened. Nevertheless, based upon the predicted amount of clad melting, it appears that the test section damage will preclude performing the planned experiment.

b) Complete Loss of Electrical Power

The loss of all electrical power to the ALIP is an extremely unlikely event because of redundancy in power supplies. Although it is possible that the previous partial loss of ALIP power faults could extend to loss of power to the third section, the probability is very small.

If this occurred, however, the ALIP could be completely lost with no transfer of power possible. Both of these accidents are limited to a Class II severity level by FEFPL-EAS scram action initiated from the low voltage subsystem. The loop thermal behavior for these cases would be identical to that for loss of commercial ALIP power accident studied in the previous section without emergency ALIP action.

The ALIP power system described in Section 5.2.4.2 is provided with a system of fuse protection in order to provide defense against conceivable primary primary vessel damage due to multiple pump power system faults. Two sets Two sets of fuses (nine fuses in each set) are provided, one set each in the feeder lines from the normal power source and the emergency power source. The EAS provides a protective function which monitors the section voltages applied to the ALIP. This function will initiate a reactor scram and transfer to emergency power on loss of the normal power source for the ALIP, including loss of power to two sections due to fuse opening resulting from a normal power surge or common mode failure of the fuses. This function is implemented using three instrument channels in a two-out-of-three protective function. Prior to installation, all the fuses will be checked at approximately 90% of full load rated current to insure that mislabeled or faulty fuses have not been obtained.

The probability of undesired failure of the fuses in the emergency power feeders is extremely low, since the normal and emergency sources are isolated by the transfer switch and the emergency power source is a fixed voltage system with a relatively high source impedance and a corresponding lower maximum fault current. This lower value permits a longer fusing time. The net result is that the normal emergency current is well below full load rated current of the emergency feeder line fuses.

c) Sudden ALIP Power Reversal Accident

With the ALIP operating normally at full or partial flow, a reversal in power is virtually an impossibility. Ad discussed previously, for this to occur would require an incorrect phasing of the pump power. The connector design incorporates mechanical interlocks to prevent an incorrect initial hookup of phase and pump section. Furthermore, verification of the correct power phasing at each connector for the two independent power sources will be a pre-operational requirement. A phase change during operation due to a commercial source error is very remote.

Nevertheless, the computer program COASTDWN, (for description see Appendix B.7), was used to determine the effect of pump power reversal on coolant flow in the FEFP loop. These calculations assume that the coolant circulation head is not a significant factor in the coolant transient response to changing pump operation, i.e., no coolant density changes during the transient.

Abrupt loss of pumping power in the FEFP loop results in a flow coastdown with the flow asymptotically approaching a level dependent on the circulation head (density difference) in the loop. Flow coastdown characteristics for the loop containing a 37-element test subassembly are shown in Fig. 11.14. Half flow is reached in the loop, test train, and bypass channel at 61 msec, 74 msec, and 46 msec, respectively, after loss of pump power.

Abrupt reversal of pump power causes a more rapid decrease in loop flow than pump trip. After a pump trip, the influence of the pump on loop flow is limited to the frictional resistance of the pump duct. After a power reversal, the pump acts like a brake on the sodium flowing down through the loop, resisting the loop flow with a pressure initially greater than the pump stall pressure. Fig. 11.15 illustrates the changing mass flow rate in the FEFP loop after pump power reversal has occurred. Half flow is reached in the loop, test train, and bypass channel at 21 msec, 26 msec, and 11 msec, respectively, after reversal of pump power.

For both loss of pump power and pump reversal, the mass flow rate in the test subassembly changes more slowly than either bypass or total loop flow. Fig. 11.15 illustrates that test section flow does not reverse until 60 msec after pump power reversal, over 20 msec later than loop flow reversal. Reversal of flow in all regions of the loop is essentially complete in 200 msec.

Thus, in terms of the time to reach sodium boiling within the test section, clearly, the sudden ALIP power reversal is more rapid than the total loss of ALIP power accident. However, the time at which test section flow reversal occurs (60 msec) is not much different than the zero flow time calculations for the instantaneous and total inlet flow blockage (80 msec) accident discussed in Section 11.3.2.2 on loop flow blockage. With the decreased scram delay time for this pump power reversal accident (80 msec delay based upon ALIP low voltage signal versus a 180 msec flow blockage accident

FIG. 11.14. FEFP Loop Flow Coastdown Characteristics

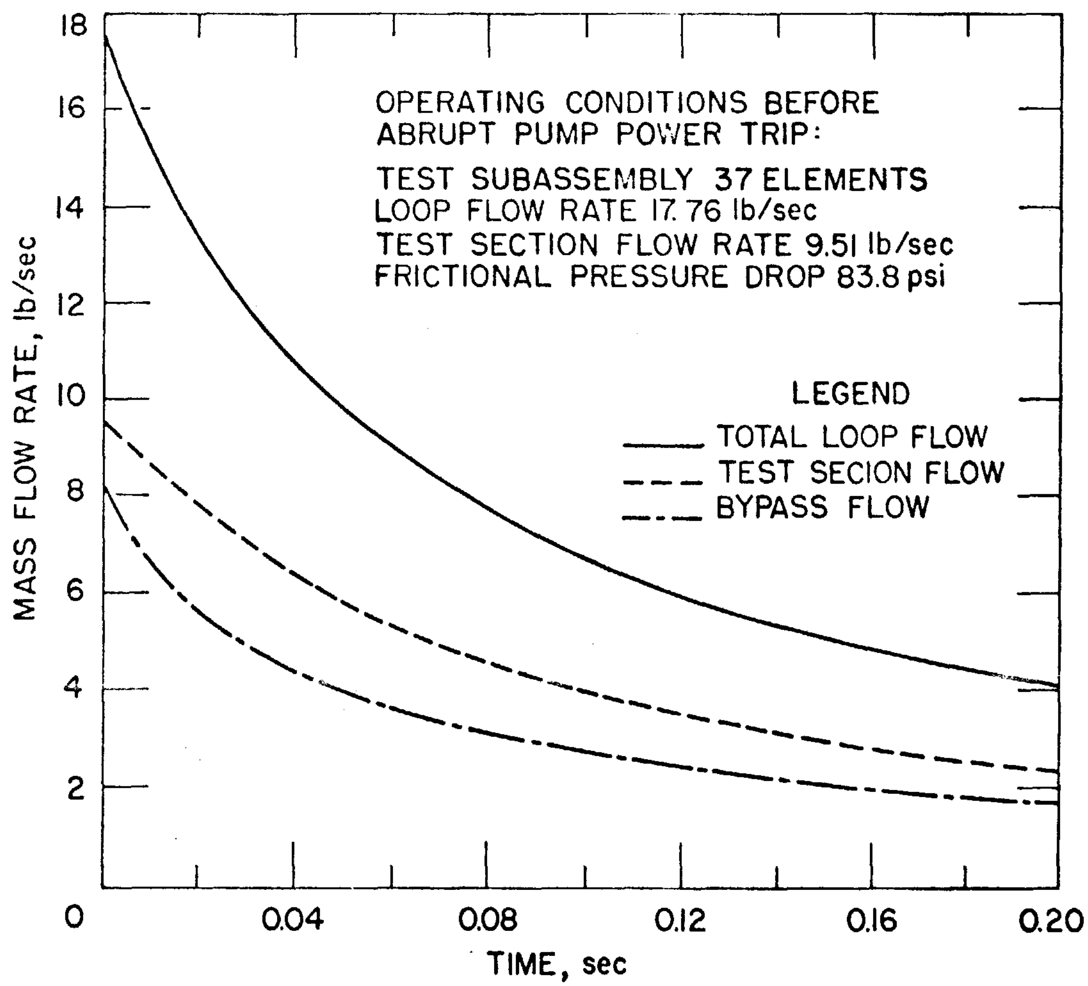

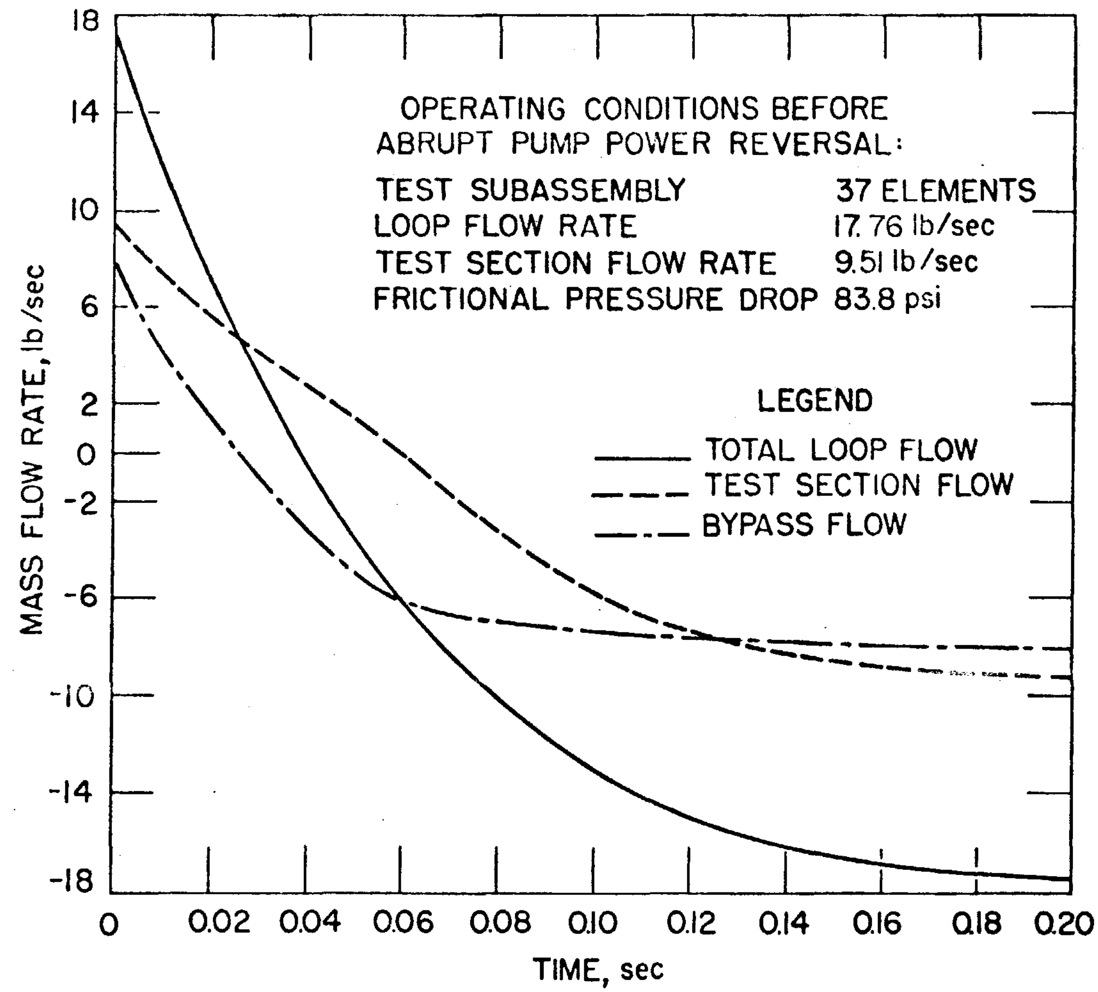

FIG. 11.15. FEFP Loop Flow Reversal Characteristics

scram delay based upon low test section flowrate) the accident consequences from the standpoint of test section damage will be less severe than the conditions presented in Section 11.3.2.2 for a total loop sodium blockage accident.

Class III - Major Test Section Damage

In order for an ALIP loss of power accident to result in major damage to the test section, the simultaneous failure of both FEFPL-EAS protective functions in the FEFPL control system must be postulated. This extremely unlikely combination of events will result in a Class III severity level accident (see Section 11.1.4.2 for definition) for only the complete loss of ALIP power and the ALIP power reversal accidents. Partial power loss (i.e., to one or two sections) will not generate molten fuel even in the event of no protective action. The ALIP power reversal accident consequences, assuming no FEFPL control system action, are expected to be quite similar to those obtained for the total flow blockage accident presented in Section 11.3.2.2 and therefore will not be discussed herein. Safety protection against excessive loop thermal conditions during this accident is provided by the scram action of the FEFPL-PPS.

For the various investigations of the complete loss of ALIP power accident with no FEFPL-EAS scram, the THYME-B code and the SAS2A code were employed. Overall loop thermohydraulic behavior was determined with the THYME-B. The details of the thermal conditions within the test section were determined with SAS2A. A brief summary of these studies is presented.

For the accident results calculated with SAS2A (assuming no ETR scram nor availability of emergency ALIP power with loop initially at Point C) the rapid reduction in test section sodium flow (flow drops to $\sim$8% of full flow after $\sim$0.6 sec) results in sodium boiling $\sim$0.6 sec after the loss of pump power. This voiding occurs at an axial location approximately 75% of the way up from the bottom of the active fueled region. The initial sodium expulsion takes about 150 msec to void the active fuel region. Thereafter, the sodium expulsion process exhibits the familiar oscillatory behavior of repeated partial liquid reentry followed by subsequent expulsion. During the 6 sec time interval over which this transient was studied, the active fuel region was almost completely voided of liquid sodium. The upper liquid-vapor sodium interface oscillated in the fission gas plenum region around the 140 cm axial elevation (active fuel region 91.5 cm long). The lower liquid-vapor interface penetrated into the fueled region, but never more than about 15 cm.

The liquid sodium film remaining on the fuel cladding outer surface initially became dry after ∿ 1.0 sec into the transient followed soon after by the inception of clad and fuel melting. Clad melting was initiated after ∿ 1.2 sec with fuel melt inception at ∿ 2.4 sec from the start of the accident. After about 4.9 sec into the accident, approximately 50% of the total test section fuel inventory was predicted by SAS to be molten.

The THYME-B thermal calculations for the total loss of ALIP power accident are presented in Fig. 11.6 and 11.11. In this analysis, it is again assumed that no corrective action is taken by the loop control system. Furthermore, the results shown assume no ETR scram action. As seen from Fig. 11.11, the primary vessel temperature would reach its 1300°F design limit about 18 sec into the accident. Based upon the previous SAS2A results, this time is considerably longer than the time needed to permit an MFCI to occur; thus, ample time is provided for preventative action. The FEFPL-PPS gives automatic scram protection thus insuring continued containment margin throughout this accident.

Several additional SAS2A runs were made investigating the influence of several factors on the previous accident predictions. The results of these studies are summarized below.

Effect of Axial Power Distribution

In the previous studies the target FFTF 1.25 peak/average cosine flux distribution was employed. To evaluate the change in accident conditions which would be realized without test section axial flux shaping, the normal unmodified ETR 1.40 peak/average flux distribution was evaluated. Fig. 11.16 shows this unmodified 1.4 power shape which was studied along with the reference 1.25 shape. Note that the ETR shape is slightly skewed toward the inlet of the test section.

For comparison purposes, the total loss of power accident was evaluated with all of the SAS2A calculational conditions remaining the same with the exception of the axial power shape and the peak flux. To operate at identical FEFP loop conditions (Point C on safety operating envelope) with the 1.4 peak/average power distribution, the peak heat flux required was 14.4 kW/ft (with 1.25 axial power shape factor, this value was 12.8 kW/ft).

The SAS2A results for this case are summarized in Table 11.5 along with the results obtained previously for the 1.25 shape. For this 1.4 shape with the same loop conditions, initial fuel centerline melting was assumed to

FIG. 11.16. Comparison of Reference 1.25 P/A FTR and 1.40 P/A ETR Axial Power Shape

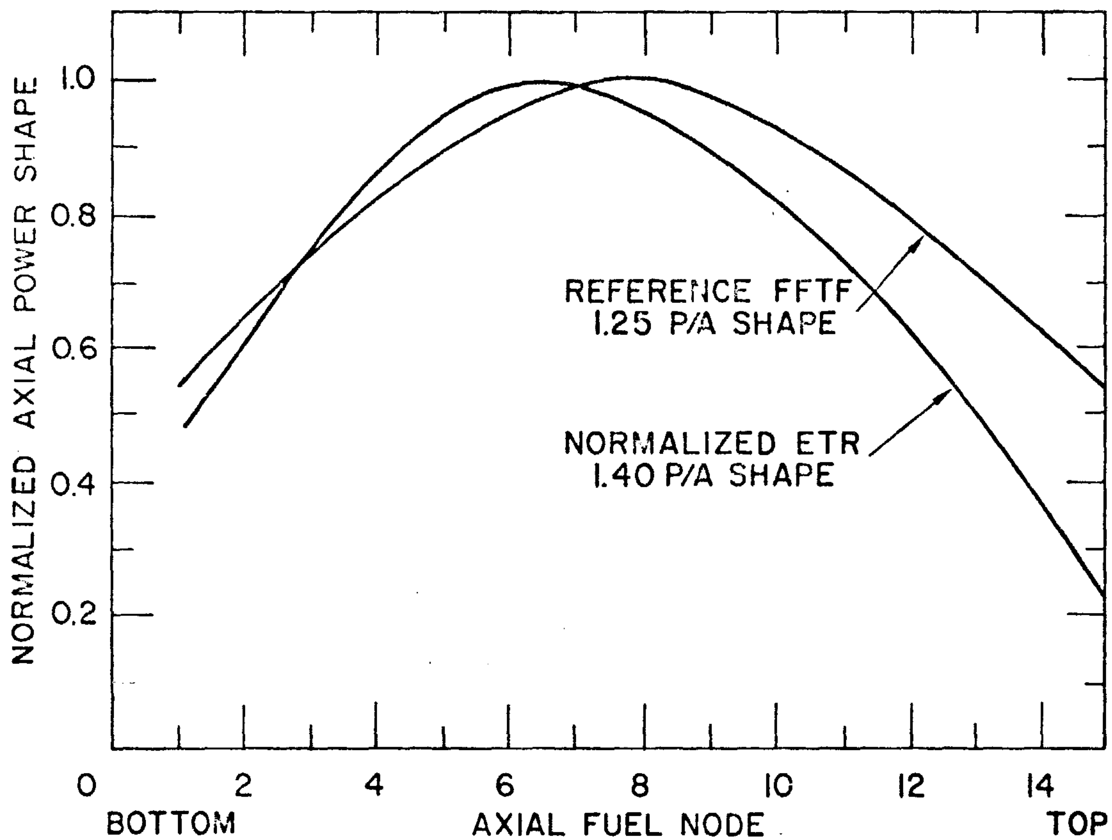

show the effect of this parameter although higher linear powers are expected before such melting actually occurs. As expected, the higher peak heat flux resulted in about a 10% reduction in the time to reach test section failure conditions. The combination of higher peak heat flux and shift in power distribution toward the inlet also resulted in a deeper sodium void initiation in the test section (59 cm vs 72 cm).

Influence of Initial Loop Conditions

Throughout this study for upper limit analyses, the loop conditions corresponding to operating Point C on the loop's safety envelope were used to define the initial state. This starting point gives the highest loop containment temperatures, but not necessarily the most adverse test section thermal conditions. Therefore, the remaining upper operating limit points (G and B of Table 11.2) of the loop safety envelope were examined using as a basis the total loss of pump power accident without scram. Point A on the safety envelope was not studied (see Table 6.4 of Chapter 6), as the loop thermal conditions were clearly less severe than the previously analyzed Point C. Initial loop conditions for these cases are presented in Table 11.2.

Results for the FEFPL-PPS protected total loss of pump power accident, starting at different initial loop operating conditions are presented in Table 11.5. The high heat flux case (Point G) results in only a 10% reduction in time to attain excessive test section conditions when compared to reference Point C. On the other hand, the lower sodium temperature case (Point B) yields almost identical conditions to Point C. It is concluded, therefore, that the long term consequences of an accident initiated at these other upper limit points will not be significantly different than the reference Point C conditions.

The results of this postulated loss of pump power accident clearly indicate that considerable clad and fuel melting will occur with extensive damage to the test section. The attainment of a molten fuel coolant interaction (MFCI) appears to be the next possible consequence of this accident. The SAS2A predictions of the accident conditions, however, are not significantly different or more severe than those used in the reference experiment as seen in Table 11.5. The potential MFCI which could result from this accident, therefore, would be well within the present design envelope containment capability of the FEFP loop.

TABLE 11.5

Effect of Axial Power Shape and Initial Loop Conditions
On the Total Loss of ALIP Power Accident Results

A. Effect of Axial Power Shape*

Accident Results	Reference 1.25 Axial Power Shape	Normal ETR 1.4 Axial Power Shape
Void Initiation Time	0.61 sec	0.57 sec
Clad Film Dry Out Time	1.01 sec	0.89 sec
Clad Melt Inception Time	1.21 sec	1.07 sec
Fuel Melt Inception Time	2.36 sec	Initially melted
Location of Void Inception	71.73 cm	59.31 cm

B. Effect of Initial Loop Conditions**

Accident Results	Upper Operating Limits			Reference Experiment
	Point C	Point G	Point B	
Sodium Void Initiation Time, sec	.61	.55	.62	.41
Clad Film Dry Out Time, sec	1.01	0.88	.96	.71
Clad Melt Inception Time, sec	1.21	1.07	1.20	.88
Fuel Melt Inception Time, sec	2.36	Initially Melted	Initially Melted	Initially Melted

* Loop initially at Point C conditions.

** For initial conditions, see Table 11.2 and for Reference Experiment description, see Chapter 10.

11.3.1.3 ALIP System Failures

In analyzing the various faults of the ALIP system, reference is made to the description of the ALIP power system, Section 5.2.4.2.B and Fig. 5.12 - ALIP Power System Schematic. The ALIP is powered with a motor-alternator through a distribution and protective system providing redundancy in event of any power system individual component failure. Following the alternator output main circuit breaker, each section of the pump has an entirely individual self-sufficient power distribution and protective scheme. The three emergency transfer switches are electrically and mechanically independent, thus a fault in one is not carried over to the adjacent one. In addition, FEFPL protection is provided by the EAS and PPS for all ALIP failures. Table 11.6 summarizes the potential ALIP malfunctions and corrective actions. Several of these faults will be discussed below. In all cases, these ALIP system failures will result in consequences no more severe than those discussed previously for the loss of ALIP power accidents.

Fault A - The loss of one phase to one section of the pump results in that section becoming inoperative with a resultant reduction in the total loop sodium flow. The loss of one phase outside of the ALIP stator results in single phase operation of the affected section, with an immediate loss of pumping force. As in the partial loss of ALIP power faults, the failure can occur in the leads or any of the components of the distribution circuitry; namely, any portion of the conductors, circuit breakers, fuses, emergency transfer switches, ratio transformers, etc. A failure in one section of the power system to ALIP will initiate corrective action automatically by increasing the power to the remaining two sections. Flow in the loop is monitored and controlled by a flow sensor which, during the normal operation, constitutes part of the control system that actuates the control of the output of the ALIP alternator power.

Fault B - The loss of one phase to each of two sections results in no pumping in two-thirds of the entire ALIP. This results in one third the pumping capacity. The comments of Fault A apply to both of the affected sections of the ALIP. Although possible, this failure is improbable because of the independent and redundant nature of the ALIP power distribution system as well as the pump sections themselves. The corrective action is the automatic increase of the power to the remaining section of the pump. An automatic EAS initiated scram may also result depending upon the initial loop conditions and selected setpoints.

TABLE 11.6

Consequences of Pump Power Circuit Faults

A.

Number of Pump Sections Affected	Number of Phases Lost Before Transfer Switches		
	1	2	3
1	cut out lost section increase power	cut out lost section increase power	cut out lost section increase power
2	cut out lost sections increase power	cut out lost sections increase power	cut out lost sections increase power
3	transfer to emergency power	transfer to emergency power	transfer to emergency power

B.

Number of Pump Sections Affected	Number of Phases Lost After Transfer Switches		
	1	2	3
1	cut out lost section increase power	cut out lost section increase power	cut out lost section increase power
2	cut out lost sections increase power shutdown likely	cut out lost sections increase power shutdown likely	cut out lost sections increase power shutdown likely
3	shutdown certain	shutdown certain	shutdown certain

C. Failures Inside Pump Windings

Number of Pump Sections Affected	SHORT (Double short which draws current)	One Phase Open	Two Phases Open
1	cut out shorted sections increase power	increase power	cut out section increase power
2	cut out shorted sections scram likely	increase power	cut out sections increase power shutdown likely
3	cut out all sections scram certain shutdown certain	increase power shutdown likely	pump is out shutdown certain

*See Chapter 5 for details of the FEFPL Experiment Assurance System which provides the primary protection function for these faults.

<u>Fault C</u> - The loss of one phase of the ALIP alternator output results in the loss of all pumping action temporarily. Protective devices in the ALIP power distribution system will transfer the pump to the emergency power system automatically upon loss of voltage on any of the phases alternator output. Automatic corrective action also includes scramming of the reactor via the FEFPL-EAS.

<u>Fault D</u> - A short in the electrical circuit to one-third of the pump results in an alarm to the operator. The entire pump system is part of an ungrounded distribution system. No adverse effect will occur with one short. However, for the sake of safety of the experiment, operator decision will disconnect the affected section of the pump to prevent possible ALIP damage resulting from a second short circuit within the same section. With the affected section inoperative, the power to the remaining sections will automatically be increased to compensate for the outage of the first section.

<u>Fault E</u> - Individual short circuits in two of the three sections of the pump will cause the alarms for each of the affected sections to alert the operator. Protection against excessive ground currents between these two sections is afforded by fuses and circuit breakers in the circuits. Automatic control action will call for an increase in the output of the unaffected pump section. In event of small ground currents, no ALIP damage will be incurred and hence no automatic interruption of the affected sections will occur. Nevertheless, operator decision will be to shut the two sections down to prevent possible ALIP damage due to the occurrence of a second short in either effected section.

<u>Fault F</u> - An individual short in each of three sections will again cause action much the same as in the preceding Fault E. With these sections faulted, the immediate manual decision will be to terminate the experiment (using normal shutdown procedures) to prevent subsequent serious damage to the loop if a second short occurs. If the ground currents are excessive, the pump will be tripped automatically by the fuses or circuit breakers in each of the circuits along with the subsequent initiation of an ETR scram.

<u>Fault G</u> - Open electrical stator winding coil in one phase of one section of the pump results in a reduction in the flow in the affected section. This condition produces an open delta configuration and pumping will be reduced by at least 40%. The control system will automatically increase the power to the remaining sections of the pump. The open winding

presents no problem to the safety of the loop. However, to guarantee against further damage to the pump winding, this section of the pump will be tripped automatically by the current overload sensing elements of the circuit breaker feeding this section of the pump.

Fault H - An open electrical circuit in one part of the delta connected stator winding in each of two sections of the ALIP will result in a reduction of the flow in the loop. The corrective action is the same as stated in Fault G.

Fault I - An open circuit in one branch of the delta connection in all of the sections of ALIP will result in a reduction of the flow in the loop. This type of fault is improbable, however, should a condition of this nature occur, the overload sensing device in each of the circuits will trip the pump and initiate an ETR shutdown.

Fault J - An open electrical coil connection in two phases of one-third of the pump winding results in reduction of flow in loop and loss of one-third of the pump. The loss of two phases within a section of stator windings, both from an open connection, reduces that section to single-phase, nonpumping operation. This corresponds to the loss of an alternator output phase (see Fault C) or the loss of pump-section power load (see Faults A and B). Here, however, there is no possibility of transferring to emergency power. The corrective automatic action is to increase power input to the remaining two-thirds of the pump, along with manual shutdown of the faulted one-third of the pump.

Fault K - An open electrical coil connection in two phases of two-thirds of the pump winding results in reduction of flow in loop and loss of two-thirds of the pump. The automatic corrective action will be to increase power to the remaining one-third of the pump and to manually shutdown the affected two-thirds of the pump. Comments in Fault J also apply here.

Fault L - An open electrical coil connection in two phases of all sections of the pump windings results in loss of all pumping action. The automatic corrective actions are to scram the reactor and control heat exchanger operations to optimize natural convective cooling of the loop.

Pump Short Consequences

As discussed above, several electrical failures and/or malfunctions occurring within the ALIP have been identified which may cause a partial or total interruption in pumping capability. For these accident situations, the behavior of the loop and the ultimate safety implications of the resultant events are identical to the loop conditions predicted for the various partial and total loss of pump power accidents. The results have been presented previously in Section 11.3.1.2.1.

Another class of failures within the ALIP which have an additional potential for loop damage are electrical shorts. Concern here is that an electrical short situation might develop within the ALIP which could conceivably result in a burnthrough of the primary vessel. The likelihood for this actually happening is very remote, for as was discussed previously, two shorts are required for current to flow in the ground loop. A ground path detector is provided in all circuits to detect the presence of a single short. Isolation of the electrical fault from input power is provided by a redundant system consisting of fuses and circuit breakers in each power input line. However, in spite of these many lines of defense against the creation of a serious short situation, it does represent a mechanism which can be postulated as causing a violation of primary loop containment. Therefore, an analysis of its burnthrough potential has been conducted with the results discussed below.

Of the many short circuit fault conditions possible, in this analysis the most severe case is assumed wherein one of the three phase feeders ground solidly to the entire metal structure of the loop. A second fault is assumed to occur in the return coil lead at one of the other phases feeding the same ALIP section. This line-to-line fault is the most severe, as it represents the highest available voltage. Figure 11.17a shows the assumed fault locations along with the coil arrangement and pump details at the center of the coils.

The current flow and hence the amount of energy available for possible damage is a complex function of the system and of the characteristics of the ground path between the location of the shorts. The current will be limited by the internal impedance of the alternator plus the impedance of the external circuit in which the fault occurs. For the FEFPL ALIP short conditions assumed in Fig. 11.17b, the symmetrical short circuit current is estimated to be 1560 amps. Under the sudden fault, the alternating current shifts initially off its zero base as though biased with a DC current. Although this effect lasts only 2 or 3 cycles, this offset current (asymmetric value) can be as high as 1.41 times the root mean square (rms) 1560 amps value. The asymmetric short circuit current then can attain a peak value of 2170 amps for this accident.

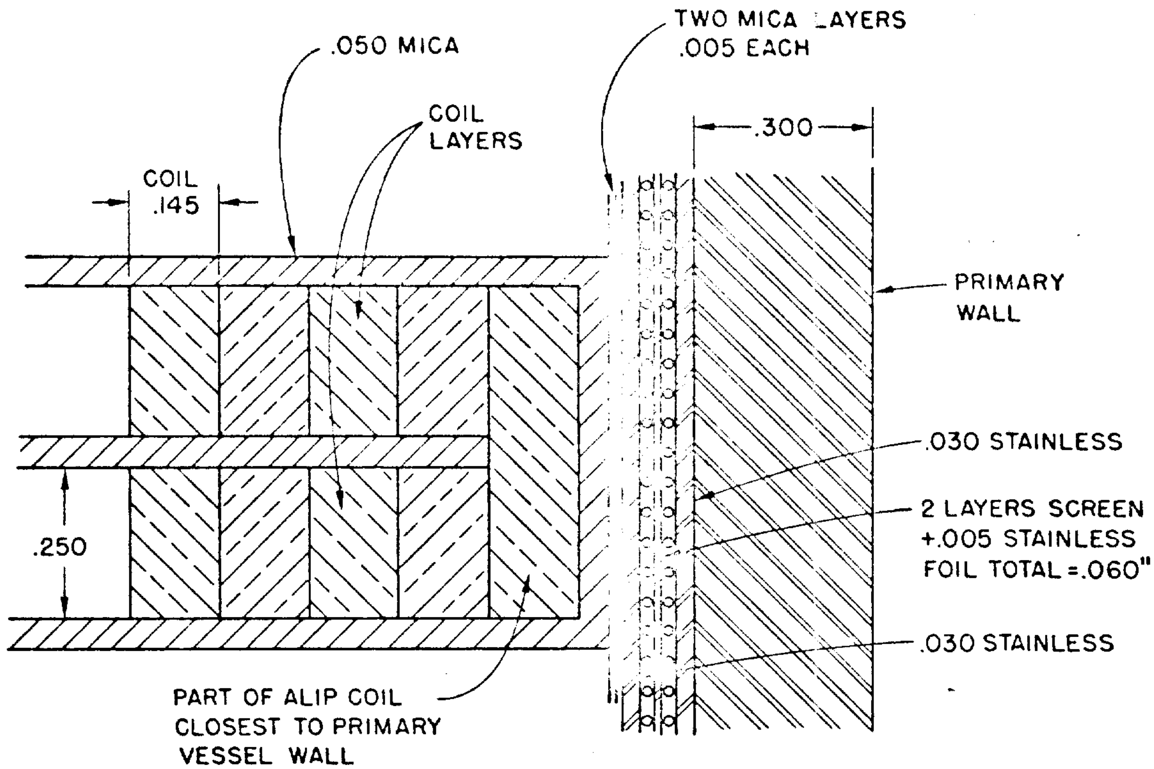

Location of Most Severe Fault

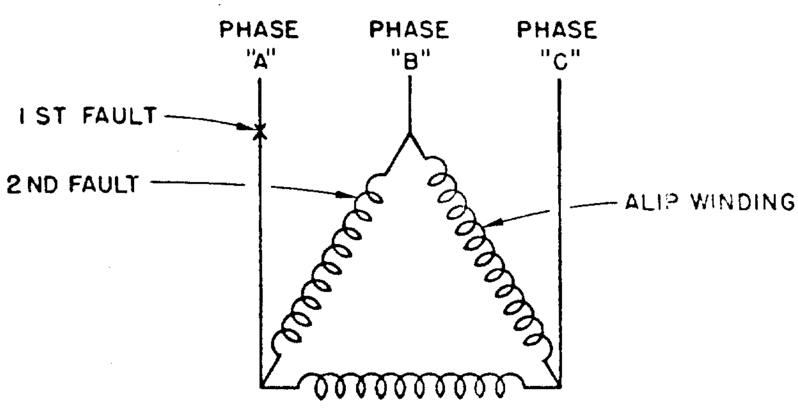

FIG. 11.17. Schematic of Most Severe ALIP Short

The ALIP power circuit contains circuit breakers in the feeders to each section which require about 3 cycles or 50 milliseconds to open the circuit and quench the arc. To reduce this time, 100 amp fuses are provided in each input line. Using a typical time current characteristics curve for this type of fuse, the fuse will melt in less than 1 millisecond when subjected to the projected 2170 amps current flow. The energy generated before the passive fuse blows is then 4.5 kjoules.

To determine whether this 4.5 kjoules energy source can burn through the primary vessel, a very simplified yet conservative analysis approach is taken. For this most severe case, it is assumed that the fault occurred at a point with melting of the copper and stainless steel proceeding in a spherical manner. Neglecting all heat losses and the heat shields between the winding of the coil and the adjacent primary wall (see Fig. 11.17a), a simple heat balance is written in which it is assumed that half of the energy is used in melting the copper and half is expended in melting the stainless steel. This assumption is overly conservative as in reality, the higher copper thermal conductivity dictates that a much larger heat flow will occur in the direction of the coils. Assuming that initially both the pump winding and the primary vessel are at 1100°F, the adiabatic spherical depth of melting is calculated to be 77 mils in the winding and 65 mils in the primary vessel. Since the primary vessel is 0.300 in. thick, even with this very conservative calculation, a considerable safety margin exists before meltthrough would be achieved.

11.3.2 Sodium Flow Blockages

11.3.2.1 Discussion of Sodium Flow Blockages

Total loop sodium flow blockage is considered a very unlikely accident. The inherent design of the FEFP, with its annular flow paths, has relatively few areas where undesirable debris can collect; in addition, a minimum number of components which could fail and cause flow blockages make a complete sodium flow blockage virtually an impossibility. The molten-fuel cup will be very securely mounted to prevent it breaking away and blocking the inlet to the test section. The loop sodium filter is designed and sized to prevent the occurrence of a total loop flow blockage in this region. The other loop internal components are also conservatively designed with the knowledge that a preexperiment structural failure could ruin the experiment. In addition, the purity and quality of the loop sodium will be fixed at an acceptable level prior to loop operation.

After an experiment, a whole range of possibilities exist for loop flow blockage. These post-experiment flow blockages are not considered as accidents, but rather as normal operating conditions as discussed in Chapter 9. The internal loop structures, in particular the in-core portions of the test train, may be deformed or fragmented. Thus, the possibility exists for blockages in the test section, bypass, downflow, or mixed test section and bypass flow above the core. When the size of the flow areas involved is considered, the possibility of a total flow blockage or even one large enough to hinder post-experimental removal of heat seems remote. The critical points with respect to flow blockages are in the heat exchanger and pump. At these locations, a flow blockage may occur, but the consequences of any credible flow blockage can be safely contained. An evaluation of the consequences of the clogging of the loop sodium filter has been presented previously in Chapter 10.

Protection against an accidental loop flow blockage is provided by the FEFPL control system. Having the responsibility for early detection will be the test section flow sensor in the Experiment Assurance System (EAS). Control action will consist of an automatic increase in electrical power to the ALIP in an attempt to increase loop sodium flow and if necessary an ETR scram (see Table 11.1 for typical set points).

For some FEFPL experiments, there will exist a large available flow reserve which may be used to recover from the loop sodium flow reductions (e.g., experiment P-1 requires an ALIP power ($\sim$60 kW) less than half of the ALIP's rated power of 150 kW). Other experiments (e.g., P-2) will operate at steady-state at or near the ALIP's rated conditions with essentially no additional pumping capacity available. Analyses of partial flow blockages for both of the above situations which bracket the test conditions to be employed during the FEFPL program are presented in this section.

Loop safety protection against a flow blockage accident also is provided by the FEFPL-PPS. In this system, thermocouples ensure that the loop containment temperatures do not become excessive while pressure sensors detect excessive pressure pulses. For both systems, an ETR scram is the required protective action. These protection subsystems are described in detail in Section 7.

11.3.2.2 Analysis of Sodium Flow Blockages

In spite of the precautions which will be taken in the loop design and during the preoperational testing period to ensure that flow blockages are not initially present within the loop or occur during power operation, they cannot be ruled out completely. Therefore, the consequences of this occurrence have been studied. The results of these investigations are discussed below in terms of the three classes of accident severity levels defined in Section 11.1.4.2. Both partial and total sodium flow blockages have been studied as discussed below.

Class I Accident - No Test Section Damage

The magnitude of postulated sodium flow blockages which do not result in test section damage has been established for both test section and loop blockages. The COASTDWN and THYME-B computer codes (see Appendix B for descriptions) were employed. These studies considered two cases. The first (Case A) assumed the loop contained 37 full-length test fuel elements and was initially operating at experiment P-1 thermal-hydraulic conditions. In the second case (Case B), the loop was assumed to be operated with 19 full-length test fuel elements at P-2 conditions. As discussed below for the two kinds of sodium flow blockage accidents the loop has a tolerance without test section damage for even a very massive type of flow restriction. Blockages more severe than those identified below must be classified as hypothetical as they represent flow area reductions for which no initiating cause of mechanism can be postulated.

a) Partial Test Section Sodium Flow Blockages

Presented in Table 11.7 are parametric results of postulated test section flow blockages as obtained using the COASTDWN code. These calculations are somewhat idealized in that the test section blockage effects were treated only as a flow area reduction in the fuel element support grid. No additional effects such as increased test section flow maldistribution were considered. Also, the COASTDWN code is based upon an isothermal model. However, in spite of these limitations, the analysis results of Table 11.7 nevertheless indicate that the flow reductions created by rather massive test section blockages are not as large as one might first suspect.

As seen in Table 11.7 (Case A) for typical P-1 test conditions without an increase in ALIP power (uncorrected flowrate), an areal test section inlet blockage of 80% will reduce the test section sodium flowrate to 64% of that present initially. The rather large total loop flow resistance of 85 psi accounts for this relative insensitivity to local blockage.

THYME-B analyses indicate that an instantaneous test section flowrate reduction of greater than 50% of rated flow is required to cause boiling and test section damage. Therefore, this 36% flow reduction will not result in sodium boiling even without an expected ETR scram from the low test section flow subsystem of the FEFPL-EAS. (From Table 11.7, and the typical FEFPL-EAS set point of 20% of rated flow as tabulated in Table 11.1, an ETR scram is assured for test section blockages greater than ~60% for Case A).

With successful ALIP control action (increase power to ALIP) as Table 11.7 for Case A indicates, an areal test section inlet blockage of about 90% can be tolerated without exceeding the Class I accident severity level, even without an ETR scram. The increase in ALIP power from its initial 78 kW level to the rated 148 kW level will allow the test section flowrate to recover to ~50% of its initial flowrate. This flow is adequate to preclude test section fuel damage for a P-1 type test.

Partial test section inlet blockage results obtained for the assumed initial P-2 test conditions are shown in Table 11.7 as Case B. For these conditions, the ALIP initially is at approximately its rated 150 kW operating limit and hence no reserve pumping capability is available to compensate for a blockage flow reduction. However, as the results of Table 11.7 for Case B indicate, the tolerance for test section flow blockages is comparable to that obtained for Case A P-1 type conditions with ALIP control action (a 90% areal test section inlet blockage reduces the test section flow to 55.6% of that initially whereas for P-1 for the same 90% blockage, an increase in ALIP power to its rated 148 kW power returned the test section flowrate to 49.3% of that initially). The larger initial P-2 loop impedance of ~157 psi versus ~85 psi for P-1 explains this reduced P-2 test flow blockage sensitivity.

The range of test section inlet flow blockages discussed above and tabulated in Table 11.7 are larger than those which can be credibly postulated to occur in the FEFP loop. To illustrate this, for comparison purposes, a pressure sensor (0.5 in. dia) blocking the inlet element grid results in about a 7% areal blockage. This occurrence, although not expected to happen, nevertheless is still about an order of magnitude below the blockage size required to cause minor test fuel damage.

b) Partial Loop Sodium Flow Blockages

The parametric results of assumed partial loop blockages are also presented in Table 11.7. The COASTDWN results were obtained by decreasing

TABLE 11.7

Partial Sodium Flow Blockage Results

Case A - 37 Element P-1 Type Conditions

Assumed Areal Blockage (%)	Uncorrected Flowrates: Test Section Flow (% of initial)	Uncorrected Flowrates: Total Loop Flow (% of initial)	Conditions after ALIP Control Action: Pump Power (kW)	Conditions after ALIP Control Action: Test Section Flow (% of initial)	Conditions after ALIP Control Action: Total Loop Flow (% of initial)
a) Test Section Inlet Blockage*					
50	93.9	97.1	90.2	100.0	103.3
60	88.8	94.5	101.3	100.0	106.1
75	73.4	86.6	148.0	98.4	115.6
80	64.0	81.7	148.0	85.9	109.1
90	36.7	67.1	148.0	49.3	89.9
b) Loop Blockage**					
50	98.8	98.9	81.7	100.0	100.0
60	97.2	97.3	84.6	100.0	100.0
70	93.8	94.0	91.2	100.0	100.0
80	85.0	85.3	112.1	100.0	100.0
90	59.7	60.4	148.0	80.6	81.1
95	33.8	34.8	148.0	45.8	46.9

Case B - 19 Element P-2 Test Conditions

Assumed Areal Blockage (%)	Test Section Flow (% of initial)	Total Loop Flow (% of initial)
a) Test Section Inlet Blockage*		
50	97.9	99.3
60	96.0	98.6
70	91.7	97.3
80	81.7	94.2
90	55.6	85.8
b) Loop Blockage		
50	99.4	99.3
60	98.5	98.7
70	97.0	97.2
80	92.8	93.0
90	76.4	76.9

* Inlet blockage of fuel element support grid.

** Outlet blockage of ALIP

Initial Conditions Prior to Blockage:

Case A - 37 element P-1 conditions (see Table 11.2)
Pump Power - 78 kW
Test Section Flow - 9.353 lb/sec
Loop Flow - 15.825 lb/sec

Case B - 19 element P-2 conditions[3]
Pump Power - 145 kW
Test Section Flow - 4.87 lb/sec
Loop Flow - 13.38 lb/sec

the flow area of the 0.5 in. long exit region of the ALIP. Noticeable in Table 11.7 are the slightly larger loop blockages which can be tolerated compared to the previously discussed test section inlet flow blockages. Without ALIP control action and without an ETR scram, an areal loop blockage of about 90% would be acceptable from the standpoint of producing no test section damage (test section flows of less than 50% are required). If possible, increasing the ALIP power to its rated 148 kW level will extend the loop blockage capability to almost the 95% areal blockage case. As was the case for test section blockages, the P-2 test loop configuration was less sensitive to a total loop blockage than a P-1 type loop (Case B results versus Case A results of Table 11.7). Loop blockages of this magnitude do not appear to be conceivable yet, as illustrated, their safety consequences are nevertheless acceptable.

Class II Accident - Minor Test Section Damage

Based upon the analyses in the previous section, sodium flow blockages capable of producing minor test section damage from the standpoint of loop safety must necessarily be large (i.e., areal blockages greater than 90%). Although even for these a successful FEFPL-EAS scram initiated from the test section sodium flow subsystem will limit their consequences to a Class II accident severity level. To provide an upper-bound estimate for this condition, a total and essentially instantaneous test section inlet sodium flow blockage was studied.

This complete FEFPL test section inlet flow blockage accident was studied using SAS2A as described in Appendix B.2. For these calculations, the blockage was simulated in the one channel SAS2A model by introducing a very large test section inlet hydraulic resistance. An L/D_e of 10^7 was used with the time constant for blockage assumed to be 0.10 sec. All other initial test section conditions remained identical to those used in the previous upper-bound loss of pump power studies (Point C of operating envelope). For this flow blockage accident, a FEFPL-EAS scram (initiated by the loop sodium flowmeters) was assumed to occur with an expected 180 msec time delay after the start of the event. Scram delays of up to the 500 msec design value shown in Table 11.1 would have only a minor influence on the accident predictions.

For this EAS protected accident boiling is predicted to occur at 0.525 seconds. Initial liquid film dryout is reached ∿ 0.9 sec into the accident. With reactor scram the cladding is rewet; then complete dryout is attained and clad melting occurs after 1.725 sec.

The corresponding fuel temperatures reveal that an ETR scram is sufficient to prevent the generation of molten test fuel. The centerline temperature decreased over the ∿ 5 sec period studied. The volume average fuel temperature decreased for the first ∿ 2 sec of the accident, then gradually increased. Although this case was not analyzed beyond ∿ 5 sec, a leveling off in average fuel temperature before fuel melting would be expected.

Therefore, prevention of fuel melting by a FEFPL-EAS scram will result in loop conditions much less severe than those predicted for the reference experiment as discussed in Section 10.2. However, the test section damage resulting from this extremely unlikely total sodium blockage accident may be enough to preclude the subsequent conduction of a meaningful experiment.

Class III Accident - Major Test Section Damage

In order for a sodium flow blockage accident to progress to a level which creates major test section damage, a coincidental failure of the FEFPL-EAS to take preventative scram action is required. The probability of this combination of events happening is very low, but even for this eventuality the loop safety is not compromised. The FEFPL-PPS provides the assurance that an ETR scram will occur before the loop containment margin is reduced. Furthermore, predictions of the total sodium blockage accident (as discussed below) are less severe than those projected in Chapter 10 for the reference experiment.

In the SAS2A calculations a constant power curve was assumed for this flow blockage accident without FEFPL-EAS protection. The SAS2A analysis predicts initially the growth of cavitation bubbles in the inlet section of the test section. The initial cavitation bubble is formed almost immediately (@ ∿ 20 msec into accident) at the -115 cm location due to the inertia of the long liquid leg. After two cavitation bubbles form and collapse, boiling within the test section actually begins after 0.477 sec into the transient. From then on, the upper liquid-vapor interface exhibits the familiar oscillatory behavior. With the inlet blockage there is no signficant inlet liquid reentry nor liquid-vapor interface oscillations. The active fueled region as a consequence stays completely voided throughout the accident. The liquid film initially drys out at ∿.75 sec, but the cladding is subsequently rewetted. Final film dryout is completed then after about 1.5 sec. At this time (about 1.5 sec), the cladding melts.

Quite evident from the fuel temperature predictions at the axial midplane of the test section is the redistribution of heat across the fuel pin. A significant increase in centerline temperature does not occur until almost 5 sec into the event, due to melting which starts at ∿2.4 sec. The volume average fuel temperature on the other hand continuously increases, reaching the melting temperature after about 3.3 sec. Complete fuel melting at the test section midplane is completed approximately 4.5 sec after the start of the accident with 50% of the total fuel inventory becoming molten after 5 sec.

These predicted results resemble those obtained for the Reference Experiment studied in Chapter 10. However, the slower rate of molten fuel generation for this total flow accident suggests that a potential molten-fuel-coolant interaction (MFCI) would be less severe. Comparisons are presented in the next section.

11.3.3 Summary of Loss of Loop Sodium Flow Accident Results

The SAS2A studies of the two major FEFPL accidents (loss of ALIP power and total loop flow blockage) suggests that the results will be quite similar to previous SAS2A predicted results which were used for the Reference Experiment molten-fuel-coolant interaction (MFCI) studies (presented in Section 10.2). In Fig. 11.18, the fraction of test fuel melted as a function of time is presented for the two FEFPL-PPS protected accidents. Also shown in Fig. 11.18 is the reference molten fuel generation curve used as a basis for the MFCI source term delineation studies. Evident in Fig. 11.18 is the less rapid fuel melting obtained for the two upper limit accident cases (no EAS scram) relative to the reference experiment prediction. Therefore, it is concluded that with a slower production of molten fuel, these accidents will not yield an MFCI of greater intensity than predicted for the reference experiment as discussed in Section 10.2.2.

The SAS2A predictions of the time for the significant accident events are summarized in Table 11.8 for the two major accidents along with the reference experiment. The major conclusions are:

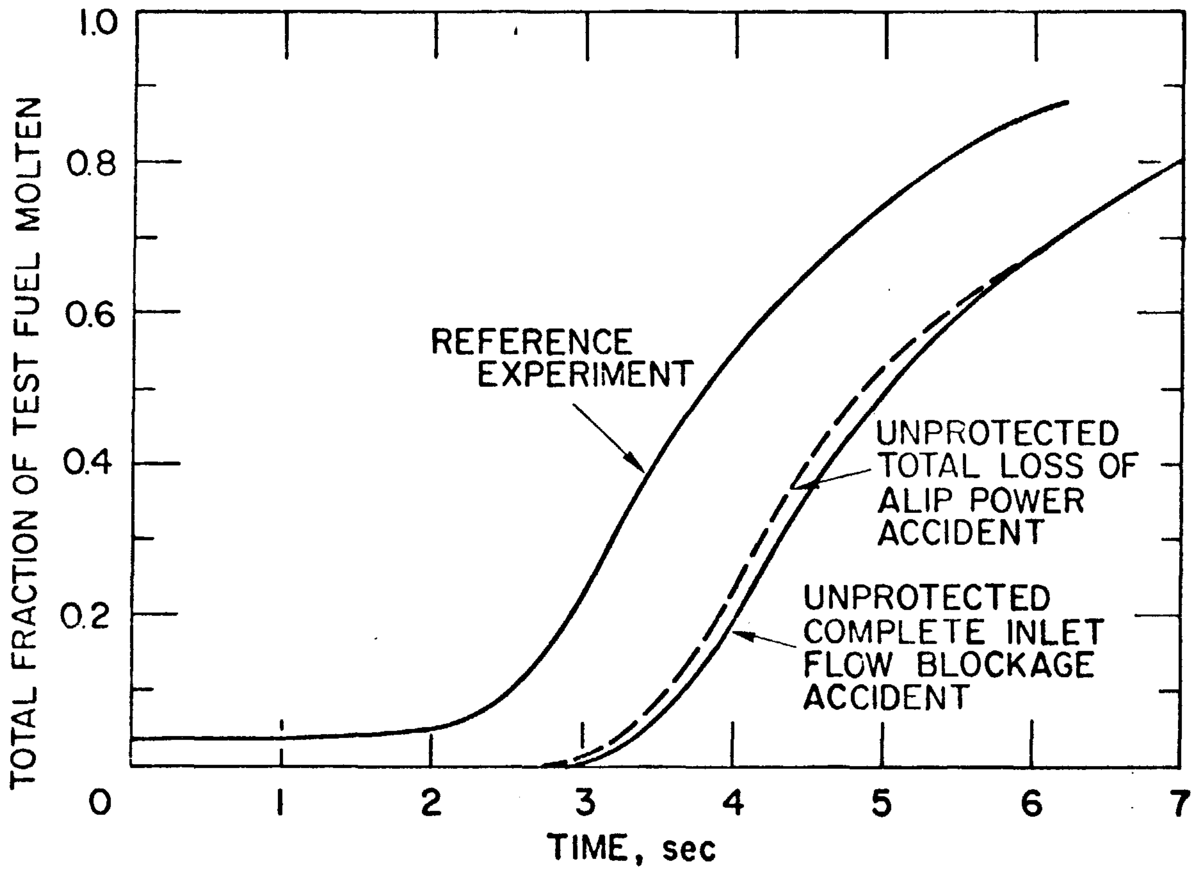

FIG. 11.18. Total Fraction of Molten Fuel versus Time for Loss of Sodium Flow Accidents

TABLE 11.8

Comparison of SAS2A Upper Limit Accident Analyses Results

Accident Sequence Times	Reference Experiment	Total Loss of ALIP Power Accident			Complete Inlet Flow Blockage Accident	
		FEFPL-PPS Protected	FEFPL-EAS Protected	EAS Scram & Emer. Power	FEFPL-PPS Protected	FEFPL-EAS Protected
Void Initiation, sec.	.41	.61	.69	Never	.48	.53
Clad Film Dryout, sec.	0.71	1.0	1.2	Never	1.3	1.6
Clad Melt Inception, sec.	0.88	1.2	1.8	Never	1.4	1.7
Fuel Melt Inception, sec.	Initially Molten	2.4	Never	Never	2.3	Never
Time to Reach 50% Fuel Melt	3.8	4.9	Never	Never	5.0	Never

. The severity level of the loss of sodium flow accidents are greatly reduced with a FEFPL-EAS initiated scram that prevents melting fuel. Some test section damage could be expected in the worst case of 100% flow blockage (which is not expected) due to the loss of cladding integrity, which may preclude running the planned experiment.

. Emergency power, plus an FEFPL-EAS scram are sufficient to prevent clad melting for the loss of pump power accident. A peak clad temperature of < 1600°F is reached, hence significant test section damage is not likely.

. The sequence and time scale of events for the total loss of pump power and the complete inlet test section flow blockage are quite similar to the reference experiment. For the two accidents, the upper limit analyses (no FEFPL-EAS scram) indicates that large quantities of molten fuel would be generated rapidly suggesting that an MFCI may occur.

The SAS2A predictions, however, are no more severe than the reference conditions used previously in the MFCI studies. As discussed in Chapter 10, this MFCI can easily be tolerated by the FEFPL system.

11.4 Loss of Heat Dump

This section presents the safety evaluations associated with the heat exchanger (HX) system of the FEFP loop. Treated herein are the safety of both the FEFP loop's primary HX and the out-of-reactor secondary HX helium system. An analysis of a failure of the HX power system is also presented in this section.

For the purposes of this section, the in-reactor primary HX is considered to consist of the secondary containment and all its internals between the two welds of the FEFPL primary containment at elevations 92 ft 10-7/8 inches and 99 ft 7-7/8 inches (except the outer test-train tube described in Section 5.2.2.1). The in-reactor primary HX safety discussion is divided into two parts: 1) events originating within the HX, their effect upon the HX and the disturbance transmitted to the rest of the system; 2) the consequences, within the HX, of perturbations originating in other parts of the system.

The safety aspects of the loop out-of reactor helium system are considered as to how their malfunctions might affect containment integrity. The basic faults examined are: 1) low helium flow; 2) high helium temperature;

3) helium pressure out-of-range; 4) impurtities in the helium system; and 5) structural failures.

The results of accident studies are presented. The ability of the FEFPL plant protection system to cope with these accidents is demonstrated.

11.4.1 Description of Heat Exchanger System

11.4.1.1 FEFP Loop Heat Exchanger

The functions of the FEFP in-pile loop HX are: 1) removal of heat generated by the experiment; 2) containment of primary coolant, secondary coolant, and radioactive products during normal and abnormal operating conditions.

The heat exchanger is an annular tube-and-shell type with helium on the shell side and sodium on the tube side. The geometry is straight tube, once-through with countercurrent flow. The HX is located between the pump and top closure. Design parameters are summarized in Table 11.9.

Sodium at temperatures up to 1050°F flows upward through a 3-5/8 in. dia. central tube to the loop reservoir. There the direction of the sodium flow is reversed, and the hot sodium enters the heat exchanger upper plenum. The tubes are of 0.750 in OD with a 0.048 in wall and are spaced in five concentric circles, 18 tubes per circle, except for 36 tubes in the outermost circle. The lower 18 in of the tube bundle is spiralled to provide for differential expansion between the heavy center tube and the smaller heat-transfer tubes. The center tube is insulated from the hot sodium flow to reduce the differential expansion. This thermal insulation is contained within a thin-walled shell. The sodium leaves the tubes and mixes in the lower plenum of the heat exchanger before passing downward to the pump.

Secondary helium coolant at 150°F, flowing at rates up to 5750 lb/hr and pressures up to 260 psia, enters the annular space between the helium-flow divider and the helium-containment jacket near the top of the loop. The jacket is sized to contain the high-pressure helium and provides double containment for the gas. The cold helium passes inside the jacket and down the outer portion of the heat exchanger to the lower plenum where it reverses direction and flows upward on the shell side of the heat exchanger, counterflow with respect to the sodium. The helium is heated to temperatures up to 1050°F as it passes through the heat exchanger. Eight baffle zones are provided to direct the helium flow across the tubes. The helium leaves the heat exchanger through the annulus between the upper sodium plenum and the helium flow divider.

11.4.1.2 Secondary Helium Coolant System

The secondary (helium) coolant system removes heat from the sodium in the FEFP in-pile loop heat exchanger and transfers the heat to high-pressure demineralized water (HDW), the helium heat exchanger, and aftercooler (see Fig. 5.8). As the hot helium leaves the FEFP in-pile loop heat exchanger, it first passes through a 2 μ shielded filter and then rejects its heat to HDW at the helium heat exchanger. In order to maintain a constant inlet temperature to the gas circulators with changing helium-outlet temperature in the heat exchanger, a 3-way control valve regulates the amount of helium that bypasses the heat exchanger.

The gas circulators are operated in series to obtain sufficient differential pressure at maximum required flow. Four circulators operated at 88% speed supply the required 5750 lb/hr of helium at a system ΔP of 77 psi, with an inlet pressure and temperature of 190 psia and 200°F.

The helium leaving the gas circulators is water cooled in an aftercooler before entry into the FEFPL heat exchanger. A bypass around the aftercooler is used to regulate the helium temperature at the loop heat-exchanger inlet. Helium flow can be varied from 2000 to 5750 lb/ hr for the temperature and pressure conditions given previously. Flow control within the helium circuit is provided by varying the speed of the gas circulators.

Startup and shutdown of the system are manual. Steady-state operation is automatically controlled. Reactor scram does not require shutdown of the helium-coolant system for the safety of the ETR, however, loop conditions may sometimes require the adjusting of the helium temperature or flow if a power shutdown occurs.

Banks of gas cylinders supply helium directly to the main piping, as required. The helium makeup and exhaust subsystem is basically an exhaust tank of 25 cu ft., which receives excess helium vented from the main piping, and a 40 cu ft makeup tank, which feeds the main piping. The volume of helium in the main piping must be varied as required to stablize pressure as the temperature varies. The makeup tank is normally operated at about 80 psi, receiving its helium from the exhaust tank via compressors having a capacity of 5 lb/hr at 1200 psi.

TABLE 11.9

Design Parameters for FEFPL Heat Exchanger

	750°F Sodium Inlet Temp.	1050°F Sodium Inlet Temp.
Heat-removal rate, kW	950	1500
Sodium flow rate, gpm	125 @ 600°F	135 @ 850°F
Helium flow rate, lb/hr	5750	5750
Max. sodium pressure drop,psi	5	5
Max. helium pressure drop, psi	50	50
Helium inlet pressure, psia	260	260
Sodium inlet pressure, psi	12 to 72	12 to 72

11.4.1.3 Helium Circulator Power System

The helium system circulators are powered from the existing ETR commercial and diesel electrical power distribution systems. A schematic of the FEFPL secondary helium coolant system wiring diagram is presented in ANL Rept. ETD-PD-0949. Commercial power is fed from the commercial "C" bus to 4160-V motor control center MCC "B" (E-127) of the gas circulator. Diesel power is fed from the diesel "E" bus to the 4160-V MCC "A" (E-126) of the gas circulator. Interchanging the power source between MCC "A" (E-126) and MCC "B" (E-127) is possible through a manually operated key-interlock selector switch.

Power is supplied by MCC "A" (E-126) and MCC "B" (E-127) to variable frequency motor-generator sets E-114 and E-115, respectively. The motor-generator sets consists of a 4160-V, 60 cycle induction motor driving a 312 kVA, 100-400 cycle generator through a variable-speed magnetic coupling. Each motor-generator set supplies and controls two circulators. The 4160-V feeders are protected against short-circuit phase and ground-fault currents by protective relaying.

Power, control and protective equipment for the circulators are in switchgear panels MCC "A" (E-116) and MCC "B" (E-117). During loop operation, both motor-generator sets run continuously in order that both power sources are available. A maximum of two circulators may be powered from either source. On loss of either power source, one circulator will be automatically transferred to the remaining running generator, if at the time the generator is supplying power to a single circulator. Interlocking prevents simultaneous operation of three circulator motors from a single motor-generator set.

11.4.2 Evaluation of Loop HX Failure

Potential malfunctions of the HX are of two types: 1) loss of heat-removal capacity and 2) loss of structural integrity. Both types of malfunctions have been evaluated. The consequences of both accident types are discussed in the next two sections.

11.4.2.1 Heat Transfer Malfunctions

In the FEFPL heat exchanger, reduction of heat transfer can result from one of three causes: 1) reduced mass flow of the primary fluid, 2) reduced mass flow of the secondary fluid, and 3) fouling of heat-transfer surfaces.

Reduced sodium flow can be caused by a malfunction of the ALIP, as discussed in Section 11.3.1, or by flow blockages in the HX or other portions of the loop. The protective system action as described in Section 11.1.2 will shutdown the loop before high temperatures occur in the HX.

Reduced helium flow can be caused by a malfunction of the secondary system. The precautions to prevent such malfunctions and to minimize the consequences thereof are described in Section 11.4.3.1.

Fouling of the heat-transfer surface during the FEFPL test is not considered significant. A slight reduction in heat removal efficiency may result which will affect the performance of the planned experiment. Any major introduction of impurities into the sodium, such as during sample failure, is likely to cause other, more important events such as partial flow blockage. The precautions to minimize impurities in the secondary helium are discussed in Section 11.4.3.4.

The inability of the HX to cool the sodium adequately, for whatever reason, will result in higher structural temperatures and higher structural temperature gradients in the HX, particularly at the HX outlet. These temperatures do not directly present a threat to the double-containment integrity of the FEFP loop. They might, however, contribute to structural failure of certain HX components. These structural failures are discussed in the next subsection.

11.4.2.2 Structural Failure

The likelihood of structural failure in the HX is minimized by designing it in accordance with Standard RDT E4-6T, the ASME Section III Code as supplemented by ASME Code Case 1331-7, and by Standard RDT E15-2T to withstand the anticipated and postulated cyclic conditions. In addition, a prototype model of the HX will be subjected to field testing. Preliminary calculations have been completed verifying the safety margins of the design. These interim calculational results are presented in Ref. 7.

The consequences of a structural failure in the heat exchanger, even if it were to occur, are very unlikely to involve damage to the secondary containment vessel, because, except in the lower helium plenum, sodium is separated from this vessel by two barriers. The containment is provided to the sodium-filled HX tubes by the bottom tube sheet and by the baffle between the plenum and the spiral-tube section. Thus, damage to the secondary containment from even a catastrophic tube failure is not likely. Such a tube failure will most likely result in helium leaking into the sodium system. The consequences of such leakage are discussed below.

Leak In Heat Exchanger

The presence of a leak in the primary containment vessel in the heat exchanger (HX) does not result in the loss of double-containment of the loop sodium with respect to the ETR Primary cooling water, since the helium annulus gas in the containment gap completely surrounds the heat exchanger. The barrier between these two helium systems is the HX helium-containment vessel. This stainless steel vessel has a wall thickness of 1/4 in. Violation of this barrier in addition to the HX tube containing the primary loop sodium would be required to allow sodium to reach the containment gap. Even if this extreme situation developed, the presence of secondary containment vessel will prevent a reaction between sodium and water.

Several design features of the HX reduce the probability of the potential release of sodium from the primary loop. The triple-containment concept (HX tube, helium-containment vessel and secondary vessel) has been described (see Section 11.4.1.1). In addition, the presence of the HX helium-flow baffles along with the arrangement of the HX tubes themselves will limit direct impingement of hot sodium upon the helium-containment vessel.

In addition to the safety features present in the loop design, normal operating conditions in the loop are such as to make a sodium leak into the HX containment gap virtually an impossibility. The helium pressure in the HX during normal operating conditions will always be greater than that in the loop sodium. The helium in the HX can enter at pressures up to 260 psia with the helium system bleed-off to an exhaust tank normally operated at 80 psia. The sodium in the HX is at the low-pressure side of the ALIP, having at most the pressure of the gas plenum at the top of the loop, a maximum initial pressure of 50 psia, and a pressure of 72.2 psia after the release of all the gas contained in all 37 fuel elements. In addition, a head of up to 8 ft of sodium is present. Thus, under steady-state operation, without reduction of secondary pressure (requiring loss of both power sources to the circulators), helium gas can be expected to pressurize the primary system indicating a heat exchanger leak and scramming the reactor rather than sodium leaking into the secondary system. If, however, an undetected heat exchanger crack exists, and the heat exchanger is subjected to a MFCI-type pulse, it is possible that some sodium could be injected into the secondary system. The extent of the Na leakage would be limited by crack size and the ~100 msec duration of the pulse to considerably less than that considered in Ref. EDF-718 for an offset shear of the heat exchanger tubes.

Under either condition, the reactor will be scrammed, automatically from primary system pressure or manually in the event of alarm of the secondary system radiation detectors. Following reactor shutdown, the loop will be frozen. Notwithstanding the low probability of such an occurrence under steady-state or transient conditions, the consequences have been studied.

The extent of contamination and radiation level is a function of experiment history prior to the event, i.e., sodium or sodium plus fuel and fission products. In either event, the spread of contaminants will be limited to the TRC and outlet helium piping down to the removable shielded filter. Gaseous fission products will be vented to the ETR stack consistent with approved effluent guidelines.

Analysis contained in Ref. EDF-789 (Rev. A) confirms that the design consideration inherent in the loop, secondary coolant system, and handling equipment will permit loop removal and reactivation of the facility.

With the reactor shut down and the loop frozen, a walk-away situation has been achieved which precludes further consideration of reactor and personnel safety. Loop handling and facility operational restoration for subsequent tests is addressed in Chapter 12, Section 12.2.1.4.

The evaluation of the thermal shock and stress consequences of a sodium leak impinging directly upon both the helium containment barrier is discussed below. The resulting stresses are all thermal stresses and depend upon the temperature gradient.

The assessment of the safety consequences of a flaw in the secondary containment vessel around the HX is presented in Section 13. A breach in the HX secondary-containment barrier provides a path for either:

1) ETR water to leak into the containment annulus, requiring simultaneous loss of AGS pressure which is considered extremely unlikely, or
2) the containment gap helium to leak out into the ETR coolant system, which is more credible as the annulus gas system pressure is greater than the ETR pressure.

Leak detection and ETR scram initiation action represent a protective element of the FEFPL-PPS.

Thermal Shock

The weld joining the HX to the ALIP presents the one place where a failure could bring sodium into direct contact with the secondary containment vessel. A failure here, therefore, has potentially the greatest possibility for damage of the secondary containment. A discussion of the structural consequences of a leak is presented below to show that this postulated failure will not propagate.

A change in temperature imposed on the secondary vessel by a hot slug of sodium will cause a local thermal stress that, depending upon the size of the region influenced, will be relieved by thermal expansion. In this event, two principal factors must be considered in order to ensure that the integrity of the vessel is not affected adversely.

First, the basic question is whether the load imposed by the differential pressure across the wall is sufficient to cause failure at the elevated temperature. The addition of a thermal stress to a vessel, already subjected to a pressure load, does not change the pressure at which the volume yields other than by the direct influence of temperature on the material mechanical properties. Assume that sodium leaks from the heat exchanger at its maximum temperature (inlet, 1100°F), and heats a given volume of the secondary vessel to the same temperature. Normally, the difference in pressure between the FEFPL annulus gas and the ETR primary water is small - about 100 psid. This is well below the value required to produce a significant stress in the vessel (the elastic limit of 1450 psid is reached at 1100°F).[9] Further, if the assumption is made that the "upper limit" MFCI ($\sim$1000 psia) occurs in coincidence with the postulated sodium leak in the heat exchanger, even these coupled events fall within the secondary vessel design limits.

The second possible effect on a vessel undergoing a change in temperature is thermal strain. At the maximum ΔT, due to sodium impingement, the local strain is of the order of 0.01 or 1%. This is fully plastic, but far removed from the 20 to 30% usually required for failure in uniaxial tension. Finally, as backup to the foregoing rationale, it should be noted that neither the ASME Boiler and Pressure Vessel Code nor High Temperature Code Case 1331-7 require analysis of thermal loads for plastic or faulted conditions.

11.4.3 Evaluation of Secondary HX System Malfunctions

The safety implications of potential secondary HX system malfunctions and accidents are discussed in the next several sections. In general, these accidents are a lesser challenge to the loop protection system than the accidents discussed previously. Analyses show that the loop response is slow and rather insensitive to minor perturbations in the HX helium system. In addition, alarms will indicate the presence of abnormal conditions in the secondary HX system due to component failures. Adequate time exists for corrective or preventative action before conditions develop which challenge the loop protective systems. The FEFPL experiment assurance system will limit all credible secondary HX system malfunctions to a Class I severity level (see Section 11.1.4.2 for definition). However, even in the event of failure of this FEFPL Control and EAS action the FEFPL-PPS will terminate the accident before a Class III severity level is reached.

The accident discussions presented in this section concentrate on the Level I design features which are provided to mitigate and/or prevent the malfunctions. In addition, results of analytical investigations are presented for certain upper limit accident cases. The ability of the FEFP loop to tolerate safely any conceivable secondary HX accident is demonstrated.

11.4.3.1 Low Helium Flow

The helium is circulated by four General Electric gas circulators connected in series. Any two circulators will furnish sufficient mass flow and delta P to meet the demand of the FEFPL loop. The circulators are powered by two variable frequency motor-generator sets, each of which operates two circulators. One MG set is powered by ETR diesel power, one by commercial power. The system is designed for maximum reliability in meeting mass flow requirements.

Frequency output of the MG sets controls circulator speed and therefore mass flow. Frequency output is controlled from a manual control located at the console by a milliamp signal proportional to the mass flow desired.

Flow through the sodium helium heat exchanger is sensed by measuring delta P across a venturi flow element, correcting delta P with temperature and pressure inputs, and linearizing the computed value. Two redundant systems furnish mass flow signals to the redundant flow recorders. Low and high flow annunciators will alert the operators if the system malfunctions. Total flow through the circulators is calculated by a system similar to the system above, with the exception that an orifice flange is used instead of the venturi.

Factors that can cause low or loss of helium flow are: 1) flow-line blockage or restriction; 2) compressor or circulator failure; 3) low pressure; 4) power failure; or 5) control-system failure. A discussion of each of the above malfunctions along with the analysis of the consequences of the low helium flow accidents follows.

Flow-line Blockage

The possibility for flow-line blockage will be lessened by periodic inspections for mechanical damage and by the care taken in the design and fabrication of the orifice, reducer, filter and other areas where blockages could occur. The most likely point for blockage is at the 2-μ shielded filter. A pressure recorder alarm will alert the operator should differential pressure across the filter exceed a certain limit.

Differential pressure across the circulators will be normally regulated to 77 psi. An alarm alerts the operator should the differential pressure exceed approximately 85 psi (+ 10% increase). The exact alarm set point will be established after completion of detailed control studies.

In order to show that the helium system can tolerate a filter blockage, a hypothetical sequence of malfunctions that lead to this event are postulated and the consequences examined.[10] The assumption is made that the FEFPL primary vessel fails and sodium enters the annulus in spite of the higher helium pressure. There the sodium would be cooled by the helium and the loop secondary tube. The entire inventory of sodium (4 cubic feet) could be contained in the 5 ft^3 annulus between the primary and secondary tubes. Although it is not expected to occur, some release of unfrozen sodium to the helium is postulated. Any sodium entering the helium system would be forced by helium velocity and gravity to the subpile room, where a horizontal section with a volume of 5 cubic feet would trap most of the sodium. The remaining sodium would pass into the shielded filter. The Rigimesh filter would trap the remaining molten sodium reducing helium flow and pressure at the inlet to the circulators. This will result in an over-speed of the circulators followed by activation of the over-speed trip to prevent off-design operation.

Circulator Failure

The flow rate is automatically adjusted between 2000 and 5750 lb/hr by a speed controller regulated by flow measured at an orifice on the downstream side of the circulators. Four gas circulators, operating at 88% of full speed, circulate helium at 5750 lb/hr. This rate is equivalent to a 3-sec helium cycle. During normal operation, two circulators, operate on commercial power and two on diesel-generator power. The maximum of two circulators may be powered from either source. On loss of either power source, one circulator will be automatically transferred to the remaining running generator, if at that time the generator is supplying power to a single circulator. The two operating circulators will provide ample cooling to remove residual heat from the loop sodium when the reactor is shut down.

In the event of circulator failure, the remaining circulators will speed up and maintain the required flow and the faulted circulator is automatically bypassed. Gas flow is bypassed around each circulator by an associated bypass valve. Interaction between valves and circulator is automatic. Turning the valve to the through position starts the circulator. Conversely, if the circulator stops, the valve turns to the bypass position. Normal coastdown time from full speed for the circulator has been estimated to be within one or two minutes.

Low Pressure

Loss of helium loop pressure would make the helium circulators much less efficient, resulting in low helium mass flow. This could result in increased FEFPL loop sodium temperatures and possible failure of the test.

Low loop helium pressure could be caused by a rupture, a failure of the pressure-control system, low pressure in the makeup system, or a failure of the pressure-relief system. Pressure-actuated alarms will be provided at the flow orifice and at the outlet of the gas circulators to alert the operator of either a high- or low-pressure situation. Low pressure at either the helium bottle supply or makeup tank will also signal an alarm at the control console. Redundancy is provided in makeup compressors, makeup bottles, and the makeup control system to minimize the possibility of low pressure in the helium makeup system.

Power Failure

A failure of the power system for helium system gas circulator is defined as the loss of system capability to supply power to at least two circulator motors. A failure analysis based on the FEFPL helium system power supply fault tree presented in Appendix A.4 was performed to determine the probability of such an occurrence. The simultaneous failure of both the ETR commercial and diesel power sources to the helium circulator is extremely unlikely, and was not considered. The consequences of this accident, however, are less severe than the total loss of all electrical power accident to the loop which was presented previously in Section 11.2.2.1. Any failure in either of the two power-distribution systems for a helium system circulator that could prevent power from being supplied by the other system was examined.

The ETR diesel and commercial power sources feed power to the two system motor generator sets through separate motor-control centers (MCC's). Interchanging of the power source between these MCC's is possible through a manually operated key-interlock selector switch. Prior to motor-generator startup, selection of a power source is required. Movement of the selector switch during operation is prevented by a key-interlock system. The switch is physically enclosed in the MCC panels, which are located within an enclosed room. Mechanical damage to this switch is, therefore, unlikely. Power to both motor-generator MCC's will be verified prior to FEFP loop operation.

The motor-generator (MG) sets provide variable-frequency power to the two circulators MCC's. These MG sets are independent with respect to power source, control power, and protective instrumentation. Each MG set incorporates an exciter-regulated, eddy-current-coupling device to permit an adjustable frequency output. Control of both MG speed regulators is provided by a common controller to maintain equal frequncy to each circulator motor. A failure of this controller will be detected, and manual switching to the standby controller or manual control can be made. The failure of the cooling water supply to both eddy-current couplings will cause removal of their excitation fields and both MG attenator speeds will decay to zero. Eddy current coupling cooling water is supplied by the ETR utility Cooling Water (UCW) System. A minimum of two of the four UCW pumps are normally in operation, one on diesel the other on commercial power supply, thus requiring the loss of both power sources to effect a total loss of secondary cooling to the loop. As a sudden loss of flow is considered improbable versus a decay in flow, the time frame of the accident is less severe than the loss of all circulators analyzed in a subsequent section. During FEFP loop operation, both the MG sets will be operating supplying power to their respective gas circulator MCCs.

The two circulators MCCs provide the power distribution, control, and protection equipment for the four gas circulators. The power to each circulator is distributed through individual circuit breakers and motor contacts located in separate MCC sections. Two of the circulators, however, can be powered from either MCC and separate circuit breaker and motor contactors, for these motors are located at each MCC. Interlocking prevents the simultaneous operation of three circulator motors from a single MG set. The cables from each MCC to the respective circulator motors are run in separate cable trays, reducing the probability of a single failure interrupting power to more than two circulators.

Control-System Failure

As presently designed, temperature-controlled, pneumatically-operated valves bypass helium flow past the helium heat exchanger and aftercooler as required in order to maintain a constant inlet temperature to the FEFPL heat exchanger. Failure of either of these two valves would not restrict flow, as either or both flow paths would remain open, but a change in the inlet helium temperature to the loop would occur.

Fracture of the rupture disc and subsequent pressure relief valve action will vent the helium system to ETR stack exhaust until such time as the relief valve reseats. Failure of the relief valve to reseat and system pressure reduction to 230 psi will result in automatic sequential introduction of helium makeup tank and gas cylinder flow for a period of 15 min, followed by a decay to atmospheric conditions. Therefore, this event, though similar, is less severe than the consequences associated with loss of helium flow previously addressed.

A loss of instrument air or control electrical current will cause the test section temperature control valve to fully open. The helium flow to the loop will increase to the rated 5750 lb/hr (valve time constant is 1.67 sec). This action has the potential for causing an excessive loop heat sink condition to develop. Therefore, the possibility of excessive thermal gradients in the nonremovable top closure region exists. For this reason, this accident has been selected as one of the upset conditions requiring detailed ASME Section III code analyses (see transients J of Ref. 1 for thermal-hydraulic results).

Analysis of Low Helium Flow Accident

Loss of helium flow was analyzed to determine the importance of the accident with respect to loop safety. The two major types of helium flow interruptions are: 1) loss of the helium circulators, and 2) helium flow blockage have been studied. Both realistic analyses have been made in which initially the loop is assumed to be at experiment P-1 type conditions (see Table 11.2), as well as upper limit type calculations. For the realistic accident studies, the expected FEFPL control system action is considered. In the upper-bound analyses, the loop is assumed to be initially at the limit of the loop performance envelope (Point C of Table 11.2), and the accident occurred simultaneously with the failure of the FEFPL test fuel damage protection systems.

a) Loss of Helium Circulator Accidents

Maximum helium flow reductions of about 13, 29, 50, and 100% would result if the loss of one to four of the helium circulators occurred and were uncorrected by FEFPL control action. The required protective action would be an increase in speed of the remaining circulators and/or opening of the helium bypass valve. Of these four possible circulator accidents, the simultaneous loss of three or four circulators is unlikely and will not be discussed in this section. However, an upper-bound appraisal of their accident consequences can be obtained from the discussion in the next section dealing with helium flow blockages.

In Fig. 11.19, the total loop helium flowrate for the loss of one circulator accident is presented. The uncorrected 13% total flow reduction curve assumes the speed of the effected circulator decreases to 1% of that initially in one minute.[11] Control system action commencing at 90% of rated flow with a 3.3 sec helium flow controller time constant as specified in Ref. 3 reestablishes full flow after 2.6 sec (see Fig. 11.19).

With the loop operating initially at experiment P-1 type thermal-hydraulic conditions, the FEFPL control action will effectively return the loop to the initial steady-state conditions after only a very minor thermal perturbation. THYME-B calculations indicate that this condition will be attained after about 40 sec. Maximum temperature increases in the loop during this transient are less than 10°F. Based upon the typical FEFPL-EAS set points presented in Table 11.1, this accident would not initiate an automatic ETR scram.

The simultaneous loss of two helium circulators could occur upon loss of commercial electrical power. However, the more likely event would be a loss of commercial power to the entire loop accident as presented in Section 11.2.1. Nevertheless, the consequences of this loss of two circulator power accident has been investigated assuming the loop initially at experiment P-1 type conditions. The helium flowrate is established at about 80%

FIG. 11.19. Helium Flowrate for Loss of One Helium Circulator

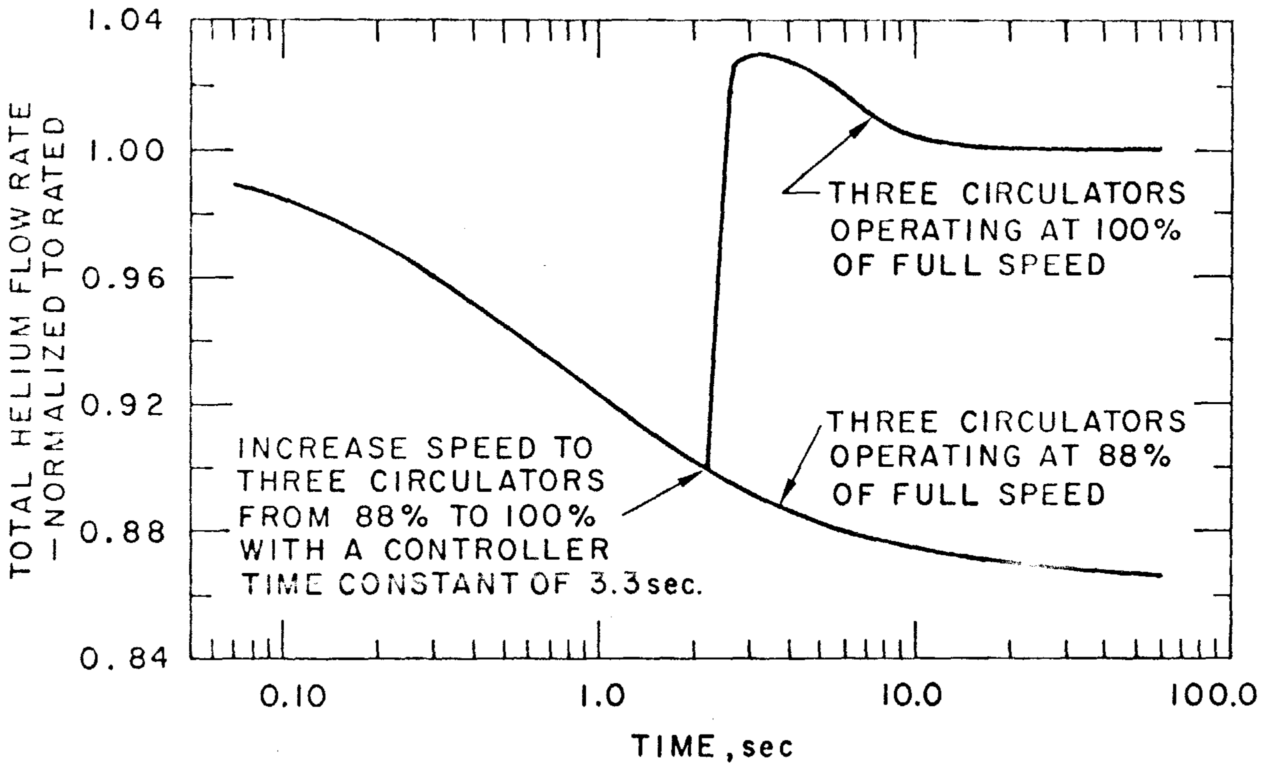

of rated helium flow by speeding up the remaining two circulators from their initial 88% full rated speed to 100% (see Fig. 11.2). No change in ALIP conditions is assumed.

THYME-B results for this loss of two helium circulators accident indicate that the FEFPL-EAS system will terminate loop operation well before excessive conditions develop. The loss of heat removal effectiveness results in a gradual increase in loop temperatures for about 90 sec. At this time, the HX sodium outlet temperature set point of 837°F is reached and a FEFPL-EAS scram occurs. A maximum test section sodium temperature of only ~1275°F is indicated - well below the level at which test section damage would be expected. Loop metal temperatures are also acceptable. An average primary vessel temperature at the core midplane of about 1025°F is indicated (about a 75°F increase from steady-state).

Even in the event that helium control action was unsuccessful, no safety problem for this accident exists. The FEFPL-EAS system can effectively cope with the uncorrected 30% helium flow reduction. The THYME-B results for this case indicate that the FEFPL-EAS scram would occur somewhat earlier at ~45 sec. Again, the HX sodium outlet temperature subsystem would provide the scram signal. Loop thermal conditions at the time of scram were almost identical to those predicted for the accident where helium control action occurred. A maximum test section sodium temperature of 1268°F and a primary vessel temperature of 1017°F were predicted. Hence, the consequences of this accident result in acceptable loop thermal conditions without any test section damage.

b) Helium Flow Blockage Accidents

A very conservative analysis of the consequences of potential flow blockage in the helium system has been made. Instantaneous helium flow reductions of 13, 29, 50, and 100% were studied. No credit was taken for helium system control or FEFPL-EAS scram action. The loop was initially assumed to be at the upper limit of the loop operating envelope (Point C of Table 11.2) prior to the flow disturbance. The results, therefore, provide an upper-bound for the consequences of a helium loss of flow accident. These sudden flow reduction cases encompass the reduced helium flowrate spectrum which could be attributed to a blockage. They also represent very conservative estimates for the uncorrected loss of one to four of the helium circulators.

The response of the FEFP loop was evaluated using the THYME-B code. The temperature predictions for the four assumed helium flow reduction cases have been calculated assuming no FEFP-EAS scram.

The analyses results indicate that the FEFPL-PPS primary vessel set point is reached for only the two large flow reduction cases (100% and 50% flow reductions) for the 50 sec accident time period studies. The 1200°F FEFPL-PPS scram set point at the primary vessel midplane would be reached at ∿ 22 sec for the 100% helium flow reduction and at ∿ 48 sec for the 50% helium flow reduction accident. The primary vessel set point at the molten fuel cup location will be exceeded somewhat earlier for these two accident cases. The test section sodium inlet temperature (approximate primary vessel temperature in the lower loop region) reaches the 1050°F set point at ∿ 17 sec for the 100% reduction and 35 sec for the 50% flow reduction. Scram at these times will terminate these accidents before an excessive loop containment system temperature is incurred. However, due to the resulting 1400°F -1500°F test section sodium temperatures minor test section damage may be incurred. But, the results indicate that even without FEFPL-EAS protective action, sodium boiling and fuel melting are not attained within the loop after 50 sec with even the most severe total helium flow reduction transient. It can, therefore, be concluded that no damage to the primary containment would occur as a result of low or complete loss of helium flow in the secondary (helium) coolant system as sufficient time exists to scram ETR.

11.4.3.2 High Helium Temperature

The two major elements used to control helium temperature are the helium heat exchanger located before the circulators, and the aftercooler located after the circulators. In both, thermal energy is transferred from the helium to high-pressure demineralized water. A temperature-controlled valve is located at the inlet of both the heat exchanger and aftercooler. These valves are controlled either manually or automatically and act to control bypass flow through the heat exchanger, aftercooler, or both, as required.

The maximum design helium temperature at the outlet of the FEFP in-pile loop heat exchanger is 1050°F. The normal operating temperature is 1000°F. Factors that could contribute to helium temperatures above design values are: 1) low helium flow (see Section 11.4.3.1); 2) failure or malfunction of the high-pressure demineralized-water system; 3) malfunction of the temperature-controlled valves.

Helium temperatures are sensed by thermocouples located on the outlet sides of the helium system heat exchangers. These sensors actuate an alarm at the control console should the temperatures exceed an established set point. Helium temperature also is measured upstream of the gas circulators, and will be used to pneumatically operate three-way valves regulating both flow through and around the primary heat exchanger.

An alarm is provided at the control console to alert the operator should the temperature at the outlet of any gas circulator exceed a preset value. The operating speed of the circulator is regulated by a flow sensor corrected for pressure and temperature by means of sensors located downstream of the aftercooler. Complete redundancy will be provided in sensors, transducers, transmitters, and controllers.

Temperatures will be monitored at the inlet and outlet of the aftercooler, and at the inlet to the FEFP in-pile loop heat exchanger. An alarm at the control console will be activated for any excessive temperature at the outlet of the FEFP in-pile loop heat exchanger.

Adequate instrumentation and controls are provided to allow corrective action for the occurrence of excessively high helium temperatures at the exit of the helium heat exchanger.

Analysis of High Helium Temperatures

Of the factors which could cause a high helium temperature, the failure or malfunction of the high-pressure demineralized-water system (HDW) could produce high helium temperatures without a reduction in helium flow. Helium flow accidents were discussed previously in Section 11.4.3.1. An evaluation of potential HDW accidents are presented herein.

Another accident which potentially can cause an increase in helium temperature to the loop HX is the malfunctioning of the helium control system. This accident (an instantaneous step change in helium inlet temperature from 150 to 400°F with a scram after 2 sec) has been studied and reported in Ref. 1 (upset case G-1). The loop thermal conditions for this case are less severe than those obtained below for the HDW accidents.

The high pressure demineralized water comes from existing valves on the HDW supply and return headers south of the cubicle. The cooling water manifold located high on the outside of the south cubicle wall distributes the water to the various cooling systems. Each distribution system consists of inlet and outlet block valves, a flow measuring device, an exit water thermocouple, and a relief valve. Low cooling water flow or high cooling water exit temperature on any subsystem actuates annunciators at the loop console and in the reactor control room.

Total loss of the HDW system supplying water to the loop is not likely. Normal system operation is maintained by one operating pump on commercial power with alarm action and automatic pickup of the standby pump on diesel power in the event of low system pressure. Misoperation of valves is not likely since the system water flow is adjusted before helium system operation starts. Any change in water flow that could lead to operating problems is annunciated. Blockage of HDW lines is considered improbable, since demineralized water is flowing through stainless steel piping. Relief valves protect each heat source from accidental overpressurization or valve misoperation.

The two heat exchangers, the primary (M-7) and the aftercooler (M-18) supplement each other in accident situations. If heat removal from M-18 ceased, M-7 would still remove all heat from the helium system, except heat of compression. If M-7 failed, M-18 would not remove all the system heat. Although this failure would subject the helium circulators to higher than design temperatures, it would not constitute a hazard to the sodium system. Annunciators would alert operating personnel in any case, and prompt corrective action applied.

Faults and malfunctions expected in the HDW system are expected to be of a minor nature and require only operational corrections. These events (i.e., leaky valves) will not result in a hazard to the loop. However, as described below, an analysis of the influence of HDW accidents on the loop behavior has been performed to determine the time scale for preventative action.

Analysis of High Helium Temperature

Two types of failures in the HDW system have been analyzed as to their effect on the loop's thermal behavior: 1) loss of HDW flow to the heat exchanger, and 2) loss of HDW in the heat exchangers. The first accident represents an interruption in water flow situation which does not result in the loss of water inventory contained in the heat exchangers. This situation would represent a flow stoppage accident in which the integrity of the HDW system was not violated.

In the second type of accident, the water contained in the heat exchanger is assumed to be lost with only the tube metal within the heat exchanger furnishing the heat sink. A pipe break draining the HDW from the system could lead to this accident situation.

Both types of accidents have been conservatively analyzed using the THYME-B code. The loop steady-state operating point before the accident was again taken as the upper loop operating point. No credit was taken for the cooling ability in the HDW system other than the heat sink provided by the material contained within the heat exchanger (coastdown or blowdown cooling effects neglected).

a) Loss of HDW Flow to the Heat Exchangers

Three unprotected loss of HDW flow situations were studied: 1) loss of HDW flow to aftercooler (M-18); 2) loss of HDW flow to primary heat exchanger (M-7); and 3) loss of HDW flow to both M-7 and M-18 heat exchangers. The mass of water (heat sink) was taken to be 318 lbs for the aftercooler and 383 lbs for the primary heat exchanger. The overall film heat transfer coefficients used for the two exchangers were their respective steady-state values (3.5×10^4 Btu/hr-°F for M-18 and 2.6×10^4 Btu/hr-°F for M-7). Figure 11.20 shows the resulting change in loop helium inlet temperature versus time for the three accident cases. The total loss of HDW system flow accident change in inlet helium temperature represents the sum of the temperature increases of the two heat exchangers.

THYME-B results for the three loss of HDW flow accident cases indicate that these unprotected transients produce only very minor thermal perturbations in the in-reactor portion of the FEFP loop. After 50 sec into the accident, loop sodium temperature increases are at most 35°F for the total loss of HDW system flow accident.

Loop metal temperature increases are also minimal. The heat exchanger region undergoes the largest temperature changes, but these also do not amount to more than 35°F. At 50 sec, the primary containment temperature at the core midplane has increased only 20°F for the total loss of flow to both heat exchangers.

It is concluded from these studies that the loss of HDW flow to the helium system heat exchangers does not constitute a safety problem. The slow rate of loop temperature increase provides ample time for corrective action.

b) Loss of HDW in the Heat Exchangers

For this analysis, all water in the heat exchangers was assumed to be lost. The only heat sink available was taken to be the metal of the heat exchanger tubes. Again, three accident cases were studied: 1) loss of HDW in the aftercooler heat exchanger (M-18); 2) loss of HDW in the primary heat exchanger (M-7); and 3) loss of HDW in both M-18 and M-7 heat exchangers. The calculations performed to determine the inlet helium temperature changes to the loop were identical to that for the previous loss of flow accidents.

FIG. 11.20. Helium Inlet Temperature Change versus Time after Loss of HDW Flow to Heat Exchangers

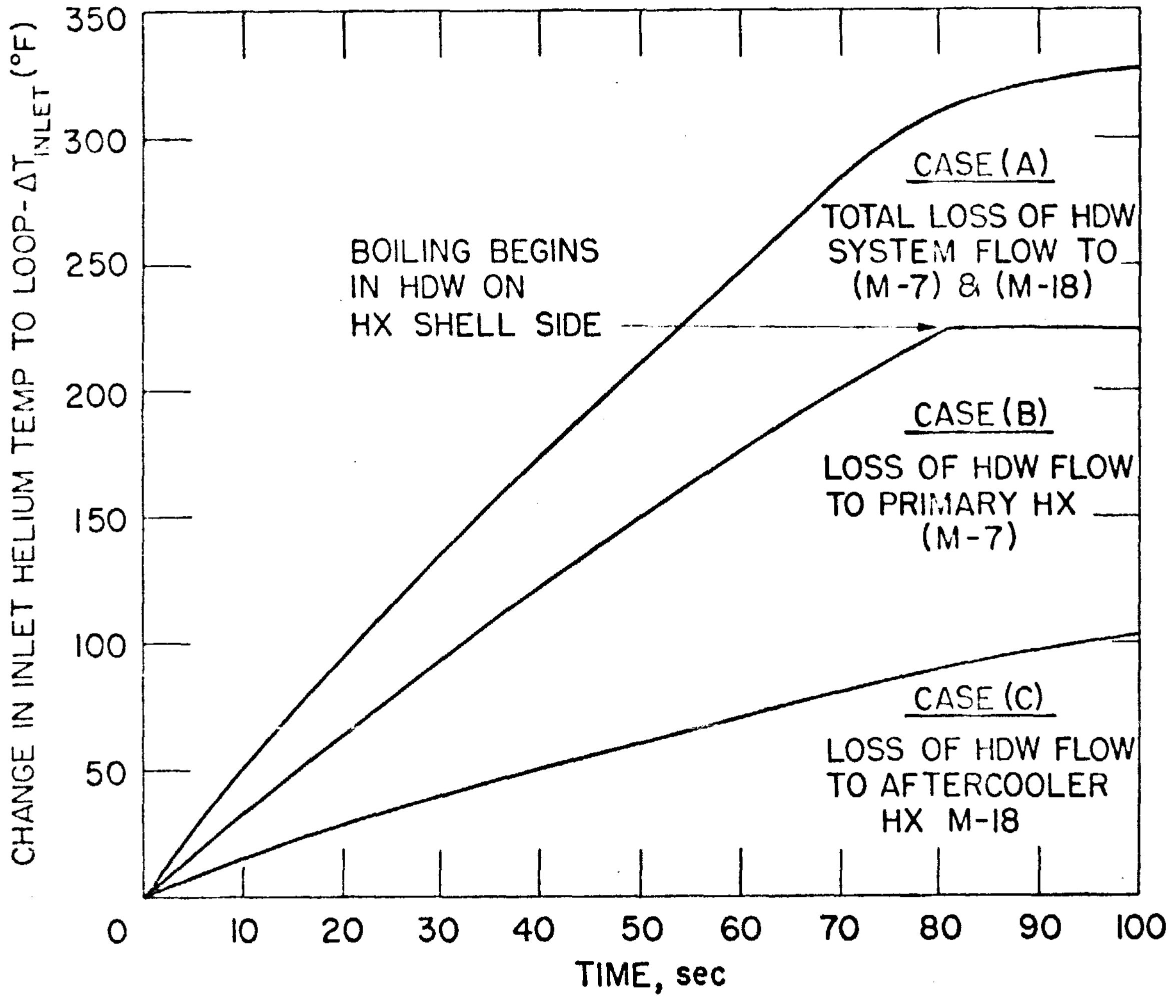

However, rather than water being the heat sink in each exchanger, the 745 lbs of tube metal in M-7 and 467 lbs in M-18 provided the heat sinks.

Figure 11.21 shows the change in inlet helium temperature to the loop for the three loss of water accidents. A comparison of these increases with those shown in Fig. 11.20 for the loss of flow accident indicates that the loss of water accidents result in a factor of three larger helium inlet temperature changes. The factor of ten reduction in stainless steel heat capacity compared to water account for the majority of this difference. These large inlet temperature changes also resulted in larger loop helium outlet increases requiring several THYME-B iterations to arrive at the inlet helium temperature changes shown in Fig. 11.21.

As expected, results of the THYME-B loop temperature predictions for the three loss of HDW accidents are more severe than for the loss of water flow accident results discussed previously. However, even for these loss of water accidents after 50 sec into the transient, thermal conditions are also not excessive. No sodium boiling is indicated within the loop and primary containment temperatures are well below the FEFPL-PPS set point values. As was the case for the loss of water flow accidents, the rate of loop sodium and metal temperatures change is slow enough to provide time for operator corrective action before the loop EAS is challenged.

Should loss of cooling water occur and warnings be ignored, the temperature of the helium will increase until the loop sodium heat exchanger efficiency is impaired to the point that a reactor scram is initiated by the Experiment Assurance System due to a "loss of heat dump." The limit condition for loss of heat dump would be the case where the inlet helium temperature to the sodium loop heat exchanger equals the maximum sodium temperature. This maximum temperature would be 1050°F.

The sodium loop boundaries affected by helium system overtemperature are: the removable top closure, the primary tube above the heat exchanger, the heat exchanger helium shell, the heat exchanger tubes and the heat exchanger center pipe. For the design pressures, the maximum allowable temperature for the loop components which form the helium boundary is 1150°F, based on ASME Section III Code allowables for normal operations. Since this is above the maximum helium temperature that can be envisioned, no damage to the loop structure will result from helium overtemperature.

FIG. 11.21. Helium Inlet Temperature Change versus Time after Loss of HDW to Heat Exchangers

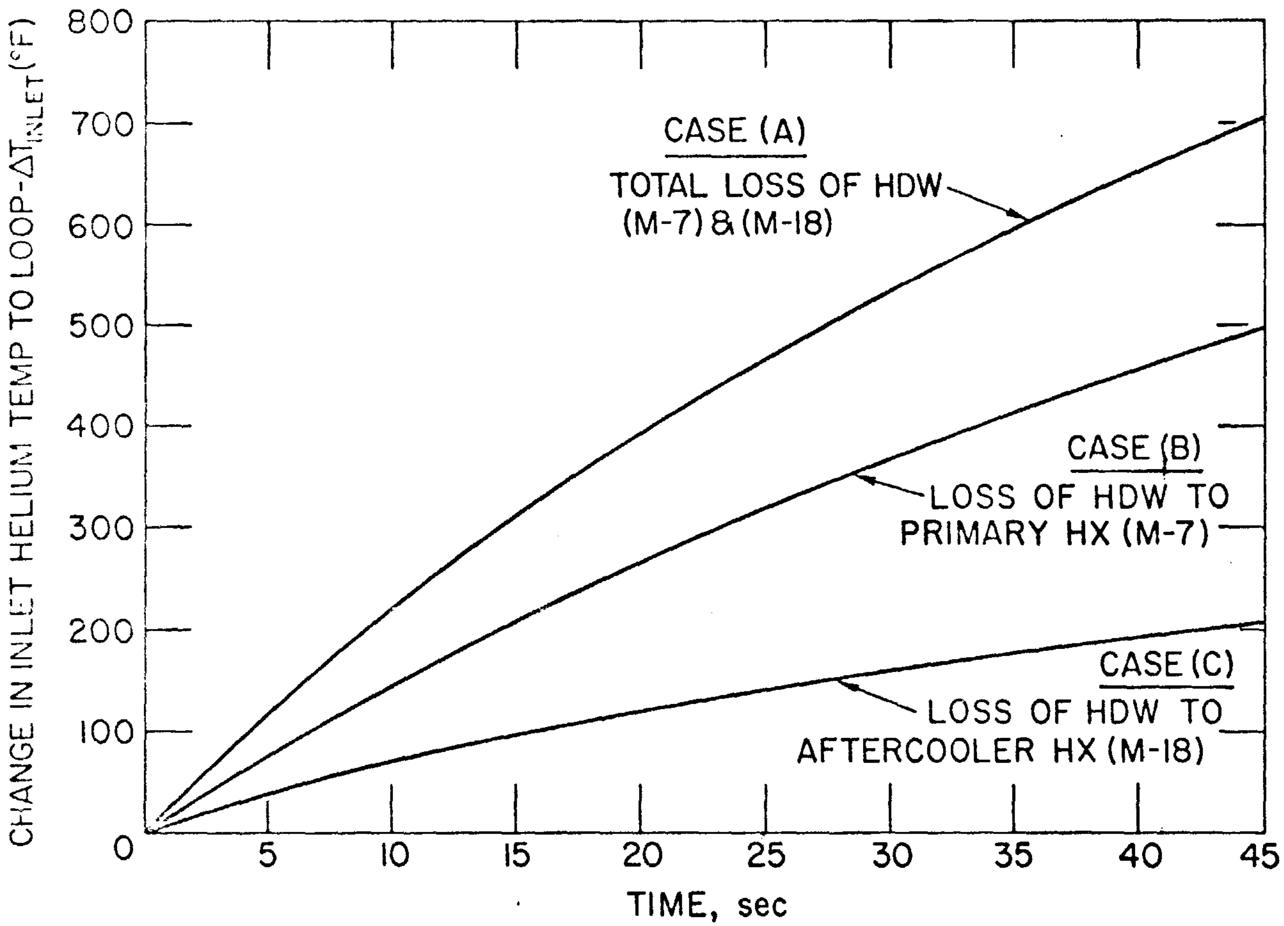

11.4.3.3 Helium Pressure Out-of-Range

High Helium Pressure

Helium enters the system from a manifold through two pressure control valves. The manifold is charged by either the makeup tank or one of two racks of six helium bottles. Pressure control valves are used on each of the two helium bottle racks and on the makeup tank in order to limit the manifold pressure. These valves are fail-safe because failure of electrical power or control air pressure will close the pressure control valves on the makeup tank and on the manifold of each helium bottle rack.

A malfunction of one of three makeup system pressure control valves and one of two system pressure control valves combined with the simultaneous failure of the system pressure relief valve would be required to provide a mechanism for overpressurizing the helium system. The makeup system maximum pressure is limited by a pressure relief valve.

Failure of each of the above control devices would introduce the contents of 12 helium bottles or a fully charged makeup tank into a previously pressurized helium system. The sodium loop boundaries affected by helium system pressure are the removable top closure, the primary vessel above the heat exchanger, the heat exchanger helium shell, the heat exchanger tubes, and the center pipe of the heat exchanger. The maximum allowable pressure, for the components which form the loop boundary, based on the ASME Section III Code allowables at the design temperature is greater than the maximum from the overpressure postulated; therefore, no damage to the loop structure will result.

Low Helium Pressure

Low helium loop pressure is annunciated by two parallel separate systems. It can be caused by a system rupture, valve misoperation, failure of helium system controller, helium bypass control valve malfunction, or loss of makeup helium.

Loss of makeup helium could be caused by mechanical failure, valve misoperation or controller failure. However, two redundant supplies, the makeup tank and the makeup bottle manifold, must fail before the helium system is affected by lack of makeup helium.

The transfer of waste helium from the exhaust tank to the makeup tank may be accomplished by either of two redundant positive displacement compressors.

The effect on loop performance of low helium pressure would be a reduction in the efficiency of the helium circulators with a decrease in helium flowrate. The consequences of low helium mass flow on loop thermal behavior are discussed in Section 11.4.3.1.

11.4.3.4 High Helium Impurity Level

Three types of impurities - water, air, and sodium, are of concern in the helium system. Online analyses are performed to determine oxygen and moisture content. A helium bleed flowrate of about 100 cc/min will provide a rapid indication of excessive levels. Nitrogen content is determined by periodic chemical analysis. Sodium is detected downstream of the helium outlet of the FEFP in-pile loop heat exchanger by means of the activity monitors.

Requirements for the coolant helium system have been established to maintain water pressure lower than helium pressure to preclude entry of water into the helium system. These requirements include periods when the system is charged with helium as well as when it is depressurized. In addition, water monitors will be used to verify continuously that the system is dry. Before initial startup, the system will be evacuated to ensure that there is no entrapped water. A simplified plastic stress analysis of a hypothetical case where water reaches the loop heat exchanger clearly shows that thermal stresses from a one time thermal shock cannot cause sufficient plastic strain to cause rupture. This conclusion is confirmed by the rules of ASME Code Case 1331-5.

Leakage of air into the system from a breach is unlikely since the helium is normally at 260 psi. The continuous oxygen monitor will determine the presence of air.

The only path for sodium to enter the system is through the FEFPL heat exchanger tubes. The presence of sodium will be detected and annunciated by radiation monitors located near the helium filter.

Problems associated with impurities in the helium system are not expected to occur in the FEFPL system. However, if they do occur, their consequences are more of an operational nature which may tend to reduce the heat removal effectiveness of the system. Moisture levels far in excess of the detection limits are required before adverse thermal and/or erosion effects are encountered in the in-pile heat exchanger and the helium circulators. The long time period required for these conditions to develop also allows ample time for their detection before a safety problem would exist. In addition, filters are provided to trap particulate matter.

11.4.3.5 Structural Failure

Extensive engineering studies have been conducted to prevent the occurrence or to minimize the consequences of structural failures in the helium system. The engineering effort on this system was threefold:[12]

1) Determining if the existing gas cooled loop (GCL) system components met the requirements of the FEFPL helium system.
2) Conducting detailed analyses of the FEFPL equipment arrangement in the ETR to insure that the system could function as required in the allotted space.
3) Preparation of detailed modification, installation, and checkout information.

The primary consideration in equipment layout was avoidance of high stresses due to high temperature operation. The piping route inside the subpile room and vertical sleeve was dictated by the necessity to minimize expansion stresses. Specifically fabricated pipe sections using very long radius bends were used to minimize stresses. The location of the system components was also dictated by the need to maximize the isolation of critical items. For example, the location of the makeup and exhaust tanks in the northeast corner of the cubicle provides isolation for the makeup tank, which is at a high pressure (1200 psig) during periods when the remaining portions of the helium system are at atmospheric pressure and below.

Of the several types of structural failures in the helium system, a catastrophic failure of a helium circulator (blades ejected through casing) would probably be the most severe as it would occur quite rapidly. A discussion of this postulated failure is presented below.

Catastrophic Failure of Helium Circulator

The impeller is a precision casting of S.A.E. 4335 steel modified for increased thermal creep resistance. At full design speed, 24,000 rpm, the design stress in the impeller is 50,000 psi compared to a 1000 hr creep rupture stress at 800°F of 100,000 psi. One circulator during initial acceptance testing was operated at an inlet temperature of 700°F for 60 hrs with speed varied from low range to design maximum. Considering the conservative design, development, and test results, the catastrophic failure of the impeller by brittle fracture at FEFP operating conditions is unlikely but still possible.

The circulator vessel and casing are designed to the requirements of the 1963 ASME Boiler and Pressure Vessel Code, Section III for Class A vessels. The design conditions were 400 psig and 750°F for the pressure retaining vessel code case. For the FEFP experiment, the helium design pressure is 260 psia.

For purposes of analysis, an impeller failure is assumed to result in high velocity shrapnel penetrating the circulator scroll and casing. Damage from flying fragments, deaccelerated by the scroll and casing, will be confined to the helium cubicle.[13] No equipment or lines except those belonging to the helium system are located in this space. The helium system is lost to the experiment but no other systems damage results from an impeller failure.

The catasrophic failure of a helium circulator will at worst result in a rapid depressurization of the helium circuit and loss of cooling to the in-reactor loop. Failure of the impeller without penetration of the circulator casing will result in loss of only that circulator. The loop's transient behavior for both of these eventualities has been discussed previously. The thermal response of the loop during both of these sudden loss of helium type flow accidents (see Section 11.4.3.1) is relatively slow allowing ample time for operator intervention.

During the postulated failure of the helium circulator, a number of service lines within the cubicle would be exposed to possible damage. None of these items, however, are associated with critical systems such as the FEFPL or ETR protection systems. Also, several of these service lines are associated with ETR experimental facilities that are not scheduled for operation; consequently, possible damage to them is not of immediate programmatic or safety concern. A discussion of the possible impact of circulator failure on cubicle service lines follows.

A. ETR Experimental Facilities Not In Use - No Effect
   1. Westinghouse DAS cooling water lines
   2. Westinghouse DAS calibration impulse lines
   3. Westinghouse C-13/6-16 experiment impulse lines
   4. Loop drain header

B. Plant Fire Lines

The FEFPL helium cubicle fire system is supplied from one 1 1/2" fire line penetrating the south cubicle wall. At a nominal supply pressure of 80 psi, a severed line would result in a flowrate of 600 gpm. This flowrate can be sustained without any adverse effects on any other plant system until the supply source has been shutdown. All sprinkler heads (six) discharging into the cubicle would result in a flowrate of 400 gpm. Floor drains in the cubicle and outside would be needed to drain the water.

C. Loop and Plant Electrical Leads

All non-FEFPL conduits and junction boxes mounted inside the FEFPL helium cubicle are empty and not in use.

D. Plant Protection System

There are no signal leads or sensors in the vicinity of the FEFPL helium cubicle.

11.4.4 ETR Core Filler Piece Water Flow Accidents

ETR cooling water flow is required to remove the gamma heat generated in the FEFPL secondary vessel and cadmium filter. Two types of ETR accidents have the potential for interrupting this essential ETR water flow and thus reduce the effectiveness of the heat removal from the loop:

- Whole core ETR accidents
- Local flow blockages in loop core filler piece (CFP)

The effect of whole core ETR accidents on the thermal performance of the loop have been studied and are presented in Section 11.6 in this report. A discussion of the consequences of an ETR water flowrate stoppage due to a loss of electrical power accident was presented previously in Section 11.2. The thermal effects on the loop of the ETR loss of cooling and reactivity insertion design basis accidents are evaluated in Section 11.6. For these major ETR accidents, the ability of the loop to survive without compromising the safety of ETR has been demonstrated.

A local flow blockage in the core filler piece annulus surrounding the FEFPL secondary vessel has been considered. The annular flow geometry and use of splines in the core filler piece provides protection against a total inlet blockage caused by debris in the ETR coolant. Holes drilled in the core filler piece guarantee that a minimum of 36% water flow of minimum allowable core delta P shall be maintained in the vent of an inlet blockage (Fig. 11.22). Furthermore, THYBE-B calculations indicate that instantaneous flow blockages resulting in an ETR cooling water flow reduction of up to 50% can be tolerated without boiling in the ETR core filler piece (CFP). For this large flow reduction, the secondary vessel temperature increases relatively slow (required about 50 sec to increase 25^{o}F without reactor scram). Temperature increases internally within the loop were minimal due to the helium insulation between the containment vessels. It is, therefore,

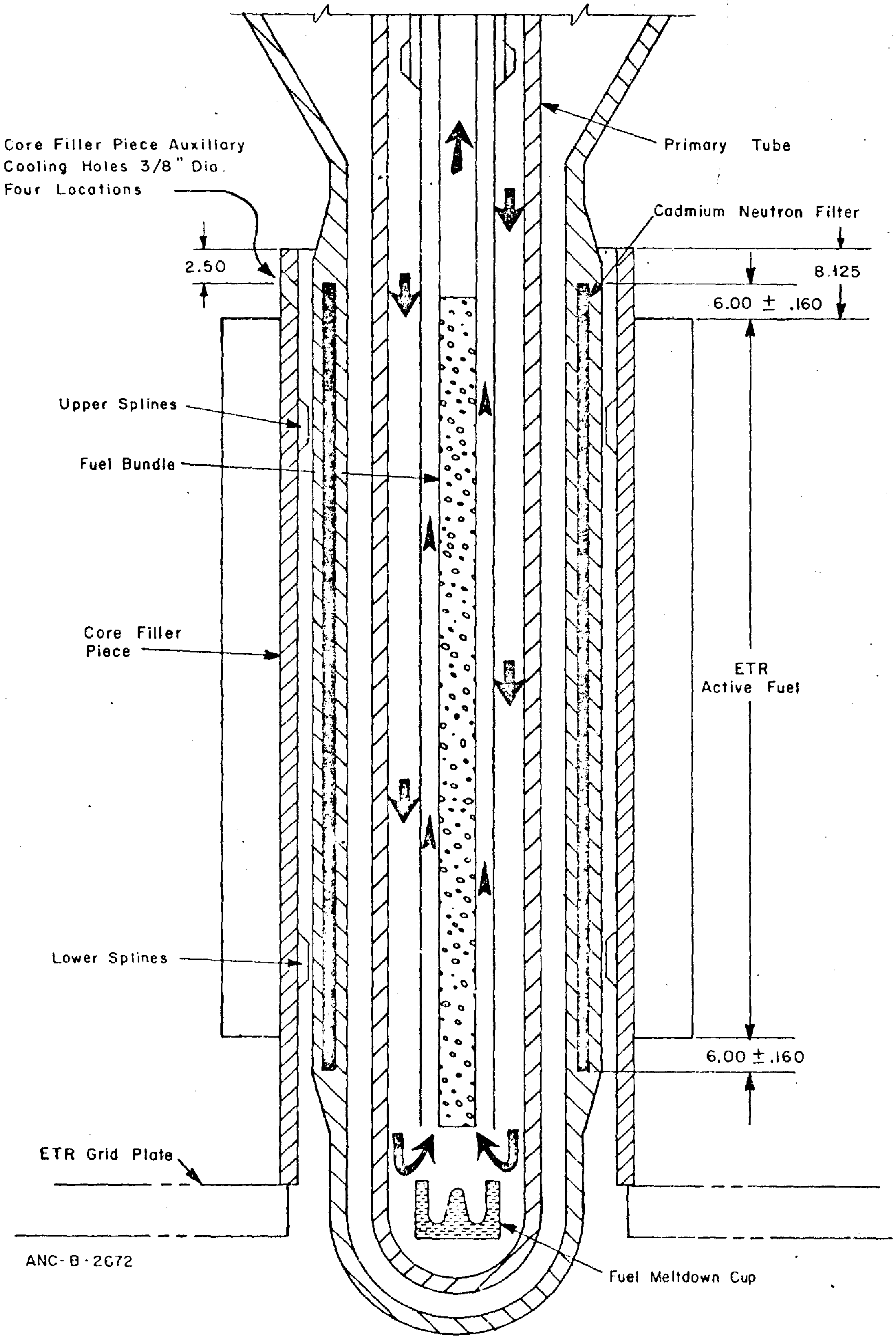

FIG. 11.22 - ETR/FEFPL Inpile Tube & Core Filler Piece Elevation Crossection

concluded that even for relatively massive flow blockages, ample time is available to scram ETR. In addition, automatic ETR scram protection is provided for this accident via the secondary vessel thermocouples provided in the FEFPL PPS (Function C), and hence, the safety of ETR will not be threatened.

11.5 Failure of FEFPL Control System

The functions of the loop control and data acquisition systems are to provide: 1) adequate instrumentation and control of the loop temperature, flow, and pressure during normal operation and experimental testing; 2) adequate instrumentation for operation surveillance for monitoring the variables controlled by the FEFP Operational Control System; 3) alarms to warn the operator of variables outside the required range; and 4) test fuel damage protection by ETR scram action as initiated from the experiment assurance control subsystem (FEFPL-EAS).

The range of safe loop operation is discussed in Section 6.0. Normal operation of the loop lies within the boundaries of safe loop operating conditions. A failure of the automatic loop control system to maintain the loop temperatures, flow and pressures required during loop operation will set off an alarm, warning the operator. Operator monitoring of system variables will be required during loop operation to preclude an alarm being required. Complete failure of the loop control system, including operator action, may lead to operating states exceeding normal operating conditions. One of the purposes of the safety systems described in Section 7.0 is to provide a backup to the loop control system to insure that the loop conditions are always safe. Postulated control system malfunctions in addition to the occurrance of various accidents were investigated and are discussed in previous sections. The safety provided by the FEFPL-PPS for these unlikely events is demonstrated.

Note that the control system will provide a line of defense for all loop initiated accidents. Total failure of both the heat exchanger and the pump or the loop control system could lead to partial loop freezing. The strength of the loop is such that loop freezing or plugging due to oxygen presents no safety problem.

11.6 ETR Design Basis Accidents

The ETR has recently undergone an extensive safety evaluation and review.[4] This detailed study, which evaluated potential ETR accidents and conditions, provided the basis for the set of technical specifications for the reactor and associated experimental loops which are presented in Ref. 8. These technical specifications have been used to define the FEFPL safety operating envelope as described previously in Chapter 6. Compliance with these ETR specifications, then, guarantees that the FEFPL operation will fall within the set of design basis conditions identified for the requirements of the protective subsystems of the ETR-PPS. The two major ETR design accidents identified in the Ref. 4 study:

- design basis reactivity insertion
- design basis loss of cooling

have been analyzed as to their effect on FEFPL to provide additional confidence that FEFPL can indeed operate safely in ETR. The consequences of these two events as to their influence on the FEFP loop and subsequent potential for additional ETR damage are discussed below.

11.6.1 Design Basis Reactivity Insertion

This design basis reactivity insertion accident has been studied in detail in Ref. 4 (see Pages 184 to 201). In spite of the extremely low probability of this accident occurring, it is analyzed to determine whether the FEFPL test fuel will melt or disassemble in such a way as to add to its severity. Of concern is creation of conditions more severe than postulated for the reference design FEFPL experiment presented in Section 10.2.1. In particular, the potential for generating an MFCI more violent than the design envelope source term is assessed. A further consideration is whether the FEFPL test fuel could conceivably reassemble into a configuration that would add reactivity in excess of the ETR Technical Specification limit (see Chapter 6). Also considered is the capability of the cadmium filter to withstand the excursion without melting and hence establish further confidence in its integrity.

The power excursion studied was a 1.3$ step reactivity accident with no positive feedback. This accident reactivity insertion and resultant ETR power and energy release time behavior are shown in Fig. 11.22 (as reproduced from Fig. V.5.1.I of Ref. 4). The transient conditions are slightly

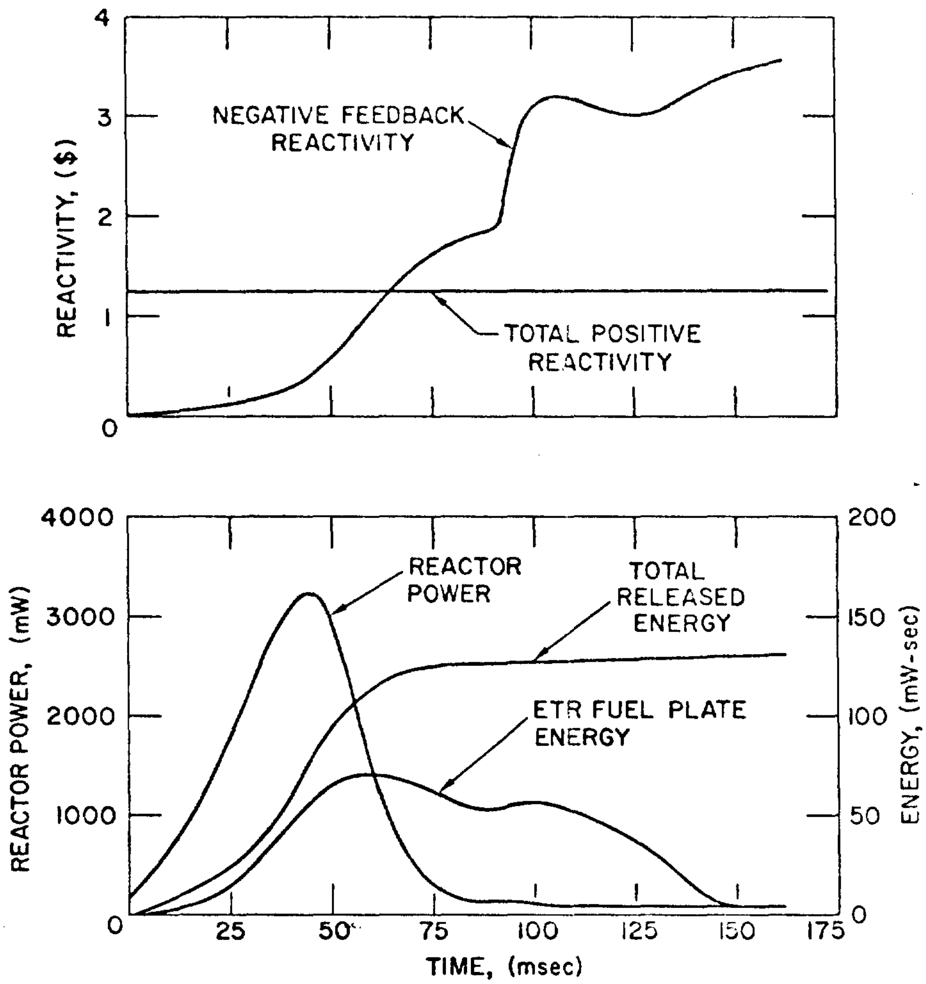

FIG. 11.23 - ETR Power Excursion for 1.3$ Step Reactivity Accident with No Positive Feedback

more severe than the prescribed 1.21$ step reactivity insertion for which the maximum fuel plate energy of 62 MW's can be tolerated without melting the ETR cladding. The details of the thermal and neutron kinetics calculations along with associated parametric studies which were conducted to generate the results shown in Fig. 11.22 are presented in Ref. 4.

The thermal-hydraulic response of the FEFPL test fuel to the power excursion shown in Fig. 11.22 is obtained using the SAS2A computer program. Initial conditions prior to the accident were again those of Point C of the loop operating envelope (Table 11.2). The maximum sodium coolant temperature experienced within the FEFPL test section during this reactivity excursion is 1444°F. This temperature represents only about a 127°F rise over the steady-state 1317°F value and is almost 360° below the local saturation temperature. The peak coolant temperature occurs at ∿ 0.25 sec into the transient after which time a rapid temperature decrease is obtained due to the large decay in reactor power level (see Fig. 11.22). This indicates that sodium boiling will not occur during this accident if loop sodium flow is maintained. Therefore, the small additional reactivity insertion contribution possible due to test section voiding (see Section 10.3.5.2) will not be available to affect the ETR transient.

For this accident, SAS2A predictions indicate that test section damage would also be minimal. A peak test fuel pin cladding temperature of ∿ 800°C (1475°F) is predicted. This temperature, occurring at ∿ 0.2 sec, is well below the 1600°F damage threshold value predicted for FFTF type fuel.[5] Molten fuel generation during the transient is also insignificant. Although centerline melting is predicted to occur at four axial nodes (out of a total of 15), the maximum amount of molten fuel generation is only 0.4% of the total fuel inventory. This maximum quantity of molten fuel occurs after about 0.4 sec, but quickly refreezes at 1.4 sec into the accident. Thermal conditions within the test fuel pins would be below those at the initial full-power level about 1.75 sec after the initiation of the accident.

The thermal analysis of the cadmium filter also indicates that this reactivity accident will not result in excessive temperatures in this loop region. The reference power generation of Fig. 11.22 is equivalent to ∿ 2/3 of a second of full power. Even assuming this is added adiabatically to the neutron filter, a cadmium temperature of 520°F ± 50°F would result. The maximum temperature is below the 609°F melting point of cadmium and hence no loss of filter due to melting is possible.

It is concluded from these analyses of the ETR design basis reactivity accident that FEFPL will not present an additional safety burden on ETR. ETR. In fact, it appears that the FEFPL test section has an excellent chance of experiencing the consequences of this accident without any major damage that would affect is operating performance.

11.6.2 Design Basis Loss of Cooling Accident

This design basis accident has been evaluated for ETR on pages 558-574 in Ref. 4. Protection is provided for this accident with the following existing ETR subsystems: inlet pressure (low), outlet pressure (low), and surge tank level. The subsystems provide sufficient protection against the consequences of this accident by providing a low pressure scram and/or adequate reactor building containment to keep radiation release at levels less than the 10 CFR 100 limits.

The ETR accident analysis results presented in Ref. 4 indicate that the severity level reached is acceptable for this design basis accident. The severity level is 3 standard deviations away from a 10% core meltdown which is acceptable for this accident. The decompression wave resulting from the double-ended piping rupture is estimated to be a 26 psi wave in the vessel upper plenum. The peak pressure increase generated by the thermal energy transfer to coolant by the maximum probable fuel melt for this accident (10% of the core fuel) is calculated to be 70 psi, taking into account the cushioning effect of the 4.1% steam fraction present.[15] Even for the hypothetical case of a closed, liquid-fuel system, the maximum pressure is 580 psi, which is well below the loop containment capability (see Chapter 13).

Loop Thermal Behavior

The THYME-B code was used to estimate the effect of this accident on FEFP Loop behavior. For this analysis, the loop was again assumed to be operating initially at the upper limit of the loop operating envelope (Point C in Table 11.2). The ETR flow rate reduction corresponding to this double-

ended break of a 36 in. primary coolant inlet pipe was obtained from Ref. 4, and is shown in Table 11.10. Also shown in Table 11.10 are the power and saturated ETR water temperature histories. The power reduction shown before an ETR scram occurs at 0.455 sec is due entirely to the negative void reactivity effect. In these THYME-B analyses, two cases are studied; the first considers the ETR flow reduction without the attendant ETR power reduction, whereas in the second case a constant full power is assumed until ETR scram at 0.455 sec followed by the reference ETR power scram reduction curve. No credit is taken for the heat sink at saturation temperatures.
The conservatism of these assumptions can be seen in Table 11.10, where the predicted reductions in both power and saturation temperatures are presented.

The THYME-B temperature results are tabulated in Table 11.11. Temperature results are presented for only the secondary vessel and the adjacent ETR coolant. Other loop temperatures remained virtually constant during this accident due to the good thermal insulation provided by the helium containment gap. As these secondary vessel temperature results indicate, the thermal conditions imposed on the FEFPL are not excessive. At 27 sec into the transient, at which time ETR core damage is predicted due to metal/water reaction, no cadmium filter melting is expected even in the event heat generation rates associated with ETR power operation continue. Assuming a successful ETR scram at 0.455 sec, there will be no problem in safely removing the gamma heat from the secondary vessel via nucleate boiling of water. It is, therefore, concluded that the FEFP loop can easily tolerate the thermal load from this accident without containment failure.

Analyses to evaluate the effect on FEFPL of the pressure pulses from this design basis accident have also been conducted. Both the initial decompression wave pressure pulse of 26 psi and the 70 psi pulse generated during core melt were assessed. In both cases, as discussed below, the resulting loop stresses were found to be well within the allowable buckling stress range.

Effect of Decompression Pressure Pulse

To analyze the 26 psi step decompression wave, the STRAP-D program is employed (see Appendix B.9). The model incorporated the major features of the secondary vessel, primary vessel, test train, and flow divider, and is basically identical to that used in the seismic analysis discussed in Section 11.7. The top end of the loop is considered fixed and roller supports were placed 24 in. below and above the core centerline and at the point where the

TABLE 11.10

Double Ended 36-in. ETR Inlet Pipe Break Accident Conditions

ETR Reductions					
Flow		Power		Sat. Temperature	
Time (sec)	W/Wo	Time (sec)	P/Po	Time (sec)	Tsat (°F)
0.0	1.0	0.0	1.000	0.0	376.
0.014	1.0	0.025	.975	0.015	375.
0.027	0.764	0.50	.950	0.020	359.
0.076	0.481	0.075	.925	0.070	240.
0.126	0.388	0.10	.910	0.140	234.
0.217	0.338	0.20	.825	0.20	228.
0.300	0.266	0.30	.770	0.29	232.
0.434	0.049	0.40	.720	0.40	236.
0.455	0.0	0.455**	.666	0.45	236.
0.487*	-0.06	0.635	Decay Heat	0.60	239.

* ETR flow reversal occurred

** ETR scram occurred

TABLE 11.11

THYME-B Secondary Vessel Temperature Predictions for Double Ended ETR Inlet Pipe Break Accident

	Constant ETR Power		ETR Scram after 0.455 sec	
Time (sec)	Secondary* Vessel Temp. (°F)	ETR Water** Temp. (°F)	Secondary* Vessel Temp. (°F)	ETR Water** Temp. (°F)
0	632	116	632	116
2	633	135	602	132
4	637	155	567	148
6	642	175	537	162
8	650	194	513	175
10	659	213	492	187
12	669	232	475	197
14	680	251***	462	206
16	692	269	451	216
18	705	287	442	225
20	719	305	435	233***
22	733	322	429	240
24	747	340	425	247
26	762	359	422	254
27	769	367	421	257

* Radial average secondary vessel temperature at core axial midplane.

** Average ETR H_2O temperature of secondary vessel heat sink.

*** Sink temperature exceeds saturation temperature after this time.

secondary vessel changes diameter. Members have been included to simulate the splines between the primary and secondary vessels and between the primary vessel and the flow divider. The flow divider and test train were assumed to act together and were modeled together in members representing the test train. Members were included to simulate the spring-loaded heat conductors between the ALIP stator and the secondary vessel.

The maximum reactions at the support locations for this 26 psi load were determined to be:[16]

top flange support	1850 lb lateral force and 73.4 in. lb moment
in-tank support	80,000 lb lateral force
top of core	2,000 lb lateral force
bottom of core	1,500 lb lateral force

The maximum stress occurs at the transition from the in-pile tube section of the secondary vessel to the pump section. This stress was approximately 3,000 psi. This represents a faulted condition for which the allowable stress is 1.2 S_t, or 21,000 psi. The maximum reaction force is at the loop support and is within allowable values.

Effect of Pressure Pulse from Molten-fuel Dispersion

Refined analyses have been conducted to determine the ETR pressure pulse emanating from the DBA loss of coolant accident.[15] The results indicate a 70 psi pressure pulse (with 4.1% initial voids at 10% core melt point) instead of the 580 psi calculated by conservative methods of Ref. 4. As presented below, this design basis 70 psi pressure pulse has been converted to equivalent static pressures acting on the FEFPL system in the regions of the top head, top dome flange, and loop.

Section III buckling analyses have been performed for the loop.[17] As shown below, the secondary vessel in the region of the HX was found to have the lowest faulted buckling pressure:

Section	Design Buckling Pressure	Faulted Buckling Pressure
HX	308 psi	770 psi
Pump	367 psi	918 psi
Transition	707 psi	1,768 psi
In-pile Tube	571 psi	1,458 psi

The equivalent static pressure in the design limiting region of the loop HX shell for the design basis 70 psi pressure pulse has been calculated to be 100.5 psi.[18] As this is less than the 308 psi design buckling pressure, the loop design is acceptable.

The equivalent static pressures in the region of the reactor vessel top head and top dome flange were calculated to be 95 psi and 175 psi, respectively.[19] Since both of these values are below the upset design condition value of 250 psi as identified for these areas in the FEFPL design specifications, a satisfactory design is indicated.

11.7 Earthquakes

Due to the evidence of seismic activity near NRTS within recent geological times, an earthquake of damaging magnitude is potentially a credible accident during the period of the FEFP program. The most recent activity of large seismic-induced displacements near the NRTS has been placed at 4,000 to 30,000 years ago.[21] This conclusion was based on geological studies of the Arco and Howe scraps.

In a review of this study, the largest earthquake that may be expected to occur near the NRTS would not exceed magnitude 7 (Richter scale). This was based on the nearest active fault, the Arco Scrap, with an epicenter assumed to be approximately 16 miles from ETR.

A magnitude 7 earthquake with a maximum ground acceleration of 24% of gravity has been used to define the Safe Shutdown Earthquake (SSE) for ETR. A spectrum intensity of 29 in. was chosen as representative for scaling the SSE. It was based on the Housner average velocity spectrum curve for an oscillator damping ratio of 0.05. Resulting horizontal scale factors for four earthquakes are shown in Table 11.12.[22] Vertical scale factors are 2/3 of the horizontal scale factors.

TABLE 11.12

Safe Shutdown ETR Horizontal Motion Scale Factors[22]

Earthquake Record	Unscaled Spectrum Intensity (in.)	Scale Factors for SSE
1940 El Centro (NS Component)	50.2	.58
1934 El Centro (EW Component)	21.6	1.35
1952 Taft (S69E Component)	27.0	1.08
1949 Olympia (NO6W Component)	33.0	.89

The seismic analysis discussed herein is based on a single spectrum: the 1940 El Centro time history. This spectrum was selected since it represents the most intense ground motion recorded to date and exhibits a greater distribution of high level response over the frequency range of interest.

While it would be ideal to conduct response analyses for several other earthquake spectra, it is felt that the use of amplification factors (to be discussed) to obtain upper stress bounds should provide adequate conservatism.

Time history accelerograms for the ETR-FEFPL interface reflecting the structural dynamic response of ETR to various seismic event records are not presently available (i.e., a detail dynamic model of ETR is not available). However, an alternative approach has been elected to determine an upper limit for maximum stresses rather than predict the expected stresses for a given accelerogram input. The analysis approach provides for the accelerogram input being applied to a structural dynamic nodal model of the FEFP loop at the attachment interface with the ETR. Stresses within the structure are determined based on the loop response characteristics. These stresses are then adjusted to account for the site scale factor and the transmissibility and for the amplification factors of the supporting concrete shield and the upper reactor vessel which supports the FEFP loop.

Damping factors used in the amplification factor and in the lumped parameter analyses have been selected based on values shown in RDT standard F9-2T.[23] Summarized, these are:

1) FEFP loop and ETR upper vessel considered as welded steel structures; 2.0% of critical damping.
2) Reinforced concrete shield supporting the reactor: 5.0% of critical damping.

The shield transmissibility factor was estimated to be 10.[24] This magnitude conservatively assumes that the shield resonant frequencies are identically coincident with those of the FEFP loop as the latter is supported within the reactor. The vessel amplification factors were found to be 1.04 (vertical) and 1.13 (horizontal).[25] These factors were determined by applying an earthquake accelerogram (1940 El Centro) at the shield-vessel support and obtaining an output response at the ETR-FEFPL interface. Hence, a factor was computed by:

$$F = \frac{\text{peak ground acceleration + peak output acceleration relative to ground}}{\text{peak ground acceleration}}$$

The loop was modeled as concentric tubes and consisted of 79 elements.[26] With the El Centro accelerogram as input, earthquake stresses were determined within the loop using the ANC STRAP-D computer code.[27] (For description, see Appendix B.9). The vertical and horizontal adjustment factors to account for the SSE scale factor and ETR transmissibility amplification were 6.03 and 6.55, respectively. The earthquake bending stresses were multiplied by these factors and added to the axial stresses caused by operating pressures. The resulting axial stress is used as one principal stress and a stress intensity is found by combining this with the circumferential and radial stresses caused by operating pressures.

Stress intensity and margin of safety results are summarized in Table 11.13 for the primary and secondary vessels. As can be seen, the stresses in the loop are below Section III allowable values[28,29] at all locations. Therefore, it is not expected that the loop would be damaged in the event an earthquake similar to the El Centro earthquake were to occur near ETR.

Subsequent to the completion of the FEFP loop detail seismic model analysis just discussed, a finite element model simulation of the ETR biological shield and vessel and the loop with its supports to the ETR was developed for use with the SAP computer program.[30] The primary objective was to obtain seismic loads for the loop attachments to the reactor vessel. Due to the complexity mass and stiffness node, simulation of the loop was limited to provide interacting effects with the supports. A secondary objective of the analysis was to provide seismic loads to the loop interface with its supports based on the earthquake input being applied at the ETR foundation.

The seismic model and results of the analysis are presented in Ref. 31. The 1940 El Centro earthquake accelerogram and scale factors previously discussed were again used. Due to model complexity, results were obtained using the spectrum response method. Seismic loads have been determined for the vessel top head, top dome flange, in-reactor lateral supports, core filler piece including the grid plate and the loop secondary coolant lines. Resulting stresses are to be determined and reported in the ASME Code Section III stress analysis for each component. (These reports will be made available upon completion.) To date, results are available on the vessel top head where the combined design and earthquake stress (24,390 psi) were shown to be less than the elastic analysis limits (34,650 psi).[32]

As presented in Ref. 31, the interface loads between the top dome flange and the loop showed a marked decrease in this analysis compared with the detailed loop analysis presented in Ref. 26. The difference is attributed to a filtering action of the ground acceleration by the concrete

TABLE 11.13

FEFPL PRINCIPLE STRESSES FOR COMBINED

SEISMIC AND OPERATING CONDITIONS [7]

	Section	Axial Stress*	$Pr/_t$	$P/_2$	Stress Intensity (max)	1.2 St or 1.2 Sy	Margin of Safety **
SECONDARY VESSEL	Bottom of core	+ 3798 - 3274	500	-50	3848	36,000	8.36
	Core ℄	+ 3403 - 2859	500	-50	3359	36,000	9.72
	Point 19	+ 545 + 21	500	-50	595	36,000	59.50
	Section C-C	+ 361 + 33	340	-50	411	36,000	86.59
	Loop Support Ring	+ 2037 - 307	1680	-50	2087	36,000	16.25
	Support	+ 1433 + 254	1680	-50	1483	36,000	23.28
PRIMARY VESSEL	Bottom of core	+ 3345 - 4646	-1420	-280	4765	20,400	3.28
	Top of Pump Stator	+ 5295 - 7215	-2020	-280	7315	21,800	1.98
	Plenum below lower tube sheet	- 916 - 1924	-3640	-280	3360	21,800	5.49
	Outer shell of HX	- 5822 + 5182	-1320	-280	6502	36,000	4.54
	HX center tube	+ 5948 - 4428	-2400	-280	7348	20,700	1.82
	Plenum above upper tube sheet	- 1587 - 1993	-3640	-280	3360	20,400	5.07
	Support of HX shell	+ 8908 - 9628	- 800	-280	9708	36,000	2.71

* (Earthquake Bending)(factor) + Pr/2t + weight + (Earthquake vertical) Factor

** $\text{Margin of Safety} = \frac{\text{Stress Intensity Allowable}}{\text{Calculated Stress Intensity}} - 1$

shielding rather than amplification by a factor of 10 as assumed in Ref. 24. It is concluded that the results of this analysis validate the assumptions presented in the loop detail seismic analysis presented in Ref. 26, which showed that the loop design was adequate.

To provide additional safety, ETR has a two-channel seismic scram subsystem.[8] The reactor safety rods are released upon the tripping of either one of the two seismic switches. These switches, which are firmly anchored to bedrock, are critically damped pendulums with a natural period of 1.0 sec. The subsystem is designed to trip within 200 milliseconds of the detection of an earthquake with a Modified Mercalli Intensity (MMI) of 4.0 or greater.[8] An MMI of 4 is a level of no damage and is equivalent to an acceleration of 0.01g.

References:

1. K. H. Liebelt, "Loop Thermal-hydraulic Analysis of the FEFPL Upset Conditions," ANC Technical Report - TR-346 (Jan 1973).

2. D. H. Thompson, et al., "Test Requirements for Fuel Element Failure Propagation In-reactor Experiment P-1," ANL/RAS 72-9 (Rev. 1) (Nov 1972).

3. J. R. Burris, "Preliminary DRAFT ATR Gas-cooled Loop Control Study," BAW-1310 (Jan 1967).

4. "Design Basis Analysis for the ETR Phase II Technical Specifications," Aerojet Nuclear Co., CI-1231 (Feb 1972).

5. J. E. Hanson, et al., "Technical Basis FFTF Fuel, Cladding Damage Criteria," BNWL-CC-2500 (Feb 1970).

6. D. H. Thompson, et al., "Test Requirements for Fuel Element Failure Propagation In-reactor Experiment P-2," ANL/RAS 72-22 (Rev. 1) (June 1973).

7. H. M. Minami, "FEFPL HX Interim Design Report Stress Analysis," AI Report - TI-542-370-007 (July 28, 1972).

*8. "ETR Technical Specifications," Aerojet Nuclear Co., CI-1233 (July 1971).

9. D. H. Lennox, et al., "Containment Study for the FEFP In-pile Loop," ANL/RAS 71-36 (Nov 1971).

10. A. A. Oare and L. H. Jones, "Helium System Filter Flow Blockage," ANC Report EDF-550 (Rev. A)(Feb 27, 1973).

11. L. H. Jones, "Helium System Operational Manual," ANC Report FR-158 (Aug 8, 1972).

12. "FEFPL Helium System Design Analysis Report," ANC Report FDR-12 (3.2 FR-67)(June 23, 1972).

13. A. A. Oare, "Catastrophic Failure of Helium Circulator," ANC Report EFT-528 (Rev. B)(Feb 27, 1973).

14. R. W. Thomas, "Core Filler Piece Design Requirements," ANC Report EDF-918 (July 5, 1973).

15. R. W. Thomas, "Pressure Pulse Related to the Water-aluminum Interaction during an ETR Design Basis LOCA," ANC Report EDF-707 (Feb 28, 1973).

16. B. L. Harris, "Stress in In-pile Loop due to 26 psi Lateral Pressure Pulse and Transporting Loads," ANC Report EDF-562 (Dec 22, 1972).

17. B. L. Harris, "Secondary Vessel Allowable Pressures at Design Temperatures," ANC Report EDF-560 (Dec 7, 1972).

18. H. L. Magleby, "Equivalent Static Pressures for Loop from ETR Pressure Pulse from Double Ended Pipe Break," ANC Report EDF-814 (Apr 27, 1973).

*Under Revision

19. H. L. Magleby and B. L. Harris, "Equivalent Static Pressure of ETR Water-aluminum Interaction Pressure Pulse," ANC Report EDF-896 (June 19, 1973).

20. "Design Specification for the FEFPL-ETR Top Dome Flange," ANC Report 70010A (Apr 27, 1973).

21. H. E. Maulde, "Geologic Investigation of Faulting Near the National Reactor Testing Station," U. S. Geological Survey Open File Report (1971).

22. V. W. Gorman, "TRA Seismic Analysis Method and Determination Evaluation Input," Aerojet Nuclear Co. Engineering Report TR-336 (Nov 15, 1972).

23. USAEC RDT Standard F9-2T, "Seismic Requirements for Design of Nuclear Power Plants," Draft (June 1972).

24. R. W. Thomas, "Seismic Transmissibility for ETR Foundation to Vessel Support," Aerojet Nuclear Co. FEFPL Report EDF-558 (Nov 21, 1972).

25. B. L. Harris, "ETR Vessel Earthquake Stress Amplification Factors," Aerojet Nuclear Co. FEFPL Report EDF-534 (Nov 14, 1972).

26. B. L. Harris, "Seismic Stress Analysis of FEFP Loop," Aerojet Nuclear Co. FEFPL Report EDF-563 (Dec 29, 1972).

27. J. A. Dearien, et al., "STRAP, A Computer Code for Static and Dynamic Structural Analysis and Studies Made Using the Code," Idaho Nuclear Corp. Report IN-1362 (June 1970).

28. "Boiler and Pressure Vessel Code, Section III - Rules for Construction of Nuclear Power Plant Components," American Society for Mechanical Engineers (July 1, 1971).

29. "Interpretations of the ASME Boiler and Pressure Vessel Code (1971) - Case 1331-5 - Nuclear Vessels at High Temperature Service (Aug 4, 1971), Replaced by Case 1331-6 (May 1, 1972)," American Society of Mechanical Engineers.

30. R. W. Wilson, "SAP - A General Structural Analysis Program," Structural Engineering Laboratory Report No. 70-20, University of California at Berkeley (Sept 1970).

31. B. L. Harris, "ETR-FEFPL Seismic Analysis," ANC Report TR-398 (June 26, 1973).

32. T. K. Burr, "ETR Top Head (FEFPL Installation) Section III Design Stress Analysis," ANC Report TR-407 (July 9, 1973).

CHAPTER 12.0

TABLE OF CONTENTS

LIST OF TABLES

LIST OF FIGURES

12.0 FEFP Loop Handling System

12.1 Scope

This section presents the safety evaluations associated with assembly, charging with sodium and handling of the FEFP Loop within the confines of ETR. These evaluations have been categorized as: (1) Handling System Analysis, (2) FS&R Operational Hazards Analysis and (3) Industrial Safety Analysis.

The Handling System Analysis presents the safety evaluations associated with handling (1) the test train, (2) the assembled loop, (3) the loop handling machine, and (4) other related handling equipment. This handling study covers potential handling operation hazards, accidents, or malfunctions from the time of delivery of the primary/secondary containment vessel and the test train to the ETR building until the irradiated loop leaves the ETR building. The study identifies the single failures which can cause handling accidents and evaluates the consequences of these accidents.

The FS&R Operational Hazards Analysis treats the hazards which result from the presence of sodium in the FS&R Facility.

The Industrial Safety Analysis treats the hazards related to normal industrial operations excluding: handling of test train, handling a loop charged with sodium and the operational sodium loop in the FS&R. It includes handling of loop components during assembly and other activities in the FS&R until the test train has been installed and sodium has been introduced into the loop.

12.2 Handling System Analysis

12.2.1 Handling Operations

The FEFP loop handling system, described in Section 5.3 is a transfer-transport system of equipment used to (1) handle the FEFP loop or its components at various NRTS facilities, and (2) transport the FEFP loop or its components between the NRTS facilities. The handling operations described herein are limited to the operations performed in the ETR reactor building. Separate hazards studies will be performed for HFEF and transportation between ETR and HFEF.

The handling operations described in this section have been categorized into six major areas: (1) movement of equipment or the loop handling machine (LHM) to the filling, storage, and remelt (FS&R) area; (2) handling operations in the FS&R; (3) movement of the LHM and loops between the FS&R and the reactor top; (4) insertion and removal of the FEFP loop into and from the ETR reactor vessel; (5) movement of the LHM between the reactor top and the transporter; and (6) movement of the transporter into or out of the ETR building.

The flow chart, Fig. 12.1, shows the handling events which occur during normal handling of the FEFP loop or its components. The sequence of events and handling operations will be subject to change or modification as assembly techniques are established and handling procedures developed. The flow chart starts with the arrival of the separate loop containment vessels at the ETR reactor building freight door and ends with the irradiated loop loaded in the LHM and on the transporter leaving the ETR reactor building for the Hot Fuel Examination Facility (HFEF). Each step lists the general operations that must occur for that step to be completed; a precursor for the next step.

12.2.1.1 Movement of Equipment or the Loop Handling Machine to the FS&R

The major handling activities for this category are: (1) the entry of equipment into the ETR reactor building; (2) the handling and transfer of the secondary containment vessel to the FS&R; (3) the handling and transfer of the primary containment vessel to the FS&R; (4) the handling and transfer of the cold/clean test train to the FS&R; (5) the handling and transfer of the irradiated test train to the FS&R; and (6) the handling of the LHM.

The progression of loop components entering the ETR reactor building are shown on the flow chart. All components enter the reactor building through the freight door located on the north side of the building. An operating limit on the reactor building[1] requires that this door remain closed except during transfer of equipment. The LHM transporter with tractor is too long to fit entirely within the ETR reactor building and consequentely, the tractor will have to be disconnected from transporter and removed from the reactor building so that the freight door can close.

The primary and secondary containment vessels will be delivered in separate shipping containers. The erection tower is used to remove the shipping containers from the loop components. The erection tower is also used as assembly stand during installation of thermocouples on the primary containment vessel. The secondary containment vessel is transferred from the erection tower to the FS&R oven. The primary containment vessel is then

FIGURE 12.1
LOOP HANDLING FLOW CHART

inserted into the secondary containment vessel in the FS&R oven.

Two different methods will be used to handle the test train. A cold/clean test train will arrive at the ETR reactor building in a shipping container, whereas an irradiated test train will arrive in a shielded cask (the LHM). The cold/clean test train will be attached to the erection tower for removal of the shipping container before it is inserted into the assembled primary and secondary containment vessel. When handling the irradiated test train, the LHM will be located on the FS&R oven hatch so that the test train can be lowered into the assembled primary and secondary containment vessel. This completes transfer of equipment to the FS&R.

12.2.1.2 Handling Operations in the FS&R

Assembly operations to attach the primary vessel to the secondary vessel are performed in the FS&R. The two vessels are welded together at the top closure of the primary vessel and inspected in accordance with the ASME Boiler and Pressure Vessel Code for Class 1, Section III vessel and RDT E 15-2T. Dimensional checks will also be made to verify that the weld did not compromise the dimensional requirements for the assembled vessel.

The test train is inserted into and attached to the primary containment vessel to complete the enclosure of the primary vessel with the exception of the sodium fill and cover gas lines. Post-assembly checkouts may be performed prior to or following filling the loop with sodium to verify that the multiple instrument leads and test train/primary vessel closure connections have not been damage.

The assembled loop is prepared for filling with sodium by installing a glove box adapter on the top flange of the loop. The sodium fill and cover gas lines are then attached.

All electrical and instrument lines are connected for pre-fill checkouts. The primary containment vessel is evacuated and inert gas is added to the annulus between the primary and secondary containment vessel to prevent oxidation of the EM pump coils during heating of the assembled vessel.

The assembled loop will then be heated to the fill temperature by the the heaters in the FS&R oven (see Section 4.10.9 and Fig. 4.15). After the fill temperature has been reached, the loop is filled with sodium and purified until the sodium contaminants are reduced to acceptable levels (see Section 5.2.3.2). The operation of the EM pump and the instruments are checked out.

The welding equipment and glove box are installed on the glove box adapter and the glove box inerted. The sodium fill lines are then cut, seal welded and inspected. The argon cover gas line is then cut, seal welded and inspected. The glove box, welding equipment, and glove box adapter are removed from the top flange of the assembled loop. Pre-operational tests are then performed on the loop in the FS&R oven. The assembled loop is now complete and ready for insertion into the ETR reactor vessel.

12.2.1.3 Movement of the LHM Between the FS&R and the ETR Reactor Vessel

The loop handling machine (LHM) will normally be used to handle an assembled loop. The LHM and transporter will normally be stored outside the ETR reactor building when not in use because of the storage area required and the floor loading limits the units impose around the truck aisle.[2,3,4] When the assembled loop is ready for transfer to the reactor vessel, the LHM and transporter are brought into the reactor building observing the precautions noted in 12.2.1.6. The LHM is moved to the FS&R hatch. All electrical and instrument lines are disconnected from the loop prior to attaching the LHM grapple to the loop. The loop is raised into the LHM where transporter power and instrument connections are made with the loop. The EM pump operation is then verified. After closing the bottom door and engaging the lateral supports the LHM is ready for transfer to the reactor top.

Prior to transferrring the LHM, several operations must be performed on the reactor vessel. These include all pre-operational testing of the ETR reactor, pre-operational testing and checkout of the loop support systems, and preparation of the reactor top for accepting the LHM. All tank preparations including alignment verification of in-tank components and installation of remote viewing equipment must also be made prior to locating the LHM on the ETR biological shielding above the reactor top.

When the transfer is made using a cold/clean test train in the loop, plant personnel on the reactor top directing the operation will not be exposed to any radiation above the background from the reactor.* For the case of test train containing preirradiated fuel, the calculated radiation field on the outside surface of the LHM is less than 680 mr/hr. This calculation is based on a fuel inventory of 37 pins preirradiated to 7% burnup at a rate of 12 kW/ft and cooled six months, and the shielding level on the

* The maximum background radiation above the biological shielding during shutdown is 10 to 20 mR/hr at 3 feet.

40-ton LHM.

By use of administrative procedures which prescribe specific placement of personnel, the estimated radiation dose[5] of personnel involved in the final alignment of the LHM on the biological shield will be approximately 110 mr. This exposure is below the value of 300 mrem set by the Administrative Exposure Guide.[6]

After the LHM is properly aligned on the biological shielding, the loop is ready for insertion into the reactor vessel.

Normal handling of the loop between the FS&R and the reactor top will encompass transfer of the loop from the FS&R and the reactor vessel. Off-normal conditions will involve either returning the loop to the FS&R for corrective maintenance or to the LHM transporter for storage until the off-normal condition has been corrected.

12.2.1.4 Insertion and Removal of the FEFP Loop Into and From the ETR Reactor Vessel

The insertion and removal of the FEFP loop from the ETR reactor vessel is considered the most critical handling operation to be performed. Emphasis will be placed on procedures and training for these operations to ensure that there is no damage to the loop or the reactor.

The insertion and removal sequence of events are listed below.

The LHM is located on the biological shielding and aligned. The loop lateral supports and bottom door on the LHM are then moved to their full open position. All LHM operations are controlled from a portable control panel separate from the LHM. The loop is lowered into the reactor vessel and onto the in-vessel supports. The grapple is disconnected from the loop and raised into the LHM so that the LHM can be removed from the biological shielding. The auxiliary power supply is connected to the loop. The auxiliary power supply will power the EM pump, providing heat to maintain the sodium molten until the main power and instrument connections are made to the loop.

The gland seal ring is inserted over the top of the loop and attached to the ETR top dome flange and the loop. Dual seals allow a leak check to be made before the reactor is pressurized. The main power and instrument connections are then attached to the loop and electrical continuity and instrument operation are verified. The removable top closure is located on the loop top flange and secured. The helium piping is attached to the removable top closure. This also connects the test train instrumentation to the acquisition system. The loop is now connected to all support systems and the final pre-operational testing can be performed to verify that the loop is in an operational condition. The reactor vessel openings are closed prior to filling and pressurization of the reactor vessel. All shielding plugs are installed in the biological shielding prior to operation of the reactor.

After the reactor has been shutdown, a period of time will be allowed for decay of fission products and activated sodium before operations are started for removal of the loop. Activity generated in the loop will be monitored by a remote area monitoring head located under the biological shielding, in addition to monitors installed within the FEFPL system.

Calculations were made,[7,8,9] to estimate the sodium and fission product activities in the loop assuming three modes of fuel dispersion:

1) two-day decay with no fuel dispersion,
2) four-day decay with 20% fuel dispersion, and
3) ten-day decay with 100% of the fuel uniformly dispersed in the sodium.

The fuel inventory for these calculations represented the conditions for the most severe planned test and was 37 pins exposed to a power level of 16 kW/ft (two ETR cycles, 60 days exposure) and containing 1800 kW fission power. Biological dose rates for various spatial configurations encountered in loop and LHM transfer operations are tabulated in Table 12.1 for each fuel dispersion mode. The dose rates listed in Table 12.1 for 4 day decay and 20% fuel dispersion change very little with additional six days decay because the short-lived sodium activity is already negligible and the fission product decay curve is relatively flat over this period.

For two-day decay of the sodium, the radiation field above the loop and under the biological shielding could reach 16 R/hr. After ten-day decay with 100% dispersion of fission products, the radiation field above the loop and under the biological shielding could reach 580 R/hr. The removal operation, remotely conducted under administrative handling procedure, and the design of support handling equipment are based on the ten-day decay condition

TABLE 12.1

Dose Rates (R/hr), External to the LHM

Fuel Inventory: 37-pin Bundle
Exposure: Two ETR Cycles, 60 days
Power Level: 16 kW/ft
Fission Power: 1800 kW

A. Dose Rates (R/hr) with FEFPL Loaded in the LHM [8,9]

Locations and Conditions	Auxiliary Shielding, pb (in.)	Dose Rates (R/hr) 2 day No Fuel Dispersion Into Sodium	4 day 20% Fuel Dispersion Into Sodium	10 day 100% Fuel Dispersion Into Sodium
Top of LHM, on C.L.	None	1.12	2.34	7.76
Opposite Hx C.L.	None	2.23	4.31	14.2
Opposite Core C.L.	None	6.8	4.75	0.23
At Bottom of LHM, on C. L.	None	1.32	2.53	7.5
At Lower Steel Annulus	None	0.10	0.13	0.56
At Door Gaps	None	0.00	0.00	0.00
At Lower Clamps	None	3.2	4.81	16.3
	1.0"	1.0	1.5	4.30
At Upper Steel Annulus and Steel-Uranium Gap	None	0.7	1.1	3.7
Center of Top of Grapple	None	0.17	0.27	0.70
At Construction Gaps	None	Twice surrounding dose for less than 0.2 inch width.		
	None	120% of surrounding dose at 15 inches from surface.		
	0.5"	Equal surrounding dose rate.		
Exposure to personnel through bottom door with loop loaded in transporter. (1" steel transporter base included)	None	0.41	0.75	2.8
Exposure to personnel adjacent to core with LHM loaded on transporter (through 1" steel of transporter).	None	1.36	0.9	0.05
Top of Grapple (at end of annulus between LHM and loop-grapple combination).	None	90.0	200.0	620.0
	2.0"	4.0	9.3	28.0

B. Maximum Dose Rates (R/hr) As the FEFPL is Raised Into the LHM [9]

Locations and Conditions	Auxiliary Shielding, pb (in.)	Dose Rates (R/hr) 2 day No Fuel Dispersion Into Sodium	4 day 20% Fuel Dispersion Into Sodium	10 day 100% Fuel Dispersion Into Sodium
As heat exchanger passes lower steel annulus (general)	None	1.30	1.98	7.435
As heat exchanger passes door guide (corners)	None	11.	15.	67.5
	2"	.80	1.2	4.55
As heat exchanger passes the door gaps	None	.25	1.2	4.10
As heat exchanger passes lower clamps	None	3.1	4.3	14.9
	1"	0.9	1.3	3.9
As heat exchanger passes upper steel annulus and steel-uranium gap	None	17.8	36.7	126.0
	2"	0.8	1.7	5.76
As heat exchanger passes upper clamps	None	18.1	36.8	126.4
As core passes lower steel annulus (6.4" section)	None	225.	156	8.4
	2"	16.6	11.	.6
	3"	4.2	2.9	.04
As core passes door guide corners (15° arc)	None	3430	2320	130
	4"	16.0	11.	.60
	5"	4.58	3.1	.04
	8"	.090	.06	.001
As core passes door gaps	None	50.7	34.0	1.84
	2"	3.25	2.2	.11
As core passes lower clamps	None	484.	325.	17.5
	3"	8.53	5.7	.3
	4"	2.33	1.6	.1

Note:

The dose rates and auxiliary shielding thicknesses listed above were used for sizing of the LHM. The current clamshell shielding design provides 3 inches of lead shielding around the lower steel annulus and 5 inches of lead at the door guide corners. See EDF-1079 for auxiliary shielding radiation study.

C. Exposure Rates at Transporter Cab Calculated Using Assumptions Designed to Give a Maximum Possible Value. (Source Equal to Integrated Flux in Gap Between LHM and Loop-grapple Combination).[9]

Locations and Conditions	Auxiliary Shielding, pb (in.)	Dose Rates (R/hr) 2 day No Fuel Dispersion Into Sodium	4 day 20% Fuel Dispersion Into Sodium	10 day 100% Fuel Dispersion Into Sodium
At cab (straight)	None	0.06	0.09	0.32
	2"	0.002	0.003	0.012
Cab at right angles to transporter	None	0.010	0.016	0.054
	2"	<0.001	<0.001	0.003

D. Dose Rates with Loop in Air

Vertical Location	Radius From Center Line (in.)	Dose Rate (R/hr)		
Heat Exchanger	15.7	6.2×10^2	5.0×10^3	1.4×10^4
Core Center	15.7	3.5×10^5	2.4×10^5	1.4×10^4
Core Center	2.73	2.2×10^6	1.6×10^6	8.0×10^4
At Bottom on C.L.	0	5.0×10^2		9.5×10^3
At Bottom on C.L.	12			1.8×10^3

Note:

The 7.76 R/hr dose rate in Table 12.1A is at contact on top of the LHM @ centerline. This value increases to 260 R/hr above the grapple due to streaming through the thinly shielded annulus between the outer diameter of the grapple and inside diameter of the LHM. The 2-inch thick transporter shield will reduce this value to 28 R/hr at contact on the shield and to 0.012 R/hr at the transporter cab on a straight line.

ANC safety policy requires the completion of a Radiation Hazards Analysis (RHA) prior to any operation with the potential for personnel radiation hazards. This analysis establishes prior to the operation, the potential hazard, the expected radiation levels, a level at which the operation will be terminated, and contingency measures.

since this condition produces the highest radiation field in which the plant personnel would be operating. The radiation field on the external surface of the biological shielding has a maximum strength of 200 mr/hr and less than 1 mr/hr four feet from the loop vertical centerline.[3]

Handling operations for removal of the loop under these conditions will involve the following equipment:

- Additional LHM shielding (sizing and design of this additional shielding has not been completed)
- 6-inch thick motor driven "sliding shield plate" mounted on the reactor biological shielding
- 3-inch to 5-inch thick auxiliary "clamshell" shields, rail mounted on reactor biological shield
- 2-inch thick auxiliary "block shielding" set in place around LHM base
- 3-inch lead "handling tool shield" used during disconnection and removal of instrument/power leads, gland seal and loop clamps, and loop removable top closure (RTC).

The sequences of removal operations is as follows:

The reactor biological shield plug over the loop is raised to allow the shield plate to be driven over the loop. The handling tool cask is positioned over the shield plate and lowered onto the biological shield as the shield plate is retracted.

Through the tool shield ports the helium piping, test train connectors, and RTC clamp are disconnected. The RTC is raised into the tool shield which is then raised as the shield plate is driven into place.

After the RTC is moved to storage, the tool shield is again positioned over the loop and lowered into place as the shield plate is retracted.

Using the tool ports and viewing equipment in the tool shield, auxiliary power is established to the EM pump, the main power and instrument connectors are disengaged and the gland seal ring removed. The tool shield is raised and the shield plate positioned over the loop.

The shield plate is extracted as the special biological shield plug and leveling plate are installed and the loop is now ready for removal.

The LHM is moved into position and lowered as the shield plate is extracted.

Auxiliary shield blocks providing ~2-inches of shielding are positioned around the bottom of the LHM and the clamshell shielding positioned around the shield blocks.

Additional shielding can be clamped to the body of the LHM if required. (Sizing and design of the additional shielding has not been completed.)

After installation of the LHM, the auxiliary loop power is disconnected and the LHM grapple attached to the loop. The loop is raised into the LHM where power is restored to the EM pump. The lateral supports in the LHM and the bottom door are closed to secure the loop in the LHM. The LHM is now ready for transfer to the transporter.

Personnel access to the reactor top will not be permitted during the extraction of the loop into the LHM.

Total radiation exposure during the preceding operation is estimated to be 1020 mr.[5] This total exposure will be spread over a number of persons and working shifts to insure that individual radiation exposures will not exceed 300 mrem per week.[6]

During operation of the loop in ETR, two abnormal conditions have been postulated to occur which can affect the normal removal operations of the loop. The abnormal conditions are: (1) removal of the loop with a failed primary containment vessel; and (2) removal of the loop with a failed heat exchanger. Either of these conditions is detected by the plant protection system and results in an immediate scram of the reactor.

Failure of the loop primary containment vessel can result in sodium entering the annulus between the primary and secondary containment vessel. Depending on the circumstances involved with failure of the primary vessel, the sodium within the loop may be permitted to freeze. Freezing will prevent further release of sodium into the annulus. The annulus gas system, which provides helium gas flow through the annulus for leak detection, is equipped with special connectors at the loop which seal the connector whenever the connector is disconnected from the annulus gas system. Thus, during removal of the loop from ETR, the annulus gas system connection is disconnected and the annulus between the two containment vessels is sealed air tight. Removal operations would proceed as with removal of a normal loop, except that no power would be required for the loop pump if the sodium is permitted to freeze.

Failure of the heat exchanger is discussed in Chapter 11 as a low probability accident, terminating with the reactor shut down, the loop frozen and no attendant safety problems.

The extent of the contamination and direct radiation (a function of the quantity of sodium released and the test history prior to the accident) are conservatively bounded by the analysis contained in Refs. EDF-789, Revision A, and EDF-718. Based on an off-set shear of a heat exchanger tube, a maximum of .35 gal. of sodium will be released after a 100% fuel meltdown and uniform dispersion through the loop volume. This released volume is contained in the RTC* as the source terms for direct radiation and contaminants considered during loop removal. With the loop frozen and the helium system shutdown, the contaminants will be isolated and shielded. The helium system will be exhausted to the ETR stack to remove gaseous fission products.

After installation of the handling shield, an expandable semi-rigid foam will be injected into the RTC and helium lines to secure contaminants and prevent particulate release as closure joints are broken. A mechanistic, procedure outline has been developed for the subsequent removal of the RTC and loop. While special precautions and handling techniques will be required, no insurmountable handling problem has been identified which would preclude the removal of the loop without hazards to personnel and restoration of the facility for operation of subsequent tests.

12.2.1.5 Movements of the LHM Between the Reactor Top and the Transporter

With the loop secured in the LHM it is moved to the transporter using the ETR crane. The LHM is then secured to the transporter and ready for transfer to the HFEF.

During mid-cycle shutdowns of the ETR reactor, it may be required that the loop be removed so that maintenance work can be performed within the reactor vessel. These shutdowns may not occur at the end of the loop test cycle. This will require that the loop be removed and stored in either the LHM or FS&R Storage Oven until maintenance work has been completed. After this storage period, the loop will be returned to the ETR reactor vessel. These removals and reinsertions will follow the sequences previously listed.

12.2.1.6 Movements of the Transporter Into or Out of the ETR Reactor Building

The LHM transporter, described in Section 5.0, transports the LHM to various NRTS facilities. The transporter provides the control panels and

* Removable Top Closure

a self-contained diesel power system for operation of the LHM by umbilical cabling. Operation of the LHM requires it to be continuously attached to the LHM portable control panel.

While in the ETR reactor building, power to the LHM control panel will normally be supplied from the ETR commercial utility, with operation of the diesel power system limited to periods of transporter entry and just prior to exit of the transporter from the reactor building. The ETR roof exhaust fans have been demonstrated as adequate to handle the diesel exhaust and will be activated during periods of diesel operation.

Trained fire brigade personnel and portable fire extinguishing equipment are available in the reactor building during periods when the transporter diesel generator is started and operating.

The weight of the transporter with LHM is within the allowable floor loading limits of the truck aisle in the ETR reactor building. The weight[38] of the transporter with the LHM and the loop is 172,340 lbs., with axle loadings of approximately 26,140 lbs with the cask in the traveling position, and 29,070 lbs with the cask in an upright position. These loadings are based on a maximum cask weight including accessories of 55 tons.

An analysis was performed on the permissible floor loading capacity for the ETR reactor building.[4, 10, 39] It was determined that the floor could support an axle loading of 30,000 lbs. The analysis considered the truck aisle floor slab, first floor - floor beam B-3, basement walls between column lines E-24 and E-25 on column line N-32, foundation of the experimental air exhaust structure, and the basement wall of Building ETR-647 adjacent to the truck apron. The analysis showed that the truck aisle floor slab, floor beams, and pipe tunnel will support the design loads with stresses below the American Concrete Institute code values. Stresses in (a) the horizontal reinforcing steel in the outside face of the basement wall between the console and basement floors; (b) the vertical steel in the outside face of the bottom nine feet of the foundation of the air exhaust structure; and (c) the horizontal reinforcing steel in the outside face of the basement wall of ETR-647 at column lines all exceeded code values by not more than 10% while the transporter is backing into the ETR reactor building. The overstresses are well below yield values and also within the 33% increase allowed for transitory wind loadings. The tractor and transporter loadings may be considered transitory since the loadings occur infrequently and are applied at a rate which reduces the effect of impact. The transporter will not be allowed to remain in this area except for maneuvering operations required to assure proper alignment during entry into the ETR reactor building.

Floor loading around the transporter will be limited to foot traffic only when the LHM is on the transporter. The ETR biological shielding is normally stored adjacent to the east side of the truck aisle. The II, III, IV, and V shielding blocks have a combined weight of 147,300 lbs. These shielding blocks will be supported over the pipe tunnel. Analysis[33] has been performed to show that the ETR main floor can support these shielding blocks in their storage position in addition to the transporter with the LHM on the truck aisle.

The defined floor limits of the truck aisle extend to the south wall of the pipe tunnel under the main floor. Beyond this location, the floor loading limits are markedly reduced to the east and to the west of the center of the truck aisle. Movements of the transporter beyond this point could cause structural damage to the ETR reactor building. To ensure that the transporter axles will not extend into the lower load limit areas, a guard rail with wheel blocks will be erected. These precautions plus administrative controls while the transporter is entering the reactor building will prevent the transporter from entering the lower floor loading areas. The transporter movements within the ETR building will be at minimum speed to prevent excessive "live" loading of the truck aisle.

12.2.1.7 Movements of the Transporter Between the ETR and TRF Main Gate

The route for the transporter with and without the loop handling machine between the ETR reactor building and the TRF main gate will always be the same to preclude the possibility of movements over the MTR piping tunnel. The same route will be followed during either entry or exit from ETR.

The transporter will enter the TRF area through the main gate on Perch Avenue. The transporter will make a 180 degree right turn into the MTR-ETR area onto Marlin Avenue. The transporter will then make a left turn onto Whitefish Street and travel down this street to the concrete slab exit between the MTR-ETR maintenance shop and the hot cell. The transporter will then be maneuvered between the ETR reactor building and reactor services building for alignment and entry into the ETR reactor building.

All vehicular traffic will be excluded from the route to be followed by the transporter during its movements within the TRF area. Also, the maximum speed of the transporter will be less than 5 miles per hour. The proposed route has been checked for structural strength and upgraded with a 2-inch course of plant mix during the 1972 Road Program. The proposed route has been reviewed with the transporter designer to ensure that corners and turning radius will be compatible with the transporter. The corner at Whitefish and Marlin was considered to be tight and as a result, the pavement was extended to the edge of the roadway.

12.2.2 ETR Handling Requirements

Handling requirements for test loops and equipment at the ETR facility are established on an individual loop basis. Handling studies are performed and reviewed by ANC for each loop. Procedures and training, as described in 12.2.4 are used to ensure that the FEFP Loop and equipment are handled correctly. All hoisting and rigging will be in accordance with RDT Standard F 8-6T, "Hoisting and Rigging of Critical Components and Releated Equipment" to insure that handling operations requiring rigging conform to good management and quality assurance practices.[11]

12.2.3 FEFP Loop Handling System

This section presents a description of the safety features for the major components of the FEFP Loop handling system. This information provides background for the Handling Hazards Analysis discussion in 12.2.5.

The following are the major components of the loop handling system:

- ETR 50-ton Crane
- Loop Handling Machine (Figures 12.2 and 12.3)
- Transporter (Figure 12.4)
- Auxiliary Shielding
- In-vessel Supports
- Accessories
  - Handling Slings
  - Special Grapples

12.2.3.1 ETR 50-ton Crane

The ETR 30-ton crane is being replaced with a 50-ton dual hook crane to provide sufficient crane capacity for handling the FEFP Loop Handling Machine (LHM). The new crane will be designed and installed in accordance with ANC Equipment Specification 642.8.

To ensure that safe design and manufacturing practices are employed, the following standards and specifications, among other, are invoked:

(a) American National Standard Institute (ANSI) B30.2, Safety Code for Cranes, Derricks, and Hoists, Jacks and Slings.

(b) National Electric Manufacturers Association (NEMA) IC-4, Industrial Control.

(c) Crane Manufacturers Association of American INC (CMAA) No. 70, Specifications for Electrical Overhead Traveling Cranes, 1971.

(d) Occupational Safety and Health Administration (OSHA) 1919.179 Overhead and Gantry Cranes.

In addition to the above, standard RDT F8-6T titled "Hoisting and Rigging of Critical Components and Equipment" is being incorporated to insure that the new 50-ton crane will comply with the RDT requirements. In addition to crane replacement, the crane runways or rails are being replaced to ensure safe operation of the 50-ton crane.

The 50-ton crane is comprised of two 25-ton hooks, each having a separate cable system reeved such that failure of one hoist hook, sheave or cable will not propagate to the second hook and cabling system. A minimum safety factor of five applied to each hook and cabling system will permit either of the 25-ton hooks to support the 47-ton LHM with loop with a dynamic load factor of two and prevent dropping the LHM into the reactor or onto the ETR reactor room floor.

The control and braking features of the 50-ton crane are designed to prevent uncontrolled lowering of the loaded hoist hooks. Over-speed trips on the crane hoist motor controls will limit the main hoist lowering speed to a maximum of 25 feet per minute. Over-speed trips are used to terminate electrical power to the hoist motor and set the hoist brakes in event an over-speed occurs. The 50-ton hoist will be equipped with two independent, automatic, electric brakes consisting of spring-set electrical solenoid released shoe or disk brakes, each brake having a minimum rating of 100% of full rated crane capacity. The electric brakes automatically set at any interruption to the hoist motor power. In addition to the electrically activated hoist brakes, the hoisting machinery is equipped with a mechanical load brake to positively lock and prevent free spooling of the load. Brakes and limit switches on the bridge travel, trolly travel, and hoist travel will prevent over-travel. The braking system and over-travel limit switches used on the ETR 50-ton bridge crane are standard features of overhead bridge cranes used for reactor servicing equipment that have proven high reliability.

Administrative controls including de-energizing and tagging out the 50-ton crane when the LHM has been located on the FS&R oven hatch and on top of the reactor will be applied. Such action will preclude lateral movements of the LHM and crane during raising and lowering the loop out of the LHM.

Following installation of the new 50-ton bridge crane in the ETR building, acceptance tests will be conducted to insure proper operation of all components. A load test to insure load carrying capability will be conducted at 125% of the crane's rated capacity. Following acceptance of the crane by ANC, periodic maintenance inspection, and testing in accordance with ANC policies and procedures and RDT F8-6T will be conducted. Proper training, qualification and administrative control of crane operators coupled with the design, installation, maintenance and testing of the crane will ensure against failure and accidents involving the crane.

12.2.3.2 Loop Handling Machine

A description of the loop handling machine is provided in Section 5.0. The standards and provisions used or applied to the design of the LHM include among others:

(a) Radiation protection within the personnel limits prescribed in AEC Manual Chapter 0524 and the AEG.[6]

(b) Nuclear criticality safety prescribed in AEC Manual Chapter 0530.

(c) USAEC Immediate Action Directive 0529-24, "Guidance Statement Regarding Shipping Containers for Fissile and Other Radioactive Materials," dated March 23, 1971.

(d) USAEC -IDO, Appendix 0500-1, Annex L, "Safe Transport of Radioactive and Fissile Materials," dated March, 1972.

(e) IDO - 12044, Health and Safety Design Criteria Manual.

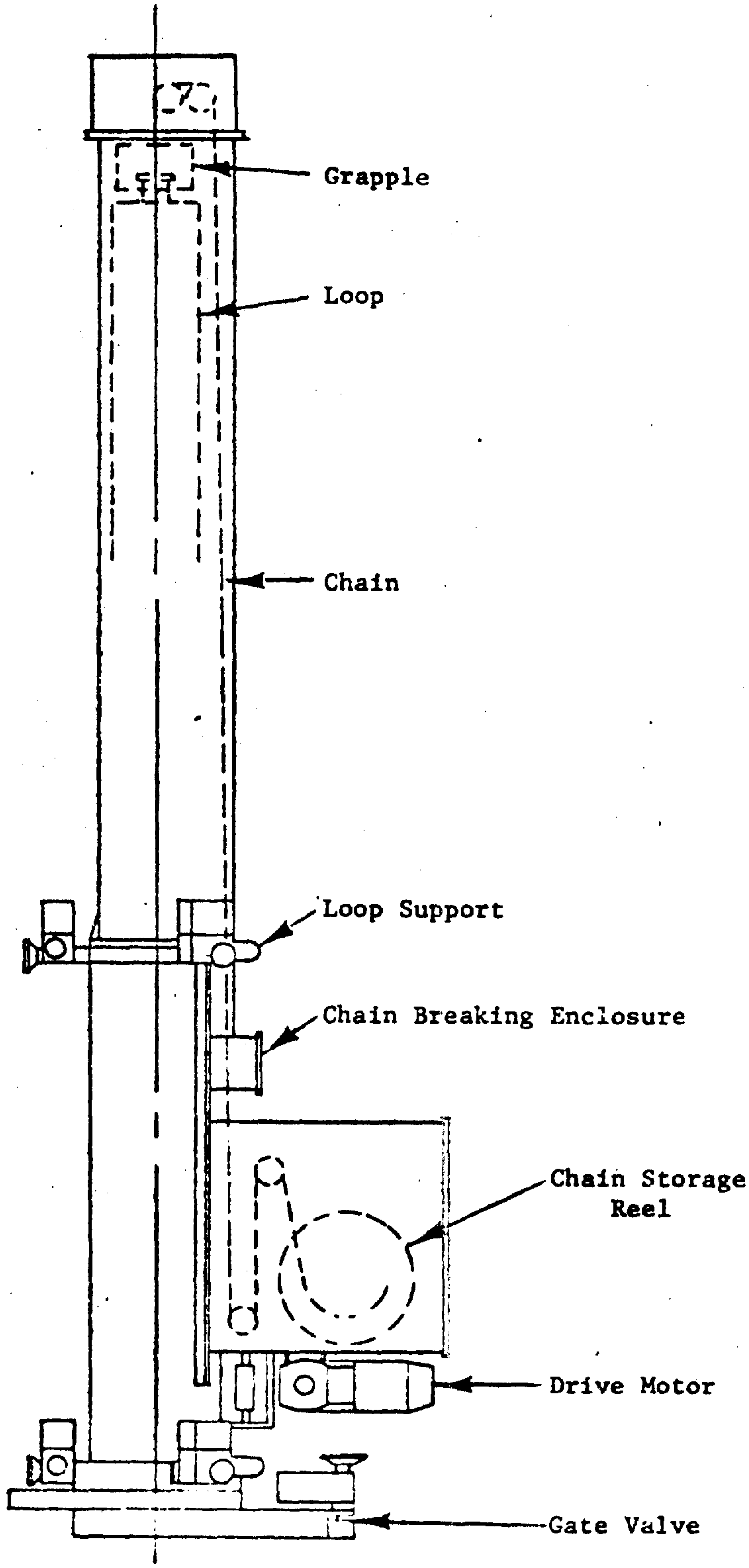

FIG. 12.2 - Loop Handling Machine

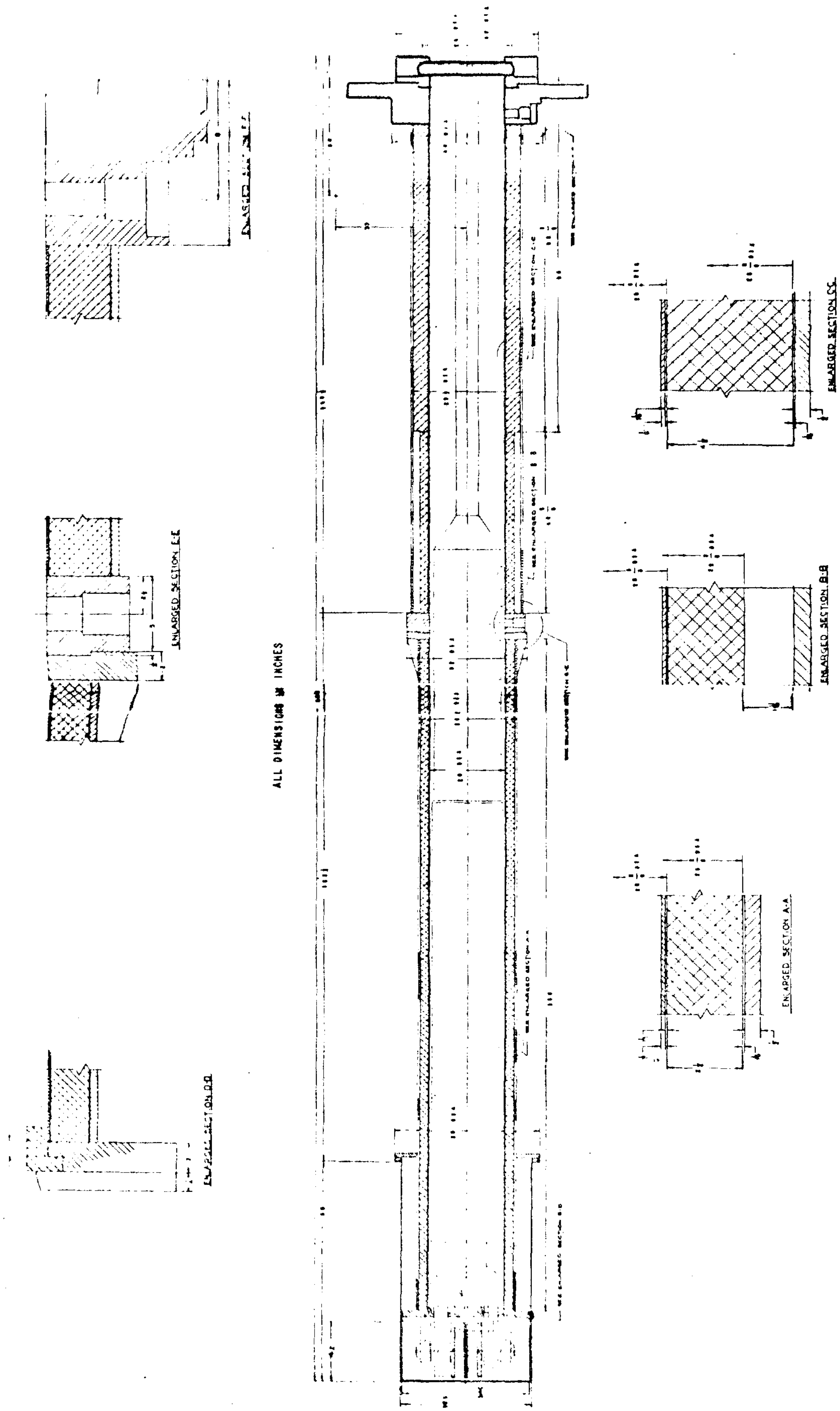

FIG. 12.3 Shielding of Loop-handling Machines

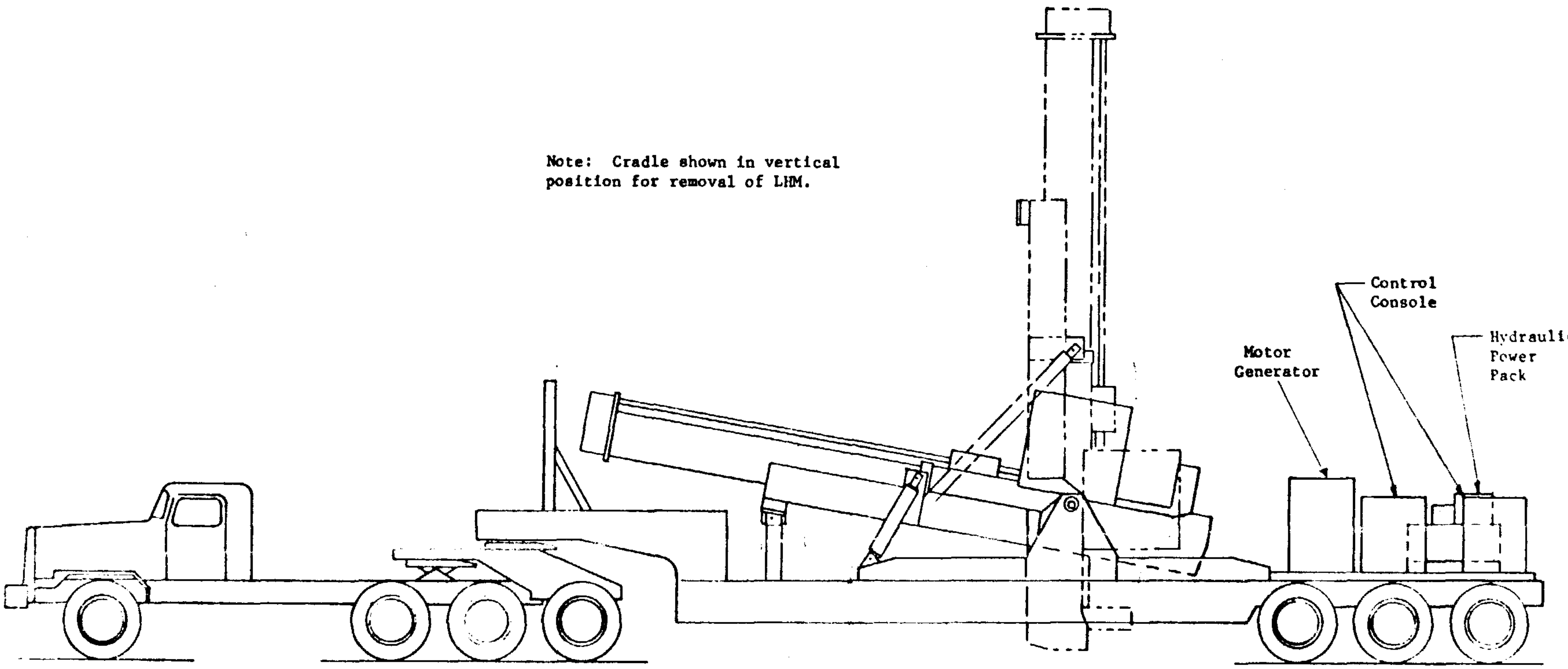

FIG. 12.4 - FEFPL Handling Machine Transporter

(f) ORNL- NSIC 68, Cask Designers Guide.

(g) RDT Standard F8-6T, Hoisting and Rigging of Critical Components and Equipment.

The safety features of the following subassemblies which comprise the loop handling machine are given in the following paragraphs:

(a) Main Body

(b) Bottom Door

(c) Loop Lateral Supports

(d) Loop Hoist Gear

(e) LHM Safety Instrumentation and Interlocks

(a) Main Body

Radiation shielding of the loop within the LHM is attained in accordance with limits set by AEC Manual Chapter 0524 using depleted uranium cylinders encased in the annulus between the inner and outer steel shells. The steel shells are sealed and the uranium is surrounded and periodically purged with an inert gas to prevent uranium deterioration. The top closure is gasketed to permit removal and access to inside of the LHM and to provide a gas tight closure.

Two lifting lugs, each located on opposite sides of the LHM, are welded to the outer shell at a position above the LHM center of gravity. The lifting lugs and linkages are designed for direct attachment to the 25-ton dual hooks on the 50-ton crane. As required by AEC Manual Chapter 0529, each lifting lug and linkage is designed with a safety factor of three imposed on the total LHM weight and the material yield strength. Either lifting lug and linkage is thus capable of supporting the loaded LHM weight of 47-tons with a dynamic load factor of two.

Tie down lugs are provided to secure the LHM to the transporter cradle during transport between various NRTS facilities. As required by AEC Manual Chapter 0529, the tie down lugs are designed for a 2 G vertical, a 10 G longitudinal, and a 5 G lateral acceleration of the LHM without generating stresses in any material of the LHM and cradle in excess of the material yield strength. The tie downs used for transport of the LHM are separate from the LHM lifting lugs and cannot be interchangeably used.

The LHM main body and all other LHM radiation shielding are designed to reduce personnel radiation exposures to comply with AEC Manual Chapter 0524 requirements. For an FEFP loop with fission power of 1.8 mW that has been irradiated in the ETR reactor for two cycles, the loop can be removed after the following decay periods: (a) 48 hours after reactor shutdown if no fuel has dispersed into the sodium, (b) four days after shutdown if 20% of the fuel has been dispersed into the sodium, and (c) ten days after shutdown if 100% of the fuel is uniformly dispersed into the sodium.

Computer studies[8,9] of the radiation dose rates that can be expected at the external surfaces of the LHM for the above condition have been made and the results are shown in Table 12.1.

(b) Bottom Door

At the lower end of the LHM a retractable shield door serves the dual purpose of providing radiation shielding as well as a lower LHM closure to prevent inadvertent dropping of the LHM contents when it is being transferred between the transporter, the FS&R, the ETR reactor top, and the HFEF unloading station. Since the door is non-sealing, provisions are made for a gasketed cover plate which will seal the door opening and prevent spread of contamination during LHM transfer operations.

The sliding door contains a 2-inch thick slab of depleted uranium for radiation shielding. The depleted uranium shielding is encased in steel plate. The sliding door is powered by an electric motor driven valve operator which contains torque cutout and limit switches for the open and closed positions. A manual over-ride (hand crank) is provided to permit door operation in the event of a failure in the power drive system.

(c) Loop Lateral Supports

Retractable loop supports are provided above the bottom door and again about one-third of the way up on the LHM. Each retractable support system consists of three supports spaced at 120° intervals around the periphery of the LHM. The top of the loop is supported by the grapple which interfaces with an insert located in the top of the LHM. These supports will stabilize the loop within the LHM in the vertical mode and support the loop when the LHM is lowered to the near-horizontal travel mode on the transporter.

The retractable loop support components are designed for 2 G vertical, a 10 G longitudinal and a 5 G lateral acceleration (consistent with AEC Manual Chapter 0529) of the supported loop in the near horizontal travel mode without generating stresses in any material of the LHM in excess of yield strength. Support pads on the end of each lateral support provide a bearing area to prevent damage to the loop secondary containment vessel for the above specified loading conditions. Each retractable loop support is powered by an electric motor driven valve operator which contains torque cut-out and limit switches for the extended and retracted position. A manual over-ride is provided to permit operation of the support screws in the event of a failure in the power drive system.

(d) Loop Hoisting Gear

The loop hoisting gear consists of the grapple located within the LHM, sprockets, and the chain drive mechanism located in a sealed enclosure affixed to the side of the LHM to control the spread of radioactive contamination. The LHM hoist is designed for 1200 duty cycles. One cycle is defined as extending the lifting chains to their full extension and then returning them to the fully retracted position. The entire hoist system was designed in conformance to RDT Standard F8-6T.

The hoist drive is provided with instrumentation for continuous monitoring of (a) the force applied to the grapple chains, with provision for stopping grapple motion if pre-established force limits are reached, and (b) the elevation of the grapple. The functional design requirements of the hoist drive are presented in Ref. 12.

The grapple is equipped with six lifting fingers which engage the underside of the in-pile loop top flange. The fingers are locked in place by over-center cams, which are driven by a single common gear shaft. An external tool must be applied to the grapple to operate the fingers. Access to the drive shaft can only be attained by extending the grapple out of the LHM. Each grapple finger is designed with a safety factor of 8 multiplied by a shock factor of 1.5, based on one-sixth of the loop weight. The above safety factor plus an inherent guide in the grapple design which prevents the loop from slipping aside and disengaging a single grapple finger will permit hoisting of the loop with one grapple finger should any five of the fingers fail.

The grapple is connected to the LHM hoist by two parallel hoist chains. Each hoist chain is a one-inch pitch triple strand roller chain with a minimum breaking strength of 37,500 lbs to give an overall safety factor of 7.5. A failure of one chain will not drop the loop as the remaining chain will support the loop with a safety factor of 3.7. This safety factor provides adequate margin for a dynamic load factor of two on the chain.

A load sensing cell is inserted in each hoist chain pathway to detect overload or underload of the hoist chains. A 10% deviation from the in-pile loop normal weight will interrupt the power to the hoist drive motor and lock the hoist brake. Each load cell is spring loaded to absorb shock and dynamic loading due to start and stop of the hoist drive systems. The load cells are adjustable to compensate for variation in the different in-pile test assembly weights.

The hoist drive system is equipped with an electric release, spring-set brake and a "no-back" mechanical brake. The electric brake is a spring-set disc brake which is solenoid-operated to release the brake during hoist-motor operation. Any loss of power to the hoist motor releases the solenoid and the brake is applied by the springs. The "no-back" mechanical brake is a mechanical device which will lock up and prevent shaft rotation should input torque to the "no-back" be interrupted.

This device also prevents external torques on the output shaft from over-riding or reversing the input shaft. The output shaft is free to move only with the rotational direction of the input shaft. This will prevent free spooling of the chain drive and thereby prevent uncontrolled or fast insertion of the loop into the reactor.

A slip clutch is located between the torque input (motor or manual) and the "no-back" coupling. This clutch will prevent excessive torque from being applied to the load carrying components.

The hoist system drive shafts are designed with a minimum safety factor of five. This coupled with allowances for keyways and torsional loading will result in a minimum safety factor of seven.

From the above, it is obvious that multiple failures would be required to overload and fail the LHM hoist system. Failures would have to occur in both load cells simultaneously with the slip clutch failure in order to load the hoist system components and reduce the factor of safety below 10. The probability of failure of the LHM hoist system would be extremely low.

Following assembly of the LHM, acceptance tests will be conducted to ensure proper operation of all components. A load test to ensure load carrying capability will be conducted at 125% of the rated capacity of the LHM hoist. Following acceptances of the LHM by ANC, periodic maintenance inspection and testing in accordance with ANC policies and procedures will be conducted (see Chapter 8). Proper training, qualification and administrative control of operators coupled with design, assembly, maintenance and testing of the LHM will ensure against failure and accidents involving the LHM.

(e) LHM Safety Instrumentation and Interlocks

The control system for operation of the Loop Handling Machine components provides limit switches and interlocks to prevent unsafe operation of the LHM components. The LHM electrical and instrumentation system consists of the following components;

- Power from the building source
- Power from the transporter mounted diesel generator.
- Power distribution panel.
- Portable LHM control console.
- LHM mounted items.
- Portable Loop Control Console with power and T.C. readout from the loop.

A discussion of each item is as follows:

Building Power Source

Normal power supply to the LHM and transporter when located inside the ETR building will be from the ETR commercial power source by plug-in to the nearest building outlet. Loss of the building power will stop operation of all LHM and transporter components. The component being operated at the time of the power loss will stop and lock in place. As previously stated, manual over-rides for the LHM door, loop clamps, and loop hoist mechanism are provided for use in emergency situations.

Transporter Mounted Power Source

A diesel generator set (45 KVA) is mounted on the rear of the transporter trailer to provide power for loop pump operation and display of loop temperature during over the road transfer of a sodium filled loop. Power to the pump is provided to make up heat losses and keep the sodium in a molten state. In the event of a loss of the building power, the trailer mounted diesel-generator could be used as the power source for completing the interrupted operation involving the LHM or transporter.

Power Distribution Panel

The LHM and transporter power distribution panel is a standard or commerical grade weather-proof enclosure containing breakers, transformers, relays, and wiring as required for operation of the LHM and transporter mounted equipment. All components are fabricated and installed to IEE standard requirements for equipment of this service (National Electric Code 1971, and NEMA Standard ICS-1970).

LHM Control Console

Two LHM control consoles are provided which can be located convenient to the LHM location at ETR and HFEF. All enclosures are weather-proof with wiring and electrical equipment being fabricated and installed in accordance with the applicable IEEE standards and safety codes (National Electric Code 1971, and NEMA Standard ICS-1970).

The control consoles include an instrument and control panel for control of each of the operating systems on the LHM. The consoles include control switches and position indicator lights for operation of the upper loop supports, lower loop supports, and LHM bottom door and the LHM hoist system. Since the four systems are interlocked, a key locked position switch for "normal" and "test" is in each circuit. When in the normal position, the system interlocks are in the circuit. When switched to "test", the interlocks are by-passed and that particular circuit can be independently tested for proper operation, however, the "test" position will not nullify the limit switches for a particular circuit system. The loop hoist circuit is controlled through a raise - lower selector switch, a start - stop button, and a speed control rheostat. The hoist speed control contains a "dead man" spring return feature which returns the rheostat to the zero speed position whenever the operator releases the rheostat control knob.

The hoist motor circuit is interlocked to permit hoist motor operations only when the following conditions are complied with:

1. Loop pump power off
2. Three upper loop supports out
3. Three lower loop supports out
4. Bottom door open
5. To lower the hoist, the grapple "Lo Limit" switch must be closed and each switch in the chain load sensors must be closed.
6. To raise the grapple, the grapple "Up Limit" switch must be closed and the switch in each chain load sensor must be closed.

Since the above interlock and limit switches are all wired in series, the incorrect position or malfunction of any one switch will prevent operation of the hoist motor.

The control circuits for the upper and lower loop supports are identical but separate. Control for each loop support is from the LHM control console. In addition to the "normal" and "test" mode switch, the controls include an "in" push button switch, "out" push button switch, and "stop" switch. Indicator lights to show the "in" or "out" position on each of the three lower loop supports and on each of the three upper loop supports are included.

The light activator switches are arranged so that both lights on each of the three lower and upper supports are on whenever the supports are not in either the full open or full closed position. The loop support indicator lights must show each of the supports either "in" or "out" before the operator proceeds to the next operation. The loop hoist grapple must be in the full up position to close the hoist upper limit switch before the loop supports can be operated. A torque limit device is provided in each support drive motor system to limit the load exerted on the in-pile loop by the supports. Each torque limit switch has a load limit switch to stop the support travel when the preset loading is reached. Limit switches and interlock switches are wired in series, therefore, the incorrect position or malfunction of any one switch will result in stoppage of the support drive motors. By having each of the three lower supports (or upper supports) equipped with a travel limit switch and a torque limit switch and by having all six limit switches on the lower support (or upper support) wired in series, a single limit switch will interrupt power to all three of the lower support (or upper support) drive motor systems. Consequently, even with failure of up to five of the limit switches, the drive motor system will still be controlled by the sixth limit switch.

The control circuit for the bottom door operator is similar to that for the support clamps. The control panel is equipped with a "normal" and "test" operating mode switch, and "open" "close" and "stop" switch and indicator lights for the open and closed position. The position indicator lights are arranged so that both lights are on whenever the door is not fully opened or closed. The loop hoist grapple must be in the full raised position to close the hoist upper limit switch before the door can be operated. A torque limit device is provided in the door drive motor system to limit the driving torque applied to the door. In addition, the door drive is equipped with limit switches to stop the drive motor when the door reaches its full open or full closed position. The limit switches and interlock switches are wired in series, therefore, the incorrect position or malfunction of one switch will result in a shutdown of the drive motor.

Other than the described position indicator lights, there is no system for automatic detection of limit switch failure in the current LHM control circuitry. However, a complete functional system checkout is required prior to each use of the LHM.

LHM Mounted Items

All electrical equipment mounted on the LHM are enclosed in weather-proof containers or enclosures and are designed and installed in accordance with applicable IEEE standards and safety codes.

LHM/ALIP Control Console

The portable loop control console provides a rheostat to control the power input to the in-pile loop sodium pump (up to 15 kW). Circulation losses plus heat losses from the pump are used to keep the sodium liquid and circulating during transport. The portable loop control console also provides for read-out of temperatures from 12 thermocouples located in the in-pile loop. Adjustment of pump power to increase or decrease the loop temperature is an operator manual adjustment made based on displayed temperature. All electrical equipment for the portable LHM/ALIP loop control console are mounted in a weather-proof enclosure and are designed and installed in accordance with IEEE Standards and Safety Codes - (National Electric Code 1971, and NEMA Standard ICS-1970).

12.2.3.3 LHM Transporter

The transporter trailer is designed and built to commercial DOT standards and practices and is equipped with the required number of axles, wheels and other safety features to permit operation over the NRTS roadways and those portions of the Idaho State Highways that are inside the boundaries of the NRTS.

The LHM transporter is designed for 600 duty cycles. One duty cycle is defined as insertion of the loop into the LHM, transport of the LHM to a discharge location, discharge the loop, and secure the system.

A support cradle is mounted on the trailer to permit transporting the LHM in a near horizontal position. The cradle includes saddles to support the LHM, locking devices to lock the LHM into the cradle, and hoisting mechanism to raise the LHM to a vertical position. The cradle and the LHM-to-cradle tie downs are designed for a 5 G lateral, 2 G vertical and 10 G longitudinal acceleration of the LHM as required in AEC Manual Chapter 0529.

A fluid power system on the transporter is used to operate the cradle up lock, the cradle down lock, the LHM-to-cradle attachment locks, and the cradle elevating and lowering system. The cradle elevating and lowering system includes dual hydraulic cylinders. In the event of a single failure of a cylinder or cylinder feed lines, the remaining cylinder will hold the load in position, and permit safe lowering of the cradle and LHM to the near horizontal position. Interlocks in the fluid power system will prevent unsafe operation of the system. The dual-cylinder arrangement coupled with proper training and administrative control of the system operators will preclude the possibility of dropping the LHM and cradle while being raised or lowered. The hydaulic system is designed, fabricated, and installed on the transporter in accordance with the National Fluid Power Association, Fluid Power Standards, January 1972.

12.2.3.4 Handling Tool Shield (HTS)

The handling tool shield (HTS) is used on top of the ETR reactor shielding to permit preparation of the loop for removal from the ETR reactor. The radiation emitted from the loop after operation is sufficiently high to preclude direct personnel contact during disassembly (see Section 12.2.1.4). The HTS will provide radiation shielding for personnel preparing the loop for removal. Administrative procedures which prescribe specific placement of personnel and timing of tasks will be employed in all operations. In addition, all tasks will be performed using remote-handling devices. The HTS is also used for removal of the removable top closure from the loop and provides shielding in the unlikely event the removable top closure should become contaminated.

Access ports are provided for insertion of handling tools into the dome flange region to remove support hardware which is attached to the loop during operation. An integral hoist will normally be used to remove the removable top closure from the loop and also the gland seal ring. The hoist complies with RDT F 8-6T requirements.

Leaded glass windows and additional light sources are incorporated in the HTS to provide visibility in the top dome flange during handling tool operations.

Three integral lifting lugs are provided for sling attachment to the 50-ton overhead crane. The lifting lug design and capacity comply with the design requirements of RDT F 8-6T.

12.2.3.5 In-vessel Supports

The in-vessel supports provide the only support for the loop within the ETR reactor vessel during release of the LHM grapple and prior to securing the loop to the top dome flange. The in-vessel support collar, which engages the loop, is attached to the ETR reactor vessel by three arms approximately 120 degrees apart. These arms are attached to the lower in-pile tube support brackets which straddle the inlet coolant flow divider in the reactor vessel. The redundant support arms permit complete failure of one of the support arms without failure of the two remaining arms. Thus, a single failure on the in-vessel supports will not result in a drop of the loop within the reactor vessel. The in-vessel supports are designed in accordance with Section III of the ASME Boiler and Pressure Vessel Code for Class I nuclear components. Fabrication and inspection in accordance with Section III, plus periodic inspection and testing during the lifetime of the supports will ensure safe operation of this hardware.

12.2.3.6 Accessories

The accessories which will be used during handling of the FEFP loop will include slings for hoisting of equipment which cannot be directly attached to overhead crane and special grapples or lifting tools used to hoist the individual containment vessels prior to assembly into the FS&R oven.

The special grapples or lifting fixtures are designed for a minimum safety factor of five. These fixtures that require the use of lifting pins to engage the containment vessels or the test train are provided with redundant pins such that the failure of any one pin will not release the component being lifted.

The slings that are used for lifting FEFPL components will have a minimum safety factor of eight. In addition, the RDT Standard F8-6T requirements for testing and maintenance of lifting slings will be adhered to.

12.2.4 FEFPL Handling Procedures and Training

All critical FEFPL operations will be performed using Detailed Operating Procedures (DOP). Where warranted, a check list will be provided for operator signature after completion of each step or series of steps in the procedures. Deviations from the DOP's by the operators are not permitted without the approval of appropriate ANC personnel as detailed in Chapter 8. The DOP's will be rigorously correct, complete in detail, verified using mock-ups where necessary, and reviewed such that they represent a high degree of operational safety and efficiency. Other FEFPL documents which provide information, system description, and operating instructions such as operating manuals and preventive maintenance procedures will be used to supplement the DOP's.

Each FEFPL handling operation will be reviewed and approved by ANC. Formal procedures will be written and approved by the Reactor Operations and the Nuclear and Operational Safety Divisions. These procedures will form the basis for the training program for the operating and maintenance personnel.

The operation and maintenance of the FEFPL in-pile loop and its subsystems and support facilities will be performed by trained operating and maintenance personnel as described in Chapter 8. The training will include classroom training supplemented by field training (as conditions permit) on that specific information required for a proper understanding of the theory, hardware, operating principles, and procedures for each system. The training periods are followed by formal, written examinations. An oral examination is then administered by the TRA Qualification Review Board to determine the general awareness of the candidate toward the operational position.

Reactor plant work will normally be performed by the teams of ANC personnel who have received prior job related training. When use of other ANC personnel is required due to work load, the Job Supervisor will assure that the individuals are briefed in detail and understand the requirements of the task prior to having them perform the task.

Individual FEFPL components that will be checked out at TRA by ANC personnel will be done in accordance with Construction Component (CC) tests which are written by the responsible engineer. The tests are reviewed by ANC before issuing to the field. A comprehensive crew briefing will be conducted by the Job Supervisor for all personnel who will participate in the CC tests before the test is initiated. This is done to make certain all personnel are familiar with the work task, to organize the job, and to review job safety. The extent of this briefing will be determined by the Job Supervisor, based on the training and experience level of his crew and on the difficulty of the task.

FEFPL systems or subsystems will be checked out in accordance with Systems Operational (SO) tests which are drafted by the responsible engineer. SO tests are reviewed and formally issued by ANC. All personnel participating in SO tests will have completed the qualification program as discussed in Chapter 8.

A demonstration or proof test will be performed in each area at ETR that involves the loop before the sodium-filled loop is handled. This will be done as part of the SO tests with the purpose of proving the handling operations before handling the sodium-filled loop. A dummy (shell) loop which simulates the weight and center of gravity of the FEFP loop will be used for this and will include the following areas of testing:

1. Alignment and mechanical fit-up tests of the ETR in-tank supports and modifications, including the in-tank support, core filler piece, top dome flange, instrument and helium line connections, and V-C shield block.

2. Demonstration check of all loop insertion and removal handling operations at the ETR reactor top.

3. Demonstration tests of the Loop Handling Machine for all insertion and removal procedures between the transporter and the ETR.

Subsequent to CC and SO testing, FEFPL handling operations are considered within the scope of normal and emergency operations. Operations of a critical nature, such as handling the loop or test train, handling of the LHM, sodium handling operations, or work that is hazardous or complex and not associated with routine operation of a system, will be performed using Detailed Operating Procedures (DOP). DOP's are supplemented by Operating Manuals for those operating instructions that are routine or repetitive in nature and by general work instructions for providing additional support information to the DOP's and manual. Examples of Operating Manual instructions include normal operation of the helium, data acquisition, or FS&R facility support systems. Critical work under the Preventive (or Planned) Maintenance (PM) program, such as some of the work associated with the LHM, sodium system equipment or Plant Protection System will be done using Standard Maintenance Procedures.

Modifications or emergency Maintenance work on FEFPL systems are performed under written instructions called a Maintenance Job Release (MJR). The work will be performed under a DOP if the modification is hazardous or complex or to a critical component or system. Examples of the latter include modification to the FEFPL Plant Protection System or to a secondary system element which controls a primary loop system parameter.

12.2.5 Handling Safety Analysis

An analysis of FEFPL handling operations within the ETR building was conducted to: (1) identify accidents that may have undesirable consequences, (2) identify failures that might lead to these accidents, (3) determine whether the accident could be caused by a single failure, (4) assess the likelihood of occurrence of single failures, and (5) evaluate the consequences of single failure accidents even though their likelihood may be remote.

Even for low probability failures, the consequences of the accident were analyzed. Multiple independent failures, however, were considered to be incredible and no further analysis was made.

12.2.5.1 Fault Tree Analysis

A fault tree analysis was used to provide a systematic and comprehensive evaluation of potential accidents. The fault tree resulting from this study is shown in Appendix A-2.

The fault tree was prepared for incidents that could occur in the ETR reactor building proper. It begins with an end-system fault condition; that is, an undesirable consequence that could occur if the system fails to perform as designed. The undesirable consequences have been defined to be: (1) damage to the Engineering Test Reactor or facility that is serious enough to cause a prolonged interruption of operation; (2) a general hazard to ETR plant personnel or the public.

The analysis provides a determination of all logical combinations of faults that can cause an accident, establishes their inter-relationship, and identifies basic faults. Basic faults are considered as either primary failure, secondary failure, design errors, or operator errors. Design error and operator error nomenclature is self-explanatory. A primary failure is a random failure of a component that occurs when it is operating within its design envelope. It is shown on the fault tree as a circle. A secondary failure is one that occurs when a component is subjected to environmental, mechanical or operational conditions outside its design rating. It is shown on the fault tree as a diamond. The study was not concerned with the total system reliability but rather was directed toward identification of single failures that can result in undesirable consequences.

Inspection of the fault tree shows that many single failures are prevented from causing an accident by use of dual or redundant systems and components. This is identified by "and" gates on the fault tree which indicate that simultaneous failure of two independent systems and/or components must occur in order to cause an accident. Single failures that enter "and" gates are therefore considered to stop at that point on the fault tree.

The remaining single failures can progress to an undesirable consequence since they are not inhibited by redundant systems or components; this is indicated by passage through "or" gates on the fault tree. These failures require additional evaluation to verify that an accident is prevented by sufficient safety margins or administrative controls. The identification of a failure as proceeding through an "or" gate does not necessarily imply that the failure causes an undesirable consequence. Since failures can occur at any time, it is possible for a failure to occur at a time when the affected equipment could withstand it without damage. However, the consequences of single failures discussed in Section 12.2.5.3, assumes they occur when greatest damage might result.

Evaluation of the fault tree for the loop handling system resulted in the identification of the single failures which result in undesirable consequences. Table 12.2 lists the single failures and their immediate consequences. Safeguards employed to prevent these failures and their consequences are presented subsequently.

12.2.5.2 Safety Assessment

Safety of FEFPL handling operations is assured through application of a defense in depth design philosophy. By this means, basic safety is provided through intrinsic features in the design; the quality, redundancy testability and fail-safe features of components; and through rigorous control of approved operating procedures. This approach can be expressed in terms of the three levels of safety in the same manner as that cited in Chapter 3.0, Safety Philosophy. Those general considerations are summarized here as follows:

The first level of safety provides accident prevention through conservative design according to applicable codes and standards, design reviews, redundancy, fabrication quality assurance and control, proof testing, operator training and qualification, preventive maintenance, and in-service inspection programs. This provides for unquestionable safety during normal operation and maximum tolerance for malfunctions.

TABLE 12.2

SINGLE FAILURES

Components	Single Failure	Immediate Consequences
Overhead Crane	Failure of crane drum drive gear while handling the LHM	Drop of item being hoisted
	Failure of crane drum drive shaft while handling LHM	
	Structural failure of crane while handling LHM	
	Failure of building structural support for crane while handling LHM	
	Failure of crane drum or sheave while handling LHM	
	Failure of crane cable when one hook used for handling tool cask or removable top closure	
Reactor Building Floor	Structural failure of truck aisle floor while supporting LHM transporter	Floor failure
Loop Handling Machine	Failure of one grapple chain while lowering loop into reactor vessel	Swinging of the loop
Operator Error	During insertion of loop into ETR reactor vessel	Loop Lowered onto in-vessel components
	During installation of auxiliary shielding	Radiation streaming

The second level of safety provides protection against incidents that are assumed to occur in spite of the care taken in design, fabrication and operation. Safety devices and detailed operating procedures provide assurance that protection is provided against secondary failure of components and operator errors.

The third level of safety supplements the first two through analysis of hypothetical failures and demonstrates that the design margin provides protection to the general public.

The fault tree analysis identified components or structures whose failure would not be arrested by a redundant structure or system. These are examined in terms of the three levels of safety in the following paragraphs.

Overhead Crane

First Level of Safety: Safe operation of the overhead crane is assured by complete conformance to the general first level considerations for design, fabrication and operation as delineated above. The crane is designed and built to the codes and standards listed in Section 12.2.3.1. This imposes a minimum safety factor of three, based on material ultimate strength for the structural support members. The primary load-bearing parts (drive gear, drive shaft, cable drum, or sheave) of the hoist are designed with a minimum safety factor of five, based on minimum ultimate strength and all cabling is designed with a minimum safety factor of six for lifting the fully loaded LHM. The training program for operators was previously described in Section 12.2.4.

Failure of a crane cable or hook, when a single hook is used to lift loop components (removable top closure, secondary containment shell, etc.) is extremely unlikely because the weight of such components is small relative to the crane capacity. This will result in a significant increase in the factor of safety (S.F. of 30 for the assembled loop) during these operations.

The overhead crane will also see limited service in support of FEFPL handling operations; this will reduce the in-service wear and damage below that normally associated with cranes in frequent use, and will also increase the fatigue life of primary load-bearing components.

Periodic proof testing and in-service inspection in accordance with RDT F8-6T will ensure that the original integrity of the overhead crane is maintained. Periodic preventive maintenance performed in accordance with approved ANC practices and policies will ensure continued proper operation of the overhead crane equipment.

Second Level of Safety: Protection against assumed incidents is assured by providing safety systems and rigorous adherence to approved detailed operating procedures for crane operation during all critical operations of FEFPL handling. Individual limit switches will prevent either the raising or lowering of crane hooks beyond their design travel, and raising or lowering speeds in excess of established limits, thereby ensuring that components (biological shielding, FS&R oven hatch, etc.) can adequately support the hoisted item (LHM) even if it should be impacted at the maximum lowering speed. The limit switches and procedures ensure that operation is within the normal design envelope for the crane and interfacing hardware.

Third Level of Safety: Failure of the overhead crane cable drive system, which includes the drive shaft, structural members, cable drum or sheave, is considered extremely unlikely based on operating experience with similar cranes at ETR and elsewhere. Nevertheless, the consequences are evaluated to demonstrate protection to the public. This is discussed in Section 12.2.5.3.

Reactor Building Floor

First Level of Safety: A structural analysis was made of the building elements which will be subjected to loading by the LHM and transporter. Following are the conclusions of this analysis:

1. The floor slab, floor beams and pipe tunnel will support the design loads with stresses below the American Concrete Institute (ACI) code values.

2. Stresses in the horizontal reinforcing steel in the outside face of the basement wall between the console and basement floors of MTR 647 will exceed code values as will the concrete shear stress. These stresses are still within the 35% increase allowed for transitory wind loads. Since the truck loading is of a transitory nature itself, it is felt over stressing of the steel is acceptable.

3. Stresses in the vertical steel in the outside face of the bottom nine feet of the foundation of the Air Exhaust Structure will exceed code values by approximately 5%.

4. Stresses in the horizontal reinforcing steel in the outside face of the basement wall of MTR 647 at column lines will exceed code values by approximately 10%.

All conditions give stresses in small localized areas only that are well below yield values. Thus, it is concluded that the structures can safely accommodate the imposed loading.

The analysis performed is considered sufficiently conservative that no load testing of the floor is required. An independent finite element analysis of the main floor and basement walls will be performed prior to entry of the transporter into the ETR reactor building to verify the previous analysis that has been performed.

Second Level of Safety: Safety is provided by strict adherence to approved procedures that is assured by use of appropriate administrative controls. Maximum travel speed, the use of a load distribution plate under the transporter landing gear, and positive identification of the travel lane are examples of specific items that will be included in the operating procedures. Administrative controls will be employed to prevent additional simultaneous loading of the truck aisle floor by other components.

Third Level of Safety: Safety of the public is provided even if floor failure should occur. This is demonstrated through an assessment of the consequences of this extremely unlikely event as presented in Section 12.2.5.3.

Loop Handling Machine

Levels of safety for the failure identified in Table 12.2 is presented below. The failure considered is of one grapple chain during insertion or removal of the loop from the reactor vessel.

First Level of Safety: Safety operation of the LHM is assured by complete conformance to the general first level considerations for design, fabrication and operation as delineated above. Each chain has a safety factor of 7.5, based on minimum breaking strength, during normal hoisting operations involving an assembled 5-ton loop. The LHM hoist drive system (drive shafts, etc.) has a safety factor of ten when hoisting the loop. This safety factor increases significantly when a 400 lb test train is being handled by the LHM. Periodic proof testing and in-service inspection in accordance with RDT F 8-6T ensures that the integrity of the grapple chains and the hoist drive system is maintained. Preventive maintenance performed periodically in accordance with ANC practices and policies ensures correct operation of all components and safety devices.

Second Level of Safety: Safety devices are employed to provide safe operation of the LHM hoist. Two load cells are provided to prevent overloading of the grapple chains and hoist drive system, thus ensuring that loads exceeding the design loads are not permitted to be hoisted by the LHM. Single limit switches are used to prevent unspooling of all the grapple chain and to prevent raising the grapple beyond its upper stop which would cause overloading of the grapple chains and hoist drive system. The load cells act on both high and low load and, as such, provide a diverse backup for the single upper and lower limit switches. Detailed operating procedures will be adhered to for all phases of LHM hoist operations to insure that the hoist system is operated in a safe manner within its design envelope.

Third Level of Safety: Safety of the public is assured even if the aforementioned failures should occur. These failures are considered extremely unlikely; nevertheless, their consequences have been evaluated to demonstrate ultimate public safety. This assessment is presented in Section 12.2.5.3.

Operators Errors

Potential operator errors as identified in Table 12.2 can result in improper alignment of in-vessel components, improper alignment of the loop prior to insertion, and misalignment of shielding or failure to install required shielding. Safety provided for these potential errors are given below:

First Level of Safety: Safety is assured through extensive operator and qualification programs at ANC. As stated in Section 12.2.4, operators are trained and tested so that they are completely knowledgeable of the correct procedures and aware of hazards that can occur if those procedures are not properly followed. Development of methods for verification of correct alignment of in-vessel components and the loop prior to insertion will provide added safety assurance. Similar controls will be developed for the installation of shielding.

Second Level of Safety: Safety is assured through use of the detailed operating procedures which must be followed without deviation and the incorporation of safety devices. For critical operations, supervisory checks and approval of operations will provide redundancy for decision and action processes. The LHM hoist system is equipped with load cells that stop and lock the hoist system whenever a 10% deviation of load occurs. Thus, misalignment of in-vessel components will register as a decreasing of load on the load cells and prevent loading of those components in excess of 10% of the load weight. Radiation monitors and health physics surveillance during loop handling will record any radiation streaming from the shielding. This will result in immediate notification to plant personnel that insufficient shielding or misalignment of shield has occurred and proper corrective action will be taken.

Third Level of Safety: Safety of the public is demonstrated by analyzing the consequences of hypothesized operator errors. Assessment of these events and consequences is presented in Section. 12.2.5.3.

12.2.5.3 The Third Level of Safety:

Single failure accidents that are not avoided by redundant systems or components have been identified in Section 12.2.5.1. The likelihood of occurrence of such accidents is very small due to the methods employed in developing the first two levels of safety as described in Section 12.2.5.2. Thus, accidents evaluated in this section are considered extremely unlikely based upon the following rationale.

Using past experience as a measure, ETR has had highly reliable heavy equipment handling systems, specifically the main reactor building overhead cranes. Over the years of its operation ETR has not experienced major malfunctions, handling mishaps, or accidents due to failure of crane components. Reliability is built into these systems prior to their being put into service. This is accomplished primarily through sound design and specification requirements. Supporting documentation on existing equipment is available in the ANC maintenance files or in the AEC documents storage. These include inspection and certification documents which insure that the crane and it components (hooks, hoists, structural members, and controls) did meet or exceed the requirements of the original design specifications as purchased and installed. Beyond the original design, installation, operational checkouts, and certification that the equipment was properly installed and operational, assurance of continued reliability is the responsibility of Aerojet Nuclear Company. This is done by means of a preventive maintenance program which requires that at periodic intervals the equipment undergo tests on controls, drive/brake systems, load tests, visual inspection of all equipment for signs of wear or damage, and non-destructive tests on load-bearing parts to establish their integrity.

The ETR administrative and procedural safeguards that will be used to guard against operator error are described in Chapter 8. For FEFPL, critical handling operations will be performed according to detailed operating procedures (DOP's).

The specification of equipment to provide large design margins based on approved codes and standards, the redundancy of structural components, controls and interlocks to preclude erroneous sequencing, quality assurance and control in manufacture, installation and maintenance, and strict adherence to procedures will be used to ensure safe handling of FEFPL components and equipment. These measures have been implemented in the first two levels of safety to make the handling operations as safe as possible.

In spite of all these precautions, a third level of safety is developed based upon analysis of assumed severe extremely unlikely accidents to demonstrate that even their consequences do not jeopardize public safety.

Overhead Crane

The crane accidents identified in Table 12.2 not withstanding, the failure of the 50-ton crane, is considered extremely unlikely based on the following factors:

- New crane designed, fabricated, installed and performance tested in accordance with Standard and Specification identified in Section 12.2.3.1.
- Comprehensive preventive maintenance, inservice inspection, and load testing in accordance with RDT F 8-6T.
- All critical lifts performed in accordance with approved detailed operating procedures based on requirements of RDT F 8-6T.
- Documented comprehensive training and qualification required for all personnel involved in operation of the 50-ton crane.
- Low frequency of handling operation involving the LHM, i.e., (loop insertion or removal operations conducted once every three to four months).
- Further reduction in probability of occurrence due to the short duration of critical lifts, i.e., (several minutes) within the previously identified low frequency of three to four months for these handling operations.

Thus, the preceding factors are considered to demonstrate the margin of safety in protection of the public for these extremly unlikely bounding accidents associated with handling of the LHM.

The possible locations for such accidents are divided into two areas; the first is over the reactor top and the second is any other potentially affected location. Locations west of the reactor top, such as the ETR canal, are excluded since administrative controls will prohibit operation of the overhead crane with LHM in this area.

The LHM can be hoisted by the overhead crane above the reactor top in either of two conditions: 1) With the loop in the LHM prior to loop insertion or following loop removal; and 2) with the loop in the reactor vessel prior to loop removal or following loop insertion. Analysis of free falls of the LHM for these two conditions is presented below.

Drop of LHM and Loop Over the Reactor Top[43]

An LHM lift of one foot over the reactor biological shielding is required during loop removal. This lift height is required only during loop removal to clear the sliding shield plate and will be limited to a short duration once every three to four months. This height and maximum weight of 47 tons for the LHM would result in 94,000 ft-lbs of energy at time of impact should a free fall occur. The first component impacted would be the biological shielding. The shielding will absorb 9450 ft-lbs of energy prior to its collapse. The shielding and LHM would next contact the top flange on the ETR reactor vessel. The top flange of the reactor vessel will be crushed or sheared as it is the prime point of contact for the LHM. However, the dome shape of the reactor vessel top is ideally suited for absorbing the remainder of the energy of the falling LHM, and is expected to platically deform approximately 6 inches. It has sufficient strength to prevent entry of the LHM into the reactor vessel.

The top end of the LHM extends through an opening in the overhead crane trolley. This will maintain the LHM in a vertical position during and following failure of the biological shielding and collapse of the top dome.

The bottom door on the LHM will always be closed during hoisting operations of the LHM with loop. Although it will be crushed on impact, it will prevent escape of the loop from the LHM.

The LHM hoist system employs dual, triple-strand chains that will absorb 2700 ft-lbs energy prior to their failure. Failure of these support chains is expected to occur since the energy of a 5-ton loop for a 1-foot free fall is 10,000 ft-lbs. Therefore, a secondary free fall of the loop within the LHM is also expected. The loop will impact the bottom door of LHM and plastically deform the secondary vessel approximately 1.5 inches leaving a clearance of 1.25 inches between the primary and secondary vessels.

Although a free-fall drop of the LHM through a distance of one foot will result in damage to the shielding, the reactor vessel and loop secondary vessel, no failure of loop primary vessel or damage to ETR fuel will occur. Thus, this accident would not result in any release of fission products and, therefore, no hazard to the general public.

LHM Drop Over Reactor Top with Loop In-vessel[43]

The second drop accident analyzed for the LHM is with the FEFP Loop located in the reactor vessel. Although the LHM weight is approximately 10% less when it does not carry the loop, much of the same damage described previously is expected to occur to the biological shielding and reactor vessel. As stated previously, the lift of the LHM to a height of one foot over the reactor will be required only during loop removal involving the sliding shield plate and will be of short duration once every three to four months.

The removable top closure (RTC) and gland seal ring are removed prior to the use of the LHM over the reactor top. In this configuration, the top of the loop is recessed approximately 24 in. below the top of the top dome flange. Thus, it would require an additional 18-in. vertical collapse of the top dome flange and reactor top dome, beyond that shown to occur from a loaded LHM drop over the reactor, in order to apply a vertical load to the loop. Thus, it is shown that vertical loading of the loop will not occur.

Modeling of this accident for an off-center drop is difficult due to the uncertainties associated with the configuration following initial impact with the biological shielding. Analysis was performed to establish the horizontal translation required to fail the primary vessel at the weakest location (pump to test train transition).

This analysis indicates that lateral movement of the reactor top dome flange base and the top of the loop by 1.46 in. is required for an equivalent lateral deflection of 0.7 in. at the pump to test train transition which is required to exceed the ultimate strength of the primary vessel. Based on the assumption that the loop supports and grid plate remain rigid, a lateral deflection of 0.7 in. at the weak point is improbable. Thus, the loop integrity is maintained and there is no resultant damage to ETR fuel.

Based on the low probability of such an accident and the improbability of displacement of the vessel resulting in failure, the consequences associated with such an accident are considered acceptable in terms of damage to the reactor and protection of the general public.

The supporting analysis for the preceding two LHM accidents is based on hand calculations.[43] A task is in progress to establish the scope of computer modeling to provide more precise structural failure margins for these accidents.

LHM Drop With or Without Loop Onto ETR Floor

The final postulated LHM drop accident that is analyzed involves an assumed failure of the crane when the LHM is being moved over the ETR floor. Administrative controls will be employed to limit maximum heights and prevent movement into restricted areas. Under this procedure, the LHM will be lowered over the south wall of the pipe tunnel under the main floor which is the strongest floor area and will preclude penetration of the main floor by the LHM should a free-fall drop occur. Therefore, the consequences without a loop in the LHM would be limited to its damage, plus some floor damage but would in no way present a hazard to the general public.

The critical phase of LHM movement will be limited to a few minutes duration as it is moved from over the top of the reactor and is then lowered to a minimum distance above the floor. At a point in this operation, the LHM will be raised to a maximum height of 10 feet above the floor and contain a maximum energy of 940,000 ft-lbs. The bottom door of the LHM will always be closed whenever the LHM is moved with the loop. This provides double barriers (grapple chains and bottom door) against escape of the loop from the LHM.

The maximum expected consequences of a free-fall drop from a height of 10 feet are evaluated, assuming no added safety systems. The LHM will impact the floor on the closed bottom door and the grapple chains will fail, thereby allowing a secondary free fall of the loop within the LHM. After impact with the floor, the LHM would be expected to fall laterally onto its side, since for this drop distance the LHM falls farther than its extension length through the hole in the crane trolley.

It is considered unlikely, that even if such an event did occur, that it would rupture both the primary and secondary loop containment. However, since prevention of FEFP Loop containment rupture has not been demonstrated analytically, it is assumed rupture of both vessels occurs and that the loop sodium inventory flows out of the LHM, onto the ETR concrete floor, carrying with it entrained particles of fuel and fission product activity.

Program objectives may dictate that the loop sodium be frozen to maintain the post-test experiment configuration, however for this analysis, the sodium is assumed molten and maintained at less than 500^{o}F. Sodium at this temperature is expected to freeze when it comes into contact with the large heat sink presented by the relatively cold LHM and/or concrete floor. However, since the floor is concrete, the possibility of a sodium reaction with the water of hydration in the concrete exists. Therefore, it is assumed that the sodium spreads over a 40 sq ft area and burns with no attempt being made to extinguish the fire. Experiments conducted for FFTF indicate that for sodium at a temperature of 1080°F, the reaction with the water of hydration in concrete is not violent.[24] The sodium is now assumed to burn as a sodium pool at temperatures from 1000° to 1400°F with appropriate air circulation to maximize the release rate of airborne materials from the fire.

Plutonium release into the sodium during the Design Basis Experiment (DBE) may occur by two postulated mechanisms. The first is by fragmentation which occurs as the molten fuel is quenched by the sodium coolant. The second is from the formation of a low density reaction product which occurs from the reaction between sodium and oxide fuels in the presence of dissolved oxygen[25].

Following the test, the loop will remain sealed for several days in the reactor with the sodium in intimate contact with the refrozen fuel. For fission product release assumptions, it is assumed that 100% of the noble gases, 25% of the solids, and 100% of the halogens are released from the fuel to the sodium.

For release from the sodium fire, it is assumed that 100% of the noble gases are released. All of the halogens are expected to be reacted with the sodium to form sodium iodide, NaI. Experiments show that less than 50% of the NaI is released during a fire with optimum ventilation. All other radioactive material, including the finely divided plutonium, is assumed to release from the sodium pool in the same fraction as the sodium iteslf, namely that 40% becomes airborne[26].

The previous discussion gave a general model of the loop handling accident. In this section, the technical basis for each of the major factors are developed.

From a radiological standpoint, the maximum experiment postulated for the FEFP Loop is pre-irradiated 37-pin test which is limited to less than 7.2 kg of UO_2-PuO_2. (Actually less than 2.5 Kg because pre-irradiated pins are 13.5-in. long.)

The most applicable data on the behavior of the fuel and sodium coolant during the meltdown phase were obtained from the multi-rod TREAT S and L series experiments conducted with oxide fuels. These tests approach conditions expected in the FEFP Loop. The S series are expected to be somewhat more severe from a fuel coolant interaction standpoint than would occur in the FEFP Loop, since the creation of molten fuel prior to sodium voiding as obtained with TREAT-ramp experiments is a condition not possible with FEFP Loop loss-of-flow tests in the ETR. The S series experiment data, therefore, would be expected to show a higher degree of mixing between the molten fuel and sodium.

Upper limit measurements available from test L-2[27] indicate that less than 0.5% of the fuel disperses into the sodium coolant as tiny particles (less than 1000 μ in diameter). The remaining portions, 99.5% resolidifies into massive agglomerates of fuel and cladding and is not available for mixing with sodium. Since sodium fires burn with temperatures on the order of 1400°F which are significantly below the 4126°F melting point of PuO_2, no further effect on the particles is expected from the involvement of the sodium and particles in a fire.

The S series experiments show that the fraction of fuel dispersed in the sodium is distributed in a range of particle sizes illustrated in Figure C.3, Appendix C. Even for the most severe case, S-5 (which was less typical than other tests because S-5 was run with evacuated rods), more than 80% of the mass of dispersed fuel was contained in particles of greater than 40 microns in diameter.

Since the fuel material enters the sodium as UO_2 and PuO_2 and is quenched to the sodium temperature in the FEFP Loop prior to removal from the reactor in much the same way as did the fuel in the S test series, it would be expected to behave in a similar manner. Thus, the fuel particles released with the sodium to the ETR floor could conservatively be estimated to be 1% of the total contained in the experiment, or approximately 72 grams. This fuel would be distributed in particle sizes such that 80% of the mass was contained in particles of 40 microns diameter or larger. This leaves 20% or a total of 14.4 grams of the fuel material in particles of small sizes. Since the fuel is a mixture of 22% PuO_2 and 78% UO_2, these 14.4 grams of fuel would contain 3.2 grams of PuO_2 which, after accounting for the oxygen fraction, leaves a total of 2.8 grams of plutonium.

An additional source of finely divided plutonium is from the formation of a low density reaction product with a generic formula of Na_3MO_4 between sodium and oxide fuels, where M is either Pu or U. The extent of reaction of the formation of this product is dependent upon the amount of dissolved oxygen in the sodium.[28]

Nominally, the FEFP Loop will have an oxygen content of 2 ppm for a total of ∿0.25 grams of oxygen in the 24 gallons of sodium in the loop. Oxygen is also released from the burnup of the fuel. Most of the oxygen (probably greater than 99%) released during burnup is combined with fission products in the fuel and is not available for further reaction. However, an exact thermodynamic model of the oxygen behavior during the accident situation is difficult to construct. Therefore, a conservative value of

1% of the total oxygen released from the burnup (1 MW for one year) is assumed to be released in the sodium at the time of the experiment meltdown. This adds an additional 0.43 grams of oxygen for a total of 0.68 grams.

Essentially, 10 grams of reactor product, Na_3MO_4, forms for every gram of dissolved oxygen. This leads to a total of 6.8 grams of reaction product.[28]

The plutonium fraction in the fuel is 0.22; thus, only 1.5 grams of the reaction product involves plutonium. The weight fraction of plutonium in the reaction product is 0.78, which yields a value of 1.1 grams of plutonium from the reaction product available for airborne release.

Thus, from the two sources, a total of 3.9 grams of finely divided plutonium (<40 microns) is available for airborne release.

Sodium burns relatively slow giving off dense vapors of sodium oxide particles, which rapidly agglomerate and settle out in the vicinity of the fire. The larger agglomerated particles fall back onto the surface of the burning sodium to form a thick crust over the surface. Because of the agglomeration and subsequent deposition, much of the material (60%) released from the burning sodium is trapped and removed from transport pathways. Nominally, finely divided material dispersed in the sodium would be expected to fractionate in the same manner as the sodium itself, with only about 40% becoming airborne.[26]

The sodium is assumed to burn at a rate of 0.4 $lbs/hr\text{-}ft^2\text{-}\%O_2$ (8.4 $lbs/hr\text{-}ft^2$ for air containing 21% oxygen) at a temperature ranging from 1000^oF to 1400^oF.[26] This is consistent with optimum ventilation rate of 150 cfm per square foot of sodium surface. This ventilation rate, while somewhat higher than would be expected for the ETR building geometry, maximizes the release of airborne materials from materials from the fire.

Particles not classed as finely divided would be expected to remain intact and stay with the liquid sodium and residue as the fire proceeds. Since sodium burns slowly and without violent updrafts, bouyant forces for lifting particles into an airborne trajectory would be small. It is anticipated that few particles larger than 10 microns would be transported from the fire surface. For conservatism, it is assumed that the mass of fuel contained in particles less than 40 microns are lifted by updrafts from the fire into the building atmosphere. Particles larger than 40 microns would fall out within 3 miles of the ETR stack even if released at the top of the 250 ft stack in a 30 mph wind, and as such, would not pose an off-site exposure potential.

For conservatism, it is assumed that 100% of the halogens and noble gases are released from the fuel to the sodium. In most accident analyses, the fraction of iodine release from the fuel is taken to be only 50% but with the extensive melting and possible vaporization in the DBE, a conservative release of 100% is postulated. One hundred percent of the iodines are assumed to react with the sodium to form sodium iodide, NaI.

The NaI release fraction varies according to burn temperature and ventilation flow rate across the burning sodium pool. For example, the NaI release fraction for a 3 sq ft sodium pool burning at 1000°F and with a 20 cfm flow rate over it is 0.25. With a burn temperature of 1200° to 1300°F and a flow rate of 90 cfm, the NaI release fraction varies from 0.15 to 0.2. For the same burn temperature, 150 cfm increases the NaI to 0.5 - the one chosen for analysis purposes.[26]

The noble gases are assumed to be released from the loop and the sodium as the fire progresses. Due to the several day decay following the DBE, these radioactive gases contribute little to the calculated radiation exposure.

Solid fission product material has been assumed to be released from the fuel to the sodium in the amount of 25%. This again is very conservative in that a release of 1% is usually used under accident conditions. The 25% is selected to be conservative in the absence of analyzed experiments which more clearly approximate the DBE. The solid fission products contained in the burning sodium are also assumed to follow the partitioning of sodium itself with 40% being released as airborne.

To calculate off-site exposures, the sodium fire is calculated to last 34 minutes with the fission products and plutonium being dispersed into the ETR building. Following the fire, another 30 minutes is allowed for the fission products to leak from the ETR building making the release time over a period of approximately one hour.

Based on a release time in excess of 30 minutes, the Markee diffusion parameters developed for the NRTS are used in the Pasquill diffusion calculations to account for off-site concentrations. The transport plume is assumed to travel in a straight line with a velocity of 2 mps. No ground deposition from the plume was considered in these calculations. Further assumptions used for the dose calculations are as follows:

A. The dose receptor remains in the plume centerline breathing at an exceptionally high breathing rate of 3.47×10^{-4} cubic meters/sec for the total passage of the plume.

B. The plutonium lung dose was calculated using the model of the ICRP Task Group on Lung Dynamics as documented in Ref. 29 and as illustrated in Ref. 30. The lung dose was calculated for a ten-year old with a dose commitment to age 70 and the appropriate dose conversion constant for each plutonium isotope. All the released plutonium has been assumed to be of 0.5 μM diameter such that 25% of the inhaled quantity is retained in the pulmonary compartment of the lung.

C. Plutonium is distributed isotopically in the fuel as shown below:

Isotope	Grams in 37-Pin Test	Curie Quantity
Pu-238	8.05	135.500
Pu-239	1421.00	87.900
Pu-240	178.80	40.100
Pu-241	3.70	425.400
Pu-242	1.70	0.007
AM-241	∿2.00	6.510

Radiological doses have been calculated for an individual at the nearest site boundary (NSB) which is 1.0×10^4 meters distant from ETR and for an individual at Arco which is 2.4×10^4 meters distant from ETR and are tabulated in Table 12.3.

The foregoing demonstrates that the essential objective of the third level of safety is achieved, viz., that protection of public health and safety is assured even if this extremely unlikely accident should occur. Nevertheless, continued study will be made and results of the study implemented to further mitigate the consequences, with a major goal of preventing failure of FEFPL containment. Examples of added safety features in this respect, whose feasibility and effectiveness are currently under study, are in the use of impact cushioning materials or devices and the development of positive means for maintaining the LHM erect at all times when it is the normal orientation.

Failure During Use of Single Hook

The remaining identified single failure that involves the overhead crane is that of a single cable when only one hook of the crane is employed. Because the weight of components lifted by one crane hook is small, the resultant damage potential will also be small in comparison to that associated with LHM drops. Although some damage may be inflicted on the dropped item and the impacted item, no release of fission products or other hazardous materials would result should such an accident occur.

Reactor Building Floor

The LHM transporter will be backed into the ETR reactor building for LHM transfer. Floor failure under the supporting wheels of the transporter

TABLE 12.3

Scoped Radiological Doses for an Individual in Arco[34] and the Nearest Site Boundary (NSB)

	Guide Value[31] (rem)	ETR DBA* Arco (rem)	FEFPL** Arco (rem)	FEFPL** NSB (rem)
Thyroid Inhalation[31]	300	223.4	25.6	60.8
Strontium Bone[32] (soluble strontium)	150	1.6	6.0	14.3
Strontium Lung[32] (insolube strontium)	100	0.4	0.4	0.95
Cloud, gamma[31]	25	0.0294	0.01	0.024
Plutonium Lung***[32]	100	None	0.54	1.15

*For the ETR DBA, 15% of the core (∿140 fuel plates) was assumed melted. Of this value, 100% of the noble fission gases, 25% of the halogens, and 1% of the solids were assumed to be released from the reactor building to the environment in a one hour period.

**Calculated with the RSAC Computer Code[33] for a 100% melt of a 37-pin test bundle that has been operated at a power level of 1 MW for a period of one year, decayed for a period of six months and then operated in the ETR for five days at a power level of 1.5 MW. The test bundle comprises ∿7.2 kg of fuel, of which ∿1.6 kg is Pu. (It is assumed that all airborne fission products are released from the building.)

***Plutonium is in insoluble form of PuO_2.

has been identified as a potential single failure accident. This would cause the transporter to settle until its weight is distributed over its undercarriage. Cross-beams located under the floor will prevent complete floor failure or collapse and the distance between the cross-beams is such as to prevent the transporter from dropping through the floor.

Although the building floor and undercarriage of the transporter would be damaged during this accident, tilting of the transporter sufficient to cause the LHM to fall would not occur. Thus, no significant damage would occur to the LHM or an included loop.

Loop Handling Machine

The single failure accident identified for the loop handling machine is failure of one LHM grapple chain while lowering or raising a loop from the reactor vesssel.

The consequences of failure of one LHM grapple chain would not result in a free-fall drop of the loop since the remaining chain would provide adequate support. Slight swinging of the loop would occur as it moves to locate its center of gravity under the remaining chain. The in-vessel supports and clearance between the grapple and the LHM would limit swinging motions. Thus, only minor damage would occur, such as scraping between the loop and in-vessel supports as the loop is lowered into the reactor vessel so that the failed chain can be repaired. Failure of loop containment would not occur, and hence no hazardous materials would be released.

Operator Errors

Two operational errors have been identified as potential initiators of single failure accidents. Although other operational errors are possible, they are prevented from causing an accident by limit switches, safety devices, and other redundant structures. Therefore, the following discusses the consequences of operational errors that are not protected by redundant systems, other than the administrative or procedural control.

The first such error can occur during insertion of the loop into the reactor vessel. This error is misalignment of the in-vessel components or the LHM, that could cause lowering the loop onto an in-vessel component. The load limit switches, which are set to detect both high and low load limits, would interrupt the lowering operation and prevent the total loop weight from being imposed on in-vessel components. This would limit the damage to minor levels, such that failure of the ETR fuel elements or failure of FEFPL containment would not occur. Thus, this error would not develop into any hazardous condition.

The second operational error studied is misalignment of or inadequate shielding around the bottom of the LHM during loop removal from the reactor vessel. The consequence would be excessive radiation streaming from the inadequately shielded loop. Health Physics surveillance and radiation monitors would immediately make this condition known to plant personnel and approved protective emergency actions instituted, the development of which is described in Chapter 8, and summarized in Section 12.2.4, above. The associated hazard would be limited to the ETR facility.

12.3 FS&R Sodium Fire Hazards Analysis

12.3.1 General

The objective of this section is to present the results of an analysis of the hazards associated with sodium in the FS&R Facility. Discussions related to handling of an FEFP Loop charged with sodium and industrial safety for the loop assembly are presented in Sections 12.2 and 12.4, respectively.

The Test Cell and the Charging Facility areas of the FS&R System were assessed. These facilities are located in the southeast end of the ETR building. A summary of the system functional requirements and description is presented in Chapter 5.2.3.2. Further detail for design requirements and design configuration are presented in References 13 and 14.

The FS&R sodium fire hazards analysis for the two facilities will be presenced in the following order:

1. Design Basis Accident (DBA) Selection,
2. DBA Analysis Conditions,
3. The Analysis Method,
4. Results and Consequences of the DBA Analysis for Each Facility.

Similar discussion for the hypothetical FS&R sodium fire cases is presented in Chapter 13.3.

12.3.2 Design Basis Accident Selection

A study[15] performed to select the DBA for the FS&R System determined that the maximum credible accident is a failure of the facility sodium loop which spills its contents and results in a sodium fire. A double-ended pipe rupture spill was the largest credible spill and, hence, was selected as the DBA for both the Charging Facility and the Test Cell. The analysis of this limiting accident takes no credit for operator action to initiate discharge of the facility sodium inventory to the dump tank, which, based on the location of the break and immediate action could substantially reduce the size of the spill. Other credible accidents considered (e.g., valve bellows failure, instrumentation penetration failures) caused less spill than postulated for the pipe rupture. The sodium spill may be either radioactive (a contamination on pre-irradiated test train) or non-radioactive.

The selection evaluation showed that a potentially larger spill than for the pipe rupture could occur due to failure of the tanks; however, it was concluded that this event was incredible. This determination was based on the criteria that the tank was designed to Section III (Class 2) requirements, fabricated under code stamp, routine vendor facility conditions, and operated at low stress conditions.[15] Other sodium loop programs have made the same selection, and, therefore, a guiding precedent has been established. Some of these are SNAP-8 and the CCTL facility at ANL.[15]

12.3.3 DBA Analysis Conditions

The DBA sodium spill quantities due to the postulated pipe rupture were determined to be 108 lbs. and 90 lbs for the Charging Facility and the Test Cell Enclosure, respectively.[16] The first case quantity represents an upper bound that may be present in the facility loop including the expansion tank under facility operating conditions. The second case quantity considers that 68 lbs of the sodium from the Charging Facility is transferred to the Test Cell and combined with an additional 22 lbs of sodium present in the Test Cell piping.

For both DBA spills, the accident is assumed to occur as a sodium pool fire.[16] Spray fires were determined to be incredible due to the low FS&R system operating pressure (40 psig) and lack of an adequate nozzle configuration arising from the possible failure.[17] Nevertheless, analyses show that a postulated spray fire to be of less consequence than the DBA.

The DBA sodium pool burn areas were determined to be 80 sq. ft and 40 sq. ft for the Charging Facility and Test Cell Enclosure, respectively.[16] The first case was based on the area within four egg crate sections (10 sq. ft total), which can contain the spill quantity, multiplied by a factor of 8 to account for uncertainty in the manner of sodium release from the pipe. For the second case the same egg crate area was multiplied by a factor of only 4, since 40 sq. ft is the maximum size of the burn pan. For any spill that reaches the lower portion of the Test Cell, the sodium will run into a self-extinguishing (area limiting) catch pan.

Ventilation air flow is normally provided to each of the facilities by the FS&R Ventilation System, (see schematic in Fig. 12.5) The air blower for this system has two operating fan speeds; high and low. Table 12.4 shows a range of vent rates available to each facility based on fan speed and cell inlet louvre and vent positions. Normal and emergency ventilation rates for DBA and non-DBA conditions are summarized below:[16]

Facility	Normal (low fan speed)	Emergency (high f.s.)	Isolation
Charging Facility	1,500 cfm	10,380 cfm	100 cfm
Test Cell	5,500 cfm	13,840 cfm	100 cfm

The emergency condition is intended for use to clear smoke upon detection of a fire if such action is desired. However, there may be situations in which the fire fighting personnel feel that a lower vent rate is preferable to control the burn rate. Hence, three vent rates have been considered for the DBA analysis. In the event that the cell is to be isolated, the inlet louvres will be shut with the fan at low speed and the in-leakage is 100 cfm to each facility. This vent condition has been included in the DBA analysis.

12.3.4 Sodium Fire Analysis Method

The pressures and temperatures generated during a sodium pool fire were computed by using the SOFIRE II code developed at Atomics International (AI). A brief summary of the method is presented herein; for a more detailed presentation, see Appendix B.

The fires in the Charging Facility were evaluated with the existing one cell version. A special version of the one cell model was written for the fires in the Test Cell since the burn pan is suspended in the air of the cell and heat can be transferred to the cell gas from the sodium surface and the bottom of the burn pan. All cases were computed assuming the conversion of sodium to sodium monoxide since this reaction generates the most heat per unit weight of oxygen consumed and therefore produces the maximum pressures and temperatures.

The aerosol release calculations were performed for the maximum sodium spill case in each facility. An aerosol agglomeration code, HAA-3, developed by AI, was used for these calculations.

12.3.5 Sodium Fire Analysis

12.3.5.1 Charging Facility

The results from the SOFIRE II analysis for the DBA cases are shown in Table 12.5 (cases 9, 9N, and 10). To represent the most severe temperature conditions, Fig. 12.6 presents the transient pressure and temperature curves for cases 9N (1500 cfm ventilation rate). Data from cases 3 through 6 have also been presented in Table 12.5 to show the sensitivity of a lesser spill quantity (68 lbs) and a lesser pool burn area (10 sq. ft).

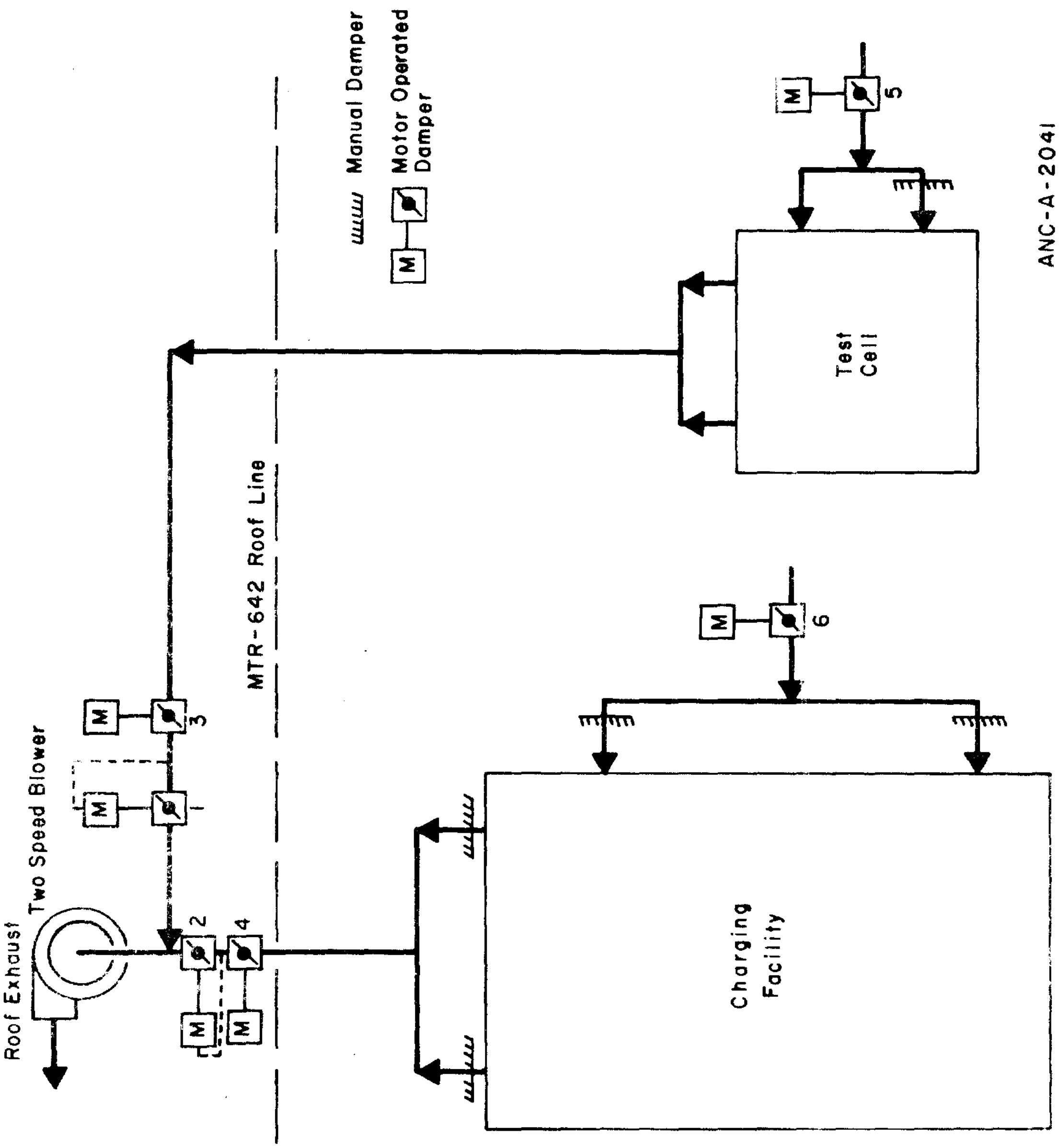

FIG. 12.5 - Ventilation Schematic

TABLE 12.4

FS&R VENTILATION AIR FLOW RATES
FOR VARIOUS SYSTEM OPERATING CONDITIONS (Note 1)

A. Charging Facility

CF Air Flow Rate and ΔP Across Cell Wall	Fan Speed	Louver Position
0 cfm @ 0" H_2O	Low	CF louvers closed
1,500 cfm @ 0.15" H_2O	Low	All louvers open in both cells
3,000 cfm @ 0.25" H_2O	High	All louvers open in both cells
6,800 cfm @ 2.6 " H_2O	Low	TC vents shut, CF vents open
10,350 cfm @ 3.6 " H_2O	High	TC vents shut, CF vents open

B. Test Cell

TC Air Flow Rate and ΔP Across Cell Wall	Fan Speed	Louver Position
0 cfm @ 0" H_2O	Low	TC louvers closed
5,500 cfm @ 0.4" H_2O	Low	All lovers open in both cells
7,100 cfm @ 0.6" H_2O	Low	CF vents shut, TC vents open
11,000 cfm @ 1.6" H_2O	High	All louvers open in both cells
13,840 cfm @ 2.27" H_2O	High	CF vents shut, TC vents open

Notes: 1) Reference 18.

In comparing results for the different cases, several trends were observed:[16]

1. For the same spill and burn area, increasing the ventilation rate decreases the maximum temperatures and pressures experienced. However, the ventilation shutdown case does provide lower temperatures than obtained for the normal ventilation flow rate. This suggests that for a given spill, there is a ventilation rate that causes the burn rate/heat removal capability ratio to maximize resulting cell temperature.

2. Burn area has a great effect on the length of burn time and on the maximum temperatures and pressures experienced.

3. Use of emergency ventilation compared to normal ventilation depresses the rate of temperature rise.

12.3.5.2 Test Cell

The results from the SOFIRE II analysis for the DBA cases are shown in Table 12.6 (cases 1, 1N, and 2). To represent the most severe temperature conditions, Fig. 12.7 presents the transient pressure and temperature curves for case 2 (100 cfm ventilation rate). Data from cases 3 and 4 have also been presented in Table 12.6 to show the sensitivity of a lesser burn area (10 sq. ft).

12.3.5.3 Aerosol Release to the Atmosphere

The atmospheric release of sodium oxide was calculated for the DBA of each facility. The results for emergency ventilation conditions are shown below:[19]

	Sodium Spill	Sodium Oxide Released
a. Charging Facility	108 lbs	73 lbs
b. Test Cell	90 lbs	60 lbs

For these calculations it was assumed that 50% of the burned sodium was released from the fire as sodium monoxide.

In the analysis it was determined that aerosol loss by settling and wall plating would be negligible in the Charging Facility. This conclusion was attributed to the high enclosure removal rates of 0.36 and 2.5 volume changes per minute under normal and emergency flow rate conditions, respectively.[19] Oxides not given off in the aerosol form will remain in the catch pan. Results for the Test Cell Enclosure would be the same.

TABLE 12.5

SUMMARY FOR CHARGING FACILITY ENCLOSURE ANALYSIS RESULTS FOR CREDIBLE SODIUM FIRES[4]

Characteristics	Case 3	Case 4	Case 5	Case 6	Case 9[1]	Case 9N[1]	Case 10[1]
Sodium Spill, pounds	68	68	68	68	108	108	108
Spill Area, ft^2 [2]	80	80	10	10	80	80	80
Ventilation Rate, cfm [3]	10,350	100	10,350	100	10,350	1,500	100
Time of Burn, hours	0.22	0.34	1.08	1.56	0.34	0.48	0.72
Initial ΔP, inches water	-3.60	+0.40	-3.10	0.0	-3.10	-0.14	+0.16
ΔP At End of Burn	-2.04	-0.45	-2.82	-0.80	-1.92	-0.07	-0.60
Maximum Gas Temperature, °F	230	356	124	206	254	410	380
Maximum Ceiling Linear Temperature, °F	142	195	108	155	164	275	256
Maximum Burn Pan Temperature, °F	1,200	960	1,410	1,247	1,218	1,063	960
Maximum Concrete Floor Temperature, °F	95	95	120	133	95	95	95

Notes: 1) Design Basis Accident

2) Total spill is assumed to occur instantaneously.

3) Vent rate during the fire is assumed to be conducted as a step change at the same time as the spill.

4) Data from Reference 15.

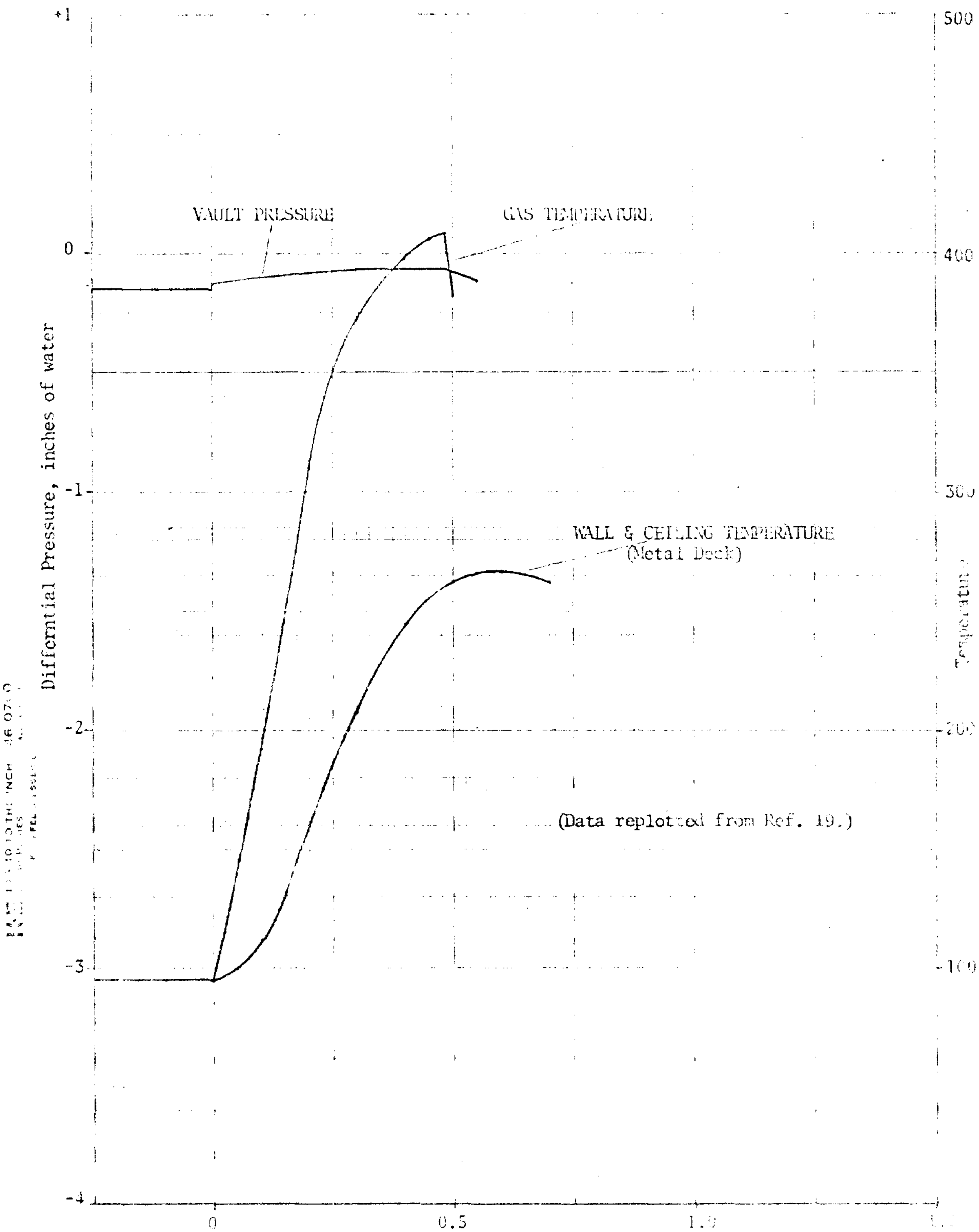

FIG. 12.6 - Pressure-Temperature History for Charging Facility DBA Sodium Pool Fire (Case 9N)

With the facility isolated (closed louvers, 100 cfm ventilation rate) excess pressure will be vented. Aerosol release to the atmosphere will be very small for this case.

12.3.6 Consequences of DBA Sodium Fires

12.3.6.1 Charging Facility

As indicated by the data in Table 12.5, the DBA sodium fire is satisfactorily contained within the Charging Facility Enclosure with any of the ventilation rates studied. This conclusion is confirmed by:

a. The maximum wall Δ pressures are less than the ± 4 inches of water design limit. Peak positive ΔP was 0.16 inches (case 10) and peak negative ΔP was -3.1 inches (case 9)

b. Temperatures are well below material limits. Insulation laid on the metal roof decking was less than 100°F in all cases; hence, well below softening of the asphalt (∿ 300°F). Expected maximum ventilation temperatures would not exceed 275°F in all cases, which is below the 400°F design temperature. The actual temperature experienced by the ventilation system would be similar to the maximum ceiling liner temperature rather than the bulk temperature.

c. The maximum concrete floor temperatures are significantly lower than the burn pan temperatures. The burn pans are supported off the floor; resulting in a floor heat sink of a greater magnitude than the conductance path to the floor. The temperatures in the burn pan may be high enough to cause some warpage but will not cause loss of structural integrity. Therefore, spillage of sodium to the floor due to a burn through is prevented.

12.3.6.2 Test Cell

As indicated by the data in Table 12.6, the DBA sodium fire is satisfactorily contained within the Test Cell Enclosure with any of the ventilation rates studied. This conclusion is confirmed by:

a. The maximum wall Δ pressures are less than the ± 4 inches of water design limit. Peak positive pressure was 0.55 inches (case 2) and peak negative ΔP was -2.06 inches (case 1).

b. Temperatures are well below material limits. Maximum wall temperature reaches only 184°F. At most, the burn pan may warp.

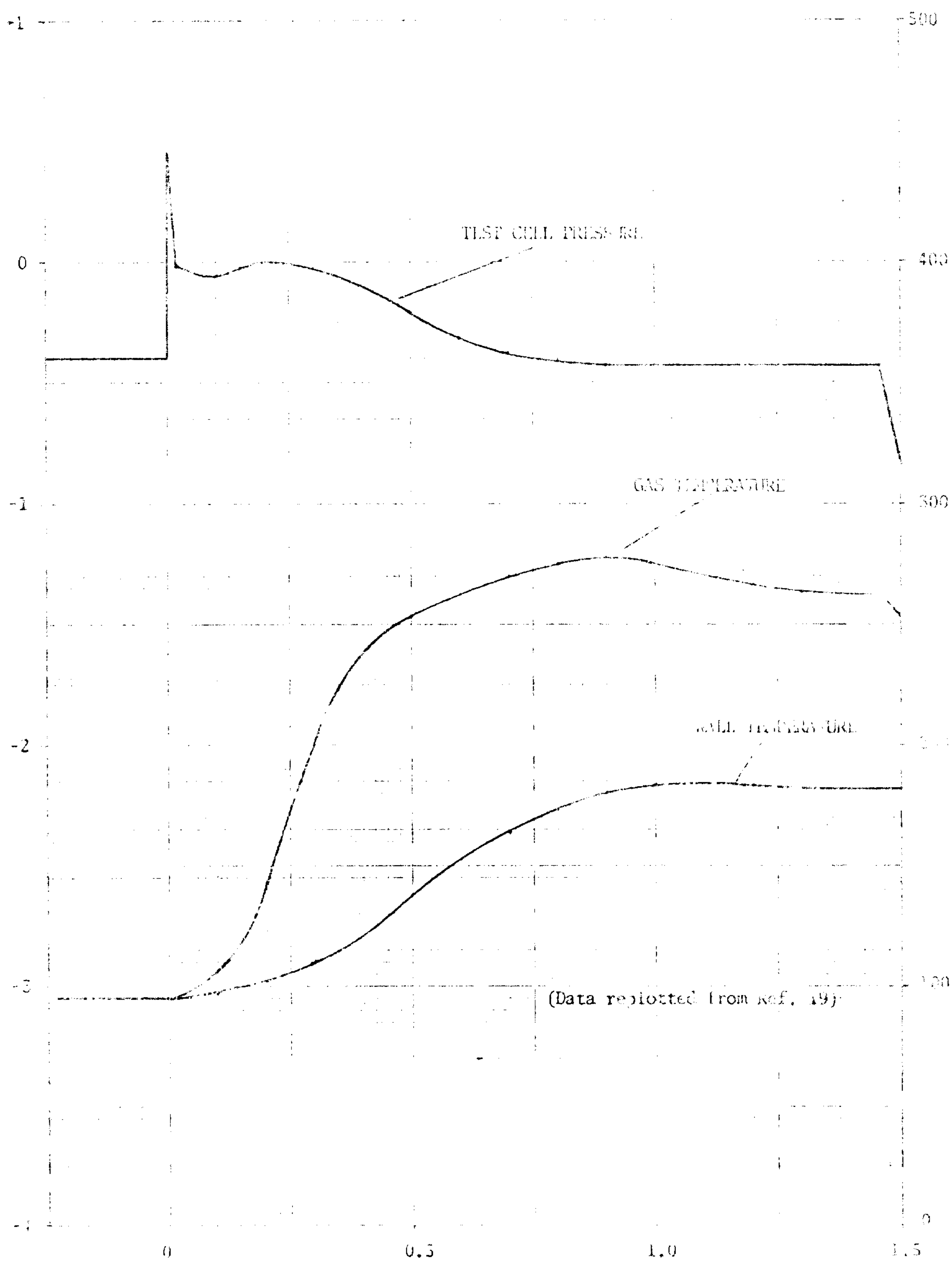

FIG. 12.7 - Pressure-Temperature History for Test
Cell DBA Sodium Pool Fire (Case 2)

TABLE 12.6

SUMMARY FOR TEST CELL ANALYSIS RESULTS FOR CREDIBLE SODIUM FIRES

Characteristics	Case: 1[1]	IN[1]	2[1]	3	4
Sodium Spill, pounds [2]	90	90	90	90	90
Spill Area, ft^2	40	40	40	10	10
Ventilation Rate, cfm [3]	13,840	5,500	100	13,840	100
Time of Burn, hours	0.66	0.67	1.46	2.35	2.55
Initial ΔP, inches water	-2.06	-0.39	+0.55	-2.10	-0.10
ΔP at End of Burn, in water	-2.06	-0.38	-0.45	-2.10	-0.57
Maximum Gas Temperature,°F	103.5	111	277	98.5	147
Maximum Wall Temperature,°F	96.0	96.8	184	95.0	112
Maximum Burn Pan Temperature, °F	566	570	309	592	354

Notes: 1) Design Basis Accident

2) Total spill is assumed to occur instantaneously.

3) Vent rate during the fire is assumed to be conducted as a step change at the same time as the spill.

4) Data from Reference 19.

12.3.6.3 Aerosol Release

Sodium oxide given off in aerosol form presents two problems for consideration: α contamination and toxicity. The former represents the contamination condition where a pre-irradiated test train is installed in the FEFP Loop, and will be discussed first.

Based on data[20] provided from HFEF operational experience, the α contamination level of the pre-irradiated test train prior to assembly into the FEFP Loop was calculated to be about 1.34×10^{-4} μCi/100 cm^2.[21] This magnitude is based on a decontamination reduction factor of 10 prior to leaving HFEF.[20] Assuming that the sodium can remove all the remaining contamination on test train surface area during the activities in the FS&R, the total α source circulating in the sodium is equivalent to about 0.7 μCi. In the spill sodium oxide release analysis model, the following assumptions were made:[22, 34]

a. The contamination is considered to be primarily plutonium.

b. The contamination is thoroughly distributed throughout the sodium volume of 480 lbs.

c. The total release occurs linearly during .34 hours.

d. The release effluent goes from the FS&R facility to the ETR roof vent.

e. The release from the roof vent occurs during a Class F (inversion) meteorological condition with an attendant windspeed of one meter per second.

f. Upon release from the building roof vent, the meteorological building wake brings the effluent to ground level at the closest point of release.

Therefore, the α contamination available for venting from the Charging Facility is about 7.7×10^{-2} μCi (e.g., 108 lbs DBA spill, 50% aerosol assumption). The model results show that the ground level concentration at the point of concern to be about 1.29×10^{-13} μCi/ml. If one pessimistically assumes that all the contamination is due to isotopes of plutonium, a comparison can be made with the allowable plutonium (insoluble form) concentrations for restricted areas:[23]

Pu-238	3×10^{-11} μCi/ml
Pu-239	4×10^{-11} μCi/ml
Pu-240	4×10^{-11} μCi/ml
Pu-241	4×10^{-8} μCi/ml
Pu-242	4×10^{-11} μCi/ml

The results show that the ground level concentration is at $\sim 10^{-2}$ below the AEC limits.

A model similar to the radiation model was used to determine sodium oxide toxicity concentrations.[22] For a 73-lb release of sodium oxide vented from the roof, the concentration at ground level is 0.055 gms/m^3. Information received from Atomics International[42] indicates that 80 mg/m^3 of NaOH is the limit for short term unprotected exposure and they are using this value as the limit to be applied at their site boundary. No on-site limits are defined for accidental conditions. A review of the test reactor facility plot plan shows no possible areas where personnel could be trapped in a high concentration area. It is concluded that additional engineered features to limit amounts of sodium oxide releases from an accidental condition are not required. The facility can be sealed to prevent release of sodium oxide if conditions warrant such action.

12.3.6.4 Summary

It has been shown in the foregoing discussions that the DBA sodium fires for the two FS&R System facilities remain contained within the respective enclosures; hence, the ETR is not damaged. Also, personnel within the building are not affected since any air flow will be into the enclosure and out the vent.

From the aerosol release studies it has been established that the contamination exposure levels are well below AEC limits permitted for personnel in the area around the ETR, even if maximum ventilation rates are used.

In conclusion, adequate protection is provided in the event a DBA level sodium fire should occur. Further, there is no need to place restrictions on ventilation rate. The ventilation rate should be the choice of the operational personnel based on their observations of the particular situation.

12.4 Industrial Safety Analysis

The following industrial safety analysis addresses the major industrial hazards and presents the safety aspects for handling and operation of the FEFPL experiment and its subsystems. This analysis does not address the radiological hazards, the loop handling machine, or the loop as they are treated elsewhere in the SAR.

12.4.1 General

Sodium has been manufactured and used in industry for years with a consistently high safety record. This is indicative of the sound handling methods employed by both manufacturers and users. Based on this experience, and through proper application of sodium technology and handling procedures, the probability of accidents in ETR can be maintained at low levels. Detailed descriptions of safe-handling procedures and practices are available in Refs. 35, 36, and 37 and in the industrial literature. Among the items considered particularly important are the use of protective clothing when working with and around sodium, and the provision of adequate safety equipment.

Attendent to the use of sodium at ETR is the need to provide and maintain appropriate records. Since the sodium-containing systems will be operated by several persons, permanent records must be maintained on the following subjects:

1. Complete descriptions of all equipment, including modifications.
2. Operating procedures, verified by use and kept updated. These include startup, shutdown, and emergency procedures.
3. Maintenance procedures developed by job safety analysis, verified by use, and kept updated.
4. Daily records of use, including operating conditions, descriptions of difficulties, repairs and adjustments.
5. Radiological records, including personnel exposure, disposition of contaminated material and movement of shielding.

Each design and work package is reviewed for safety implications in accordance with ANPP 6.40, Independent Nuclear and Operational Safety Review, and ANPP 6.02, Safe Work Permit Usage. Under these directives, all hazardous or potentially hazardous activities are reviewed for safety, including all phases of facility and system (procedural and hardware) design and requisition, and that approved preventive or protective measures are taken prior to and during the performance of all hazardous work. This is supplemented by job safety analysis, field tests of written procedures, and field observations.

12.4.2 Filling Storage and Remelt Facility

Sodium Handling

Sodium from commercial sources can be received in the form of reagent grade 1-lb bricks in sealed cans, bricks packed in steel drums, filled 55-gallon drums (440 lb net), and railway tank cars (80,000 lbs). All containers are designed to meet DOT specifications for handling and shipping.

Sodium shipped in DOT approved containers has no restrictions against outside storage. A yard storage area will be designated in the Test Reactor Area for the storage of these shipments. The storage area will be checked on a regular basis while sodium is being stored. When needed, the sodium will be moved from the storage area directly into the Charging Facility at ETR.

The possibility of removing contaminated sodium from the system and shipping it to ANL at EBR-II exists. Requirements for shipping will depend upon the contaminants involved. Radioactive contaminants will require shielded shipping containers with the amount of shielding dependent upon the activity of the contaminant. Non-radioactive contaminated sodium shipments will be evaluated on the basis of the contaminant and will be handled in accordance with the evaluation. In all cases, NRTS on-site shipping regulations will apply.

The movement of the drums in the ETR will be directly into the Charging Facility which is designed specifically for the purpose of handling sodium. The cell is provided with curbs to prevent water from the reactor area entering the facility. The facility is equipped with a steel liner. The walls of the facility are constructed of certified cement block with a UL rating of three hours. Openings into the facility are protected with approved fire doors rated equal to the walls of the facility.

Existing water lines (including Fire Water) have either been removed from the facility or are double-contained to prevent leakage into the facility. A provision for monitoring the facility at all times during its operation is provided by a closed circuit television system. Fire detection is accomplished by the use of photoelectric and ionization detectors and by visual means.

Sodium Systems

Inherent in the design of the sodium system are several instruments for detecting sodium leaks. These include a remote television monitor which will continuously display the inside of the Charging Facility Enclosure, and a system of ionization and photoelectric smoke detectors. Any detection of a sodium leak will initiate shutdown of the system, and the implementation of fire-control equipement should a fire develop. Sodium fire-control will involve the manual application of metal fire-extinguishing agents such as calcium carbonate, or dry sand to the burn area. Personnel will be equipped with protective clothing, self-contained breathing apparatus, and other special equipment required in combating sodium fires.

Sodium System Repair

The general approach to system repair will be as follows:

1. Determine the condition of the system. This would include such things as: whether the system is completely drained or not, temperature and pressure, oxides or other impurities present, and the inert gas situation.

2. Define the problem in terms of: is the work at hand the result of an accident, equipment failure, planned modification and/or routine maintenance.

3. Formulate an approach to accomplish the objective and write the procedure.

4. Field test the procedure, updating it as needed before proceeding with the job.

Generally, the major work on the sodium system involves the cutting of pipes to make modifications, remove an item of equipment, pipe weld, defective pipe, temperature and flow instrumentation or plugged sections of pipe.

Before such work is started, the system either is drained or freeze plugs established. The system will be depressurized and the temperature reduced to room temperature.

In pipes 4 inches or less in diameter and empty, a flow of inert gas will be established, and a pan containing dry Calcium Carbonate will be placed under the area where the cut is to be made. Cutting will then be done dry. The fires generated by the cutting will be continually covered with an extinguishing agent. When the first cut is completed, it will be taped to assure gas flow. After the second cut is completed, the pipe section will be removed and the open ends of the system plugged by using rubber pipe plugs or tape to exclude foreign material from the system.

Pipes containing frozen sodium will be handled in the same manner except that special attention will be given to avoid ignition of the fires and the cut ends will be completely taped closed.

Welding of pipe sections on equipment containing sodium can be performed safely. What is required is that the weld area must be cleaned of traces of sodium, and that chill blocks be used to prevent melting of sodium in adjacent pipe sections.

All work on sodium systems that involves cutting, welding, etc., requires that a fire watch (equipped with protective clothing and fire extinguishment equipment) be in the area until the job is secured in a safe configuration. The NRTS Fire Department will act as the fire watch upon request.

Dangerous Materials

It is important to note that certain commonly available solvents and cleaning fluids are highly dangerous to use with sodium. These include:

1. Water
2. Carbon Tetrachloride
3. Trichloroethylene
4. In general, any chlorinated hydrocarbon

The use of these materials will be excluded from use or storage in operating areas where they may come into contact with sodium. Other materials prohibited for use in areas where they may come into contact with internal or external surfaces of in-pile loops are identified in FDR-03, Section 3.5.

Cleaning for Reuse or Storage

Almost every modification or repair of an in-service sodium system will involve the clean-up of equipment and/or pipe. Small parts can be cleaned by soaking in ethanol or Dawanol EB. Heavier alcohols (ethyl, butyl) can be used for slower reaction and less chance of fires, but the butyls form a barrier film before all the sodium may be reacted. In any case, hydrogen gas is a reaction product. Thus, the cleaning of small parts will be by procedure and will be carried out in an area where proper ventilation and fire protection is provided.

Dry steam may also be used providing a rapid but messy method of cleaning and will be confined to large rugged parts that can withstand the resulting hydrogen oxygen reactions that occur during the steaming. Nitrogen may be used as cover gas to dilute and minimize the reactions. Steam lance barriers will be provided in addition to protective clothing in steaming operations. A by-product of steam cleaning, sodium hydroxide, (a caustic) will be collected and neutralized before disposal.

Personnel Protection

Types of protective clothing provided for personnel protection against possible sodium burns will include, but is not limited to, the following:

1. Flame retardant coveralls preferably without pockets, cuffs, rolls, or openings which sodium could enter and become trapped. If such coveralls are not available, all openings will be taped shut.

2. Full length chrome tanned leather coats, pants, leather leggings, and leather shoes.

3. Two-piece aluminized asbestos suits which can be equipped with cooling devices and breathing air supply.

4. Full brim, phenolic resin hard hats with full face shields, Jones goggles, or chemical splash goggles, and poly vinyl chloride long gauntlet gloves.

5. Self-contained breathing apparatus.

6. Rite-White Guard type units equipped with either clear or welding shade visors, chrome leather shoulder shroud and supplied air. These units are for personnel comfort.

The type of personnel protective equipment used for a particular job will be evaluated and specified for each job before the job begins. Equipment for emergency use (such as a sodium fire) will be specified in the procedures on fire fighting. All personnel connected with the operation of FEFPL will be trained in the use of the protective equipment used.

First Aid for Sodium Burns

The proven emergency first aid for sodium burns is to try to knock off or scrape off all the large sodium pieces from the skin and clothing as quickly as possible and the person showered immediately in a safety shower. The water dilutes the caustic reaction products and will limit skin damage.

All clothing should be removed if possible before showering as the clothing can trap pieces of sodium. Sodium trapped in clothing will react violently and harmfully as the hydrogen gas released from the burning sodium will explode, with the force of the explosion directed in toward the body due to its confinement in the clothing.

After showering personnel receiving sodium burns will be immediately transported to the dispensary for treatment.

First aid materials and supplies are kept in the ETR Health Physics Office for the field treatment of sodium burns.

References

*1. Technical Specification CI-1233.

2. The ETR floor limits are specified on Phillips Dwg. ETR-D-1584.

3. Loads imposed by transporter and LHM are given in ANC letter CLAY - 12-72.

4. Memorandum, H. B. Perkins to W. Kaspic, ANL Report ETC/FE-1066, (April 20, 1973).

5. FEFPL/ETR Handling Study TR-295.

6. ANC NOS Manual 6.3.A and 6.8.A.

7. T. E. Young, ETR Biological Shielding Radiation Study for FEFPL, ANC Report EDF-398, (July 3, 1972).

8. Loop Handling Machine Shielding Analysis, ANC Report CRS-104-71, (December 13, 1971).

9. Loop Handling Machine Radiation Streaming Analysis, ANC Report CRS-95-72, (May 8, 1972).

10. R. R. Halstead, ETR Buildings Structural Check, ANC Memo Report HALS-2-73, (January 4, 1973).

11. FDR-05

12. FEFPL Loop Handling System Functional Design Requirements, ANL Report R-103-1023-SE, (March 1973).

13. "FEFPL Filling, Storage and Remelt System Design Requirements," ANC Report FDR-03, Rev. 2, (June 19, 1973).

14. H. D. Killian, "FEFPL Filling, Storage and Remelt System Preliminary Design Report," ANC Report FR-193, (July 3, 1973).

15. R. W. Marshall, "Rationale Used in Determining the Design Basis Accident for the FS&R," ANC FEFPL Project EDF-526, (November 9, 1972).

16. W. R. Bird, "Charging Facility Enclosure and Test Cell Sodium Fire Evaluation," ANC FEFPL Project EDF-848, (June 15, 1973).

17. W. R. Bird, "Sodium Fire Analysis, Spill Evaluation," ANC FEFPL Project EDF-1052 (September 6, 1973).

18. R. R. Piscitella, "FS&R - Ventilation Air Flow Rates for Various System Operating Conditions," FEFPL Project EDF-687, (February 9, 1973).

19. L. Baurmash and R. L. Koontz, "Evaluation of Sodium Pool Fires in FEFPL," Atomics International Report, AI-73-32, (April 30, 1973).

20. W. E. Stephens, "Estimate of Surface Contamination Levels of Test Trains Containing Pre-irradiated Fuel," ANL Memorandum, (December 20, 1972).

21. W. R. Bird, "FEFPL, FS&R Exhaust Duct Filter, Determination for Need of," ANC Memorandum Bir-1-73, (January 12, 1973).

*Under revision.

22. H. K. Peterson, "FEFPL Contamination Sodium Spill", ANC Memorandum HKP-47-72 (December 22, 1972).

23. AEC Manual, Chapter 0524, Standards for Radiation Protection, (November 8, 1968).

24. R. K. Hilliard and J. M. Yatabe, FFTF Secondary Sodium Fire Protection System Test F1, HEDL-TME-73-48, (April 1973).

25. C. E. Johnson, et al., "Effects of Oxygen Concentration on Properties of Fast Reactor Mixed-Oxide Fuel", Reactor Technology, Vol. 15, No. 4, (Winter 1972-73) pp 303 fdw.

26. R. L. Koontz, C. T. Nelson, and L Baurmash, Modeling Characteristics of Aerosols Generated during LMFBR Accidents, "Treatment of Airborne Radioactive Wastes", IAEA, Vienna (1968), SM-110/19, pp 53.

27. D. H. Lennox, Argonne National Laboratories, Personnel Communications, February 1974.

28. D. L. Smith, "Oxygen Interactions Between Sodium and Uranium-Plutonium Oxide Fuel", Nuclear Technology, Vol. 20, (December 1973), pp 190-198.

29. Task Group on Lung Dynamics (P. E. Morrow, et al.,) "Deposition and Retention Models for Internal Dosimetry of the Human Respiratory Tract", Health Physics Journal, Vol. 12, pp 173-207 (1966).

30. B. R. Fish, et al., "Calculation of Doses Due to Accidentally Released Plutonium from an LMFBR", ORNL-NSIC-74, November 1972.

31. Title 10, Code of Federal Regulations, Part 100.

32. "Plutonium Dose Criteria for Reactor Safety Analysis", Memorandum, G. L. Voelz, M.D., Idaho Operations Office, USAEC (February 14, 1965).

33. R. L. Coates and N. R. Horton, "RSAC-A Radiological Safety Analysis Computer Program", IDO-17151 (May 1966).

34. ANC Report EDF 689, "ETR/FEFPL Potential Hazard Comparison - Radiological Source Terms for Dose Calculations", (February 14, 1973).

35. Liquid Metal Handbook, Sodium NaK Supplement, Atomic Energy Commission, Department of the Navy, 3rd Edition, C. B. Jackson (Ed.), (1955)

36. M. Sittig, "Sodium, Its Manufacture and Uses", Reinhold Publishing Co., New York, N.Y., (1956).

37. J. W. Mausteller, F. Tepper and S. J. Rodgers, "Alkili Metal Handling and Systems Operating Techniques", Gordon and Breach Science Publishers, New York, N.Y., (1967).

38. A. A. Oare, "FEFPL Transporter Loading at NRTS Facilities", ANC Report EDF 928, (July 10, 1967).

39. T. J. Hill, "ETR Floor Loading Limits - LHM Transporter and Tractor", ANC Report EDF 1090, (October 3, 1973).

40. T. J. Hill, "ETR Floor Loading Analysis", ANC Report EDF 1028, (August 21, 1973).

41. W. R. Bird, SAR Chapter 12 Revision, ANC FEFPL Project EDF 1184, (December 14, 1973).

42. Criteria for Allowable NaOH Release Rates for Operation of the AI Steam General Module and Operation of the Large Leak Test Facility, SRR-001-140,032, Safety Review Report, (January 1973).

43. T. J. Hill, "SAR Accident, LHM Drop on Reactor Top", ANC Report EDF 556, Revision A, (May 1974).

CHAPTER 13.0

TABLE OF CONTENTS

LIST OF TABLES

LIST OF FIGURES

13.0 Hypothetical Events

A hypothetical event is a condition for which no real sequence of causative events can be identified, but which is nevertheless considered in order to assess margins relative to protection of the public. The FEFPL/ETR system is not specifically designed to tolerate hypothetical events, however, these events are arbitrarily imposed on the loop as a test of its capability to function safely into a range well beyond the Reference Experiment.

Three principal mechanisms that are a potential source for accidents are discussed in this chapter, namely: a) containment system failures, b) reactivity addition, and c) sodium fires. Given first is the approach used to prevent such initiating mechanisms; second, it is shown that should they occur, the consequences are limited and present no unusual risk to Operations personnel, the ETR, or the public; and third, conditions for which no real sequence of precursor events can be identified, are arbitrarily postulated to demonstrate margin of safety. Also identified are the extensive analyses that have been carried out to verify understandings and confirm phenomenology.

13.1 Loss of Sodium Containment

The FEFPL containment system evolves from a "defense in depth" design philosophy which embodies the following multiple levels of safety.

First, the loop has two barriers between sodium and water everywhere except in the region of the heat exchanger, where there are three. Acting together, both vessels are designed to contain, without deformation, internal pressures at least a factor of four higher than postulated for a molten fuel-coolant interaction much more severe than expected. The FEFPL secondary vessel will not buckle if exposed to the external pressure loads that may result from the ETR loss-of-cooling DBA which involves dispersion in water of 2.55 Kg of U-235 as molten particles. (As will be discussed later, the loop also can tolerate other potential side effects of the DBA.)

Second, during in-pile operation, the FEFPL Plant Protection System will continuously monitor the containment system to ensure that the safety margin is maintained. If a leak, overtemperature, or overpressure occurs in either vessel, the ETR will be shut down automatically.

Third, should it be postulated that one vessel fails for a reason not explained, and without detection by the FEFPL-PPS, an effective barrier still will separate the loop sodium from the ETR water. Each of the two containment vessels, primary and secondary, is designed to safely withstand alone the design envelope pressure pulse or the thermal effects of molten fuel. Additionally, analyses show that failure of one vessel will not propagate to the other.

Finally, it is shown that the loop containment system can withstand arbitrarily imposed hypothetical events. When parametrically tested against hypothetical events that have even higher pressures than the accidents mentioned previously, the loop containment system maintains its integrity. Should, again for an unexplained reason, failures develop in both vessels that are not detectable, the potential sodium leak would not be great enough to endanger ETR or personnel.

13.1.1 Integrity of the Primary Containment Vessel

The boundary established by the primary containment vessel passes through three regions that include the heat exchanger, test section and pump. The likelihood of failure in each is discussed.

Heat Exchanger

The design, fabrication and testing of the primary containment in the region of the heat exchanger (HX) are such that no failure should occur during the FEFP program. If a failure should occur in this region of the primary boundary, it probably would not leak sodium because the helium pressure in the heat dump system exceeds the sodium pressure. Even if sodium could escape through such a failure, it would be prevented from entering the annulus between the primary and secondary containments by a shroud around the heat exchanger. Therefore, the containment in this region consists of two barriers between sodium and the loop secondary vessel. If a failure should occur in the shroud as well as in the heat exchanger, it also should not leak sodium because the annulus gas system is at a higher pressure than the helium heat dump system.

Should a failure occur in the shroud alone, or in both the shroud and heat exchanger, it will be detected by the FEFPL-PPS and result in an automatic shutdown. Two additional gamma monitors, not part of the PPS, will alarm should radioactive sodium from the heat exchanger enter the helium coolant. One is located at the shielded filter, the other near the helium circulators.

Multiple, independent malfunctions would be required to permit operation with reduced containment integrity in the heat exchanger area: 1) failure of the heat exchanger, 2) probable failure of two gamma monitors, 3) failure of the shroud, and 4) failure of the FEFPL-PPS.

ALIP

The primary containment vessel in the pump region is a 7.18 in. OD by 0.3 in. thick tube inside the pump stator, surrounding the pump core. It is designed to withstand, without excessive permanent deformation or failure, all predicted mechanical loads that may result from planned experiments or potential malfunctions. Also, the pump core will attenuate and minimize the direct load from a pressure pulse generated within the test section.

The coils in the pump stator are doubly insulated from the containment vessel to preclude the possibility of electrical shorts that might lead to local overheating. To effect an I^2R heating path through the vessel, a double failure of insulation must first occur in the region of one coil, then a similar failure must occur near a second coil in the same pump section to complete the circuit. A ground-fault detector, however, is provided that will alarm if an initial failure occurs. If this happens, the operator is required to deenergize the defective section of the ALIP and thus remove a possible avenue for a short circuit. In addition, a backup system of fuses and circuit breakers provides automatic protection against currents high enough to jeopardize the integrity of the containment vessel.

No mechanism has been identified that would fail the primary containment in the ALIP region. Nevertheless, if failure occurs, the higher pressure of helium within the annulus should prevent sodium leakage.

Test Section

This section of the primary vessel also is designed with a large protective margin for thermal or mechanical loads. As mentioned previously, the primary vessel is designed to withstand without excessive deformation pressures many times greater than those considered to be realistically obtainable from a possible molten fuel-coolant interaction. The vessel is protected from direct exposure to molten fuel that may arise in the test section by two barriers that are normally sodium cooled by forced convection. These barriers, the hex can surrounding the fuel pins (it will have double walls for many experiments), plus the flow divider are expected to retain their integrity if in direct contact with molten fuel that may tend to travel radially.

Current evidence from TREAT L-series experiments indicates that the molten fuel produced in flow-decay tests freezes at the upper and lower boundaries of the fuel zone to prevent further axial migration. If this should not occur, however, in the FEFP loop, fuel will be trapped in a coolable geometry in other regions of the test train. Fuel debris that may fall downward will be contained in the refractory metal meltdown cup at the bottom of the test section. Particles that may be swept upward will normally be caught in a filter located at the upper end of the test train, which is out of the active region of the ETR core. Cooling of fuel trapped in either location can be effected by natural circulation of sodium, although the ALIP is designed to provide forced circulation under all anticipated experimental conditions.

To prevent loss of containment protective margin for mechanical loads, the primary vessel temperature is monitored by the FEFPL -PPS; an ETR scram is automatically initiated to prevent an MFCI should the primary vessel temperature approach 1300°F. Simultaneously, the annulus gas cooling system is actuated to limit the temperature rise of the vessel.

If fuel debris from the test section should concentrate in the meltdown cup, there would be no criticality hazard. Analysis indicates that about ten times the total quantity of fuel available in a 37-pin test section would remain subcritical in optimum geometry with an infinite water reflector.

Although the primary vessel can withstand without failure all anticipated consequences of either planned experiments or possible loop malfunctions, an additional FEFPL-PPS function is the continual monitoring of the vesssel integrity. Consequently, it is considered extremely unlikely that a failure could occur and remain undetected.

13.1.2 Integrity of the Secondary Containment Vessel

Although it is not likely that such a need will arise during the FEFP in-reactor experimental program, the secondary vessel is designed to withstand alone, without permanent deformation, the mechanical loads that may result from a design basis MFCI unattenuated by the presence of a primary vessel. It is also designed to withstand, without buckling, pressure loads that may be generated by disturbances external to the loop. The postulated ETR Design Basis LOCA Accident establishes an upper limit pressure pulse to test analytically the loop containment margin.

The faulted buckling pressure in the weakest part of the secondary vessel, which is in the HX region, is 770 psi above the Annulus Gas System (AGS) pressure.[1] During reactor operation, the AGS pressure is nominally 280 psia;[2] therefore, buckling would not be expected for pressure pulses below 1050 psia. (To protect against the possible operation of the loop with low annulus gas pressure, the FEFPL-PPS will alarm at 260 psia and initiate an ETR scram at 250 psia.) As indicated in Section 11.6.2, the peak pressure that would be expected from the ETR DBA is only 70 psi. Thus, the design gives a large safety margin for external pressure loads. Side effects that may accompany the DBA include: blowdown from the ruptured pipe, and the melting of aluminum at clad hot spots. Water vapor from the first is not expected to indirectly affect the FEFPL by causing a breakdown in a primary loop support function, such as control or heat removal. The first barrier between FEFPL components and the ruptured ETR primary inlet pipe is the reactor biological shielding that surrounds the top dome and forms the walls of the pipe tunnel. Second, the instrumentation racks for the loop control and PPS systems are mounted on a raised floor in a separate, closed, air-conditioned room that provides an additional barrier against moisture. The helium circulation equipment that is part of the loop heat dump system also is located in a closed cubicle; however, some of the associated switchgear is in external cabinets. If steam or water vapor were to eventually reach and manage to cause a malfunction resulting in loss of power or loop heat sink the potential for damage to FEFPL fuel is expected to be less severe than the Class I accidents already discussed in Chapter 11. This is because the ETR PPS would sense the DBA and effect a scram trip within 0.3 to 0.35 seconds.[3] Consequently, this scram should precede any possible loop malfunctions that might be caused by the relatively slow spread of water vapor. (For the accidents discussed in Chapter 11, the postulated malfunction occurs first, then an ETR scram is initiated.).

Molten aluminum produced by the ETR DBA is not expected to pose a thermal challenge to the loop secondary vessel. During and after the DBA, the core remains covered with about 18 feet of water;[3] consequently, significant migration of molten aluminum without freezing is unlikely. In addition, the loop is surrounded in the core region by aluminum shroud and filler pieces which enclose a water filled annulus. This system provides a protective wall against molten material. Finally, should any material reach the loop secondary vessel, it would be unlikely that it contains enough stored heat to thermally damage the stinaless steel wall. The maximum clad temperature is estimated to fall within 1700°F and 2459°F.[3] Heat loss during transit of this material to the loop could only reduce its temperature range below the values given. Thus, there appears to be no possibility of melting the stainless steel vessel.

Other potential sources of stress in the secondary vessel include the pressurized annulus gas system, and thermal gradients. The pressure in the annulus is normally about an order of magnitude below the design requirements for the vessel. In addition, the gas system has a diverse relief system to prevent overpressure which includes two different types of pressure relief valves in parallel.

There are no apparent sources for large thermal stresses in the secondary under any normal circumstances. Insertion of the loop into the ETR water will be done with the sodium some 400°F cooler than during operation. The stresses during this, as well as other operational transients, fall within the values allowed by the ASME Section III Code for Nuclear Pressure Vessels.

During ETR power operation, the in-reactor section of the secondary will be subject to gamma heating, but cooled by external water flow. Circumferential variations in this heating due to power skewing will be held to less than a ± 7.5% departure from average during normal operation by the ETR core loading and control rod program. Bowing to the limits given does not pose either thermal or mechanical conditions that are unacceptable (see Section 9.1.1.1).

In summary, there appears to be no identified mechanism to cause failure of the secondary vessel.

13.1.3 Containment Vessel Failure Propagation

The previous discussion indicated that a failure of either containment vessel would be extremely unlikely. Nevertheless, to show that the system has the necessary safety margin to tolerate low probability events, failure of either vessel - for any unknown reason - is postulated to determine whether such a failure will propagate to the other.

First, the assumption is made that a failure occurs in the primary vessel during normal loop operation prior to a planned experiment. As mentioned previously, the annulus gas system is designed to maintain a pressure gradient that would prevent the leakage of sodium from the primary. Also, the FEFPL-PPS continuously monitors both vessels and automatically initiates ane ETR scram upon loss of integrity. In the hypothetical event that a failure occurs, remains undetected, and an experiment is performed that may develop pressures high enough to force sodium into the annulus, the secondary vessel could experience either a local impingement or general flooding with hot sodium. Analyses show that neither case would produce harmful thermal stresses.[4,5]

To create a situation whereby the secondary vessel might be exposed to more severe thermal transients, it is necessary to postulate the escape of molten fuel from the primary into the annulus. As described in Section 13.1.1, the test section is designed to control fuel migration and sodium cooling is provided to remove sensible and decay heat. The primary receptacle for molten fuel, the meltdown cup, is designed to withstand the thermal shock associated with the receipt of molten fuel; out-of-pile experiments have verified this capability.[6] It is also designed to accommodate the mechanical loads that may stem from a MFCI within the test section.

In the event of a small crack developing in the meltdown cup, the surrounding sodium will freeze molten fuel that may tend to escape. Even should a large failure of the cup occur, without blocking all circulation of sodium, the primary will not overheat to the point of failure. Therefore, a catastrophic failure of the meltdown cup must be hypothesized in order to cause possible failure of the primary (several of the FEFPL-PPS scram set-points would be exceeded if molten fuel were to penetrate the primary). If such a failure is then coupled with the series of previous events, the secondary vessel may face a thermal transient from contact with molten fuel. This situation is analyzed (in Chapter 10) and it is determined that the normal flow of ETR cooling water outside the secondary vessel is sufficient to prevent meltthrough and failure. Thus, there does not appear to be a credible chain of events that could lead to a failure of the primary vessel that would propagate to the secondary.

Next, it is assumed that the secondary instead of the primary, fails from an unknown cause. Again, the question to be answered is whether such a failure will propagate.

The annulus gas system also is designed to maintain helium pressure above that of the ETR core water; therefore, a small leak in the secondary would cause helium to flow out rather than water into the annulus. The annulus gas system pressure is monitored continuously to ensure that it exceeds the loop sodium pressure and the ETR water pressure - a drop below a preset limit automatically effects an ETR scram. In order to parametrically test the capability of the loop to maintain containment integrity under conditions that are unlikely and overly severe, the following hypothetical sequence is postulated. Although the loop containment vessels are tested for possible leakage before the loop is inserted in the ETR and then again before operation at power, the assumption is made that an unidentified mechanism suddenly causes a hole or crack to develop. This would normally be detected by the FEFPL-PPS which automatically calls for an ETR scram; immediately, the loop power and temperature start dropping. The higher pressure annulus gas system would be expected to prevent an inward leakage of ETR water. If, however, water flows in to contact the primary vessel whose temperature has fallen from the hot operational value, the resultant thermal stress would not affect the integrity of the primary vessel.[5] The water from initial leakage would rapidly boil to bring the annulus pressure up to equilibrium with the core water pressure to further limit the leakage with only a pressure of about 250 psia on the primary (and secondary) vessels. This is well below the 1145 psid minimum buckling pressure[5] for all the regions of the primary vessel except for the heat exchanger shroud, which is rated at 440 psia. The latter, however, would receive support from the helium flow divider should it deform; also, should the shroud develop a leak, the heat exchanger still provides another barrier to sodium flow into the annulus. If the water should flash, or chug, several times before equilibrium is established, the repeated thermal stress will not approach the lower cyclic limit for fatigue failure (see NB-3113, 4, ASME Boiler & Pressure Vessel Code, Section III).

Based on the foregoing, it is concluded that under the extremely unlikely circumstances that a leak develops in either the primary or secondary containment vessel, it will not propagate to the other. For the first line of defense against this type of accident, the containment system is designed to tolerate loads well in excess of those anticipated in order to prevent failure. Second, the integrity of both vessels is continuously monitored; should a reduction in containment margin occur, the ETR is automatically shut down. Finally, analysis has shown that even if a leak develops - and goes without detection - this failure will not propagate.[5]

13.1.4 Containment System Safety Margin

To verify that the loop containment system has extra safety margin to protect both the ETR and personnel, its response to hypothetical conditions is considered. It is shown that the loop can tolerate internally generated events much more severe than could be reasonably anticipated, such as molten fuel-coolant interactions that give pressures higher than the design basis experiment (see Fig. 7.6, Chapter 7). The ability of the loop to withstand hypothetical external pressure loads is examined.

The maximum postulated pressure source that may arise from an accident outside the loop system stems from the ETR design basis LOCA. This is the pressure pulse generated during the dispersion of molten fuel following loss of coolant. Under these circumatances, it was predicted* that $\sim$ 4% of the core would melt; however, this value was increased to 15% for the reference ETR DBA that provides the basis for calculations of the amount of radioactivity that may be released. This reference accident results in a MFCI peak pressure of 54 psia at the ETR top head[7] which can be withstood easily by all portions of the loop. The lowest allowable faulted buckling pressure for the FEFPL is about 1050 psia (with 280 psia annulus gas pressure) in the vicinity of the HX.[1]

To define the safety margin of the loop, parametric studies were performed whereby it is postulated that a much larger fraction of the ETR core melts and is dispersed. It was found, for example, for an arbitrarily choosen core melting fraction as high as 50%, the peak pressure was 701 psia based upon SPIRT computer code analyses.[8] Technical details of the model are given in Ref. 7. When a conservative dynamic amplication factor of slightly more than 50% of the ETR core must melt before the FEFPL secondary vessel would be subjected to loads (1050 psia) that might cause buckling. Even if this should occur, it does not follow inevitably that the secondary crack or the primary also buckle.

Because it is necessary to postulate that such a large fraction of the ETR core be damaged before FEFPL design loads are approached, it is concluded that the presence of the loop does not pose any significant additional risk.

* Calculations performed previously in support of ETR safety analysis.

13.1.5 Consequences of Undetected Failure of Both Containment Vessels

The multiple lines of defense employed to ensure the integrity of both containment vessels makes the failure of either extremely unlikely. If failure should occur, the pressure gradient imposed by the annulus gas system acts to prevent liquid leakage. The system also is monitored continuously for possible loss of integrity by the FEFPL-PPS; in the event of a failure, an ETR scram is effected and the experiment terminated.

Nevertheless, the consequences of a hypothetical series of events is examined to determine the possible risk to ETR or personnel.

Although no mechanism that is likely to cause a sudden failure of either vessel has been identified, it is first postulated that a small failure develops in the primary vessel.

To prevent leakage into the annulus, the helium pressure is held at a level at least 50 psia greater than the sodium pressure during normal loop operation (see Section 7.1.3.3). If it drops below this value, the PPS effects an automatic ETR scram. In spite of the fact that the FEFPL-PPS is designed and built to conform with the applicable standards for reactor protection systems, it is further assumed that two additional, independent, failures occur: a) the annulus helium pressure unexplicably drops below the pressure within the primary vessel without makeup action, thus permitting radioactive sodium to leak into the annulus, and b) the FEFPL-PPS low helium pressure function fails to alarm and scram the ETR.

Next, it is assumed that a small failure occurs in the secondary vessel. In order for sodium, however, to leak into the ETR coolant requires still an additional independent failure, namely, loss of pressure in the ETR primary coolant system. Thus, at least four independent failures must occur in order for sodium to enter the ETR without detection and action by the FEFPL-PPS.

If sodium flows into the ETR water, the resultant increase in ph normally would be expected to activate the ETR ph alarm upper set point of 5.7 within a few minutes, depending upon the mixing and diffusion that may occur. In order to examine the potential consequences of a sodium leak, it is postulated that this alarm is observed and a quantity of radioactive sodium, arbitrarily taken to be about one pound, enters the ETR primary coolant before remedial action is taken.

Associated with this hypothetical event, there are four potential problems: a) a pressure pulse from a possible sodium-water reaction, b) hydrogen generated from this reaction, c) an increase in the radioactive content of the ETR primary system due to Na^{24} (it is assumed that this hypothetical sequence of events occurs during the relatively long period of loop operation at temperatures prior to a planned experiment), and d) an increase in ph of the ETR primary system water. None of these appear to pose a serious hazard to either the ETR or personnel.

Pressure Pulse

Experimental data have been obtained to determine the magnitude and duration of major pressure pulses associated with the nearly instantaneous release of over three pounds of hot NaK into cold water.[9] These measurements showed that the energy contained by the pressure spikes was very small leading to no structural damage in a GETR-type core. Although the GETR design is somewhat different from the ETR, it should have about the same sensitivity to mechanical loads due to similar core structural characteristics. The GETR core is a two-foot by two-foot matrix with an active length of three feet. Flat plate, aluminum clad, uranium-aluminum alloy fuel plates are assembled into three-inch by three-inch elements with side plates. This heterogeneous, water-cooled core is contained within a slender aluminum pressure vessel. Thus, it can be concluded that the release of one-third as much liquid metal would not give rise to mechanical loads of destructive significance to the ETR core, pressure vessel, or primary piping. In addition, they would not approach the allowable external buckling pressure for the FEFPL secondary vessel. Prior calculations[10] indicate that even if the entire sodium inventory of the loop were released in a relatively short period (100 - 1000 seconds), the resultant pressure pulse, conservatively calculated, would not exceed the ETR pressure vessel design rating.

Hydrogen Gas

A study of limited sodium leak rates shows that small leaks could be tolerated by an ETR coolant system with no serious consequences. A leakage rate of up to 16 pounds of sodium per hour would produce hydrogen at under the allowable rate of 2.2 SCFM given in the ETR Technical Specifications. For a leak below the ETR core, where greater gas injection would be less of a ETR fuel blanketing hazard, a limiting sodium flow of approximately 46 pounds per hour would be acceptable before the hydrogen generated would form an explosive mixture in the purge air through the degassing tube of the ETR coolant system. Thus, a total flow of sodium of one pound for the hypothetical, undetected, failure of both FEFPL containment vessels does not present a hydrogen explosion hazard from the limited sodium-water reaction that may occur. Also, because the leakage of sodium would be expected to occur near the bottom of the loop, no significant gas blanketing in the region of the loop cadmium filter would be expected.

Radioactivity

The saturated specific activity of the FEFPL Na^{24} is estimated to be about 0.12 curies/cc.[10] For the hypothesized release of one pound of sodium, a total of about 70 curies would be released to the ETR primary coolant. Because this release occurs over a period of an hour, it is reasonable to assume that the NaOH is uniformly dispersed in the ETR water; therefore, the concentration approaches $\sim$ 0.46 microcuries/cc. This is well below the accepted concentration limits for the ETR primary coolant of 20 microcuries/cc for continous operation and 200 microcuries/cc for operation up to 24 hours.[11]

Corrosion

The NaOH formed by the sodium-water reaction in the immediate vicinity of the leak would increase the alkalinity of the water until corrective action were taken. A standard-procedure reactor water flush at 1000 gpm, started within 1/2 hour after shutdown would prevent significant corrosion of the aluminum clad fuel elements (the corrosion rate of aluminum at 190°F is less than 0.3 mils/day at ph of 9).[10] The other material as sensitive to corrosion as aluminum that is exposed to the ETR primary coolant, namely beryllium, is likewise unaffected by the small, transient increase in ph. The remainder of the materials, stainless steels and iron alloys, would suffer negligible weight loss or caustic embrittlement. For a slow increase in ph, corrective action would be taken to restore it to the normal operating range by the ETR operators.

13.2 Loss of Cadmium Thermal Neutron Filter (TNF)

Because a positive reactivity addition of 1.48% $\Delta k/k$ would result from the loss of the cadmium filter, which is used to attenuate the ETR thermal neutron flux to the experiment, a filter design has been developed Fig 13.1 which assures that it cannot move from its as-fabrication position.

As shown in Figure 13.1, the TNF is an integral part of the secondary containment assembly. It is 48-in. long and extends 6-in. above and below the ETR Core. The filter consists of a nominal 0.040-in. thickness of cadmium which is sandwiched between the secondary containment outer wall and a nominal 0.060-in. thick stainless steel protective sheath. The lower end of the sheath, as installed, is flush with the outside diameter of the secondary tube to preclude interference during insertion and removal operations.

The filter is fabricated by placing a flash coat of nickel (less than 0.0005 in.) on the inside surface of the sheath. The steel sheath is then electroplated with a nominal 0.040-in. thick cadmium layer. The sheath is then assembled to the secondary tube with a shrink fit providing 1.5 to 3 mils radial interference under all operational conditions (Fig 13.2).

The described configuration provides sufficient interference to prevent vertical displacement of the cadmium should the outer sheath vanish. The outer sheath is, however, welded at either end to the secondary tube, outside the ETR Core region, to seal the cadmium in place. Containment is thus assured even in the event the cadmium were to melt due to excessive gamma heating or loss of ETR cooling water flow through the core filler piece annulus.

The described process for encapsulation and quality control during fabrication should preclude the possibility of voids between the filter and surrounding stainless steel, thereby eliminating possible sites for water nucleation should a failure of the sheath occur. If, however, it is postulated that the sheath fails, the most likely area would be at the top or bottom weld. Water leaking into these relatively cold regions would not likely mitigate to the filter midplane because of the design features mentioned previously. Nevertheless, it is assumed that water does find a path between the secondary tube and cadmium to reach the midplane, or hottest region. This would tend to cool the filter, but ignoring this effect the resulting saturated steam pressure corresponding to the maximum hot spot temperature at the inner cadmium to stainless steel interface would be 500 psi. The resultant hoop stress in the sheath is well below the elastic limit and no yielding would occur that would affect the cadmium bond. Thus, the postulated water leak would not provide a mechanism for displacement of the cadmium filter.

As shown in Fig. 13.1, the FEFPL core filler piece is a 44-1/8 in. long aluminum block which adapts the circular loop to the square ETR core grid configuration. Splines at two elevations on the internal surface of

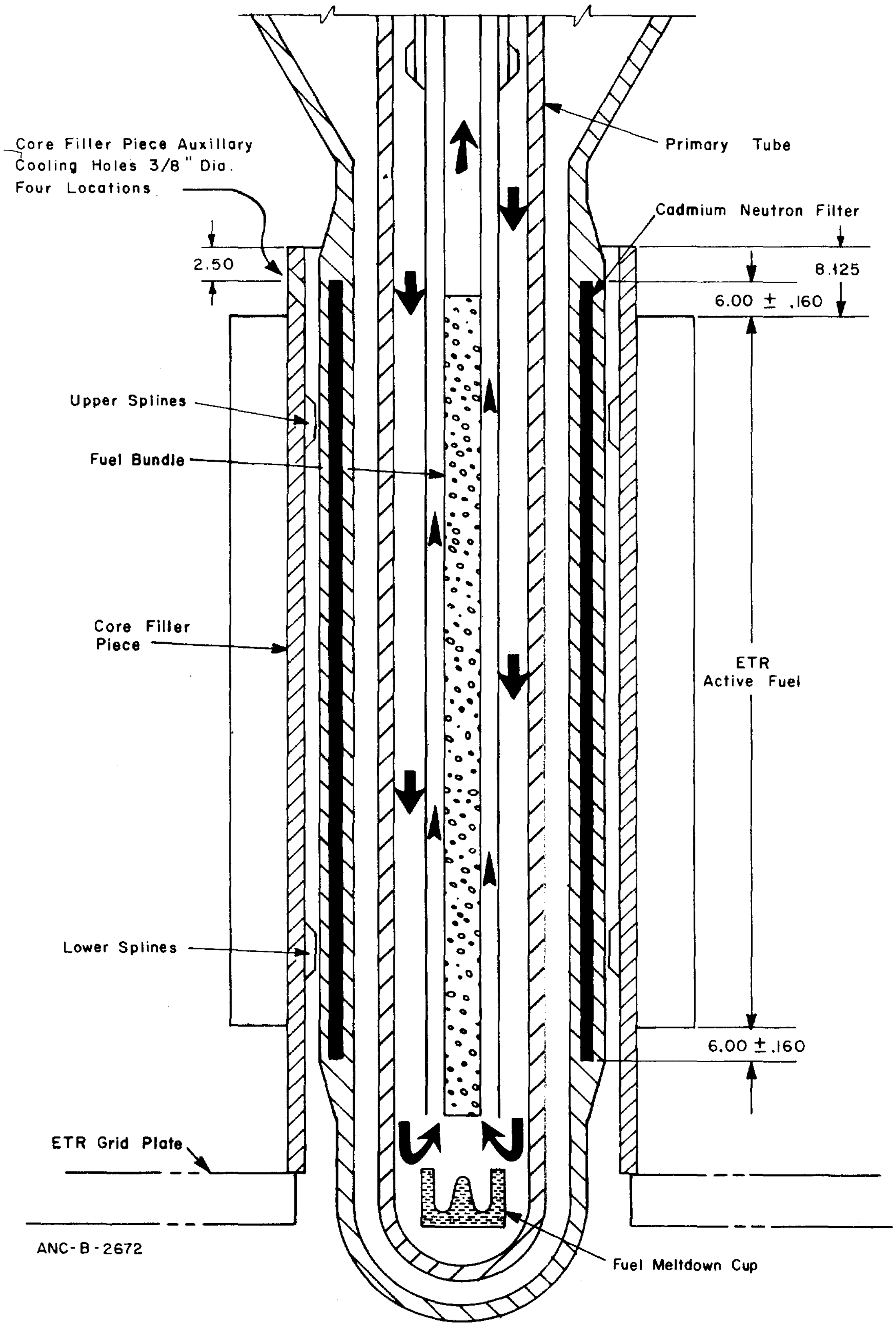

FIG. 13.1 - ETR/FEFPL Inpile Tube, Neutron Filter and Core Filler Piece Schematic

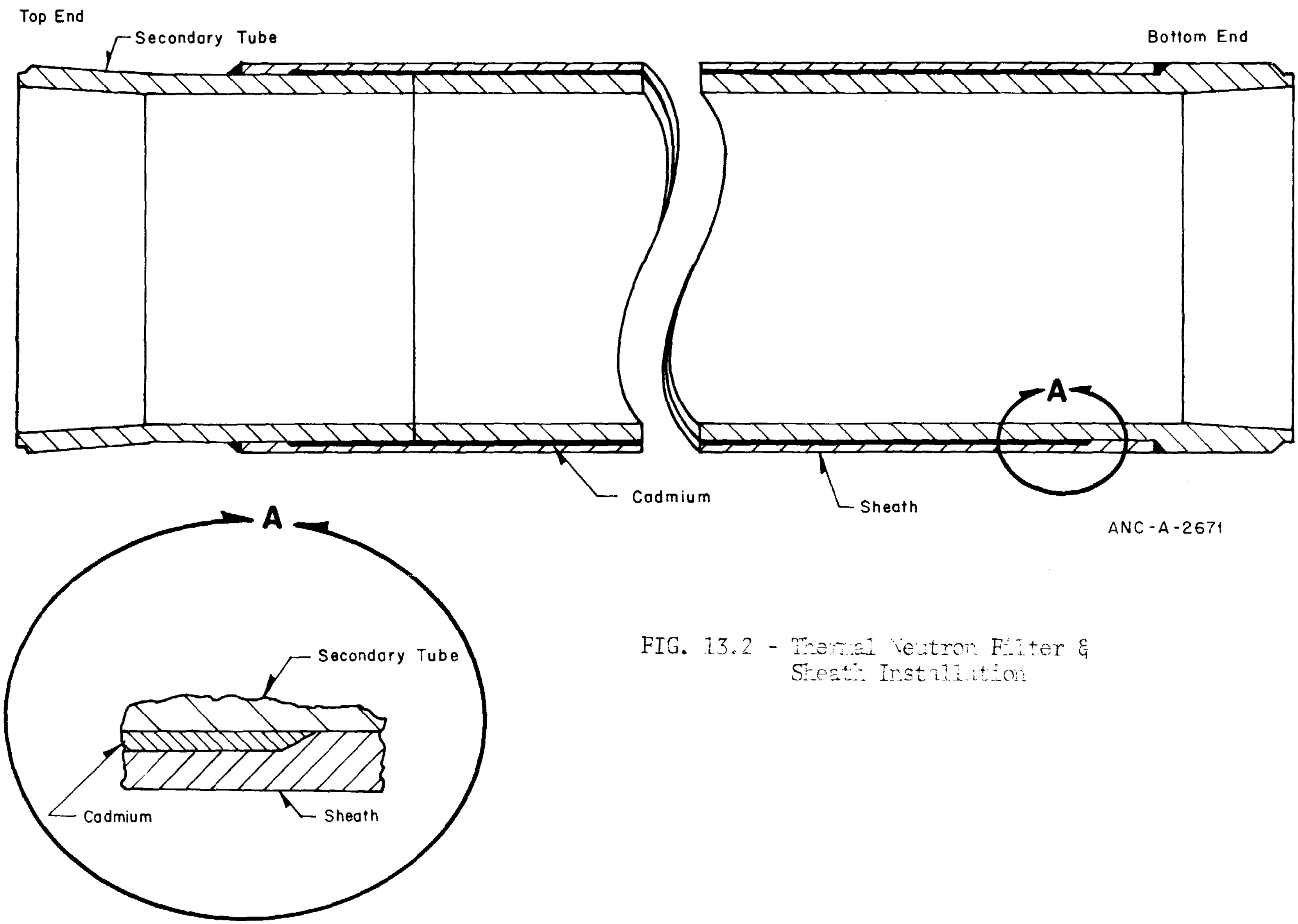

FIG. 13.2 - Thermal Neutron Filter & Sheath Installation

the core filler piece, center the tube and maintain the cooling water flow annulus between the tube and filler piece.

The top of the core filler piece is elevated approximately 8 in. above the active core to minimize the possibility of blockage of the flow annulus.

The core filler piece design incorporates four 3/8-in. diameter auxiliary cooling holes 2-1/2 in. below the top of the core filler piece which provide a minimum of 36% normal annulus cooling water flow at the minimum core ΔP in the unlikely event of complete blockage of the flow annulus inlet.

Protection against cadmium melting is provided by FEFPL-PPS Function C which monitors secondary containment temperature near the core midplane. As demonstrated in the Chapter 7 discussion of this protective function, even for the extreme accident condition summarized below, a substantial positive margin to cadmium melting is maintained without ETR scram.

Accident	Max. Cd Temp.	Margin to Melting without Scram
a) 131% step overpower with 20% flux tilt	412°F	197°F
b) 80% CFP flow blockage with 20% flux tilt	472°F	137°F

As discussed in Chapter 7, it was thus necessary to assume a 150% axisymmetric gamma heating rate in addition to the 80% flow blockage with 20% flux tilt in order to establish a relationship between the threshold of cadmium melting at the hot spot and the monitored variable and thus a worst case setpoint. Under these conditions, only 7.3 in. of cadmium axial length at the hot spot orientation would reach the critical variable limit of 609°F if unprotected.

Based on a study[19] conducted in conjunction with the design of the TNF, it is concluded that the temperature required for attack of the stainless steel sheath by molten cadmium is unachievable under the accident conditions described, and further, that if attack were to occur it would not be sufficient to impair the integrity of the sheath over a 70-day full power operating life.

The preceding discussion strongly supports the conclusion that complete loss of the TNF is hypothetical, however, this accident is pursued to its completion to assess the inherent safety margins relative to protection of the reactor facility and general public.

To provide a path for loss of cadmium, the following hypothetical sequence of events must be postulated:

a) nearly complete blockage of cooling water around FEFPL secondary containment with reactor overpower

or

ETR loss of flow or power excursion without scram,

b) failure of FEFPL-PPS to sense overheating of cadmium or failure of ETR-PPS to respond to scram signal,

c) whole or partial melting of cadmium,

d) failure of stainless steel protective sheath at a site that permits significant loss of molten cadmium.

Four low-probability failures must occur in a mutually compatible fashion in order to lose cadmium, thus, this accident is considered to be hypothetical. Nevertheless, even if this should happen, it can be shown that tolerable reactivity additions result for physically realistic rates of cadmium motion. For holes in the stainless steel protective sheath that are postulated to be large, the melting rate can be controlling; whereas, for smaller ones, the exit and falling times may dominate.

Although not considered credible based on the conditions identified as required, it is assumed that TNF does become molten without detection. Thus, in a stagnant coolant condition, it would take in excess of one second due to gravity alone for the cadmium to leave the core region assuming it is lumped at the core midplane. Further time would be required for the molten cadmium to move within the 0.040-in. thick containment sheath to the site of a possible fault, thus, instantaneous loss of the cadmium filter is considered incredible. Compared to the allowances made for ramp insertions in the Technical Specifications, which deals in msec, any postulated hypothetical FEFPL ramp would be considered as slow, and hence, is not presently restricted by specific requirements.

An analysis[12] using the ANC PARET computer code has been performed to determine the effect of cadmium loss for various ramp insertion rates. Due to the difficulty of postulating a feasible mechanism for losing the filter, it was assumed that the loss would be radially linear with time. Only the scram rod insertion was considered for negative reactivity insertion (i.e., the negative temperature coefficient was neglected, which is conservative). The energy generated for the time period that the reactor was above 150% of 175 MW (262.5 MW) was shown to be less than 11 MW sec for ramp times of 2 sec or more. Duration above this power level trip point was 0.165 sec for the 2 sec ramp and .040 sec for ramps of 3 sec or longer. Peak power levels were less than 266 MW or only 2% above the trip level. These results indicate that the reactor control system greatly attenuates the effect of ramp cadmium loss. Thus, no damage to the ETR core or FEFPL fuel would result.

13.3 FS&R Sodium Fire Analyses for Hypothetical Conditions

13.3.1 General

Sodium fire analysis for the FS&R Charging Facility and Test Cell Enclosure are presented in SAR Section 12.3 for the postulated design basis accidents. None of these endanger the ETR or operating personnel by propagating to other portions of the ETR facility. In this section, margins beyond the design basis analysis are assessed by considering hypothetical sodium spills and pool burn areas that are larger than previously discussed.

Because this analysis represents conditions beyond the DBA analysis, it is suggested that Section 12.3 be reviewed for background information on test train contamination, accident basis, pool burn area, ventilation operation and method of analysis. As before, the AI SOFIRE II and HAA-3 codes are used for sodium pool fire and aerosol release analyses, respectively. Therefore, the approach to be taken in this section is to present the analysis followed by a discussion of the consequences to the ETR facility and operating personnel.

13.3.2 Sodium Fire Analysis

13.3.2.1 Charging Facility

The maximum hypothetical spill for the Charging Facility is determined to be 492 pounds of sodium that spills over an area of 278 square feet.[13] This represents the entire sodium inventory within the Charging Facility. The area represents the entire burn pan area.

The SOFIRE II analysis for ventilation rates of 10,380 cfm, 1,500 cfm and 100 cfm (closed inlet louvre) are presented in Table 13.1 (Cases 1, 1N, and 2, respectively). The most severe pressure condition, Case 2 (100 cfm), represents a condition in which the inlet louvre is closed with the fan on low speed. The peak ΔP reaches +8.2 in. of water for a brief period.

The trends discussed in Section 12.3.5.1 generally apply in this analysis as well.

13.3.2.2 Test Cell

A hypothetical sodium spill in the Test Cell is less severe than the foregoing event postulated for the Charging Facility because:

a) the quantity of sodium that can be released is less than for the Charging Facility,

b) the maximum Test Cell burn pan area is less than available in the Charging Facility, and

c) the Test Cell enclosure volume is greater than for the Charging Facility.

13.3.2.3 Aerosol Release

The atmosphere release of sodium oxide was calculated for the Charging Facility hypothetical spill of 492 pounds of sodium. The resulting sodium monoxide release for maximum ventilation rates is calculated to be 330 pounds.[14] Aerosol release concentrations are calculated using a 1500 cfm ventilation rate, as this rate represents minimum dilution thus the highest concentration even though the burn time is longer. As discussed in 12.3.5.3, it is assumed that 50% of the burned sodium is released from the fire as sodium monoxide.

13.3.3 Consequences

13.3.3.1 Charging Facility

As shown in Table 13.1, the hypothetical spill sodium fire is satisfactorily contained within the Charging Facility enclosure during normal or large ventilation flowrates. This conclusion is confirmed by:

a) The maximum wall Δ pressures are less than the ±4 in. of water design limit. A negative peak ΔP of -3.60 was the most severe case (#1).

b) As indicated by the ceiling liner temperature results, concrete block wall and ventilation ducting temperatures fall within acceptable material limits.

c) Because an intumescent mastic coating (ALBI-89) is used as a fire retardant and insulator for the ceiling, softening of the asphalt roof is prevented. The amount of maximum temperature reduction that can be expected due to this design feature is shown in the comparison cases of 2 and 2A. The latter, which represents the coating case, shows 114°F for the maximum ceiling liner temperature.

d) The burn pan and concrete floor temperatures are less than shown for the DBA cases.

For the condition where the ventilation flowrate is 100 cfm, the pressure conditions are the most severe. In particular, this applies to the wall differential pressure which reaches +8.2 in. of water. As shown

TABLE 13.1

Summary of Charging Facility Enclosure
Analysis Results for Hypothetical Sodium Fires[1]

	Case 1	Case 1N	Case 2	Case 2A[4]
Sodium spill, lbs	492	492	492	492
Spill area, ft^2[2]	278	278	278	278
Ventilation rate, cfm[3]	10,350	1,500	100	100
Time of burn, hrs	0.72	1.24	2.61	2.33
Initial ΔP, in. of water	-3.60	-0.11	+8.2	+8.1
ΔP at end of burn	-1.00	-0.03	-0.90	-0.89
Max gas temp, °F	470	605	650	336
Max ceiling liner temp, °F	307	414	465	114
Max burn pan temp, °F	1,017	880	676	696
Max concrete floor temp, °F	95	95	95	95

Notes:

(1) Data from Ref. 2 (AI-73-32).

(2) Total spill is assumed to occur instantaneously.

(3) Vent rate during the fire is assumed to be conducted as a step change at the same time as the spill.

(4) Includes intumescent mastic coating on the ceiling liner.

in Fig. 13.1, the ±4 in. of water ΔP design criteria is surpassed for a period of about 40 sec. Actual strength of the wall allows for 6.9 in. of water ΔP before containment breeching would occur.[18] This pressure spike has been conservatively calculated since all 492 pounds of sodium within the system is assumed to spill instantaneously. Based on the conservatism of this analysis, actual breech of the facility wall would be extremely unlikely even in the event of the described hypothetical charging facility sodium spill. As discussed for the other ventilation rates, the enclosure temperatures remain within the material limits.

13.3.3.2 Test Cell

Because the test cell has a larger volume and smaller sodium inventory, a hypothetical spill can be safely contained.

If the hypothetical spill should occur with the hatchway open (e.g., hatchway opening is due to damage caused by a hypothetical drop of the LHM) the pressure pulse is sufficiently attenuated and temperatures will be lower than for an enclosed Test Cell. Although the ventilation system could be used to draw the smoke out the roof vents, some release within the ETR facility would be likely.

13.3.3.3 Aerosol Release

As mentioned in Section 12.3.6.3, sodium oxide given off as an aerosol may present two potential problems: alpha contamination when a preirradiated test train is installed in the FEFP Loop and toxicity due to sodium monoxide. The hypothetical Charging Facility spill represents a release of about 10 times the sodium monoxide that is discussed in Section 12.3.6.3 for the DBA spill; however, the burn time is longer by 2 to 3 times for the same ventilation rate.

For the release due to the DBA spill, it was shown that the ground level concentration at the point of concern outside the ETR facility was 1.29×10^{-13} μCI/ml. The hypothetical spill would increase this concentration to about 1×10^{-12} which is a factor of ten below the AEC limits for plutonium in a restricted area.[16, 17]

For the hypothetical release of 330 pounds of sodium monoxide from the roof vent, the concentration at ground level is about 10 times greater than the amount shown for the DBA case in Section 12.3.6.5 or

FIG. 13.3. Pressure-temperature History for Charging Facility Hypothetical Sodium Pool Fire (Case 2)

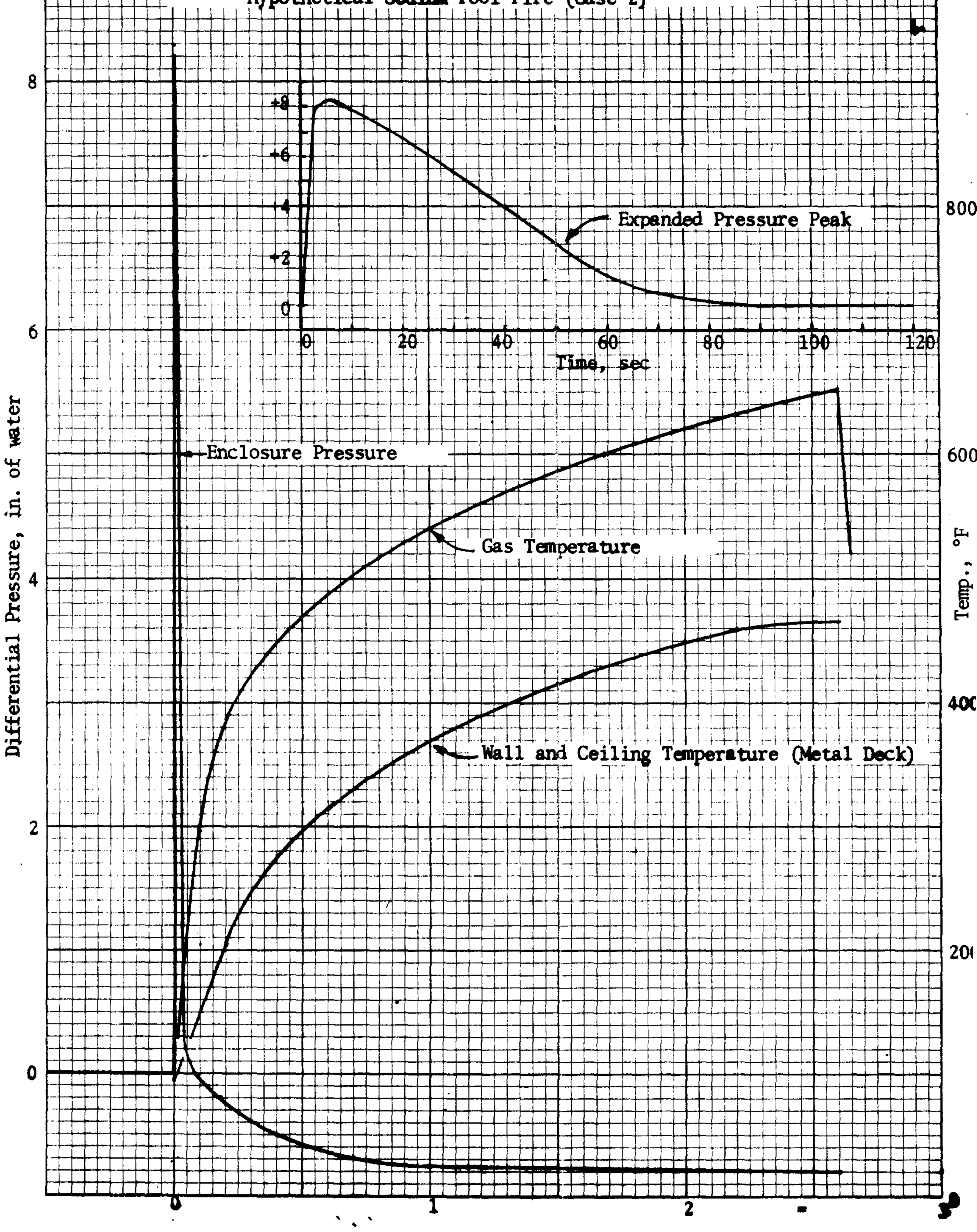

about 0.47 gms/m^3. There are many areas exterior to the facility that can be reached where personnel could go to avoid the sodium monoxide aerosol.

For the Test Cell hypothesized spill with the damaged hatchway, some of the aerosol settles within the ETR facility. If a preirradiated test train were installed in the loop, alpha contamination would be present. The previous discussion indicates that the magnitude is small. However, radiation monitoring would be used to detect any activity. If the levels should reach facility operating limits, the ETR emergency evacuation plan would be implemented.

13.3.3.4 Summary

It has been shown in the foregoing discussions that the hypothetical fires remain within the respective enclosures and do not propagate to the rest of the ETR facility; hence, the ETR is not damaged. Also, personnel within the building are not affected since the air will flow into the enclosure and out the vent. In the event of a damaged hatchway as discussed for the Test Cell, smoke will likely enter the ETR facility. Radiation monitoring will provide warning of activity to personnel, so evacuation measures can be implemented if deemed necessary.

The hypothetical spill provides greater contamination and sodium monoxide in the aerosol release compared to the DBA spill. However, the conclusions reached for the DBA analysis summary still apply. The contamination exposure concentration outside the ETR is well below the AEC limits.

References

1. B. L. Harris, "Secondary Vessel Allowable Pressures at Design Temperatures," ANC FEFPL EDF-560 (December 7, 1972).

2. ANC FDR-10, FEFPL Annulus Gas System Design Requirements, (April 3, 1972).

3. S. A. Atkinson, et. al., "Design Basis Analysis for the ETR Phase II Technical Specifications," CI-1231, (February 1972)

4. R. C. Gottula, "Analysis of Hypothetical Accident Leaks of Sodium and Water in FEFP Loop," ANC-GOTT-7-72 (December 19, 1972).

5. H. L. Magleby, "Leak of Primary and Secondary Tubes," ANC FEFPL EDF 494A, (October 11, 1972).

6. R. D. Pierce, et. al., "Design Criteria and Evaluation of a Meltdown Cup for the Fuel Element Failure Propagation Loop," (to be published).

7. L. J. Siefken, "Pressure Pulse Related to the Water-aluminum Interaction During an ETR Design Basis LOCA," ANC FEFPL EDF-707, (February 28, 1973).

8. L. J. Siefken, "Water-aluminum Pressure Pulse Calculations for Hypothetical Core Meltdowns," ANC FEFPL EDF-736, (March 8, 1973).

9. E. E. Walker and G. W. Tunnel, "Fast Ceramic Reactor Development Program Soda-Pop Testing," NEDM-12063, (December 31, 1969).

10. "Safety Study for the Fuel Element Failure Propagation Loop in the ETR," ANL/RAS-04, (October 30, 1970).

11. S. A. Atkinson, et al., "ETR Technical Specifications," CI-1233, (July 22, 1971).

12. J. H. Lofthouse, "Summary of ETR-FEFPL Accident Calculations of Cd Filter Melt and Annulus Flooding," Attachment 1 to ANC FEFPL Project EDF-727, (March 2, 1973).

13. W. R. Bird, "Charging Facility Enclosure and Test Cell Sodium Fire Evaluation," ANC FEFPL Project EDF-848 (June 15, 1973).

14. L. Baurmash and R. L. Koontz, "Evaluation of Sodium Pool Fires in FEFPL," AI Report AI-73-32 (April 30, 1973).

15. W. R. Bird (EDF report to be published).

16. AEC Manual, Chapter 0524, Standards for Radiation Protection (November 8, 1968).

17. W. R. Bird, Revised Aerosol Release Input for SAR, ANC EDF-1195, December 17, 1973.

18. N. Smith, Review of Charging Facility Wall for Maximum Uniform Load, ANC EDF-1189, December 17, 1973.

19. ANC Report, FR-189, Section 8 Thermal Neutron Filter Design Report, Vol. 1, (March 1974).

APPENDIX A

TABLE OF CONTENTS

LIST OF TABLES

LIST OF FIGURES

A.0 Safety Fault Trees

A.1 Summary

This appendix is a compilation of fault trees that have provided a framework for the accidents analyzed in Chapter 11.

These fault trees provide insight into the inter-relationships among possible events and, as such, serve as one tool to assist in the safety analysis of the overall system. Because the individual accidents identified by the fault trees are considered in the body of the report, no further discussion of each tree is provided here.

In addition, this chapter contains an Accident Summary Table. This table is based on the formalism outlined in RDT Standard C 16-1T which requires identification of fault events, classification as to probability and comparison with consequences. Table A.1.1 combines fault events described in the SAR text, the previous accident summary table which A.1.1 supersedes and additional events logically related to events identified in the text. With the fault events thus identified, probability of occurrence (likelihood) has been assigned. These assignments are, in some instances, made subjectively, but are considered conservative. The consequences assigned in the table are those derived from the accident discussions in the text. Where a particular accident is not explicitly treated, an analysis is identified which bounds the event considered. Finally, the accidents discussions are cross referenced by SAR page number.

TABLE A.1.1

FEFPL ACCIDENT SUMMARY TABLE

Fault Event	Assumed Mitigating Systems and Conditions	Net Likeli-hood	Analysis	Experiment Consequence	Vessel Integrity Primary	Vessel Integrity Secondary	Treated
1. He Flow Blockage 10%	EAS-control and/or PPS or none	A	Bounded by 5, 6, and 7	Class I	OK	OK	Yes
2. He Flow Blockage 30%	EAS-control and/or PPS or none	U	Bounded by 8, 9, and 10	Class I	OK	OK	Yes
3. He Flow Blockage 50%	EAS-control and/or PPS or none	EU	Bounded by 11, 12, and 13	Class I or II	OK	OK	Yes
4. He Flow Blockage 100%	EAS-control and/or PPS or none	H	Bounded by 14, and 15	Class I or II	OK	OK	Yes
5. Loss of one He Circulator	EAS-control PPS	A	Treated 11-93	Class I	OK	OK	Yes
6. Loss of one He Circulator	PPS only	U	Treated 11-96 Scram not reached	Class I	OK	OK	Yes
7. Loss of one He Circulator	None	H	Same as 6	Class I	OK	OK	No
8. Loss of two He Circulators	EAS-control PPS	A	Treated 11-95	Class I	OK	OK	Yes
9. Loss of two He Circulators	PPS only	U	Treated 11-96 Scram not reached	Class I	OK	OK	Yes
10. Loss of two He Circulators	None	H	Same as 9	Class I	OK	OK	No
11. Loss of three He Circulators	EAS PPS	U	Treated 11-96	Class I	OK	OK	Implicitly

Fault Event	Assumed Mitigating Systems and Conditions	Net Likelihood	Analysis	Experiment Consequence	Vessel Integrity Primary	Vessel Integrity Secondary	Treated
12. Loss of three He Circulators	PPS only	EU	Treated 11-96	Class II	OK	OK	Yes
13. Loss of three He Circulators	None	H	Bounded by 19	Class III	OK	OK	No
14. Loss of All He Circulators	EAS PPS	EU	Treated 11-96	Class I	OK	OK	Implicitly
15. Loss of All He Circulators	PPS only	H	Treated 11-96	Class II	OK	OK	Yes
16. General He System Breach	EAS and/or PPS	U	Same as 17, 18	Class I or II	OK	Failed Out-of-vessel	No
17. Breach at Circulators	EAS PPS	U	Treated 11-106 Bounded by 14	Class I	OK	Failed Out-of-vessel	Yes
18. Breach at Circulators	PPS only	EU	Bounded by 15	Class II	OK	Failed Out-of-vessel	No
19. Breach at Circulators	None	H	Bounded by 49	Class III	OK	OK	No
20. He Flow Control Failure-with Bypass	EAS PPS	A	Treated 11-92 No effect	Class I	OK	OK	Yes
21. He Flow Control Failure-without Bypass	EAS PPS	U	Bounded by 14, 15	Class I or II	OK	OK	No

Fault Event	Assumed Mitigating Systems and Conditions	Net Likeli-hood	Analysis	Experiment Consequence	Vessel Integrity		Treated
					Primary	Secondary	
22. Actuate He Relief Valve with Makeup	EAS PPS	A	Bounded by 5, 8, 11, or 14	Class I	OK	OK	No
23. Actuate He Relief Valve with Makeup-No Reseat	EAS PPS	U	Bounded by 5, 8, 11, or 14	Class I	OK	OK	No
24. Actuate He Relief Valve with Makeup-No Reseat	PPS Only	'EU	Bounded by 6, 9, 11, or 15	Class I or II	OK	OK	No
25. Actuate He Relief Valve with No Reseat or Makeup	PPS Only	EU	Bounded by 15	Class II	OK	OK	No
26. Loss of Comm. Power to Circulators for He	EAS and/or PPS or none	A	Bounded by 8, 9, 10 Treated 11-95	Class I	OK	OK	Yes
27. Loss of Diesel Power to Circulators	EAS and/or PPS or none	A	Bounded by 8, 9, 10 Treated 11-95	Class I	OK	OK	Yes
28. Loss of All Power to Circulators	EAS and/or PPS	EU→H	Bounded by 14, 15	Class I or II	OK	OK	Yes
29. Overpressure of He from Makeup with Relief Valve	EAS and/or PPS	A→H	Bounded by 22, 23, 24, 25	Class I or II	OK	OK	No
30. Overpressure from He Makeup-No Relief Valve	EAS and/or PPS	U→H	Bounded by 16	Class I or II	OK	OK	No
31. Loss of He Makeup from Loss of Control Power	EAS and/or PPS	A→H	Bounded by 5 through 10	Class I	OK	OK	No

Fault Event	Assumed Mitigating Systems and Conditions	Net Likeli-hood	Analysis	Experiment Consequence	Vessel Integrity		Treated
					Primary	Secondary	
32. Water in He System	EAS and/or PPS	U→H	Bounded by 38, 39 Treated 11-104	Class I or II	OK	Failed Out-of vessel	Yes
33. Loss of Water from Secondary HX	EAS PPS	A	Treated 11-101	Class I	OK	OK	Yes
34. Loss of Water from Secondary HX	PPS Only	U	Treated 11-101 No PPS Scram Req'd	Class II	OK	OK	Yes
35. Loss of Water from Secondary HX	None	H	Same as 34	Class II	OK	OK	Implicitly
36. Loss of HDW Supply for Secondary HX	EAS and/or PPS	A→H	Treated 11-99 Bounded by 33, 34, 35	Class I or II	OK	OK	Yes
37. Failure He Temperature Control	EAS and/or PPS	A→H	Treated 11-97 Bounded by 33, 34, 35	Class I or II	OK	OK	Yes
38. Failure of One Secondary HX	EAS and/or PPS	U→H	Bounded by 33, 34	Class I	OK	Possibly Failed Out-of-vessel	No
39. Failure of Both Secondary HX's	EAS and/or PPS	EU→H	Bounded by 33, 34	Class I or II	OK	Possibly Failed Out-of-vessel	No

Fault Event	Assumed Mitigating Systems and Conditions	Net Likeli-hood	Analysis	Experiment Consequence	Vessel Integrity		Treated
					Primary	Secondary	
40. Leak in Primary Side of FEFPL Heat Exchanger	PPS/Positive Pressure	U	Treated 11-86	Class II	Failed	OK	Yes
41. Leak in Primary Side of FEFPL HX & Na Out	None	EU	Treated 11-87	Class III	Failed	OK	Yes
42. Design Error Failing to Get Sufficient He Cooling	EAS-Control and/or PPS	A→H	Bounded by 5 through 15	Class I, II, or III	OK	OK	No
43. Loss of One Section of ALIP	EAS-Control	A	Treated 11-40	Class I	OK	OK	Yes
44. Loss of One Section of ALIP	None	U	Treated 11-41	Class I	OK	OK	Yes
45. Loss of Two Sections of ALIP	EAS-Control	U	Treated 11-42	Class I	OK	OK	Yes
46. Loss of Two Sections of ALIP	None	EU	Treated 11-42	Class I	OK	OK	Yes
47. Loss of Three Sections of ALIP	EAS-Control and Power Transfer	A	Treated 11-42	Class I	OK	OK	Yes
48. Loss of Three Sections of ALIP	EAS-Control or Power Transfer	U	Treated 11-52	Class II	OK	OK	Yes
49. Loss of Three Sections of ALIP	None	EU	Treated 11-59	Class III	OK	OK	Yes
50. Two ALIP Shorts to Enable Attack of Primary Cont.	Circuit Breaker EAS	U	Treated 11-67	Class II	OK	OK	Yes

Fault Event	Assumed Mitigating Systems and Conditions	Net Likeli-hood	Analysis	Experiment Consequence	Vessel Integrity		Treated
					Primary	Secondary	
51. Two ALIP Shorts to Enable Attack of Primary Cont.	EAS Only	EU	Treated 11-67	Class II	Failed	OK	Yes
52. Two ALIP Shorts to Enable Attack of Primary Cont.	None	H	Treated 11-68	Class III	Failed	OK	Yes
53. Power Reversal to ALIP	EAS	H	Treated 11-58	Class II	OK	OK	Yes
54. Up to 90% Test Section Blockage	EAS PPS	A	Treated 11-72	Class I	OK	OK	Yes
55. Up to 90% Test Section Blockage	PPS Only	U	Treated 11-72 PPS Not Needed	Class I	OK	OK	Yes
56. Up to 90% Test Section Blockage	None	H	Same as 55	Class I	OK	OK	Yes
57. Up to 90% Loop Blockage	EAS PPS	A	Treated 11-74	Class I	OK	OK	Yes
58. Up to 90% Loop Blockage	PPS Only	U	Treated 11-74 PPS Not Needed	Class I	OK	OK	Yes
59. Up to 90% Loop Blockage	None	H	Same as 58	Class I	OK	OK	Yes
60. Total Test Section Blockage	EAS PPS	U	Treated 11-74	Class II	OK	OK	Yes
61. Total Test Section Blockage	PPS Only	EU	Treated 11-75	Class III	OK	OK	Yes

Fault Event	Assumed Mitigating Systems and Conditions	Net Likeli-hood	Analysis	Experiment Consequence	Vessel Integrity Primary	Vessel Integrity Secondary	Treated
62. Total Loop Blockage	EAS PPS	EU	Treated 11-74	Class II	OK	OK	Yes
63. Total Loop Blockage	PPS Only	H	Treated 11-75	Class III	OK	OK	Yes
64. Excessive ALIP Vibration	-	-	Yet to be Performed	-	-	-	No
65. Overpower to ALIP Coil	EAS-Control and/or PPS or None	A→H	Bounded by 54 through 63	Class I or III	OK	OK	No
66. Design or Control Error Failing to Provide Sufficient Flow	EAS and/or PPS or None	A→H	Bounded by 54 through 63	Class I or III	OK	OK	No
67. Sodium Filter Failure	EAS and/or PPS or None	A→H	Bounded by 54 through 59	Class I	OK	OK	Implicitly
68. Primary Vessel Failure or Seals	PPS/Positive Pressure	U	Treated 13-7	Class II	Failed	OK	Yes
69. Primary Vessel Failure or Seals	None	H	Treated 13-8	Class III	Failed	OK	Yes
70. Design Error for Primary Within Design Margin	PPS/Positive Pressure or None	A	No Effect	Class I	OK	OK	No
71. Design Error for Primary Outside Design Margin	PPS/Positive Pressure or None	U→H	Bounded by 68, 69	Class II or III	Failed	OK	No
72. High Primary Internal Static Pressure	PPS or None	A→H	Bounded by 70, 71	Class I, II or III	OK or Failed	OK	No

Fault Event	Assumed Mitigating Systems and Conditions	Net Likelihood	Analysis	Experiment Consequence	Vessel Integrity Primary	Vessel Integrity Secondary	Treated
73. Error for γ Heating of Primary Vessel	PPS or None	A→H	Bounded by 70, 71	Class I, II, or III	OK or Failed	OK	No
74. Faulty Construction of Primary	PPS/Positive Pressure or None	U→H	Bounded by 68, 69	Class II or III	Failed	OK	No
75. Chemical Attack of Primary	PPS or None	A→H	Bounded by 70, 71	Class I, II, or III	OK or Failed	OK	No
76. Secondary Vessel or Seals Failure	PPS/Positive Pressure	U	Treated 13-9	Class I	OK	Failed	Yes
77. Secondary Vessel or Seals Failure	None	H	Treated 13-9	Class I	OK	Failed	Yes
78. Design Error of Secondary Vessel-Within Design Margin	PPS/Positive Pressure or None	A	No Effect	Class I	OK	OK	No
79. Design Error for Secondary Vessel-Outside Margin	PPS/Positive Pressure or None	U→H	Bounded by 76, 77	Class I	OK	Failed	No
80. High Annulus Pressure	PPS or None. Regulators and Two Reliefs	A→H	Bounded by 78, 79 Treated 13-7	Class I	OK	OK or Failed	Yes
81. Chemical Attack on Secondary Vessel	PPS or None	A→H	Bounded by 78, 79	Class I	OK	OK or Failed	No
82. Error for γ Heating of Secondary Vessel	PPS or None	A→H	Bounded by 78, 79	Class I	OK	OK or Failed	No

Fault Event	Assumed Mitigating Systems and Conditions	Net Likeli-hood	Analysis	Experiment Consequence	Vessel Integrity		Treated
					Primary	Secondary	
83. Faulty Construction of Secondary Vessel	PPS/Positive Pressure or None	U→H	Bounded by 76, 77	Class I	OK	Failed	No
84. Leak of FEFPL HX of He to Annulus Side	PPS/Positive Pressure	U	Treated 11-86	Class I	OK	OK	Yes
85. Leak of FEFPL HX of He to Annulus Side	PPS Only	EU	Treated 11-86	Class II	OK	OK	Yes
86. Failure of FEFPL HX	EAS, PPS	U→H	Treated 13-3 Bounded by 84, 85, 16, 40, 41	Class I, II, or III	OK or Failed	OK	Yes
87. Design Error in FEFPL HX Within Design Margin	None	A	No Effect	Class I	OK	OK	No
88. Design Error in FEFPL HX Outside of Margin	EAS, PPS	U→H	Bounded by 86	Class I or II	OK or Failed	OK	No
89. Overpressure of ETR Water Relative to Annulus	PPS/Positive Pressure or None	A→H	Bounded by 78, 79	Class I	OK	OK or Failed	No
90. Air or Argon in Gas Annulus	EAS and/or PPS	A→H	To be Examined	-	-	OK	No
91. Blockage or Overtemp. of ETR Water Cooling Second.	PPS or None	A→H	Treated 11-107	Class I	OK	OK	Yes
92. Loss of ETR Water Cooling for ALIP	EAS	EU	No Cooling Req'd	Class I	OK	OK	No

Fault Event	Assumed Mitigating Systems and Conditions	Net Likelihood	Analysis	Experiment Consequence	Vessel Integrity		Treated
					Primary	Secondary	
93. Failure of Annulus Cooling System	None	A	Treated 10-67	Not Applicable	OK	OK	Yes
94. ETR DBA Loss-of-Cooling	PPS/Positive Pressure ETR PPS Annulus Relief Valves	H	Treated 13-6 and 11-112	Class I	OK	OK	Yes
95. Excessive Power Generation in Test Within Design Envelope at Full Power	EAS-Control PPS	A	Within Control Envelope Treated 6-13	Class I	OK	OK	Implicitly
96. Excessive Power Generation in Test Within Design Envelope at Full Power	PPS Only	U	Bounded by 49	Class II or III	OK	OK	No
97. Excessive Power Generation in Test Within Design Envelope at Full Power	None	H	Same as 96	Class II or III	OK	OK	No
98. Excessive Power Generation in Test Outside Design Envelope at Full Power	EAS Control PPS	U→EU	Bounded by 95, 96	Class II or III	OK	OK	No
99. Excessive Power Generation in Test Outside of Design Envelope at Full Power	None	H	Bounded by 96	Class II or III	OK	OK	No

Fault Event	Assumed Mitigating Systems and Conditions	Net Likeli-hood	Analysis	Experiment Consequence	Vessel Integrity		Treated
					Primary	Secondary	
100. FEFPL Support Loading During Handling and Operation	Loop Lateral Supports	A	Treated 12-31, 11-117, and 9-22	Not Applicable	OK	OK	Yes
101. FEFPL Support Loadings with One Failed Support	Remaining Supports	U	Handling Treated Treated 12-31	Not Applicable	OK	OK	Yes No
102. ETR Reactivity Excursion	EAS-Control PPS	A→EU	Less than 103	Class I	OK	OK	Implicitly
103. ETR DBA Reactivity Excursion	EAS or PPS and ETR PPS	EU	Treated 11-111	Class I or II	OK	OK	Yes
104. ETR DBA Reactivity Excursion	ETR PPS Only	H	Same as 103	Class I or II	OK	OK	Yes
105. Incorrect Sample Per-formance Prediction	EAS-Control and/or PPS or None	A→H	Bounded by 95 through 99	Class I, II, or III	OK	OK	No
106. Water in Gas Annulus	PPA/Pos. Pressure-None	EU→H		Class I to III	OK	Failed	Yes
107. Incorrect Neutron Filter Performance	EAS-Control and/or PPS or None	A→H	Bounded by 95 through 97	Class I, II, or III	OK	OK	No
108. Reactor Operational Error	EAS-Control and/or PPS or None	A→H	Bounded by 95 through 99	Class I, II, or III	OK	OK	No
109. Incorrect Sample Composition	EAS-Control and/or PPS or None	A→H	Bounded by 105 see also 10-13	Class I, II, or III	OK	OK	Implicitly

Fault Event	Assumed Mitigating Systems and Conditions	Net Likeli-hood	Analysis	Experiment Consequence	Vessel Integrity		Treated
					Primary	Secondary	
110. Loss of Commercial Power to Loop and ETR	EAS PPS	A	Treated 11-23	Class I	OK	OK	Yes
111. Loss of Commercial Power to Loop and ETR	ETR PPS Only Direct on Power Loss	U	Treated 11-24	Class II	OK	OK	Yes
112. Loss of Commercial Power to Loop and ETR	ETR PPS Only or ETR Indirect	EU	Treated 11-26	Class III	OK	OK	Yes
113. Loss Of Commercial Power to Only Loop	EAS PPS	A	Treated 11-27	Class I	OK	OK	Yes
114. Loss of Commercial Power to Loop Only	PPS Only	U	Treated 11-29	Class II or III	OK	OK	Yes
115. Loss of Commercial Power to Loop Only	None	H	Bounded by 49	Class III	OK	OK	No
116. Loss of All Power to Loop and ETR	EAS PPS	EU	Treated 11-31	Class II	OK	OK	Yes
117. Loss of All Power to Loop and ETR	PPS Only	H	Treated 11-35	Class III	OK	OK	Yes
118. Loss of All Power to Loop Only	EAS PPS	U	Treated 11-36, and 11-29	Class II	OK	OK	Yes
119. Loss of All Power to Loop Only	PPS Only	EU	Treated 11-37, and 11-29	Class III	OK	OK	Yes

Fault Event	Assumed Mitigating Systems and Conditions	Net Likeli-hood	Analysis	Experiment Consequence	Vessel Integrity Primary	Vessel Integrity Secondary	Treated
120. Loss of Cadmium Filter	EAS and/or PPS, ETR PPS	H	Treated 13-14	Class I or III	OK	OK	Yes
121. Misalignment of LHM While Lowering or Raising the Loop-FS&R or Reactor	Training-Administrative Controls-Dual Load Cells in LHM Control Circuit	A	Treated 12-25, 12-48	None	OK	OK	Yes
122. Misalignment of LHM While Lowering or Raising the Loop-FS&R or Reactor	Training-Administrative Controls or None	EU	Treated 12-25, 12-48	Minor Damage to Loop Supports or External Galling of Sec. Vessel	OK	OK	No
123. Misalignment of LHM While Lowering or Raising an Irradiated Assembly	Training-Administrative Controls-HP Surveillance Duel Load Cells	A	Treated 12-25, 12-48	Radiation Streaming	OK	OK	Yes
124. Overspeed Lowering of LHM-Reactor or FS&R	Training-Administrative Control-Overspeed Cutout in Crane Control	A	Bounded by 130	None	OK	OK	No
125. Overspeed Lowering of LHM-Reactor or FS&R	Training-Administrative Control or None	U	Bounded by 130	Minor Damage to FS&R Reactor Top Leveling Plate	OK	OK	No
126. LHM Hoist Control Sys Failure or Malfunction While Raising or Lowering Loop-FS&R or Rtr	Training-Administrative Control-System Testing Load Cells-Automatic Break-Limit Switches	EU	Bounded by 130	Structural Damage to Reactor FS&R	OK	OK	No

Fault Event	Assumed Mitigating Systems and Conditions	Net Likelihood	Analysis	Experiment Consequence	Vessel Integrity		Treated
					Primary	Secondary	
127. LHM Hoist Mechanical Failure or Malfunction While Raising or Lowering Loop-ETR or FS&R	Redundancy (Grapple, Hoist Chains, Load Cells, Drive Shafts). Mechanical Design Safety Factors-Fabrication Standards Quality Control, Inspection Testing	EU	Treated 12-48	Restrained Movement of Loop	OK	OK	No
128. Single Failure-LHM Attachment-Crane Hook, Cable or Sheave While Supporting LHM	Redundancy Mechanical Design Safety Factors, NDT and Inspection-Low Frequency of Operation Fabrication Standards	U	Treated 12-18 Bounded by 130	Uncontrolled Movement of LHM Possible Structural Damage Rtr Biological Shielding	OK	OK	No
129. Single Failure ETR Crane Drive Gear, Drive Shaft or Drum While Supporting LHM and Drop Over Rtr Top	Mechanical Design Safety Factors Fabrication Standards and Inspection Testing-Low Frequency of Op.	EU	Treated 12-43, 12-44	Damage to ETR Core Fission Product Release	OK	OK	Yes
130. Single Failure ETR Crane Drive Gear, Shaft or Drum While Supporting LHM and Drop Over Rtr Floor	Mechanical Design Safety Factors Fabrication Standards and Inspection Testing-Low Frequency of Op.	EU	Treated 12-46	Class III plus Fire/Contaminated Aerosol Release	Failed	Failed	Yes
131. Failure of ETR Building Structure Supporting Crane While Handling LHM	Design Safety Factors NDT and Inspection	EU	Bounded by 130	Class III plus Fire/Contaminated Aerosol Release	Failed	Failed	No
132. Test Cell Sodium Spill DBA	Design-Test Cell Enclosure-Ventilation System	EU	Treated 12-49 Bounded by 134	Fire/Contaminated Aerosol Release	NA	NA	Yes

Fault Event	Assumed Mitigating Systems and Conditions	Net Likeli-hood	Analysis	Experiment Consequence	Vessel Integrity		Treated
					Primary	Secondary	
133. Charging Facility Sodium Spill DBA	Design-Charging Facility Enclosure-Ventilation Sys	EU	Treated 12-49 Bounded by 134	Fire/Contaminated Aerosol Release	NA	NA	Yes
134. Charging Facility Sodium Spill Hypothetical	Design-Charging Facility Enclosure-Ventilation Sys	H	Treated 13-16	Fire/Contaminated Aerosol Release	NA	NA	Yes
135. Earthquake	None	A	Treated 11-118	Class I	OK	OK	Yes
136. Test Dropping	EAS and/or PPS or None	U→H	Bounded by 54 through 61	Class I, II, or III	OK	OK	No

EVENT REPRESENTATIONS

The rectangle identifies an event that results from the combination of fault events through the input logic gate.

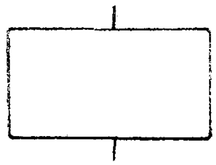

The circle describes a basic fault event that requires no further development. Frequency and mode of failure of the event so identified is derived from empirical data.

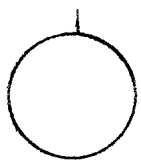

The triangles are used as transfer symbols. A line from the apex of the triangle indicates a transfer in, and a line from the side denotes a transfer out.

The diamond describes a fault event that is considered basic in a given fault tree. The possible causes of the event are not developed further because the necessary statistical data is not available, or the analyst has determined that the event will not cause a failure to the system or the occurrence of the event is not likely to occur.

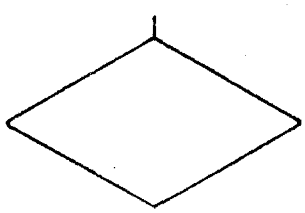

LOGIC OPERATIONS

AND GATE describes the logical operation whereby the coexistence of all input events is required to produce the output event.

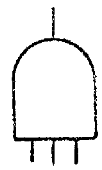

OR GATE defines the situation whereby the output events will exist if one or more of the imput events exist.

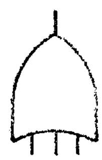

The house indicates an event that is normally expected to occur such as a phase change in a dynamic system.

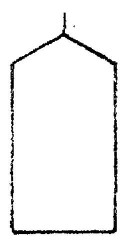

Fig. A.1.1 Fault Tree Symbolism

A.2 Loop Operational Fault Tree

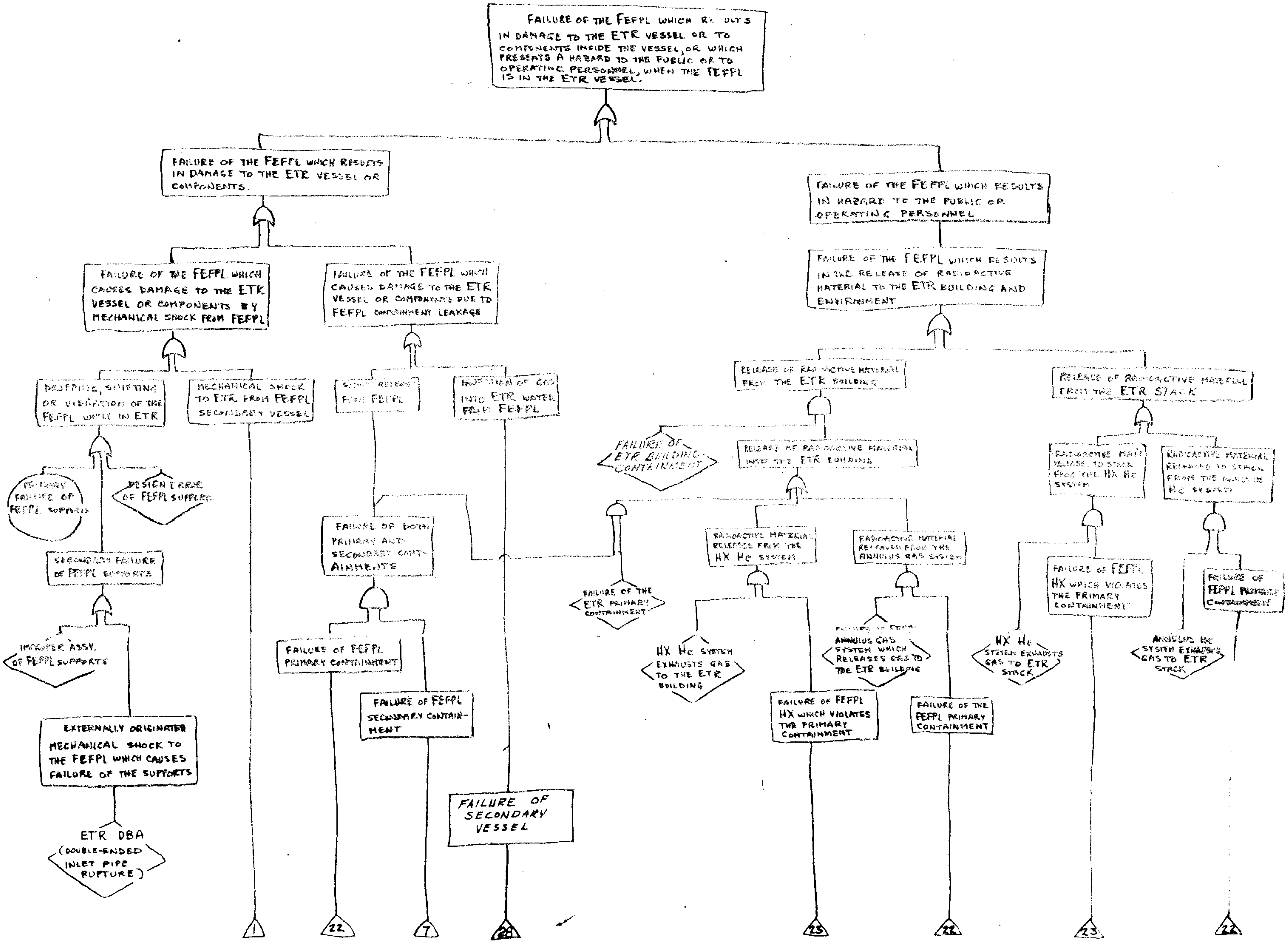
FAILURE OF THE FEFPL WHICH RESULTS IN DAMAGE TO THE ETR VESSEL OR TO COMPONENTS INSIDE THE VESSEL, OR WHICH PRESENTS A HAZARD TO THE PUBLIC OR TO OPERATING PERSONNEL, WHEN THE FEFPL IS IN THE ETR VESSEL.
FAILURE OF THE FEFPL WHICH RESULTS IN DAMAGE TO THE ETR VESSEL OR COMPONENTS.
FAILURE OF THE FEFPL WHICH RESULTS IN HAZARD TO THE PUBLIC OR OPERATING PERSONNEL
FAILURE OF THE FEFPL WHICH CAUSES DAMAGE TO THE ETR VESSEL OR COMPONENTS BY MECHANICAL SHOCK FROM FEFPL
FAILURE OF THE FEFPL WHICH CAUSES DAMAGE TO THE ETR VESSEL OR COMPONENTS DUE TO FEFPL CONTAINMENT LEAKAGE
FAILURE OF THE FEFPL WHICH RESULTS IN THE RELEASE OF RADIOACTIVE MATERIAL TO THE ETR BUILDING AND ENVIRONMENT
DROPPING, SHIFTING OR VIBRATION OF THE FEFPL WHILE IN ETR
MECHANICAL SHOCK TO ETR FROM FEFPL SECONDARY VESSEL
SHOCK RELEASE FROM FEFPL
INJECTION OF GAS INTO ETR WATER FROM FEFPL
RELEASE OF RADIOACTIVE MATERIAL FROM THE ETR BUILDING
RELEASE OF RADIOACTIVE MATERIAL FROM THE ETR STACK
FAILURE OF ETR BUILDING CONTAINMENT
RELEASE OF RADIOACTIVE MATERIAL INTO THE ETR BUILDING
PRIMARY FAILURE OF FEFPL SUPPORTS
DESIGN ERROR OF FEFPL SUPPORTS
SECONDARY FAILURE OF FEFPL SUPPORTS
IMPROPER ASSY. OF FEFPL SUPPORTS
EXTERNALLY ORIGINATED MECHANICAL SHOCK TO THE FEFPL WHICH CAUSES FAILURE OF THE SUPPORTS
ETR DBA (DOUBLE-ENDED INLET PIPE RUPTURE)
FAILURE OF BOTH PRIMARY AND SECONDARY CONTAINMENTS
FAILURE OF FEFPL PRIMARY CONTAINMENT
FAILURE OF FEFPL SECONDARY CONTAINMENT
FAILURE OF SECONDARY VESSEL
FAILURE OF THE ETR PRIMARY CONTAINMENT
RADIOACTIVE MATERIAL RELEASED FROM THE HX He SYSTEM
RADIOACTIVE MATERIAL RELEASED FROM THE ANNULUS GAS SYSTEM
HX He SYSTEM EXHAUSTS GAS TO THE ETR BUILDING
ANNULUS GAS SYSTEM WHICH RELEASES GAS TO THE ETR BUILDING
FAILURE OF FEFPL HX WHICH VIOLATES THE PRIMARY CONTAINMENT
FAILURE OF THE FEFPL PRIMARY CONTAINMENT
RADIOACTIVE MATL RELEASED TO STACK FROM THE HX He SYSTEM
RADIOACTIVE MATERIAL RELEASED TO STACK FROM THE ANNULUS He SYSTEM
FAILURE OF FEFPL HX WHICH VIOLATES THE PRIMARY CONTAINMENT
FAILURE OF FEFPL PRIMARY CONTAINMENT
HX He SYSTEM EXHAUSTS GAS TO ETR STACK
ANNULUS He SYSTEM EXHAUSTS GAS TO ETR STACK
1
22
7
28
23
22
23
22

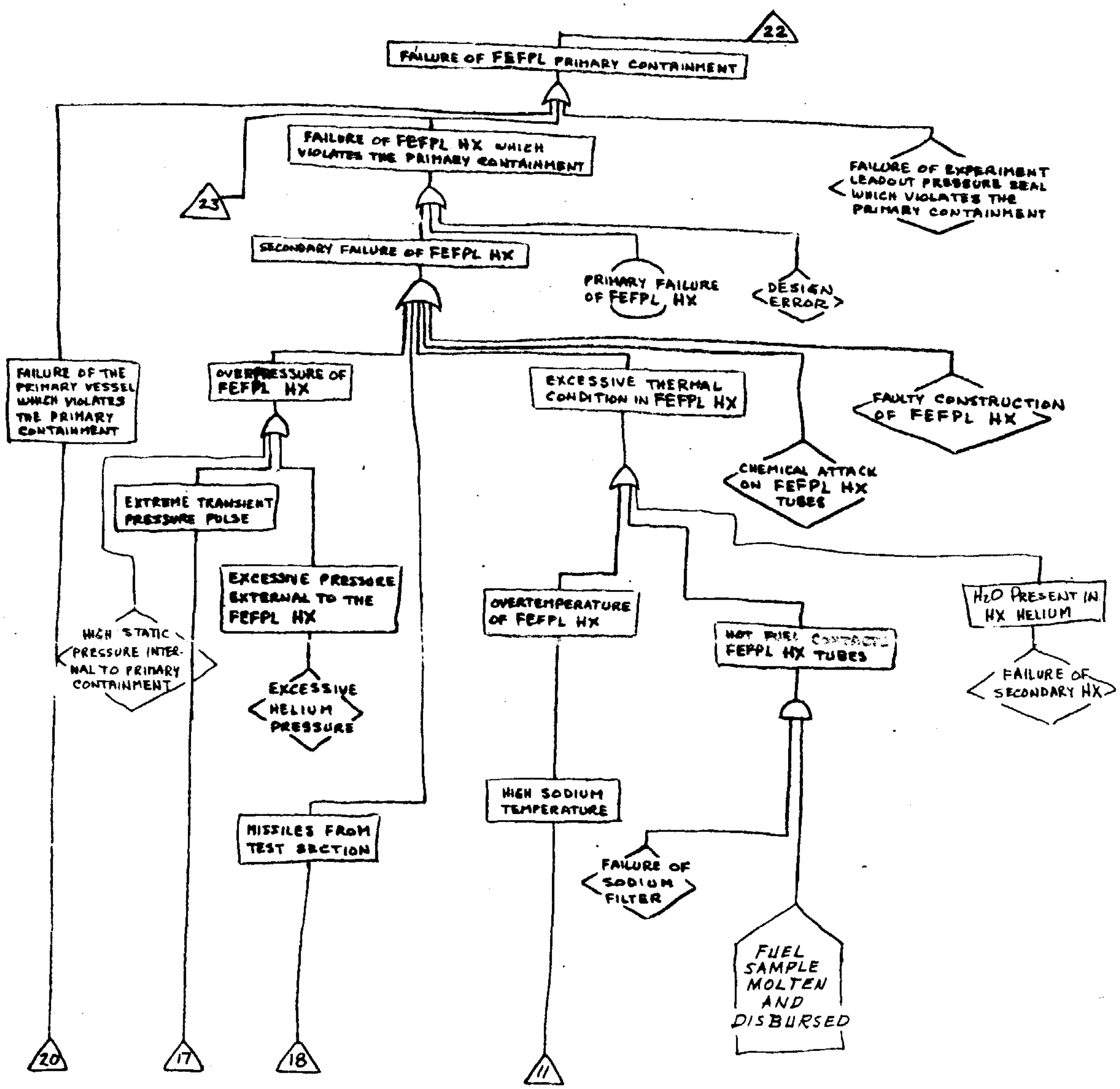
22
FAILURE OF FEFPL PRIMARY CONTAINMENT
FAILURE OF FEFPL HX WHICH VIOLATES THE PRIMARY CONTAINMENT
23
FAILURE OF EXPERIMENT LEADOUT PRESSURE SEAL WHICH VIOLATES THE PRIMARY CONTAINMENT
SECONDARY FAILURE OF FEFPL HX
PRIMARY FAILURE OF FEFPL HX
DESIGN ERROR
FAILURE OF THE PRIMARY VESSEL WHICH VIOLATES THE PRIMARY CONTAINMENT
OVERPRESSURE OF FEFPL HX
EXCESSIVE THERMAL CONDITION IN FEFPL HX
FAULTY CONSTRUCTION OF FEFPL HX
CHEMICAL ATTACK ON FEFPL HX TUBES
EXTREME TRANSIENT PRESSURE PULSE
EXCESSIVE PRESSURE EXTERNAL TO THE FEFPL HX
HIGH STATIC PRESSURE INTERNAL TO PRIMARY CONTAINMENT
EXCESSIVE HELIUM PRESSURE
OVERTEMPERATURE OF FEFPL HX
HOT FUEL CONTACTS FEFPL HX TUBES
H2O PRESENT IN HX HELIUM
FAILURE OF SECONDARY HX
HIGH SODIUM TEMPERATURE
MISSILES FROM TEST SECTION
FAILURE OF SODIUM FILTER
FUEL SAMPLE MOLTEN AND DISBURSED
20
17
18
11

3

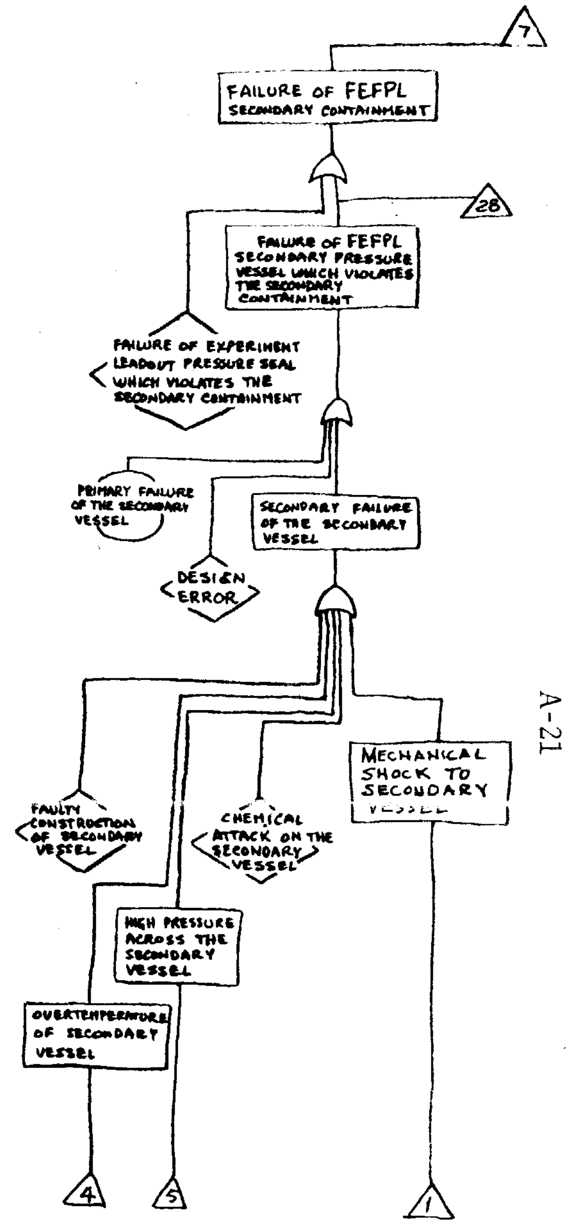
7
FAILURE OF FEFPL SECONDARY CONTAINMENT
28
FAILURE OF FEFPL SECONDARY PRESSURE VESSEL WHICH VIOLATES THE SECONDARY CONTAINMENT
FAILURE OF EXPERIMENT LEADOUT PRESSURE SEAL WHICH VIOLATES THE SECONDARY CONTAINMENT
PRIMARY FAILURE OF THE SECONDARY VESSEL
SECONDARY FAILURE OF THE SECONDARY VESSEL
DESIGN ERROR
FAULTY CONSTRUCTION OF SECONDARY VESSEL
CHEMICAL ATTACK ON THE SECONDARY VESSEL
MECHANICAL SHOCK TO SECONDARY VESSEL
HIGH PRESSURE ACROSS THE SECONDARY VESSEL
OVERTEMPERATURE OF SECONDARY VESSEL
4
5
1

2

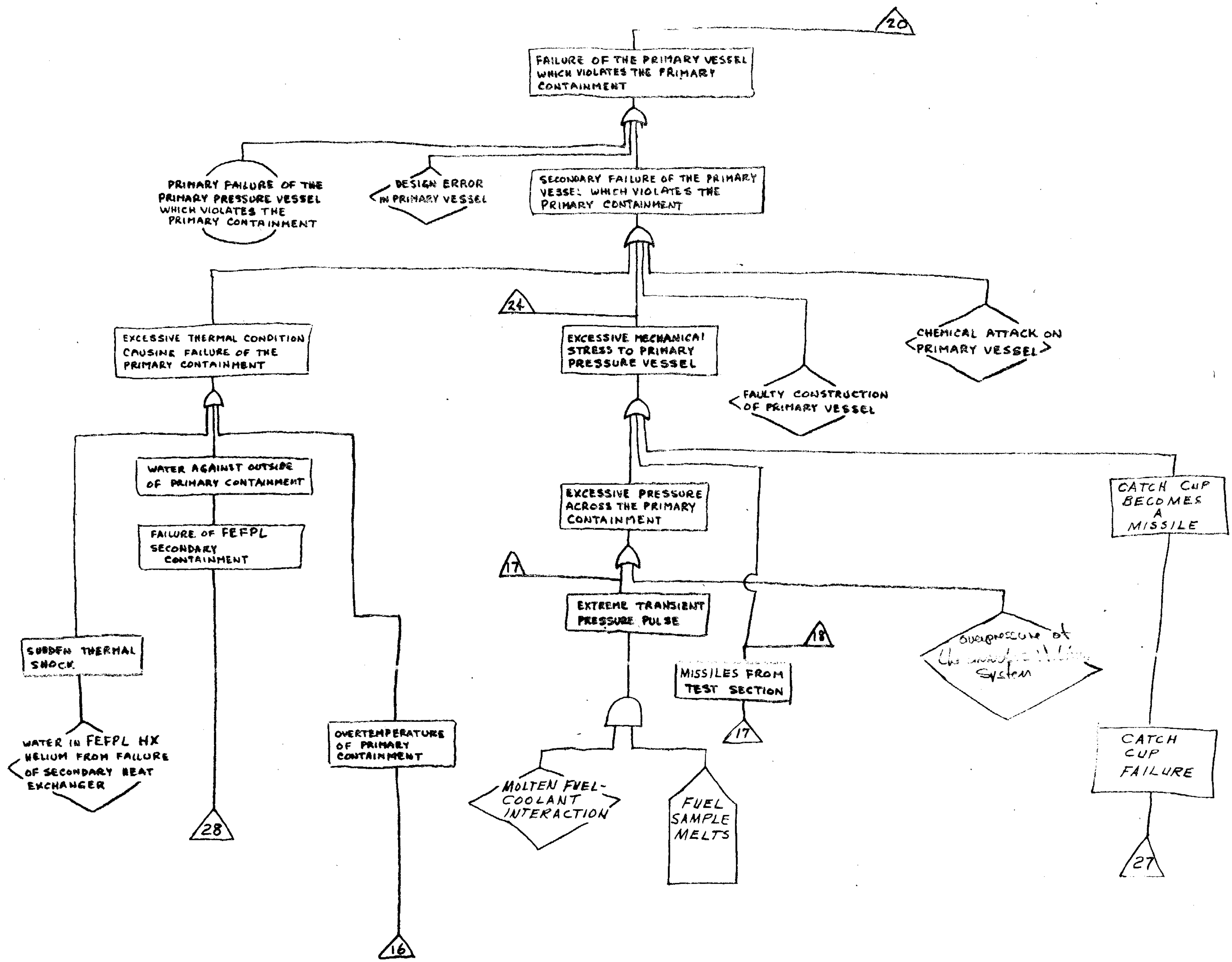

20
FAILURE OF THE PRIMARY VESSEL WHICH VIOLATES THE PRIMARY CONTAINMENT
PRIMARY FAILURE OF THE PRIMARY PRESSURE VESSEL WHICH VIOLATES THE PRIMARY CONTAINMENT
DESIGN ERROR IN PRIMARY VESSEL
SECONDARY FAILURE OF THE PRIMARY VESSEL WHICH VIOLATES THE PRIMARY CONTAINMENT
24
EXCESSIVE THERMAL CONDITION CAUSING FAILURE OF THE PRIMARY CONTAINMENT
EXCESSIVE MECHANICAL STRESS TO PRIMARY PRESSURE VESSEL
CHEMICAL ATTACK ON PRIMARY VESSEL
FAULTY CONSTRUCTION OF PRIMARY VESSEL
WATER AGAINST OUTSIDE OF PRIMARY CONTAINMENT
FAILURE OF FEFPL SECONDARY CONTAINMENT
EXCESSIVE PRESSURE ACROSS THE PRIMARY CONTAINMENT
CATCH CUP BECOMES A MISSILE
17
EXTREME TRANSIENT PRESSURE PULSE
18
overpressure of
System
SUDDEN THERMAL SHOCK
MISSILES FROM TEST SECTION
17
WATER IN FEFPL HX HELIUM FROM FAILURE OF SECONDARY HEAT EXCHANGER
OVERTEMPERATURE OF PRIMARY CONTAINMENT
CATCH CUP FAILURE
MOLTEN FUEL-COOLANT INTERACTION
FUEL SAMPLE MELTS
28
27
16

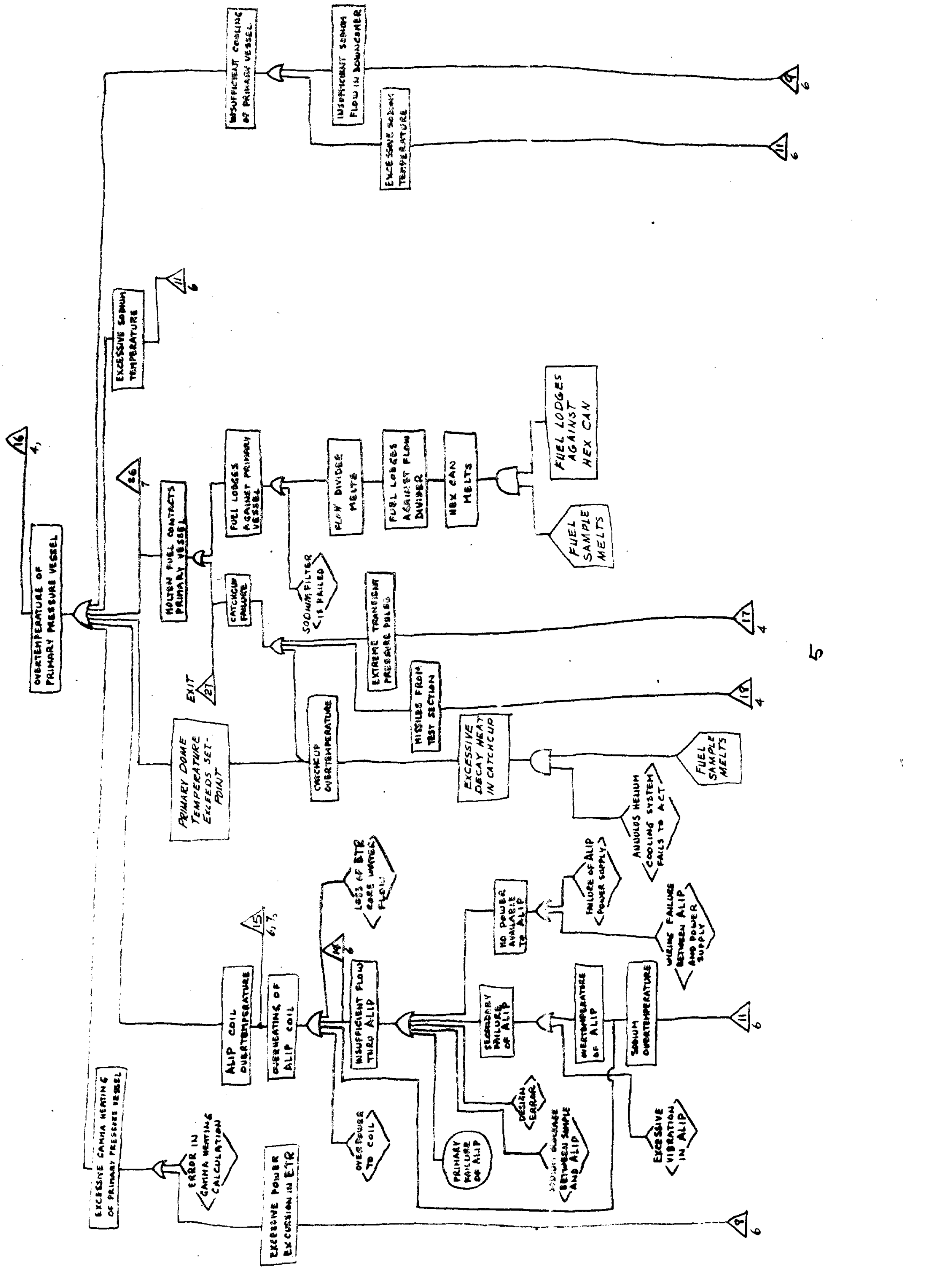
OVERTEMPERATURE OF PRIMARY PRESSURE VESSEL
16
4,
INSUFFICIENT COOLING OF PRIMARY VESSEL
INSUFFICIENT SODIUM FLOW IN DOWNCOMER
9
6
EXCESSIVE SODIUM TEMPERATURE
11
6
EXCESSIVE SODIUM TEMPERATURE
11
6
MOLTEN FUEL CONTACTS PRIMARY VESSEL
26
7
FUEL LODGES AGAINST PRIMARY VESSEL
FLOW DIVIDER MELTS
FUEL LODGES AGAINST FLOW DIVIDER
HEX CAN MELTS
FUEL LODGES AGAINST HEX CAN
FUEL SAMPLE MELTS
SODIUM FILTER IS FAILED
CATCHCUP FAILURE
EXTREME TRANSIENT PRESSURE PULSE
17
4
MISSILES FROM TEST SECTION
18
4
EXIT
21
PRIMARY DOME TEMPERATURE EXCEEDS SET-POINT
CATCHCUP OVERTEMPERATURE
EXCESSIVE DECAY HEAT IN CATCHCUP
FUEL SAMPLE MELTS
ANNULUS HELIUM COOLING SYSTEM FAILS TO ACT
ALIP COIL OVERTEMPERATURE
15
6, 7,
OVERHEATING OF ALIP COIL
LOSS OF ETR CORE WATER FLOW
6
INSUFFICIENT FLOW THRU ALIP
NO POWER AVAILABLE TO ALIP
FAILURE OF ALIP POWER SUPPLY
WIRING FAILURE BETWEEN ALIP AND POWER SUPPLY
SECONDARY FAILURE OF ALIP
OVERTEMPERATURE OF ALIP
SODIUM OVERTEMPERATURE
11
6
DESIGN ERROR
SODIUM BLOCKAGE BETWEEN SAMPLE AND ALIP
EXCESSIVE VIBRATION IN ALIP
PRIMARY FAILURE OF ALIP
OVERPOWER TO COIL
EXCESSIVE GAMMA HEATING OF PRIMARY PRESSURE VESSEL
ERROR IN GAMMA HEATING CALCULATION
EXCESSIVE POWER EXCURSION IN ETR
9
6
5

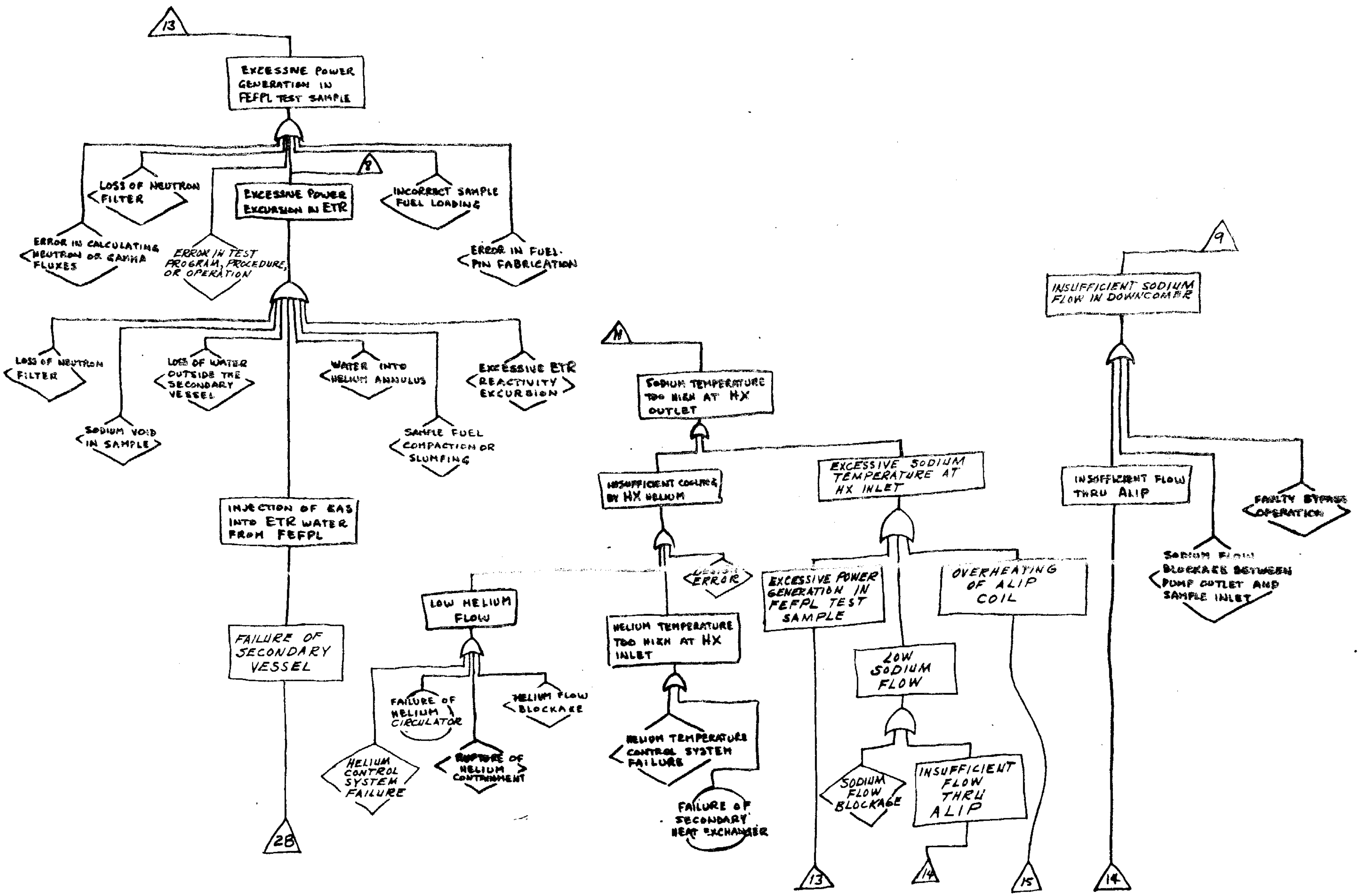

13
EXCESSIVE POWER GENERATION IN FEFPL TEST SAMPLE
LOSS OF NEUTRON FILTER
9
EXCESSIVE POWER EXCURSION IN ETR
INCORRECT SAMPLE FUEL LOADING
ERROR IN CALCULATING NEUTRON OR GAMMA FLUXES
ERROR IN TEST PROGRAM, PROCEDURE, OR OPERATION
ERROR IN FUEL-PIN FABRICATION
LOSS OF NEUTRON FILTER
LOSS OF WATER OUTSIDE THE SECONDARY VESSEL
WATER INTO HELIUM ANNULUS
EXCESSIVE ETR REACTIVITY EXCURSION
SODIUM VOID IN SAMPLE
SAMPLE FUEL COMPACTION OR SLUMPING
INJECTION OF GAS INTO ETR WATER FROM FEFPL
FAILURE OF SECONDARY VESSEL
28
LOW HELIUM FLOW
FAILURE OF HELIUM CIRCULATOR
HELIUM FLOW BLOCKAGE
HELIUM CONTROL SYSTEM FAILURE
RUPTURE OF HELIUM CONTAINMENT
11
SODIUM TEMPERATURE TOO HIGH AT HX OUTLET
INSUFFICIENT COOLING BY HX HELIUM
EXCESSIVE SODIUM TEMPERATURE AT HX INLET
ERROR
HELIUM TEMPERATURE TOO HIGH AT HX INLET
HELIUM TEMPERATURE CONTROL SYSTEM FAILURE
FAILURE OF SECONDARY HEAT EXCHANGER
EXCESSIVE POWER GENERATION IN FEFPL TEST SAMPLE
OVERHEATING OF ALIP COIL
LOW SODIUM FLOW
SODIUM FLOW BLOCKAGE
INSUFFICIENT FLOW THRU ALIP
13
14
15
9
INSUFFICIENT SODIUM FLOW IN DOWNCOMER
INSUFFICIENT FLOW THRU ALIP
FAULTY BYPASS OPERATION
SODIUM FLOW BLOCKAGE BETWEEN PUMP OUTLET AND SAMPLE INLET
14

A-24

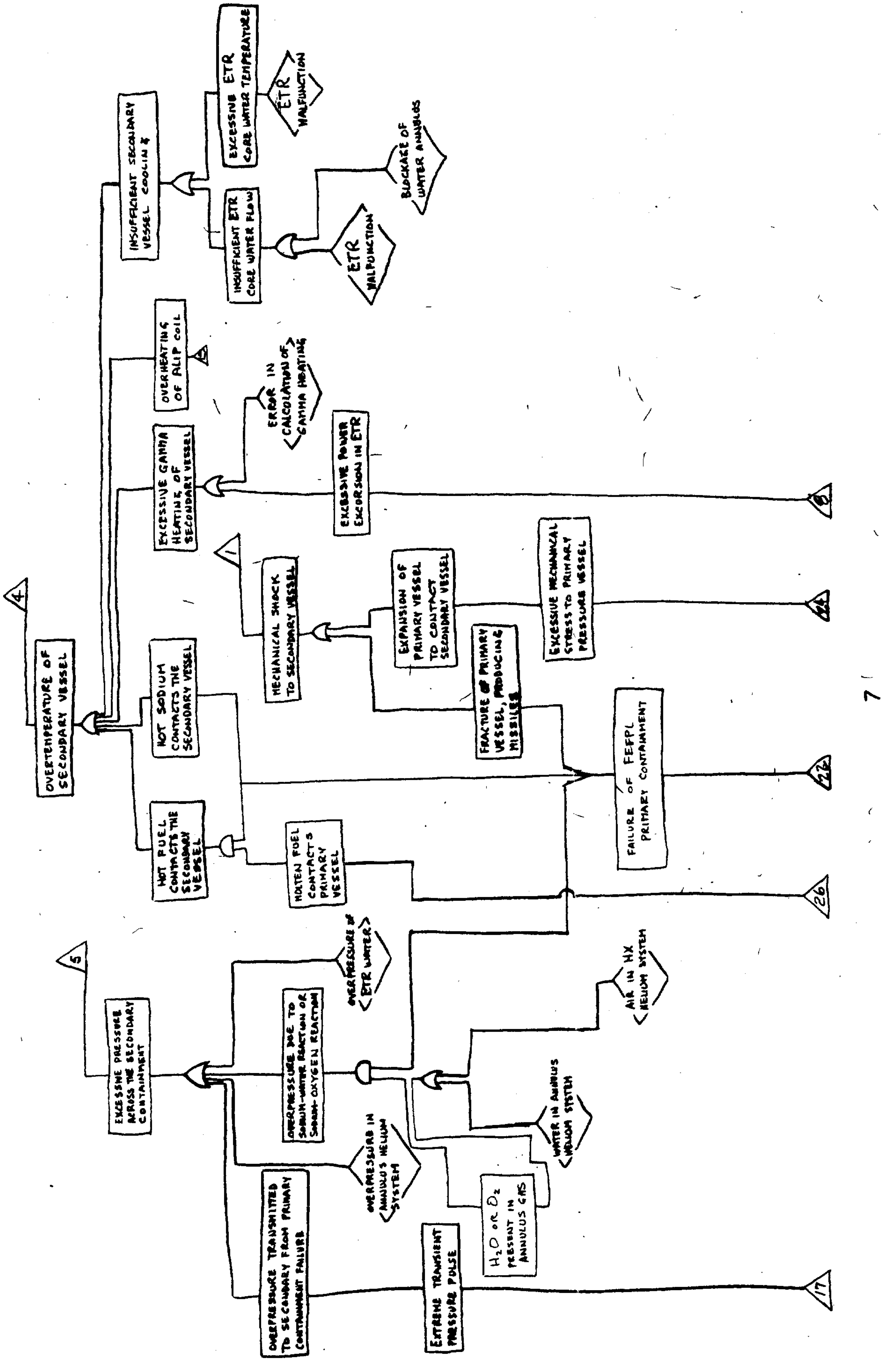
OVERTEMPERATURE OF SECONDARY VESSEL
4
INSUFFICIENT SECONDARY VESSEL COOLING
EXCESSIVE ETR CORE WATER TEMPERATURE
ETR MALFUNCTION
INSUFFICIENT ETR CORE WATER FLOW
ETR MALFUNCTION
BLOCKAGE OF WATER ANNULUS
OVERHEATING OF ALIP COIL
EXCESSIVE GAMMA HEATING OF SECONDARY VESSEL
ERROR IN CALCULATION OF GAMMA HEATING
EXCESSIVE POWER EXCURSION IN ETR
8
HOT SODIUM CONTACTS THE SECONDARY VESSEL
1
MECHANICAL SHOCK TO SECONDARY VESSEL
EXPANSION OF PRIMARY VESSEL TO CONTACT SECONDARY VESSEL
EXCESSIVE MECHANICAL STRESS TO PRIMARY PRESSURE VESSEL
FRACTURE OF PRIMARY VESSEL, PRODUCING MISSILES
FAILURE OF FEFPL PRIMARY CONTAINMENT
22
HOT FUEL CONTACTS THE SECONDARY VESSEL
MOLTEN FUEL CONTACTS PRIMARY VESSEL
26
5
EXCESSIVE PRESSURE ACROSS THE SECONDARY CONTAINMENT
OVERPRESSURE DUE TO SODIUM-WATER REACTION OR SODIUM-OXYGEN REACTION
OVERPRESSURE OF ETR WATER
AIR IN HX HELIUM SYSTEM
WATER IN ANNULUS HELIUM SYSTEM
H_2O OR D_2 PRESENT IN ANNULUS GAS
OVERPRESSURE IN ANNULUS HELIUM SYSTEM
OVERPRESSURE TRANSMITTED TO SECONDARY FROM PRIMARY CONTAINMENT FAILURE
EXTREME TRANSIENT PRESSURE PULSE
17

A.3 Loop Handling Flow Chart

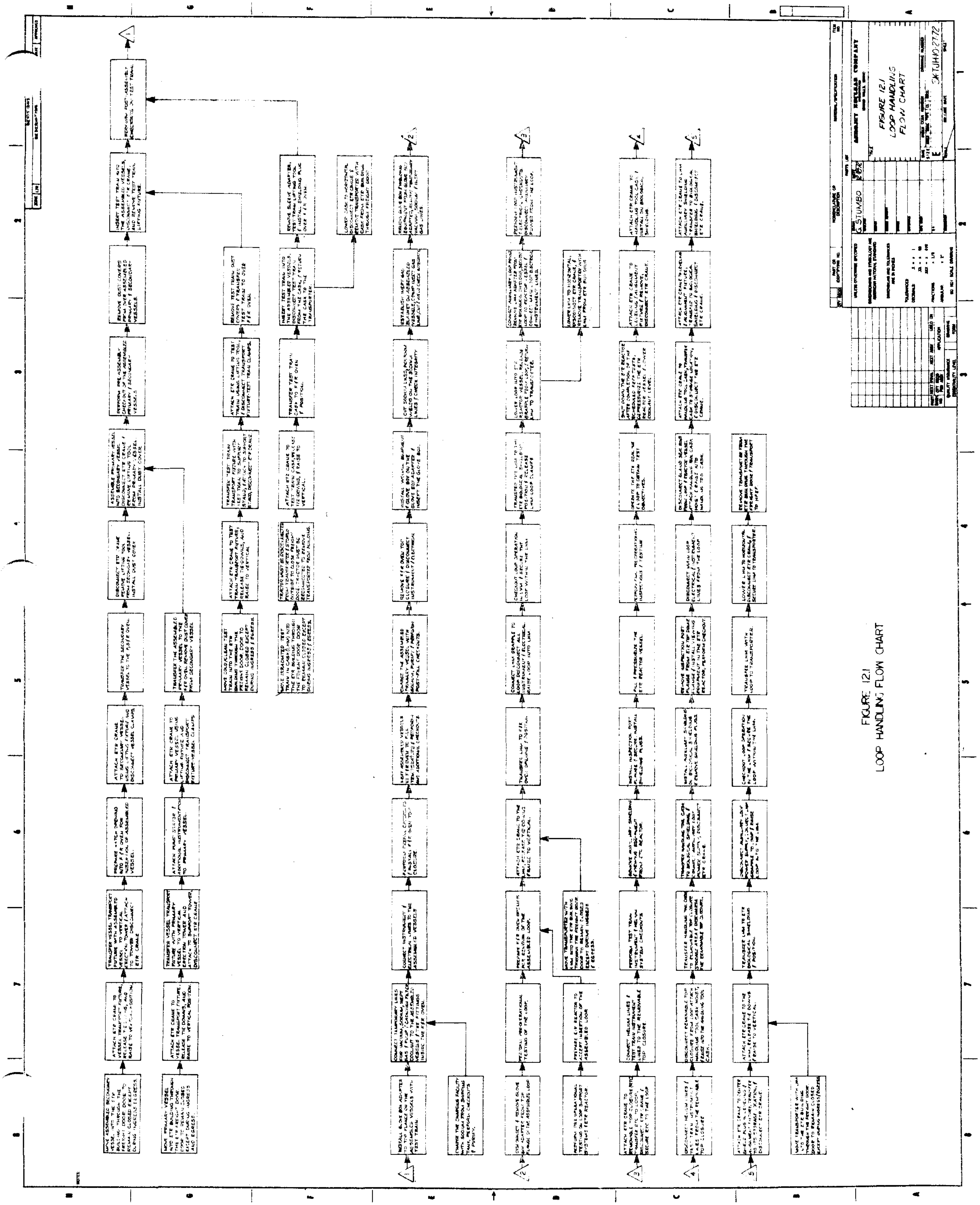

FIGURE 12.1
LOOP HANDLING FLOW CHART

A.4 Loop Handling Fault Fault Tree

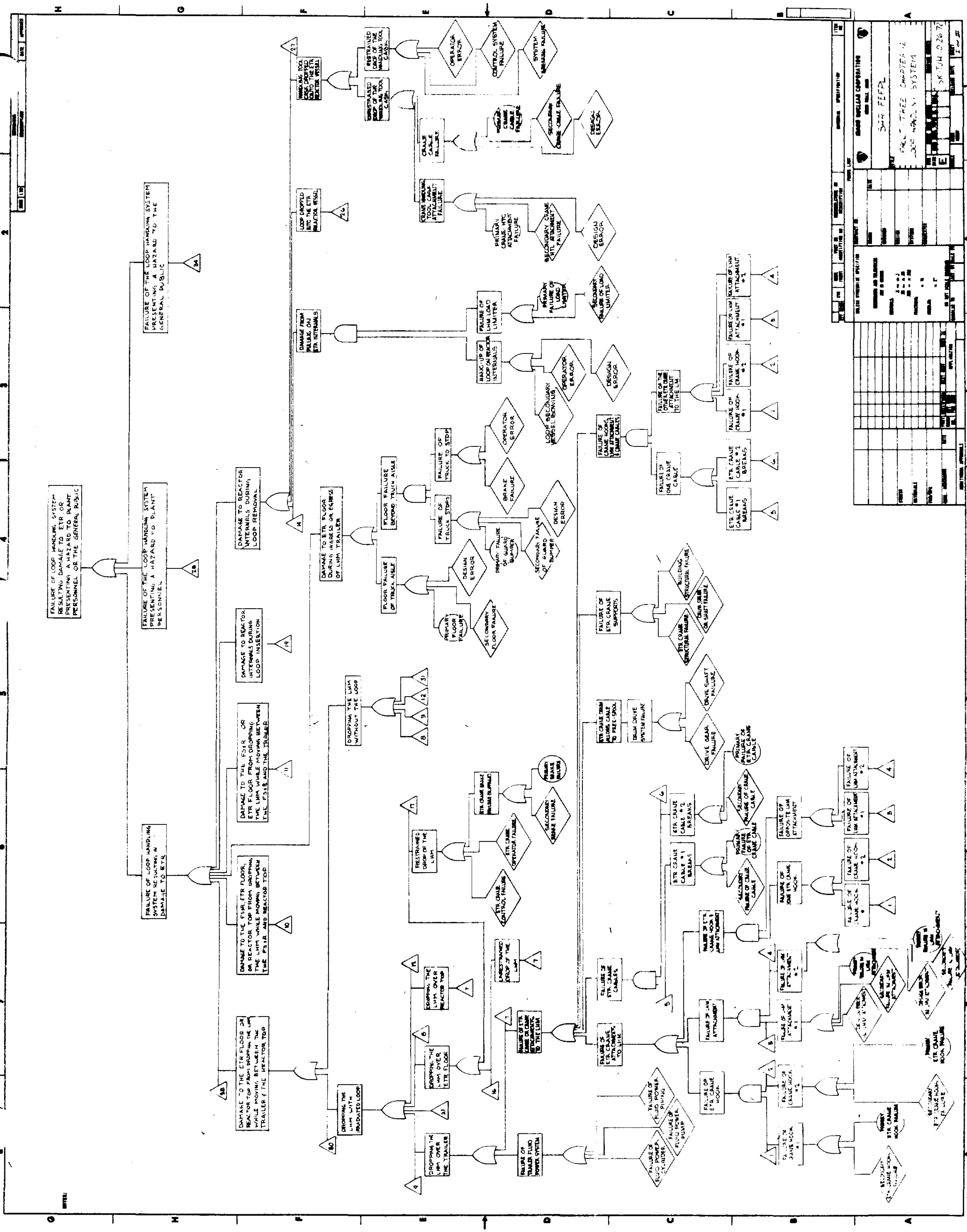
FAILURE OF LOOP HANDLING SYSTEM RESULTING DAMAGE TO ETR OR PRESENTING A HAZARD TO PLANT PERSONNEL OR THE GENERAL PUBLIC
FAILURE OF THE LOOP HANDLING SYSTEM PRESENTING A HAZARD TO THE GENERAL PUBLIC
FAILURE OF THE LOOP HANDLING SYSTEM PRESENTING A HAZARD TO PLANT PERSONNEL
FAILURE OF LOOP HANDLING SYSTEM RESULTING IN DAMAGE TO ETR
DAMAGE TO REACTOR INTERNALS DURING LOOP REMOVAL
DAMAGE TO REACTOR INTERNALS DURING LOOP INSERTION
DAMAGE TO ETR FLOOR DURING INGRESS OR EGRESS OF LHM TRAILER
DROPPING THE LHM WITHOUT THE LOOP
DROPPING THE LHM WITH IRRADIATED LOOP
FLOOR FAILURE BEYOND TRUCK AISLE
FLOOR FAILURE OF TRUCK AISLE
FAILURE OF TRUCK TO STOP
FAILURE OF TRUCK STOPS
OPERATOR ERROR
BRAKE FAILURE
DESIGN ERROR
PRIMARY FLOOR FAILURE
SECONDARY FLOOR FAILURE
LOOP DROPPED INTO THE ETR REACTOR VESSEL
DAMAGE FROM PULLING ON ETR INTERNALS
FAILURE OF LHM LOAD LIMITER
FAILURE OF ETR CRANE SUPPORTS
FAILURE OF ETR CRANE CABLES
FAILURE OF ETR CRANE HOOK
DRIVE GEAR FAILURE
DRIVE SHAFT FAILURE
FAILURE OF TRAILER FLUID POWER SYSTEM
DROPPING THE LHM OVER THE TRAILER
DROPPING THE LHM OVER ETR FLOOR
DROPPING THE LHM OVER REACTOR TOP

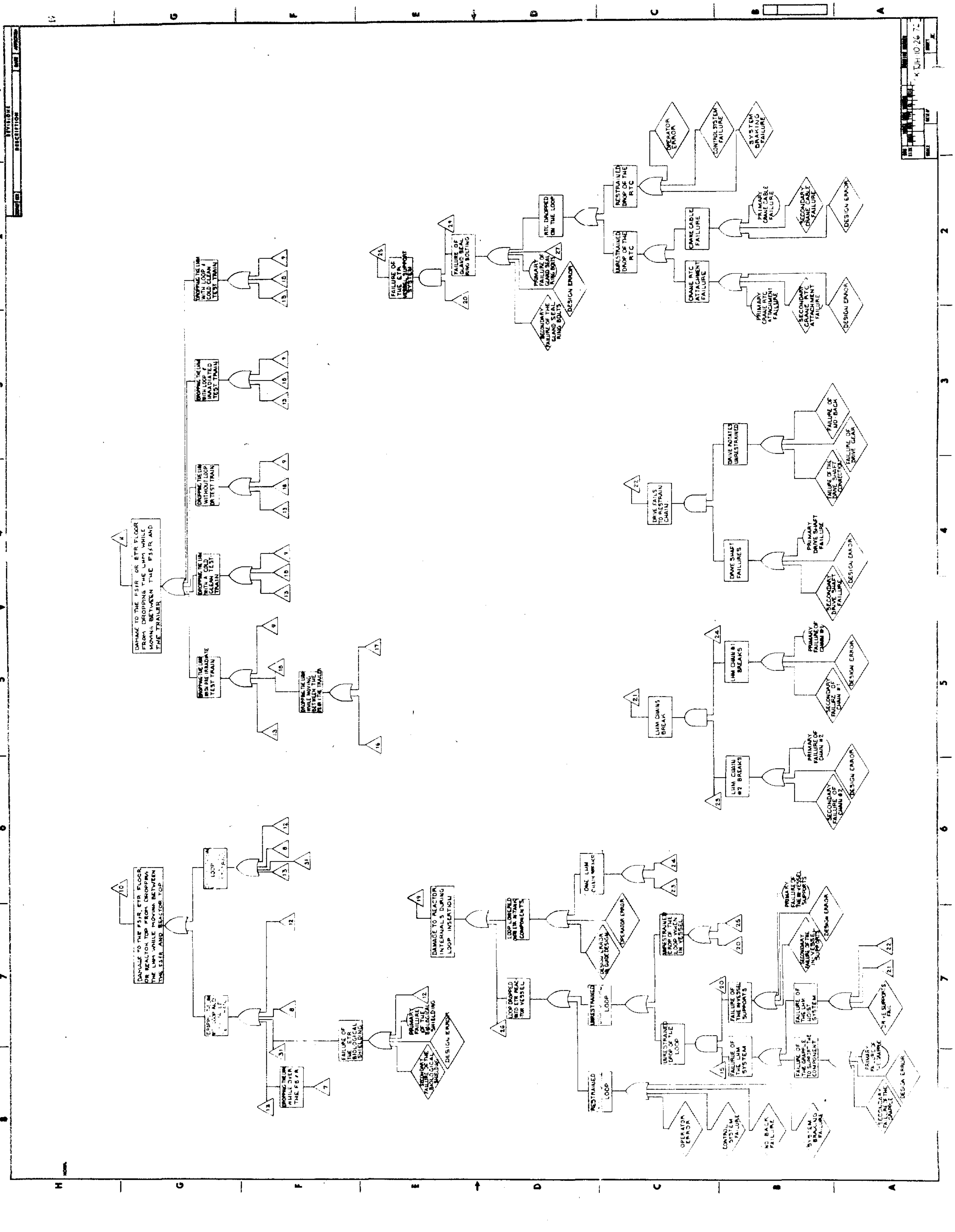
DAMAGE TO THE FSFR, ETR FLOOR OR REACTOR TOP FROM DROPPING THE LHM WHILE MOVING BETWEEN THE FSFR AND REACTOR TOP
DAMAGE TO THE FSFR OR ETR FLOOR FROM DROPPING THE LHM WHILE MOVING BETWEEN THE FSFR AND THE TRAILER
DAMAGE TO REACTOR INTERNALS DURING LOOP INSERTION
FAILURE OF THE ETR VESSEL SUPPORT SYSTEM
FAILURE OF GLAND SEAL RING BOLTING
RTC DROPPED ON THE LOOP
RESTRAINED DROP OF THE RTC
UNRESTRAINED DROP OF THE RTC
OPERATOR ERROR
CONTROL SYSTEM FAILURE
SYSTEM BRAKING FAILURE
CRANE CABLE FAILURE
CRANE RTC ATTACHMENT FAILURE
DESIGN ERROR
DRIVE FAILS TO RESTRAIN CHAIN
DRIVE ROTATES UNRESTRAINED
DRIVE SHAFT FAILURES
LHM CHAINS BREAK
LHM CHAIN #1 BREAKS
LHM CHAIN #2 BREAKS
FAILURE OF THE ETR BIOLOGICAL SHIELDING
LOOP DROPPED INTO ETR REACTOR VESSEL
RESTRAINED LOOP
UNRESTRAINED LOOP
NO BACK FAILURE

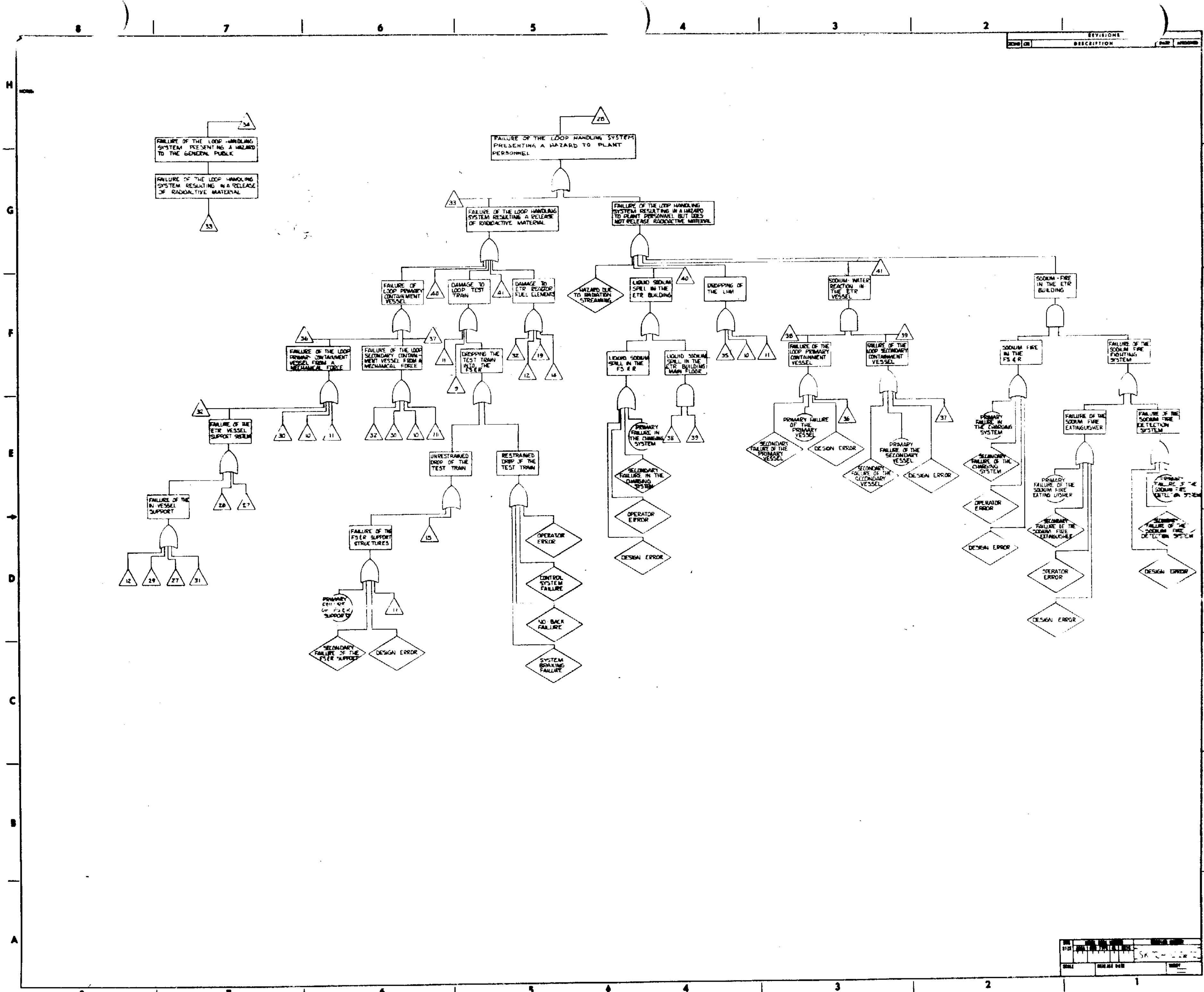
FAILURE OF THE LOOP HANDLING SYSTEM PRESENTING A HAZARD TO THE GENERAL PUBLIC
FAILURE OF THE LOOP HANDLING SYSTEM RESULTING IN A RELEASE OF RADIOACTIVE MATERIAL
FAILURE OF THE LOOP HANDLING SYSTEM PRESENTING A HAZARD TO PLANT PERSONNEL
FAILURE OF THE LOOP HANDLING SYSTEM RESULTING A RELEASE OF RADIOACTIVE MATERIAL
FAILURE OF THE LOOP HANDLING SYSTEM RESULTING IN A HAZARD TO PLANT PERSONNEL BUT DOES NOT RELEASE RADIOACTIVE MATERIAL
FAILURE OF LOOP PRIMARY CONTAINMENT VESSEL
DAMAGE TO LOOP TEST TRAIN
DAMAGE TO ETR REACTOR FUEL ELEMENTS
HAZARD DUE TO RADIATION STREAMING
LIQUID SODIUM SPILL IN THE ETR BUILDING
DROPPING OF THE LHM
SODIUM - WATER REACTION IN THE ETR VESSEL
SODIUM - FIRE IN THE ETR BUILDING
FAILURE OF THE LOOP PRIMARY CONTAINMENT VESSEL FROM A MECHANICAL FORCE
FAILURE OF THE LOOP SECONDARY CONTAINMENT VESSEL FROM A MECHANICAL FORCE
DROPPING THE TEST TRAIN INTO THE FS&R
LIQUID SODIUM SPILL IN THE FS & R
LIQUID SODIUM SPILL IN THE ETR BUILDING MAIN FLOOR
FAILURE OF THE LOOP PRIMARY CONTAINMENT VESSEL
FAILURE OF THE LOOP SECONDARY CONTAINMENT VESSEL
SODIUM FIRE IN THE FS & R
FAILURE OF THE SODIUM FIRE FIGHTING SYSTEM
FAILURE OF THE ETR VESSEL SUPPORT SYSTEM
UNRESTRAINED DROP OF THE TEST TRAIN
RESTRAINED DROP OF THE TEST TRAIN
PRIMARY FAILURE IN THE CHARGING SYSTEM
SECONDARY FAILURE IN THE CHARGING SYSTEM
OPERATOR ERROR
DESIGN ERROR
PRIMARY FAILURE OF THE PRIMARY VESSEL
SECONDARY FAILURE OF THE PRIMARY VESSEL
PRIMARY FAILURE OF THE SECONDARY VESSEL
SECONDARY FAILURE OF THE SECONDARY VESSEL
FAILURE OF THE SODIUM FIRE EXTINGUISHER
FAILURE OF THE SODIUM FIRE DETECTION SYSTEM
PRIMARY FAILURE OF THE SODIUM FIRE EXTINGUISHER
SECONDARY FAILURE OF THE SODIUM FIRE EXTINGUISHER
SECONDARY FAILURE OF THE SODIUM FIRE DETECTION SYSTEM
FAILURE OF THE IN VESSEL SUPPORT
FAILURE OF THE FS&R SUPPORT STRUCTURES
CONTROL SYSTEM FAILURE
NO BACK FAILURE
SYSTEM BRAKING FAILURE
SECONDARY FAILURE OF THE FS&R SUPPORT
DESIGN ERROR

A.5 ALIP Power System Fault Tree

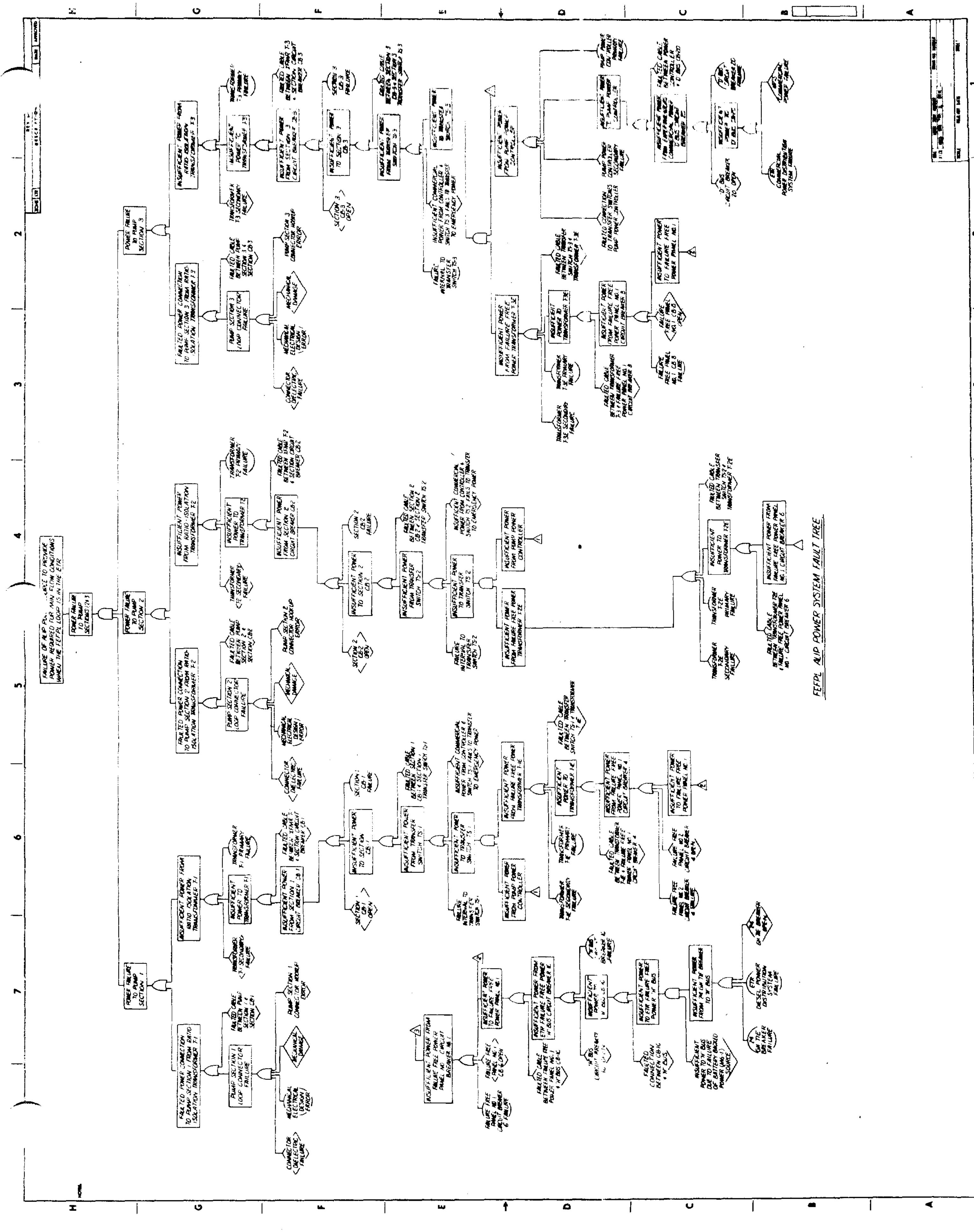
FEFPL ALIP POWER SYSTEM FAULT TREE

A.6 Helium System Fault Tree

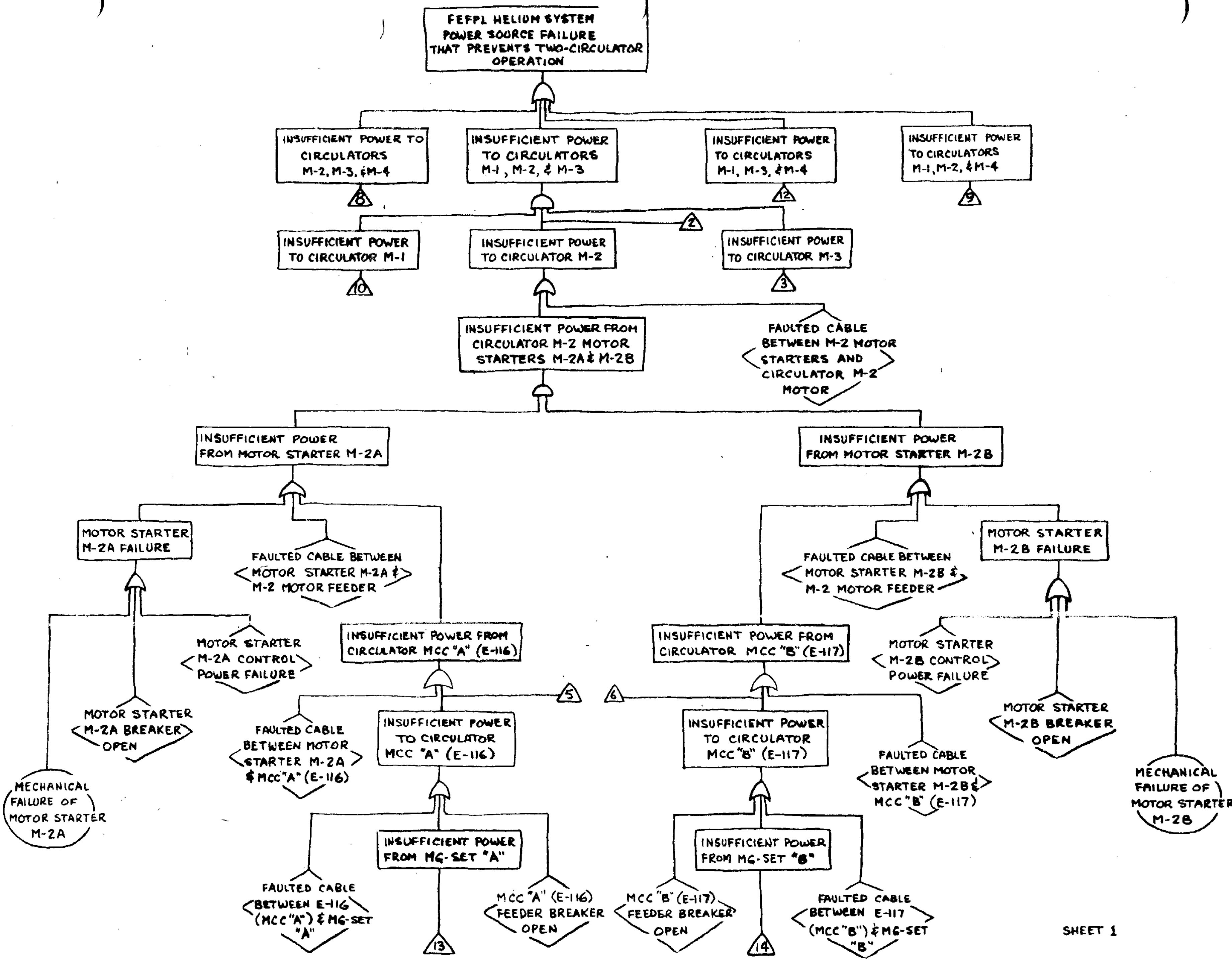
FEFPL HELIUM SYSTEM POWER SOURCE FAILURE THAT PREVENTS TWO-CIRCULATOR OPERATION
INSUFFICIENT POWER TO CIRCULATORS M-2, M-3, & M-4
INSUFFICIENT POWER TO CIRCULATORS M-1, M-2, & M-3
INSUFFICIENT POWER TO CIRCULATORS M-1, M-3, & M-4
INSUFFICIENT POWER TO CIRCULATORS M-1, M-2, & M-4
8
12
9
2
INSUFFICIENT POWER TO CIRCULATOR M-1
INSUFFICIENT POWER TO CIRCULATOR M-2
INSUFFICIENT POWER TO CIRCULATOR M-3
10
3
INSUFFICIENT POWER FROM CIRCULATOR M-2 MOTOR STARTERS M-2A & M-2B
FAULTED CABLE BETWEEN M-2 MOTOR STARTERS AND CIRCULATOR M-2 MOTOR
INSUFFICIENT POWER FROM MOTOR STARTER M-2A
INSUFFICIENT POWER FROM MOTOR STARTER M-2B
MOTOR STARTER M-2A FAILURE
FAULTED CABLE BETWEEN MOTOR STARTER M-2A & M-2 MOTOR FEEDER
FAULTED CABLE BETWEEN MOTOR STARTER M-2B & M-2 MOTOR FEEDER
MOTOR STARTER M-2B FAILURE
MOTOR STARTER M-2A CONTROL POWER FAILURE
INSUFFICIENT POWER FROM CIRCULATOR MCC "A" (E-116)
INSUFFICIENT POWER FROM CIRCULATOR MCC "B" (E-117)
MOTOR STARTER M-2B CONTROL POWER FAILURE
5
6
MOTOR STARTER M-2A BREAKER OPEN
FAULTED CABLE BETWEEN MOTOR STARTER M-2A & MCC "A" (E-116)
INSUFFICIENT POWER TO CIRCULATOR MCC "A" (E-116)
INSUFFICIENT POWER TO CIRCULATOR MCC "B" (E-117)
FAULTED CABLE BETWEEN MOTOR STARTER M-2B & MCC "B" (E-117)
MOTOR STARTER M-2B BREAKER OPEN
MECHANICAL FAILURE OF MOTOR STARTER M-2A
MECHANICAL FAILURE OF MOTOR STARTER M-2B
INSUFFICIENT POWER FROM MG-SET "A"
INSUFFICIENT POWER FROM MG-SET "B"
FAULTED CABLE BETWEEN E-116 (MCC "A") & MG-SET "A"
MCC "A" (E-116) FEEDER BREAKER OPEN
MCC "B" (E-117) FEEDER BREAKER OPEN
FAULTED CABLE BETWEEN E-117 (MCC "B") & MG-SET "B"
13
14

SHEET 1

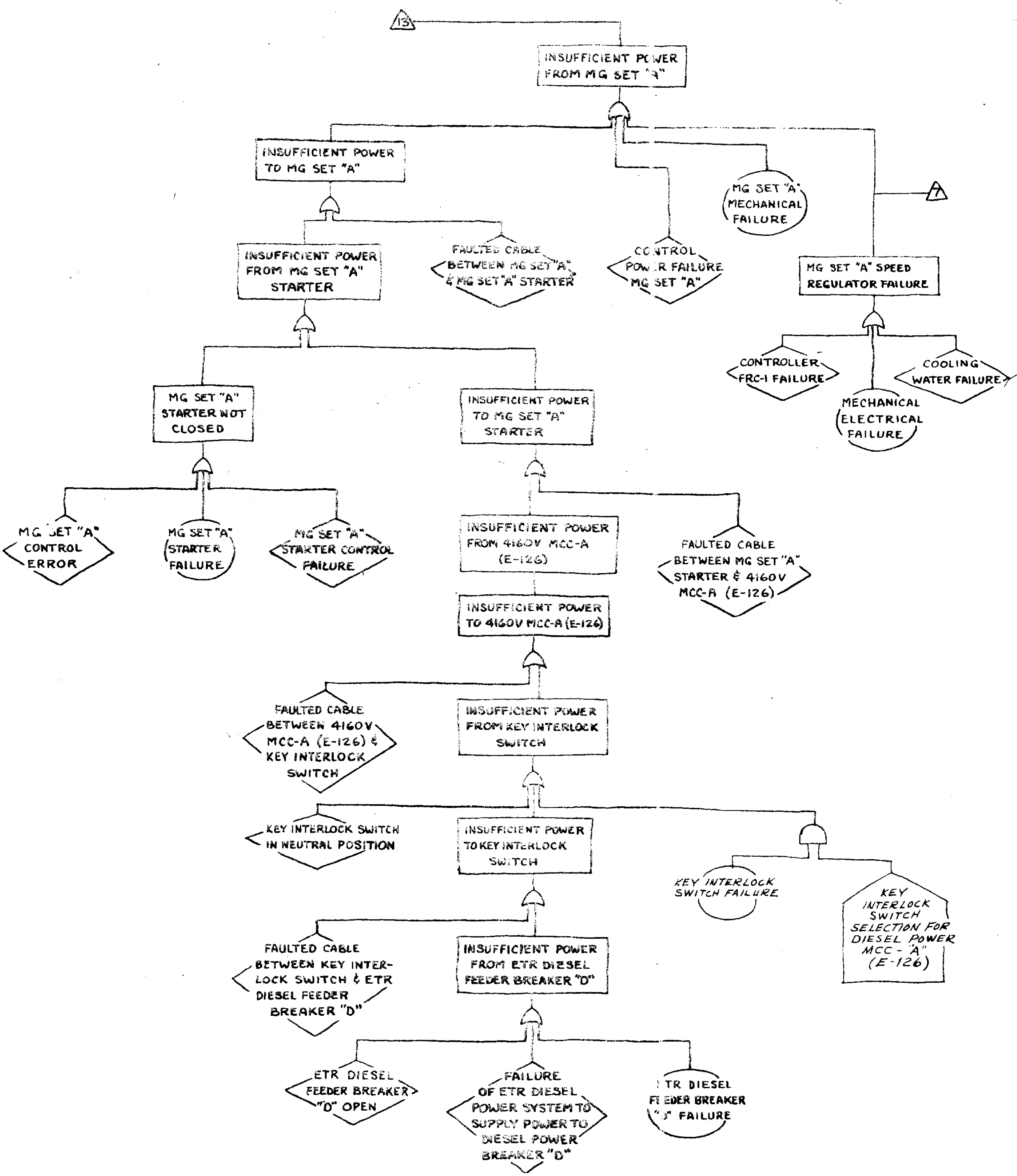
13
INSUFFICIENT POWER FROM MG SET "A"
INSUFFICIENT POWER TO MG SET "A"
MG SET "A" MECHANICAL FAILURE
7
CONTROL POWER FAILURE MG SET "A"
MG SET "A" SPEED REGULATOR FAILURE
INSUFFICIENT POWER FROM MG SET "A" STARTER
FAULTED CABLE BETWEEN MG SET "A" & MG SET "A" STARTER
CONTROLLER FRC-1 FAILURE
MECHANICAL ELECTRICAL FAILURE
COOLING WATER FAILURE
MG SET "A" STARTER NOT CLOSED
INSUFFICIENT POWER TO MG SET "A" STARTER
MG SET "A" CONTROL ERROR
MG SET "A" STARTER FAILURE
MG SET "A" STARTER CONTROL FAILURE
INSUFFICIENT POWER FROM 4160V MCC-A (E-126)
FAULTED CABLE BETWEEN MG SET "A" STARTER & 4160V MCC-A (E-126)
INSUFFICIENT POWER TO 4160V MCC-A (E-126)
FAULTED CABLE BETWEEN 4160V MCC-A (E-126) & KEY INTERLOCK SWITCH
INSUFFICIENT POWER FROM KEY INTERLOCK SWITCH
KEY INTERLOCK SWITCH IN NEUTRAL POSITION
INSUFFICIENT POWER TO KEY INTERLOCK SWITCH
KEY INTERLOCK SWITCH FAILURE
KEY INTERLOCK SWITCH SELECTION FOR DIESEL POWER MCC - "A" (E-126)
FAULTED CABLE BETWEEN KEY INTER-LOCK SWITCH & ETR DIESEL FEEDER BREAKER "D"
INSUFFICIENT POWER FROM ETR DIESEL FEEDER BREAKER "D"
ETR DIESEL FEEDER BREAKER "D" OPEN
FAILURE OF ETR DIESEL POWER SYSTEM TO SUPPLY POWER TO DIESEL POWER BREAKER "D"
ETR DIESEL FEEDER BREAKER "D" FAILURE

SHEET 2

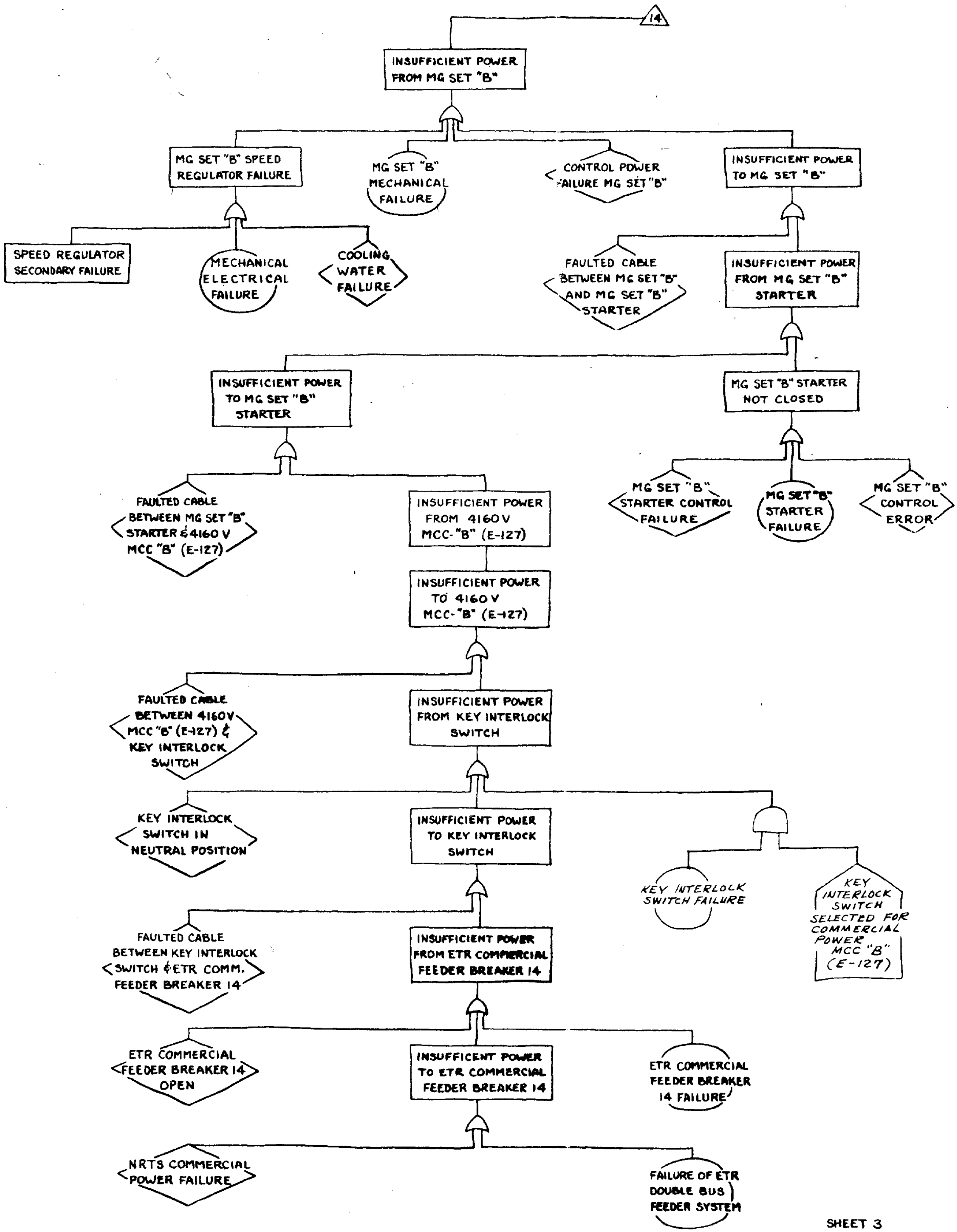
14
INSUFFICIENT POWER FROM MG SET "B"
MG SET "B" SPEED REGULATOR FAILURE
MG SET "B" MECHANICAL FAILURE
CONTROL POWER FAILURE MG SET "B"
INSUFFICIENT POWER TO MG SET "B"
SPEED REGULATOR SECONDARY FAILURE
MECHANICAL ELECTRICAL FAILURE
COOLING WATER FAILURE
FAULTED CABLE BETWEEN MG SET "B" AND MG SET "B" STARTER
INSUFFICIENT POWER FROM MG SET "B" STARTER
INSUFFICIENT POWER TO MG SET "B" STARTER
MG SET "B" STARTER NOT CLOSED
FAULTED CABLE BETWEEN MG SET "B" STARTER & 4160 V MCC "B" (E-127)
INSUFFICIENT POWER FROM 4160V MCC-"B" (E-127)
MG SET "B" STARTER CONTROL FAILURE
MG SET "B" STARTER FAILURE
MG SET "B" CONTROL ERROR
INSUFFICIENT POWER TO 4160 V MCC-"B" (E-127)
FAULTED CABLE BETWEEN 4160V MCC "B" (E-127) & KEY INTERLOCK SWITCH
INSUFFICIENT POWER FROM KEY INTERLOCK SWITCH
KEY INTERLOCK SWITCH IN NEUTRAL POSITION
INSUFFICIENT POWER TO KEY INTERLOCK SWITCH
KEY INTERLOCK SWITCH FAILURE
KEY INTERLOCK SWITCH SELECTED FOR COMMERCIAL POWER MCC "B" (E-127)
FAULTED CABLE BETWEEN KEY INTERLOCK SWITCH & ETR COMM. FEEDER BREAKER 14
INSUFFICIENT POWER FROM ETR COMMERCIAL FEEDER BREAKER 14
ETR COMMERCIAL FEEDER BREAKER 14 OPEN
INSUFFICENT POWER TO ETR COMMERCIAL FEEDER BREAKER 14
ETR COMMERCIAL FEEDER BREAKER 14 FAILURE
NRTS COMMERCIAL POWER FAILURE
FAILURE OF ETR DOUBLE BUS FEEDER SYSTEM

SHEET 3

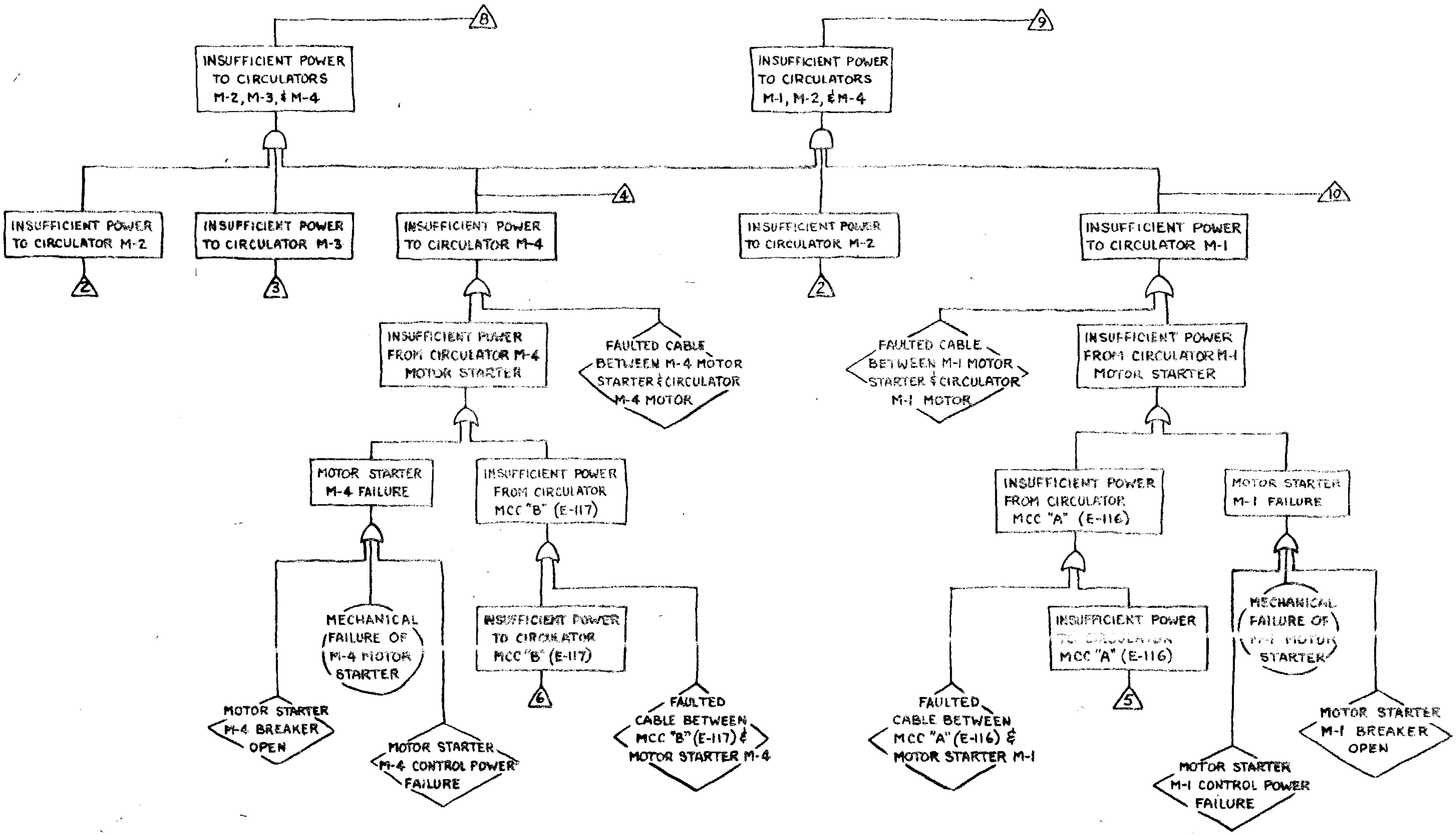

INSUFFICIENT POWER TO CIRCULATORS M-2, M-3, & M-4
8
INSUFFICIENT POWER TO CIRCULATOR M-2
2
INSUFFICIENT POWER TO CIRCULATOR M-3
3
INSUFFICIENT POWER TO CIRCULATOR M-4
4
INSUFFICIENT POWER FROM CIRCULATOR M-4 MOTOR STARTER
FAULTED CABLE BETWEEN M-4 MOTOR STARTER & CIRCULATOR M-4 MOTOR
MOTOR STARTER M-4 FAILURE
INSUFFICIENT POWER FROM CIRCULATOR MCC "B" (E-117)
MECHANICAL FAILURE OF M-4 MOTOR STARTER
MOTOR STARTER M-4 BREAKER OPEN
MOTOR STARTER M-4 CONTROL POWER FAILURE
INSUFFICIENT POWER TO CIRCULATOR MCC "B" (E-117)
6
FAULTED CABLE BETWEEN MCC "B" (E-117) & MOTOR STARTER M-4
INSUFFICIENT POWER TO CIRCULATORS M-1, M-2, & M-4
9
INSUFFICIENT POWER TO CIRCULATOR M-2
2
INSUFFICIENT POWER TO CIRCULATOR M-1
10
FAULTED CABLE BETWEEN M-1 MOTOR STARTER & CIRCULATOR M-1 MOTOR
INSUFFICIENT POWER FROM CIRCULATOR M-1 MOTOR STARTER
INSUFFICIENT POWER FROM CIRCULATOR MCC "A" (E-116)
MOTOR STARTER M-1 FAILURE
FAULTED CABLE BETWEEN MCC "A" (E-116) & MOTOR STARTER M-1
INSUFFICIENT POWER TO CIRCULATOR MCC "A" (E-116)
5
MECHANICAL FAILURE OF M-1 MOTOR STARTER
MOTOR STARTER M-1 CONTROL POWER FAILURE
MOTOR STARTER M-1 BREAKER OPEN

SHEET 4

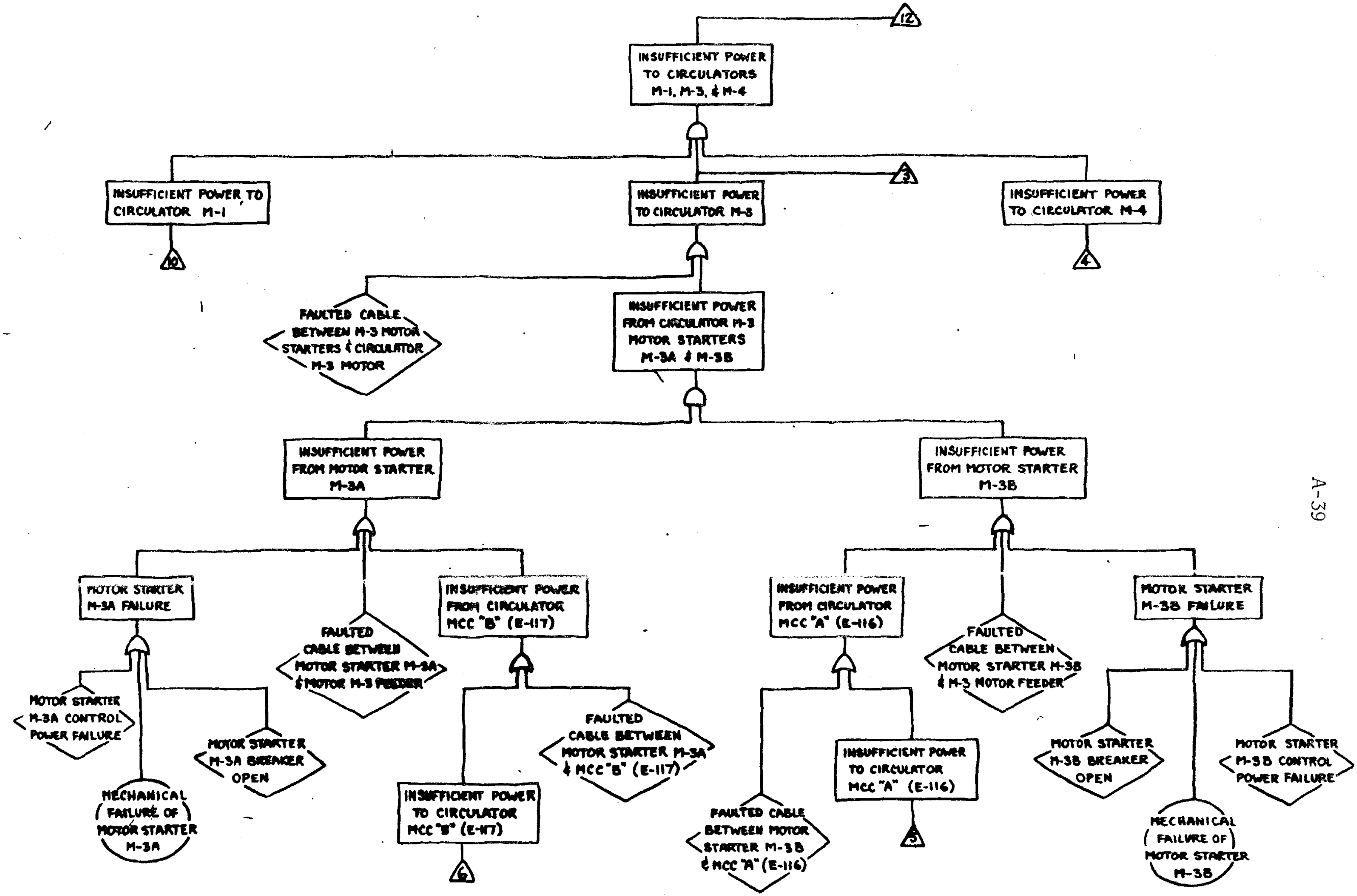

12
INSUFFICIENT POWER TO CIRCULATORS M-1, M-3, & M-4
INSUFFICIENT POWER TO CIRCULATOR M-1
10
INSUFFICIENT POWER TO CIRCULATOR M-3
3
INSUFFICIENT POWER TO CIRCULATOR M-4
4
FAULTED CABLE BETWEEN M-3 MOTOR STARTERS & CIRCULATOR M-3 MOTOR
INSUFFICIENT POWER FROM CIRCULATOR M-3 MOTOR STARTERS M-3A & M-3B
INSUFFICIENT POWER FROM MOTOR STARTER M-3A
INSUFFICIENT POWER FROM MOTOR STARTER M-3B
MOTOR STARTER M-3A FAILURE
FAULTED CABLE BETWEEN MOTOR STARTER M-3A & MOTOR M-3 FEEDER
INSUFFICIENT POWER FROM CIRCULATOR MCC "B" (E-117)
INSUFFICIENT POWER FROM CIRCULATOR MCC "A" (E-116)
FAULTED CABLE BETWEEN MOTOR STARTER M-3B & M-3 MOTOR FEEDER
MOTOR STARTER M-3B FAILURE
MOTOR STARTER M-3A CONTROL POWER FAILURE
MOTOR STARTER M-3A BREAKER OPEN
MECHANICAL FAILURE OF MOTOR STARTER M-3A
FAULTED CABLE BETWEEN MOTOR STARTER M-3A & MCC "B" (E-117)
INSUFFICIENT POWER TO CIRCULATOR MCC "B" (E-117)
6
FAULTED CABLE BETWEEN MOTOR STARTER M-3B & MCC "A" (E-116)
INSUFFICIENT POWER TO CIRCULATOR MCC "A" (E-116)
5
MOTOR STARTER M-3B BREAKER OPEN
MOTOR STARTER M-3B CONTROL POWER FAILURE
MECHANICAL FAILURE OF MOTOR STARTER M-3B

SHEET 5

APPENDIX B

TABLE OF CONTENTS

LIST OF FIGURES

LIST OF TABLES

B.0 Models and Methods

B.1 THYME-B

To simulate transient thermal and hydraulic conditions in the Fuel Element Failure Propagation Loop (FEFPL) subsequent to arbitrary perturbations of steady-state operation, the THYME-B (Thermal-Hydraulic Model for Experiments) computer code was developed. In this version of the model,[1] fluids are considered single-phase and flow is unidirectional. Spatial detail employed for temperature calculations varies with location in the loop; greatest resolution is provided in regions of major heat transfer, i.e., the fuel zone and heat exchanger.

THYME-B was developed to solve the model equations. THYME-B comprises a two-part program. The first is a FORTRAN initialization program designed to solve the system of steady-state equations for the loop model. It includes a set of subroutines that calculates overall thermal conductances, generally based upon dimensional input information, flow rates, and thermophysical properties of the fluids. Revelant steady-state data are then automatically passed to the dynamic portion of the model, thereby establishing proper initial conditions for the beginning of a specified dynamic simulation.

The dynamic portion of the program is coded via IBM S/360-CSMP.[2] At present, 84 first-order, coupled differential equations and a large number of algebraic relationships are included. Subroutines (macros) are used to compute thermophysical properties of sodium and helium, flow-dependent transport delays used in areas of negligible heat transfer, and dynamic heat-flow characteristics of the ALIP. Function generators and switching functions are used to control initiation and describe various loop transient conditions that include complete test section flow blockage, partial test section flow blockage, loss-of-flow caused either by pump failure or blockage, and reactor scram with residual fission and fission product decay heat generation. Perturbations in some parameters of auxiliary loop systems can also be prescribed as arbitrary functions of time. These include flow rate of ETR water coolant to in-pile tube, rate of flow of helium through loop heat exchanger, inlet temperature of helium flowing through the loop heat exchanger.

The THYME-B model does not contain a sodium voiding model. Sodium temperatures in the test fuel zone and HFR water temperature in the in-pile tube can be limited to their saturation temperatures.

THYME-B Modeling

The THYME-B model of the FEFPL loop is presented in Figs. B.1, B.2, B.3, B.4, and B.5. These figures provide the detailed nodal nomenclature and locations for each of the major loop regions.

General types of data input needed to establish initialization of a desired steady-state operating condition include:

1) total primary loop flow rate or pump power
2) local heat generation rates
3) flow rates and inlet temperatures of ancillary coolants
4) FEFPL dimensional data around the primary circuit, including test bundle
5) sodium inventories and heat capacities in various regions of the primary circuit, and
6) hydraulic loss coefficients for sodium flow paths

The initialization portion of THYME-B provides complete output of converged steady-state temperatures, primary system flow rate, pump power and test section-bypass flow split. Values of thermal conductances and an accounting of heat balance in the heat exchanger is supplied.

In the dynamic portion of the program, variables to be printed and/or plotted are selected by the user, as are the print-plot time intervals. Printed information is normally preformated by CSMP although the user may add his own print and format statements.

B.2 SAS2A

The detailed thermohydraulic analyses of conditions within the FEFPL test section during experimental and accident transients were performed with the SAS2A accident analysis code.[3] This latest version contains many improvements, particularly in the area of sodium voiding dynamics predictions, over the previous SAS version.[4] Application of the code to the FEFPL geometry is described below.

SAS2A Modeling.

In this SAS2A study, a single channel model of the FEFPL test section was used to describe the 37 rod test section array and is shown schematically in Fig. B.6. The prototypical FTR fuel pin was described

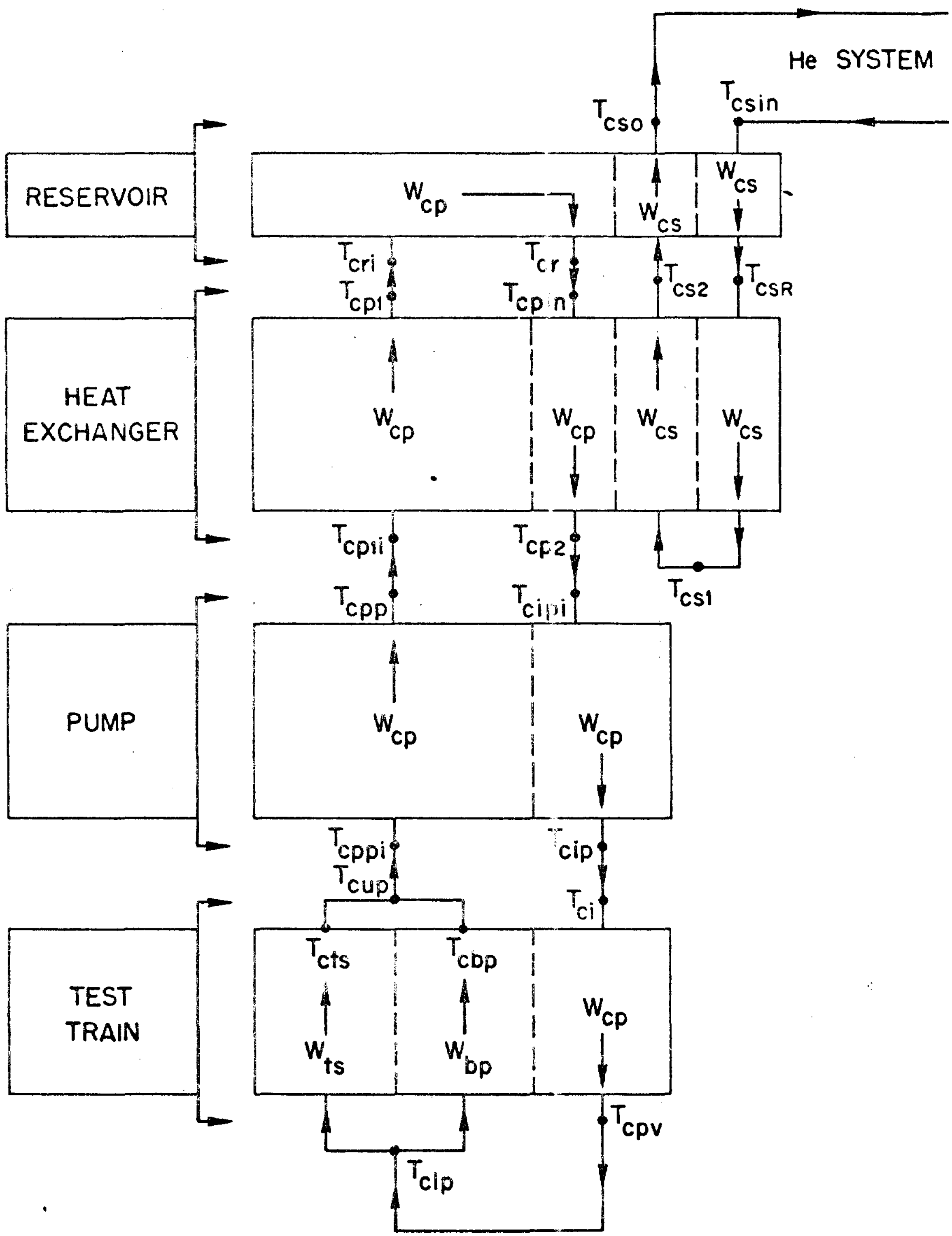

FIG. B.1 THYME-B Overall FEFP Loop Description

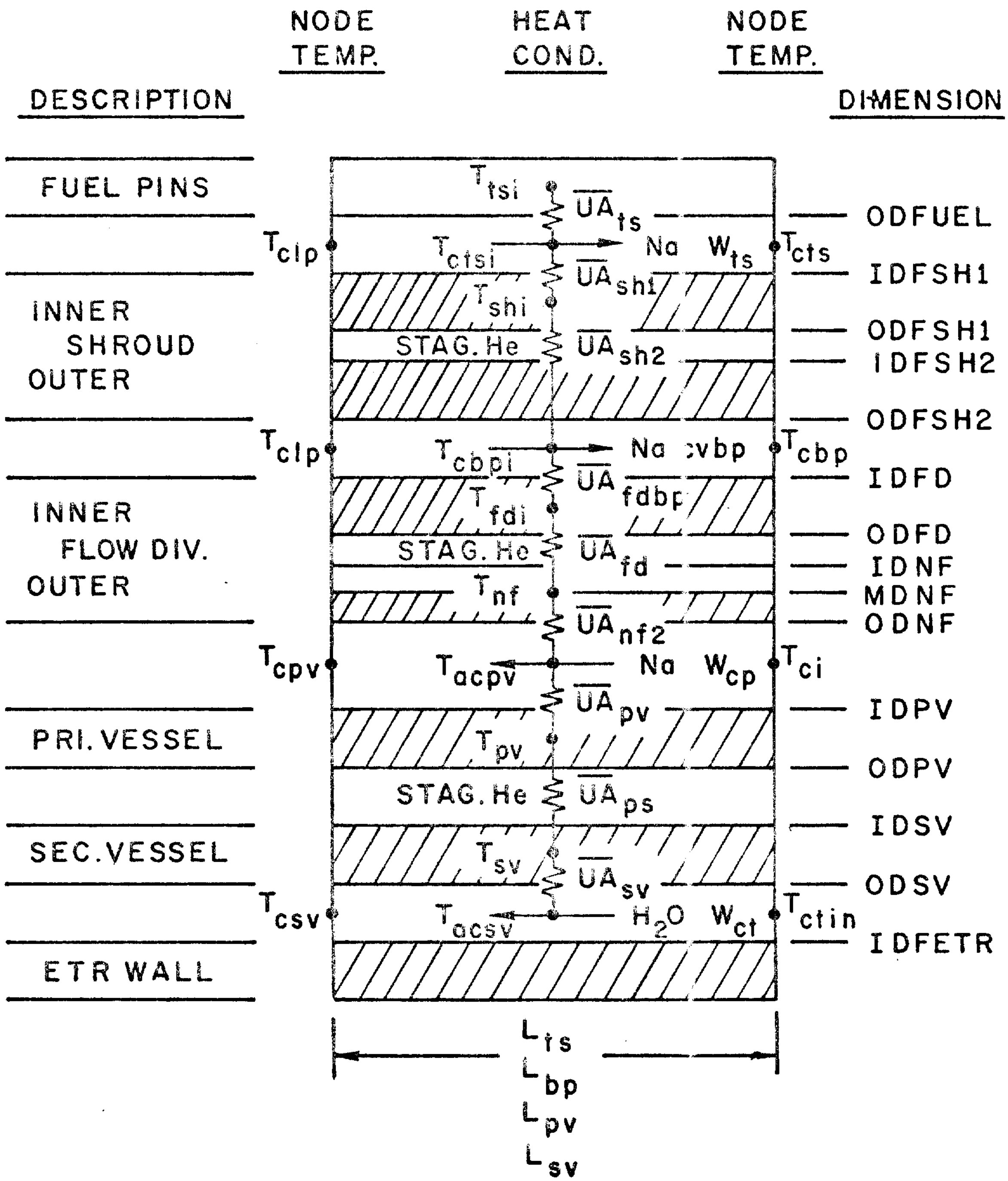

FIG. B.2 THYME-B Core Zone of Test Train Description

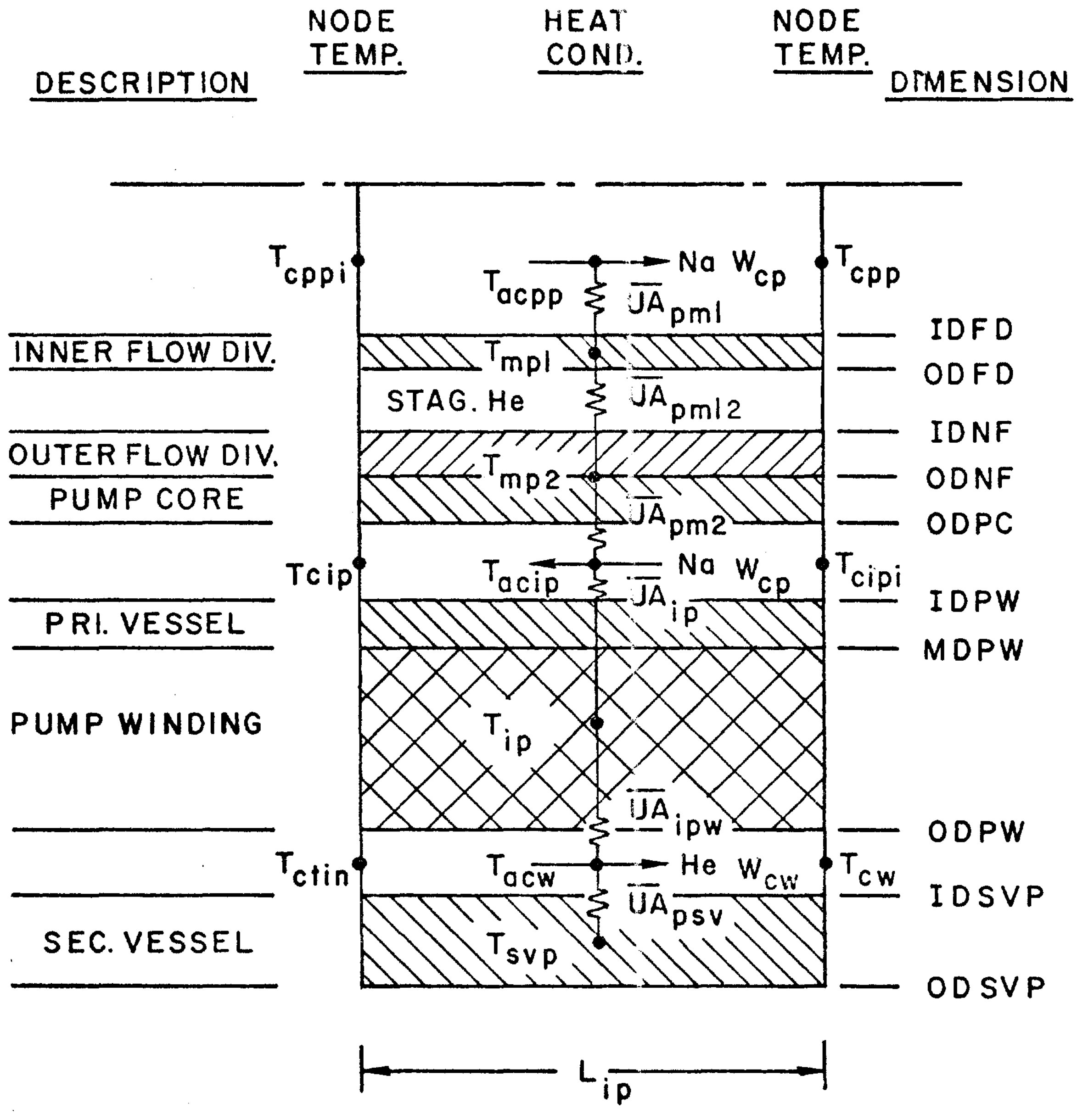

FIG. B.3 THYME-B ALIP Description

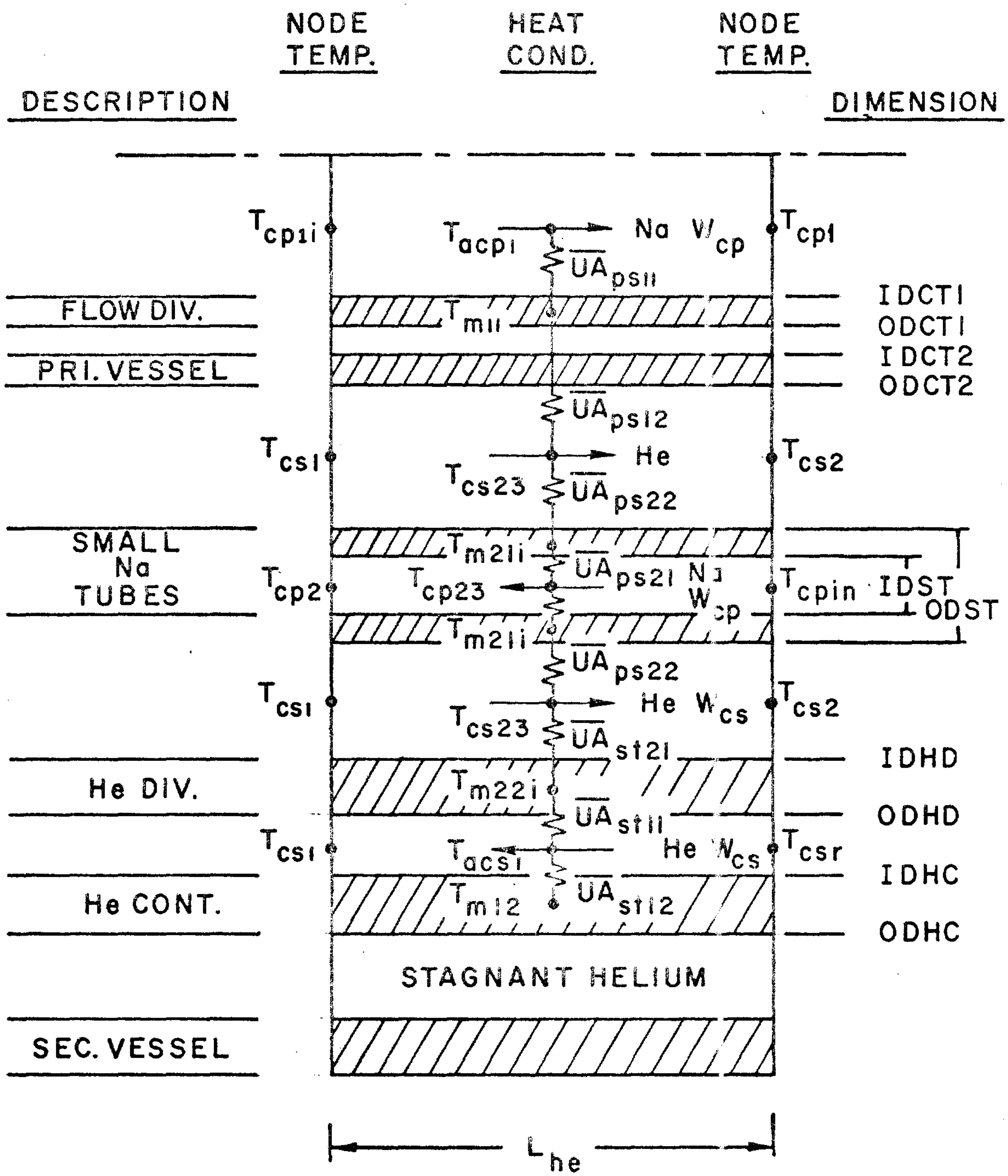

FIG. B.4 THYME-B Description of Heat Exchanger

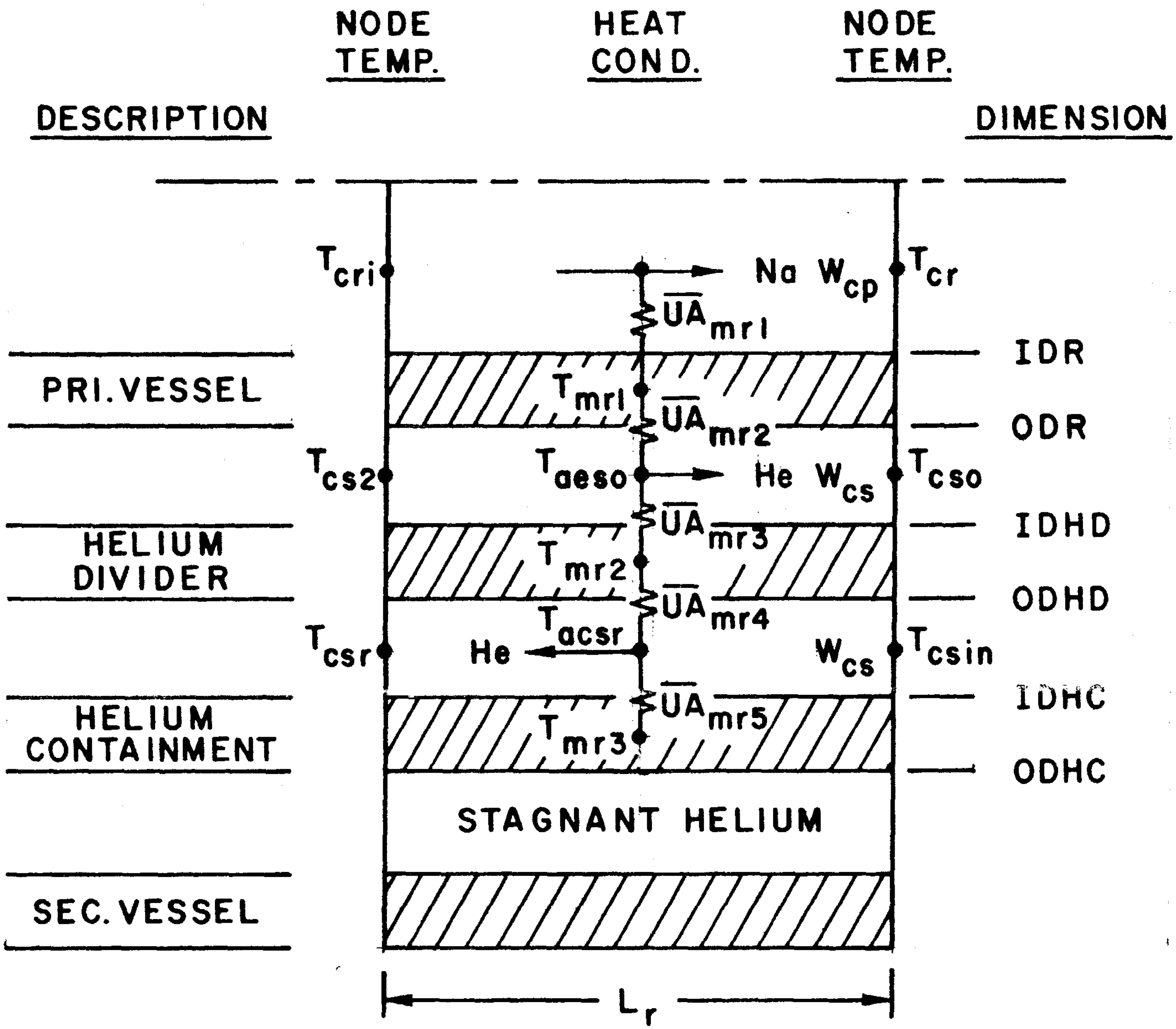

FIG. B.5 THYME-B Description of Reservoir using 10 radial temperature nodes with 15 axial nodes in the active fuel region. Pseudo lower and upper test section reflectors were utilized to describe the loop's calculated steady-state pressure drop. For the 37 fuel rod test section geometry with 150 gpm total loop flow, the frictional lengths of these reflectors were adjusted to reproduce the 77 psia total loop pressure drop value as predicted by the FEFPSTY code (see description given in Sect. B.5). As Fig. B.6 indicates, a lower reflector length of 115 cm was requred to attain the 27.2 psi loop lower leg pressure drop (pump to test section inlet) while an upper reflector length of 26.15 cm was sufficient to provide the required 6.23 psi loop upper leg pressure drop (outlet of test section to loop reservoir).

The coolant inertial lengths shown in Fig. B.6 at the inlet and outlet of the test section were selected to agree with the transient sodium expulsion characteristics as predicted for the FEFP loop by FEFPSLUG program (see Sect. B.6). The two inertial lengths were estimated with the following relationship, summing over all loop sections:

$$L_{inertial} = \sum_i L_i \left(\frac{A_{test}}{A_i}\right)$$

In Fig. B.7 a comparison is presented of the sodium ejection characteristics of the loop as obtained using SAS2A with the reference FEFPSLUG results. These results, showing liquid-vapor interface location versus time for the initial sodium ejection process, indicate that the lower liquid leg motion has been simulated almost exactly by SAS2A. However, as seen in Fig. B.7, the upper liquid leg expulsion has been overpredicted by SAS2A. As this is conservative (a more rapid expulsion leads to earlier fuel melting) no attempt was made to adjust the SAS2A upper leg inertial length in order to obtain a better agreement with FEFPSLUG.

As Fig. B.6 illustrates, the model employs an axial structure to simulate the colder nonheat generating FEFPL hex can. No heat transfer across this structure is allowed (only heat capacity effect is considered), therefore, the model only approximates the heat sink present around the FEFPL test section.

In the majority of cases studied, the 37 element FTR-type fuel bundle was evaluated with the FTR axial power distribution (peak/average = 1.25), test section sodium inlet temperature of 481°C, steady-state coolant mass velocity of 564.75 gm/cm^2 sec and steady-state peak heat flux of 12.8 kW/ft. These values were test section parameters which reflected the conditions at the loop's maximum operating capability point (point C of Fig. 6.3 as given in Sect. 6.1). A 70°C sodium superheat at initiation of sodium boiling was assumed with the upper plenum temperature of reentrant sodium taken as 800°C. Thermophysical and mechanical property data, identical to those employed in LMFBR studies, were used for the FEFPL materials.[5]

For the cases involving ETR reactor shutdown, the normalized power decay relationship developed for the FEFPL fuel region was employed. This basic curve is identical to that used in the THYME-B program and considers the retardation influence of the delayed gammas and is shown in Fig. B.8. As Fig. B.8 indicates, this power versus time relationship is for a 180 msec delay in scram, although in the SAS2A studies other scram delay times were also investigated.

Standard SAS2A input methods were used in the simulation of the test section sodium flow rate reductions for the two types of transients: (1) loss of ALIP power, and (2) inlet flow blockages. The test section flow coastdown behavior following the loss of pump power was calculated by SAS using an inputted pump head versus time relationship. This function was determined using the COASTDWN computer program (see description given in Sect. B.7) and the present FEFPL pump characteristics. Fig. B.9 compares the SAS2A predicted test section flow rate with the reference COASTDWN relationship for the case of total loss of electrical power without the emergency power assistance. As Fig. B.9 indicates, the SAS2A predicted flow decrease is more rapid than the reference value. As this is conservative, no further adjustment was attempted to bring the SAS2A prediction more in line with the reference COASTDWN relationship.

The test section flow rate versus time during loss of ALIP accident with emergency power assistance assumed that 15 kW of emergency pump power was available after a delay of 100 msec. The test section flow rate was again calculated by SAS2A for this case using a pump head versus time relationship as determined using the COASTDWN code. Fig. B.10 shows the excellent agreement between the SAS2A test section flow rate versus time prediction and the reference COASTDWN code results.

The complete FEFPL test section inlet flow blockage accidents were studied using SAS2A by introducing a very large test section inlet hydraulic

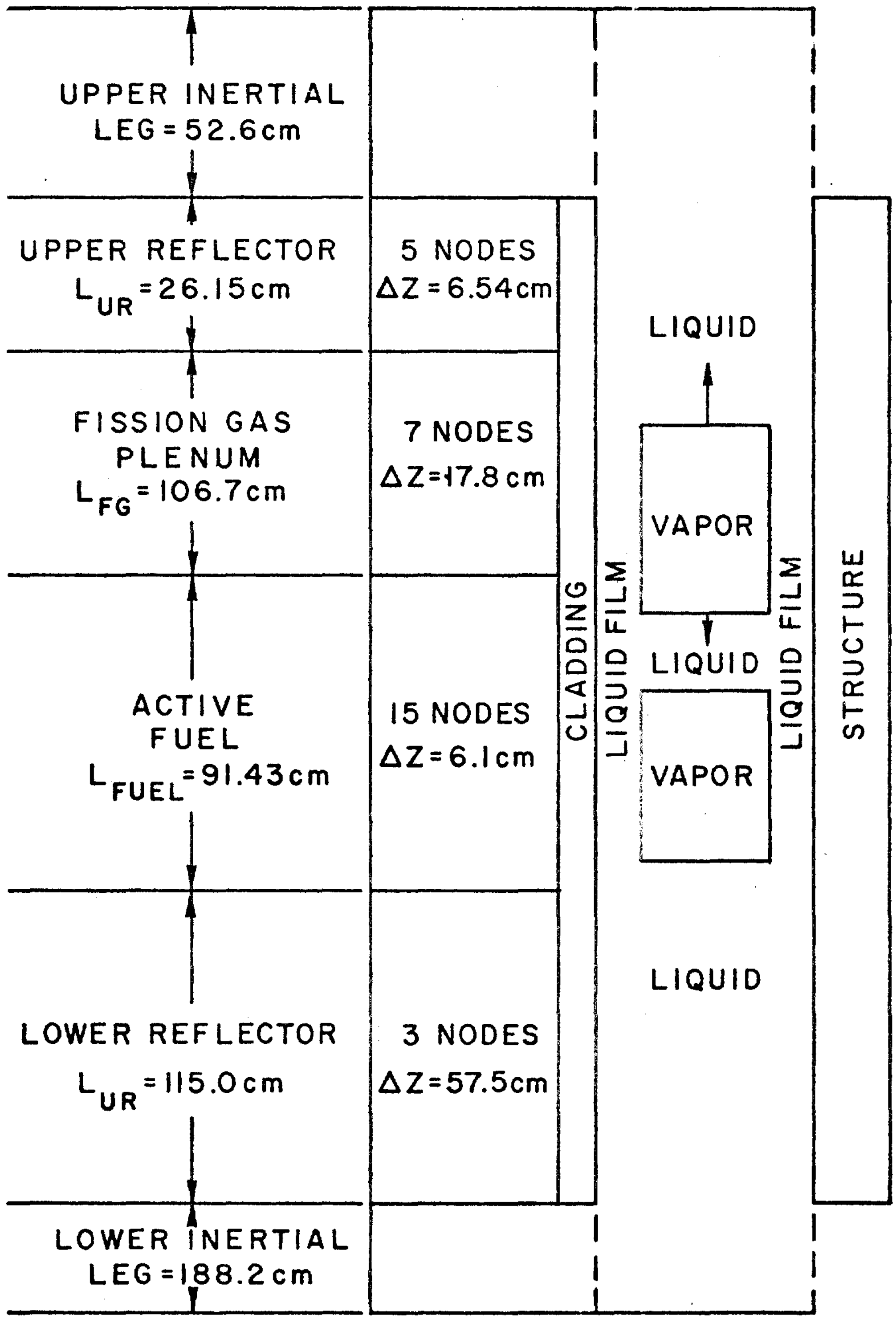

FIG. B.6 SAS2A Geometric Model of FEFP Loop

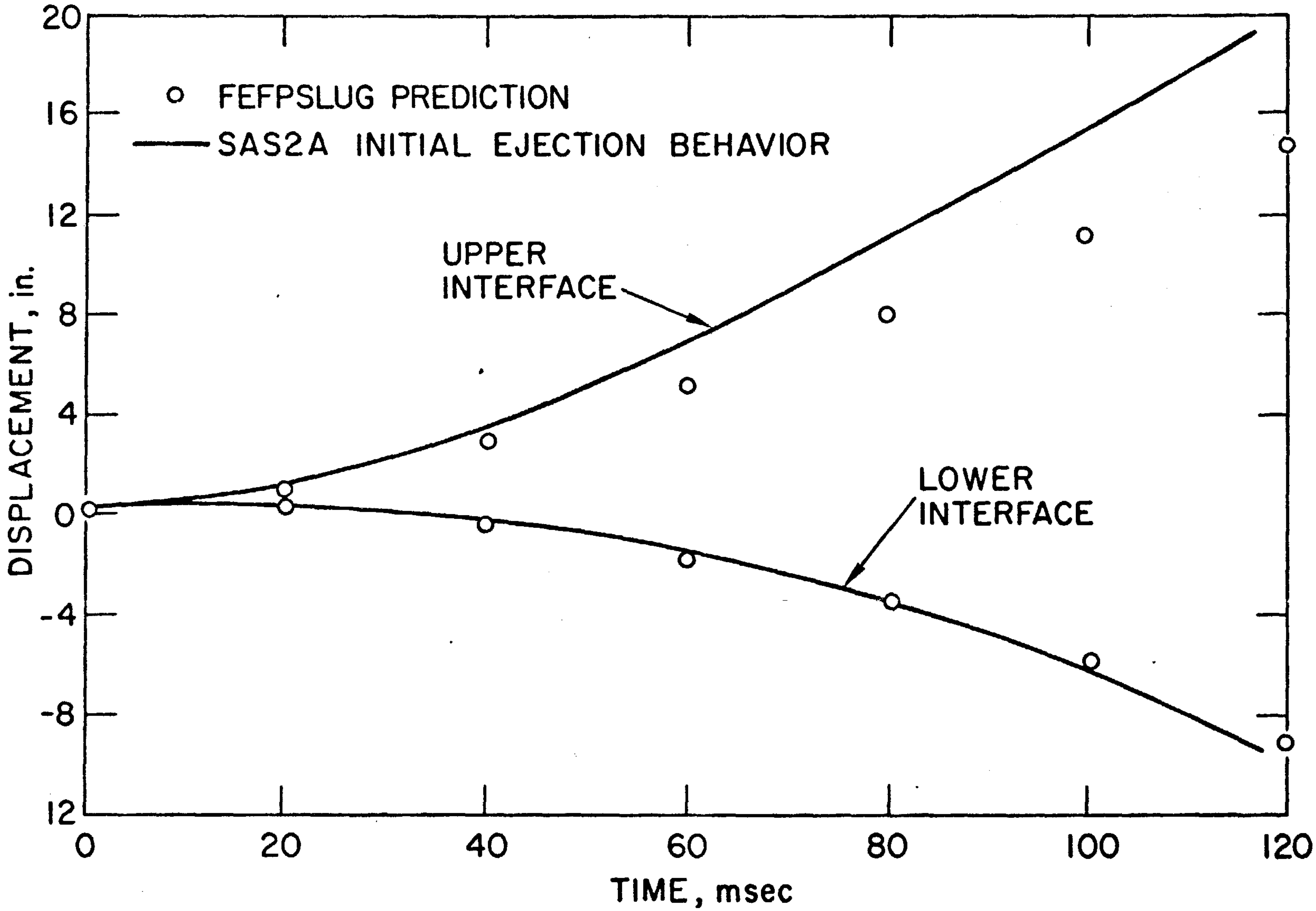

FIG. B.7 Sodium Voiding Interface Location Versus Time

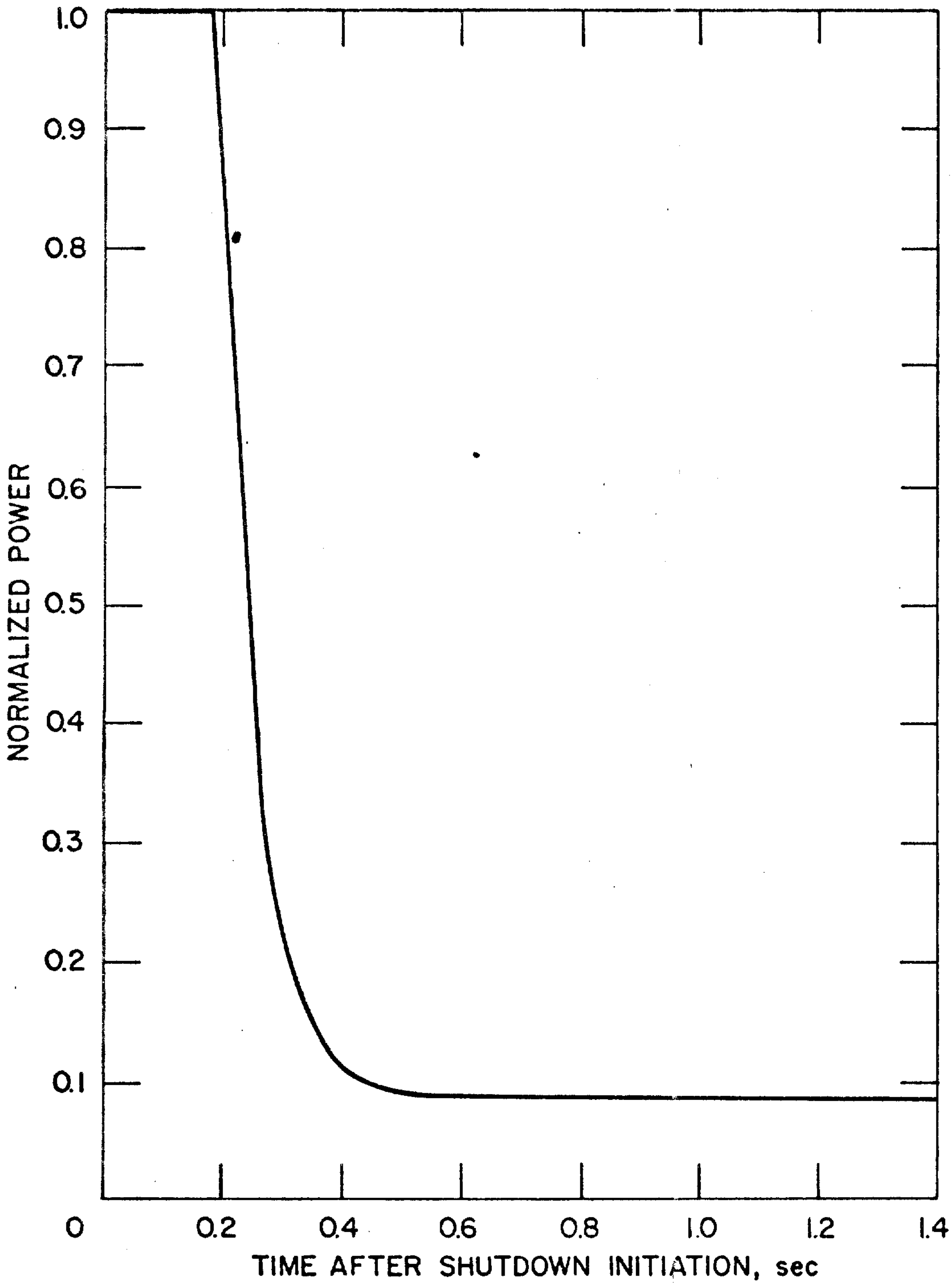

FIG. B.8 Normalized Test Section Power Versus Time After Shutdown Initiation

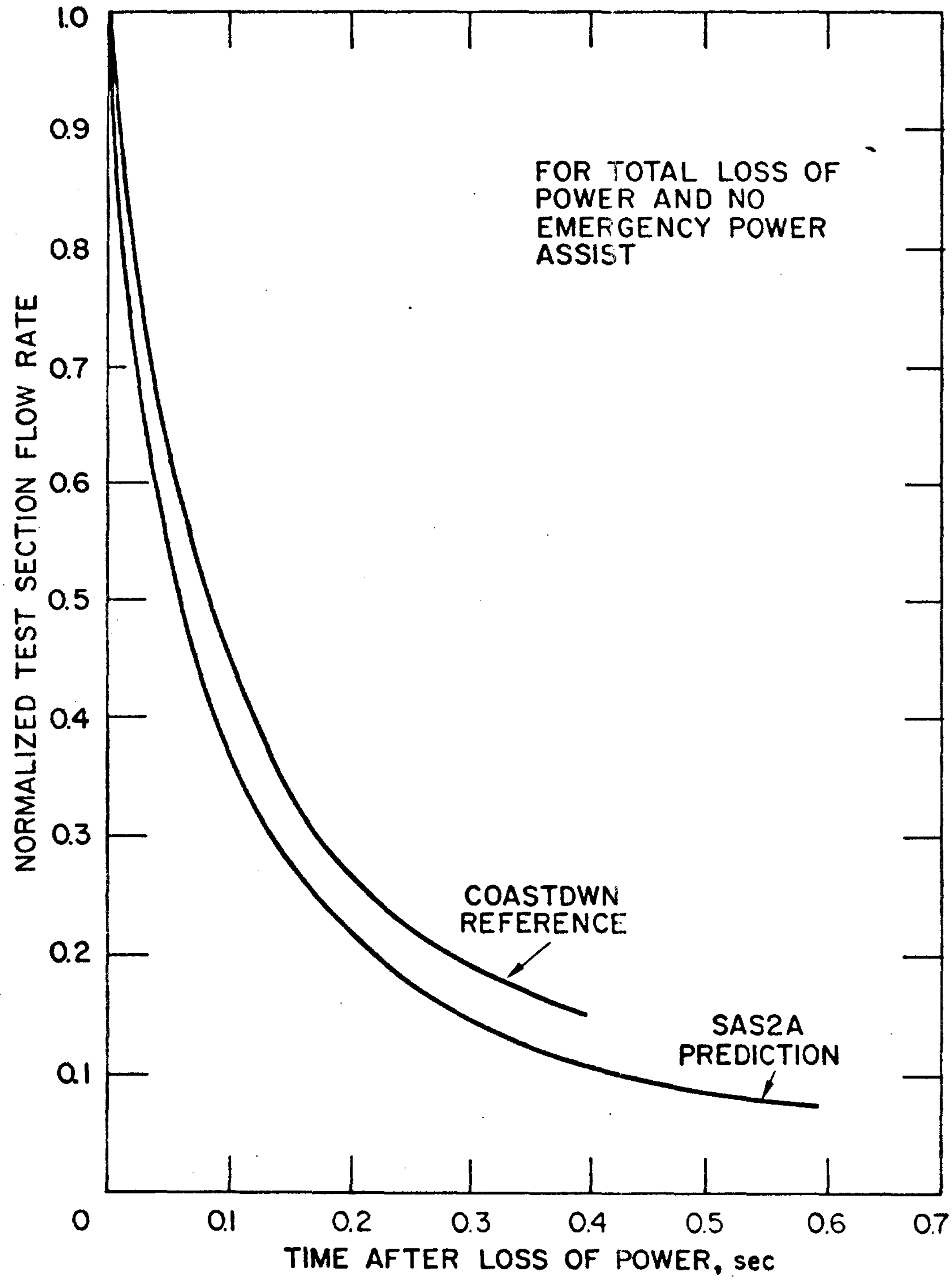

FIG. B.9 Normalized Test Section Flow Rate Versus Time After Loss of Total Pump Power

FIG. B.10 Normalized Test Section Flow Rate After Loss of ALIP with Emergency Pump Power

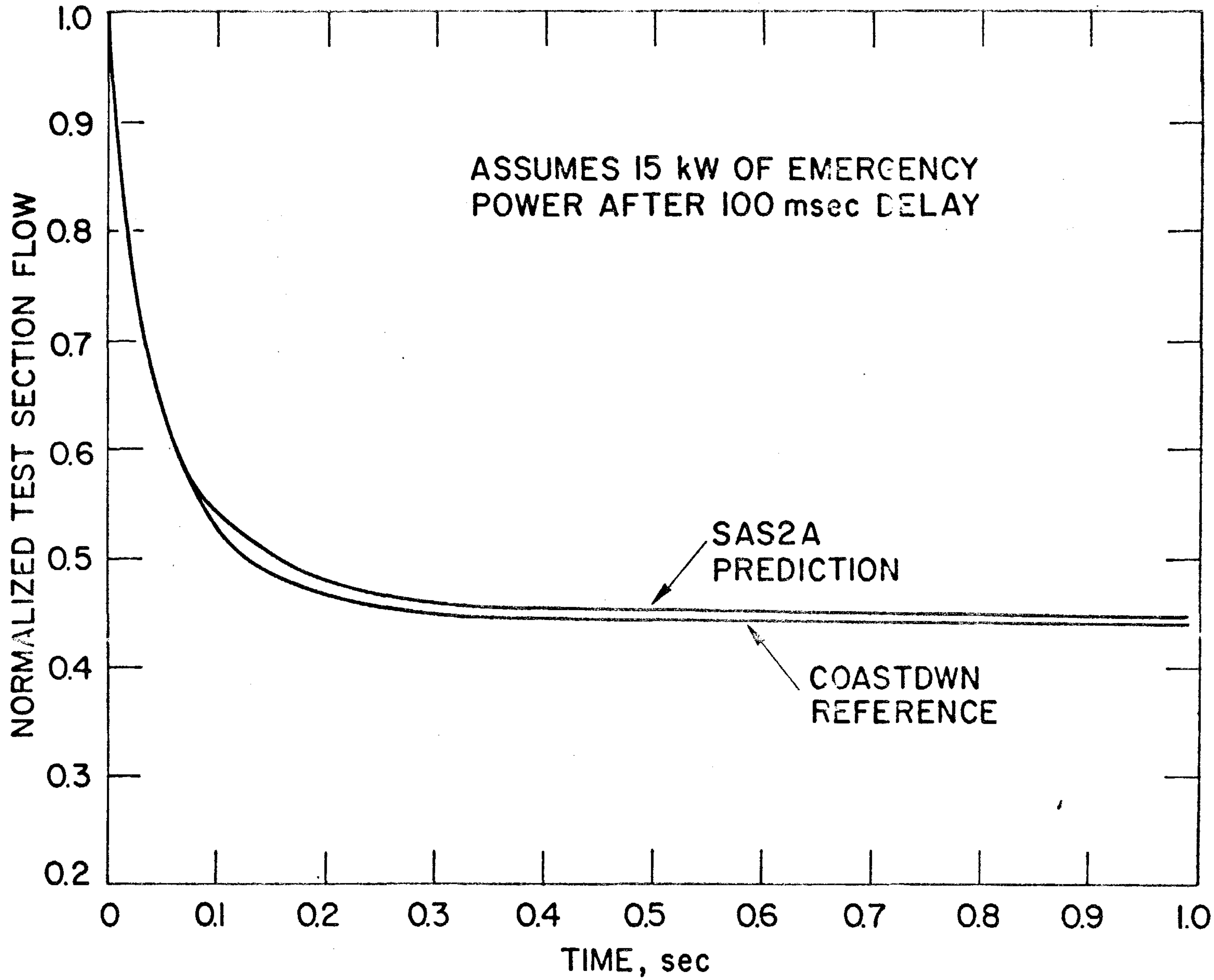

resistance. A L/D_e of 10^7 was used with a time constant for blockage assumed to be 0.10 sec. These hydraulic conditions resulted in a sodium flow stoppage to the test section inlet more rapid than probably could be physically realized in the actual system. Using this flow relationship for analyzing the reference design basis experiment (Sect. 10) and flow blockage accident (Sect. 11) is therefore conservative.

B.3 REXCO

The radial MFCI pressure distribution throughout the multi-vessel FEFP loop in the test section region was obtained using the REXCO-H computer program.[6] The REXCO-H code is a time dependent, hydrodynamic, two-spatial-dimension computer program designed to perform the numerical calculation describing the response of a primary reactor containment system to a high-energy excursion. The hydrodynamic equations and the equations of state for the reactor materials are expressed in Lagrangian form. Cylindrical symmetry is assumed. Shock discontinuities are diffused by the introduction of an artificial viscosity. The code input, or initial values, are the pressures, internal energies, and velocities generated by the accident. Over the ensuing time the code computes the responsive displacements, velocities, pressures, specific internal energies, densities, and strains at finite time intervals. The computations are cyclically repeated for any number of time steps, or until a specified terminating condition, such as a vessel failure, is reached. The code has the capability of exhibiting graphically the pressure distribution, displacements, and motions, so that the shock wave propagation, loading history, and sequential damage to the reactor components can be traced throughout the course of the excursion.

The REXCO-H model has been checked against physical data available from laboratory experiments in which reactor accidents are simulated by the detonation of small explosive charges in scaled models.[7] The results of the comparisions demonstrate that the REXCO-H code has the capability of accurately predicting the early time pressure loadings which were generated. As a consequence, it was concluded that the code can be extended to the analysis of the initial pressure loadings created by reactor core explosions of a similar nature.

REXCO-H Modeling

The physical model of the loop used in this REXCO-H analysis is presented in Fig. B.11. Only the test section region in the core is modeled in detail. The following major assumptions have been made:

1) A simplified axisymmetric model depicted in Fig. B. 11 consisting of six concentric zones in the radial direction and a total of 43 zones in the axial direction is used.

2) Lengthwise, the analytical model emcompasses roughly one-half of the test section fuel elements, including the insulator pellets and the reflector.

3) All vessels are assumed to be thin circular cylinders fixed at the bottom and free to move upwards and in the radial direction. The vessels are assumed to have only membrane stresses. Five vessels are used in the model and correspond to the hex can, the flow divider, the primary vessel, the secondary vessel, and the ETR water flow shroud.

4) The model has a rigid-body platform with a mass equal to that of the sodium above the reflector region. No additional restraints on the platform are assumed.

5) The first four zones on the bottom of the model are assumed to be steel to support the vessels. The effects of this assumption are localized and tend quickly to dissipate any actions in the vertical direction.

6) The fuel, reflectors, and insulator are composites of different materials. The equation of state of the fuel is based on the pressure-volume diagrams for the respective source MFCI terms (for example, Fig. 10.12). In simulating the MFCI source, only the portion of the pressure-volume curve following the peak pressure is used. The Mie-Grüneisen equations of state are used for insulator and reflector materials. These equations of state were determined based on the volume fractions of the respective materials.

The design envelope MFCI source term obtained from the ANL parametric model was used as input. The expected MFCI source term in Sect. 10.2.2.1 gives pressures and energies less severe than these, and hence was not evaluated with REXCO-H. No adjustment of the source pressure-volume input was made to account for compliance of the insulating gas gap in the hex can. This approximation is conservative. Any revisions in the REXCO model so that it can describe more exactly the MFCI source will reduce the values of the calculated pressures.

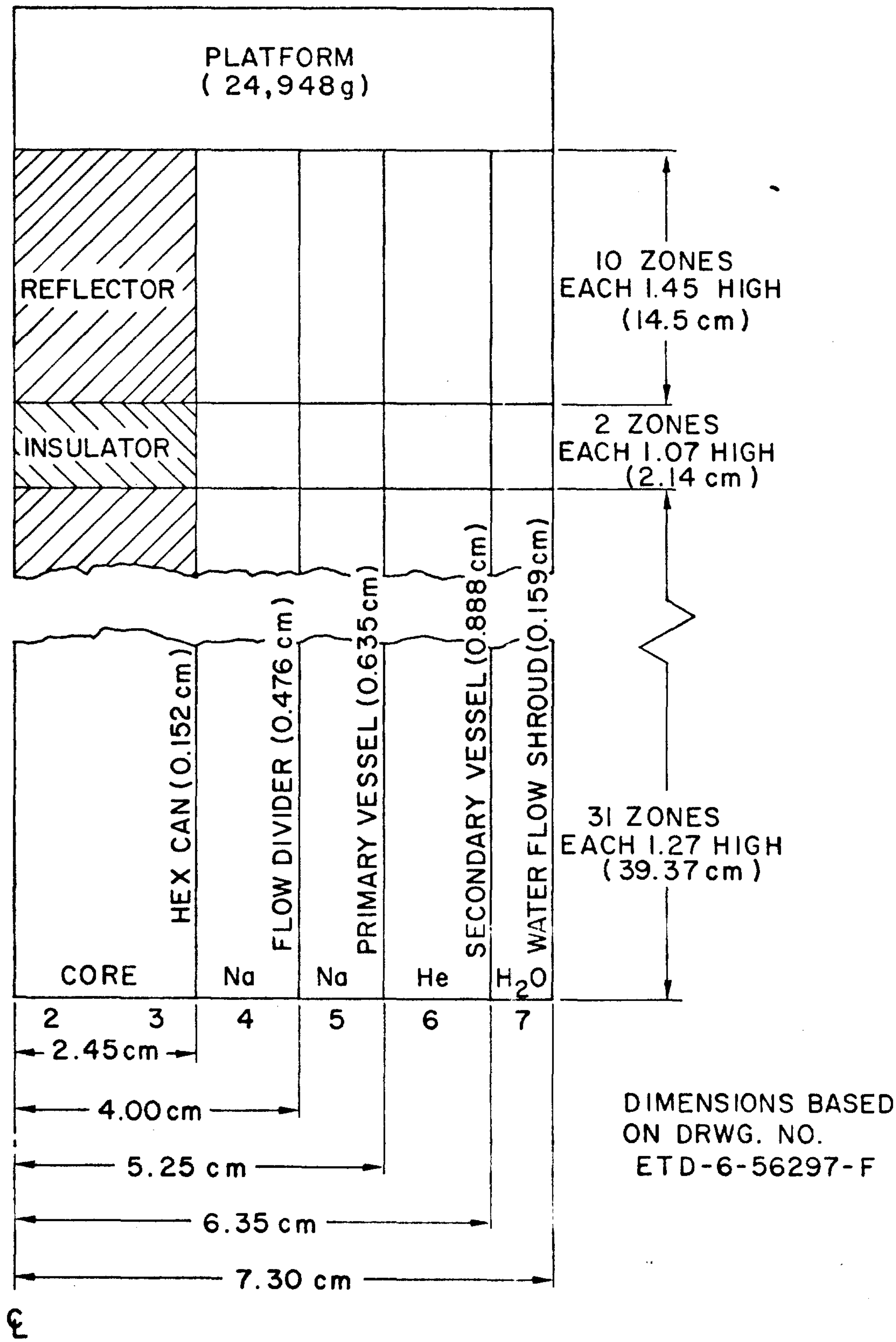

FIG. B.11 Loop Model for REXCO Analysis

B.4 FCI Parametric Model

The FCI parametric model developed at ANL is employed to calculate the pressure-temperature-work history during a molten fuel-coolant interaction.[8-10] This one-dimensional model incorporates the two major competing rate limiting processes: the heating of the coolant by the fuel (which produces pressure), and the expansion of the heated coolant (which reduces pressure) against a constraint given by the surroundings. The complicated fragmentation and mixing processes of fuel and sodium along with other important effects are described and incorporated into the model as input parameters. Extensive parametric studies of MFCI's were performed for reasonable assumed ranges of these parameters and are presented in Appendix C.

In the original MFCI model[8] two different approximations were developed to describe the process of sodium heating by the fuel;

1) quasi-steady state heat transfer where a constant heat transfer coefficient was assumed,

2) transient conduction where fuel fragmentation and mixing was assumed.

The above two models were recast into a single formulation,[9] in which the heat transferred to the coolant in the reaction zone is expressed as:

$$\frac{dQ}{dt} = A(t)\left(\frac{k_f}{\sqrt{\pi\alpha_f t}} + \frac{k_f}{R}\right)(T_f - T_{Na})$$

where T_f and T_{Na} are average temperatures of the fuel and sodium, k_f and α_f and the fuel thermal conductivity and thermal diffusivity of the fuel particles of radius R, and A(t) is the time dependent characteristic fuel-sodium heat transfer area. It is assumed that A(t) has the form of:

$$A(t) = A_o\left[1 - \exp\,(-t/t_m)\right]$$

where t_m is the "mixing fragmentation" time constant to describe the increase with time of the heat transfer surface area as fuel fragments and more fuel mixes in the interaction zone with the sodium.

In the application of this thermal model, when molten, the fuel temperature is expressed with a pseudo-value which accounts for the heat of fusion. The validity of this treatment is presented in Ref. 9. Three types of one-dimensional axial constraint are incorporated in the FCI parametric model:

1) acoustic constraint due to adiabatic, and compressible coolant columns of infinite extent above and below the reaction zone of length Lm,

2) inertial constraint of an unheated and incompressible coolant column of given length above the reaction zone,

3) acoustic constraint up to the acoustic unloading time and a finite inertial constraint for continuation to longer times. The unloading time corresponds to the round-trip time to the nearest free surface, and may result in a cutoff in the heat transfer due to the flashing of the sodium.

The acoustic constraint, valid only up to the acoustic unloading time of 2 L/Co, where L is the distance from the mixing zone boundary to the nearest free reflecting surface and Co is the sonic velocity, is accurate during the initial shock phase of the MFCI. The expression for the change in reaction zone volume with the acoustic constraint (neglecting the volume change of the fuel) is:

$$\frac{dV}{dt} = \frac{S}{\rho_o C_o} (P-P_o) + \frac{P_o^{1/n} V_{go}}{nP^{[1+(1/n)]}}$$

where S is the flow area per gram of heated coolant, P is the pressure in the mixing zone, P_o , ρ_o are the initial pressure and sodium density throughout the system, V_{go} is the initial gas volume in the reaction zone, and n is the adiabatic exponent. The second term in the right hand side, then, represents the compliance of any noncondensable gas present initially in the mixing zone.

Under the inertial constraint condition, the heated coolant in the mixing zone expands against the inertia of the upper heated coolant column (one way expansion). A macroscopic momentum balance give the motion of this loading coolant column:

$$\frac{dU}{dt} = - g + \frac{P-P_{ex}}{\rho_o (Z_{ex}-Z)} - (1/2)\, U^2 \frac{f}{R_h}$$

Where P_{ex} is the exit gas plenum pressure, Z_{ex} is the position of the exit gas plenum, Z is the position of the mixing zone - upper coolant column interface, U is the ejection velocity of the upper coolant column, g is the acceleration due to gravity, f is the friction factor, and R_h is the hydraulic radius of the coolant channel.

The reaction zone volume change, again neglecting the volume change of the fuel, and considering the compliance volume of the noncondensable gas is:

$$\frac{dV}{dt} = \frac{SU}{2} + \frac{P_o^{1/n} V_{go}}{nP^{[1+(1/n)]}} \frac{dP}{dt}$$

Several additional features have been implemented into the basic FCI parameter model as outlined above. The details of these calculational options are described in Ref. 10 and 11, and include the effect of:

1) gas blanketing of heat transfer rate (in addition to compliance effect),

2) fuel particle size distribution,

3) elastic deformation of vessel wall,

4) finite transport rate of reactants into mixing zone.

A listing of the FCI parametric model is presented in Ref. 11.

FCI Modeling

A wide range of MFCI conditions and parameters were studied using the FCI parametric model. The exact values employed for the MFCI parameters are presented in the discussion pertaining to each specific MFCI study (see Appendix C). In general, however, it was assumed that the center of the reaction zone is located at the midplane of the FEPL test fuel. The length of the unheated upper sodium column to the loop gas reservoir is then 610 cm with a density of 0.754 gm/cc. A cover gas pressure of 1.18 atm was assumed with an initial reaction zone pressure of 1.6 atms. A list of the required conditions necessary to run the FCI parametric model are presented below:

Initial Conditions	Problem Parameters
. system pressure	. mass ratio of UO_2/Na
. fuel temperature	. fuel particle radius
. sodium temperature	. amount of inert gas
. sodium quality and vapor volume	. acoustic impedance
. specific volume of sodium	. fuel heat capacity
	. fuel time constant

Physical property data for sodium which were extrapolated from the data of Ref. 12 are built into the program.[8]

Results from the FCI parametric program are provided at specified time steps and include the value and calculational error estimate for:

(1) temperatures of coolant and fuel within reaction zone

(2) pressure and specific volume of reaction zone

(3) vapor quantity and inert gas volume if applicable

(4) work and impulse caused by interaction

(5) velocity and location of reaction interface

The model is programmed for IBM 360 in FORTRAN IV. For integration of the model's differential equations, ANL's double precision programs DFBND-DIFI[13] and DFBRDV[14] are employed.

B.5 FEFPSTY

FEFPSTY is a computer program that applies a hydraulic model incorporating the equation of motion for one-dimensional flow of incompressible fluid to describe the closed-system fluid flow conditions in the FEFP loop during steady flow operation. FEFPSTY calculates the loop frictional pressure drop, the net sodium circulation head, gross and net pump head, the required pump power input, and bypass orifice requirements.

The loop is described as a chain of distinct connected regions. Each region is described by a specific length, flow area, equivalent diameter, and flow expansion/contraction loss coefficient. Net loop frictional pressure drop is the summation of the frictional pressure drop and form losses for all the loop regions, with adjustments for the sodium circulation head existing because of coolant temperature and density differences around the loop.

Pressure levels at locations within the loop are calculated as a function of the loop flow, sodium circulation head, and cover-gas pressure. Bypass orifice requirements result from a matching of the total pressure difference between the bypass orifice and point of flow combination for the parallel test subassembly and bypass flow paths.

An ANL-developed pump model is incorporated in FEFPSTY to estimate the pump power required to maintain steady loop flow. This model is keyed to mathematical pump performance predictions for the "interim" annular linear induction pump, and will be verified against experimental data after pump calibration tests are completed.

FEFPSTY Modeling

Steady-state flow in the FEFP loop is described as one-dimensional, variable temperature, and incompressible for solution of the equation of motion in the hydraulic model. Pressure drop calculations are performed by identifying the flow conditions in each of ∿75 different geometrical regions in the FEFP loop and determining the friction factor, frictional pressure drop, and form losses (pressure drop due to area changes, change in flow direction, etc.) associated with each distinct loop region. Individual regions range in length from 0.16 to 79.6 in. and in cross-sectional area from 0.44 to 132.7 in.^{2}. Flow paths and relative locations of components in the FEFP loop are illustrated in Fig. B.12.

The Colebrook relationship for fluid friction in turbulent flow[15] is used to calculate the friction factor for flow in each of the regions of the loop. This relationship is as follows:

$$\frac{1}{\sqrt{f}} = 2 \log_{10} \left(\frac{\varepsilon}{3.7D} + \frac{2.51}{R\sqrt{f}} \right)$$

where

f = turbulent flow friction factor

ε = roughness of the flow passage

D = equivalent diameter of the flow passage

R = Reynolds number

Form losses associated with gradual and abrupt changes in flow area and flow direction in the loop are evaluated from information found in the Piping Handbook,[16] Reactor Handbook,[17] and Handbook of Fluid Dynamics,[18] and are part of the code data input. Sodium properties required for the friction factor and pressure drop calculations are evaluated from Golden and Tokar[12] sodium-property relationships in a FEFPSTY subroutine.

Coolant distribution and pressure drop in the test subassembly are calculated by procedures reported by Sangster.[19] Central, side and corner coolant subchannels in the test subassembly are identified and described by flow area and equivalent diameter. A subassembly flow distribution is then determined that satisfies the requirement of equal axial pressure drop in all subchannels. Smooth-tube pressure drop results are adjusted by two factors, one a function of the fuel element pitch to diameter ratio, and the other a function of the spacer-wire lead-to-diameter ratio, to yield the pressure drop in the wire-wrapped test element subassembly.

Loop pressure drop and flow rate identify the pump operating condition. Pump power input is determined from an ANL-developed pump model that uses the "interim" pump design condition (150 gpm, 150 psi, 148 kW) and geometrical parameters (length = 65 in., flow area = 2.93 in.^{2}, duct roughness = 100 micro in., field velocity = 71.3 fps) to calculate a performance parameter relating pump power and stall pressure. This parameter is then used to estimate the pump power requirements at the loop operating conditions.

B.6 FEFPSLUG

The FEFPSLUG code simulates dynamic coolant response in the FEFP loop to determine coolant expulsion characteristics resulting from a pressure transient occurring in the test subassembly. FEFPSLUG solves equations of motion for one-dimensional, unsteady flow of incompressible, single-phase sodium constrained by inertia and fluid friction while responding to pressure perturbations that produce distinct source-fluid interfaces. The FEFPSLUG analyses are based on a single pressure source in the test section and on a rigid loop system.

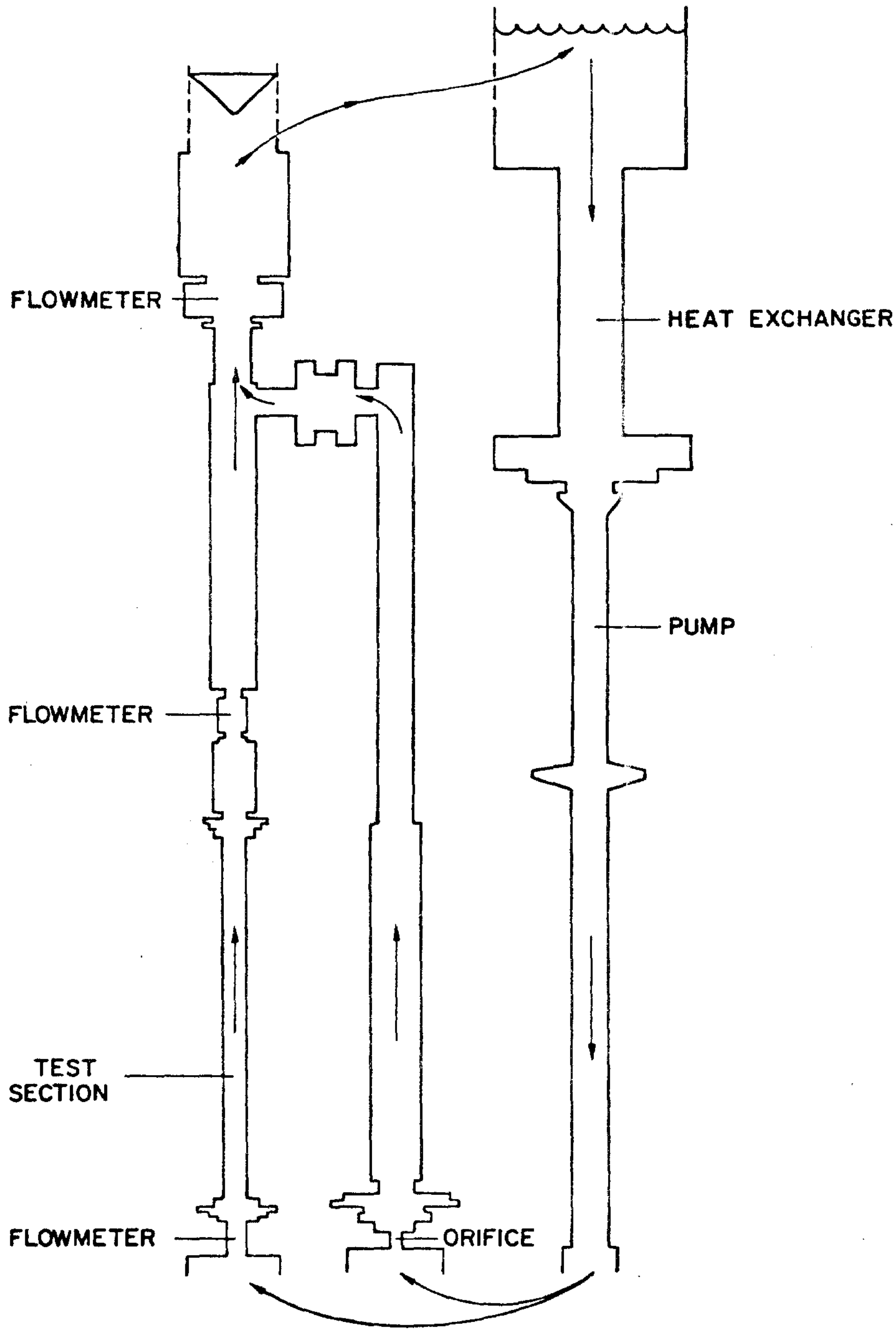

FIG. B.12 Loop Model for Hydraulic Calculations

FEFPSLUG is a combination of two computer codes, one (FEFPSTY) for steady-state pretransient analysis, and the other for dynamic analysis. Calculation of pressure drop and pressure level is made by FEFPSTY and supplied to the dynamic code as initial conditions.

The dynamic analysis calculates the time-varying mass flow rate of multiple fluid columns in the loop, the coolant kinetic energy, and the displacement of fluid from the test subassembly as a function of the test subassembly size and pressure-time history of the transient. Inherent in this analysis is the calculation of time-varying frictional pressure drop and pump pressure head during the transient. Pump operating characteristics are described in a general manner that permits the pump head to be calculated for any flow regime, including reverse flow through the pump. Pressure in the gas plenum is assumed to increase adiabatically as coolant is displaced from the test assembly.

FEFPSLUG Modeling

Five bodies of fluid (slugs) are required to describe the motion of coolant in the FEFP loop during transients causing expulsion. These fluid columns, illustrated in Fig. B.13, are the downcomer, the lower test section, the upper test section, the bypass, and the combined flow in the upper flow divider.

The hydraulic model in FEFPSLUG is comprised of five first-order, coupled differential equations, one differential equation of motion for each of the individual fluid columns in the loop, and supporting relations defining interface pressures, coolant expulsion, pump performance, and cover-gas compression. The equation of motion for the fluid column extending from the gas plenum down through the heat exchanger, the pump, and the in-reactor tube to the bottom of the loop is as follows:

$$\frac{1}{g_c}\left(\sum_i \frac{L_i}{A_i}\right)_d \frac{dW_{down}}{dt} = P_{plenum} + \Delta P_{pump} + \frac{g}{g_c}\left(\sum_i \rho_i L_i\right)_d - \frac{1}{2g_c}\left[\sum_i \left(f_i \frac{L_i}{D_i} + K_i\right)\rho_i V_i^2\right]_d - P_{bottom\ of\ loop}$$

where

W = fluid column mass flow rate

L = flow passage length

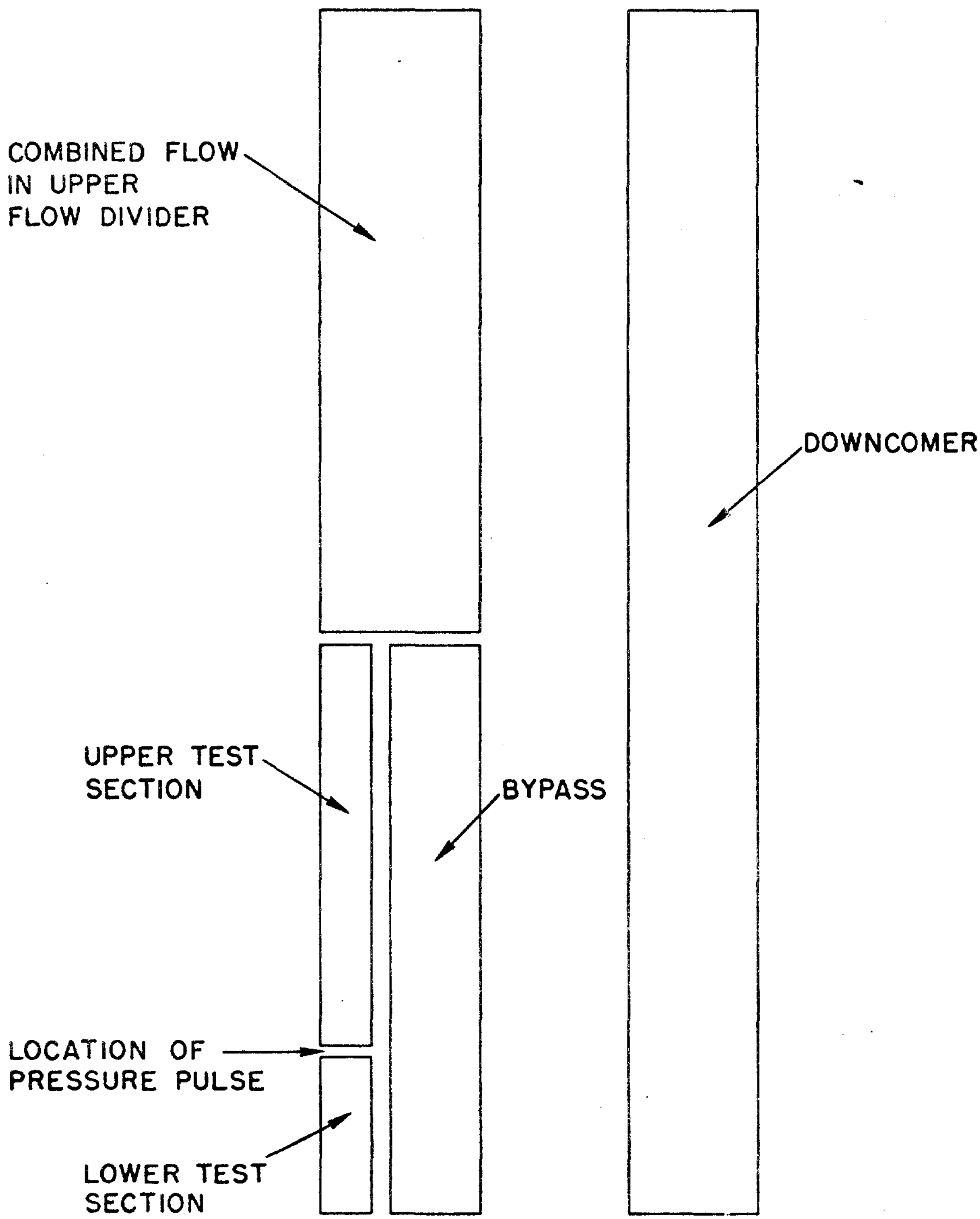

FIG. B.13 FEFPSLUG Loop Model

D = equivalent diameter

A = cross-sectional area

K = expansion/contraction loss coefficient

V = coolant velocity

ρ = coolant density

f = friction factor

g = gravitational constant

P = pressure

i = index defining a specific flow passage

Solution of the dynamic hydraulic model of the FEFP loop is obtained by using the Continuous System Modeling Program (CSMP).[2]

Most of the input data to the dynamic code is from the steady-state initialization program FEFPSTY, described in Section B.5. These data include loop and test subassembly geometry (~75 different regions are used to describe loop and test subassembly geometry), steady-state loop flow rate, regional coolant temperatures, pump operating conditions, bypass orifice dimension, gas plenum volume, initial gas pressure, and gas specific heat ratio.

The pressure-time history of the transient pressure pulse is specified in the dynamic code in subroutine form. Location of the pressure transients is a variable; it can be described as occurring in the test subassembly at any position between the lower and upper end caps of the test element bundle.

A choice of integration techniques for performing the dynamic analysis is available in CSMP. Output data from the dynamic analysis includes total frictional resistance, total elevation pressure head, and mass rate of flow for each of the fluid columns as a function of time. Also output are the coolant displacements in the test subassembly, pump pressure head (if continued pump operation is assumed), and the pressure levels at the heat exchanger, pump, bypass orifice, bottom of the loop, location of bypass and test section flow combination, and gas plenum during a pressure transient.

B.7 COASTDWN

The COASTDWN code simulates dynamic coolant response in the FEFP loop to determine transient flow characteristics resulting from gradual or abrupt changes in pressure drop, coolant temperature, pump power or other perturbations in operating conditions that do not result in coolant expulsion. COASTDWN solves equations of motion for one-dimensional, unsteady flow of incompressible, single-phase sodium constrained by inertia and fluid friction while responding to changes in loop operating parameters. The transient-initiating mechanism may be a single event or simultaneous or staggered occurrence of multiple events.

COASTDWN is a combination of two computer codes, one (FEFPSTY) for steady-state pretransient analysis, and the other for dynamic analysis. Calculation of pressure drop and pressure level is made by FEFPSTY and supplied to the dynamic code as initial conditions.

The dynamic analysis calculates the time-varying mass flowrate of multiple fluid columns in the loop. These flowrates are a function of the loop initial operating conditions, the test subassembly size, and the flow-perturbing events. Inherent in the dynamic analysis is the calculation of time-varying frictional pressure drop and pump pressure head during the transient. Pump operating characteristics are described in a general manner that permits the pump head to be calculated for any flow regime, including reverse flow through the pump. Initial gas pressure in the loop plenum remains unchanged during flow transients described by COASTDWN, but is used to determine pressure levels throughout the loop during a transient.

COASTDWN Modeling

Four fluid columns are used to describe the motion of coolant in the FEFP loop during flow transients that do not result in coolant expulsion. The four fluid columns, illustrated in Fig. B.14 are the downcomer, the test section, the bypass, and the combined flow in the upper flow divider. COASTDWN is applicable for nonexpulsion transients, including those stemming from loss of pump power, reversal of pump power, gradual or sudden blockage of flow through the test subassembly, changes in geometry of coolant flow passages, etc.

The hydraulic model in COASTDWN is comprised of four first-order, coupled differential equations, one differential equation of motion for each of the individual fluid columns in the loop, and supporting relations defining interface pressures and pump performance. COASTDWN is similar to FEFPSLUG, described in Section B.6, but does not require procedures to calculate coolant expulsion or cover gas compression. Lack of coolant expulsion in the transients described by COASTDWN permits the test section flow to be described by one equation of motion instead of the two equations required in FEFPSLUG.

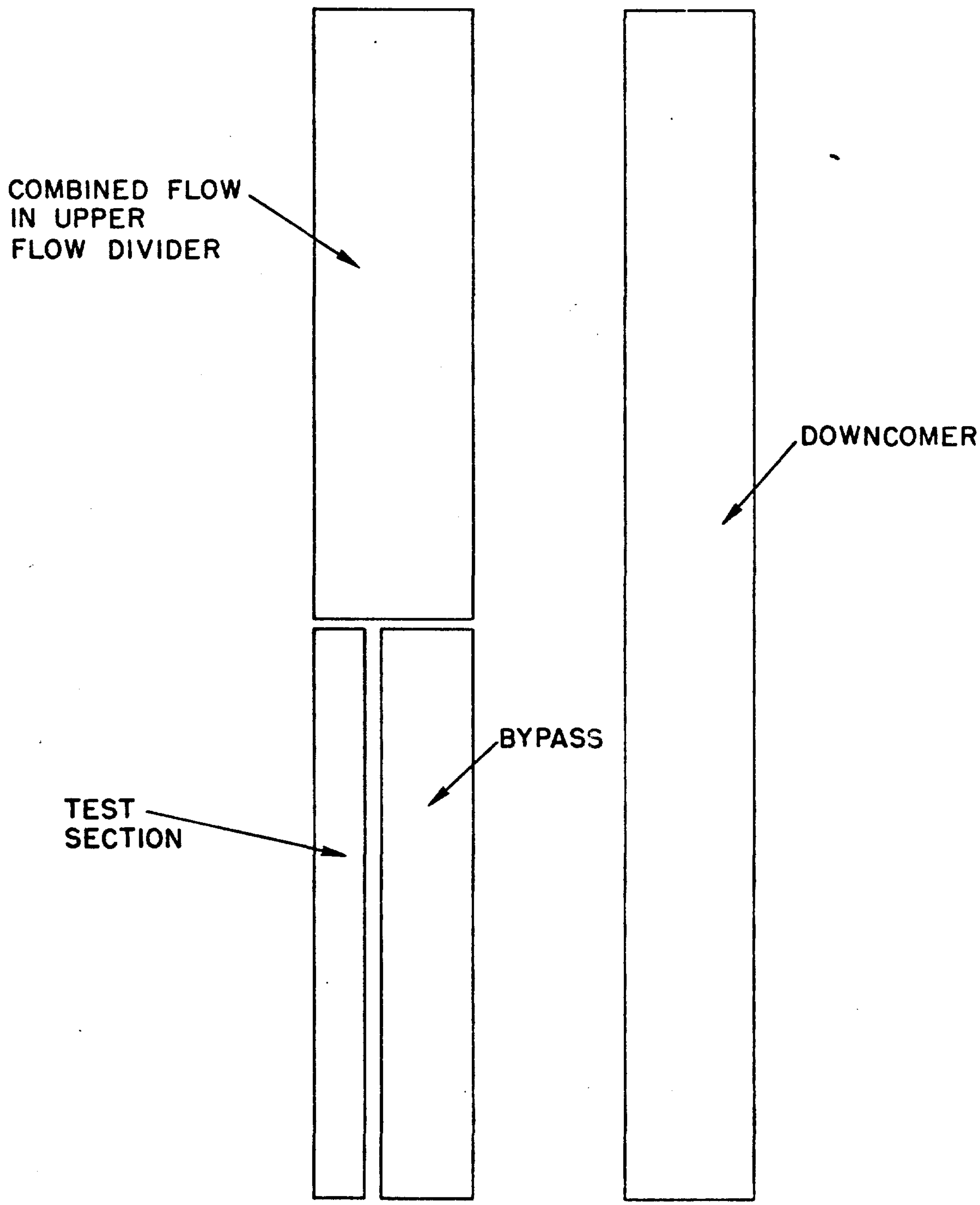

FIG. B.14 COASTDWN Loop Model

B.8 NAHAMMER

The NAHAMMER code describes acoustic transmission of a pressure pulse in a closed hydraulic system consisting of series or parallel piping, pipe junctions, and gas-filled plenums or reservoirs. NAHAMMER is based on water-hammer theory and uses a superposition method to solve the equations of mass and momentum for one-dimensional, unsteady-isentropic flow of compressible, subcooled sodium in a rigid system containing a single pressure source. Coolant motion resulting from a pressure pulse is assumed to occur without frictional resistance.

Water-hammer equations are derived by neglecting the convection terms $u \frac{\partial \rho}{\partial z}$ and $u \frac{\partial u}{\partial z}$ in the general one-dimensional equations of mass and momentum. Neglecting these terms in the simplified equations of mass and momentum,

$$\frac{\partial p}{\partial t} + \frac{\rho C^2}{G_c} \frac{\partial u}{\partial z} = 0$$

$$\frac{\partial u}{\partial t} + \frac{G_c}{\rho} \frac{\partial p}{\partial z} = 0$$

where

- p = pressure
- ρ = fluid density
- C = sonic velocity
- G_c = gravitational constant
- u = fluid velocity
- t = time
- z = position

limits NAHAMMER application to systems in which the sodium velocities are small relative to the sonic velocity in the sodium. The solution of the equations is of the form

$$u - u_o = \frac{G_c}{C\rho} F(z + ct) - f(z - ct)$$

$$P - P_o = F(z + ct) + f(z - ct)$$

where F and f are pressure waves traveling in opposite directions. Additional detail on the formulation and application of NAHAMMER can be found in Chen and Thompson.[20]

NAHAMMER contains an ANL model for molten fuel-coolant interaction,[8] but a separate pressure-time history may also be input as the source. The NAHAMMER calculations trace the pressure perturbation as the MFCI occurs, and the resulting change in magnitude of the pressure waves as they are transmitted and reflected through the system at sonic velocity. These calculations account for energy losses of the pressure waves in the subcooled sodium coolant at diameter discontinuities, elbows, tees, partial blockages, dead-ends, tanks, and in regions of temperature change.

NAHAMMER Modeling

The pressure perturbation of interest in the FEFP loop is the molten fuel-coolant interaction (MFCI). Appendix C describes the numerous MFCI studies that were made. NAHAMMER analyses were based on the design envelope MFCI, which reaches a 194 atm peak pressure at 5.7 msec from the start of the interaction, followed by a gradual pressure decrease.

Approximately 40 sections were used to describe the FEFP loop for the MFCI pressure pulse calculations. This loop model is illustrated in Fig. B.15. The geometry is defined by assigning an identification number to each section of the system, identifying the type of junction connecting adjacent sections, and calculating the number of nodes and distance between nodes in each section. Section lengths ranged from 0.2 to 55 in., and the number of nodes in each section varied between 2 and 62. The MFCI source region was described as a 12 in. length of the test subassembly bounding the fuel midplane, or similar-length sections of the adjacent bypass channel or downcomer, that experience a pressure increase resulting from test-train structural displacement in the radial direction.

Temperature of the source-pressure region was assumed to be up to 650°F higher than the temperature of the rest of the system. This produces an abrupt change in sonic velocity at the axial boundaries of the source region, and causes partial reflection of the propagating pressure waves, a condition called acoustic impedance. In the FEFP loop calculations, the MFCI pressure was not influenced by pressure waves reflected back into the source region.

NAHAMMER calculates on a node by node basis, the magnitude of the pressure waves in the positive and negative directions, and the local coolant pressure and velocity. It serves a bookkeeping role in accounting for all the pressure waves propagating in the system in both directions, and from these

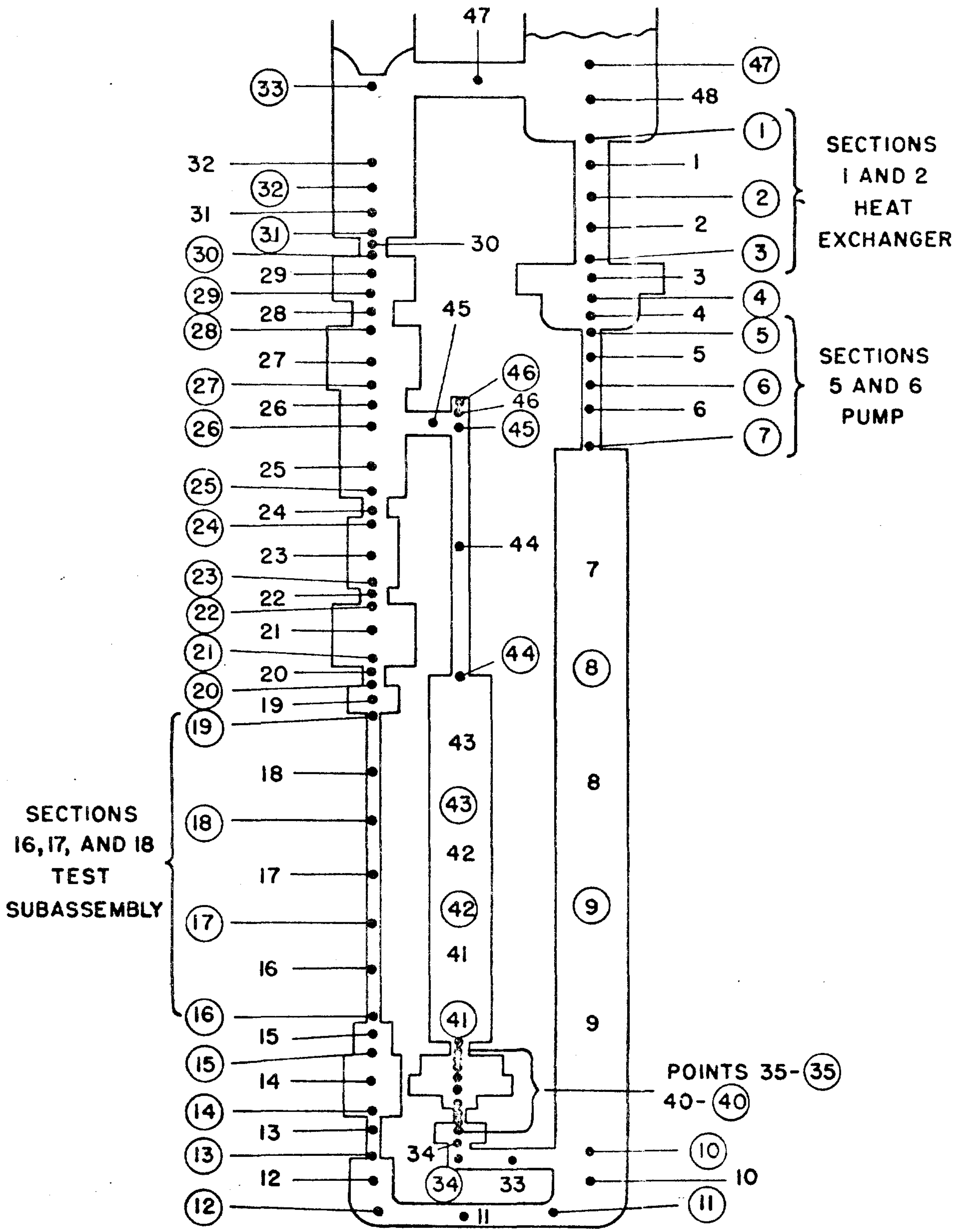

FIG. B.15 Model of FEFP Loop for NAHAMMER Analysis results calculates the attenuation of the pressure pulse in the system. In the FEFP loop, the peak pressure at the bottom of the loop, the pump, and the heat exchanger were 1880, 932, and 230 psi, respectively, an appreciable reduction from the 2855 psi peak source pressure.

B.9 STRAP

The dynamic structural response of the loop when subjected to seismic excitations, ETR pressure loadings, and handling loads, is analyzed with the STRAP (STRuctural Analysis Package) computer code.[21] This code was originally developed to calculate the structural behavior of water reactor systems under decompression loads, seismic excitation, various forms of externally applied time-dependent forcing functions, and static loads. The code performs static and dynamic analyses of structural systems using either a displacement or stiffness method to model the structure and an uncoupled modal summing procedure to perform the dynamic analysis. STRAP is a three-dimensional structural analysis code and can be used in the static and dynamic analysis of structures having up to 250 degrees of freedom. With STRAP, a structure can be described with up to 100 members, using up to 100 nodes. This model has been checked against experimental results obtained in the subcooled blowdown thrust studies with good agreement indicated.[21]

The mathematical model of the structural system, as formulated in STRAP, describes the continuous structure with a finite number of concentrated mass points (elements) connected by massless members. The force response relation is represented by a set of ordinary differential equations. The nodes of the structure, representing the connection points of the finite elements, have specified directions of motion (degree of freedom) the number of which are determined by the complexity of the structure (dimensionality of model). The relationship between the static forces applied to the structure and the resultant static deflections of the structure are determined using a stiffness matrix. When the structure is subjected to time-dependent loads, the mass and damping effects of the structure are included in the analysis.

For the dynamic analysis of a structure, the STRAP input and output specifications which are required are summarized in Table B.1. Further details concerning the STRAP code are presented in Ref. 21.

TABLE B.1

STRAP Model Input and Output Description Summary

Input: (1) Definition of structure
- Type of structure
- Number of members
- Number of nodes

(2) Coordinates of structural nodes

(3) Definition of structural members
- Member type
- Material constants
- Section properties such as areas and inertias
- Nodes which define member ends
- Adjustments in member length

(4) Mass of structure

(5) Damping function

(6) Forcing function
- Pressure histories
- Force histories
- Acceleration histories (earthquake)

(7) Definition of member forces desired as output

Output: (1) All input information

(2) Fundamental vibrational frequencies of system

(3) Displacements, velocities, accelerations, and member forces for each time step

(4) Maximum forces in members and times at which they occur

(5) Plots of member forces and structural displacements with respect to time

STRAP Modeling

The FEFP loop, as shown schematically in Fig. 1.1, is modeled by STRAP as a frame to simulate concentric tubes and consisted of 79 elements. The model included the secondary vessel, primary vessel, test train, and flow divider. The test train and flow divider were modeled together. A schematic of the STRAP model is shown in Fig. B.16. The numbers which appear on the sketch are nodal points. An attempt has been made in this schematic to show what each section of the model represents. In the case of the splines between the primary and secondary vessels or between the primary vessel and flow divider, the degree of freedom in the vertical direction was released to simulate the ability of a sliding motion to occur. These members were made very short to simulate the actual structure. The area of the members representing the splines were taken to be large enough to give a high stiffness for those members. The spline members are only an approximation of the FEFPL contraint because of clearances between the splines and the FEFPL components. Spline members were also employed to simulate the spring loaded heat sink in the ALIP region. A spring constant of 688 lb/in. for the heat sink was used when calculating the area for those members. The upper end of the primary and secondary vessels were assumed to be fixed. Roller supports were placed at different locations to represent the supports for the three different cases analyzed.[22]

In the pressure pulse analysis,[23] a virtual mass term was calculated to account for the hydrodynamic effect of motion in water and added to the weight of the members of the secondary vessel. In all four analyses, the weight of the sodium was added to the elements which make up the test train and flow divider. Also, in the plenum sections above and below the heat exchanger, a portion of the sodium weight was added to the primary vessel. The damping value was taken to be 2% of critical.

B.10 SINDA-3G

A detailed and comprehensive thermal and hydraulic model of the FEFPL loop has been developed by ANC using the SINDA-3G[24] computer package. This

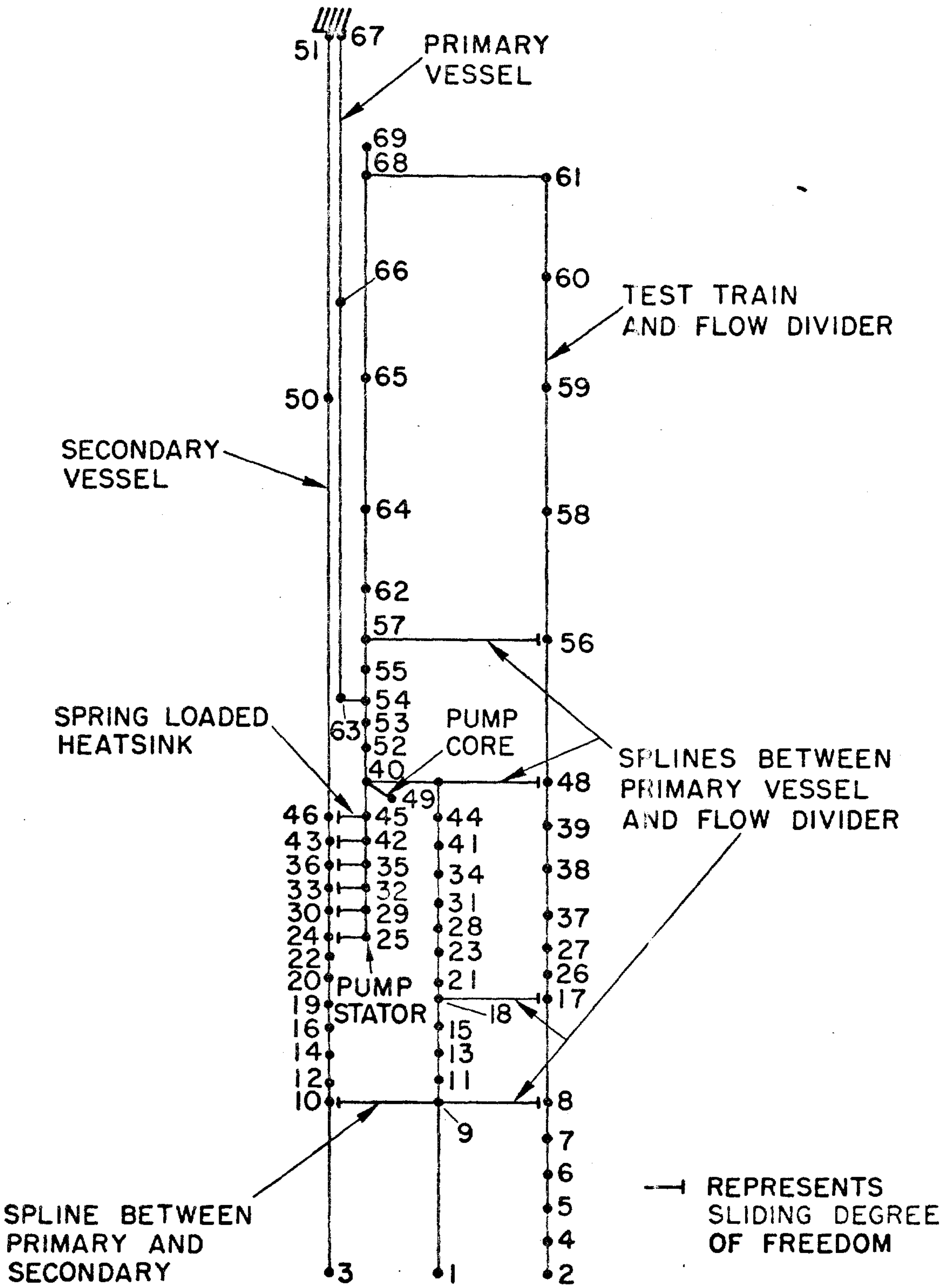

FIG. B.16 STRAP Model Schematic of FEFPL elaborate steady-state and transient model, called SINDA-3G, is described in Ref. 25 and provides a more in-depth description of the FEFPL thermohydraulic behavior than the THYME-B code (for description see Appendix B.1). It, therefore, is applied extensively in design to calculate boundary conditions for other detailed models of specific loop components which in turn yield temperature data for the loop stress analyses. Good predictive agreement between SINDA-3G and THYME-B has been obtained for several benchmark problems.[26,27] This agreement confirms the adequacy of both computer models, thus providing the necessary assurance in the validity of the calculational results.

SINDA-3G uses a lumped parameter approach wherein the physical masses are represented by nodes, each with uniform properties, uniform response, and uniform input (e.g., heat sources). The heat transfer processes are represented by interconnecting conductors. In addition to the availability of time and temperature-dependent quantities, the versatility of the code is greatly enhanced by the ability of the programmer to include auxiliary programming statements as part of the input data. This option has been used extensively in the present work for calculating various film coefficients and hydraulic properties, and for altering the solution routines by inclusion of Fortran logical statements. It is noted that the present model does not consider either boiling or freezing of the liquid sodium. No inherent limitations of the code would prevent extension of the model to these conditions; however, this would involve a considerable effort.

SINDA-3G Modeling

As in any modeling effort, numerous approximations were required to describe a geometry as complex as FEFPL. Listed below are the major ones:

(1) Purge helium - inlet temperature of 150°F assumed at bottom of loop.

(2) Meltdown cup - a diametral helium gap of 0.010 in. is assumed between the meltdown cup and its tungsten liner.

(3) Cadmium filter - no contact resistance and no end effects considered.

(4) Fuel pins - a void is assumed inside the cladding above reactor core.

(5) Test train - flow divider not insulated at fuel pin level. Upper test train internals (flowmeters, leads, screen, etc.) are replaced with equal

volumes of additional flowing sodium in the thermal portion of the model; however, hydraulically their presence is considered.

(6) Pump - the entire stator assembly is modeled very coarsely by only six nodes. The stator assembly is assumed separated from the secondary vessel by a diametral helium gap of 0.006 in.

(7) Axial heat transfer is, in general, ignored in both the structure and the fluids.

A SINDA-3G nodal layout diagram of the FEFP loop is presented in Fig. B.17. The dimensions for the current FEFPL geometry used in this modeling effort are presented in Ref. 25. The thermal model contains 693 nodes of which 94% have temperature-dependent heat capacity. Three nodes representing boundary conditions are used; they specify the inlet conditions of (1) the heat exchanger helium (150°F at sodium reservoir level), (2) the purge annulus helium (150°F at bottom of loop), and (3) the ETR core cooling water (110°F above the reactor core). Axially, in the present model, the nodes are distributed as shown below:

Item	Location	# Axial Levels	# Nodes
1	Meltdown Cup	1	14
2	Above Cup, Below Core	2	36
3	36" Heated Core	9	207
4	Above Core, Below Pump	5	88
5	Pump	3	48
6	Above Pump, Below HX	2	24
7	HX (w/tube sheets)	13	260
8	Above HX	1	13
9	Boundary Nodes	-	3
		36	693

The present model contains 765 conductors of which more than 80% are temperature and/or flow dependent. The conductors are listed by function below:

Function	# Conductors
Radial Conduction	
Fuel Pins	34
Primary Vessel (w/HX tubes)	50
Secondary Vessel (w/cadmium filter)	56

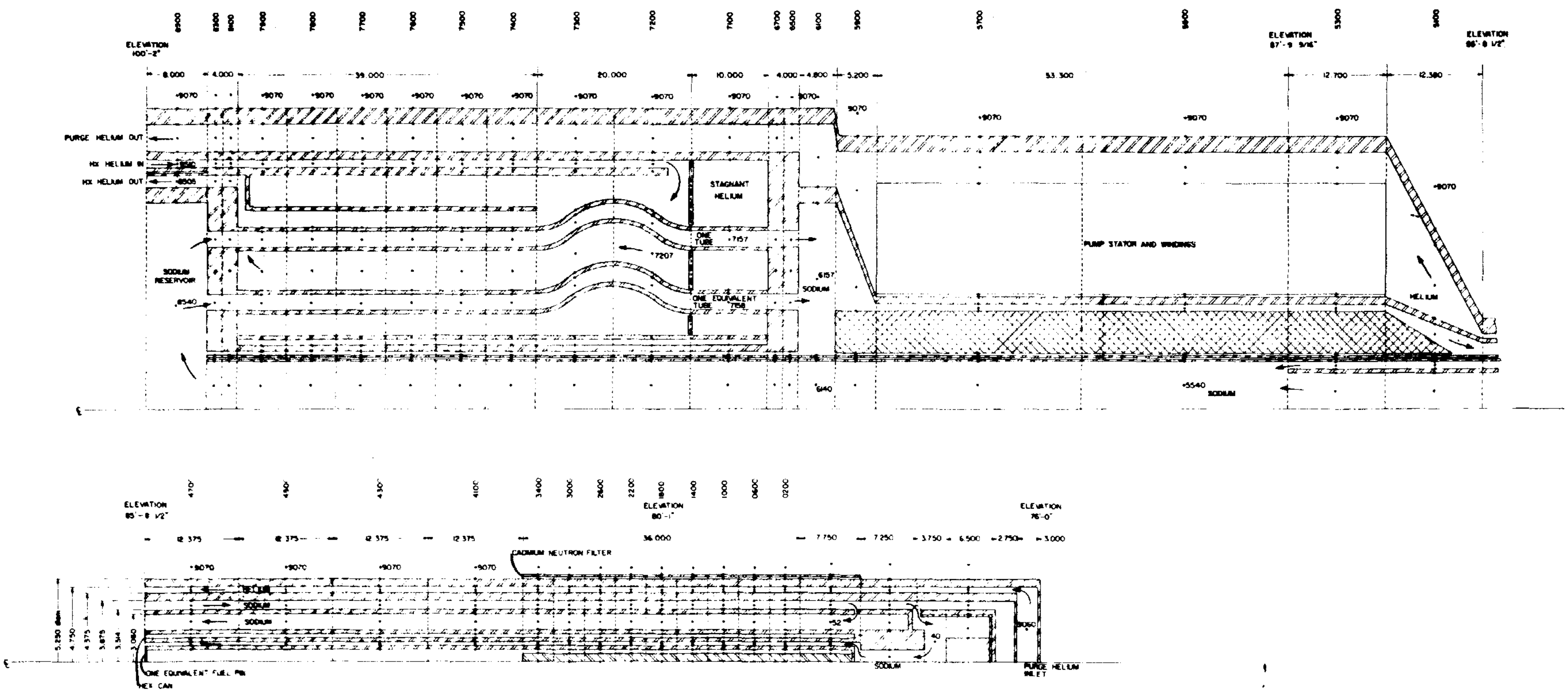

FIG. B.17 SINDA-3G Node Diagram for 19 and 37-pin FEFPL Thermal-hydraulic Loop Model (Models 19-A and 37-A)

Other	219
Vertical Conduction	
Primary Vessel (w/HX tubes)	20
Secondary Vessel (w/cadmium filter)	28
Film Coefficient	
Sodium	159
HX Helium	61
Purge Helium	72
ETR Core Water	36
Fluid Flow	
Sodium	5
HX Helium	1
Purge Helium	1
ETR Core Water	1
Radiation	22
	765

Two versions of the model have been developed to handle both the 19- and 37-pin geometries. They differ in the number of fuel pins, size of the hexagonal can containing the pins, heat source distribution, and orifice size at the test section inlet. In both cases, all fuel pins are located internal to the hexagonal can.

Execution time for the model includes a basic data read and compilation time of about six minutes on the IBM 360-75. This is followed by a steady-state solution which may take as long as 15 minutes depending on the accuracy of the initial temperature estimates. Finally, the transient solution is begun, proceeding at the rate of approximately one to two seconds per minute of computer time with hydraulic calculations or three to four seconds per minute of computer time when the hydraulic calculations are bypassed (constant sodium flow and pump power) and larger time steps are allowed. Typically, convergence criteria of 0.05 and 0.10°F maximum temperature change per iteration are used in the steady-state and transient routines, respectively.

Twenty-nine various temperatures and flows are plotted versus time on three graphs to enable easy scanning of the results. In addition to complete temperature printouts at desired intervals, the model punches 30 temperatures and flows versus time for input to three detailed models; the cadmium filter, lower tubesheet and upper transition, and nonremovable top head models. Although no standard restart option is available, programming has been included to (1) store the steady-state temperatures on magnetic tape to serve as initial guesses for subsequent transient runs beginning from the same initial conditions, and (2) store transient temperature data from selected cases in order to extend the run at a future date without rerunning the initial portion of the transient.

Further details of the SINDA-3G model of the FEFP loop and its operational features are presented in Ref. 25.

B.11 SOFIRE II

A. General

The pressures and temperatures generated during a sodium pool fire were computed by using the SOFIRE II code developed at Atomics International (AI).[28] The code provides a pressure-temperature history of the containment following a postulated sodium spill, which developes into a fire. The pressure is the result of heat from the reaction of spilled sodium with oxygen in the atmosphere above the sodium and to the sensible heat contained in the spilled sodium. This process is a transient one and the maximum pressure is a function of the sodium burning rate and the enclosure ventilation configuration.

B. Experimental Verification

Experimental verification of the code was conducted in a 30 ft high, 10 ft. diameter vessel with pool fires of 6 sq. ft.[29] Average initial combustion rate was found to be 0.17 lb O_2/hr-ft^2-% O_2. In additional studies conducted in a 6 ft high, 2.5 ft diameter vessel with pool fires of 0.03 to 0.2 sq. ft in area in various oxygen atmospheres, the average initial oxygen consumption rate was found to be 0.15 lb O_2/hr-ft^2-% O_2. These test results, which were conducted at sodium temperatures of about 1000°F, together with results of small open pool fires, have been used as the basis for conservatively predicting the pressures resulting from potential sodium accidents.

C. Charging Facility Pool Fires[28]

The analytical model used for the FS&R Charging Facility Sodium pool fire analysis is composed of a series of equations, based on an energy and mass balance, employed to calculate the energy and flows resulting from a fire within a cell. These equations have been programmed in the SOFIRE II one cell code for calculation by digital computer to give temperatures, sodium burning rates, and cell volume pressures as a function of time.

Fixed input conditions to the code include the spill facility geometries and the atmospheric conditions inside the building. The wall material thermal properties are assumed to be independent of temperature. Variable conditions which require initial input values include gas and wall temperatures, oxygen concentrations, initial sodium pool temperature, and ventilation rate.

During each chosen time increment, the calculations are made of: (1) the sodium burning rate, which is directly dependent on the oxygen concentration within the system at that time point, (2) the temperature of the sodium and the heat transferred to the system gas or downward to the pan, (3) the heat transferred from the system atmosphere to the wall, (4) the sodium node temperatures based on the heat balance on the input heat and that lost to the floor, (5) the gas densities and pressure, (6) the gas flow in and out of the cell, and (7) the oxygen concentration based on the sodium burning rate established at that time. The calculations are conservative since no allowance is made for heat being transferred to metal structures and components within the enclosure. The relative effect is dependent on the heat capacity of these internal components,but the gas temperature and pressure would be lower than shown.

D. Test Cell Pool Fires[28]

In the test cell cases, the code was slightly modified because it was specified that the burn pan was suspended in the air of the cell. Thus, heat is also transferred to the cell atmosphere from the bottom of the pan by convection and radiation. A special version of the SOFIRE II one cell code was written to include this pathway of heating the cell gas. Since no heat is transferred to internal components, these cases are also conservative.

E. Aerosol Releases[28]

The quantity of sodium oxide released to the atmosphere through the ventilation system is a function of the ventilation rate and the airborne concentration of sodium oxide in the vault or cell. The airborne concentration is related to the rate at which sodium oxide is released from the pool fire, the rate at which the aerosol particles agglomerate, and the rate at which the agglomerates settle to the floor. This aerosol behavior is dynamic and has been modeled with the HAA-3 aerosol agglomeration code.[30] It was assumed that 50% of the oxidized sodium is released to the cell gas in the form of particles with a log-normal distribution described by a mass median radius of 0.5 μm and a standard deviation of 2.0. The source rate was obtained from the oxidation rate of sodium computed with SOFIRE II.

References:

1. W. W. Marr, et. al., "Thermal-hydraulic Dynamic Simulation Model for FEFP," ANL/RAS 71-21 (May 1971).

2. System/360 Continuous System Modeling Program (360A-CX-16X) Users Manual, IBM.

3. "The SAS2A LMFBR Accident Analysis Code," Proc. Conf. on New Developments in Reactor Mathematics and Applications," CONF-710302 (March 1971).

4. J. C. Carter, et. al., "SAS1A, A Computer Code for Analysis of Fast Reactor Power and Flow Transients," ANL-7607 (October 1970).

5. W. Bohl, et. al., " A Preliminary Analysis of the FFTF Flow Coastdown Accident," ANL/RAS-7139 (December 1971).

6. Y. Chang, J. Gvildys, and S. H. Fistedis. "Two-dimensional Hydrodynamics Analysis of Primary Containment," ANL-7498 (November 1969).

7. J. E. Ash and R. T. Julke, "Comparison of a Two-dimensional Hydrodynamics Code (REXCO) to Excursion Experiments for Fast Reactor Containment," ANL/RAS 71-14 (January 1971).

8. D. H. Cho, et. al., "A Rate-limited Model of Molten Fuel/Coolant Interactions: Model Development and Preliminary Calculations," ANL 7919 (March 1972).

9. D. H. Cho, et. al., "A Parametric Study of Pressure Generation and Sodium Slug Energy from Molten Fuel-Coolant Interactions," ANL/RAS 71-5 (January 1971).

10. D. H. Cho, "Preliminary Assessment of Fuel-Coolant Interactions Following a Voided-core Disassembly," ANL/RAS 72-14 (April 1972).

11. W. L. Chen, et. al., "Recent Additions to the Parametric Model of Fuel-Coolant Interactions," ANL/RAS 72-17 (May 1972).

12. G. H. Golden and J. V. Tokar, "Thermophysical Properties of Sodium," ANL-7323, Argonne National Laboratory, 1967.

13. K. A. Paciorek, "Fortran IV Precision Routines Which Estimate the Error in the Bulersch-Stoer Method for Solution of a System of First-Order Ordinary Differential Equation," ANL-D255S (October 1967).

14. K. A. Pacioreck, "Fortran IV Double Precision Routines Which Provides Input/Output and Control for Use with Double Precision Routines," ANL-D255S (October 1967).

15. Turbulent Flow in Pipes with Particular Reference to the Transition Region Between Smooth and Rough Pipe Laws, Journal Inst. Civil Engs. (London) 11, 133-156, (February 1939) Original not seen, found in L. F. Moody, Friction Factors for Pipe Flow, Trans. ASME, 66, 671-684 (1944).

16. Piping Handbook, Second Edition, McGraw-Hill Book Co., New York, N.Y. (1967) S. Crocker and R. C. King.

17. Reactor Handbook, Second Edition, Vol. IV, Engineering Interscience Publishers (John Wiley & Sons), New York, N.Y. (1964) S. McLain and J. H. Martens.

18. Hanbook of Fluid Dynamics, McGraw-Hill Book Co., New York, N.Y. (1961) V. L. Streeter

19. W. A. Sangster, "Calculation of Rod Bundle Pressure Loss," ASME paper 68 WA/HT-35, presented at the ASME Winter Annual Meeting, December 1-5, 1968, New York, N.Y.

20. W. L. Chen and D. H. Thompson, "NAHAMMER, A Computer Program to Study The One-dimensional Pressure-pulse Propagation Resulting from a Molten Fuel-Coolant Interaction in a Hydraulic System,"(in preparation).

21. J. A. Dearien, et. al., "STRAP, A Computer Code for Static and Dynamic Structural Analysis and Studies Made Using the Code," IN-1362 (June 1970).

22. B. L. Harris, "Seismic Stress Analysis of FEFP Loop," ANC FEFPL Report EDF-563 (December 22, 1972).

23. B. L. Harris, "Stress in In-pile Loop Due to 26 psi Lateral Pressure Pulse and Transporting Loads," ANC FEFPL Report EDF-562 (December 22, 1972).

24. P. F. O'Brien, et. al., "Workshop in Heat Transfer Computer Programs," Sec. 1, Engineering 896.3, Lecture notes for ten day short course, May 19-30, 1969, Engineering and Physical Science Extension, UCLA.

25. K. H. Liebelt, "Revised Thermal-hydraulic Loop Model for Fuel Element Failure Propagation Loop (FEFPL)," Technical Report TR-337 (November 1972).

26. K. H. Liebelt, "Compariosn of ANL and ANC FEFPL Thermal-hydraulic Loop Models," ANC Interoffice Correspondence to A. A. Oare KHL-5-72 (March 1972).

27. A. A. Oare, "Summary of Thermal-hydraulic Meeting with ANL Personnel," ANC Interoffice Correspondence to C. R. Snyder, AAO-15-72 (April 1972).

28. L. Baurmash and R. L. Koontz, "Evaluation of Sodium Pool Fires in FEFPL," Atomics International Report AI-73-32 (April 30, 1973).

29. P. Beiriger, et. al., "SOFIRE II User Report," Atomics International Report AI-AEC-13055 (March 1973).

30. R. Hubner, et. al., "HAA-3 User Report," Atomics International Report AI-AEC-13038 (March 1973).

APPENDIX C

TABLE OF CONTENTS

LIST OF FIGURES

LIST OF TABLES

C.0 Interaction of Core Materials and Liquid Sodium

C.1 Interaction of Fuel and Liquid Sodium

Hypothetical accidents will be simulated in the Fuel Element Failure Propagation Loop to be inserted in the ETR. These simulations include situations where molten fuel will be generated. The presence of hot molten fuel and liquid sodium becomes, therefore, of concern in assuring loop integrity. This concern stems from the fact that a number of industrial incidents have shown that large-scale vapor explosions (a vapor explosion occurs when the vapor produced cannot be relieved quickly enough to prevent pressurization and the formation of shock waves) can occur when hot molten materials encounter cool liquids (examples: Al-H_2O and stainless steel-H_2O). These vapor explosions have for many years represented an unsolved problem of extremely hazardous and destructive consequences.[1] However, recent results from a large number of prototypic experiments involving meltdown of oxide fuel pins in the presence of liquid sodium suggest that large-scale vapor explosions are not possible with LMFBR materials (UO_2-Na) in the FEFPL environment. This is further substantiated by a recent hypothesis[2] which suggests that the explosive mechanism apparently requires a rate of energy release which can result only if the vapor generation is a result of exceeding the stability limit (i.e., spontaneous nucleation limit*) of the more volatile liquid, i.e., the occurrence of spontaneous or explosive boiling. A discussion on vapor explosions in terms of available information is presented in Section C.1.1. Presented in subsequent sections are analytical results based upon the earlier information used to establish the MFCI source terms presented in Section 10.2 and defined in Appendix D.

C.1.1 Current Status

A survey of experimental and analytical studies indicates that the following conditions must be satisfied in order to produce large-scale physical explosions:

1. Direct liquid-liquid contact,
2. The contact temperature must be substantially above the boiling point of the more volatile liquid; a recent hypothesis suggests that this temperature must exceed the stability limit.[2]

*Spontaneous nucleation refers to homogeneous or vapor free heterogeneous nucleation (resulting from density fluctuations) as compared to nucleation at preferred sites.

The phenomenon of direct contact between a hot and cold liquid can be evaluated by examining the requirements for film boiling. Much improved correlations have recently become available to predict the Leidenfrost and minimum temperatures.[3,4] The latter correlation is largely based upon the "foam limit" as proposed by Spiegler, et al.[5] These correlations are based on data obtained with solid-liquid systems including liquid metals. However, since large differences in nucleation characteristics exist between solid-liquid and liquid-liquid systems[6] and since the nucleation and wetting phenomena are believed to play an important role in determining the appropriate boiling regime, an alternate method based upon the above correlation is suggested for evaluating the minimum temperature for film boiling in a liquid-liquid system. The approach includes the thermal properties of the more volatile liquid as well as the hot liquid following the method proposed by Henry,[3] and the stability limit (T_S) is calculated based upon the well-known kinetic approach rather than from Van der Waals equation as used by Spiegler. In this way, the possibility of spontaneous nucleation at the liquid-liquid or solid-liquid interface (i.e., vapor-free heterogeneous nucleation) as compared to the bulk liquid (i.e., homogeneous nucleation) can be accounted for if the interfacial tension or the contact angle (ϕ) for the particular system in question is known. If ϕ (measured through the liquid)is zero, the stability limit corresponds to the homogeneous nucleation limit. As ϕ becomes larger, the stability limit is correspondingly reduced.[6] In the absence of mechanical (external forces) and/or hydrodynamic (no subcooling) disturbances, repeated liquid-liquid contact would appear difficult when the contact temperature, T_i, exceeds the stability limit, T_S. However, in the case where the more volatile liquid is subcooled with respect to the ambient pressure, repeated liquid-liquid contact can occur despite the fact that T_i exceeds T_S. This form of boiling in a liquid-liquid system is referred to as "continuous explosive boiling." The repeated occurrence of direct liquid-liquid contact is provided by the overexpansion (the vapor growth stage) and the generation of subambient pressure which is only possible in the presence of sufficient subcooling. The subsequent collapse and acceleration of the more volatile liquid towards the hot liquid results in hydrodynamic forces sufficiently large to cause enhancement in the liquid-liquid contact area. The occurrence of this process in a liquid-liquid system with proper geometric configuration and constraint will escalate into a large-scale vapor explosion. This picture of the vapor explosion is similar to that suggested by Board, et al.[7] with the additional requirement that T_i exceeds T_s.

The above criterion for the minimum temperature of the hot surface that will support film boiling in a liquid-liquid system in the absence of subcooling of the more volatile liquid, indicates that molten UO_2 (2800°C) can readily come into direct liquid-liquid contact with liquid sodium (T_{min} = 5000°C). (For the UO_2-Na system, assuming $\phi \sim 0°$, saturated sodium and molten UO_2 at 3000°C, T_i is ∿1200°C and T_s is ∿2050°C.) The contact angle (ϕ) for this system at temperatures of interest would appear to be essentially zero.[8] This is indeed consistent with experimental observations since molten UO_2 fragments extensively when dropped or injected into liquid sodium (based on numerous out-of-pile and in-pile experiments) while at the same time, coherent vapor explosions have never been observed in these experiments. (These are discussed further below.) For the UO_2-Na system in the absence of nucleation sites, a local superheat explosion is possible. Basically, liquid sodium globules can be entrained and wet the UO_2 surfaces. The lack of nucleation sites in the liquid-liquid-like system results in the overheating of the liquid sodium until vapor free heterogeneous or homogeneous nucleation occurs. When the superheat limit is reached, vaporization is rapid enough to produce shock waves. However, in the presence of nucleation sites, molten UO_2 encountering liquid sodium will lead to ordinary nucleate boiling, where the vapor generation rate is many orders of magnitude smaller. This is so because the contact temperature is much closer to the nominal boiling point than the stability limit of liquid sodium (T_i ∿1200 and T_s ∿2050°C). For the Al-H_2O and stainless steel-H_2O systems, the minimum temperatures fall well below the nominal melting temperatures of these materials (T_{min}, stainless steel-H_2O ≈350°C, T_{melt}, stainless steel ≈1450°C, T_{min}, Al-H_2O ≈310°C, T_{melt}, Al ≈660°C). This finding is consistent with observations that molten Al and stainless steel when dropped into saturated water do not fragment or explode,[1] indicating the existence of film boiling well beyond the occurrence of solidification. On the other hand, large coherent vapor explosions have been observed with the same materials when the water has been sufficiently subcooled, in agreement with the qualitative evaluation of the requirements for liquid-liquid contact and that the contact temperature must exceed the stability limit of the more volatile liquid. The latter requirement appears to be in qualitative agreement with recent scoping experiments involving the requirements for vapor explosions between Freon 22 and water.[9] The above considerations are also consistent with observations on molten tin explosions in subcooled water where temperatures of tin less than 400°C did not produce vapor explosions.[7] It, therefore, appears from available experimental data that liquid-liquid systems, like UO_2-Na with property combinations that readily result in direct liquid-liquid contact (based upon film boiling considerations) at the same time are not sufficient to produce large-scale explosive interactions. Further detailed experiments involving several suitable liquid combinations are in progress to determine if $T_i > T_s$ is a general and necessary requirement for coherent vapor explosions.[10]

Both in- and out-of-pile experiments have been conducted to provide data on UO_2/sodium interactions for use in analysis of hypothetical fast reactor accidents. Simulations have included both whole-core (loss-of-flow and overpower transients) and local-core incidents (local blockages and overenrichment errors). These results support the above discussion.

Two different test vehicles have been used for TREAT meltdown tests that involve the interaction of molten fuel and coolant. A stagnant sodium autoclave that contains an inertial loading piston has been used for the S-series tests. These tests have been made to investigate fuel-coolant interactions under the extreme conditions of a hypothetical prompt-disassembly burst in an unvoided core. The generation of 100-atmosphere fuel-vapor pressures before clad failure (S-11 and S-12) did not produce a significant interaction of the molten UO_2 and liquid sodium. The interaction associated with the first pressure pulse was small, and the first pressure pulse can be explained as the release of high-pressure UO_2 vapor with negligible contributions from sodium vaporization.[11] Apparently, the fuel vapor in this case prevents direct liquid-liquid contact and the liquid sodium acts as an energy-dissipating source rather than a working fluid by absorbing the heat from the rapidly condensing fuel vapor.

The Mark-II flowing sodium loop has been used for power excursion meltdown tests of oxide pins (E- and H-series) as well as for flow disturbance tests (L-series). Clusters of up to seven pins can be accommodated and simulations have included both fresh and old fuel. Tests completed to date involving sample power rises comparable to 50¢/sec and \$3/sec LMFBR excursions (H- and E-series tests, respectively) have all resulted in very mild interactions,[12] illustrating that nucleate or intermittant boiling occurs rather than explosive boiling. The feasibility of analytical interpretations of these TREAT experiments in terms of mild UO_2-Na interactions has been demonstrated.[13] The main features responsible for the low pressure generation as compared to what can be calculated based upon thermodynamic arguments[14] and proposed rate limiting source term models[15,16] are as follows: 1) no all liquid heating, vapor present while fragmentation takes place and no explosive boiling, all of which prevent formation of high shock pressures, and 2) heat transfer between fuel and sodium is sufficiently slow, i.e., by nucleate boiling, that heat losses and condensation play a very important role in reducing available work energy. Three "L-series" tests have also been completed to study failure consequences arising from complete loss of flow without reactor shutdown. Test L-2 was run with seven fresh pins, while L-3 used seven pins irradiated to about 3.5 a/o in EBR-II at power levels insufficient to produce a well-defined central void, and the L-4 sample consisted of seven pins irradiated to about 4.3 a/o in EBR-II at power levels high enough to produce a well-defined central void. No fuel-coolant interaction could be identified in any of these three experiments,[12] which is consistent with the current understanding of the loss-of-flow sequence that provides for saturated sodium-out condition and no coherent liquid reentry prior to fuel melting, and thus coherent mixing is precluded. The occurrence of nucleate boiling further prevents intimate contact and results in a relatively slow quenching process of the molten UO_2.

To treat the case of a hypothetical whole-core accident with sodium out, kilogram-scale out-of-pile experiments with reactor materials have been carried out to study heat transfer and incoherence effects of larger masses of interacting fluids. Experiments have involved up to 3 kilograms of molten UO_2 (produced by the thermite method) injected into subcooled liquid sodium.[17] No violent coolant vaporization events of the "vapor explosion" type occurred. The observed boiling events were generally very mild and can be classified as nucleate or transition boiling.

In summary, in over twenty prototypic experiments that have been performed to date, it has been observed that the reaction between the molten fuel and liquid sodium is very much smaller than that which is theoretically possible.[14-16] These experimental findings relating to LMFBR materials are consistent with current understanding of vapor explosion phenomena.

C.1.2 Earlier Analytical Studies

Discussions contained in the subsequent sections are based on the available information of fuel-coolant interactions at the time the FEFPL design was initiated. The ANL FCI parametric model was used to establish the molten fuel coolant interaction source term. This is an improvement over the classical Hicks-Menzies thermodynamic analysis in that time dependent interaction processes are considered. In addition, consideration was given to the time delay in heating the coolant caused by the mixing and fragmentation of fuel within the reaction zone. The effects of sodium compressibility as well as the presence of vapor and/or inert gases on the reaction rate were also described. The influence of constraints, both acoustical and inertial, were treated in one dimension. The formulation of the ANL FCI parametric model and resulting computer code are summarized in Appendix B.4.

C.1.2.1 Basic Considerations

The parametric model requires input identification by the user of several parameters. Computations with the SAS model (described in Appendix B.2) help establish the initial conditions and the state of fuel and coolant just prior to a postulated MFCI. Other parameters, such as the fuel particle size, must be determined from experimental data.

The following sections present the rationale, along with supporting analyses and experimental evidence, behind the selections of the FCI model parameters, initial conditions, and variables used in arriving at the MFCI source terms developed in Section 10.2. In these studies, the major model input parameters were studied using as a baseline the FEFPL expected design values:[18]

Initial temperature of molten fuel	= 3661°K
Initial sodium coolant temperature	= 1100°K
Optimum fuel to liquid sodium mass ratio	= 11.11
Length of reaction zone	<3 ft
Expected fuel to liquid sodium mass ratio	<1/2 optimum
Fuel to coolant heat transfer cutoff time	<5.7 msec
Fuel particle radius	>117 μ
Mixing and fragmentation time	>3 msec
Vapor/liquid ratio	>1
Amount of molten fuel participating	<1/2 total inventory

The above values are based upon the following considerations of the FEFPL geometry and the loss-of-flow reference experiment described in Section 10.2.2.

1) Sodium vapor and/or inert gas will be present in or near the reaction zone during the MFCI.
2) The reaction will take place in the presence of excess liquid.
3) The amount of molten fuel reacting will not exceed half of the total fuel inventory.
4) A fuel to coolant heat transfer cutoff time will be realized upon attainment of two-phase conditions within the reaction zone.
5) Conservative values are selected for the fuel particle radius and the mixing and fragmentation time-constant based upon the limited experimental data.

C.1.2.2 Initial Reaction Zone Conditions

Influence of Initial Gas and/or Sodium Vapor

The presence of large amounts of sodium vapor and/or inert gas within or near the reaction zone is a certainty for the conditions predicted for the FEFPL reference transient, because sodium boiling will occur prior to fuel melting during all loss-of-flow accidents, according to SAS results. This type of transient is not a necessary condition to insure sodium voids, but rather a sufficient one (it appears that overpower transients also initially can have large amounts of sodium vapor present). Sodium vapor volume at least equivalent to the volume of molten fuel is expected. (The volume ratio of fuel to sodium in the test section is about one: during dryout and melting, the liquid sodium must be replaced by vapor). In addition, several sources of inert gas, such as the inherent fuel void volume, the gas volume in the upper fission gas plenum, and the compliance volume built into the hex can assembly are also present.

The source of voids and expansion volume in the FEFPL is as follows:

		Gas/liquid Volume Ratio
Gas in fuel voids		0.15
Fission plenum gas volume		1.00
Hex-can thermal insulation (60 mils)		0.25
Hex-can strain		0.35
Sodium vapor in active fuel region		1.00
Sodium vapor in fission gas plenum region		1.20
	Total	3.95

The sodium vapor present is equivalent to the test section being almost completely voided. This is consistent with the SAS predictions for the reference experiment (see Fig. 10.4), where the upper sodium liquid-vapor interface oscillated in the fission gas plenum region around the 200 cm location (referenced to test section inlet).

It should be pointed out that in the majority of these FEFPL calculations, the physical presence of inert gas in the mixing zone is considered only insofar as its affect on the compliance of the system is concerned. The beneficial gas blanketing effect of retarding the fuel-to-coolant heat transfer has been neglected during the early phases of the reaction. Therefore, in these calculations which account for only the compliance effect, the actual mass of gas is not important, only its volume. The escape of some inert gas from these regions (i.e., fission gas plenum) is expected prior to an MFCI. However, it is highly unlikely, due to the time required to equalize the pressure, that these spaces will quickly refill with liquid sodium and hence reduce the compliance volume.

With the above sources of gas present within or near the MFCI reaction zone, it will not be possible to attain extremely high pressures during the liquid sodium expansion phase of the interaction. Figure C.1 shows the peak pressures which could conceivably occur if no gas compliance were available. As Fig. C.1 shows, with more realistic lengths of reaction zone (molten fuel participation), lower pressures result even without vapor present. The quasi-steady-state model gives about a factor of five reduction in the peak magnitude of the peak pressure (2000 atm to 430 atm) when the reaction zone length is reduced from 3 to 0.5 ft (a 3 ft zone is used in the design envelope source calculations).

The influence of cushion-gas in reducing the peak pressure can be seen in Fig. C.2. Several cases with varying amounts of initial vapor and/or gas are investigated using the set of parameters listed in Section C.1.2.1 As a comparison of the curves in Fig. C.2 shows, small amounts of gas also delay the time when the peak pressure is reached (curve 1 versus curve 2). The presence of vapor in amounts large enough to preclude complete vapor condensation shows a gradual increase in pressure to the pressure condition at the thermal cutoff time (curve 4) in contrast to the condensation effect shown by curve 3. The latter tends to approach the "all-liquid" case. Furthermore, it appears for these interaction parameters that gas/liquid volume ratios greater than one (curve 4) result in little additional reduction in peak pressure.

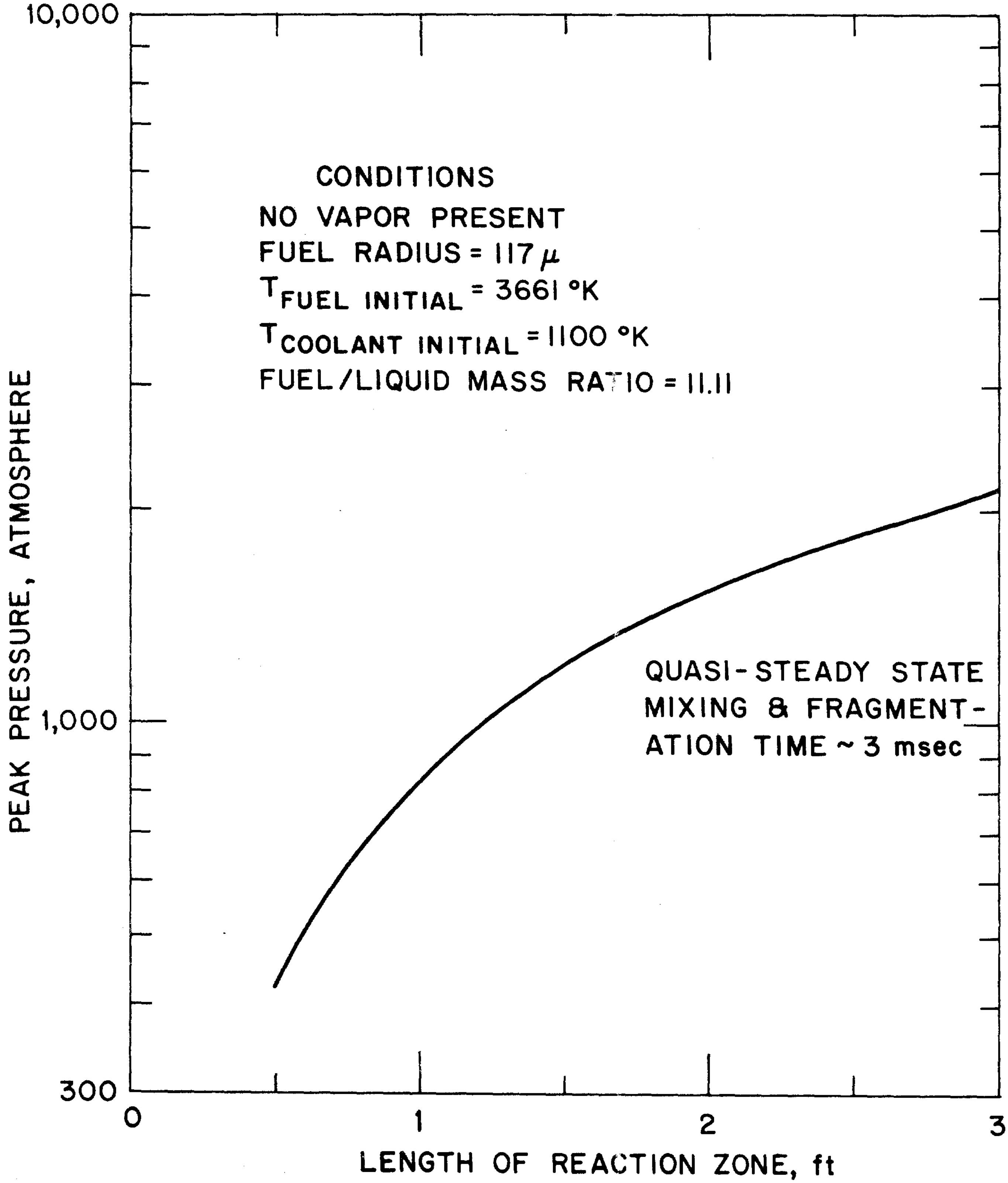

FIG. C.1 - Peak Pressure Without Compliance

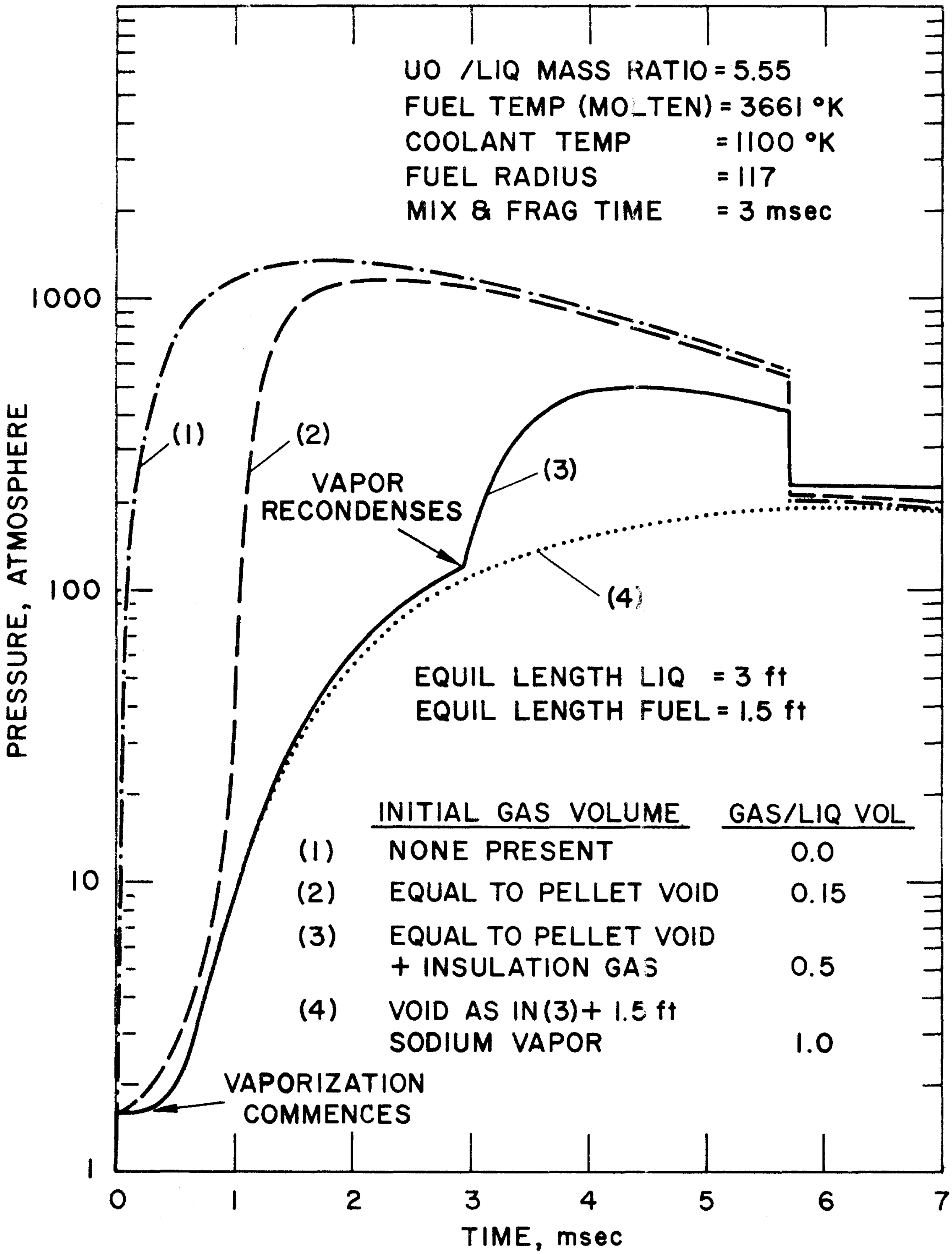

FIG. C.2 - Effect of Cushion Gas on Peak Pressure

Presence of Excessive Liquid

The fuel-to-sodium mass ratio affects the thermal to mechanical conversion efficiency which is obtained during the MFCI. The pressure-time history predicted with the ANL model reflects, therefore, the assumptions made regarding the value of this ratio within the reaction zone at the time of the MFCI. A description of the mode of fuel cladding failure and a description of the location and boundaries of the reaction zone is needed to define this quantity more exactly. At present, a firm quantitative model describing the release of molten fuel from a multirod array does not exist. Considering, however, the FEFP loop geometry, plus the results of the SAS analysis, the following observations can be made.

1) The most logical locations for the reaction to occur are in the lower extremities of the fuel bundle, or in the lower plenum region. The ability of the vapor bubble to prevent liquid reentry suggests that the fuel will slump and that the reaction cannot occur at the near optimum fuel to liquid unit-cell configuration, because the fuel fraction must increase as the fuel tends to compact.

2) If small amounts of molten fuel drop into the lower plenum region of the core, the reaction would be expected to characterize an excessive liquid situation. The noncoherent nature of the melting process suggests that only small quantities of fuel gradually would contact sodium over the time required for significant fuel melting. (Heat losses from the hex can are ignored; they contribute to the incoherence of melting by cooling the ends of the pins.)

3) If molten fuel reacts within the lower plenum region, excess liquid must be present. It is inconceivable for the original unit-cell mass of fuel to be instantaneously transported to the lower plenum in the exact optimum configuration. If 50% of the molten fuel falls to this region, the mass ratio of fuel to sodium is $\sim$4.9.

4) In the case of an MFCI occurring due to small amounts of molten fuel slumping into the nonmolten regions of the fuel bundle, the reaction heat transfer characteristics also would be expected to resemble an excessive liquid situation. The unmelted cooler fuel and cladding in the reaction zone will compete with the liquid for the molten fuel's heat. The presence of this heat sink will therefore reduce the heat available for the liquid and thus retard the liquid heatup rate.

Experimental evidence obtained from the H-2 TREAT test indicates that an excessive liquid situation existed. The interpretation of this data is presented in Ref. 13.

Quantity of Molten Fuel Participating in MFCI

In the MFCI analysis, the amount of molten fuel interacting was assumed to be 50% of the total fuel inventory. Calculations described previously in Section 10.2.1.4 indicate that this amount is conservative, because the incoherence of the melting process is not fully accounted for and because heat losses from the fuel are ignored. As discussed, it is expected that only small amounts of fuel will react instantaneously. Nevertheless, to establish an upper limit on energy generation, half of the fuel inventory is used as a conservative estimate.

The conservatism inherent in the 50% fuel participation quantity assumption is further substantiated by the results of refined mechanistic MFCI calculations presented in Section C.1.2.5.

Thermal Cutoff

A thermal cutoff that effectively terminates the transfer of heat from the fuel to the coolant results when the fuel is insulated by vapor and/or gas blanket. The value of 5.7 msec is used throughout this analysis. It is based upon the total travel time of the acoustic shock to the upper gas reservoir interface. The return of the rarefraction wave to reduce pressure in the reaction zone permits boiling, and the subsequent film blanketing of the fuel particle terminates heat transfer.

When a two-phase mixture is present in the system, the wave travel time may be considerably longer than 5.7 msec. The velocity of sound in a two-phase mixture can be retarded by an order of magnitude depending upon the void fraction. The axial wave travel time would therefore be greatly increased. For this condition, however, much lower pressures would be realized due to the softening of the pressure constraint.

Two factors, however, suggest that 5.7 msec may still be a conservative over-estimate of the time at which the transfer of heat from the fuel ceases. First, the close proximity to the reaction zone of the compliance volume at the hex can wall permits a reduction by several orders in the acoustic wave travel time in the radial direction to this free surface. Second, and probably of greater importance, is the fact that for the situation of interest, compliance volume is initially present and vapor generation is insignificant within the mixing zone. Calculations indicate that at about 5 msec, the mixture quality is about 10%. This quality gives void fractions greater than 50% in the test section; therefore, heat transfer must decrease before 5 msec.

C.1.2.3 Reaction Kinetics Parameters

Two major reaction-kinetics parameters, i.e., the fuel particle radius and the mixing and fragmentation time-constant, must rely upon experimental data for their values. The amount of information for the expected FEFPL conditions is very limited. Most of the MFCI data has been obtained from relatively small bench-scale experiments that drop either the hot material into the cold working fluid, or vice versa, although additional data has also been obtained from in-pile meltdown experiments in TREAT.

Fuel Particle Size

For an estimate of the fuel particle radius, the multirod TREAT S-series experiments appear to be the only tests that approach conditions expected in the FEFP loop. It should be pointed out that even these are at conditions which appear to be more severe than FEFPL tests that will lead to MFCI in the presence of large amounts of initial sodium vapor. The creation of molten fuel prior to sodium voiding as obtained with TREAT ramp experiments is a condition not possible with the FEFPL loss-of-flow tests in ETR. Therefore, yields lower than those in the S-series are expected during FEFPL experiments.

Nevertheless, in this study, the S-series residual fuel particle radius data is employed.[19] These particle data are shown in Fig. C.3, along with data from molten UO_2-sodium drop tests in the laboratory. The smallest mean particle diameter was found after the S-5 test, or about 200μ. Discounting the laboratory drop tests that do not simulate FEFPL conditions, and the results from test S-5 which was run with evacuated fuel pins, a mean particle size found for multirod arrays is observed. This appears to be the lowest particle size found for multirod arrays that contain fill gas; consequently this value is used as a best estimate for the "upper limit MFCI." To be conservative, however, a radius of 117μ was used as the particle size for the design envelope MFCI. To ascertain whether 117μ is a conservative fuel particle radius, a more representative analysis is required using the actual distribution of particle size found, rather than the

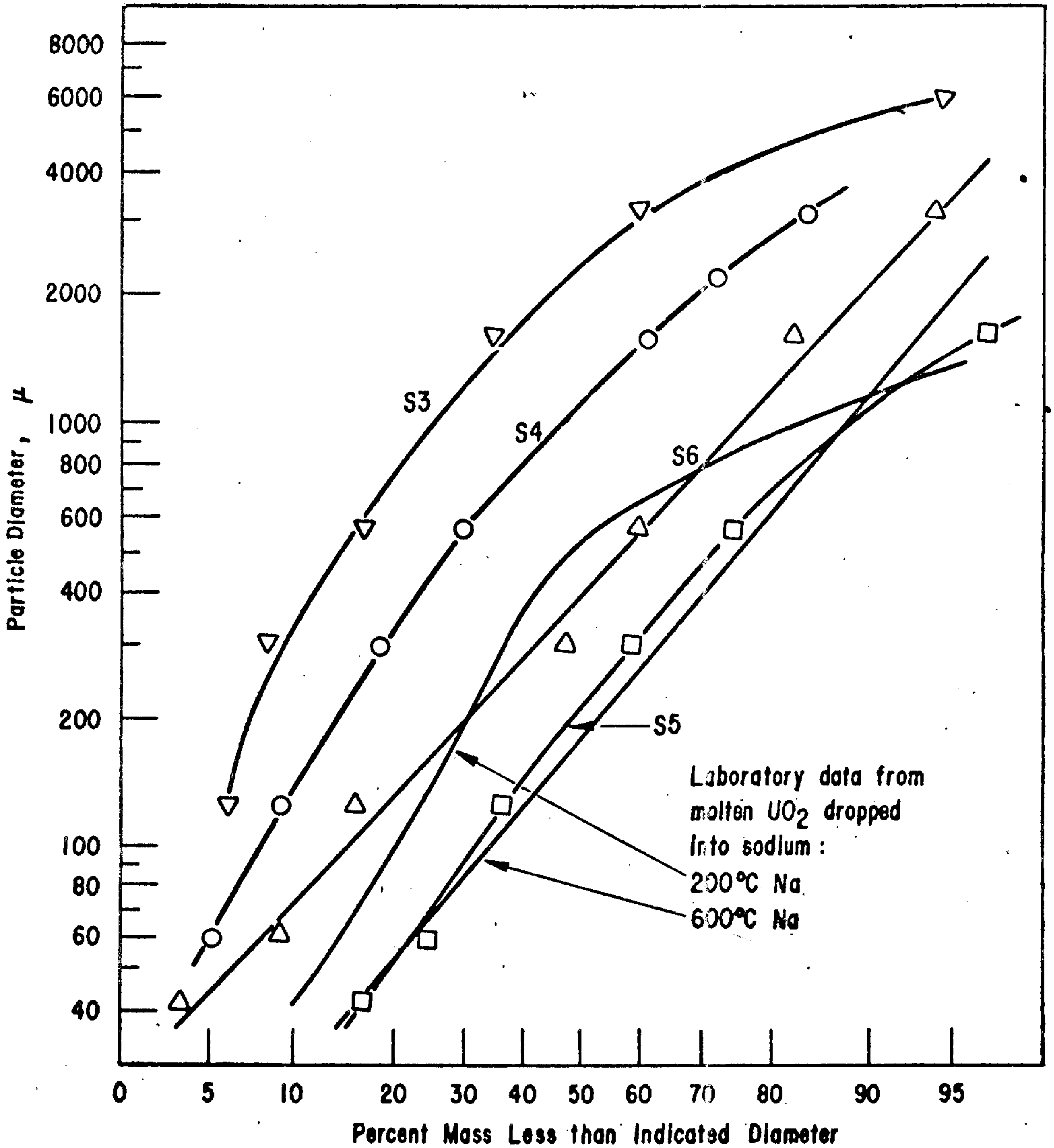

FIG. C.3 - Particle Size Distribution from S-3, S-4 S-5, S-6 and Laboratory Experiments median value. The particle size distribution used is given in Table C.1 and represents the data observed in laboratory experiments with 400°C sodium.[20] Table C.2 summarizes the initial conditions and MFCI parameters used which are identical to the FEFPL design envelope source term with the exception of the use of a zero fragmentation time-constant. For comparison, calculations have also been made using two different mean diameters; the median based on mass (234μ) and the surface-volume mean (133μ). Definitions of these mean diameters are given in Table C.1, along with the particle size distribution used. Note that the median based on mass (234μ) is the fuel particle diameter which has been used in most of the parametric model calculations.

The results of these MFCI calculations are presented in Fig. C.4 and Fig. C.5. Pressure-time histories calculated using the FCI parametric model with one-dimensional acoustic constraint are presented in Fig. C.4. The corresponding sodium temperature histories are presented in Fig. C.5.

In the pressure calculations shown in Fig. C.4, the mixing-zone sodium vaporized very early in the process due to the presence of a large amount of noncondensable gas in the mixing-zone, and the pressure rise time was relatively long (the pressure-time histories shown were calculated assuming no vapor blanketing). In this case, the use of the particle size distribution gave somewhat higher pressures for the initial period of 0.7 msec and lower pressures thereafter than those calculated with the median diameter.

These observations indicate that, when the particle size distribution is taken into account, the heat transfer rate is higher for short times, but lower for longer times, than it is when the median diameter is used. This can be seen rather easily from the sodium temperature histories given in Fig. C.5.

In this analysis, the pressure was highest when the volume-surface mean diameter of 133μ was used.

The above calculations suggest that the use of a mean particle diameter would not introduce any gross errors. In view of the uncertainties involved in fuel-coolant interactions, it seems adequate at present to use a mean particle size, such as the median diameter of 234μ in most calculations. Further details of this investigation are found in Ref. 21.

Mixing and Fragmentation Time

The concept of a mixing and fragmentation time-constant (t_m) has been employed in the ANL FCI parametric model (see Appendix B.4) to account for

TABLE C.1

Fuel Particle Size Distribution and Mean Diameter

1. The particle size distribution used was taken from Armstrong's laboratory data obtained with 400°C sodium.[20] It is given below where y_i represents the mass fraction of fuel particles having an average diameter of d_i.

d_i (cm)	y_i
0.171	0.0767
0.113	0.0894
0.072	0.0743
0.051	0.0852
0.032	0.1951
0.019	0.1054
0.013	0.1064
0.009	0.0947
0.0064	0.0600
0.00355	0.1128

2. The median or the 50% value of the above distribution is 234μ. When the distribution is log-normal, the median represents the geometric mean of the mass distribution. This is approximately the case with the distribution data given above.

3. The volume-surface mean or the Sauter mean diameter is often used in surface area determinations. Its reciprocal is proportional to the surface area per unit volume. The volume-surface mean diameter is defined as follows:

$$d_{vs} = \frac{\sum f_i d_i^3}{\sum f_i d_i^2}$$

where f_i is the frequency of particles having diameter d_i. In terms of the mass fraction, y_i, the volume-surface mean diameter becomes

$$d_{vs} = \left(\sum \frac{y_i}{d_i}\right)^{-1}$$

For the particle size distribution given above, the volume-surface mean diameter is 133μ.

TABLE C.2

Initial Conditions and Parameters Used for the Calculations of the Effect of Fuel Particle Size Distribution

Initial Sodium Temperature, °K	1100
Initial Sodium Volume, cc/g	1.35
Initial Pressure, atm	1.6
Initial Fuel Temperature, °K	3361
Fuel/Sodium Mass Ratio	5.5
Flow Area per Gram of Heated Sodium, cm^2/g	0.029
Initial Volume of Noncondensable Gas per Gram of Sodium, cc/g	1.35
Fragmentation Time Constant, sec	Zero

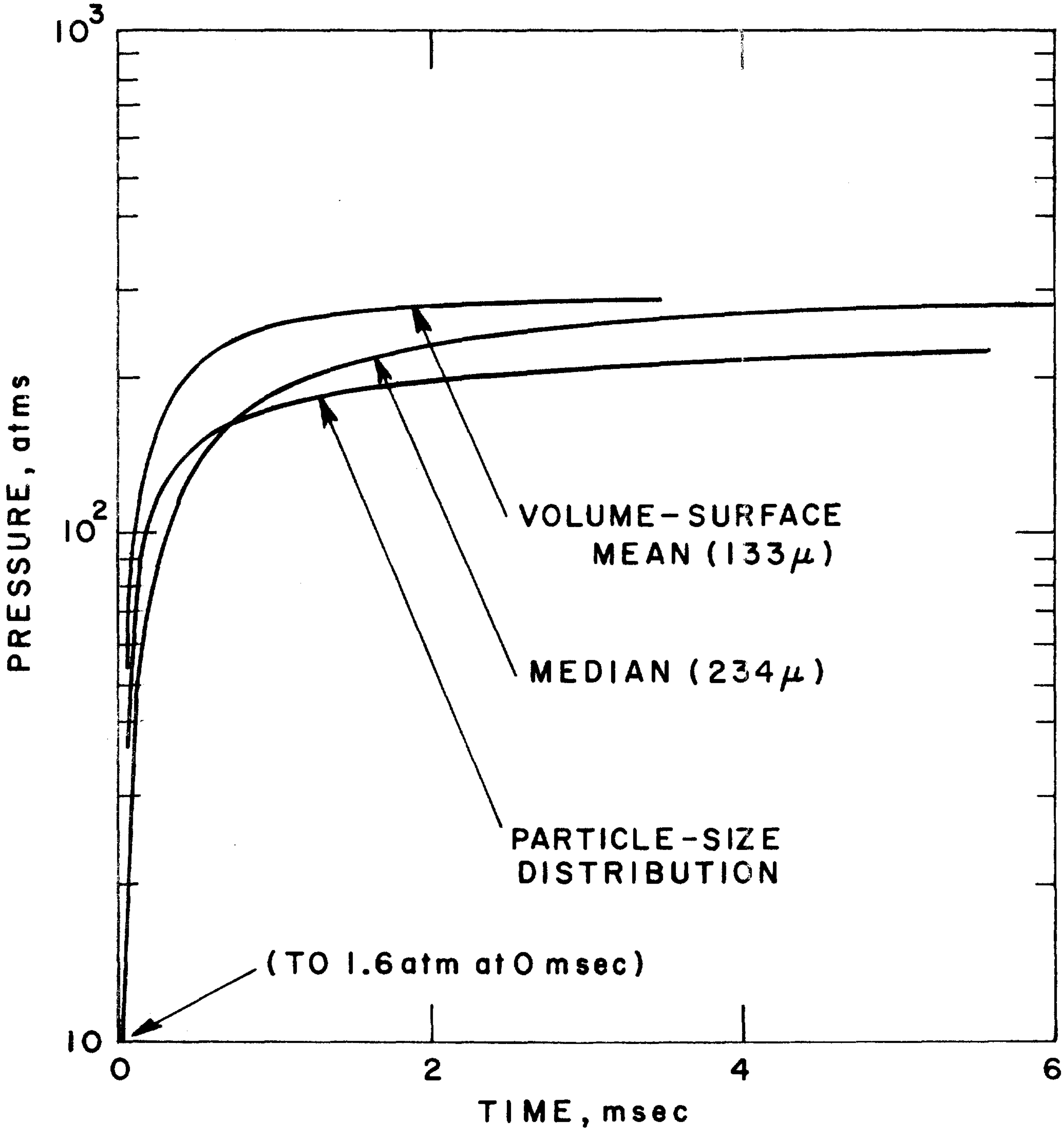

FIG. C.4 - Effect of Fuel Particle Size Distribution; Pressure-Time Histories

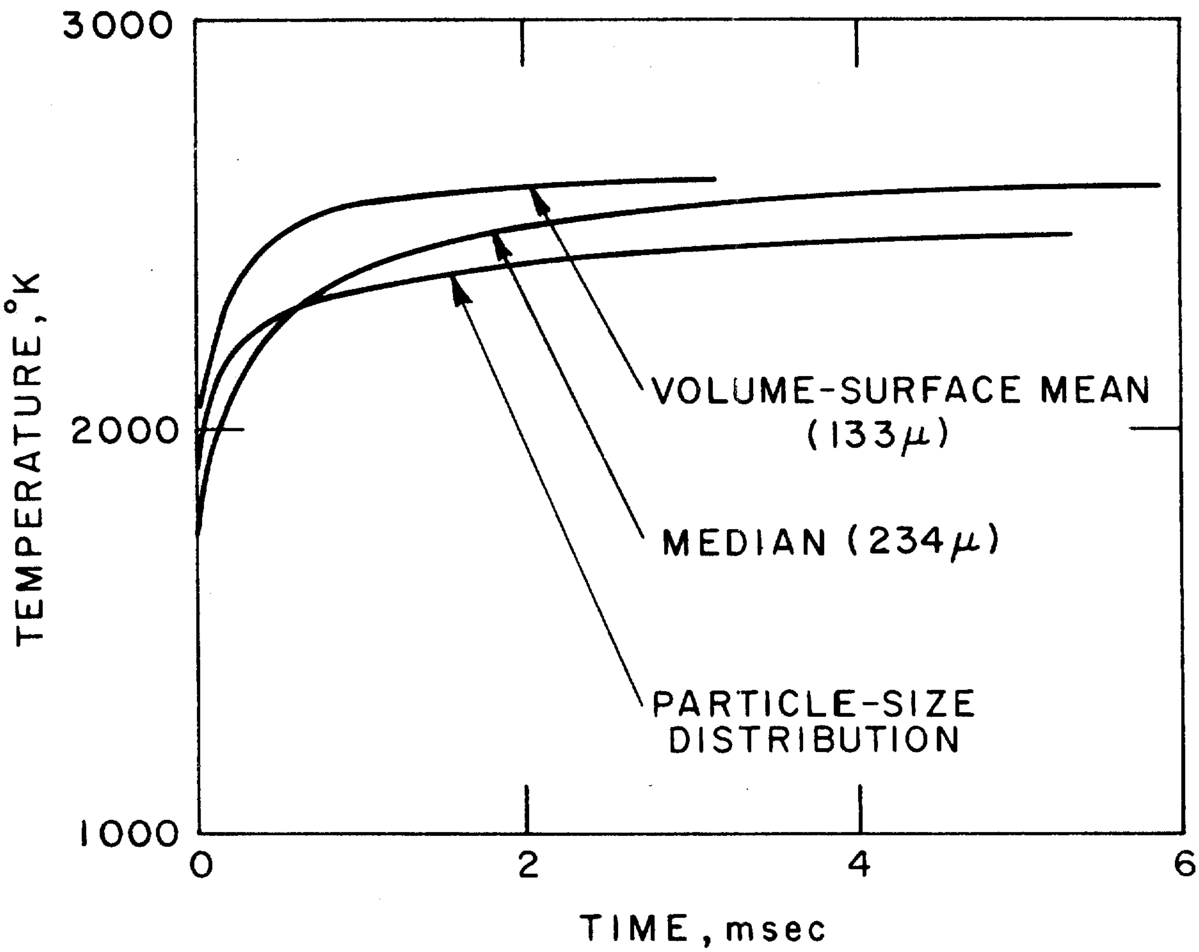

FIG. C.5 - Effect of Fuel Particle Size Distribution; Sodium Temperature Histories the time dependent processes involved in creating the small fuel particle sizes observed experimentally. There is no direct experimental data on the value of this parameter. Clearly a finite time is required as the large amounts of fuel assumed in this study (50% of total fuel inventory, or 3330 gms) escapes from the failed fuel pins and mixes and fragments in the reaction zone. The value of 3 msec used for the design envelope source term gives approximately the same results as the quasi-steady-state FCI formulation (see Appendix B.4) that did not allow explicitly for a time dependent heat transfer surface area.[22,23]

Although a mixing and fragmentation time constant of at least 3 msec is reasonable and expected, the effect on the calculational results of this parameter is examined. Shown below are typical peak MFCI pressures for various assumed fuel particle radii as calculated with a zero mixing and fragmentation time:

Fuel Particle Radius (μ)	Peak Pressure (atms)
117	220
200	190
400	121
600	88

In this study, the conditions postulated for the design envelope MFCI (see Section 10.2.4) are used, except that the mixing and fragmentation time is reduced to zero, thereby eliminating it as an input variable.

The pressures resulting as a function of fuel particle size show effectively that the pressure is reduced by the slower heat transfer from larger fuel particles. Also evident is the relatively small increase ($\sim$10%) in peak pressure when the mixing and fragmentation time is reduced from 3 msec to zero at the design basis 117μ fuel particle size.

C.1.2.4 Physical Property Data

The MFCI calculations require the use of thermomechanical property data in order to characterize the behavior of both the fuel and sodium. Throughout these investigations a consistent set of values is employed based upon the best available property data existing at this time. Where even large uncertainties exist, or the calculational results are very sensitive to the value of a given parameter, conservative values are used.

Fuel Properties

Temperature-independent fuel property data are required in an ANL FCI parametric model. No mechanical property information is employed as the pressure of fuel volume is neglected in determining the compliance of the reaction zone.

The fuel properties selected are valid for both the UO_2 and mixed-oxide fuels (PuO_2-UO_2) expected to be used in the FEFP Program and are tabulated in Table C.3. Also shown in Table C.3 are literature values for UO_2, PuO_2, and mixed-oxide (U, 20 wt % Pu)O_2.[24]

TABLE C.3

Summary of Fuel Properties

Property	FEFPL Design	UO_2	PuO_2	(U,20 wt % Pu)
Melting Point, °C	2800	2840	2400	2810
Thermal Conductivity, W/cm-°C @ 95% TD	0.031 constant	0.022 >1600°K	0.023 at 1000°C	0.021 >1600°C
Specific Heat, cal/mole, °K	26. constant	23. at 1800°K	-	24. to 26. at 1800°K
Density, gm/cc @ 100% theoretical	10.96 constant	10.3 at 1800°K	10.7 at 1800°K	10.4 at 1800°K

As shown in Table C.3, a high estimate of fuel thermal conductivity has been chosen for the FEFPL design MFCI analysis. The peak pressure that is calculated, therefore, is higher than would be realized using the more realistic lower value. The fuel heat capacity (product of specific heat times density) value of 1.05 cal/cc-°C is representative of the literature data presented in Table C.3.

Sodium Properties

The sodium property data employed in these FEFPL MFCI analyses were identical to the values used in previous FTR studies.[21-23] These high-temperature data were extrapolated from the low temperature data of Ref. 25. It is recognized that considerable uncertainties exist in these high temperature, high pressure sodium properties. This uncertainty, however, is well within the accuracy of the basic MFCI model's predictive capabilities. The conservative approach taken in other modeling areas is felt to compensate for the uncertainties in the sodium properties.

It is noted that the mechanical properties of sodium, namely the isothermal compressibility factor and the thermal expansion coefficient, are of major importance in determining the peak pressure. However, in a soft system with a large vapor compliance volume (typical of the expected FEFPL conditions) these properties are not as important in determining the peak system pressure. For this situation, the peak pressure will be primarily controlled by the vapor/inert gas in the reaction zone.

C.1.2.5 Effect of Reactant Transport on MFCI

The original ANL FCI parametric model used to establish the FEFPL MFCI source terms was formulated around a "closed system" in which a given homogeneous mixture of materials (fuel, coolant, vapor-gas) interacted. This batch-type process did not consider explicitly the transport of reactants across the reaction zone boundaries, although the fragmentation and mixing time constant does account somewhat for this effect. As the SAS predictions of the conditions for the reference experiment indicates (see Section 10.2.2), this "closed system" is not consistent with the physical situation in the melting FEFPL test section prior to an MFCI. For the coolant-actuated transients, the lack of significant quantities of liquid sodium in the vicinity of the molten fuel suggests that for a violent MFCI to occur, finite rates of mass transport of either one (or both) of the reactants to an interaction zone would be required. To explore the basic conservatism inherent in the "closed system" approach, three types of transport processes were identified and studied:

1) Molten fuel is transported to the liquid sodium below the test section at constant rate (i.e., droplet falling or film flow),

2) Significant quantities of molten fuel are held up in the test section or on the bottom flowmeter and then fall into the liquid sodium in the lower portion of the loop,

3) Liquid sodium reenters the test section at a finite rate contacting molten fuel.

The three mechanistic descriptions all start with a sudden complete flow blockage, followed by sodium voiding, clad melting and fuel melting. At this point, the molten fuel may relocate and either freeze, react with sodium, or collect in a molten pool for possible subsequent reaction. These possibilities form the basis for the three models.

To study these more mechanistic descriptions of the MFCI phenomena, a modified version of the ANL FCI parametric model, described in Appendix B.4, is employed.[26] In this analysis, it is assumed that fuel and sodium enter the reaction zone at a constant rate and in constant proportion. The following conservative model parameters and conditions are assumed:

- Optimum UO_2/Na mass ratio of 11.11
- Fuel particle radius of 117μ
- Fragmentation time of 3 msec
- Initially no gas vapor present in reaction zone
- No thermal cutoff
- Rigid container walls
- No heat loss from reaction zone
- Inertial constraint only (sodium incompressible)
- All the fuel in a 37-pin array (6660 gms) is available for interaction

Other FCI parametric model input data are identical to the values employed in the design envelope source term studies (see Section C.1.2.1). The results for the three transport models are discussed in the next sections.

Fuel Falling at Melting Rate

In this analysis, it is assumed that the fuel melts and either runs or falls under the influence of gravity into the lower sodium interface. Although continuous sodium voiding of the test section is required to sustain fuel melting, the effect of sodium vapor is neglected. The axial constraint for the reaction zone is taken to be the 609-cm liquid-sodium-column extending from the test section to the loop reservoir gas level. The physical description of this model is illustrated in Fig. C.6 as Model I.

The molten fuel-coolant interaction pressure histories are obtained for three constant fuel-transport rates of 3.33, 1.66, and 1.11 gm/msec. These rates correspond to the continuous addition of molten fuel produced by a linear melting of 50% of the total 37 fuel pin inventory (3330 gms) over a one second, 2 second, and 3 second time interval. The maximum rate at which 50% of the fuel melts has been predicted by SAS to be ∿2 seconds, based upon the reference flow blockage experiment (see Table 10.1). To account for possible heating of the liquid fuel, the molten fuel is assumed to be 100°C above the melt temperature (pseudo temperature of 3761°K is used in FCI parametric study).

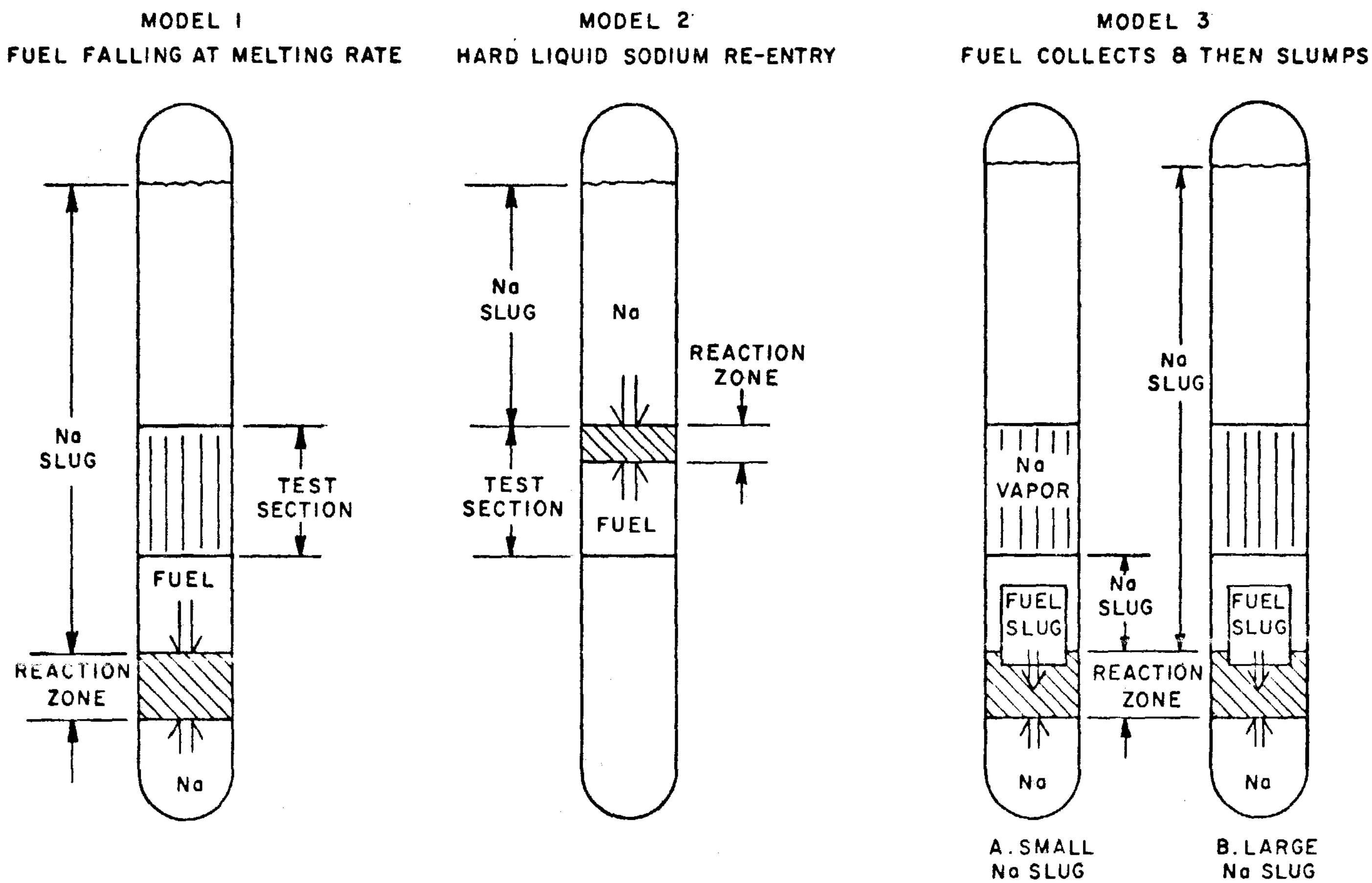

FIG. C.6 - Mechanistic MFCI Models

Pressure history results for these three cases are presented in Fig. C.7. For comparison purposes, the two FEFPL source terms described in Section 10.2 are also shown. Evident is the reduced peak pressures which are obtained for the fuel transport cases compared to the "batch" type design envelope case. Even assuming the much more conservative MFCI parameters (i.e., optimum UO_2/Na mass ratio and no compliance gas volume initially), a peak pressure of only 110 atms is realized (for a constant fuel-transport rate to the reaction zone corresponding to melting 50% of the fuel in one second). The general agreement in pressure pulse shape between the batch-type system and fuel-transport-type system is also evident in Fig. C.7. This agreement can be attributed to the "softness" of both systems. As seen from the results tabulated in Table C.4, sodium vaporization occurs quite early within the reaction zone for both the FEFPL source terms and also in Model I.

Shown in Table C.4 is a comparison of energy generation for the two models. The variable size reaction zone due to the addition of reactants results in an order of magnitude reduction in work compared to the closed system FEFPL source term values. At 5.7 msec, the amount of fuel participating is less than 20 gms for the fuel transport cases studied.

Hard Liquid Sodium Reentry

In this model, it is assumed that fuel melts and somehow remains within the voided region of the test section. This fuel may either accumulate to form a molten pool in the lower region of the test section or retain to some extent its original rodded geometry. If the fuel slumps into a larger mass, it continues to accumulate in a pool until violent boiling gives rise to an unstable geometry. Instability would occur after a maximum of about 15% of the fuel collects in the pool. Because at this point there has been no violent MFCI (fuel surface in contact with sodium vapor), the hex can is intact and cooled on the outside by the bypass sodium. Under these conditions of repeated fuel vaporization, a layer of fuel approximately 0.1 in. thick can freeze on the walls (over the full length of the hex can this represents about 50% of the total fuel inventory in a 37-pin test section). Next, it is postulated that for some unknown reason, liquid sodium reenters the test section and contacts the pool of molten fuel, or the molten fuel remaining in the rodded geometry. The rate at which sodium returns to be available for reaction is one or two g's. In this model, illustrated in Fig. C.6 as Model 2, the pressure pulse is calculated for a hard system without sodium vapor initially present.

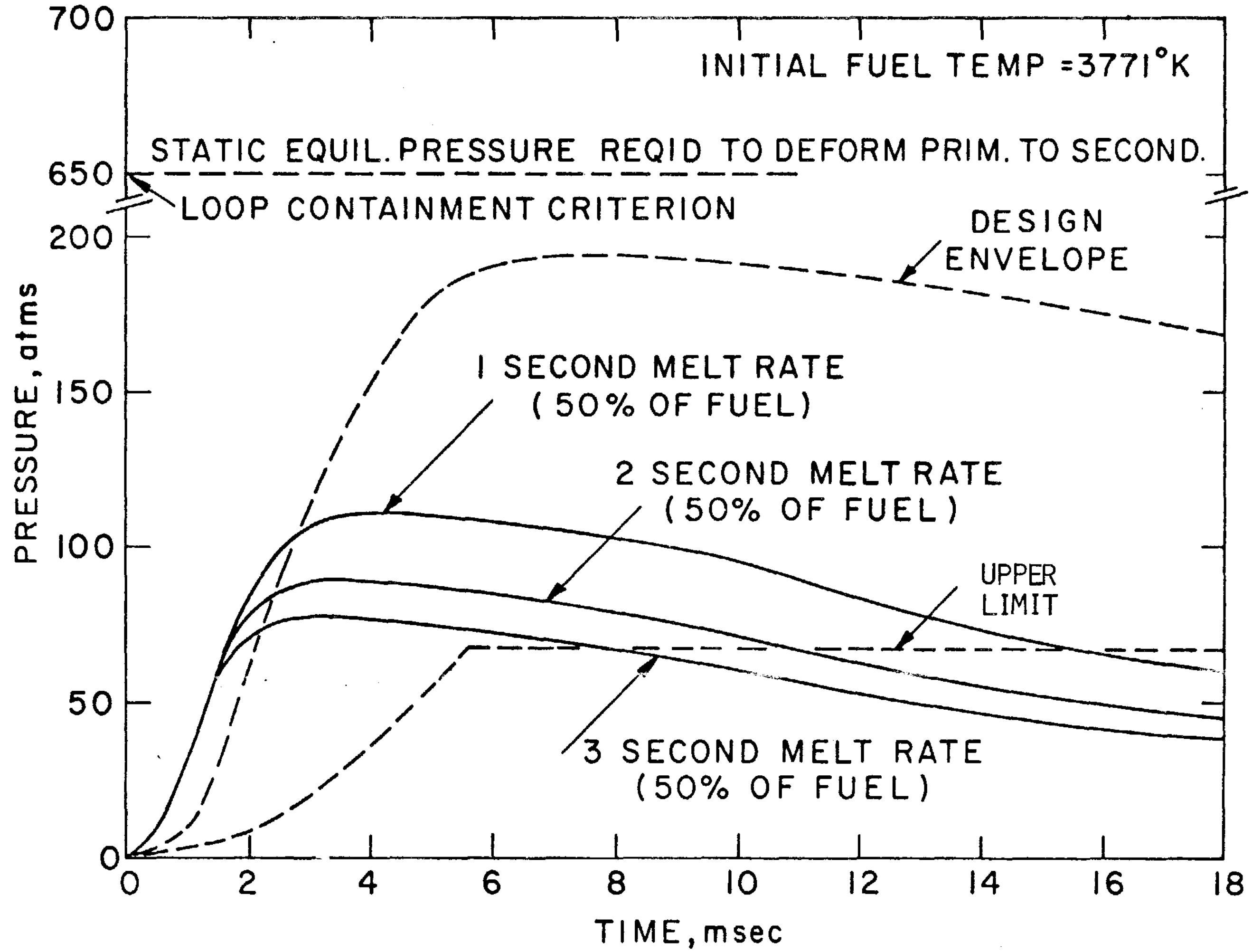

FIG. C.7 - Model 1 Pressure Histories Fuel Falling at Melting Rate

TABLE C.4

Summary of Transport Model Results

FEFPL Source Terms	Rate of Fuel Addition (gms/msec)	Vaporization Time (msec)	Peak Pressure Time (msec)	Peak Pressure Pressure (atms)	Results at 5.7 msec: Total Fuel Involved	Sodium Quality	Pressure (atms)	Total Work (joules)
Design Envelope	Infinite	0.924	5.7	194.2	3330 gms	0.095	194.2	1818.
Upper Limit	Infinite	0.426	5.7	68.9	3330 gms	0.080	68.9	1750.
MODEL 1- Fuel Falling at Melting Rates								
1 second for 50% fuel	3.33	0.586	3.990	111.2	19.0	0.54	108.7	173.
2 seconds for 50% fuel	1.66	0.433	3.396	89.3	9.5	0.61	84.7	119.
3 seconds for 50% fuel	1.11	0.362	3.091	78.1	6.3	0.65	72.6	91.
MODEL 2- Hard Liquid Reentry								
Sodium at 2000 cm/sec	119.8	2.763	0.214	520.8	683.	0.024	145.	1614.
Sodium at 1000 cm/sec	59.9	2.029	0.103	273.2	341.	.0175	84.3	491.
Sodium at 500 cm/sec	29.9	1.497	0.047	139.4	170.	.0103	45.2	174.
MODEL 3- Fuel Slump Into Sodium Pool								
Small Slug, 1 g fuel vel.	42.8	0.499	3.266	135.2	244.	0.0354	115.7	761.
Small Slug, 2 g fuel vel.	85.6	0.678	4.137	174.6	488.	1.000	169.2	5224.
Large Slug, 1 g fuel vel.	42.8	1.593	0.103	249.5	244.	0.0188	65.8	383.
Large Slug, 2 g fuel vel.	85.6	2.242	0.151	495.0	488.	0.0354	115.7	1521.

Three sodium reentry velocities are evaluated; 2000 cm/sec, 1000 cm/sec and 500 cm/sec -- corresponding to velocities of about six, three, and one and one-half times a 1.5 ft free fall velocity under gravity, and therefore are overestimations of the expected liquid reentry velocity. In all three cases, the fuel is assumed to be molten with the liquid fuel temperature 100°C above saturation (3771°K pseudo fuel temperature).

The calculated MFCI pressure histories are shown in Fig. C.8 for the three sodium reentry velocity cases. Also presented for comparison are the two FEFPL reference MFCI pressure source terms (design envelope and upper limit described in Section 10.2). As seen in Fig. C.8, a characteristic of these hard reentry cases is the sharp, rather large, initial peak pressure. However, the peak pressure of about 520 atms (obtained with 2000 cm/sec reentry velocity) is still below the $\sim$650 atms static equivalent pressure required to deform the FEFPL primary vessel to the secondary vessel. Also evident in Fig. C.8 is the subsequent rise in pressure for the three cases after the initial peak and sodium vaporization which occurs at 1.5 msec to 2.7 msec. Accounting for the expected heat losses from the reaction zone or gas blanketing due to the presence of sodium vapor will keep these pressures within the design envelope.

As tabulated in Table C.4 for this hard liquid reentry situation (Model 2), the total fuel involved in the interaction is relatively small. At 5.7 msec, the total fuel participating was 683 gm, 341 gm, and 170 gm for the 2000 cm/sec, 1000 cm/sec, and 500 cm/sec liquid reentry velocities, respectively. This represents only about 2.5 to 10% of the total fuel available in a 37-pin test bundle. The total work generated (see Table C.4) at 5.7 msec approached that obtained for the FEFPL source terms for the 2000 cm/sec reentry case (1614 joules) but was about an order of magnitude less for the 500 cm/sec liquid reentry case.

Fuel Slumps into Sodium Pool

In this mechanistic description of the MFCI process, the fuel is again assumed to melt and slump to form a molten pool, as in the previous model. Now, however, after the pool reaches a maximum stable configuration, it falls into and reacts with the sodium below at a rate determined by the acceleration of gravity. Two constraint situations are examined: a large 610 cm liquid column extending from the interaction zone to the upper loop reservoir and a small (1.5 ft) liquid slug which is between the reaction zone and the voided test section. The actual condition is probably somewhere in between these two extreme situations. Figure C.6 illustrates schematically these two fuel slumping cases as Model 3.

FIG. C.8 - Model 2 Pressure Histories Hard Liquid Reentry

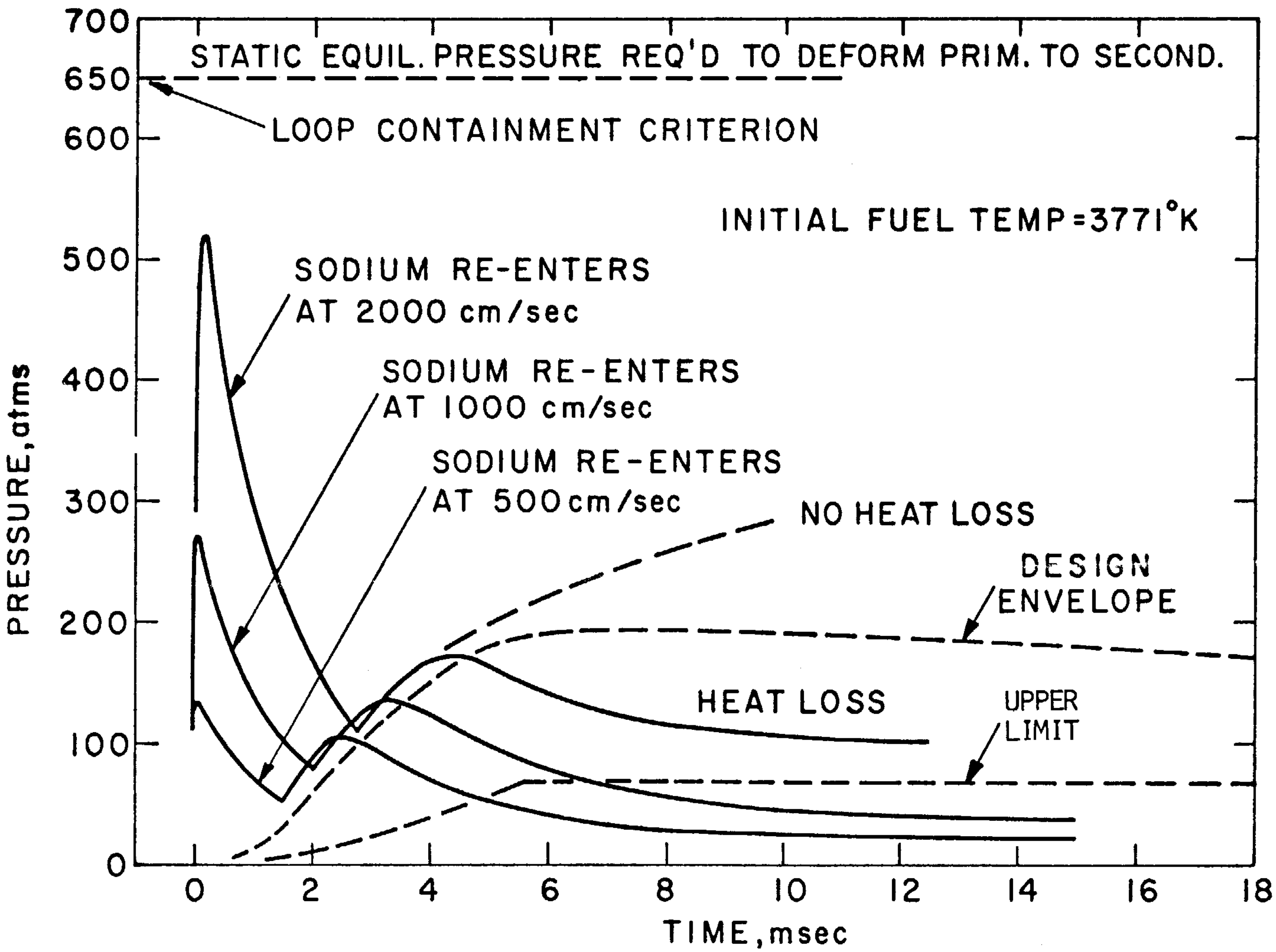

Calculations of the MFCI pressure-time behavior were performed for the two liquid constraints, each at two assigned full slumping velocity levels: a velocity corresponding to a free fall (1.5 ft) under 1 g acceleration; and a velocity corresponding to twice the 1.5 ft free fall velocity under a 1 g acceleration. For all cases, the fuel was assumed to be initially at the fuel vaporization temperature (pseudo-fuel analysis). Results of these analyses are shown in Fig. C.9 and Table C.4, identified as Model 3.

The MFCI pressure-time history for the various fuel slumping cases investigated are presented in Fig. C.9. Evident are the sharp pressure peaks exhibited by the two cases calculated assuming the large liquid slug constraint condition. The 500 atms pressure peak obtained assuming a high fuel-slump rate (85 gms/sec), however, is still below the 650 atms static equivalent pressure required to deform the primary vessel to the secondary. Interestingly, the two fuel-slumping cases examined with the small liquid slug constraint condition yielded pressure-time behaviors representative of the "soft" FEFPL design source terms (see Fig. C.9). For all cases, the pressure amplitude prediction after sodium vaporization (sharp breaks in curves of Fig. C.9) are at levels consistent with the FEFPL source term design range.

Further comparison of these slumping results with the design FEFPL MFCI source term predictions are provided in Table C.4. The fuel taking part in the interaction was only 3.7 and 7.3% of the total fuel inventory at 5.7 msec for the two fuel-slumping velocities considered. The total work generated up to 5.7 msec was, with the exception of the small slug at the high slumping-rate case, less than the FEFPL design source values. With the small slug, an unrealistically large slug velocity (21,000 cm/sec) resulted in the work generation being over twice the FEFPL design value at the 5.7 msec time of comparison. The total integrated value should not, however, exceed the 112,000 joules generated by the design envelope source term (calculated at 71 msec).

FIG. C.9 - Model 3 Pressure Histories Fuel Slump Into Sodium Pool

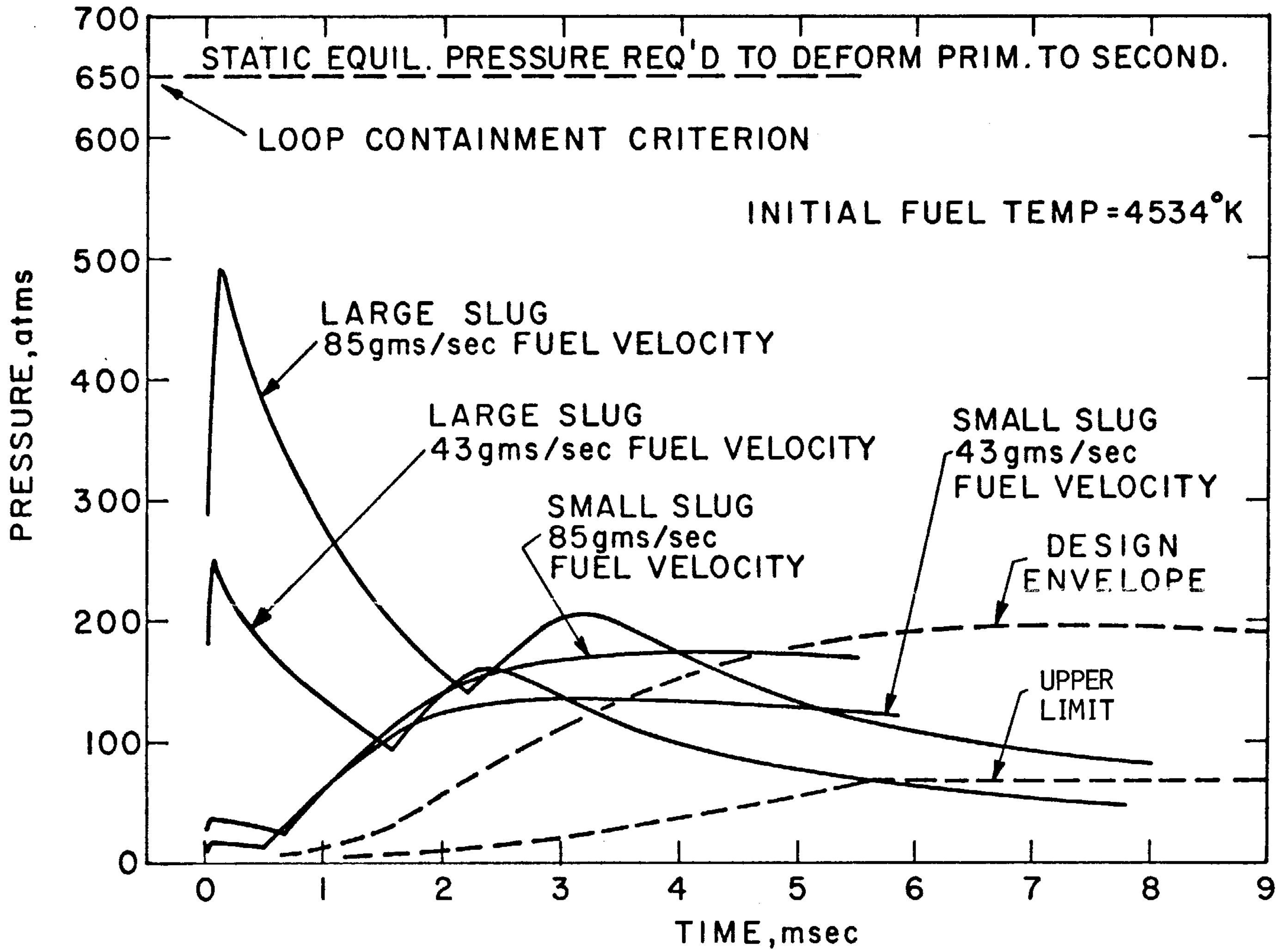

C.2 Interaction of Stainless Steel and Liquid Sodium

Although the criteria given in Ref. (2) for large scale vapor explosions does indeed indicate a potential for such explosions between sodium and stainless steel, if the steel is near boiling, the criterion itself represents one of a set of necessary, but not sufficient, conditions for large scale explosions. Other such conditions which are not easily quantified reflect the contact mode between the hot and cold fluids and the initial coherence of the two fluids.

a) To achieve a large scale explosion, the two fluids must come together in a tightly constrained manner, i.e., one fluid is entrained within the other with little gas or vapor present. In terms of the criterion given in Ref. (2), this means that a large compressible volume presents a physical barrier to the rapid mechanical transport of small droplets of both fluids which is essential to transfer large amounts of energy strictly by interface contact. Therefore, it is difficult for such a system to escalate into a large scale violent interaction.

b) The coherence of both liquid masses is not independent of the contact mode, but it has been experimentally demonstrated that, when the gross nature of the contact mode remains the same and the hot fluid is broken into small particles, systems, which normally explode, will not. (Long's aluminum-water studies.)

The available in-pile and out-of-pile experiments which have developed stainless steel temperatures necessary to satisfy the criterion of Ref. (2), have not observed any violent large scale interactions. It is felt that the two factors given above, play a major role in preventing any large scale interaction between sodium and stainless steel.

References:

1. R. P. Anderson and D. R. Armstrong, AIChE Preprint 16, presented at the Fourteenth National Heat Transfer Conference, Atlanta, Georgia (Aug. 5-8, 1973).

2. H. K. Fauske, Nucl. Sci. & Eng., 51, 95-101 (1973).

3. R. E. Henry, Trans. Am. Nucl. Soc., 15, 420 (1972).

4. K. J. Baumeister and F. F. Simon, Trans. ASME, J. of Heat Transfer, 95, 2, 166-173 (1973).

5. H. K. Fauske, J. Reactor Technol., 15, 4, 278-302 (1972).

6. P. Spiegler, et al., Int. J. Heat Mass Transfer, 6, 987-989 (1963).

7. S. J. Board, et al., Central Electricity Generating Board Report, RD/B/N2423 (Oct. 1972).

8. J. W. Taylor and S. D. Ford, UKAEA Rept. AERE-M/R-1729 (1955).

9. R. E. Henry, G. T. Goldfuss, and D. J. Quinn, "An Experimental Study of Large-scale Vapor Explosions", submitted for presentation at the San Francisco ANS Meeting (Nov. 1973).

10. R. P. Anderson, Argonne National Laboratory, private communication (July 1973).

11. S. M. Zivi, M. Epstein, and D. H. Cho, ANL/RAS 73-7 (April 1973).

12. C. E. Dickerman, AIChE Preprint 17, presented at the Fourteenth National Heat Transfer Conference, Atlanta, Georgia (Aug. 5-8, 1973).

13. A. W. Cronenberg, H. K. Fauske, and D. T. Eggen, Nucl. Sci. & Eng., 80, 53-62 (1972).

14. E. P. Hicks and D. C. Menzies, Proc. Conf. Safety, Fuels, and Core Design in Large Fast Power Reactors, ANL-7120, 654 (1965).

15. A. Padilla, Trans. Am. Nucl. Soc., 13, 375 (1970).

16. D. H. Cho, R. O. Ivins, and R. W. Wright, Proc. Conf. on New Developments in Reactor Mathematics and Applications, USAEC Rept. CONF-71-0202, 25 (1971).

17. T. Johnson, Argonne National Laboratory, private communcation (June 1973).

18. D. H. Lennox, et al., "Containment Study for the FEFP In-pile Loop", ANL/RAS 71-36 (Nov. 1971).

19. R. W. Wright, et al., "Fuel-coolant Interaction Effects during Transient Meltdown of LMFBR Oxide Fuel in a Sodium-filled Piston Autoclave: TREAT Tests S-2 and S-6", ANL/RAS 71-32 (Sept 1971).

20. D. R. Armstrong, et al., "Interaction of Sodium with Molten UO_2 and Stainless Steel using a Dropping Mode of Contact," ANL-7890 (Dec 1971).

21. W. L. Chen, et al., "Recent Additions to the Parametric Model of Fuel-coolant Interactions," ANL/RAS 72-17 (May 1972).

22. D. H. Cho, et al., "A Rate-limited Model of Molten Fuel-coolant Interactions: Model Development and Preliminary Calculations," ANL/RAS 70-05 (July 1970).

23. D. H. Cho, et al., "A Parametric Study of Pressure Generation and Sodium Slug Energy from Molten Fuel-coolant Interactions," ANL/RAS 71-5 (Jan 1971).

24. B. F. Rubin, "Summary of $(U,Pu)O_2$ Properties and Fabrication Methods," GEAP-13582 (Nov 1970).

25. G. H. Golden and J. V. Tokar, "Thermophysical Properties of Sodium," ANL-7323 (Aug 1967).

26. D. H. Cho, "Preliminary Assessment of Fuel-coolant Interactions Following a Voided-core Disassembly," ANL/RAS 72-14 (April 1972).

APPENDIX D

TABLE OF CONTENTS

D.0 Definitions

D.1 Anticipated Fault (A)

An anticipated fault is an off-normal condition which individually may be expected to occur one or more times during the system lifetime. For FEFPL, the associated consequences are judged acceptable provided that the loop conditions are within a Class I severity, both containments remain fully intact, and any radiation release is within the limits of AECM-0524. An anticipated event in conjunction with failure of either the EAS or control system is judged acceptable as above, except that loop conditions will be considered acceptable if within a Class II severity level.

D.2 Unlikely Fault (U)

An unlikely fault is an off-normal condition which individually is not expected to occur during system lifetime; however, when integrated over all systems and components, events in this category may be expected to occur. Two concurrent independent anticipated faults are defined as an unlikely fault. For FEFPL, the consequences of an unlikely fault are judged acceptable provided that loop conditions are within a Class III severity level, the fault does not cause failure of either containment, and any radiation release is within the limits of AECM-0524.

(2A = U)

D.3 Extremely Unlikely Fault

An extremely unlikely fault is an off-normal condition of such extremely low probability that it is not expected to occur during the lifetime of the system, but which nevertheless represents a limiting condition failure considered possible. An unlikely fault concurrent with an anticipated fault is defined as an extremely unlikely fault. The consequences of an extremely unlikely fault are judged acceptable provided that no containment failure is caused by the fault, at least one containment remains fully intact, and any radiation release is within the guideline values presented in 10CFR-100.

(U + A = EU)

D.4 Hypothetical Event

A hypothetical event is a condition for which no real sequence of causitive events can be identified, but which is nevertheless considered in order to assess margins relative to protection of the public. Events resulting from four or more concurrent independent anticipated events are included in this category.

(4A = H)

D.5 Design Basis Accident

A design basis accident is a specific event which bounds all consequences of a particular type or an event resulting from two concurrent independent unlikely faults. The design basis accident shall not result in radiation exposures in excess of the guidelines values presented in 10CFR-100.

D.6 Examples of Failures

The failure of either the EAS or control system is defined as an anticipated event.

The failure of the EAS and control system is also defined as an anticipated event due to commonality in the two systems.

The failure of the FEFPL PPS is defined as an unlikely event.

D.7 MFCI Source Term Definitions

D.7.1 Realistic

The realistic MFCI source term represents the maximum pressure pulse expected in the FEFPL experimental program based upon recent analytical and experimental results[1]. A value of 10 atm is indicated from this assessment.

D.7.2 Upper Limit

The upper limit MFCI source term represents the maximum expected pressure pulse based upon earlier information and was generated with the ANL-FCI parametric model using realisitic yet conservative input parameters appropriate to the FEFPL geometry and conditions. A peak pressure of 68 atms is obtained for this geometry.

D.7.3 Design Envelope

The design envelope MFCI source term represents an upper bound on the energy and pressure releases based upon initial design information using pessimistic "worst case" input parameters to the ANL-FCI parametric model. A very conservative estimate of 194 atm was obtained which enveloped the existing pertinent MFCI experimental data at the time. This term has been used in the design analysis of the loop. Comparison with the Realistic and Upper Limit values provides a measure of the degree of conservatism inherent in the source term prediction.

Reference:

1. H. K. Fauske, Nucl. Sci. & Eng., 51, 95-101 (1973).

APPENDIX E

TABLE OF CONTENTS

LIST OF TABLES

E.0 Gamma Heating in Loop Structural Materials

E.1 Introduction

Differing values of gamma heat rates appear in various sections of this report. This is a consequence of the development of changed estimates of the expected gamma heating rates that were made during the time that SAR analyses were in progress. Since the latest estimates are in the direction of reduction of earlier predictions, and the bulk of the analyses were completed at the higher, more conservative values, revised SAR calculations were considered unwarranted.

E.2 Vessel Temperatures for Containment

Initial values for gamma heating rates were provided by the calculations of McArthy.[1] These estimates were based upon an assumed highly peaked ETR fission rate in the vicinity of the loop and a 37 element test fuel bundle operating at an average linear power level of 12 kW/ft, which yielded axial average gamma heating rates of 9.6 watts/gm and 10.5 watts/gm in the FEFPL primary and secondary vessels, respectively. These values were then used in the SAR THYME-B calculations.

Later on, information was received reporting that a peak ETR gamma heating rate as high as 18 watts/gm had once been measured.[2] Since it was known that the THYME-B treatment of heat transfer through the vessel walls yields overpredictions of their average temperatures, a more accurate appraisal of average wall temperatures was made through use of a detailed thermal model.[3] The important results obtained from that study are listed in Table E.1.

TABLE E.1

Calculated Average FEFPL Vessel Temperatures at Core Midplane

	Heating Rate (watts/gm)		Temperature (°F)	
	THYME-B	Detailed Model	THYME-B	Detailed Model
Primary	9.6	18.0	1052	1012
Secondary	10.5	18.0	632	638

Both sets of calculations were performed for extreme steady-state loop operating conditions, viz., those delineated in Table 6.2 of the SAR for operating point C of the loop heat exchanger. The values tabulated above clearly show that the temperatures calculated by THYME-B are representative of gamma heating rates of 18 watts/gm in both containment vessels. Thus, as compared to the heating rates predicted by McArthy, the THYME-B calculated temperatures are highly conservative.[4]

Still later, FEFPL gamma heating rates were again estimated based upon a simple benchmark critical experiment and associated calculations. Although a precise mockup, and therefore the actual ETR core configuration for FEFPL operation was not precisely known, "best estimate" values were developed for ETR operating at 175 MW. From these values, upper limits for gamma heating in the primary and secondary vessels were established by applying a 25% increase attributed to uncertainties in the best estimate values.

Applying this factor to the best estimate or expected average peak gamma heating rate values of 7.5 watts/gm and 9.2 watts/gm in the primary and secondary vessels respectively yields the following maximum values:

Primary vessel: 1.25 x 7.5 = 9.4 watts/gm

Secondary vessel: 1.25 x 9.2 = 11.5 watts/gm

Since these are well below the equivalent of 18 watts/gm used in the THYME-B code, a generous margin of conservatism exists in the associated SAR analyses of maximum expected average vessel wall temperatures and, hence, their containment capabilities.

E.3 Influence of Lower Gamma Heating Levels on FEFPL Protective Functions

E.3.1 Function A - Primary Containment Temperature in Fuel Zone

As discussed in SAR Section 7.1.3.3-A, the critical plant variable for this protective function is the radially averaged primary vessel wall temperature, whereas the associated monitored variable is its outer surface temperature. Because of the radial temperature gradient through the wall, differences exist between the values of critical and monitored variables, the magnitude of which is dependent upon the gamma heating level. As the heating level is reduced, the outer surface temperature deviates by lesser amounts from the average and, hence, the minimum expected gamma heating rate establishes the minimum permissible limit of the monitored variable. This minimum value is established by applying the following factors to the best estimate value:

1. 10% reduction attributed to uncertainties in the best estimate values.

2. 20% reduction that accounts for an ETR power level of 140 MW as the maximum power level envisioned for FEFPL experiments.

Combining these in a multiplicative manner yields the factor, F_{min}:

$$F_{min} = 0.9 \times 0.8 = 0.72$$

Applying this factor to the best estimate or expected average peak value of 7.5 watts/gm in the primary vessel

$$7.5 \times 0.72 = 5.4 \text{ watts/gm}$$

as the associated minimum expected value. The resulting minimum temperature differential across the primary vessel wall, inferred from the data in Table II of Ref. 5, is $\sim 78^{o}F$. Thus, the permissible limit for the monitored variable is $1300^{o}F$ plus one-half of the minimum differential or $1339^{o}F$.

The worst case setpoint is conservatively established, based upon using the temperature transients calculated for a high gamma heating rate (18 watts/gm) as shown in SAR Fig. 7.3 and chosen to provide a $25^{o}F$ protective margin. Thus, for the minimum level of gamma heating cited above, a worst case setpoint of $\sim 1247^{o}F$ will initiate a reactor scram sufficiently early to provide the desired protective margin in the primary vessel.

E.3.2 Function C - Secondary Containment Temperature in Fuel Zone

The design basis for FEFPL protective function C is discussed in SAR Section 7.1.3.3-C. As stated therein, the critical plant variable for this protective function is the temperature of the cadmium filter and the associated monitored variable is the temperature of the inner surface of the secondary vessel. As for the case of protective function A discussed above, a temperature difference exists between critical and monitored variables, the magnitude of which is a function of gamma heating levels.

As indicated in the protective function C discussion, there was considerable margin shown for the two most severe postulated accidents without protective action. These results were calculated on the basis of the gamma heat sources shown in SAR Fig. 9.2, which are the recommended design levels at core midplane for ETR operating at a power level of 175 MW; they include a 25% overheating allowance for uncertainties.

Discussion on minimum expected gamma heating values is unnecessary since there is margin unprotected. Further, to simulate a condition of cadmium melting, it was necessary to increase the magnitude of gamma heating above the design rates (150%) in combination with the most severe postulated accident.

References

1. ANL Memo, A. E. McArthy to Distribution, "Calculated Gamma Ray Heating in the Fuel Element Failure Propagation Loop Irradiated in the ETR", 3/22/71.

2. ANL Memo, R. T. Curtis to D. H. Lennox, "Measured Gamma Heating Rates in ETR", 5/23/73.

3. ANL Memo, W. A. Bezella to D. H. Lennox, "Review of Containment Vessel Temperatures", 7/13/72.

4. ANC Internal Report, R. C. Young, et al., "Recommended Nuclear Specifications for FEFPL", CI-1246, 10/72.

5. Personal Communication, A. Bowman, ANC, 12/13/73.